Universiteit Leiden
The Netherlands

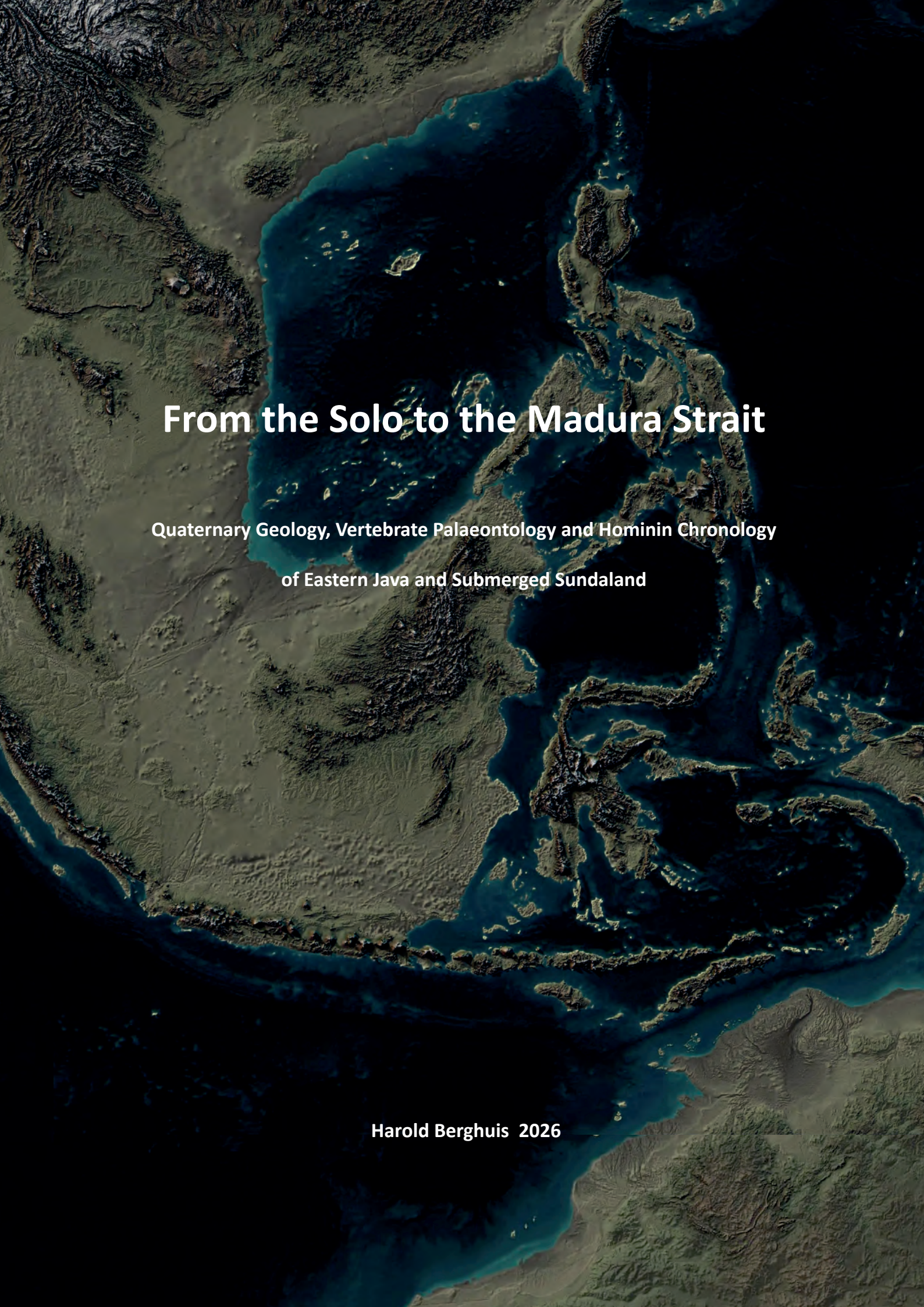
From the Solo to the Madura Strait: Quaternary geology, vertebrate palaeontology and hominin chronology of eastern Java and submerged Sundaland

Berghuis, H.W.K.

Citation
Berghuis, H. W. K. (2026, January 22). *From the Solo to the Madura Strait: Quaternary geology, vertebrate palaeontology and hominin chronology of eastern Java and submerged Sundaland*. Retrieved from https://hdl.handle.net/1887/4287856

Version:	Publisher's Version
License:	Licence agreement concerning inclusion of doctoral thesis in the Institutional Repository of the University of Leiden
Downloaded from:	https://hdl.handle.net/1887/4287856

Note: To cite this publication please use the final published version (if applicable).



From the Solo to the Madura Strait

Quaternary Geology, Vertebrate Palaeontology and Hominin Chronology of Eastern Java and Submerged Sundaland

Harold Berghuis 2026

From the Solo to the Madura Strait

Quaternary Geology, Vertebrate Palaeontology and Hominin Chronology

of Eastern Java and Submerged Sundaland

Harold Berghuis, 2026

Cover: Topography of the ice ages by the designer Vality 7 (v7x)
Artist's impression of SE Asia during the Last Glacial Maximum
Design and lay-out: Harold Berghuis
Photographs: Harold Berghuis (unless otherwise stated)
Copyright © 2026 Harold Berghuis Amsterdam
All rights reserved. No parts of this thesis may be reproduced or transmitted in any form or by any means without prior written approval by the author.

This research was self-funded, with additional funding from the Faculty of Archaeology, Leiden University, and the Dutch Research Council NWO (Grant number 016.Vidi.171.049).
The research was carried out with permission of the Indonesian Ministry of Research, Technology and Higher Education, under RISTEK permits 284/SIP/FRP/E5/Dit.KI/IX/2018 and 343/E5/E5.4/SIP/2019.

From the Solo to the Madura Strait

Quaternary Geology, Vertebrate Palaeontology and Hominin Chronology

of Eastern Java and Submerged Sundaland

Proefschrift

ter verkrijging van
de graad van doctor aan de Universiteit Leiden
op gezag van (waarnemend) rector magnificus
volgens besluit van het college voor promoties
te verdedigen op donderdag 22 januari 2026
klokke 16.00 uur
door
Harold Warner Konstantijn Berghuis
geboren te Amstelveen
in 1969

Supervisors:

Prof. dr. M. van Kolfschoten (Leiden University)

Dr. J.C.A. Joordens (Max Planck Institute for Evolutionary Anthropology, Leipzig, Germany)

Prof. dr. Ir. A. Veldkamp (University of Twente)

Doctorate committee:

Prof. dr. M.A. Soressi (Leiden University)

Prof. dr. J. Kolen (Leiden University)

Prof. dr. A.G. Henry (Leiden University)

Dr. T. Sutikna (Badan Riset dan Inovasi Nasional (BRIN), Indonesia)

Dr. F.S. Busschers (Deltaris, TNO, Utrecht)

Riwayatmu ini. Sedari dulu jadi perhatian insani.

Voor Odile, Ada, Willemijn en Zwaantje. Jullie hebben nog veel mooiere wenkbrauwen.

CONTENTS

1. Introduction and thesis outline 1

2. Plio-Pleistocene foraminiferal biostratigraphy of the eastern Kendeng Zone (Java, Indonesia), the Marmoyo and Sumberingin Sections 11
Published in: *Palaeogeography, Palaeoclimatology, Palaeoecology* (2019)

3. Hominin homelands of East Java, revised stratigraphy and landscape reconstructions for Plio-Pleistocene Trinil 31
Published in: *Quaternary Science Reviews* (2021)

4. The eastern Kendeng Hills (Java, Indonesia) and the hominin-bearing beds of Mojokerto, a re-interpretation 63
Published in: *Quaternary Science Reviews* (2022)

5. Response to the comment of Huffman and Zaim 93
Published in: *Quaternary Science Reviews* (2023)

6. A late Middle Pleistocene lowstand valley of the Solo River on the Madura Strait seabed, geology and age of the first hominin locality of submerged Sundaland 99
Published in: *Quaternary Environments and Humans* (2025)

7. First vertebrate faunal record from submerged Sundaland: the late Middle Pleistocene, hominin-bearing fauna of the Madura Strait 119
Published in: *Quaternary Environments and Humans* (2025)

8. The taphonomy of the Madura Strait fossil assemblage, a record of selective hunting and marrow processing by late Middle Pleistocene Sundaland hominins 175
Published in: *Quaternary Environments and Humans* (2025)

9. The late Middle Pleistocene *Homo erectus* of the Madura Strait, first hominin fossils from submerged Sundaland 201
Published in: *Quaternary Environments and Humans* (2025)

10. The Pleistocene stratigraphy, biozonation and hominin chronology of eastern Java, a synthesis 217

Samenvatting 250
Summary 253
Dankwoord - Ucapan terima kasih - Acknowledgements 256
Curriculum Vitae 258
References 259



Drone view of the Solo at Trinil. The shallow zone is the historic excavation site of Dubois. The blue plastic cover is where a small part of the bone-bearing beds have remained. The museum is on the opposite bank (red roofs). The volcano Lawu lies in the distance. Picture by Eduard Pop.



Chapter 1

Introduction

CHAPTER 1

Introduction

1. Discovery of the Madura Strait site and research questions

Between 2010 and 2016, I worked as a geotechnical consultant for the Port of Surabaya (Indonesia), on the deepening and expansion of the harbour. The work involved the development of land reclamations along the coast. One of these reclamations was the BMS-site, a 100-ha artificial island in the Madura Strait, along the coast of Gresik **(Fig. 1A-B)**, which was planned to become a new cargo handling area. For its construction, we used sand that was extracted from the nearby seabed. In June 2015, the sand suppletion was completed. The island was left for dewatering and compaction, and was completely desolated. As I walked over the site, I noticed that the surface was strewn with bone fragments, beautifully mineralized and obviously old. I called local museums, but I could not find someone to investigate the material. Within a couple of months, further construction work would start. I decided to collect the bones, before they would be lost forever. It took me several lonely weeks to search its surface, collecting more than 6,000 fossils.



Fig. 1. A: The BMS island in the Madura Strait shortly after reclamation, June 2015. View to the east, toward Madura. **B:** Surface of the BMS-island during the dewatering stage. **C:** Ordering specimens in the Geological Museum Bandung.

The boxes with fossils had been piling up in my Surabaya office. In 2016, I sent everything to Iwan Kurniawan, vertebrate palaeontologist at the Geological Museum in Bandung. Together, we cleaned and numbered the material and did some provisional taxonomical ordering **(Fig. 1C)**. For a full analysis of the assemblage, we needed funding and a team of skilled zoologists, which would be hard to arrange. However, I liked the fossils and appreciated my time in the

museum, so why wouldn't I do it myself? I only needed osteological training and supervision. Back home, I called Thijs van Kolfschoten, professor zooarchaeology at Leiden University, and yes, he was willing to receive me in his lab. Surrounded by mounted skeletons, I showed him pictures of my fossils. A bit to my surprise he said, 'Alright, let's do it!'.

So I became a PhD-student of Professor Van Kolfschoten. He introduced me to Professor José Joordens, an expert on hominin evolution. She was preparing a study of the Dubois excavation site in Trinil, eastern Java, and proposed to integrate my Madura Strait study into her larger project. Together, we formulated six research questions:

1. What is the species composition of the Madura Strait assemblage?

2. What is the taphonomic background of the assemblage?

3. What can we say of the vertebrate community structure and the former landscape?

4. Is there evidence of hominin presence?

5. What is the geological setting and age of fossiliferous deposits?

6. How does the Madura Strait site relate to the famous find sites of Java, in terms of stratigraphy, age and biostratigraphy?

The first four research questions are reasonably straightforward and may largely be based on a thorough analysis of the assemblage. Research question five is more difficult to answer due to the subsea setting of the setting of the site. However, as an engineer at the port of Surabaya, I had access to a wealth of unpublished geotechnical data, including dredging reports, sonar surveys and logs of deep drillings, which appeared to be of great help for reconstructing the geological build-up of the site. However, after reading through more than 100 years of palaeontological and geological publications of eastern Java, I realized that research question number six would be the most challenging.

2. The stratigraphy and biostratigraphy of eastern Java

T*he excavations of Dubois*

Eastern Java is renowned for its rich Pleistocene vertebrate localities. The fossils had sparked the imagination of the Javanese for centuries. Large, petrified bones were regarded as the remains of giants from a mythical past, with bone beds as the remains of their battlefields. In the 1850's, the *Natuurkundige Vereeniging van Nederlandsch-Indië* gained interest in this matter. On their initiative, Junghuhn and Raden Saléh surveyed several fossil-rich sites. Both wrote short notes on their work (Saléh, 1867; Junghuhn, 1857). Later, Martin (1886) elaborated on their findings in more detail. He noted that the fossil species are similar to those from the Siwalik Hills of India, described by Falconer and Cautley (1846).

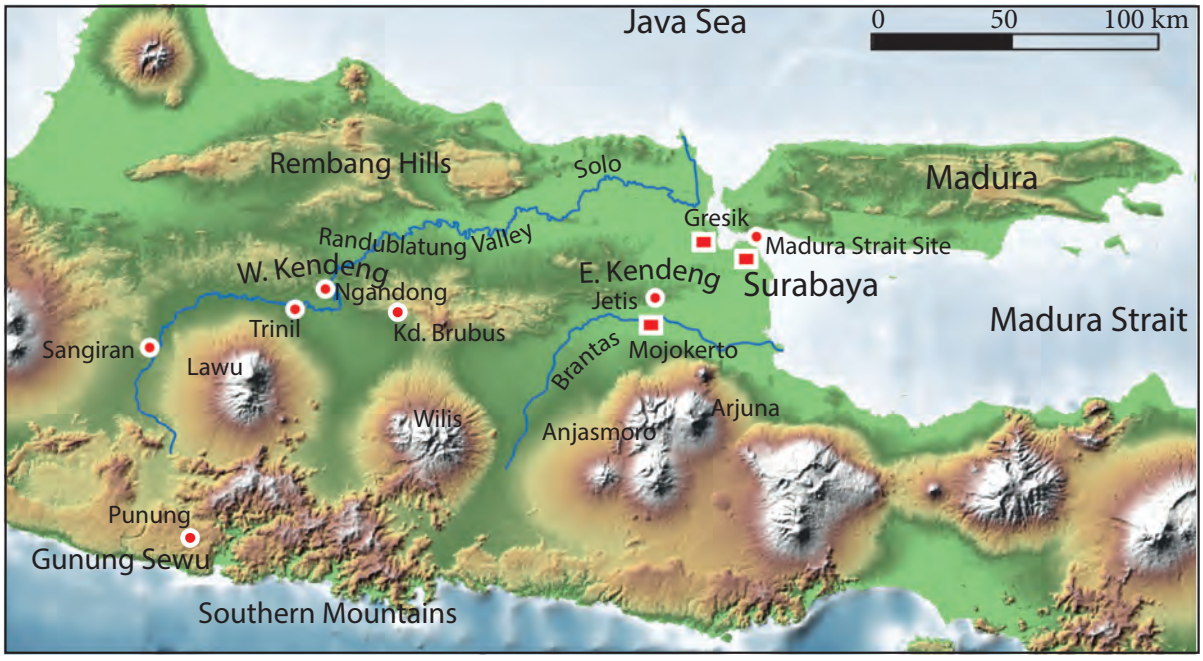


Fig. 2: Eastern Java, with the Madura Strait subsea site and on-land sites mentioned in the text. The Kali Glagah Section lies in Central-Java, outside the range of this map. The site has not been included in this study. Its significance for this study lies in the projection of its fossil fauna to the Sangiran site, as proposed by Leinders et al. (1985).

In the 1890s, Eugène Dubois came to Java on his quest for fossil evidence of a transitional form between apes and humans. He made large excavations in outcrops of fluvial sandstones, exposed in the gentle southern footslopes of the Kendeng Hills **(Fig. 2)**, collecting many thousands of vertebrate bones. His most productive site was Trinil, along the banks of the Solo River. Here, he found the hominin fossils that brought him fame (Dubois, 1894a). Originally described as *Pithecanthropus erectus*, the Trinil skullcap is nowadays regarded as the type specimen of *Homo erectus* (Pop et al., 2024; Mayr, 1950). Dubois referred to the fossil-bearing fluvial sandstones in this region as the Kendeng Schichten. He regarded the vertebrate fossils from these strata as one homogenous fauna, the Kendeng Fauna or the Trinil Fauna, with an estimated Late Pliocene or Early Pleistocene age (Dubois, 1907, 1895).

The vertebrate faunal stages of Von Koenigswald

Three decades later, relevant new vertebrate sites were discovered in the eastern part of the Kendeng Hills near Djetis and Mojokerto (Cosijn, 1932, 1931), in the Glagah Valley near Bumiayu (Van der Maarel, 1932) and in a terrace of the Solo near Ngandong (Ter Haar, 1934; Oppenoorth, 1932). The latter site yielded a spectacular discovery of 12 partial hominin crania and two hominin tibiae. Von Koenigswald (1935, 1934) analysed the fossil assemblages from these sites and found relevant differences in species composition, which he regarded as a reflection of the changing local vertebrate community over time. He defined several faunal stages for eastern Java **(Table 1)**, which he provisionally dated by faunal comparisons with dated fossil assemblages from the Asian mainland.

T*he stratigraphy of Duyfjes*

Around this same period, the geologist Duyfjes was assigned to map the Kendeng Hills and its surroundings. He chose the ~1,500 m thick depositional record exposed in the eastern part of the hill range as his standard section, subdividing this section into four stratigraphic units **(Fig. 3)**. The base of the series consists of calcareous and diatomaceous mudstones, which he referred to as the Lower and Upper Kalibeng Formations, with an assumed Pliocene age. These are overlain by several hundred meters of marine clays, which Duyfjes named the Pucangan Formation, with an assumed Early Pleistocene age. The clays are overlain by deltaic sandstones and finally by fluvial sandstones and conglomerates, by Duyfjes regarded as a deltaic sequence. In the fluvial top of this sequence, Duyfjes resorted to Von Koenigswald's vertebrate biostratigraphy. He noted that the lower part of these fluvial strata yields vertebrate fossils of the Jetis Fauna, whereas the upper part contains the Trinil Fauna. This justified the incorporation of the basal fluvial strata into the Early Pleistocene Pucangan Formation. For the overlying fluvial strata he proposed a new unit: the Kabuh Formation, which he assumed to be of Middle Pleistocene age.

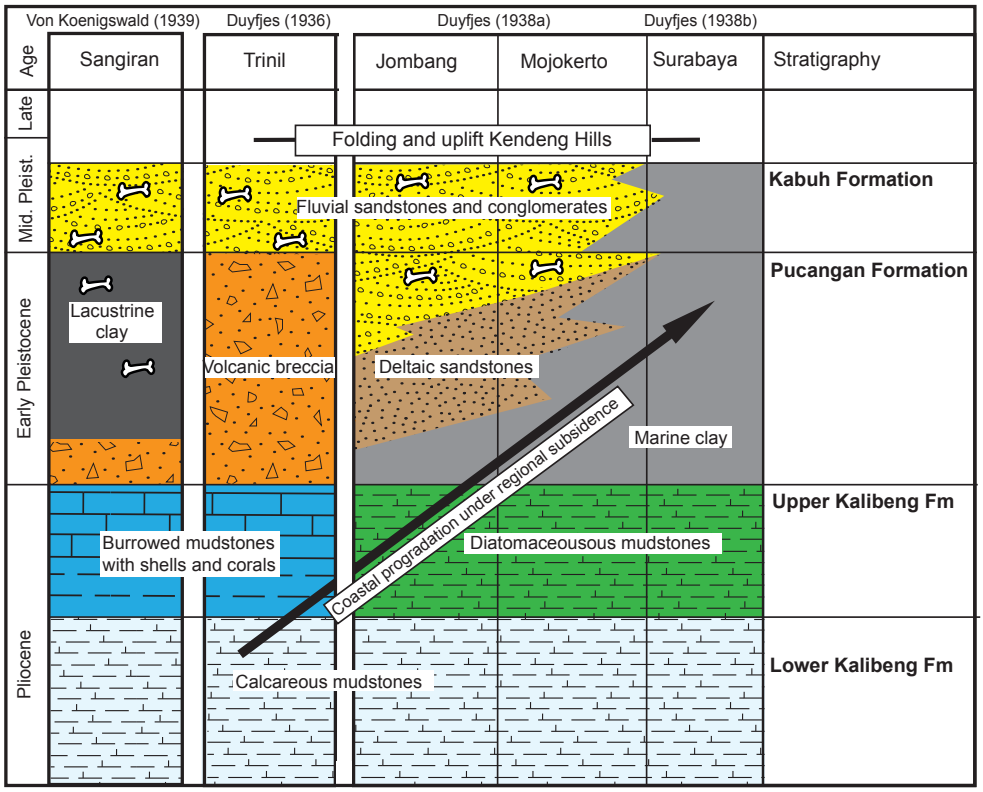


Fig. 3: Published and commonly accepted Pliocene and Pleistocene stratigraphy of eastern Java, for the Kendeng Hills and surroundings, based on Duyfjes (1936,1938a,b). For Sangiran, Duyfjes' units are also referred to under local names, as proposed by Itihara et al. (1985): Upper Kalibeng Fm = Puren Fm; Pucangan Fm = Sangiran Fm; Kabuh Fm = Bapang Fm.

As was normal in those days, Duyfjes' units have a chronostratigraphic significance. For his interpretations, he assumed that eastern Java, north of the volcanic arc, had been a subsiding basin throughout the Pliocene and the Early to Middle Pleistocene, and that this area had been subject to uninterrupted deposition in this period. He thus regarded his standard section as an uninterrupted regressive record, reflecting deltaic progradation driven by volcanic supply (Duyfjes, 1938a). He further assumed that the folding and uplift of the Kendeng Hills postdate this prolonged period of continuous deposition. This model allowed him to correlate his units over the hill range. If lithologies changed, he based his correlations on thickness measurements (he speaks of 'parallelization'), combining strata of different facies in the same unit, assuming that the strata have the same age and that the changing facies represent lateral changes of the depositional landscape.

Moving westwards, the Kendeng Hills consist almost entirely of folded calcareous mudstones, which Duyfjes referred to in his stratigraphic framework as the Lower Kalibeng Formation. Younger strata appear along the southern foothills, and consist of mollusc-bearing mudstones, volcanic breccias and fluvial sandstones. Duyfjes (1936) correlated these one by one with his eastern-Kendeng units **(Fig. 3)**. For the fluvial sandstones at the top of this series, he had an important palaeontological justification for this correlation: these sandstones yielded Dubois' Trinil Fauna and thus, by default, form the Middle Pleistocene Kabuh Formation. Von Koenigswald (1939) extended Duyfjes' correlations further westward to Sangiran. At this site, he described fluvial sandstones with a Trinil Fauna underlain by black clays with dispersed vertebrate fossils, which, according to his observations, belong to the Jetis Fauna. Within Duyfjes' chronostratigraphic framework, this implies that the clays are part of the Early Pleistocene Pucangan Formation.

The revised faunal stages of de Vos et al. and Sondaar

In the 1980s, De Vos et al. (1982) and Sondaar (1984) reviewed the faunal units of Von Koenigswald, through a re-inventory of museum collections and excavation reports. The authors concluded that Von Koenigswald's units had been based on mixed finds with a poorly documented provenance. They proposed a new vertebrate biostratigraphy based on fossil material with a well-described provenance **(Table 1)**. The Satir and Ci Saat Faunas form a subdivision of the previous Kali Glagah Fauna, distinguishing between fossil species from the base and the top of this Glagah River excavation site. The Trinil HK Fauna refers only to the fossil species of the *Haupt Knochenschicht* of Trinil, which forms the base of Dubois' excavation site. The authors introduced the Kedung Brubus Fauna as a new unit, containing the fossil species that Dubois excavated at this site, ca. 35 km east of Trinil. According to the authors, it records the arrival of new species and therefore must be younger than the Trinil HK Fauna. Remarkably, the authors recognized this Kedung Brubus Fauna also in the basal fluvial strata of the eastern Kendeng, around Mojokerto and Jetis. This implies an inverted age relationship compared to Von Koenigswald's previous interpretations, in which the fossils from Jetis were considered to be older than those from Trinil.

Von Koenigswald 1	Age range	Sondaar 1984	Age range
Sampoeng	Holocene	Wajak	>37.4 – 28.5 ka[1]
		Punung	128 – 118 ka[2]
Ngandong	Late Pleistocene	Ngandong	140 – 90 ka[3]
Trinil	Middle Pleistocene	Kedung Brubus	< 900 ka[4]
Djetis	Early Pleistocene	Trinil HK	~900 ka[4]
Kali Glagah	Late Pliocene	Ci Saat	1.3 - 0.9 Ma[4]
		Satir	< 1.9 Ma[4]

Table 1: Vertebrate biostratigraphy of eastern Java. Age ranges from: 1: Storm et al. (2013). 2: Westaway et al. (2007). 3: Rizal et al (2019). 4: Matsu'ura et al. (2022). All age ranges are based on dating studies of type localities, except Matsu'ura et al. (2022), which is based on dating studies of the Sangiran depositional record.

The Punung and Wajak Faunas are new units in the biostratigraphic framework of Sondaar (1984). They are based on fossil assemblages collected from caves in the Southern Mountains. The material from Punung was excavated by Von Koenigswald in the 1930s, who had regarded the fossils as a representant of the Trinil Fauna. Badoux (1959) and De Vos (1983) recognized the fossils as a younger assemblage. The Wajak Fauna is a cave fauna excavated by Dubois in the 1890s and described by Van den Brink (Van den Brink, 1982).

Leinders et al. (1985) projected most of the new faunal units onto the depositional record of Sangiran, referring to find lists from the excavations by Aimi and Aziz (1985). According to these authors, the lower part of the black clays contains the Satir Fauna, whereas the top contains the Ci Saat Fauna. Subsequently, the authors noted that the basal conglomerate of the overlying fluvial strata (the *Grenzbank*) contains the Trinil HK Fauna, whereas the overlying fluvial sandstones contain the fossil species of the Kedung Brubus Fauna. Referring to the available numerical ages of the Sangiran depositional record, Leinders et al. (1985) were able to provide age ranges for the faunal units. Van den Bergh et al. (2001) updated the species lists and the age ranges. **Table 1** offers a new update of these age ranges, based on recent dating studies.

Contradictions

The new faunal units have become widely accepted. Meanwhile, Duyfjes' Pucangan and Kabuh Formations, which are based on the older biostratigraphy of Von Koenigswald, have remained in use, obviously leading to contradicting ages.

This is not the only contradiction between the local biostratigraphy and the stratigraphy. Duyfjes' stratigraphy is based on continuous deposition, whereas De Vos et al. (1982), Sondaar (1984) and Van den Bergh et al. (2001) relate the faunal stages to alternating island conditions and mainland connections. In this model, island conditions are linked to highstands, causing isolation of species and endemism. These alternate with lowstand-related stages of mainland connection, allowing new species to migrate to Java. Today, these climate-related sea-level cycles are referred to in terms of Marine Isotope Stages (MIS). As a geologist, I would argue that it should be possible to trace this cyclicity in the depositional record. In fact, recognizing depositional cyclicity is likely easier than detecting subtle changes in the vertebrate fossil record.

This highlights a fundamental flaw in Duyfjes' stratigraphy: the model of continuous deposition is a grave oversimplification. Throughout the Pleistocene, eastern Java must have been subject to tectonism, climate change, intermittent eruptions, developing drainage systems and sea-level fluctuations. It is essential that we regard the Pleistocene deposits of Java as a record of this dynamic landscape. Instead of 'uninterrupted and laterally continuous', the depositional record is probably incomplete and laterally variable.

The Madura Strait coastline of Surabaya and the submerged shelf

In this respect, it is interesting to zoom in on the Surabaya coastline, with the new vertebrate locality below the seabed of the Madura Strait. Duyfjes (1938b) also correlated his units with the depositional record of this area. Deep drilling data had shown him that the local subsoil is made up of marine clays, overlying at, a depth of ~200 m, a substrate of calcareous mudstones. He concluded that the area has remained outside the maximum range of Pleistocene deltaic progradation. Holding on to his stratigraphic model, he assigned the lower half of the clays to the Pucangan Formation and the upper half to the Kabuh Formation, with a projected, invisible unit boundary, assumed to represent the Early to Middle Pleistocene boundary **(Fig. 3)**. This peculiar stratigraphic procedure is exemplary of Duyfjes' chronostratigraphic approach.

Interestingly, seismic surveys of the deeper Madura Strait and the Java Sea reveal a sub-seabed depositional record of stacked marine sequences separated by unconformities. This features a distinct signal of alternating highstands and lowstands. But where are the traces of these Pleistocene sea-level changes in the coastal record of Surabaya?

The subsiding Sunda Shelf

I had just started thinking about these issues when some relevant new publications came out. Husson et al. (2020) and Sarr et al. (2019) showed that the Pleistocene Sunda Shelf had not been a tectonically stable surface, as had commonly been assumed, but instead, has been subject to subsidence throughout most of the (Middle) Pleistocene. The authors presented a new landscape model, in which Sundaland was widely exposed during the Early Pleistocene. Middle Pleistocene subsidence gradually brought its surface within the range of sea-level fluctuations, resulting in progressive inundation of the lower reaches of the shelf during highstands **(Fig 4A-B)**. Only from MIS11 onward, this caused short periods of significant shelf-drowning, possibly leaving only the mountainous cores of Borneo, Sumatra and Java exposed. This is indeed what we see on the seismic profiles of the deeper parts of the shelf: a basal unconformity representing prolonged Early Pleistocene exposure, overlain by four or five marine cycles. Their preservation and stacking, with the basal unconformity today lying at a depth of ~ 200 m below sea level, can only be explained by shelf subsidence.

This new tectonic model of the Sunda Shelf places the Pleistocene geology and biogeography of Java in a completely new perspective. Rather than being an island with intermittent land connections, Java must have been part of continental Sundaland. Only from the second half of the Middle Pleistocene onward, there may have been several short island stages.

3. Geological investigations (2017 - 2021)

Research question 6 (*How does the Madura Strait site relate to the famous find sites of Java, in terms of stratigraphy, age and biostratigraphy?*) had been based on the idea that there is a well-defined and coherent stratigraphic and biostratigraphic framework for eastern Java. Unfortunately, this is not the case. The stratigraphy and biostratigraphy contradict each other, and neither system aligns with the offshore geology nor with the regional Sundaland landscape models.

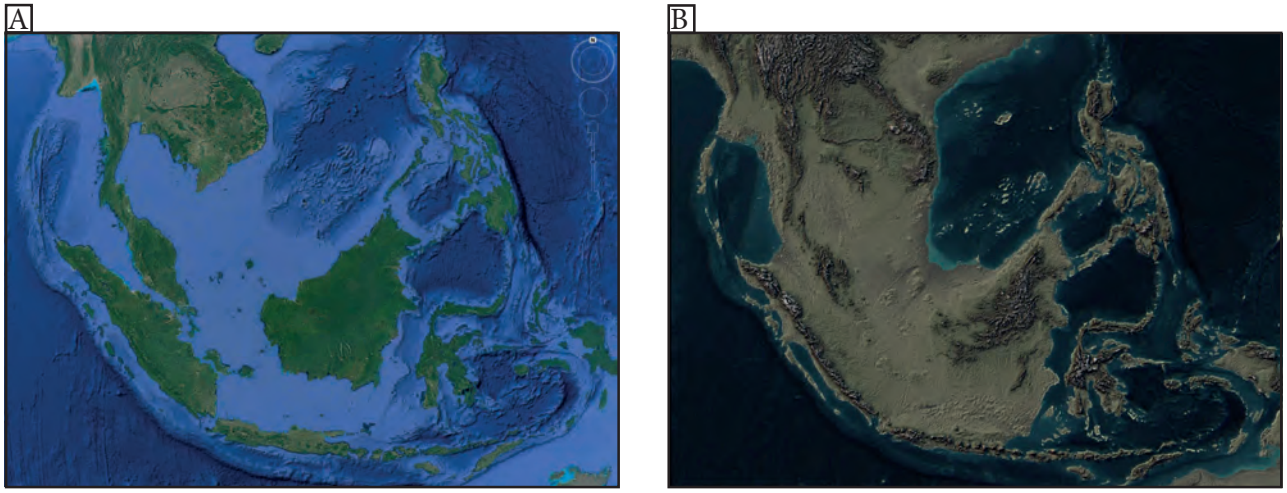


Fig. 4. **A:** The drowned Sunda Shelf, current situation, with the island of Java centrally in the south. Stages of large-scale shelf-drowning during highstands probably go back to MIS11. Map data: Google Earth. **B:** The exposed Sunda Shelf or Sundaland. The shelf was probably widely exposed during the Early Pleistocene and the beginning of the Middle Pleistocene. From MIS11 onward, this exposed state probably alternated with flooding stages. Map data: Vivid maps, coastlines of the ice age.

The problem is most urgent for the stratigraphy. We might very well say that Duyfjes' model of continuous deposition hinders our understanding of a more complex and possibly cyclic depositional record. Therefore, if I wanted to understand the position of the Madura Strait site and its fossil fauna within the larger (bio)stratigraphic framework of Java, I also had to work on the framework.

This would be a huge task, clearly beyond the scope of my studies as I had envisioned. On the other hand, the Madura Strait site offered an excellent starting point for such a broader stratigraphic study. The site, located along the Java coastline, has an intermediate position between the island and the shelf sea. If I could establish a stratigraphic connection between the onshore stratigraphy of Java and the offshore seismic stratigraphy of the deeper Madura Strait, this would not only explain the stratigraphic position of the new fossil locality, but this could also be used as a basis for a revised Pleistocene landscape model and possibly a revised stratigraphic framework for eastern Java.

'Why don't you come along?' Professor José Joordens and her counterpart Shinatria Adhityatama (ARKENAS, Jakarta) were preparing their fieldwork in Trinil, with a team of archaeologists and palaeontologists. Indeed, I had come to realize that I would not make progress with the Madura Strait site without investigating the onshore geology of Java. This was the beginning of what would become a huge detour in my studies. Between 2017 and 2019, I spent long months surveying the wider surroundings of Trinil, Jombang and Mojokerto. I followed the traces of the Brantas and the Solo rivers. I moved to Madura and mapped its southern coastline. During these months, I met Professor Tom Veldkamp, who came to visit the Trinil study team. Tom is an extraordinary geologist with a keen eye for fluvial responses to changing landscapes. His feedback has been of great help and an important motivation to continue with my geological reinterpretations.

4. Analyses of the Madura Strait assemblage (2022-2024)

The geological investigations and the subsequent publication of the results had put my work on the Madura Strait assemblage on hold. Moreover, the collection, stored at the Geological Museum in Bandung, had become inaccessible due to COVID travel restrictions.

By the end of 2022, I resumed my work on the fossils. It had taken some time, but by this point, I had a much better understanding of their age and geological context. Finally, I could truly analyse the Madura Strait assemblage and work on the first five research questions.

THESIS OUTLINE

The thesis comprises ten chapters: an introduction, eight published papers, and a synthesis. These are followed by summaries in both Dutch and English, acknowledgements, the author's CV and a list of references.

Chapters 2 to 6 of this thesis address the geology of eastern Java, chapters 7 to 9 concentrate on the Madura Strait assemblage. All of these chapters are stand-alone papers, which have been peer-reviewed and published in scientific journals. For all papers, I have been the main investigator with respect to research design, field investigation, fossil collecting, museum and laboratory analyses, manuscript writing and visualization, with of course important advice and support from the involved co-authors. Relevant exceptions are the OSL-datings, which were carried out by Tony Reimann and Alice Versendaal, and the foraminiferal determinations, which were carried out by Simon Troelstra.

The Supplementary Information of the papers has not been included in this thesis. For these documents, please refer to the (open-access) on-line publications.

Chapter 2: ***Plio-Pleistocene foraminiferal biostratigraphy of the eastern Kendeng Zone (Java, Indonesia): the Marmoyo and Sumberingin Sections***

Published in: Palaeogeography, Palaeoclimatology, Palaeoecology (2019)

The base of the eastern Kendeng exposures consists of calcareous and diatomaceous mudstones, which grade into marine clays. It represents a gradual transition from open marine conditions to coastal conditions, which is a crucial stage in the early development of eastern Java. In this chapter, we draw up a detailed foraminiferal biostratigraphy of this marine series, with an interpretation of its significance in terms of ages, depositional depths, regional landscapes, and the continuity of the depositional record.

This study was conducted in close cooperation with Simon Troelstra (Vrije Universiteit, Amsterdam), a leading expert on planktonic and benthic foraminifera.

Chapter 3: ***Hominin homelands of East Java: Revised stratigraphy and landscape reconstructions for Plio-Pleistocene Trinil***

Published in: Quaternary Science Reviews (2021)

The banks of the Solo around Trinil reveal a ~3 Ma record of coastal and terrestrial deposition. Numerous researchers have described this depositional record. In this chapter, we briefly summarise earlier depositional and stratigraphic models. We proceed with a thorough re-interpretation of the local strata, against a background of volcanism, tectonism, the development of the Solo drainage system, sea-level fluctuations and climate change. This results in a revised stratigraphic framework, representative of Trinil and its direct surroundings.

This chapter does not address the detailed build-up and numerical ages of the site excavated by Dubois, which were published in subsequent publications (Hilgen et al., 2023; Pop et al., 2023). In the synthesis of the thesis, I will go deeper into the spectacular results of these publications and their consequences for the interpretation of the Trinil fossil record.

Chapter 4: ***The eastern Kendeng Hills (Java, Indonesia) and the hominin-bearing beds of Mojokerto, a re-interpretation***

Published in: Quaternary Science Reviews (2022)

The top of the eastern Kendeng exposures consists of deltaic and fluvial strata. Duyfjes selected his reference sections for the Pucangan and Kabuh Formations in this area. Today, large sand quarries offer an unprecedented insight into this complex series.

We present a detailed description and a re-interpretation of the record against a background of volcanic supply, tectonism, ancient climates, the development of the Brantas drainage system, and sea-level fluctuations. Duyfjes' stratigraphy is revised and re-interpreted as a local framework, representative of the Jombang and Mojokerto exposures only.

The fluvial strata at the top of the eastern Kendeng exposures exhibit a cyclic build-up that can be correlated with the Middle Pleistocene sea-level sequences of the offshore Madura Strait.

Chapter 5: *Response to the comment* by Huffman and Zaim

Published in Quaternary Science Reviews (2023)

Our re-interpretation of the eastern Kendeng stratigraphy has important consequences for the age, landscape context and stratigraphic position of the *Homo erectus* child skull from Perning (Mojokerto). Our analysis was criticised by Huffman and Zaim, in a comment published in Quaternary Science Reviews in 2023. We gratefully accepted the offer by the journal to write a response.

Chapter 6: A late Middle Pleistocene lowstand valley of the Solo River on the Madura Strait seabed, geology and age of the first hominin locality of submerged Sundaland

Published in: Quaternary Environments and Humans (2025)

This chapter presents a detailed description of the coastal subsoil around Surabaya, down to a depth of ~100 m. We place the local coastal development in a larger landscape framework, by correlations with the coastal record of the nearby eastern Kendeng Hills, the upstream terraces of the Solo, and the off-shore geology of the deeper Madura Strait.

Chapter 7: First vertebrate faunal record from submerged Sundaland: the late Middle Pleistocene, hominin-bearing fauna of the Madura Strait

Published in: Quaternary Environments and Humans (2025)

Among the Madura Strait fossils, we identified 36 vertebrate species, divided into four taxonomical Classes and eleven Orders. This chapter provides an extensive and richly illustrated description of the assemblage, including measurements and specimen counts. The assemblage is interpreted in terms of vertebrate communities. A comparison is made with relevant fossil assemblages from Java, and the significance of the assemblage within the regional biogeography of Sundaland is discussed.

Chapter 8: The taphonomy of the Madura Strait fossil assemblage, a record of selective hunting and marrow processing by late Middle Pleistocene Sundaland hominins

Published in: Quaternary Environments and Humans (2025)

A systematic study of the taphonomy of the Madura Strait assemblage provides new insights into several relevant research questions, such as: What is the accumulation history of the fossils? Are OSL-ages of the sediment representative of the ages of the fossils? Can we translate the assemblage to living populations and ecosystems? And, are there signs of hominin foraging behavior?

Chapter 9: The late Middle Pleistocene *Homo erectus* of the Madura Strait, first hominin fossils from submerged Sundaland

Published in: Quaternary Environments and Humans (2025)

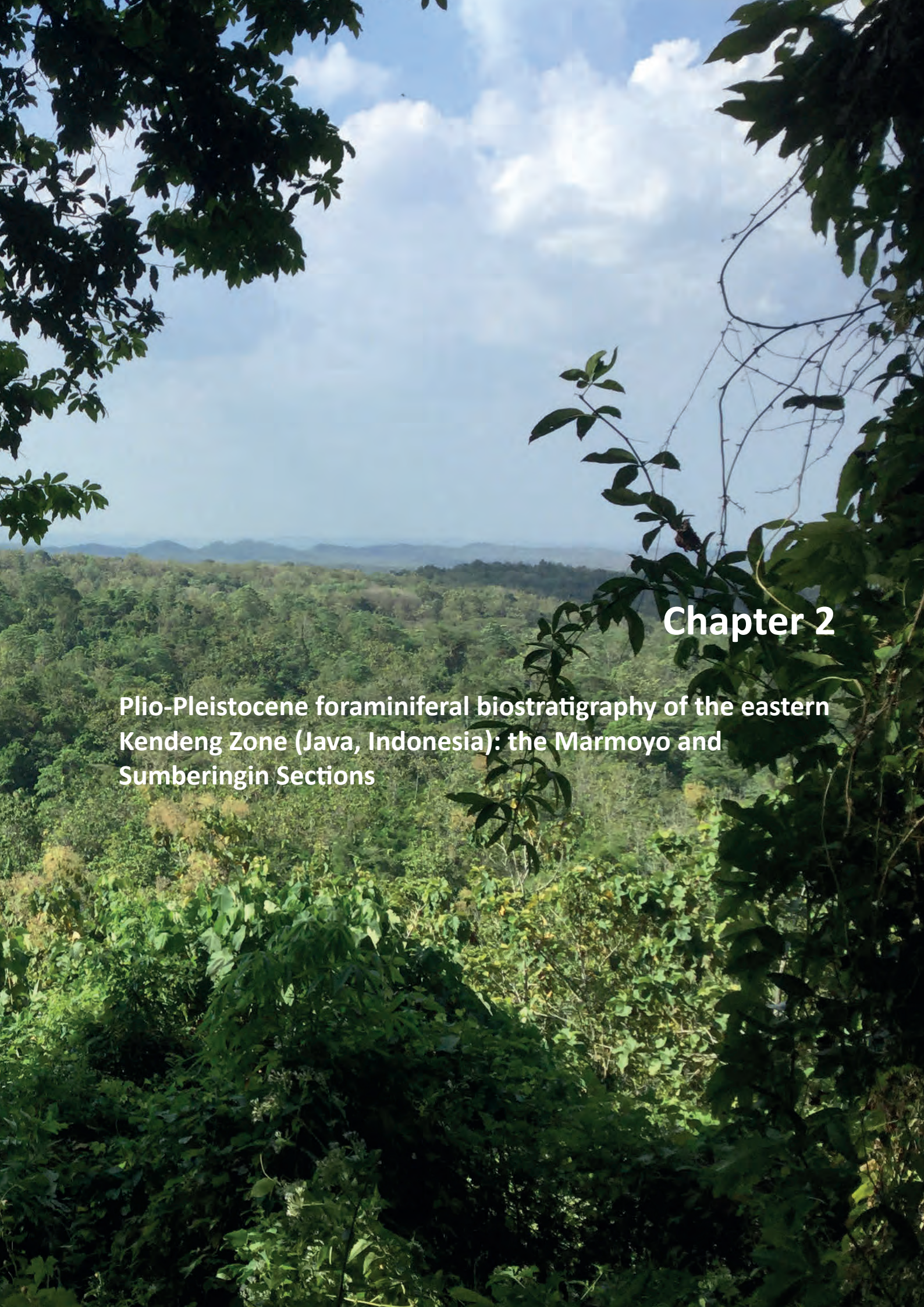
The Madura Strait assemblage contains two hominin cranial fragments: a frontal fragment and a parietal fragment. In this chapter, we provide a metric and morphological description of the two cranial fragments and compare them with Pleistocene hominin remains from Java, Flores and mainland Asia.

Chapter 10: The Pleistocene stratigraphy, biozonation and hominin chronology of eastern Java, a synthesis

The thesis concludes with a discussion and revision of the Pleistocene stratigraphy, biozonation and hominin chronology of eastern Java, against a larger 'Sundaland' landscape context.



View from Gunung Marmoyo, looking to the northwest. The Marmoyo River is beneath the canopy.



Chapter 2

Plio-Pleistocene foraminiferal biostratigraphy of the eastern Kendeng Zone (Java, Indonesia): the Marmoyo and Sumberingin Sections

CHAPTER 2

Plio-Pleistocene foraminiferal biostratigraphy of the eastern Kendeng Zone (Java, Indonesia): the Marmoyo and Sumberingin Sections

H.W.K. Berghuis, S.R. Troelstra, Yahdi Zaim

Published in: *Palaeogeography, Palaeoclimatology, Palaeoecology* (2019)

ABSTRACT

The Plio-Pleistocene of the eastern Kendeng Hills (Java, Indonesia) consists of a more than 1,250 m thick series, passing upwards from diatomaceous laminated mudstones to blue clays and deltaic sandstones. The fine-grained marine beds have received little attention from researchers. Age assumptions are based on correlations with better-studied sections in the western Kendeng Hills. In contrast, the deltaic sandstones at the top of the series have received ample attention. These beds are renowned for their fossil vertebrate fauna, including *Homo erectus*. Lately, doubts have arisen concerning the age and stratigraphic position of the fossiliferous sandstones. The aim of this study is to establish a detailed biostratigraphy of the fine-grained marine beds, which may also provide new age indications for the overlying fossil-bearing sandstones.

We selected the Marmoyo and Sumberingin Sections as suitable representatives for the local marine stratigraphy. Both sections were logged and sampled, and the samples were analysed for their foraminifera content. The sections provide sufficient biostratigraphic markers to allow for a reasonable age control. We found that the diatomaceous facies is older than previously thought: it dates from the Early Pliocene and corresponds in age with bathyal, foraminifera-rich mudstones of the western Kendeng Zone. It implies the existence of two bio-geographic zones in the Early Pliocene basin, with eutrophic, oxygen-depleted conditions in the east and normal oxygen conditions in the west. The diatomaceous mudstones change upwards into foraminifera-rich mudstones, marking a return to normal oxygen conditions later in the Early Pliocene, and eventually into blue clays, representing a shift from bathyal to outer shelf conditions in the Late Pliocene. Higher up in the blue clays, changes in the planktonic foraminifera assemblage indicate cooler water conditions, which we relate to the beginning of the Pleistocene.

Although generally regarded as a continuous regressive series, our work revealed the existence of an unconformity within the blue clays. The blue clays above this unconformity represent a shallow marine, deltaic setting. It is this second blue clay series that passes conformably into the overlying deltaic sandstones. The presence of reworked planktonic foraminifera in the upper clay-series hampers adequate biostratigraphic dating, but the stratigraphic break within the clays suggests that this second sequence is younger than previously assumed.

1. Introduction

The Kendeng is an east-west trending fold zone in East-Java (**Fig. 1**). Nowadays it is an undulating hill-range, reaching heights of around 300 m ASL, but during the Miocene it formed the deepest part of a narrow, marine retro-arc basin located north of an east-west trending volcanic arc (Lunt, 2013). In the Late Miocene, local volcano-tectonic conditions changed. Volcanic activity decreased and the basin, which had previously been subsiding, became subject to compressive conditions, marking a transition to large-scale uplift (Genevraye and Samuel, 1972; Hamilton et al., 1979; Smyth et al., 2008). This uplift is recorded in the foraminiferal fauna of the thick Pliocene mudstone series, which bears evidence of a gradual regression from bathyal to shelfal conditions. The mudstones pass upwards into coastal beds and subsequently into breccias and sandstones, marking emergence and resumption of active volcanism in the Pleistocene. On-going compression of the basin deposits caused folding and thrusting, characteristic of the present-day Kendeng Hills.

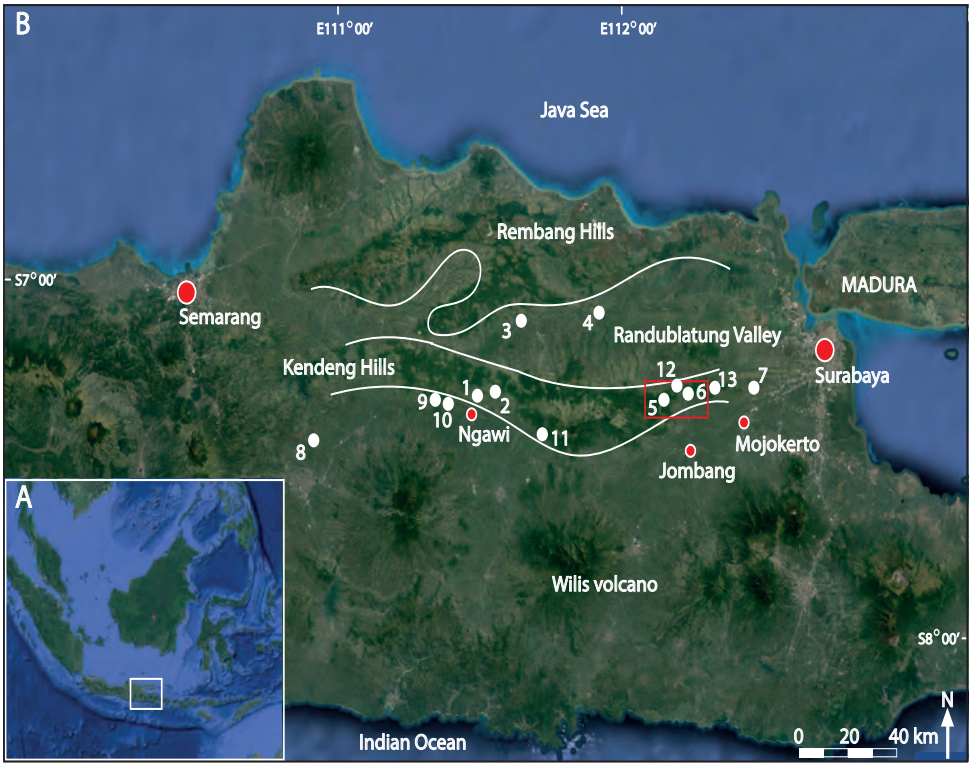


Fig. 1. A: The Indonesian archipelago with the study area on the eastern part of the island of Java. **B:** East-Java, physiographic zones, locations of the biostratigraphic sections and sites mentioned in the text. 1: Solo River Section. 2: Ngepung Section. 3: Tobo-Cepu wells. 4: Bojonegoro-1 well. 5: Marmoyo Section. 6: Sumberingin Section. 7: Perning. 8: Sangiran. 9: Sonde. 10: Trinil. 11: Kedung Brubus. 12: Kali Beng. 13: Gn. Pucangan. Red box: area shown in Figure 3. Map data: Google, DigitalGlobe.

The Plio-Pleistocene regression of the Kendeng Zone is primarily known from detailed foraminiferal biostratigraphic studies of the southwestern Kendeng Hills (Saint-Marc and Suminta, 1979; Van Gorsel and Troelstra, 1981). The local stratigraphy consists of a thick regressive series of marine mudstones, overlain by coastal beds with corals and molluscs, and capped by terrestrial breccias and sandstones. The Plio-Pleistocene series of the eastern Kendeng Hills has a different character. It consists of massive marine mudstones, overlain by several hundred metres of laminated diatomaceous mudstones, which change upwards into blue clays, which in turn change into deltaic sandstones. Except for the sandstones at the top, this series has received little attention from researchers. Based on historic mapping work by Duyfjes, the diatomaceous beds were correlated with the coastal beds of the southwestern Kendeng. The overlying blue clays were correlated with the terrestrial breccias of the southwestern Kendeng Zone.

A foraminiferal biostatigraphy of the marine series of the eastern Kendeng Zone is, so far, not available. Our study aims to establish this. It will fill an important gap in the local biostratigraphy and will allow us to test the validity of the currently used stratigraphic correlations.

The study also aims to provide a better insight into the age of the deltaic sandstones, conformably overlying the fine-grained marine series. These beds are renowned for their fossil vertebrate fauna (Cosijn, 1932, 1931; Von Koenigswald, 1935, 1934). Ever since the discovery of a *Homo erectus* skullcap in 1936, the age and stratigraphic position of the deltaic sandstones has been a source of debate (e.g. Huffman et al., 2005; Huffman, 2001a). A detailed biostratigraphy of the underlying marine series may provide a new insight into the (maximum) age of these sandstones.

2. Background

2.1 Stratigraphy, ages and correlations

2.1.1 Stratigraphy by Duyfjes

The stratigraphy of the Kendeng Zone (**Fig. 2**) was set up by Duyfjes (1936, 1938a). This author based his Plio-Pleistocene units on reference sections in the eastern Kendeng Zone. Duyfjes defined two Pliocene units, the Lower and Upper Kalibeng Formations, named after the Kali (River) Beng. The Lower Kalibeng Formation consists of massive calcareous mudstones rich in foraminifera, reaching a thickness of around 800 m. The Upper Kalibeng Formation conformably overlies this unit. It consists of several tens of metres of marine sandstones, which pass upwards into thinly laminated diatomaceous mudstones, reaching a thickness of 400 to 700 m. Duyfjes traced his Pliocene units westwards over the Kendeng Zone. The Lower Kalibeng Formation retains its facies of a massive calcareous mudstone and is well traceable in the field. In the western Kendeng Zone, this monotonous series can be seen to overly bedded sandstones and argillaceous mudstones, a transition that Duyfjes marked as the lower boundary of the unit. Mapping the Upper Kalibeng Formation from its reference area in the eastern Kendeng Zone toward the western Kendeng Zone, Duyfjes found its facies changing to slightly sandy calcareous-argillaceous mudstones and finally to the well-known reefal limestones and calcareous mudstones with marine molluscs and coral fragments, as exposed along the southwestern flanks of the Kendeng Zone. These reefal strata generally have a thickness of 100 to 200 m.

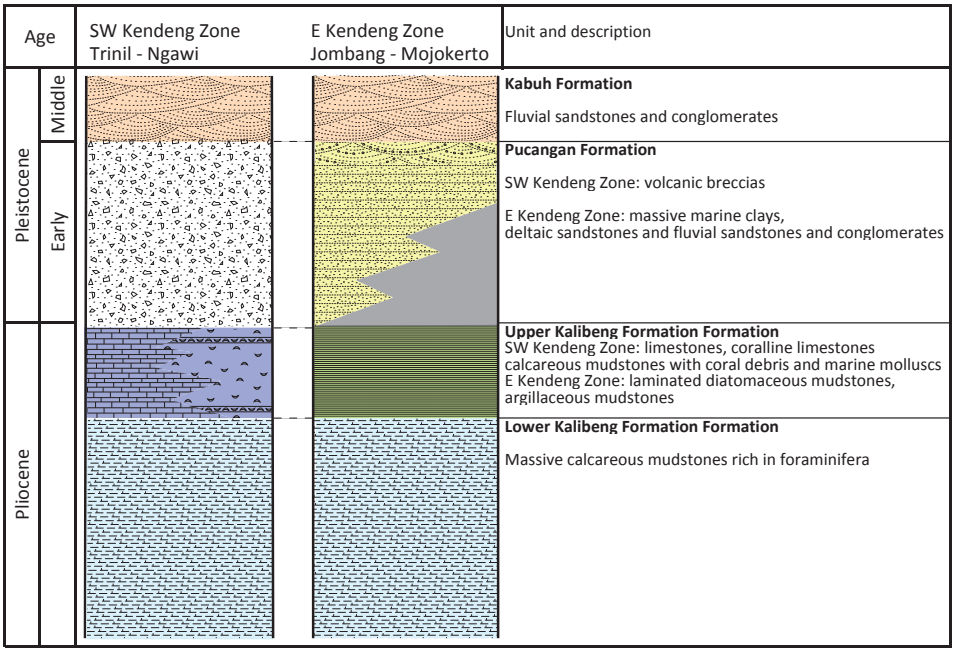


Fig. 2. Plio-Pleistocene Kendeng Zone stratigraphy. Adapted from Duyfjes (1936, 1938).

Duyfjes also defined two relevant Pleistocene units: The Pucangan and Kabuh Formations. He used the Sumberingin Section as his reference section; the names of the units refer to a nearby hill (Pucangan) and village (Kabuh). The base of the Pucangan Formation consists of marine blue clays, which Duyfjes found conformably overlying the diatomaceous mudstones of the Upper Kalibeng Formation. The clays change upward into deltaic and fluvial sandstones, which he referred to as the Volcanic Facies of the Pucangan Formation. For Duyfjes, the Pucangan Formation represented a prograding delta over a shallow muddy sea. In the Sumberingin Section, the clays reach a thickness of ca. 300 m, whereas the overlying sandstones are almost 500 m thick. Toward the northeast, the thickness of the clays increases and the sandstones eventually wedge out. The upper part of the Sumberingin Section consists of cross-bedded, fluvial sandstones and conglomerates, which Duyfjes regarded as a separate unit: the Kabuh Formation.

Tracking his Pleistocene units westward over the Kendeng Zone, Duyfjes found that the Clay Facies of the Pucangan Formation gradually disappears. Around Ngawi and Trinil, volcanic breccias directly overlie the Upper Kalibeng Formation, which in this area consists of reefal beds. Duyfjes regarded the breccias as the Volcanic Facies of the Pucangan Formation. These breccias are overlain by cross-bedded fluvial sandstones, which Duyfjes correlated with the cross-bedded sandstones in the eastern Kendeng Zone and consequently regarded as the Kabuh Formation.

2.1.2 Von Koenigswald's vertebrate biostratigraphy

Von Koenigswald (1935, 1934) developed a vertebrate biostratigraphy for the terrestrial strata of Java. Duyfjes (1936, 1938a) referred to this biostratigraphy, stating that the Pucangan Formation contains the Early Pleistocene Jetis Fauna

and that the Kabuh Formation contains the Middle Pleistocene Trinil Fauna. The timing of the publications suggests that Duyfjes drew the boundary between his two Pleistocene units based on Von Koenigswald's faunal units. However, Huffman (2005) suggested that Duyfjes defined his units earlier, based on lithological characteristics.

2.1.3 The *Homo erectus* of Perning and its age

Ever since the finding of a *Homo erectus* skullcap in Perning (Mojokerto) in 1936, the age of the deltaic sandstones of the eastern Kendeng Zone has been subject of debate (Huffman et al., 2005). The fossil was found in a conglomerate bed, which Duyfjes indicated as the Pucangan Formation (Duyfjes, 1936). Based on his stratigraphic correlations, it is older than the *Homo erectus* fossils of Trinil (Dubois, 1894a), which come from beds that Duyfjes indicated as the Kabuh Formation. Using Von Koenigswald's biostratigraphy, the Trinil fossils are of Middle Pleistocene age and the Perning skullcap is of Early Pleistocene age. Many years later, a similar debate came up after de Vos (1982) and Sondaar (1984) rejected Von Koenigswald's vertebrate biostratigraphy, indicating that it was based on fossils from mixed localities and a poorly known stratigraphic provenance. They presented a new vertebrate biostratigraphy, consisting of an Early Pleistocene Trinil HK Fauna and a Middle Pleistocene Kedung Brubus Fauna. They assigned the fossils of the sandstones near Perning to the Middle Pleistocene Kedung Brubus Fauna and the main fossil-bearing bed of Trinil to the Early Pleistocene Trinil HK Fauna. Their revision suggests that the deltaic sandstones of the eastern Kendeng Zone date from the Middle Pleistocene. Moreover, it implicates that Duyfjes' stratigraphic correlations of the Pleistocene units over the Kendeng Zone are invalid, again leading to debate (Bartstra, 1983; Hooijer, 1983; Hooijer and Kurtén, 1984). A decade later, Swisher et al. (1994) carried out $^{40}Ar/^{39}Ar$ on volcanic pumice of the Perning site, arriving at an age of 1.81 ± 0.04 Ma. This again pushed back the age of the Perning *Homo erectus* and the surrounding deltaic beds to the Early Pleistocene, however, it was rejected by others, claiming that the pumice is reworked (Langbroek and Roebroeks, 2000; Vos et al., 1994). Reworked or not, Morwood et al. (2003) conducted fission track dating on pumice at the Perning site and found an age of 1.49 ± 0.13 Ma.

2.1.4 Revisions by Pringgoprawiro and local stratigraphic practice

Pringgoprawiro (1983) renamed the Lower Kalibeng Formation as the Kalibeng Formation and the Upper Kalibeng Formation as the Sonde Formation, using a type section near the village of Sonde in the southwestern Kendeng Zone. Holding on to Duyfjes correlations, he also renamed the laminated diatomaceous mudstones of the eastern Kendeng Zone to Sonde Formation. Moreover, he separated the blue clays from the Pucangan Formation and assigned them to the Lidah Formation, which is an older name for similar clays found in the Randublatung Zone, the lowland north of the Kendeng Hills. Although international researchers generally hold on to Duyfjes' units, Indonesian researchers often follow Pringgoprawiro's revisions (Noya e.a., 1992; Sukardi, 1992).

2.2 Foraminiferal biostratigraphy

Foraminiferal biostratigraphic studies have greatly contributed to our understanding of the Kendeng Zone stratigraphy. Calibration using the magnetostratigraphy acquired by regional deep-sea drilling has provided detailed ages for first occurrences (F.O.) and last occurrences (L.O.) of planktonic foraminifera species (Berggren et al., 1995, 1985; Wade et al., 2011). Unless specified, biostratigraphic ages mentioned in this paper are based on Wade (2011). Below we summarize and briefly discuss several relevant biostratigraphic studies from different localities.

The Bojonegoro-1 well (Bolli, 1966) is located in the Randublatung Zone, north of the Kendeng Hills. During the Mio-Pliocene, this area formed the slope north of the deeper Kendeng Basin. The base of the well reaches calcareous mudstones with a Miocene planktonic foraminifera fauna. These are overlain by argillaceous-calcareous mudstones containing Late Pliocene biostratigraphic markers, implying a latest Late Miocene – Early Pliocene hiatus. The Late Pliocene mudstones above the hiatus represent upper bathyal to outer shelf conditions (Boomgaart, 1949; Lunt, 2013).

The Ngepung Section (Saint-Marc and Suminta, 1979) is a river section located in the southwestern Kendeng Zone, covering 650 m of massive calcareous mudstones representing Duyfjes' Lower Kalibeng Formation. The mudstones provide a continuous depositional record, starting in the Late Miocene and covering the entire Pliocene, without the hiatus of the Bojonegoro-1 well. The mudstones are overlain by reefal limestones (Upper Kalibeng Formation), which the authors date as Early Pleistocene.

The Solo River Section (Van Gorsel and Troelstra, 1981), re-evaluated by Lunt (2013), offers the most detailed foraminiferal biostratigraphy of the western Kendeng Zone. It covers approx. 800 m of massive calcareous mudstones, rich in well-preserved foraminifera and contains a fine array of relevant biomarkers. The mudstones form an uninterrupted series, starting in the Late Miocene age and covering the entire Pliocene. The regressive nature of the upper part of this series is reflected by its benthic fauna and a decreasing ratio between planktonic and benthic foraminifera (P/B-ratio). The reefal limestones overlying the mudstones contain several datum levels suggesting an Early Pleistocene age: the F.O. of *Globorotalia* cf. *truncatulinoides* (1.93 Ma), the last occurrences of *Globigerinoides extremus*

(1.99 Ma) and *Globigerinoides fistulosus* (1.88 Ma), as well as a dextral to sinistral coiling change in *Globorotalia menardii*.

Biostratigraphic data are also available for several wells near Tobo - Cepu, in the western Randublatung Zone. Although not very detailed and relatively far from the eastern Kendeng Zone, the sections are relevant because they cover the blue clays that Pringgoprawiro (1983) correlated with the blue clays of the eastern Kendeng Zone (as the Lidah Formation). In this area, the clays occur from the surface down to depth of approx. 350 m. The clays overlie a coarse lag of sandstones with marine molluscs, locally known as the Selorejo Formation. The base of this coarse interval is an unconformity above the Pliocene calcareous mudstones. Several researchers report the first arrival *G. truncatulinoides* (F.O. 1.93 Ma) in the base of the clays, directly above the Selorejo Formation (Pringgoprawiro and Baharuddin, 1979; Sanyoto, 2009).

3. Methods

3.1 The sections

After an elaborate inspection of local river sections, we concluded that a continuous section, running through the entire marine series, from the diatomaceous mudstones to the blue clays and the overlying sandstones, is not available. This is mainly due to a poor exposure of the blue clays. We selected two river sections, which together provide the best possible coverage of the local stratigraphy: The Marmoyo Section and the Sumberingin Section (**Fig. 3**). Both sections were described by Duyfjes (1938a) and form key sections in his original stratigraphy.

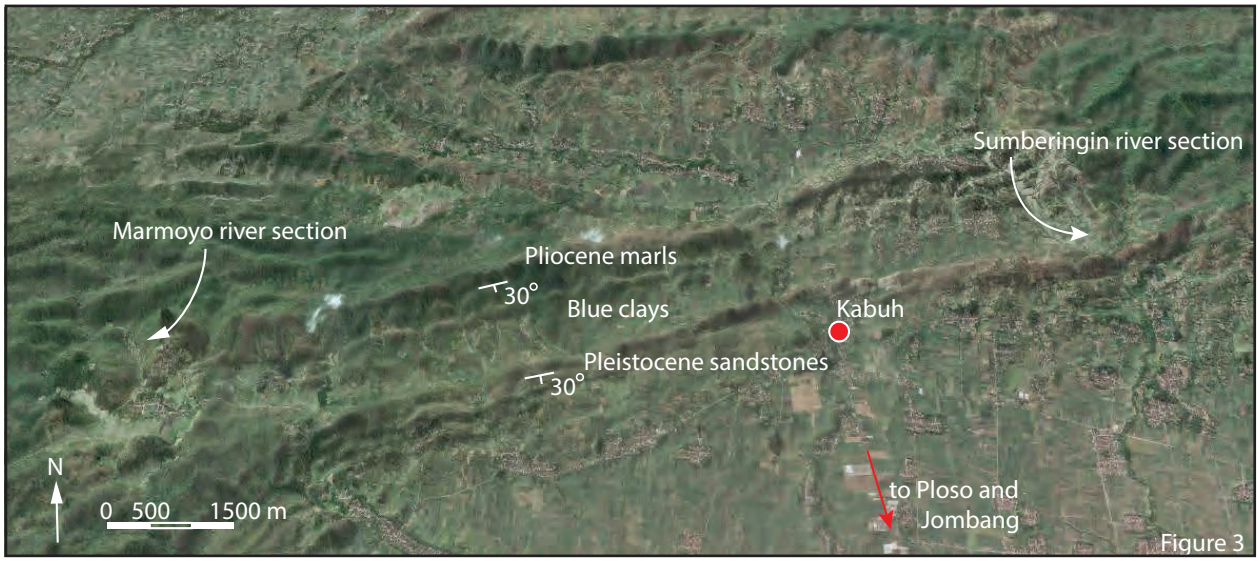


Fig. 3. Location of the Marmoyo and Sumberingin Sections and local geological structure. For location see **Figure 1**. Map data: Google, DigitalGlobe.

The studied river sections cut through the southern flank of a large anticline. North of Marmoyo, this flank of the anticline is thrusted northwards over younger strata. The Marmoyo Section exposes a marine series of ca. 600 m. The series is undisturbed by the thrustzone, which is located just north of the section, and the beds have a constant dip of approx. 30 degrees to the south. The base of the section consists of bedded marine sandstones, regarded by Duyfjes as the base of the Upper Kalibeng Formation in its eastern facies. Moving southwards, the sandstones pass into the overlying laminated diatomaceous mudstones, which dominate this section. The laminated mudstones pass into massive calcareous-argillaceous mudstones rich in foraminifera, which in turn change into massive blue clays, regarded by Duyfjes as the Clay Facies of the Pucangan Formation. The clays form the top of the section and are exposed in the creek just before it enters a wider, east-west trending valley. The blue clays make up the subsoil under this valley, although poorly exposed.

Moving approx. 10 km to the east, parallel to the axis of the anticline and following this wide valley, we find the Sumberingin creek cutting a gully through the fields and exposing the local blue clays. The creek continues to the south where it cuts through another ridge, representing the sandstones overlying the blue clays. The gradual transition from clays to deltaic sandstones is well exposed. The sandstone section was first described by Van Es (1931) and later by Duyfjes (1938a). Duyfjes used it as the standard section for his Pleistocene units, the Pucangan and Kabuh Formations. Both authors mentioned the underlying clays, but did not include them in their detailed descriptions, merely describing the clays as 'homogenous'. We found the exposed clays in the base of this section to have a thickness of almost 300 m. Unfortunately, the creek does not expose the lower boundary of the clays. The blue clays, as exposed in the creek, generally dip southward by ca. 30 degrees, following the dip of the flank of the anticline. But the dip of

the strata also reveals the existence of a gentle superimposed fold, forming a small local anticline. The core of this gentle fold represents the lowest stratigraphic level of the clays exposed in the creek. In the fields, near the core of this small anticline, there is an isolated hill consisting of lighter coloured calcareous mudstones, indicating that we are very close to the lower boundary of the clays.

The Sumberingin Section stratigraphically overlies the Marmoyo Section. Together, the sections form a marine record with a thickness of ca. 1,400 m. Our biostratigraphic study includes the combined stratigraphic section, up to the base of the deltaic sandstones, covering more than 800 m. The sandstones were left out of the biostratigraphic study, as they are largely made up of transported erosion products.

We attempted to ensure a stratigraphic overlap between the two sections, in order to provide a good stratigraphic fit. However, appearances of new species in the base of the Sumberingin Section indicate that there is a minor gap between the two sections **(Section 5.3.1)**. For detailed charts of the sections and field pictures reference is made to supplemental figures S1 to S4.

3.2 Field and laboratory procedures

We measured, described and photographed the sections in detail and sampled with an interval of 10 – 20 m. Sample preparation was carried out in the Laboratory for Sediment Analysis of the Vrije Universiteit, Amsterdam. To retrieve the foraminifera, the samples were emerged in petroleum ether for two days, after which the fluid was decanted. Subsequently, boiling water was poured over the samples, disaggregating the material. This method provided reasonable residues which, after sieving through a >63 µm mesh and drying on a hotplate, were studied under a binocular microscope.

We studied a total of 43 samples for their foraminiferal content. We listed the total occurrences per sample of planktonic and benthic foraminifera and diatoms as poor, moderately rich or rich. Diatom occurrences mentioned in this paper only include the >63 µm specimens. Diatoms were not included in further identification work. Preservation of the foraminifera is generally reasonable, allowing for proper identification. Planktonic species strongly dominate the assemblages. Benthic species are scarce and often occur as single specimens. The faunal analysis was carried out semi-quantitatively, with occurrences per species listed as scattered, common or abundant. P/B-ratios were determined based on actual counts, however note that there are large differences in total foraminifera occurrences per sample, affecting the significance of the P/B-ratios. A sample may for example be rich in planktonic foraminifera and poor in benthic foraminifera and have a P/B-ratio of 95%, whereas another sample may be poor in planktonic foraminifera and extremely poor in benthic foraminifera, and yet also have a P/B ratio of 95%.

3.3 Nomenclature for fine-grained rocks

The studied sections are dominated by clay to silt sized marine sediments. In previous publications on the Kendeng Zone, similar sediments where either named marls (Duyfjes, 1938a, 1936) or mudstones (Lunt, 2013), the latter referring to a carbonate-classification system such as proposed by Dunham (1962). The studied sediments have a varying composition, which makes the description ‘mudstones’ insufficient. We follow Lazar et al. (2015) and refer to all indurated sediments with more than 50% of the grains being clay or silt-sized (< 63 µm) as mudstones. The mudstones have been given an attribute for their dominant composition (calcareous, argillaceous or diatomaceous). In cases of mixed composition, sediments were given two attributes (e.g. calcareous-argillaceous). Composition of the sediments was determined by field observation and laboratory analysis. Carbonate content was estimated with hydrochloric acid (10%). Not indurated, clay-dominated, plastic sediments have been referred to as clays.

4. Results: facies and fauna

We divided the combined biostratigraphic section into 11 zones, each with a characteristic facies and microfauna (**Fig. 4**). Zones I – V represent the Marmoyo Section; Zones VI – XI the Sumberingin Section.

4.1 Zone I (917 – 940 m)

Lower boundary: not exposed. Facies: Brownish-yellow, bedded, fine to medium grained sandstones and interbedded calcareous-argillaceous mudstones. Sand grains are mainly of terrigenous origin, with admixture of foraminifera and sporadic fine shell debris. Sandstone beds range in thickness between 10 and 40 cm and are massive or vaguely planar laminated. Interbedded mudstones are massive and have an average thickness of 10 cm. Rich in foraminifera, P/B-ratio: 99%.

Planktonic foraminifera: Rich. Abundant occurrences of *Globorotalia tumida*, *Globorotalia menardii* (dextral), *Globigerinoides trilobus* and *Globigerinoides ruber.* Common occurrences of *Globigerina bulloides*, *Dentogloboquadrina altispira* and *Sphaeroidinella dehiscens.* Scattered occurrences of *Neogloboquadrina* cf. *pachyderma* and *Pulleniatina obliquiloculata.*

Benthic foraminifera: Poor. Scattered occurrences of *Cibicidoides wuellerstorfi, Uvigerina peregrina, Pullenia bulloides*, *Gyroidina* sp., *Bulimina marginata*, *Eponides* sp. and *Lenticulina* sp.

4.2 Zone II (793 – 917 m)

Lower boundary: Gradational. Facies: Greyish-white, planar laminated diatomaceous mudstones. Rich in diatoms in the > 63 µm fraction. Slightly calcareous. Poor to moderately rich in foraminifera, P/B-ratio: 99%.

Planktonic foraminifera: Poor to moderately rich. Common occurrences of *G. tumida* and *Globigerinoides trilobus*. Scattered occurrences of *G. menardii* (dex.)*, Globigerinoides ruber, G. bulloides* and *P. obliquiloculata.*

Benthic foraminifera: Poor. Scattered occurrences of *Gyroidina* sp., *Osangularia bengalensis* and *Oridorsalis tener.*

4.3 Zone III (635 – 793 m)

Lower boundary: Gradational. Facies: White, planar laminated (platy) diatomaceous mudstones. Very rich in diatoms. Slightly calcareous. Poor in foraminifera, P/B-ratio: >99%.

Planktonic foraminifera: Poor. Scattered occurrences of *G. tumida*, *G. trilobus, G. ruber* and *S. dehiscens.*

Benthic foraminifera: Extremely poor to absent. Scattered occurrences of *Hyalinea balthica.*

Zone III contains two interbedded sandstone beds (at 725 and 792 m), with a thickness of ca. 0.5 m. Facies: Brownish-yellow, fine to medium grained sandstones. Sand grains are mainly of terrigenous origin, with admixture of foraminifera and sporadic fine shell debris. Beds are internally unstructured. The sand bed at 725 m was analysed for foraminifera. The material is moderately rich in foraminifera. Many of the foraminifera are broken. P/B-ratio: 90%.

Planktonic foraminifera: Moderately rich. Abundant occurrences of *G. menardii* (dex.) and *P. obliquiloculata.* Scattered occurrences of *G. tumida, G. trilobus* and *Neogloboquadrina pseudopima.*

Benthic foraminifera: Moderately rich. Common occurrences of *Hyalinea balthica.*

Scattered occurrences of *Bulimina marginata, Lenticulina* sp., *Ammonia supera* and *Melonis barlaeanus.*

4.4 Zone IV (475 – 635 m)

Lower boundary: Conformable, but sharp. Facies: Light grey, massive calcareous-argillaceous mudstones. Upward, detrital clay content increases and colour changes from white to light grey. Rich in foraminifera, P/B-ratio: 99%.

Planktonic foraminifera: Rich. Abundant occurrences of *G. menardii* (dex.), *N. pseudopima, G. trilobus* and *G. bulloides*. Common occurrences of *G. tumida, G. tumida flexuosa* (abundant in the lower part of this zone)*, P. obliquiloculata, G. ruber, Pulleniatina primalis, Orbulina universa, S. dehiscens, S. subdehiscens* and *Neogloboquadrina acostaensis*. Scattered occurrences of *Globorotalia miocenica, Globorotalia multicamerata*, *Neogloboquadrina humerosa* and the *Globorotalia crassaformis–tosaensis* group.

Benthic foraminifera: Poor. Scattered occurrences of *Cibicidoides wuellerstorfii, Pullenia bulloides*, *Gyroidina* sp., *Bulimina marginata*, *Bolivina robusta*, *Globocassidulina subglobosa* and *Sigmoilopsis schlumbergeri*.

Zone IV contains a well arranged series of first (F.O.) and last occurrences (L.O.) of index species: L.O. of *Globorotalia margaritae* (3.84 Ma), F.O of *G. miocenica* (3.76 Ma), L.O. of *Globorotalia plesiotumida* (3.76 Ma), L.O. of *Sphaeroidinellopsis seminula* (3.67 Ma), L.O. of *P. primalis* (3.65 Ms), L.O. of *S. subdehiscens* (3.57 Ma), L.O. of *D. altispira* (3.46 Ma), F.O. of *Globigerinoides fistulosus* (3.33 Ma) and the F.O. of *Globorotalia pertenuis* (3.1 Ma).

4.5 Zone V (393 – 475 m)

Lower boundary: gradational. Facies: Bluish-grey, massive clays. Very low admixture of silt, plastic, slightly calcareous. Poor to moderately rich in foraminifera, P/B-ratio: 95%.

Planktonic foraminifera: Base is poor in planktonics. Upwards the fauna recovers to moderately rich. Common occurrences of *G. tumida, G. trilobus, G. ruber, G. bulloides* and *N. acostaensis.* Scattered occurrences of *G. menardii* (dex.), *N. pseudopima* and the *G. crassaformis-tosaensis group*.

Benthic foraminifera: Poor. Scattered occurrences of *Lenticulina* sp., *Bulimina marginata, Ammonia* sp., *Hoeglundia elegans, Hyalinea balthica, Brizalina* sp., *Bolivina quadrilatera* and *Pseudorotalia gaimardii.*

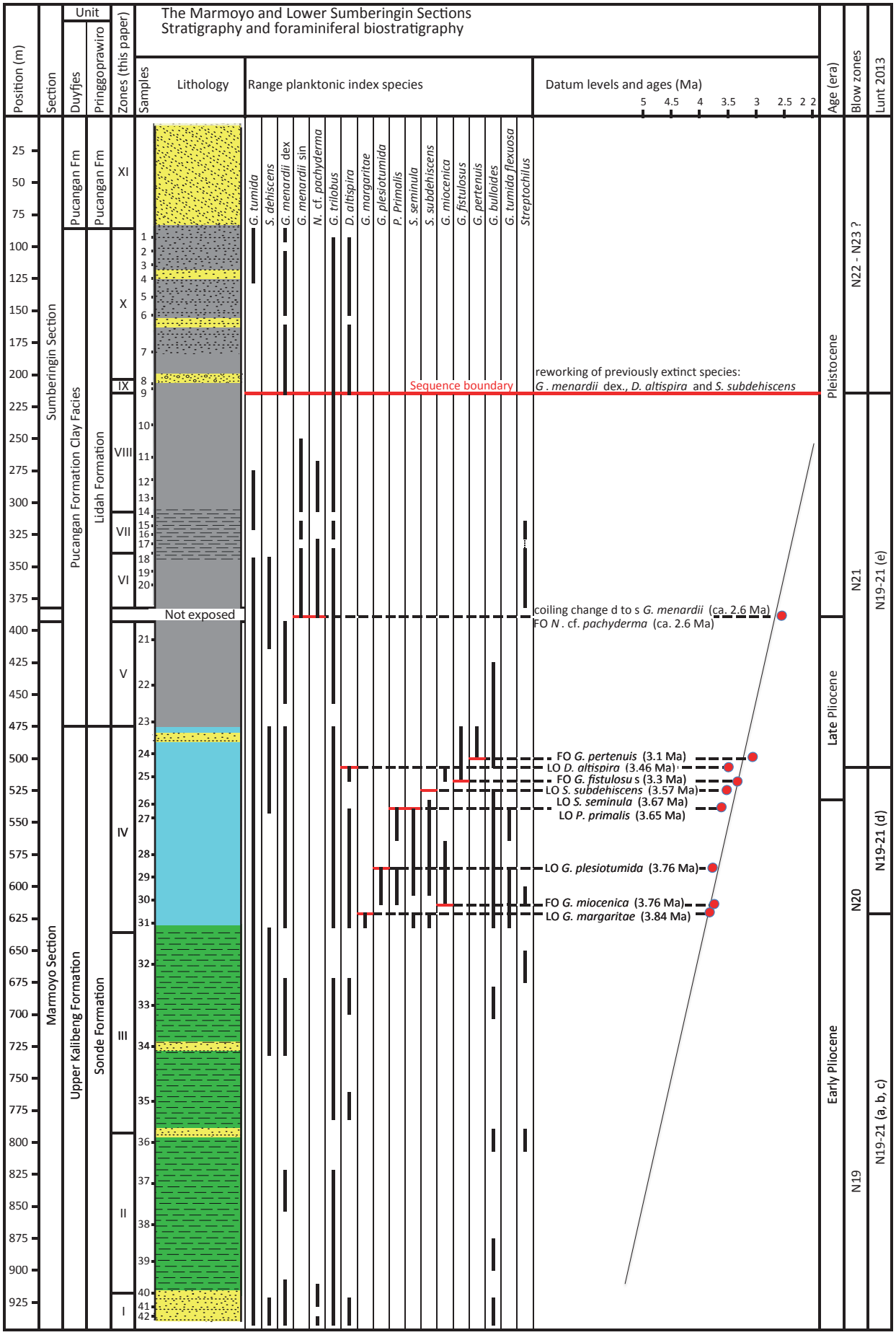


Fig. 4. Planktonic foraminifera biostratigraphy of the combined Marmoyo-Sumberingin Section. Note: only a selection of planktonic index species is shown. See text for full assemblage descriptions. Lithology legend: see **Fig. 5**.

4.6 Unexposed interval: (383 – 393)

Zone V forms the top of the Marmoyo Sections and Zone VI forms the base of the Sumberingin Section. Differences in the foraminiferal fauna indicate that there is an unexposed interval between the sections. We provisionally assumed a thickness of 10 m for this unexposed interval (see section 5.3.1).

4.7 Zone VI (340 – 383 m)

Lower boundary: Not exposed. Facies: Bluish-grey, massive clays. Very low admixture of silt, plastic, moderately calcareous. Contains carbonate concretions. Rich in foraminifera, P/B-ratio: 95%.

Planktonic foraminifera: Rich. Abundant occurrences of *G. menardii* (sin.), *N. pseudopima, N. humerosa, G. trilobus, G. ruber* and *Streptochilus* sp. Common occurrences of *P. obliquiloculata* and *N.* cf. *pachyderma.* Scattered occurrences of *G. tumida, O. universa* and *S. dehiscens.*

Benthic foraminifera: Poor. Scattered occurrences of *Ammonia* sp., *Sphaeroidina bulloides, Gyroidina* sp*., Brizalina* spp*., Hyalinea balthica, Bulimina marginata, Uvigerina* sp*.* and *Hoeglundia elegans.*

4.8 Zone VII (306 – 340 m)

Lower boundary: Conformable, but sharp. Facies: Light grey, laminated argillaceous-diatomaceous mudstones. Rich in diatoms and radiolaria. Poor to moderately rich in foraminifera, P/B-ratio: 99%.

Planktonic foraminifera: Poor to moderately rich. Scattered occurrences of *N. pseudopima*, *N. humerosa*, *G. trilobus*, *G. ruber*, *Streptochilus* sp*., G. menardii* (sin.) and *N.* cf*. pachyderma.*

Benthic foraminifera: Poor. Common occurrences of *Brizalina* spp. Scattered occurrences of *Bulimina marginata* and *Bulimina aculeata.*

4.9 Zone VIII (215 – 306 m)

Lower boundary: Conformable, but sharp. Facies: Bluish-grey, massive clays. Very low admixture of silt, plastic, rich in organic matter, moderately calcareous. Rich in foraminifera, P/B-ratio: 95%.

Planktonic foraminifera: Rich. Abundant occurrences of *G. menardii* (sin.), *N. pseudopima* and *N. humerosa.* Commom occurrences of *P. obliquiloculata*, *G. ruber, G. trilobus* and *N.* cf*. pachyderma.* Scattered occurrences of *G. tumida* and *G. crassaformis ronda.*

Benthic foraminifera: Poor. Scattered occurrences of *Ammonia* sp*., Sphaeroidina bulloides, Gyroidina* sp*., Brizalina* sp*., Hyalinea balthica, Bulimina marginata, B. aculeata, Uvigerina* sp*., Hoeglundia elegans, Nodosaria* sp*., Lenticulina* sp*., Eponides* sp. and *Baggina indica*.

4.10 Zone IX (210 – 215 m)

Lower boundary: Erosive. Facies: Mottled greyish-red, conglomerate. Matrix of coarse sand (moderately rounded), sand grains mainly of terrigenous origin, but with abundant shell fragments, highly calcareous. Gravel pebbles up to 3 cm, moderately rounded, polymict composition (mainly andesitic). Vaguely bedded, channel-fill structures. Moderately rich in foraminifera, P/B-ratio: 50%.

Planktonic foraminifera: Moderately rich. Common occurrences of *G. trilobus* and *P. obliquilocuta.* Scattered occurrences of *G. menardii* (dex)*, G. ruber, G. obliquus, D. altispira* and *S. subdehiscens.*

Benthic foraminifera: Moderately rich. Abundant occurrences of *Brizalina* sp., *Pseudorotalia conoides* and *Asterorotalia trispinosa.* Scattered occurrences of *Elphidium* sp. and the larger foraminiferal species *Amphistegina lessonii* and *Gypsina* sp*.*

4.11 Zone X (85 – 210 m)

Lower boundary: Gradational. Facies: Bluish-grey, massive clays, low admixture of silt and fine sand, plastic, rich in organic matter, highly calcareous. Upward, the sand content increases, with lenses and laminae of fine sand and fine shell debris. In the upper part of this zone, sandbeds of several cm thickness occur, locally showing small scale loading structures. The upper part of this zone also contains two hard, calcareous sandstone beds with abundant marine molluscs (single valves). Moderately rich in foraminifera, P/B-ratio: 75%.

Planktonic foraminifera: Moderately rich. Abundant occurrences of *G. trilobus* and *D. altispira*. Common occurrences of *G. menardii* (dex.) and *P. obliquiloculata.* Scattered occurrences: *S. subdehiscens*, *G. tumida, N. pseudopima* and *G. obliquus*.

Benthic foraminifera: Moderately rich. Common occurrences of *Ammonia* sp., *Pseudorotalia conoides* and *Asterorotalia trispinosa.* Scattered occurrences of *Elphidium* sp. and the larger foraminiferal species *Amphistegina lessonii* and *Gypsina* sp.

4.12 Zone XI (0 – 85 m)

Lower boundary: Gradational. Facies: Fine-grained, bedded sandstones. Sand grains are mainly of terrigenous origin. Most beds are internally massive and have a thickness of 20 to 40 cm. The beds are separated by mud drapes and show frequent dewatering and loading structures. The fine-grained sandstones change upward into bedded medium-grained sandstones, with beds that are finely laminated and normal graded. Locally the beds show a hummocky or wavy cross-stratification. Note that the marine sandstones have a total thickness of app. 400 m. Only the base of the sandstones has been included in our descriptions. No foraminiferal analysis was carried out on samples from this zone.

In general the sandstone series shows a coarsening upward trend, with upward thickening beds. The sandstones pass into fluvial conglomerates and cross-bedded sandstones. For detailed accounts of the overlying sandstones, see Van Es (1931) and Duyfjes (1938a).

5. Discussion

5.1 Dating

Zone I does not provide clear biodatums, but the presence of *G. tumida* (F.O. 5.51 Ma), and *S. dehiscens* (F.O. 5.48 Ma) indicates that the sediments are not older than Pliocene. The dextral coiling direction of *G. menardii* forms another indication of a Pliocene age of this zone, as this species changes its coiling direction from sinistral to dextral near the Miocene-Pliocene boundary and remains dextral throughout the Pliocene (Blow, 1969; Bolli et al., 1989). Zones II and III are low in planktonic foraminifera and contain no distinct marker horizons. Zone IV is rich in planktonic foraminifera and contains a good succession of first and last occurrences of index species (**Fig. 4**). A plotted timeline provides a uniform deposition rate of 18 cm/ka for the calcareous-argillaceous mudstones of Zone IV, which is relatively high, but agrees nicely with the rate of 17 cm/ka found by Van Gorsel and Troelstra (1981) for the mudstones of the Solo River Section of corresponding age. The timeline provides a good age estimate of 4 Ma for the base and 3 Ma for the top of zone IV.

The ages found for the calcareous-argillaceous mudstones of Zone IV show that the underlying diatomaceous mudstones are older than 4 Ma. Assuming a uniform deposition rate of 18 cm/ka throughout this series, we come to an age of approx. 5 Ma for the base of the diatomaceous mudstones (base of Zone II). As commonly the deposition rate of diatom ooze is lower than the deposition rate of calcareous ooze and detrital clays (Hüneke and Henrich, 2011), the base of the diatomaceous mudstones may be even older. However, the Pliocene planktonic content of the sandstones at the base of the section confines the entire section to the Pliocene. With an approximate age range of 5 to 4 Ma, the laminated diatomaceous series dates from the Early Pliocene, which makes it older than previously assumed based on Duyfjes' extrapolations. It is interesting to note that an Early Pliocene age of these beds was already postulated by Reinhold (1937) based on diatom analyses.

With an estimated age of 3 Ma, the base of the blue clays, represented by Zone V, is of Late Pliocene age. This zone, which forms the top of the Marmoyo Section, does not contain age diagnostic markers. But the dominant coiling direction of *G. menardii* remains dextral throughout this zone, indicating that it pre-dates the Plio-Pleistocene boundary. In the overlying blue clays of Zone VI, forming the base of the Sumberingin Section, the coiling direction of *G. menardii* is reversed to sinistral. This coiling change, regarded as an indicator for a change to cooler water conditions, is used regionally to mark the base of the Pleistocene (Blow, 1969; Bolli et al., 1989). Zone VI also shows the appearance of a new species: the cool-water immigrant *N.* cf. *pachyderma*. The arrival of this species in the equatorial waters of the Kendeng Zone points to changing ocean currents and influx of cooler water from high latitude regions, which can also be linked to the beginning of the Pleistocene.

The overlying blue clays of Zones VI, VII and VIII are of Early Pleistocene age. The age of the blue clays of Zone VIII is of special interest as it underlies an unconformity and represents the end of a long depositional sequence. Zones VI, VII and VIII do not contain clear age-diagnostic horizons. However, these zones do contain scattered occurrences of *Globigerinoides obliquus extremus* (L.O. 1.99 Ma) and *G. fistulosus* (L.O. 1.88 Ma). Although these occurrences are not very consistent over these zones, they provide an indication that Zone VIII predates the last occurrences of these species. It agrees with the projected timeline as plotted in **Fig. 4**, assuming a deposition rate of 18 cm/ka. It gives a rough age estimate of 2 Ma for the top of Zone VIII, directly below the unconformity.

The conglomerates and blue clays overlying the unconformity (Zones IX and X) contain a mixed planktonic fauna which includes Pliocene species such as *D. altispira*, *S. subdehiscens* and dextrally coiled *G. menardii*, species for

which we found extinctions much lower in the stratigraphy. The re-appearance of these species indicates reworking of older planktonics, which implies nearby exposure and erosion of older strata. The presence of reworked planktonics impedes dating with planktonic bio-horizons.

5.2 Blow's zonation

Biostratigraphic studies in Indonesia generally use Blow's zonation (1969). The base of the Marmoyo-Sumberingin Section is not older than N18, because of the occurrence of *G. tumida* at the base of the section. The occurrence of *S. dehiscens* in the base of the section suggests an N19 age. The boundary between zones N19 and N20 is determined by the evolutionary transition from *N. dutertrei* to *N. pseudopima*. This transition is hard to identify in many Indo-Pacific sections, as was already noted by Lourens et al (2004). We referred to all members of this lineage as *N. pseudopima.* Hence, the boundary between zones N19 and N20 cannot be identified. For the boundaries between Zones 20, 21 and 22, Blow's system relies on the *G. crassaformis-tosaensis-truncatulinoides* lineage. Again, the evolutionary forms of this lineage are hard to identify in the Pliocene – Pleistocene of the Indo-Pacific. Moreover, the members of this lineage are scarce in local sections. Both features were noted by Lourens et al. (2004) and Lunt (2013). It makes the lineage not very useful for biostratigraphic purposes in this region. It also raises questions about the significance of ages or correlations based on species of this lineage in previous studies in the vicinity. In **Fig. 4**, the boundary between N20 and N21 was provisionally drawn at the last occurrence of *D. altispira.* The boundary between N21 and N22 was drawn at the last occurrence of *G. fistulosus* and *G. extremus*, which coincides with the unconformity within the blue clays.

Lunt (2013), recognizing the difficulties to indicate the boundaries between Blow's Mio-Pliocene Zones, proposed a revised subdivision of Blow's Zones N19-21 for the Indo-Pacific region (N19-21 a to e). In the same publication, he used this zonation for a discussion of the Solo River Section. We added his zonation, as far as applicable, to our stratigraphic column of **Fig 4.**

5.3 The unexposed interval and the unconformity within the marine clays

5.3.1 The unexposed interval

The faunal changes in the base of Zone VI show that there is no overlap between the top of the Marmoyo Section (Zone V) and the base of the Sumberingin section. There probably is a stratigraphic gap between the sections. The thickness of this missing interval is unknown, but there are reasons to assume that it is a minor interval only. In the first place, the total thickness of the blue clays investigated in the two sections is 390 m (Zones V – X). This is very near to the total thickness of the blue clays as can be deduced from the width of the east-west trending valley between the two ridges (**Fig. 3**). This valley has a width of ca. 675 to 700 m. Based on a constant dip of 30 degrees measured in this flank of the anticline, the valley roughly represents a clayey interval of 395 m. In the second place, calcareous mudstone outcrops right beside the Sumberingin creek (see **Fig. S2**) indicate that the basal clays as exposed in the creek have a stratigraphic position very close to the unit boundary. We provisionally estimate an unexposed interval of 10 m between Zones V and VI.

5.3.2 The unconformity

As noted in section 5.1, the base of the conglomerate bed of Zone IX forms an unconformity. It has a sharp, erosive lower boundary over the massive marine clays of underlying Zone VIII. The unconformity is also marked by a sudden change in foraminifera fauna. The clays below this level contain a marine fauna, with benthics representing upper bathyal to outer shelf conditions. The conglomerate and overlying clays of Zone X are characterized by near-coastal benthic species and the occurrence of previously extinct planktonic species, indicating reworking. The time hiatus represented by the unconformity is unknown; the overlying deposits may be of Early or Middle Pleistocene age.

5.4 Correlations with other biostratigraphic sections

Fig. 5 shows the correlation of marker horizons between the Marmoyo-Sumberingin Sections, the Solo River Section and the Bojonegoro-1 well. The laminated diatomaceous mudstones of the Marmoyo Section correspond to the middle part of the massive mudstones of the Solo River Section, both dating from the Early Pliocene. The overlying calcareous-argillaceous mudstones have a number of biomarkers that can be directly correlated to the Solo River Section, i.e. the L.O. of *G. margaritae* (3.84 Ma), the L.O. of *Sphaeroidinellopsis* spp. (3.57 Ma) and the F.O. of *G. fistulosus* (3.33 Ma), indicating that these strata correspond to the higher parts of the massive mudstone series of the Solo River Section and date from the latest Early Pliocene and Late Pliocene.

Remarkable is the upward continuation of *D. altispira* in the Solo River Section, up to the overlying limestones. In the Marmoyo Section, as well as in the Bojonegoro well, the L.O. of this species (3.46 Ma) is recorded close to the F.O. of *G. fistulosus* (3.33 Ma), but in the Solo River Section, it continues upwards until well above the first appearances of

this species and the first appearance of *G. tosaensis* (3.35 Ma). This occurrence of *D. altispira* high in the stratigraphy of the Solo River Section, also noted by Lunt (2013), is not consistent with the other biomarkers. We regard the occurrences of *D. altispira* in the limestones of the Upper Kalibeng Formation as reworked. Note in this respect that the same species is found as reworked specimens in the top of the Sumberingin Section. Here, its reworked origin is easily recognizable, as the extinction of the species was recorded lower in the stratigraphy.

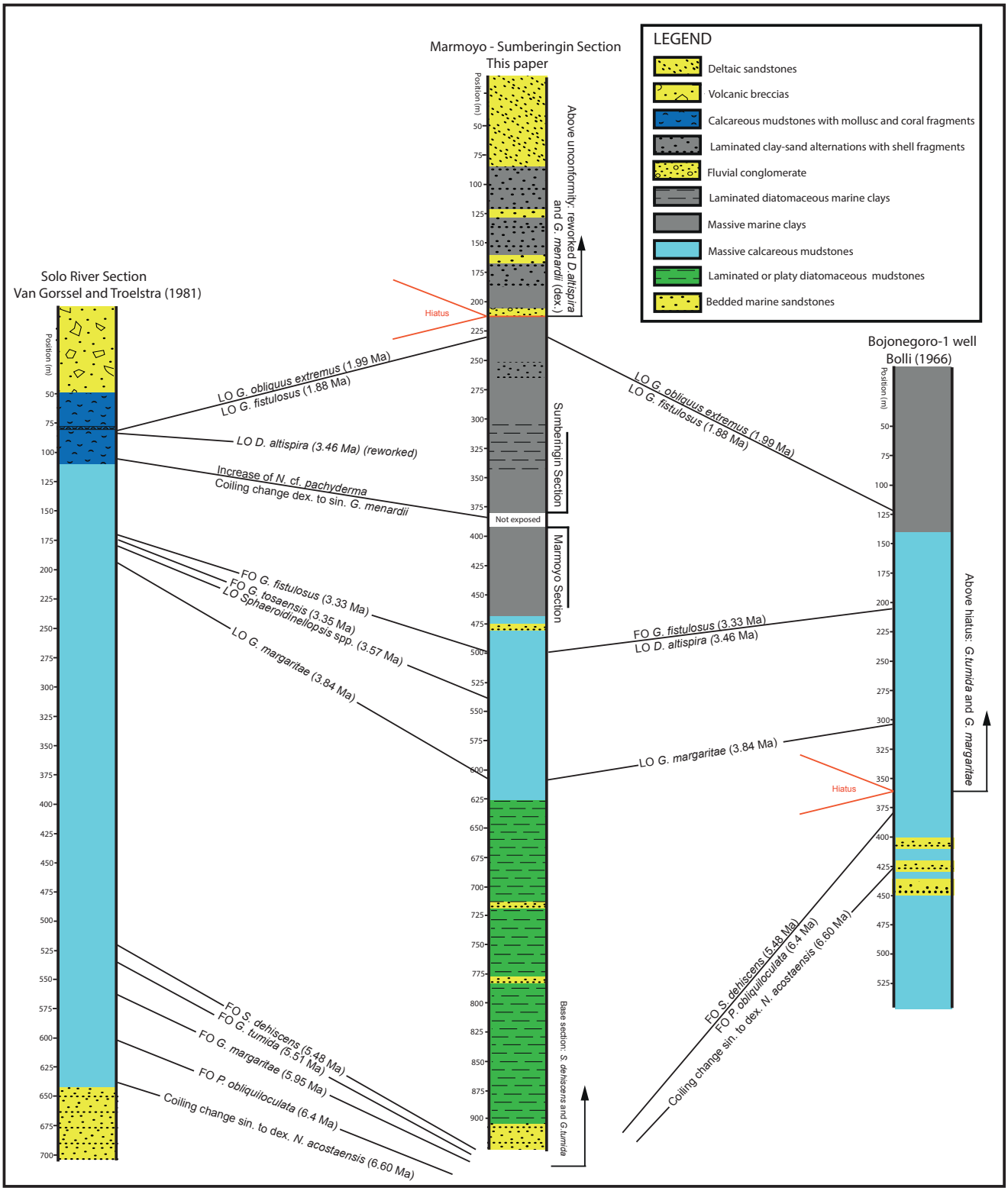


Fig. 5. Biostratigraphic correlations between the Solo River Section, the Marmoyo-Sumberingin Section and the Bojonegoro-1 well.

We conclude that all mudstones of the eastern Kendeng Zone form the lateral equivalent of the Lower Kalibeng Formation of the western Kendeng Zone. Duyfjes' correlation with the coastal strata of the western Kendeng Zone (Upper Kalibeng Formation) was incorrect. Looking at the Bojonegoro-1 well, we find that the laminated diatomaceous mudstones of the Marmoyo Section largely correspond to the depositional hiatus in the Bojonegoro-1 well. The overlying calcareous-argillaceous mudstones of the Marmoyo Section correspond to the mudstones above the hiatus in the Bojonegoro-1 well.

The Late Pliocene base of the blue clays, as exposed at the top of the Marmoyo Section, still forms the lateral equivalent of the top of the Lower Kalibeng Formation of the Solo River Section. The overlying clays of Early Pleistocene age, as exposed in the base of the Sumberingin Section, correspond in age with the reefal limestones of the Solo River Section, both containing the characteristic sinistrally coiled *G. menardii* and the increased occurrences of *N.* cf. *pachyderma*.

Correlations between the blue clays of the Bojonegoro-1 well and the blue clays of the Sumberingin Section are more complicated, due to the sparsity of biostratigraphic markers within the blue clays and the low sample density in the blue clays of the Bojonegoro-1 well. However, we found scattered occurrences of *G. fistulosus* and *G. obliquus extremus* in the blue clays of the Sumberingin Section below the unconformity, whereas these species were found extinct at the base of the blue clays in the Bojonegoro-1 well. This is an indication that the clays of the Bojonegoro-1 well are younger than the basal clays of the eastern Kendeng Zone. Possibly, this accounts for the blue clays of the entire Randublatung Zone. The clays of the Randublatung Zone may correspond to the second clay sequence of the Sumberingin Section, above the unconformity. This would be in agreement with the stratigraphic position of the blue clays in the western Randublatung Zone, overlying a similar unconformity and coarse coastal bed (Selorejo Formation).

Duyfjes (1938a) did not recognize the unconformity in the clays of the Sumberingin Section and correlated the entire clay series with the breccias of the western Kendeng Zone. Our biostratigraphic study indicates that this is incorrect: the blue clays below the unconformity are older. The clay above the unconformity and the overlying deltaic sandstones may correlate in age with the breccias of the Solo River Section, which would be more or less in line with Duyfjes' correlations. However, the unconformity within the clays may also represent a larger hiatus, which would make the overlying clays and deltaic sandstones younger.

5.5 Depositional conditions

5.5.1 Zone I

The stratigraphic position of this thin sandstone interval, interbedded between deep marine mudstones, points to a turbiditic origin. Unambiguous sedimentological features of turbidity currents have not been found. The sandstone beds are vaguely parallel laminated and alternate with thinner beds of calcareous-argillaceous mudstones. The beds are provisionally interpreted as layers D and E of the Bouma sequence, possibly representing a distal turbiditic setting. The benthic assemblage dominated by *Gyroidina* sp., *Uvigerina peregrina, Pullenia bulloides, Bulimina marginata* and *Cibicidoides wuellerstorfii* indicates bathyal conditions, which is confirmed by a P/B-ratio of 99%.

The sandstones can be correlated with thinner sandstone beds intercalated in the Solo River and Ngepung Sections at the same level. Previous authors linked these sandstone intercalations to uplift and volcanic activity of the volcanic arc during the Late Miocene and Early Pliocene (Genevraye and Samuel, 1972; Saint-Marc and Suminta, 1979) or to climatic influences (Van Gorsel and Troelstra, 1981) (see also section 5.6).

5.5.2 Zones II and III

The P/B-ratio of over 99% indicates bathyal conditions, consistent with the depositional depth of the corresponding part of the Solo River and Ngepung Sections.

The laminated mudstones are poor in foraminifera and rich in diatoms, indicating eutrophic conditions, blooming phytoplankton and reduced oxygen conditions. The extremely low benthic species diversity also indicates reduced oxygen conditions at the seabed. Zone III represents similar conditions as Zone II, but more extreme. The sediment consists primarily of diatoms; benthic foraminifera are extremely scarce or even absent. This zone represents the peak of the algal productivity.

The two interbedded sandstone layers of zone III are interpreted as turbidites. They have a similar, relatively rich foraminifera content as Zone I, with a mixed benthic assemblage of shelfal and bathyal species. The frequent occurrence of broken foraminifera indicates transport, which is in line with a turbiditic origin.

Eutrophication of marine waters is generally related to an increased supply of siliceous nutrients. It is commonly associated with volcanic activity, influx of erosion products or upwelling. The sediment of Zones II and III is very low

in clastic components, which makes the first two factors unlikely. Upwelling is the most likely explanation for the increased nutrient-supply, which is supported by the occurrence of specific, upwelling-related planktonic species (see section 5.6).

5.5.3 Zone IV

The rich planktonic foraminifera fauna of this zone, and the sharp reduction in diatoms, mark a return to normal oxygen conditions. The more homogenous nature of this material indicates increased benthic activity. Nevertheless, benthic foraminifera are still relatively scarce and the P/B-ratio remains around 99%, pointing to deep-water conditions. The benthic assemblage contains similar bathyal species as were found in the underlying zones, but also some new species occur: *Bolivina robusta*, *Globocassidulina subglobosa* and *Sigmoilopsis schlumbergeri*. The higher species diversity points to a better oxygenation of the bottom waters. The introduction of *Bolivina robusta* may indicate slightly shallower conditions, which we postulate as upper bathyal.

5.5.4 Zone V

The plastic, argillaceous nature of this material indicates an increased supply of fine detrital clay, a trend that was already visible in the calcareous-argillaceous mudstones of Zone IV. The planktonic assemblage is similar to the underlying zone IV, but with reduced abundances. The P/B-ratio of 95% indicates a minor further shallowing. This is supported by the benthic assemblage, consisting of a mixture of upper bathyal species and shelfal, muddy-substrate species such as *Ammonia supera* and *Pseudorotalia gaimardii.* We postulate an outer shelf environment for this zone, which is consistent with the corresponding part of the Ngepung and Solo Sections.

5.5.5 Zone VI

The benthic assemblage of this zone is dominated by bathyal species, although we still find sparse occurrences of the shelfal *Ammonia* sp. The P/B-ratio of 95% indicates similar depth conditions as the underlying Zone V. However, the re-appearance of *Uvigerina* sp.*, Laticarinina pauperata* and *Gyroidina* sp*.* indicates a return to somewhat deeper water conditions, which we tentatively describe as upper bathyal to outer shelf.

The abundant occurrence of planktonic species is striking. The assemblage indicates cooler conditions as well as upwelling (see section 5.6).

5.5.6 Zone VII

The laminated argillaceous mudstones of Zone VII are poor in foraminifera and rich in diatoms, indicating eutrophic conditions, blooming phytoplankton and reduced oxygen conditions. The common occurrence of the benthic species *Brizalina* spp. also indicates low oxygen conditions at the seabed. The P/B-ratio of 99% conditions and the dominance of bathyal benthic species as *Bulimina marginata* suggest further deepening, however the extreme sparsity of benthic species is also related to the reduced oxygen conditions at the bed. We tentatively regard the depth conditions as upper bathyal to outer shelf, similar to Zone VI.

The eutrophication represented by this zone is likely related to upwelling (see section 5.6). Note that the occurrence of a diatomaceous zone within the blue clays was never reported before.

5.5.7 Zone VIII

The rich planktonic foraminifera fauna of this zone, and the sharp reduction of diatoms, mark a return to normal oxygen conditions. The facies of the clays, as well as their planktonic content, strongly resemble the clays of Zone VI, underlying the diatom zone. The benthic assemblage still contains deep-water species such as *Hoeglundia elegans, Bulimina marginata, Gyroidina* sp*.* and *Uvigerina* sp.*,* but it is dominated by shelf species as *Ammonia* sp., *Lenticula* sp.*,* and *Eponides* sp*.* Also the P/B-ratio of 95% indicates slightly shallower conditions than the underlying zone, which we tentatively interpret as upper bathyal to outer shelf.

5.5.8 Zone IX

The erosive base of this zone represents the first Pleistocene emergence of this part of the Kendeng Zone. It also represents a significant and abrupt change in the foraminifera fauna.

The conglomerates with shell fragments, overlying the unconformity, represent coastal conditions. The material is rich in planktonic foraminifera, with an assemblage that is characterized by the return of the Pliocene species *D. altispira* and *S. subdehiscens*, and the return of dextrally coiled *G. menardii.* The return of these species indicates erosion and reworking of older marine deposits, which is in line with the coastal depositional setting.

The benthic foraminifera assemblage consists of a new group of species, characteristic for deltaic, near coastal envi-

ronments: *Pseudorotalia conoides*, *Asterorotalia trispinosa, Elphidium* sp., *Amphistegina lessonii* and *Gypsina* sp.

5.5.9 Zone X

The facies of these clays, with fine sand laminae and laminae of fine shell debris, indicates (inner) shelf conditions, dominated by settling of mud and regular influx of fine sand, either by small-scale turbidites or by settling of high suspension-loads, initiated by storms or events of high river discharge. The planktonic assemblage is similar to the underlying conglomerates of Zone IX and contains reworked Pliocene species, indicating an influx of erosion products and hence a near-coastal setting. The benthic assemblage also resembles the conglomerates of zone IX. It is dominated by typical deltaic species such as *Pseudorotalia coinoides, Asterorotalia trispinosa, Elphidium* and the larger foraminiferal species *Amphistegina lessonii* and *Gypsina* sp. We postulate an inner shelf environment in a near-coastal, pro-delta setting. This is in line with the gradual transition to the overlying deltaic sandstones of Zone XI.

5.5.10 Zone XI

The fine-grained, normal-graded sandstone beds with mud drapes represent a proximal deltafront environment. The dewatering structures indicate rapid sedimentation rates. The coarsening and thickening upward trend within the thick sandstone series indicates deltaic progradation.

5.6 Water temperature and upwelling

The planktonic assemblage of the Marmoyo Section is dominated by tropical species such as *G*. *trilobus*, dextrally coiled *G. menardii*, *G*. *tumida*, and *D. altispira.* The warm, tropical conditions are consistent with the regional climate-record for the Pliocene. Occurrences of *N.* cf. *pachyderma* in the sandstones of Zone I suggest that base of the Marmoyo Section represents cooler water conditions. The species was also found in the corresponding segment of the Solo River Section. Van Gorsel and Troelstra (1981) interpreted the occurrence of this species as a sign of temporary global cooling around the Miocene-Pliocene boundary, which they associated with a less dense vegetation cover of nearby landmasses and an increased supply of coarse clastics to the basin.

Zone VI, at the base of the Sumberingin Section, bears evidence of cooler water conditions: i.e. the abundant appearance of *N.* cf. *pachyderma,* a strong decline of *G. tumida* and the change in coiling direction from dextral to sinistral in *G. menardii.* The dispersal of the cooler-water species *N.* cf. *pachyderma* to low-latitude waters is regionally linked to changing ocean currents related to global cooling at the beginning of the Pleistocene. Also the coiling change in *G. menardii,* is linked to cooling water conditions marking the Plio-Pleistocene boundary (Bandy, 1972; Ericson et al., 1955; Jenkins, 1967; Kucera, 2007). A decrease in tropical planktonic species and the appearance of *N.* cf. *pachyderma* and sinistrally coiled *G. menardii* was also found in the Solo River Section (Van Gorsel and Troelstra, 1981), at the base of the limestones overlying the massive mudstones.

Another temperature-indicative species found in the Marmoyo Section is *G. bulloides.* It is a cool-water species, but also a species known to thrive under high-productivity conditions, which makes it a good indicator for upwelling conditions (Schiebel and Hemleben, 2005; Thiede, 1975). The species is consistently found throughout the entire Marmoyo Section. Another indication of upwelling conditions is the scattered occurrence of the biserial planktonic species *Streptochilu*s sp. in the diatomaceous zones (Zones II, III and Zone VII). *Streptochilus* sp. is associated with near-coastal upwelling (Pardo and Keller, 2008; Smart and Thomas, 2006). It makes upwelling the most likely explanation for the increased nutrient-supply and algae-production as recorded in the diatomaceous strata. Another interesting feature is the common occurrence of *G. tumida flexuosa* in Zone IV. The species is an indicator for changing, suboptimal oceanographic conditions (Lamb and Beard, 1972), which can once again be associated with upwelling.

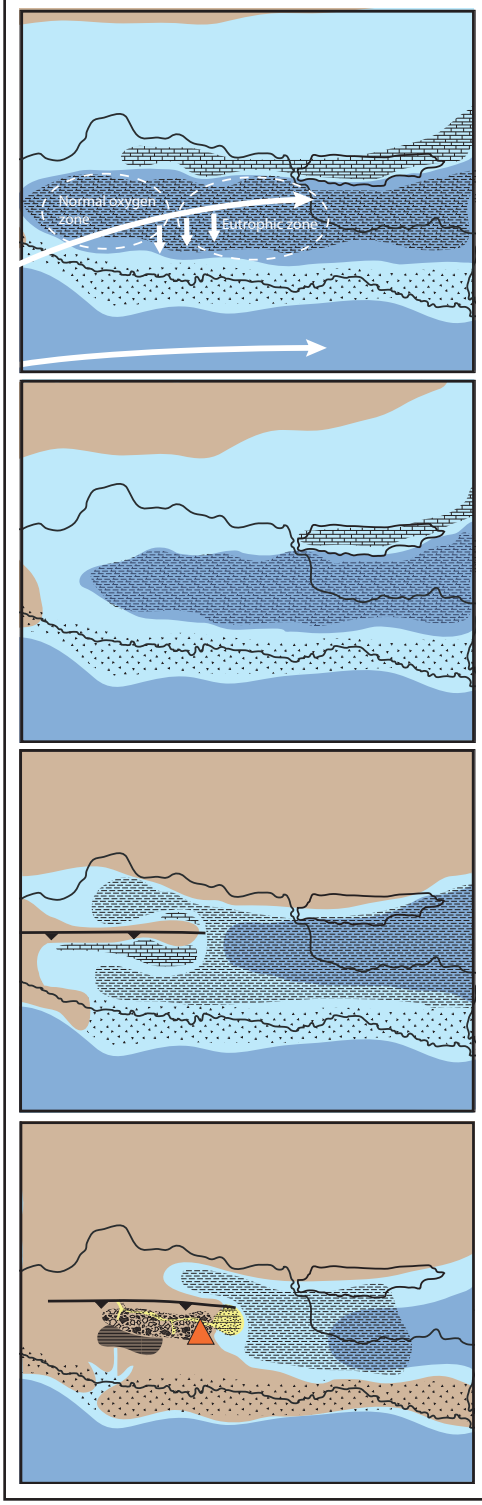
The occurrence of upwelling-conditions in the Pliocene Kendeng Zone may be explained by its oceanic setting. For much of the Pliocene, there was probably no active volcanic arc to the south and the Kendeng basin was situated along the southern margin of the large exposed landmass of Sundaland (Hall, 2013; Hall and Spakman, 2015; Morley et al., 2017). This makes the setting more or less comparable to the Indian Ocean area south of present-day Java. This area is subject to semi-annually reversing currents. During the northwest monsoon, an eastward current results in coastal downwelling and a redistribution of warm Indian Ocean water in the coastal seas. However, during the southeast monsoon, steady easterly winds drive the current westward, resulting in Ekman-induced upwelling and a drop in surface-water-temperatures (Sprintall et al., 1999; Wyrtki, 1961). Assuming a similar oceanic setting, upwelling may have been a seasonal phenomenon in the Pliocene and Early Pleistocene Kendeng Zone.

5.7 Paleogeography (Fig. 6)

5.7.1 Early Pliocene

The diatomaceous mudstones of the eastern Kendeng Zone correlate in age with the Early Pliocene massive mudstones of the western Kendeng Zone. Both series were deposited under bathyal conditions, but show a striking differ

ence in facies. The mudstones of the western Kendeng Zone have a rich and well-preserved foraminiferal fauna and are thoroughly bioturbated. The corresponding strata of the eastern Kendeng Zone consist primarily of diatoms, are laminated and have a highly reduced foraminiferal fauna. This gives an image of an Early Pliocene Kendeng Zone in which phytoplankton-blooms and resulting low-oxygen conditions were a local phenomenon, occurring primarily in the eastern part of the basin. We found coastal upwelling as the most likely cause for this eutrophication. However, there is evidence that upwelling occurred over the entire Pliocene Kendeng Zone. The admixture of *G. bulloides* was also found throughout the mudstones of the Solo River Section (Van Gorsel and Troelstra, 1981). Also, Burckle (1982) found *Thallasionema nitzschiodes,* a species indicative for upwelling conditions, in the Early Pliocene diatom assemblage of the Ngepung Section. If upwelling occurred over the entire Kendeng Zone, then additional factors must have



Early Pliocene
Bathyal depth conditions prevail in the entire Kendeng Zone. The volcanic arc has become inactive and is largely submerged, creating an open connection to the Indian Ocean in the south. In the north, the basin is bordered by the shallow Sunda Shelf and coral reefs on the uplifted Rembang - Madura high. Upwelling conditions occur, linked to seasonal eastward marine currents and off-shore directed Ekman currents. It causes the development of an eutrophic zone with high diatom productions. In the western part of the basin, normal oxygen conditions prevail and sedimentation is dominated by calcareous muds rich in foraminifera.

Late Pliocene
Compression and uplift of the Kendeng Zone result in gradual shallowing. Upper bathyal conditions prevail in most of the basin. Normal oxygen conditions return to the entire Kendeng Zone.The supply of detrital clays increases, which is marked by a transition in the depositional record to calcareous-argillaceous mudstones rich in foraminifera and finally to marine bluish clays. In the eastern Kendeng Zone, the base of the marine clays dates from ca. 3.0 Ma.

Early Pleistocene (ca. 2.6 - 2.0 Ma)
Continuing compression of the Kendeng Zone results in folding and northward thrusting of the axial part of the Kendeng Zone. In the east, the thrust belt emerges. Coral reefs develop along this emerged axial part of the Kendeng Zone. The surrounding area develops as a shallow embayment, with shelfal depth conditions in the west and upper bathyal conditions in the east. The supply of detrital clay to these shallow waters is high, marked by the deposition of bluish marine clays.

Early Pleistocene (after 2.0 Ma)
Continuing uplift of the Kendeng Zone results in further regression. In the remaining embayment, shallow marine conditions prevail. The supply of detrital clay is high and sedimentation is dominated by marine clays. Around 1.9 Ma, volcanic activity returns to the area, starting in the Wilis volcanic complex. The area south of the Kendeng thrust belt is covered with volcanic breccias. A large delta develops, prograding over the shallow marine embayment.The exact timing of this deltaic development remains unclear.

Fig. 6. Plio-Pleistocene paleogeography of the Kendeng Zone. Charts based on Hall (2013) and Lunt (2013) with addition of new data from the present study.

been involved in the development of a eutrophic biogeographic zone in the eastern Kendeng Zone. This may have been an interaction between oceanic currents and paleogeography. Possibly, the Early Pliocene eastern Kendeng Zone had a relatively sheltered position, leading to more extreme eutrophication.

5.7.2 Late Pliocene

In the Late Pliocene, normal oxygen conditions and a rich foraminifera fauna returned to the entire Kendeng Zone. Gradual uplift brought upper bathyal to outer shelf conditions to the basin. Deposition changed from predominantly calcareous to more argillaceous, indicating a higher supply of detrital clay from surrounding land surfaces. Eventually, deposition changed to blue marine clays, the base of which has been dated at 3 Ma in the eastern Kendeng Zone.

5.7.3 earliest Early Pleistocene (2.6 – 2.0 Ma)

The Plio-Pleistocene boundary (2.6 Ma) is roughly placed at the appearance of *N.* cf. *pachyderma* and the coiling change from dextral to sinistral in *G. menardii*. In the eastern Kendeng Zone, this transition lies within the marine blue clays. In this area, upper bathyal to outer shelf conditions and clay deposition continued well into the Early Pleistocene. In the southwestern Kendeng Zone, this microfaunal transition is found at the base of the reefal limestones. It shows that the limestones date from the earliest Early Pleistocene and correlate laterally with marine blue clays in the east. The limestones of the southwestern Kendeng Zone were formed as reefs fringing the axial part of the Kendeng Zone, which had been subject to folding and thrusting and emerged in this period.

5.7.4 Early Pleistocene after 2.0 Ma

This period is characterized by the return of active volcanism to this part of East Java, with the Wilis volcanic complex as the first eruption centre. Large-scale eruptions started around 1.9 Ma (Hartono, 1994), supplying volcanic breccias to a vast area south of the axial Kendeng ridge, nowadays the area around Kedung Brubus, Ngawi, Trinil and Sangiran. Continuing uplift, possibly in combination with periods of temporary sea-level drop, resulted in more widespread exposure of the Kendeng Zone.

Around Sangiran, a lagoonal or lacustrine environment developed after the first phase of highly active volcanism, followed by a phase of fluvial deposition. Fluvial deposition is also widespread in the Trinil area, where fluvial sands overlie the volcanic breccias. The breccias are regarded as the Early Pleistocene Pucangan Formation and the fluvial sands as the Middle Pleistocene Kabuh Formation (Duyfjes, 1936, 1938a).

In the eastern Kendeng Zone, we found evidence for a period of exposure, followed by a new transgression and a return to shallow marine conditions. It corresponds to what Huffman (2001b) calls the Pleistocene Randublatung Embayment. It is characterized by a nearby coastline and a large, prograding sandy delta. The northeast directed deltaic progradation over shallow marine clays can nowadays be traced in the depositional record of the eastern Kendeng Zone between Jombang and Mojokerto. This shallow marine, deltaic phase cannot be accurately dated by foraminifera biostratigraphy, due to strong admixture of reworked foraminifera. The exact timing of this deltaic phase in relation to the deposition of volcanic breccias and fluvial sandstones in the SW Kendeng Zone around Trinil and Ngawi remains unknown.

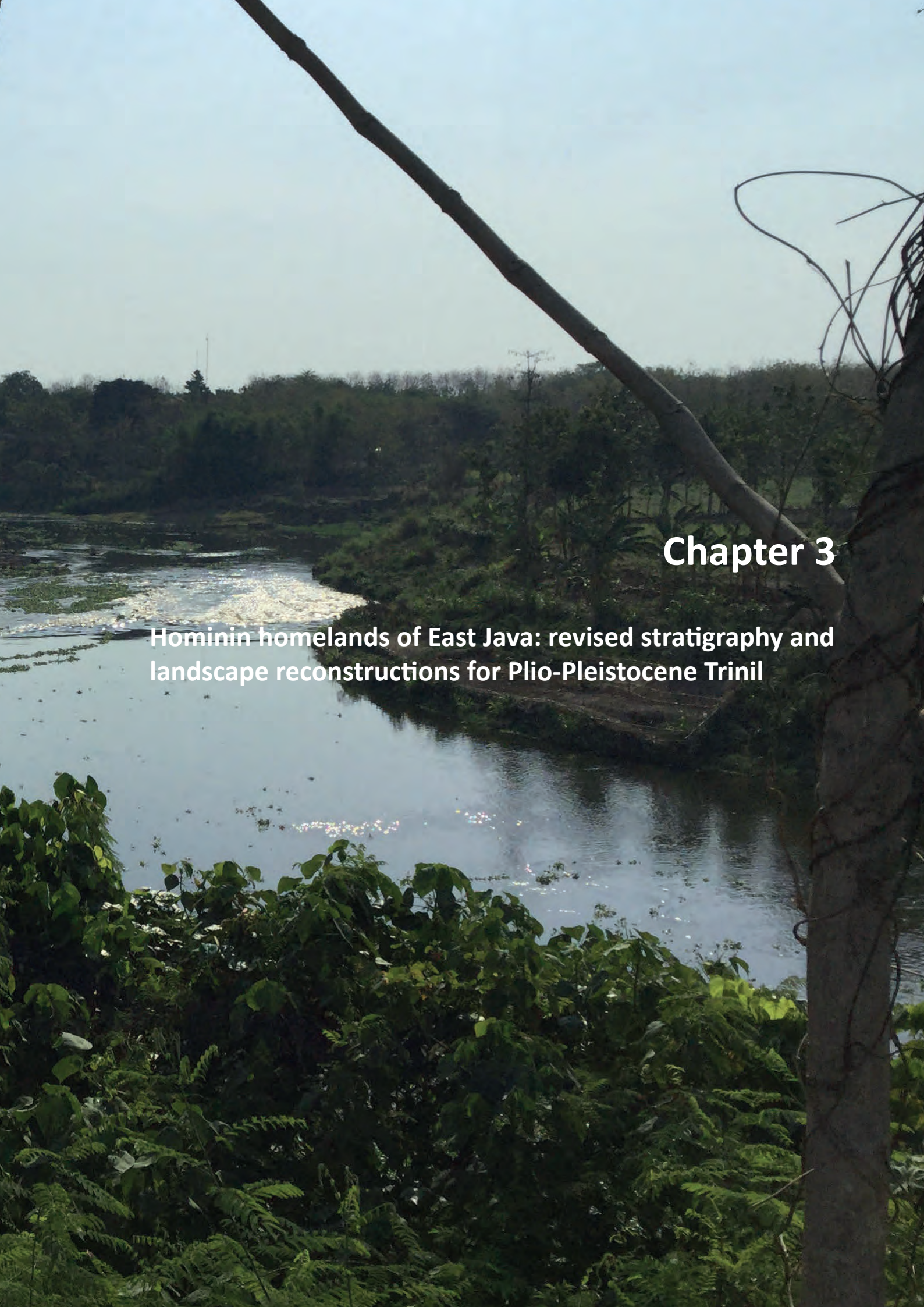
6. Conclusions

This study fills the last great gap in the local biostratigraphy. It shows that some of the previously assumed correlations (Duyfjes, 1936, 1938a) between strata of the western and eastern Kendeng Zone are incorrect. The laminated, diatomaceous mudstones of the eastern Kendeng Zone are older than previously assumed and date from the Early Pliocene. The blue clays of the eastern Kendeng Zone represent two different sequences. The lower sequence forms the continuation of the Pliocene regressive series. With an age of ca. 3 Ma, its base is older than assumed by Duyfjes, who regarded the base of the blue clays as Pleistocene. It dates from the Late Pliocene and continues into the Early Pleistocene. The second blue clay sequence postdates a period of exposure and represents shallow marine conditions and prograding sandy deltas. Its content of reworked planktonic foraminifera impedes accurate dating. It may be of Early or Middle Pleistocene age.

Although the finding of an unconformity within the blue clays puts the deltaic sandstones in a new stratigraphic context, our study does not provide a final conclusion about the age and stratigraphic position of the vertebrate fossil bearing sandstones.



The Solo, just upstream of Trinil. View direction is to the southwest (downstream). Dubois' excavation site lies at the left bank and is visible by the blue plastic. The museum lies on the opposite site of the river (not visible).



Chapter 3

Hominin homelands of East Java: revised stratigraphy and landscape reconstructions for Plio-Pleistocene Trinil

CHAPTER 3

Hominin homelands of East Java: revised stratigraphy and landscape reconstructions for Plio-Pleistocene Trinil

H.W.K. Berghuis, A. Veldkamp, Shinatria Adhityatama, Sander L. Hilgen, Indra Sutisna, Didit Hadi Barianto, Eduard A.L. Pop, Tony Reimann, Dida Yurnaldi, Dian Rahayu Ekowati, Hubert B. Vonhof, Thijs van Kolfschoten, Truman Simanjuntak, J.M. Schoorl, Josephine C.A. Joordens

Published in: *Quaternary Science Reviews* (2021)

Abstract

Trinil (Java, Indonesia) yielded the type fossils of *Homo erectus* and the world's oldest hominin-made engraving. As such, the site is of iconic relevance for paleoanthropology. However, our understanding of its larger geological context is unsatisfactory. Previous sedimentological studies are around 100 years old and their interpretations sometimes contradictory. Moreover, the existing stratigraphic framework is based on regional correlations, which obscure differences in local depositional dynamics. Therefore, a new and more local framework is urgently needed. We carried out a comprehensive geological study of the Trinil area. Using a Digital Elevation Model, we identified seven fluvial terraces. Terrace deposits were described and OSL-dated and fluvial behaviour was reconstructed. The terraces were correlated with terraces of the Kendeng Hills (e.g. the hominin-bearing Ngandong terrace) and date back to the past ~350 ka. Thus far, most of the Trinil terraces and their deposits had remained unidentified, confounding sedimentological and stratigraphic interpretations.

The exposed pre-terrace series has a thickness of ~230 m. Together with the terraces, it forms a ~3 Ma record of tectonism, volcanism, climate change and sea-level fluctuations. We subdivided the series into five new and/or revised stratigraphic units, representing different depositional environments: the Kalibeng Formation, Padas Malang Formation, Batu Gajah Formation, Trinil Formation and Solo Formation. Special attention was paid to erosional contacts and weathering profiles, forming hiatuses in the depositional series, and offering insight into paleoclimate and base-level change. The Trinil Formation provides a new landscape context of *Homo erectus*. Between ~550 and 350 ka, the area was part of a lake basin (Ngawi Lake Basin), separated from the marine base level by a volcanic barrier, under dry, seasonal conditions and a regular supply of volcanic ash. An expanding and retreating lake provided favourable living conditions for hominin populations. After 350 ka, this role was taken over by the perennial Solo River. Landscape reconstructions suggest that the Solo formed by headward erosion and stream piracy, re-connecting the Ngawi Lake Basin to the plains in the west. Our study offers a local framework, but its Pleistocene landscape record has regional significance. Most of all, it forms a much-needed basis for future, detailed studies on the build-up of the hominin site of Trinil, its fossil assemblages and numerical ages.

1. Introduction

Trinil (East Java, Indonesia, **Fig. 1**) is the discovery site of the world's first deliberately sought fossils of a transitional form between apes and humans (Dubois, 1894a). Originally named *Pithecanthropus erectus*, these specimens are now regarded as the type fossils of *Homo erectus* (Mayr, 1950). The site yielded thousands of vertebrate fossils (Dubois, 1907; Selenka and Blanckenhorn, 1911a) that play a key role in regional Pleistocene vertebrate biostratigraphy (Von Koenigswald, 1934, 1935; De Vos et al., 1982; Sondaar, 1984) and biogeography (Van den Bergh et al., 1996; Van der Geer, 2019). Moreover, a recently discovered fossil freshwater shell from Trinil, carved with a geometric pattern, is regarded as the world's oldest hominin-made engraving (Joordens et al., 2015).

Despite the importance of Trinil for faunal (including hominin) evolution, our understanding of the local geology is still based on over 100 years old sedimentological studies, often with contradictory interpretations (e.g. Dubois, 1908; Carthaus, 1911). Moreover, Duyfjes (1936, 1938) introduced a regional stratigraphy that is still in use today (e.g. Zaim, 2010; Joordens et al., 2015; Puspaningrum et al., 2020). However, this framework does not take into account the dynamic development of emerging Java, under the influence of volcanism, tectonism and sea-level fluctuations, with great differences in depositional environments across relatively short distances. Duyfjes' regional stratigraphic units are partly based on correlations between outcrops, combining strata with different facies in one unit, which deprives us of a detailed insight into local depositional processes and ages. This unsatisfactory state of the art hampers understanding of the geology in the Trinil area and confirms that a local approach is urgently needed. Our study aims to establish a comprehensive sedimentological, stratigraphic and geochronological framework for the sediments exposed in Trinil and surroundings. We use detailed field observations and modern facies models to reconstruct depositional settings and landscapes. Our study does not include a detailed re-inventory of Dubois' excavation site. This will be addressed in a separate paper (Hilgen et al., 2023).

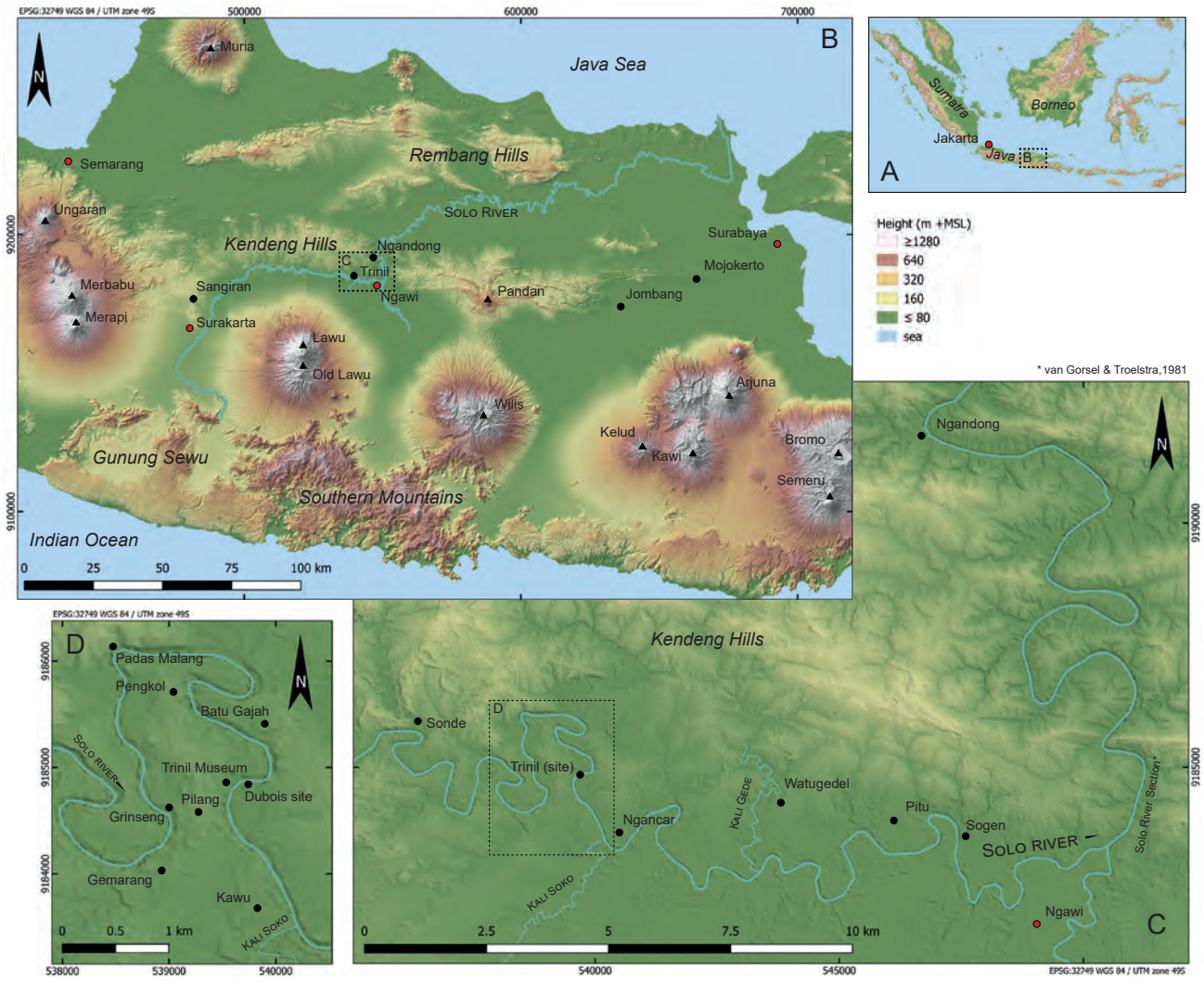


Fig. 1. A: The Indonesian archipelago with the larger study area on the eastern part of Java. **B:** Physiography of Central and East Java and sites mentioned in the text. **C:** The study area between Sonde and Ngawi. **D:** The Solo River meander of Trinil. Map data: GTOPO30 (A), ALOS (B), TanDEM-X © DLR 2019 (C and D)

2. Background

2.1 Setting, volcanism and tectonism

The Trinil area forms an inland plain, ca. 60 m above sea level, bounded in the north by the Kendeng Hills and in the south by the volcano Lawu **(Fig. 1C)**. The Solo River lies entrenched in a ca. 15 m deep channel, exposing a sedimentary series dominated by Pleistocene volcaniclastics. East of Trinil, the Solo changes course to the north and crosses the Kendeng Hills. Here the riverbanks expose folded Tertiary marine strata.

In the Miocene, most of eastern Java was part of a marine retro-arc basin located north of an east-west trending volcanic arc (Lunt, 2013). In the Late Miocene, volcanism ceased and the basin became subject to compression and uplift (Hamilton et al., 1979; Smyth et al., 2008). By the end of the Pliocene, east-west directed thrust and fold zones developed and emerged from the sea: the Rembang and Kendeng Hills and the Southern Mountains (Satyana et al., 2004; Clements et al., 2009). Between these ridges shallow marine zones prevailed, most of which gradually emerged later in the Pleistocene.

In the Early Pleistocene, volcanism returned, mainly building up stratovolcanoes in the low-lying zone between the Southern Mountains and the Kendeng Hills (van Bemmelen, 1949; Soeria-Atmadja et al., 1994). The Wilis was among the first eruption centers. Its core rocks date to 1.9-1.8 Ma (Hartono, 1994). Lawu is a young volcano, but along its southern flanks are the remains of a cone known as Old Lawu. Its core rocks were never dated, but its slopes have a dissected morphology similar to Wilis **(Fig. 1)**, suggesting a similar age.

2.2 Previous work on sedimentology and stratigraphy

Dubois collected fossils from tuffaceous strata that he called the Trinil Beds. He noted cross-bedding and interbeds of rounded gravel, which convinced him that the material is of fluvial origin (Dubois, 1894a, 1895, 1907). He related the volcaniclastic composition of the sediment to contemporaneous volcanic activity. Based on palaeontological analyses, he assigned the tuffs to the Late Pliocene or Early Pleistocene. Volz (1907) regarded the tuffs as volcanic debris flows from the Lawu, representing a long depositional phase covering most of the Pleistocene. Elbert (1908) agreed with Dubois on a fluvial depositional background, but suggested that the tuffs form two series: the lower series constitutes the actual Trinil Beds, the higher series is significantly younger and was deposited by the Solo. Carthaus (1911) described the larger geological context around Trinil and distinguished three lithological units, from old to young: calcareous beds with molluscs, volcanic breccias, and fossiliferous tuff. He recognized the calcareous strata as coastal deposits and the overlying breccias as a terrestrial lahar. He regarded the upper boundary of the breccias as the undulating lahar surface, after its flow had ceased. He claimed that the overlying fossiliferous tuffs (Dubois' Trinil Beds) formed in ponds on the lahar surface, referring to interbedded clays with leaf imprints. For him, occasional cross-bedding represents episodes of overflowing ponds. Van Es (1931) regarded the upper boundary of the marine, mollusc-bearing unit as an unconformity, representing Early Pleistocene exposure. He agreed with Dubois' interpretation of the Trinil Beds as a fluvial deposit, but in contrast to earlier researchers, he did not regard the sediment as primary volcanic material, but as fluvially supplied erosion material, referring to interbeds of well-rounded andesite gravel.

2.3 Duyfjes' regional stratigraphy

Duyfjes (1936, 1938) developed a regional stratigraphy, based on reference sections near Jombang, ca. 100 km east of Trinil. He described marine calcareous mudstones and diatomaceous mudstones, which he assigned to the Lower and Upper Kalibeng Formations, assuming a Pliocene age. These grade upwards into marine clays, deltaic sandstones and fluvial sandstones, which he assigned to the Early Pleistocene Pucangan Formation and the Middle Pleistocene Kabuh Formation, placing the unit boundary halfway the fluvial sandstones. Duyfjes used the units to map the Kendeng Hills and adjacent areas, over a distance of more than 150 km. Moving away from his reference sections, he had difficulties tracing his units and frequently relied on extrapolations ('parallelization'). The sandy marine deltas, which form the main Pleistocene landscape element of Jombang, are absent around Trinil. Nevertheless, Duyfjes applied his stratigraphic format to the Trinil series and assigned the calcareous strata to the Lower and Upper Kalibeng Formation, the breccias to the Pucangan Formation and the fossiliferous tuffs (Dubois' Trinil Beds) to the Kabuh Formation. Following Van Es (1931), Duyfjes regarded the Kabuh Formation as a fluvial deposit made up of erosion material. Higher-up in the Trinil series, he noted primary volcaniclastic sediment, which he assigned to the Notopuro Formation.

2.4 Discovery of fluvial terraces

Ter Haar (1934) described Solo terraces in the transverse valley through the Kendeng Hills **(Fig. 1C)**. One of these terraces, near the village of Ngandong, appeared to be rich in vertebrate fossils including *Homo erectus* (Oppenoorth, 1932). This shed new light on Elbert's (1908) earlier suggestion on the presence of Solo deposits around Trinil. Ter

Haar assumed that the Trinil Beds are the equivalent of the Ngandong terrace deposits. Lehmann (1936) found that the highest part of the plains around Trinil forms flat-topped, gravelly surfaces, which he referred to as the High Terrace. He regarded this terrace as the equivalent of the fossiliferous terrace of Ngandong. He noted that the gravelly surface layer truncates the Trinil Beds and concluded that the latter forms an older, pre-Solo deposit. Lehmann also recognized a 'Low Terrace': smaller surfaces that locally border the river, standing out ca. 7 m above low water level. Duyfjes (1936) added the sediment of Lehmann's terraces to his Trinil stratigraphy as 'Terrace Deposits'.

2.5 Problems, aims and objectives

The great differences between the depositional series of Jombang and Trinil reflect different depositional landscapes with unknown (age) relations. It makes the use of Duyfjes' regional stratigraphic units in Trinil inappropriate. Duyfjes regarded his Trinil stratigraphy as an uninterrupted series, which is unlikely, as it forms a ~3 Ma record of highly dynamic coastal and terrestrial deposition. Such series generally have a complex build-up, of various depositional stages and hiatuses.

A remarkable side-effect of the introduction of Duyfjes' stratigraphic framework is that it ended the previous discussion on the depositional background of the Trinil series, as if the new unit names provided final answers to earlier disputes (e.g. Soeradi et al., 1985).

Since the 1930s there have been major advances in the analysis of fluvial and pyroclastic facies and in fluvial dynamics controlling incision and deposition, allowing us to re-evaluate the complex geology of Trinil with a fresh view. This is an essential step, aiming for a better understanding of the context of the excavation sites and the excavated fossils.

The objectives of our field study are: 1) to develop coherent models of local depositional environments, against a background of volcanism, tectonism, sea-level fluctuations and climate change; and 2) to define new, local stratigraphic units, which follow major changes in depositional setting.

Special attention will be paid to the role of fluvial terraces and terrace-related deposits. Elbert's (1908) and Bartstra's (1982) suggestion of a more widespread occurrence of Solo deposits is still relevant. Recently, the terrace sequence of the Kendeng has been re-investigated and dated, revealing four terrace levels dating back to the past ~350 ka (Rizal et al., 2020). It makes a re-inventory of the Trinil terraces increasingly relevant.

3. Methods

3.1 Field study

Fieldwork was carried out in 2018 and 2019, studying riverside exposures and sand quarries between Sonde and Ngawi (Fig. 1C, D). We prepared a 12-m resolution digital elevation model (DEM) based on TerraSAR-X / TanDEM-X satellite images (© DLR 2019) to identify potential terrace surfaces. The surfaces were mapped and surveyed in the field and heights were measured by GPS and referenced with DEM-based heights. In exposures, the build-up of the terraces was studied. Terrace sediments were described and delineated, carefully documenting the position and nature of the contact between terrace deposits and pre-terrace substrate. Correlations between terraces were based on absolute and relative heights of terrace surface and (scour) base and facies of the terrace deposits, bringing to light seven terrace levels. Gravel-composition counts were carried out to obtain an additional parameter for terrace correlations (Supplement 1).

After the terrace deposits were delineated, the pre-terrace stratigraphy was studied in detail. The pre-terrace strata have a slight southward dip (2 - 10 degrees), which enables the study of stratigraphic sections along north-south directed river transects. Reference sections were selected and described, measured, and photographed. All sites and sections mentioned in the text are indicated in **Fig. 1** and Supplement 2.

3.2 Classifications, measurements and protocols

Lithological and textural descriptions are based on Dunham (1962) for carbonates, Wentworth (1922) for epiclastic and Fisher and Schminke (1984) for pyroclastic material. Deposits are regarded as pyroclastic when they consist for >75% of primary pyroclastic material. This material may be recycled by fluvial processes, but is regarded as epiclastic when eroded from older, consolidated rock. Sand- and silt-sized pyroclastic grains are referred to as ash (unconsolidated) or tuff (consolidated). Gravel-sized pyroclastic clasts are referred to as lapilli. The term lahar refers to volcanic debris flows and to the deposits thus formed. Paleosols have been described following the World Reference Base for soil resources of the Food and Agriculture Organization (FAO, 2015).

The stratigraphic units were originally referred to as Beds (e.g. Trinil Beds). In later publications, these units were re-labeled as Formation (e.g. Kabuh Formation) without further changes to the unit definition.

GPS-measured heights, referenced to the World Geodetic System 1984 (WGS84) have been recalculated to meters above mean sea level (m +MSL) using a local geoid height of 25.142 m (source: Unavco), i.e. orthometric height (m +MSL) = WGS84 height – 25.142 m.

Our interpretations follow published facies models: Miall (1996, 2014) for fluvial deposits, Ashworth et al. (1994) for braided river deposits, Hampton and Horton (2007) for sheetflow deposits, Cas and Wright (1987) and Fisher and Schmincke (1984) for pyroclastic deposits, Vallence (2005) for lahars, and Tucker (1985) and Wright (1984) for shallow marine carbonates.

3.3 Geochronology

We applied feldspar optically stimulated luminescence (OSL) dating to two representative sediment samples from the fluvial terraces. Details on sample provenance, sampling and measurement protocols and data analyses are provided in Supplement 3.

4. The fluvial terraces and their deposits

4.1 The terrace landscape of Trinil

The plains of Trinil have subtle height differences. Our DEM-analysis distinguished seven terrace levels, with heights ranging between 68 and 50 m +MSL **(Fig. 2)**. All heights represent the situation in the direct vicinity of Trinil. Moving away, terrace heights change, following the gradient of the Solo and as a result of differential uplift. The terrace margins are generally indistinct slopes, remodeled by erosion and rice cultivation. However, at a broader scale, they reflect ancient meander loops and abandoned river courses.

Terraces T7, T6 and T5 form plateaus at 68, 66 and 64 m +MSL. They have sandy surface sediments with rounded gravel and are mostly overgrown with teak forest or sugar cane. T4, T3 and T2 form wide plains, at 59, 58 and 54 m +MSL, covered with rice fields. T4 and T2 have a thin clayey topsoil, overlying a subsoil of consolidated tuffs. T3 has gravelly surface sediment.

The Solo River is deeply incised in this terraced landscape, with wide entrenched meanders. Around Trinil, its gravelly bed lies around 41 m +MSL. T1 forms small terraces at 50 m +MSL, nested along the sides of the Solo incision.

Lehmann referred to the gravel-covered plateaus (our terraces T7, T6 and T5) as the High Terrace. He also recognized T1, along the banks of the current Solo, which he named the Low Terrace. But he remained unclear about the background of the wider plains, which we identified as T4, T3 and T2, probably because he rarely found surface gravel. He left this area blank on his chart, or loose-handedly ascribed parts of the plains to his High or Low Terrace, which is definitely incorrect: The area forms separate terrace surfaces and has a different build-up, as we will show in the next sections.

The tuffs forming the subsoil of T4 and T2 have commonly been described as pre-terrace substrate, either named Trinil Beds (Dubois, 1908) or Kabuh Formation (Duyfjes, 1936), implying that these wide terraces are straths without fluvial surface sediments. This is highly uncommon. Moreover, the wide, relatively low plains do not show signs of extensive surface erosion that could have removed this fluvial cover sediment.

4.2 Sedimentology of T7, T6 and T5

4.2.1 Description

T7, T6 and T5 are made up of fluvial, flat lying surface deposits overlying a planar erosion surface. The latter is easily recognized, running parallel to the terrace surface and truncating the southward dipping substrate. It is covered with an unstructured lag of rounded andesite gravel (thickness 20 to 60 cm; main gravel size 2 – 6 cm). Pebbles with red weathering rinds are common (Supplement 1). The gravel lag grades into brown-yellow sand and conglomerates with m-scale, low-angle trough cross-bedding structures **(Fig. 4, photos 12 and 14)**. The sand is made up of well-sorted, mono-crystalline (feldspars, pyroxenes, hornblendes) and lithic (andesite) grains. The surface layer of T7 and T6 has a thickness of ca. 2 m, but the T5 sediment locally reaches greater thicknesses. Around the Trinil Museum, its thickness is ca. 4.5 m.

Of special interest are channeled incisions, which are locally found below the T7 planation surface, cutting several meters into the underlying pre-terrace substrate. The quarries of Batu Gajah and Watugedel **(Fig. 3A and C)** provide good exposures of such incisions, which are mantled with rounded andesite gravel and filled with greyish-white

tuff, dominated by vitric grains and mono-crystalline feldspars. The material has dm-scale trough cross-bedding and stacked channel structures with a lapilli-rich fill dominated by moderately rounded pumice (size range 0.5 – 3 cm). The strata do not follow the southward dip of the substrate. Moreover, the occurrence of rounded andesite gravel indicates that the deposits are part of the terrace sequence. We regard T7 as a composite terrace, made up of two series: T7A and T7B.

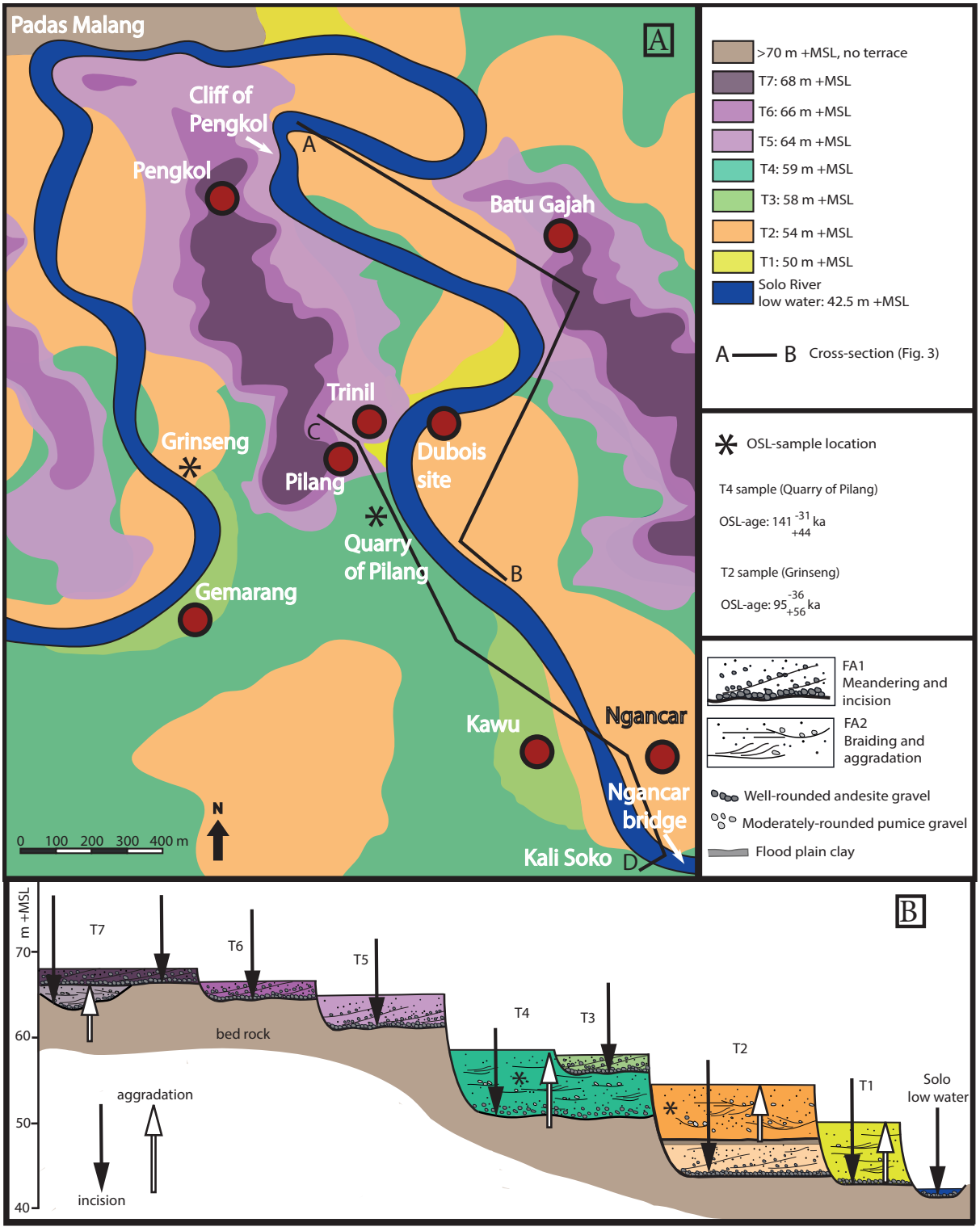


Fig. 2. A: Map of the fluvial terraces around Trinil © DLR 2019 (TerraSAR-X / TanDEM-X data). **B:** Idealized cross-section over the sequence of fluvial terraces of Trinil. FA = Facies Association, see **Table 1**; OSL datings, see Supplement 3.

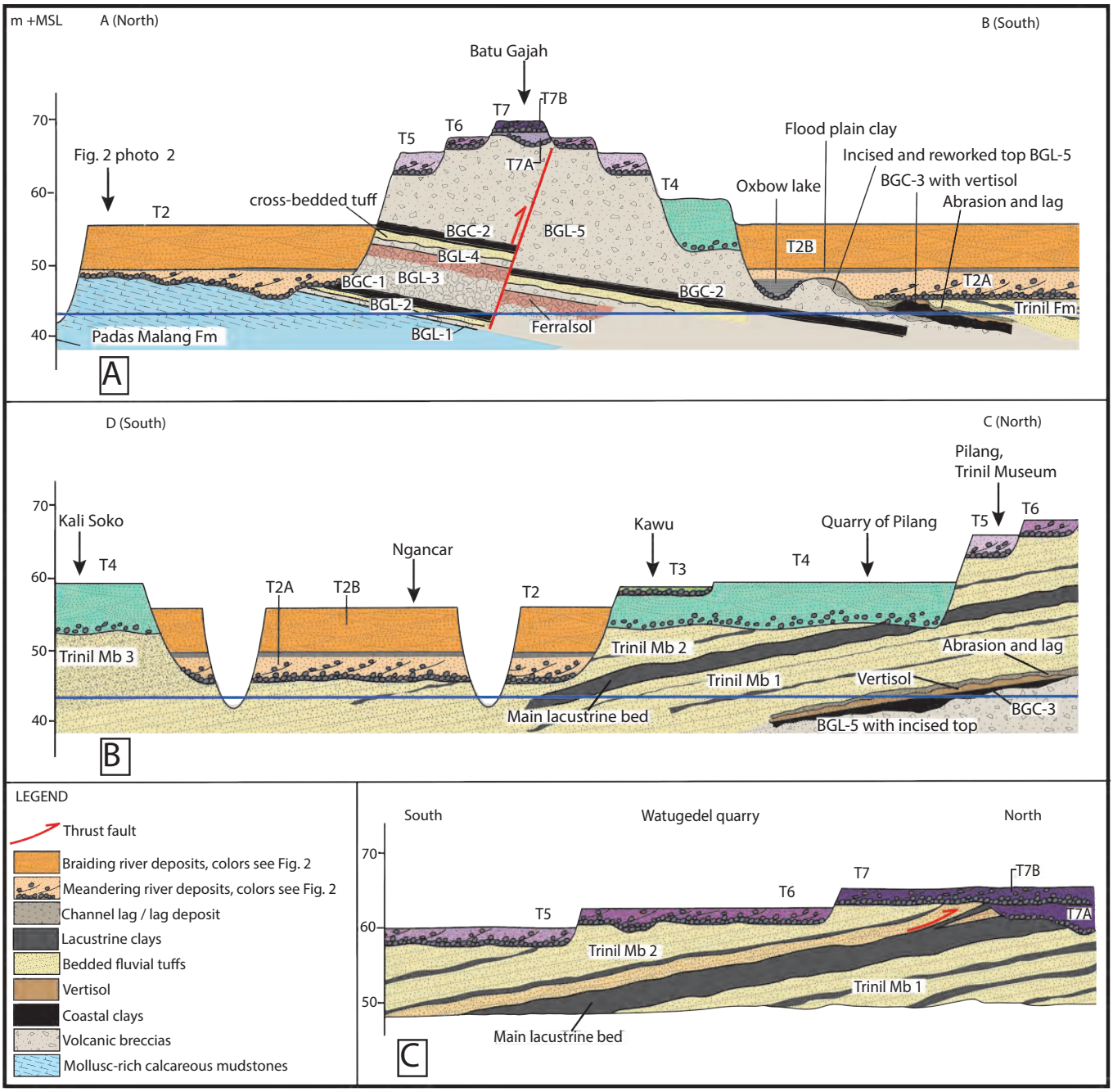


Fig. 3. Cross-sections through the Trinil area, showing schematic occurrence of the stratigraphic (sub)units. Location of the cross-sections are indicated in Fig. 2 and Supplement 2. Colors of the terrace deposits follow the terrace map **(Fig. 2)**. Horizontally not to scale. Section lengths: A and B = ca. 2 km, C = ca. 500 m. Note difference in perspective. The cross-sections follow as much as possible the natural view toward the riverbanks and quarry sides. Note that cross-section A gives a general insight in the stratigraphic situation around the Dubois excavation site. A detailed stratigraphic description of this site will be presented in a separate publication by Hilgen et al. (2023).

4.2.2 Interpretation

T7, T6 and T5 are strath terraces. The gravelly sediment forms a residual mantle, associated with the incisive stage, and represents a laterally mobile gravel-bed river. Lateral accretion structures and a fining-upward grain-size trend indicate meandering conditions. The well-rounded andesite gravel points to long-distance bed-load transport, which is confirmed by its composition, including rock types uncommon in the direct vicinity (Supplement 1). The relatively thick sediment cover of T5 was formed in conjunction with the gravel-covered scour. We regard this series as a 'working depth' deposit of material in transit, representing a situation of simultaneous deepening and widening of the valley floor (Gibbard and Lewin, 2002).

The channel structures (T7A), locally preserved under the strath of T7B, form remnants of an older fluvial stage. The gravelly lag must be associated with incision, whereas the tuffaceous fill represents subsequent aggradation. The lack of vertical grading and the occurrence of multiple, stacked channels point to braided conditions. The fill was truncated during the subsequent incisive stage of series T7B.



Fig. 4: Selected photographs of the terraces and terrace deposits (Solo Formation). See Supplement 6 for coordinates and setting.**(1)** Terrace T1, the terrace deposits overlie massive calcareous mudstones (FA3) of the Kalibeng Formation. **(2)** Terrace T2, terrace deposits T2A and T2B overlying hard calcareous mud bank (FA4) of the Padas Malang Formation. **(3)** T2A (FA1), channelling scour base and gravel lag over fine tuff (FA11) of the Trinil Formation. **(4)** T2A, abandoned channel and oxbow lake clays (FA1). **(5)** idem, zoom in to laminated oxbow lake clays. **(6)** T2A, floodplain clays (FA1), overlain by cross-bedded ash and pumice (FA2) of T2B. **(7)** Oxbow lake clays (FA1, T2A), slightly incised and covered with sandy crevasse splay deposits (FA1, T2A). **(8)** Cross-bedded tuff and pumice (FA2, T2B). **(9)** Cross-bedded tuff (FA2, T4). **(10)** Cross-bedded tuff with pumice (FA2, T7A). **(11)** Terrace T7, T7A deposits overlain by T7B deposits. **(12)** Fluvial cover sediment of Terrace 6 (meandering facies, FA1). **(13)** T5, scour base and gravel lag (FA1) over Trinil Formation. **(14)** Point bar facies (FA1) of T5. **(15)** Drone image of Dubois Site (blue tent) and Trinil Museum, with general overview of the terraces.

4.2.3 Andesite gravel as a key characteristic of Solo incision

Strath terraces T7, T6 and T5 show that, during its incisive stages, the Solo was a meandering river, carrying a bed load of far-travelled, rounded andesite gravel. The gravel-covered straths form a notable contrast with the underlying substrate, in which we never observed rounded andesite gravel. This raises an important question: Is it possible that the andesite gravel, which Dubois, Van Es and Duyfjes described as interbeds within the tuffaceous Trinil / Kabuh Formation, represent misinterpreted Solo deposits? For this question, the large quarry of Watugedel forms a good reference **(Fig. 3 C)**. It exposes ca. 40 m of planar-bedded tuffs, overlying volcanic breccias. The strata dip ca. 8 degrees to the south, confirming that they belong to the pre-terrace substrate. Dubois (1893), who collected fossils from the nearby Kali Gede, described the strata as the Trinil Beds. The tuffs are mostly planar laminated, rich in in-situ calcareous concretions, and have interbeds of light grey clay. Rounded andesite gravel is absent over the entire length of the section. The dipping beds are truncated by the straths T7, T6 and T5, forming a staircase along the top of the quarry. As expected, the scour surface of the terraces is mantled with rounded andesite gravel. This strongly suggests that rounded andesite gravel is not part of the facies of the Trinil / Kabuh Formation and that andesite gravel is a distinguishing characteristic of a Solo-related incision or planation surface. In the next sections, we will show that this is a valuable field criterion.

4.3 Sedimentology of T4 and T3

4.3.1 Description

The riverside quarry of Pilang provides good exposures of the strata below T4 **(Fig. 3B)**. Dubois and Duyfjes, who referred to the site as Kliteh, described the local tuffs as Trinil / Kabuh Formation. The base of the exposures, just above low water level of the Solo, consists of southward-dipping, planar-bedded fine tuff with in-situ calcareous concretions and interbeds of grey clay.

Halfway up the quarry profile, this dipping series is truncated by a slightly undulating erosional contact, which does not follow the southward dip of the underlying beds, but remains at a height of ca. 51 m +MSL. It is covered with greyish white tuff, consisting of vitric grains and subordinate mono-crystalline feldspars. The series continues up to terrace level and shows trough cross-bedding and stacked channel structures with lapilli-rich fills, dominated by moderately rounded pumice (main size range 0.5 – 2 cm). The base of this series, up to ca. 1 m above the erosive base, contains dispersed rounded andesite gravel (size range 2 - 6 cm).

Along the southern edge of the quarry, the surface level steps down ca. 1 m to 58 m +MSL. At the same time, a planar scour surface appears at ca. 56 m +MSL, cutting into the T4 sediment. The scour surface is covered with a lag of rounded andesite gravel (thickness 40 to 70 cm; main gravel size 3 – 7 cm). The gravel lag grades into brown-yellow sand and conglomerates with m-scale, low-angle trough cross-bedding structures. The sand is made up of mono-crystalline (feldspars, pyroxenes, hornblendes) and vitric grains.

4.3.2 Interpretation

The southward dip of the basal series relates these strata to the pre-terrace substrate. The bedded tuffs are identical to those in the Watugedel quarry and do not contain rounded gravel **(Fig. 3B and C)**. The erosion surface over these strata forms an angular disconformity and marks a previously unnoted stratigraphic boundary. The stacked channels and a lack of vertical grading in the overlying fluvial series point to braided conditions and aggradation, whereby the terrace surface appears to form the top of this aggradation stage. Returning to the base of this aggradational series, the dispersed rounded andesite gravel forms a conspicuous element, which we defined in **Section 4.2.3** as a key characteristic of Solo incision. The gravel does not form a well-defined lag over the scour surface, as would be expected, but has become dispersed over the lower meter of the tuffaceous fill sediment. We postulate that high-energy currents picked up the gravel during the onset of the aggradation stage.

We conclude that the Pilang quarry exposes two tuffaceous series. A lower, tilted series represents the pre-Solo bedrock. It is truncated by an erosion surface representing Solo incision. The overlying series represents subsequent fluvial deposition, which makes T4 a fill terrace. Previous researchers did not distinguish between the two series, due to their apparently similar composition. However, we do note facies differences: the lower series is characterized by parallel bedding and interbedded clays, whereas the upper, terrace-related series has more dynamic channel and cross-bedding structures. Moreover, the lower series is rich in in-situ calcareous concretions, whereas these were not observed in the overlying terrace-series.

The gravel-covered T3 represents a cut terrace, incising several meters into the fill of T4. Its gravelly surface sediments represent incision and lateral accretion, similar to strath terraces T7 to T5.

4.4 Sedimentology of T2

4.4.1 Description

Moving south from Pilang to the village of Kawu, we descend to terrace T2 (54 m +MSL). The base of the riverbank exposes southward dipping, bedded tuffs, with in-situ calcareous concretions and clayey interbeds, which can be traced back along the river and form the continuation of the material exposed in the base of the Pilang quarry. But here, the bedded tuffs only make up the lower 1 or 2 m of the riverbank profile. At ca. 43.5 m +MSL this dipping series is truncated by a horizontal erosional contact covered by an unstructured lag (thickness 0.1 to 0.8 m) of rounded andesite gravel (size range 3-8 cm) with admixed reworked calcareous concretions. Locally the gravel is cemented by calcite. The gravel is covered by brown-yellow sand and conglomerate, with m-scale, low-angle trough cross-bedding structures. The sand consists of mono-crystalline (feldspars, pyroxenes, hornblendes) and lithic (andesite) grains. This bedded series fines upward and is overlain by a massive, crumbly dark brown clay, with root traces and red mottling (thickness ca. 0.5 m), the top of which is found at ca. 48.5 +MSL.

The clay is sharply overlain by cross-bedded tuff and fine, moderately rounded pumice lapilli **(Fig. 4, photo 6)**, continuing up to terrace level (54 m +MSL). The tuff is dominated by vitric grains and mono-crystalline feldspars. The series lacks vertical grading and contains multiple, stacked channel structures.

The gravel-covered scour, at ca. 43.5 m +MSL, can be traced along the long river transect between Kawu and Ngancar Bridge, along both banks of the river **(Fig. 3A and B)**. All along this reach, the southward-dipping bedded tuffs, with in-situ calcareous concretions and clayey interbeds, form the lowermost one or two meters of the riverbank profile, although the southward dip gradually decreases. Interbeds of rounded gravel were not found in this dipping series, confirming our observations in the Watugedel quarry **(Section 4.2.3)**.

4.4.2 Interpretation

The tilted, bedded tuffs, exposed just above low water level, can confidently be regarded as the pre-terrace substrate**.** Along the long river transect between the Trinil Museum and Ngancar Bridge, these strata form a continuous series reaching a total thickness of around 50 m **(Section 5.3 and 5.4)**. The erosive surface at 43.5 m +MSL forms an angular disconformity over this series, associated with the overlying terrace T2. The gravel lag marks this scour as an ancient incision level of the Solo. This gravel lag forms the basis of a ca. 5 m thick fining-upward series (T2A), reflecting a gravelly channel, sandy point bars and floodplain clays. We relate this series to the incisional stage, representing lateral accretion. As we also noted for T5, the relatively thick sediment-cover points to temporary storage of material in transit, reflecting ongoing deepening and widening of the valley floor. The thickness of the series corresponds to the depth of the deeper channels on the floodplain (see also **Section 4.5**). The clay layer at ca. 48.5 m +MSL represents the ancient floodplain associated with this laterally migrating river. It has become buried by a second fluvial series (T2B), dominated by tuffaceous sediment. The stacked channels and lack of vertical grading indicate a braided style and aggradational conditions. The terrace surface represents the top of this aggradation stage, which makes T2 a fill terrace. And, as was also noted for T4, the tuffaceous fill of series T2B lacks in-situ calcareous concretions and has more pronounced channel structures than the southward-dipping tuffaceous strata of the pre-terrace substrate, offering valuable diagnostic criteria for distinguishing between terrace deposits and substrate **(see Tables 1 and 2, FA2 and FA11)**.

4.5 The T2-scour over harder substrates

4.5.1 Description

We described the T2 basal scour as a planar erosion surface over the tilted tuffaceous substrate. Along the northern margin of the study area, the pre-terrace substrate is made up of harder lithologies. Here, T2 forms smaller surfaces, roughly following the course of the current river. Often, the basal scour is more irregular. The substrate along the left riverbank opposite the cliffs of Pengkol **(Fig. 2)** consists of erosion-resistant, cemented calcareous mudstones. These are truncated by a gravel-covered, channeled scour, generally down to an incision depth ranging between 43.5 and 46 m +MSL (**Fig. 3A)**. The incision-related deposits (T2A) consist of rounded andesite gravel overlain by trough cross-bedded conglomerates, only locally capped by floodplain clays. At ca. 48.5 m +MSL, this series is buried by cross-bedded tuffs, forming the aggradational series T2B, which continues up to terrace level (54 m +MSL). Of particular interest are sites where the T2-scour forms isolated channels with a clayey fill, for example along the right riverbank south of Padas Malang and along the left riverbank just upstream of the Dubois site **(Fig. 3A; Fig. 4, photos 4 and 5)**. At both locations, the T2 scour forms a steep-sided channel, incised in massive volcanic breccias, reaching an incision depth of ca. 43.5 m +MSL. The scour is covered with a lag of rounded andesite gravel, locally cemented by calcite, and forms a conspicuous platform just above low water level. The gravel is sharply overlain by ca. 3 m of light grey, slightly plastic clays with fine silty laminae. The clays are sharply overlain by ca. 1 m of cross-bedded sands, which at their base slightly abrade the laminated clays. Around 48.5 m +MSL, the sand is buried by the tuffaceous, aggradational series T2B, which continues up to terrace level.

4.5.2 Interpretation

The spatial distribution of T2, forming wide plains south of Trinil and narrower surfaces more to the north, reflects variability in bedrock resistance. In the south, the river could easily increase valley width by cutting into the tuffaceous substrate. However, along the northern margin of this abraded platform, abrasion proceeded slower and the river formed more confined channels and meanders. This also explains the relatively thick 'working-depth' deposits of series T2A in more central areas of the former valley floor. The clay-filled, isolated channels represent abandoned channels with oxbow lakes. Silty laminae reflect episodes of flooding of the main channel. The preservation of the laminae indicates oxygen-depleted bottom waters. Trough cross-bedded sands overlying the oxbow-lake clays are part of the basal, meandering-river series and represent flooding events or crevasse splays **(Fig 4, photo 7)**.

4.6 Sedimentology of T1

4.6.1 Description

The left riverbank east of Padas Malang provides good insight in the build-up of T1. Directly above low water level, the riverbank is made up of marine mudstones. Between 42.5 - 43 m +MLS, these strata are truncated by a planar erosion surface, covered with a ca. 40 cm thick lag of rounded andesite gravel. The erosive contact can be traced along the foot of the terrace, over a distance of several hundred meters. The gravel is sharply overlain by loosely consolidated ash, dominated by vitric grains and monocrystalline feldspars. The series shows fine cross-bedding structures and stacked, shallow channel structures and continues up to terrace surface at 50 m +MSL.

4.6.2 Interpretation

The gravel-covered erosional contact forms a sharp lithological contrast with the underlying mudstones and is readily identified as the scour base of T1. It represents the mobile channel-belt characteristic of the incisive Solo. The overlying ash represents a subsequent aggradational stage, characterized by braided conditions, which makes T1 a fill terrace.

T1 follows the course of the current river. Prior to the formation of the recent Solo incision, T1 probably occupied the area of the current channel. Currently, only small plateaus remain along the riverbank. However, patchy remnants of T1-related fill sediment are more widespread, plastered against the lower part of the riverbanks, usually lacking a clear terrace surface. The same accounts for T1-related gravel. Patches of this material occur on the current valley-floor, close to low water level, only slightly higher than the gravel bed of the current river. When studying riverbank exposures, care must be taken to identify such remnants of young T1 sediment.

Description	*Interpretation*
FA1. Planar basal scour surface covered with an unstructured lag (10-80 cm) of clast-supported, well-rounded gravel (size 2-8 cm) (Fig. 4, photo 13). Gravel predominantly of andesitic composition (Supplement 1). Basal gravel covered with ca. 2 m of (fine) conglomerate and yellowish-brown sand with m-scale, low-angle trough cross-bedding (Fig. 4, photos 12 and 14). Sand dominated by mono-crystalline (feldspars, pyroxenes, hornblendes) and lithic (fine andesite fragments) grains. The sand may grade into a top layer of brown, massive clay with a crumbly structure, mottling and fine root traces, but often such fine top layer is absent. Total thickness is generally 2 to 3 m, up to terrace surface. Locally reaching greater thickness, up to 5 m.	**Incision and lateral accretion Meandering river** Material in-transit
Locally, a more irregular basal scour surface occurs, forming deep channels with high-angle banks and thick (up to 80 cm) and coarse (size up to 8 cm) gravel lags (Fig. 4, photo 3). Frequent occurrence of isolated channels cut into the pre-terrace-stratigraphy. Isolated channels may have a fill of plastic, grey, planar laminated clays (Fig. 4, photo 4 and 5).	Partly confined conditions. Oxbow lakes
FA2. Overlying an older scour surface and a lag deposit associated with a previous incision stage, or burying an older terrace. Sediment consists of greyish-white, coarse to fine ash (often consolidated to tuff) with fine, moderately rounded lapilli (size up to 4 cm, main size range 0.5 – 2 cm). No notable vertical grain-size grading. Ash dominated by vitric grains and fine pumice debris with subordinate mono-crystalline grains (mainly feldspars). Lapilli consist of vesicular pumice and sparse dacites. Frequent occurrence of stacked channel structures, with lapilli-rich fills (Fig. 4, photo 11) and high-angle, dm to m-scale trough cross-bedding (Fig. 4, photos 6 to 10). Outside these channels, the material is generally planar bedded, with fine planar lamination or cross-lamination. Terrace surface is top of aggradation.	**Aggradation under high volcanic supply Braided river**

Table 1: Terrace-related fluvial Facies Associations

4.7 Incision and aggradation, fluvial styles and volcanic supply

The terraces of Trinil reflect alternating stages of incision and aggradation, with notable differences in fluvial style. Incisive stages are characterized by gravel-bed rivers. The channel gravel is found in association with overlying point-bar structures and fining-upward sequences, indicating meandering conditions. Also the arcuate terrace margins **(Fig. 2)** point to a meandering style for the incisive Solo. Aggradational stages are characterized by sediment-laden, braided conditions. Such sequences of meandering incision and braided aggradation reflect changes in the balance of water flow and sediment load. For the Trinil terrace sequence, volcanic supply must have been the decisive factor controlling these changing conditions. The surface sediments of incisional stages consist of epiclastic material, reflecting abrasion and long-distance transport. Aggradational series are invariably made up of fresh pyroclastic material, indicating that stages of braiding and aggradation were triggered by volcanic eruptions.

We subdivided the terrace deposits into two facies associations **(Table 1)**, which are useful for field identification and distinguishing the terrace sediments from the pre-terrace substrate. For the latter, separate Facies Associations will be defined in **Section 5 (Table 2)**.

4.8 OSL dating of the terrace deposits

We selected terraces T2 and T4 for numerical dating, as these fill terraces, unnoted by previous researchers, are of primary interest for the revised stratigraphy of Trinil. We carried out feldspar OSL-dating of the tuffaceous fill of both terraces **(Fig. 2).** For a detailed discussion on measurement results and interpretations see Supplement 3. The T4 sediment was dated to 141 (-31/+44) ka, whereas the T2B sediment was dated to 95 (-36/+56) ka. These ages are within the age range of the Solo terraces in the Kendeng Hills around Ngandong, which date back to the past 350 ka (Rizal et al., 2020), confirming that the deposits are part of the Solo terrace sequence and not of the older substrate.

4.9 Correlation between the Trinil and Kendeng terrace sequences

We propose a preliminary correlation between the terraces of Trinil and the terraces of the Kendeng area, based on position within the terrace sequence, composition of terrace sediments and OSL-ages **(Fig. 5).**

The upper terrace of the Kendeng is a poorly preserved strath terrace with a ca. 1 m thick surface layer rich in rounded andesite gravel (Fauzi et al., 2016). We regard this terrace as the equivalent of Trinil-terraces T7, T6 and T5. Possibly, a detailed study of the Kendeng upper terrace may reveal a subdivision into (sub)levels, as in Trinil. Referring to the OSL ages of Rizal et al. (2020), we provisionally regard T7, T6 and T5 as a group of straths, with a rough age range of 350 – 300 ka.

The middle terrace of the Kendeng area can be correlated with Trinil-terrace T4, referring in the first place to their position within the terrace sequence and available OSL-ages. Moreover, the terrace sediment reaches a thickness of > 4 m and consists of cross-bedded sand with stacked channel structures, reflecting aggradational conditions similar to T4. An equivalent of terrace T3, cut into the surface of T4, is unknown from the Kendeng area.

The lower terrace of the Kendeng, the famous Ngandong terrace, correlates with Trinil-terrace T2, again referring to their position in the local terrace sequence, the terrace sediment and OSL ages. The lower terrace yielded numerous vertebrate fossils including hominin remains and has recently been extensively re-studied (Huffman et al., 2010; Indriati et al., 2011; Sipola, 2018). The terrace sediment consists of a basal lag of andesite gravel, covered with an aggradational series of pebbly, cross-bedded tuffaceous sands, which the authors relate to contemporaneous volcanic supply, similar to the situation described for Trinil-terrace T2. Rizal et al. (2020) provide multiple dates for the Ngandong lower terrace, indicating an age range of 140 to 92 ka. Our OSL age of series T2B, of 95 (-36 / +56) ka, fits within this range.

Finally, the lowermost terrace of the Kendeng Hills is readily correlated with T1. Both terraces form small surfaces bordering the river, ca. 7 m above low water, and are made up of a thin andesite-gravel lag covered with a fill of unconsolidated ash.

Our OSL ages from Trinil terraces T4 and T2B plot near the lower age range boundary of the corresponding Kendeng terraces, which may be related to differences in applied dating methods. However, it may also reflect differences in timing of the response to degradation or aggradation events along the longitudinal river profile (Bull, 1990).

4.10 Incision and uplift rates based on the Ngandong and Kendeng terraces

The greater heights of the Kendeng terraces compared to the corresponding terraces of Trinil reflect higher uplift rates. **Fig. 5B** plots Solo incision over the last 350 ka, as recorded by the terraces of the Trinil and Kendeng areas. For the age plots, we used the oldest available OSL ages of the Kendeng terraces, assuming that these provide the closest representation of the incision stage, preceding aggradation.

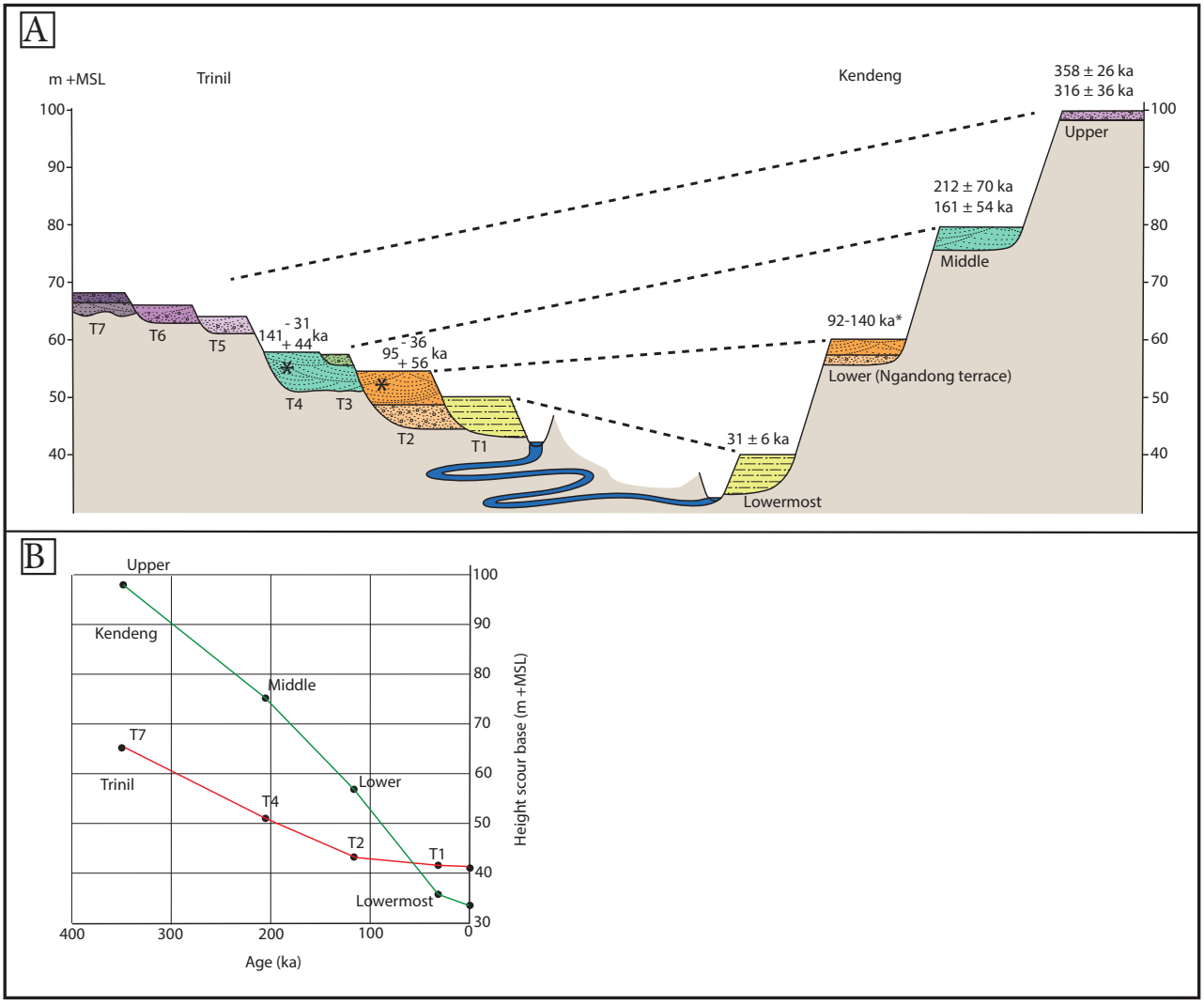


Fig. 5. A: Correlation between the Solo River terraces of Trinil and the Kendeng Hills with OSL ages. Trinil ages from this study (Supplement 3). Kendeng terrace names and ages from Rizal et al., 2020. * Bayesian modelling including ESR, U-series and Ar/Ar ages. **B:** Solo River incision rates over the last ~350 ka for the Trinil and Kendeng areas.

At Trinil, incision rates were around 90 mm/ka between 350 and 100 ka, slowing down to ca. 10 mm/ka over the last 100 ka. In the Kendeng, incision rates were much higher, reaching values of ca. 200 mm/ka. We regard this prolonged and constant net downcutting of the Solo River as tectonically controlled incision. The greater downcutting rate of the Solo River in the Kendeng Ridge compared to Trinil reflects higher uplift rates **(Section 7.2)**. The limited preservation of the Kendeng terraces may very well relate to this higher uplift rate (Veldkamp and van Dijke, 2000).

5. Sedimentology of the pre-terrace substrate

Our careful delineation of the terrace-related deposits made it possible to study the underlying substrate, without the risk of mixing up these two series. We selected four overlapping reference sections (Supplement 2), covering a total thickness of 230 m **(Fig. 9)**. The series has limited lateral variation over the study area. Marker beds are well-identifiable and facilitate correlation between outcrops that may be kilometers apart.

For our descriptions and interpretations, we distinguished 10 Facies Associations (FA2 – FA12) based on texture, sediment composition, sedimentary structures and stratigraphic position **(Table 2)**.

5.1 The Padas Malang Section

The base of the Padas Malang Section forms the lowest stratigraphic level exposed around Trinil. It consists of massive calcareous mudstones (FA3) **(Fig. 6, photos 1 and 2)**. The deposits represent open marine conditions under a low influx of terrigenous material. The rich foraminifera content and thorough bioturbation indicate normal oxygen conditions. The mudstones form the top of a thick marine unit that dominates the exposures of the Kendeng Hills.

Correlation with a nearby foraminiferal biostratigraphic section indicates that the strata as exposed around Trinil were formed under outer-shelf depth conditions (Van Gorsel and Troelstra, 1981). Moving upsection, the facies of the mudstones gradually changes, by the introduction of bedding structures and an admixture of granular calcareous material

and fine shell debris (**Fig. 6, photo 3)**, reflecting gradual shallowing and increasing energy conditions. Occasional beds are made up of sub-rounded clasts (ca. 10 cm) of calcareous mudstones, indicating nearby erosion of bottom material, likely during storms.

Description	*Interpretation*
FA3. White to light grey, massive calcareous mudstone. No bedding structures (Fig. 6, photos 1 and 2). Rich in well-preserved foraminifera, few diatoms. No macrofossils.	**Open marine, outer shelf**
FA4. White to light grey, bioclastic wackestone. Fine calcareous matrix with abundant silt or sand-sized calcareous grains and shell debris (Fig. 6, photo 4). Rich in gastropods, bivalves (mostly disarticulated), echinoids and coral debris* (Fig. 6 photos 8-10). Well-preserved crustacean burrows (Fig. 6, photos 5 and 6). Locally bedded, but generally massive and strongly affected by bioturbation (Fig. 6, photo 12).	**Sheltered calcareous lagoon**
Interbeds (1 – 5 m) of thickly bedded, strongly cemented, greyish white calcareous mudstone with sparse calcareous grains or bioclasts (Fig. 6, photo 7).	Calcareous mudbank
FA5. Greyish white, bedded packstones and grainstones. Planar bedding (5 to 30 cm), beds parallel laminated or massive. Sediment made up of sand- to fine gravel-sized calcareous grains, consisting of detrital bioclasts (shell debris and sparse coral debris), ooids and granular calcareous mud. Upward, beds occur with fine root traces and red mottling (Fig. 6, photo 11). Stratigraphic position: overlying the sheltered lagoonal facies (FA5) and underlying terrestrial strata.	**Peritidal carbonate platform**
FA6. Homogenous black clay, rich in organic matter. Sparse red mottling. Fine blocky structure, slightly plastic (Fig. 7, photos 5 and 12). Contains dispersed fine pyrite crystals (only visible by hand-lens). Occasional fine root traces. Contains occasional, poorly preserved gastropods, assigned to *Melanoides* aff. *tuberculata.* The clay forms tabular interbeds with a thickness of 1 to 3 m between terrestrial volcanic breccias (FA7 and FA8) (Fig. 7, photos 3 and 11).	**Coastal marsh**
FA7. Massive tuff breccia. Poorly sorted matrix of white-grey, fine to coarse welded tuff, practically devoid of clay. Tuff dominated by vitric and mono-crystalline grains, mainly feldspars and some pyroxenes, with subordinate lithic grains. Contains ca. 20% gravel to cobble-sized angular fragments and occasional boulders up to 1.5 m. Coarser fragments consist of hard, unweathered (pyroxene) andesite (Supplement 1). Finer fragments (up to 2 cm) dominated by angular, unweathered vesicular pumice (Fig. 7, photos 3, 4, 6, 7). Contains charred wood.	**Eruption-induced lahars**
FA8. Massive, clayey tuff breccia. Matrix of poorly sorted, grey or brown-red clay, silt and sand (Fig. 7, photos 1, 9, 10, 12). Sand dominated by lithic and crystal grains. Contains ca. 15% gravel-sized, angular to sub-rounded fragments. Diverse clast composition (Supplement 1), most in a soft, weathered state. Contains clay pebbles and uncharred plant fragments.	**Slope-collapse induced lahars**
FA9. Massive, white to yellow, moderately consolidated fine tuff (Fig. 7, photo 2), dominated by vitric grains. Subordinate crystal grains, mainly feldspar. Top generally fluvially reworked.	**Rain-induced ash lahars**
FA10. Thickly bedded (m-scale) grey, firmly welded, massive, matrix-supported lapilli-tuff. Hard and compact matrix of poorly-sorted tuff rich in mono-crystalline grains (predominantly plagioclase and pyroxene) with subordinate lithic and vitric grains. Lapilli concentration varies per bed, between 0 and 50%. Lapilli dominated by lithic fragments: sub-rounded dacite (max. clast size 6 cm, main size range 2-4 cm) and subordinate subangular andesite (max. clast size 3 cm, main size range 1-3 cm). Poor in vesiculated pumice. Subtle grading of lapilli gives an indistinct stratification (Fig. 8, photo 11). Interbeds (ca. 50 cm) of fine, wavy-laminated tuff with lenticular structures.	**Pyroclastic flows and surges**
FA11. Bedded (dm-scale) greyish white fine tuff made up of vitric grains with subordinate mono-crystalline grains (mainly feldspars, occasional laminae enriched in pyroxenes). Beds form sheets with considerable lateral continuity and are generally planar laminated, but occasionally massive, containing fine plant debris. Occasional shallow, low-angle channel structures. Channel fills of coarse tuff with fine, moderately rounded pumice or dacite lapilli and low-angle trough cross-bedding (cm to dm-scale) (Fig. 8, photo 8). Beds often separated by clay drapes or cm-scale massive, grey clay layers with limited lateral continuity. Clays drapes or layers have fine root traces and occasional vertical burrows. Clayey layers contain freshwater molluscs**. Most beds contain in-situ calcareous concretions (Fig. 8, photo 3), generally small concentric nodules (up to 6 cm), but locally forming coalescent, platy structures or larger rods (rhyzoliths). No notable vertical grain-size trend.	**Ash-covered braidplain**
FA12. Massive, grey, plastic clay, slightly admixed with fine ash. Contains fine plant debris and freshwater molluscs**. The clays are interbedded within FA11, with sharp boundaries. The upper boundary may be slightly incised, or riven by deep desiccation cracks (Fig. 8, photos 8 and 10). Clay beds range in thickness from ca. 50 to 300 cm (Fig. 8, photos 5 and 6). The beds have a similar composition to the thinner clay interbeds in FA11, but have a considerable lateral continuity. The clays are often found in association with greyish-white, massive or laminated fine ash rich in diatoms. The diatom-rich material contains plant debris and well-preserved leaf imprints (Fig. 8, photos 5, 7, 8).	**Shallow lake**

* For species, reference is made to published faunal descriptions (Felix, 1911; Martin, 1909; Staff und Reck, 1911).
**: For species, reference is made to published faunal descriptions (Carthaus, 1911; Joordens et al., 2009; Martin-Icke, H., 1911; Van Benthem Jutting, 1937).

Table 2: Facies Associations of the pre-terrace series.

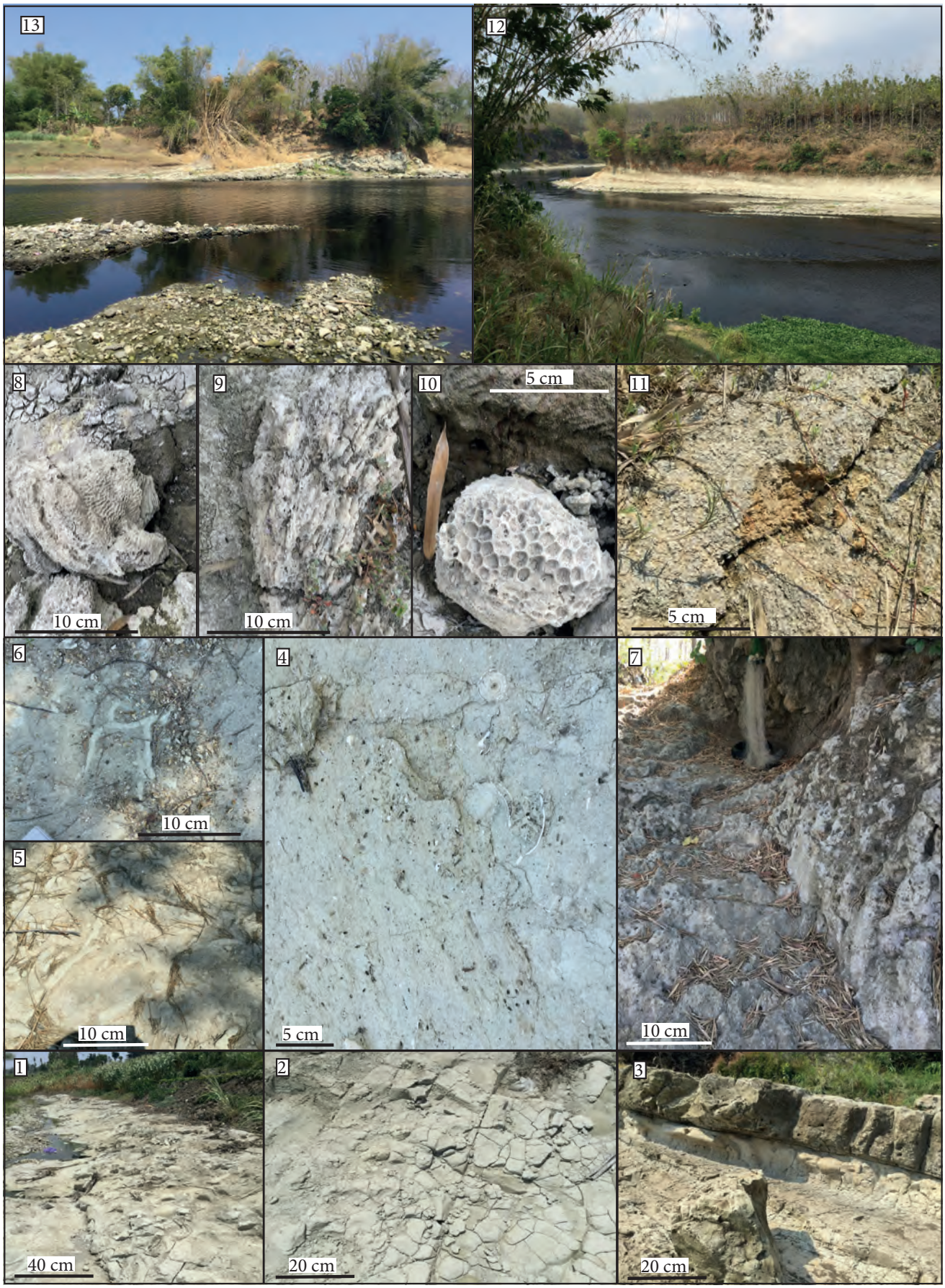


Fig. 6. Selected photographs of the Kalibeng and Padas Malang Formations. See Supplement 6 for coordinates and setting. **(1)** Massive calcareous mudstones (FA3), Kalibeng Formation. **(2)** Idem. **(3)** Bedded mudstones (FA4), base of the Padas Malang Formation. **(4)** Calcareous lagoon facies (FA4), Padas Malang Formation. **(5)** Calcareous lagoon facies with burrows (FA4), Padas Malang Formation. **(6)** Idem. **(7)** Calcareous mudbank facies (FA4), Padas Malang Formation. **(8)** Coral rubble bank (FA4), Padas Malang Formation. **(9)** Idem. **(10)** Idem. **(11)** Rooted top layer of bedded grainstones (peritidal facies, FA5), top of Padas Malang Formation. **(12)** Padas Malang, view on right bank **(13)** River side exposures of Padang Malang Formation north of Pengkol.

The bedded mudstones grade into mollusc-rich lagoonal deposits (FA4) (**Fig. 6, photo 4)**, reflecting further shallowing. The absence of bedding structures and presence of abundant burrowing traces indicates a sheltered, lagoonal setting and a limited tidal range, with an estimated depositional depth of 5 to 30 m. The frequent occurrence of coral debris indicates nearby coral reefs, but in-situ corals have not been found. A several meter thick interbed of massive, cemented calcareous mudstone is regarded as a mudbank, formed by algae or sea-grasses on the seabed, trapping and binding fine calcareous mud. The mollusc-rich, burrowed strata reach a thickness of ca. 75 m. Moving upsection through these lagoonal strata, the material becomes slightly admixed with fine, vitric ash, pointing to nearby volcanic activity. Gradually the material grades into bedded packstones and grainstones (FA5), representing further shallowing to peritidal conditions, a setting which is confirmed by its stratigraphic position: overlying lagoonal deposits and underlying terrestrial strata. The bedded coarse-grained strata represent high-energy conditions, with turbulent tidal currents and waves supplying calcareous grains and forming ooids. The top of the bedded grainstones, just below a sharp boundary with the overlying terrestrial, non-calcareous deposits, has a crumbly structure, red mottles and contains fine root traces **(Fig. 6, photo 11)**, representing the development of grassy vegetation in an intertidal or supratidal setting.

5.2 The Batu Gajah Section

The Batu Gajah Section covers most of the volcanic breccias of Trinil. Whereas this was previously regarded as one, undifferentiated series, we found that the breccias are made up of several volcanic debris flows (lahars), with differing backgrounds. Following Vallence (2005), we distinguished three types of lahars. Eruption-induced lahars (FA7) have a matrix dominated by juvenile pyroclastic grains and contain < 5% clay. They generally start as pyroclastic flows, but change into lahars when they become mixed with crater-lake water or when they enter rivers (Lavigne et al., 2007). Slope-collapse induced lahars (FA8) contain weathered fragments and have a clay-rich matrix (> 5%). These lahars are not related to primary pyroclastic eruptions, but to a collapse of water-saturated, weathered and hydro-thermally altered rock making up the slopes of a volcano. The collapse may be initiated by earthquakes or by intrusion of magma or hot gasses into the dome, driving hydrothermal water toward the flanks, resulting in an outward-directed pore-pressure gradient (Scott et al., 2001). Rain-induced lahars (FA9) are generally low-volume flows of rain-soaked ash, remobilized from surrounding slopes.

The base of the Batu Gajah Section forms a stratigraphic overlap with the top of the Padas Malang Section, consisting of a regressive series changing from lagoonal deposits (FA4) to bedded grainstones (FA5) capped with a rooted top layer of ca. 10 cm. It is overlain by a clay-rich lahar with weathered volcanic fragments (FA8) **(Fig. 7, photo 1)**. The lower boundary of this lahar forms a sharp contact with the rooted top layer of the calcareous grainstones. Except of scarce rip-up clasts, there are no indications of significant abrasion. Although a time-gap cannot be ruled out, the absence of a thicker weathering profile suggests that the debris flow overrode the coastal, grassy landscape.

The breccia is rich in fine plant remains and the matrix has a characteristic reddish-brown color. This indicates that the surface rocks of the upstream volcanic slopes were chemically weathered prior to slope-collapse and associated lahar-flow, suggesting humid, tropical conditions. The material contains red, nodular iron concretions (up to 10 cm), which are concentrated along horizontal levels, indicating post-depositional redox accumulations related to groundwater fluctuations. A clayey topsoil associated with this weathering stage is absent, indicating soil truncation.

The basal lahar is overlain by a massive fine tuff layer, representing a rain-induced lahar (FA9) **(Fig. 7, photo 2)** and reflecting volcanic activity. Its upper surface has been subject to fluvial reworking, as witnessed by ca. 40 cm deep, low-angle channel structures. The channel fill contains reworked calcareous concretions (1-3 cm), indicating a climate with pronounced wet and dry seasons.

A black clay layer (FA6) with a thickness of ca. 2 m overlies the two basal debris flows, **(Fig. 7, photos 3 and 5)**. It forms a laterally continuous marker level that can be traced over the entire study area. The massive and blocky-structured clays indicate thorough bioturbation and intermittent flooding. The clay contains dispersed fine pyrite crystals, which generally form under intermittent brackish water conditions, in combination with high bioavailability of organic matter and a dominant anaerobic environment (Pons et al., 1982; Weaver, 1989; Roychoudhury et al., 2003; Ferreira et al., 2015). This setting is supported by the occurrence of *Melanoides* aff. *tubercalata,* a species common in coastal marshes (Farani et al., 2015). It is interesting to note that coastal marshes with high accumulation of organic matter and pyrite are common in present-day Indonesia (Moormann and van Bremen, 1978). The clay contains a remarkable lens (ca. 60 cm thick) of well-sorted, well-rounded gravel (6 -7 cm) with an open structure. The pebbles consist of hard, calcareous material, which must have been eroded from the underlying marine series. Based on their position in the coastal clays and lithological composition, which excludes fluvial supply from the volcanic hinterland, the gravel is regarded as a beach bar.



Fig. 7. Selected photographs Batu Gajah Formation. See Supplement 6 for coordinates and setting. **(1)** Clay-rich lahar (FA8) with admixed red-coloured ferralitic weathering material (Batu Gajah Lahar 1). **(2)** Massive tuff, rain-induced lahar (FA9) with incised top and reworked calcareous concretions (Batu Gajah Lahar 2). **(3)** Coastal marsh clay (FA6, Batu Gajah Clay 1) overlain by eruption-induced lahar (FA7, Batu Gajah Lahar 3). **(4)** Eruption-induced lahar (FA7, Batu Gajah Lahar 3). **(5)** Sample of coastal marsh clay (FA6, Batu Gajah Clay 1). **(6)** Eruption-induced lahar (FA7, Batu Gajah Lahar 3). **(7)** Idem, zoom in to matrix. **(8)** Saprolite (truncated Ferralsol) in the top of Batu Gajah Lahar 3. **(9)** Remnant of the humic top soil of the Ferralsol along the top of Batu Gajah Lahar 3, overlain by Batu Gajah Lahar 4. **(10)** Clay-rich lahar (FA8) with admixed yellowish-red ferralitic weathering material (Batu Gajah Lahar 4). **(11)** Batu Gajah Clay 2 and (overlying) Batu Gajah Lahar 5. **(12)** Coastal marsh clay (FA6, Batu Gajah Clay 2) overlain by clay-rich lahar (FA8, Batu Gajah Lahar 5). **(13)** Incised and reworked top of Batu Gajah Lahar 5.

The black clay layer is sharply overlain by a volcanic breccia (FA7) reaching a thickness of 8 to 12 m. It has a matrix of white tuff, consisting of partly welded vitric grains and is practically devoid of clay, indicating an eruption-induced background. The underlying clay does not show signs of excessive soil formation, indicating that the lahar directly overran the coastal marsh. The base of the lahar contains wavy streaks of ripped-up clay. The mixed composition of the volcanic fragments points to explosive dome disruption. Vesicular pumice fragments are regarded as juvenile, eruption-related material, while non-vesicular fragments represent older dome rock. The latter includes andesite boulders up to ca. 1.5 m **(Fig. 7, photos 4, 6, 7)**. Charred wood fragments suggest an origin as a pyroclastic flow.

Toward its top, the tuff breccia becomes intensely weathered **(Fig. 7, photo 8)**. The color changes from greyish white to mottled reddish brown and the texture changes from consolidated vitric tuff to crumbly clay. Also the volcanic fragments, still visible in the weathered matrix, have completely altered to clay. Large root traces filled with massive brown clay penetrate the material. The weathering profile has a thickness of at least 3.5 m and represents a regolith. Thin (ca. 20 cm) patches of the humic topsoil have remained (**Fig. 7, photo 9)**, consisting of massive, crumbly, dark brown clay with fine concretions and root traces. It suggests that the original soil profile was a Ferralsol, indicative of a humid tropical climate and well-drained conditions. The largely missing topsoil indicates that the soil profile was truncated. Assuming a weathering rate of 1 to 2 cm/ka (Evans et al., 2019), the soil profile represents a timespan of (at least) 175 to 350 ka.

The paleosol is overlain by a thin clay-rich lahar (FA8) with a characteristic reddish yellow color **(Fig. 7, photos 9, 10)** that indicates incorporation of soil material in the lahar flow. Referring to the underlying weathering profile, the occurrence of reddish, weathered rock on surrounding volcanic slopes is not surprising. The material contains weathered and unweathered volcanic fragments (generally < 10 cm) consisting of andesite and pumice (Supplement 1). The top of this lahar has been subject to fluvial reworking, as witnessed by low-angle channeling structures with a crudely cross-bedded, poorly sorted fill of a similar yellowish breccia.

The reworked breccia is overlain by a ca. 1 m thick layer of massive, greyish white, poorly consolidated tuff, which we regard as a flow of rain-soaked ash (FA9). The material is poorly exposed and the contact with the underlying reworked breccia could not be observed. Along its top, the tuff is fluvially reworked and well-exposed as a ca. 2 m thick, cemented tuff layer with fine pumice lapilli and dm-scale trough cross-bedding.

The fluvial tuff is sharply overlain by another black clay layer with pyrite crystals (FA6), identical to the clay found lower in the section **(Fig. 7, photos 11 and 12)**, representing a return to coastal backswamp conditions. Again this clay layer, as well as the underlying cross-bedded tuff, forms a well-recognizable marker bed, which can be traced over the entire study area.

The clay is overlain by an up to 15 m thick, clay-rich lahar (FA8) with dispersed angular volcanic clasts of mixed composition: weathered and unweathered pumices, andesites and clay pebbles **(Fig. 7, photos 12 and 13)**. The material is rich in N-S oriented, uncharred logs. The clayey lahar represents a voluminous collapse of water-saturated dome rock, which suggests that the lahar event was triggered by volcanic activity. Fragments of unweathered vesicular pumice in the flow material probably represent syneruptive components. The top of this thick lahar layer is strongly incised, with steep channels cutting meters deep into the lahar surface. The incision surface is covered with crudely cross-bedded, poorly sorted sand and conglomerates, containing semi-rounded volcanic fragments of a mixed andesitic, dacitic and pumice composition **(Fig. 7, photo 13)**.

The incised surface is covered by black clays with fine pyrite (FA6), indicating renewed coastal backswamp conditions. The clay reaches a thickness of several meters and fills the incisions. In the top of the black clay, a ca. 100 cm thick paleosol has formed, reflecting base-level lowering and drainage of the coastal marsh. It consists of pale yellow clay with a blocky structure, red mottles and calcareous concretions (up to 5 cm) **(Fig. 8, photo 1)**. Upwards, slickensides appear, as well as desiccation cracks and small tree-root traces filled with dark grey topsoil material. The weathering profile is characteristic of a Vertisol, pointing to a climate with pronounced dry and wet seasons. The soil profile is truncated and the truncation surface is covered with a ca. 30 cm thick lag of trough cross-bedded coarse ash rich in calcareous concretions. The latter must have been reworked from the eroded soil. The lag deposit is overlain by a thick series of planar laminated fine vitric tuff (FA11).

5.3 The Sogen Section

The base of the Sogen Section mirrors the upper part of the Batu Gajah Section, revealing a remarkably consistent build-up of the stacked series of lahars and interbedded clays. We started our measured section at the base of the thick, clay-rich lahar (FA8) with wood fragments. Again, this lahar is deeply incised and covered with massive black clays (FA6) representing the development of a coastal marsh. The clay contains dispersed fine pumice, which may represent an accumulation of floating pumice, or slumping of slope material from the steep-sided incisions. The clay is capped with a truncated Vertisol, covered with a lag of coarse ash rich in reworked calcareous concretions.

The lag deposit is overlain by a thick series of moderately consolidated planar and locally cross-laminated fine tuff (FA11). The sheet geometry of the beds and planar lamination reflect unconfined, sheetflow-like conditions, with shallow water depths and high current velocities **(Fig. 8, photo 4)**. Occasional shallow channel structures (W: 5 to 10 m, D: 10 to 15 cm) represent unconfined, braided channels on the floodplain, with insignificant incision. Cross-lamination, mainly in the channel fills, points to unidirectional, eastward flow. Sheetflow conditions and unconfined braided streams are generally associated with episodic flooding over a wide floodplain (Hampton and Horton, 2007). This setting is confirmed by clay drapes and clay lenses with burrows and desiccation cracks, representing a gradual drying-up of shallow ponds after flooding events. Abundant calcareous concretions indicate a seasonally fluctuating groundwater table or water content, generally associated with pronounced dry and wet seasons **(Section 7.5)**. Horizons with fine rootlets point to a (seasonal) grassy vegetation cover.

The vitric grains and occasional moderately rounded pumice lapilli form juvenile pyroclastic material, indicating a rich volcanic supply. The dominance of well-sorted, fine vitric tuff points to an origin as fallout ash. The material must have been remobilized from surrounding slopes by surface run-off and debris-flows. Interbedded massive, fine tuff layers with plant debris represent small debris flows, which have occasionally been preserved on the floodplain.

The bedded tuffs contain several laterally continuous interbeds of plastic, light grey clays (FA12). The lighter color and absence of pyrite crystals distinguishes these clays from the black coastal marsh clays (FA6). The lighter color relates to an admixture with fine vitric ash and a lower organic content. The absence of pyrite crystals indicates depositional conditions not influenced by intermittent brackish conditions. The clays contain occasional fresh-water molluscs, representing stagnant conditions such as lakes or ponds (Van Benthem Jutting, 1937). The stratigraphic position of the clays, interbedded between sheets of fluvially reworked volcanic tuff, reflects intermittent lacustrine stages **(Section 7.6)**. The plasticity of the clay and the absence of calcareous concretions or mottling indicate that the material was formed under (semi)permanent waterlogging. The massive, well-bioturbated facies rich in plant debris represents a shallow, marginal lacustrine environment or freshwater swamp. The admixture of ash within the lacustrine clays points to ongoing (fluvial) supply of fine pyroclastic material.

The clay interbeds generally have a thickness of 50 to 100 cm. They may be capped with a thin Vertisol, or have shrinkage cracks along their upper surface, reflecting lake withdrawal. A thicker lacustrine interbed occurs ca. 20 m above the base of the tuff series. The clay layer has a thickness of ca. 3 m and grades into white, massive and laminated fine ash rich in diatoms. The algal blooms indicate nutrient-rich conditions, likely caused by dissolved silica. Increasing eutrophication occasionally led to oxygen-depleted bottom conditions, recorded by non-bioturbated, laminated diatomite (Sáez et al., 2007). The diatomite contains frequent leaf imprints, showing that the lake had forested margins. Euphorbiaceae and Malvaceae tree taxa (Supplement 4) point to a relatively open, sunny tropical forest. Trees of these families are usually pioneering species and are indicative of a disturbed setting (pers. comm. Huang Jian, June 2020). Environmental disturbance may be related to volcanic supply or fluctuating lake levels.

Above this ca. 5 m thick lacustrine interval, the bedded tuff series continues, with frequent interbeds of lacustrine clays (**Fig. 8, photo 9)**. Toward the top of the section, the facies of the tuffs gradually changes: its color becomes greyish as a result of an increasing content of mono-crystalline pyroxenes. Moreover, there is an increasing occurrence of isolated, sub-rounded, low-weight dacite lapilli (up to 3 cm). This announces a more significant facies change in the overlying strata.

5.4 The Kali Soko Section

The upward continuation of the bedded tuff series can be observed along the riverbanks south of Padas Malang and south of Trinil. These Solo transects are made up of the same bedded tuff series as the Sogen Section, but the exposures are disturbed by deeply incised terrace bases. South of Trinil, the bedded tuffs are only exposed in the lower one or two meters of the riverbank exposures, below the T2 scour surface **(Fig. 3B)**. Approaching Ngancar Bridge, the same facies change can be observed as in the top of the Sogen Section: an increase of monocrystalline pyroxene and admixture of dispersed, moderately rounded dacite gravel. Channel structures become more prominent, reflecting more dynamic flow conditions.

South of Ngancar Bridge, the series can be traced along the banks of Kali Soko (Supplement 2). Its facies gradually changes to grey, matrix-supported lapilli-tuff, with a rhythmic bedding and subtle grading of lapilli (FA10) **(Fig. 8, photo 11)**. This points to deposition by pyroclastic flows rather than water-saturated flows. The matrix is intensely welded, which also points to an origin as hot pyroclastic flows. The richness of lithic lapilli indicates that the pyroclastic flows must be associated with dome explosions rather than rapid vesiculation of magma. The sub-rounded shape of the clasts may be caused by repeated extrusion and fallback in the vent, preceding eruption (Fisher and Schmincke, 1984). Several ca. 50 cm thick interbeds of wavy laminated tuffs are regarded as base surges or ash cloud surges.

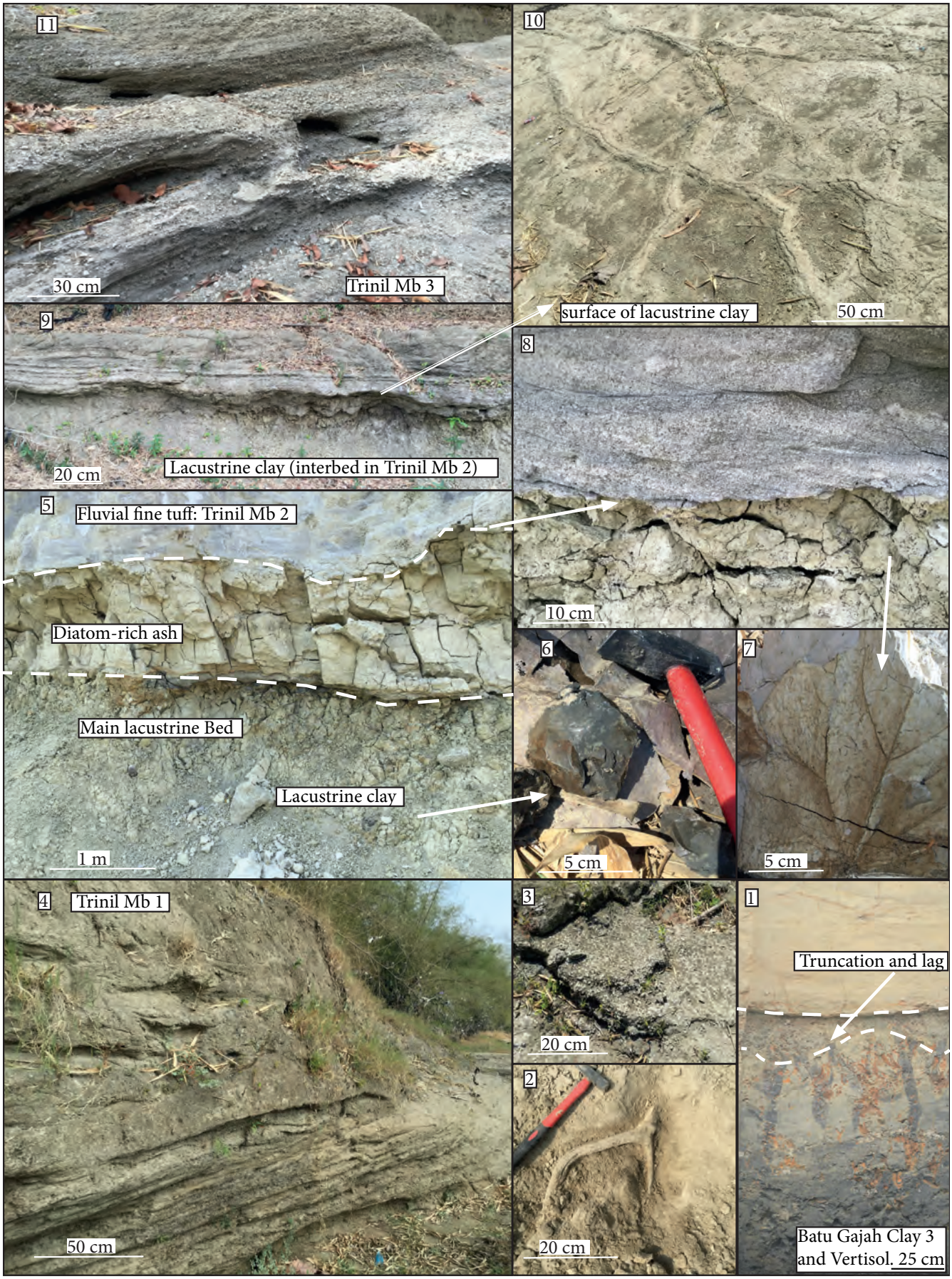


Fig. 8. Selected photographs of the Trinil Formation. See Supplement 6 for coordinates and setting. **(1)** Batu Gajah Clay 3 with Vertisol, truncation surface and lag deposit, overlain by terrace T1 sediment. **(2)** Fossil antler (Axis lydekkeri) in Trinil Mb 1. **(3)** Planar bedded tuff (FA11) rich in (in-situ) calcareous concretions (Trinil Mb 1). **(4)** Planar bedded tuff (FA11, Trinil Mb 1). **(5)** Lacustrine clay and lacustrine diatomite (FA12, Main lacustrine bed) overlain by fluvial tuff (FA11, Trinil Mb 2. **(6)** Sample of lacustrine clay (FA12). **(7)** Leaf fossil from lacustrine diatomite (FA12). **(8)** Contact surface between Main Lacustrine Bed (diatomite) and overlying tuffs of Trinil Mb 2. **(9)** Lacustrine interbed in Trinil Mb 2. **(10)** Top of lacustrine interbed with desiccation cracks. **(11)** Pyroclastic deposits (FA10, Trinil Mb 3).

Pyroclastic flow deposits were frequently fluvially reworked, as witnessed by channeling structures and dm-scale trough cross-bedding along the top of massive beds. Occasional lenses of clay or fine ash, often with desiccation cracks and fine root traces, represent small ponds. Their upper boundary is frequently convoluted and shows asymmetrical deformation structures, indicating northward-directed shear from overriding pyroclastic flows.

6. Stratigraphic revision

We propose a new, local lithostratigraphy for the Trinil area, with reproducible unit boundaries, following major changes in depositional conditions. Most units have been subdivided into (numbered) subunits.

The relation to the former stratigraphic practice is briefly discussed. Although some of the new units (partly) run parallel to the former units, they should not be regarded as synonyms, because the former units have connotations linked to unfounded regional correlations.

6.1 Kalibeng Formation (revised unit)

6.1.1 Definition

The massive calcareous mudstones (FA3) at the base of the Trinil series are assigned to a redefined Kalibeng Formation.

6.1.2 Former practice

Duyfjes (1936, 1938) defined the Lower and Upper Kalibeng Formations, consisting of massive calcareous mudstones overlain by diatomaceous mudstones. Berghuis et al. (2019) showed that the diatomaceous strata form a local facies of the larger pelagic series. We therefore propose to discard the prefixes 'Upper and Lower' and regard all pelagic mudstones of the Kendeng Hills as one regional unit: the Kalibeng Formation.

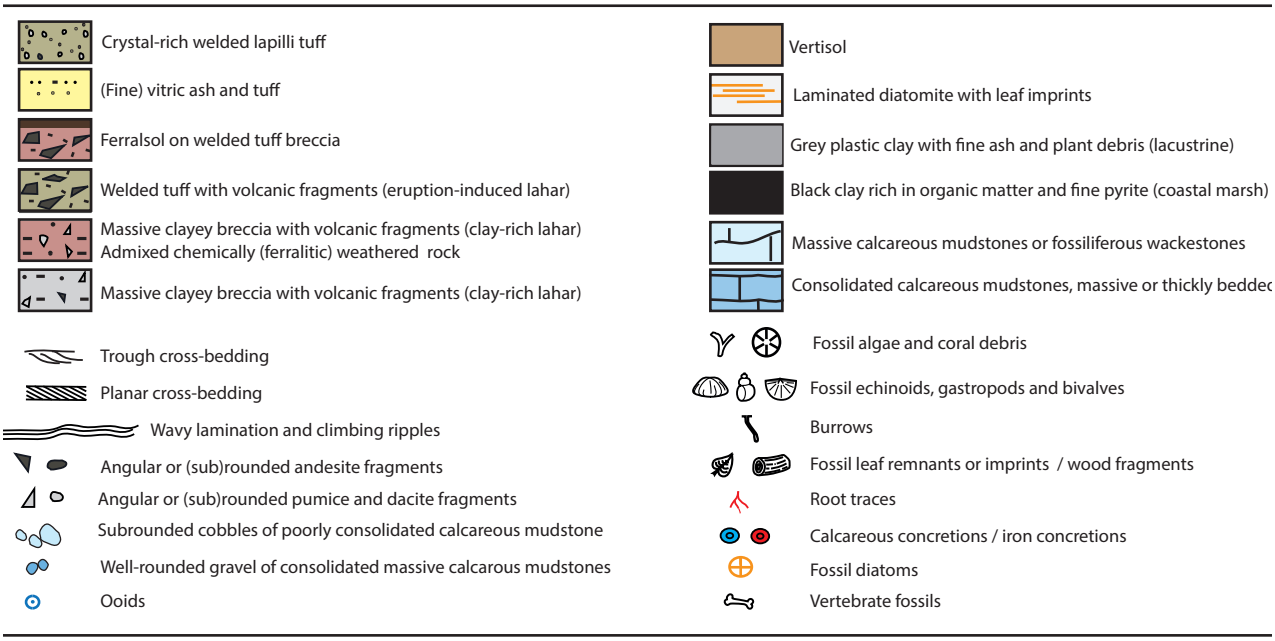
6.2 Padas Malang Formation (new unit)

6.2.1 Definition

We propose the Padas Malang Formation as a new unit for the bedded and / or mollusc-rich calcareous mudstones of Trinil. We define the introduction of bedding structures and the admixture of fine granular calcareous material as the base of the unit. The unit covers all lagoonal and peritidal calcareous deposits up to the first terrestrial, non-calcareous debris flow.

6.2.2 Former practice

Duyfjes (1936) attributed the lagoonal deposits of Trinil to his Upper Kalibeng Formation, correlating the beds with the diatomaceous deposits of the eastern Kendeng Hills. This correlation is incorrect. The diatomaceous strata are significantly older, largely dating from the Early Pliocene, and were formed under bathyal depth conditions (Berghuis et al., 2019).



Legend to **Fig. 9**.

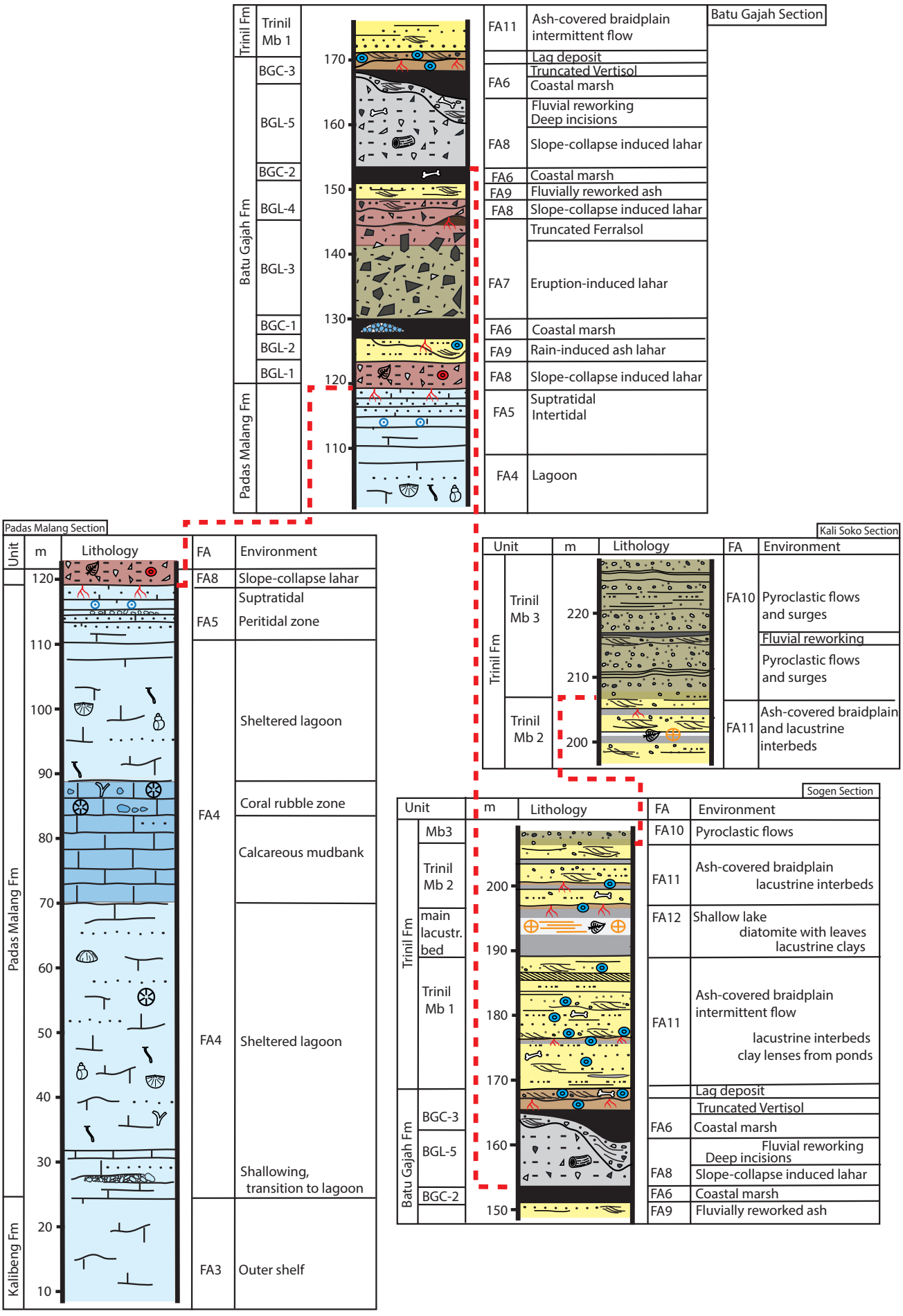


Fig. 9. Pre-terrace stratigraphy of the Trinil area in 4 reference sections, with correlated marker beds. For location of reference sections see Supplement 2. FA = Facies Association, see **Table 2**. Revised stratigraphy based on this paper. Subunit codes: BGL = Batu Gajah Lahar. BGC = Batu Gajah Clay. Legend: previous page.

6.3 Batu Gajah Formation (new unit)

6.3.1 Definition

We propose the Batu Gajah Formation as a new unit for the stacked volcanic breccias and interbedded black clays. The sharp contact between the calcareous strata (Padas Malang Formation) and the lowest non-calcareous debris flow forms the base of the unit. The unit continues upwards up to the base of the bedded tuffs. The unit consists of five debris flows, which we numbered Batu Gajah Lahar 1 to 5 (BGL1-5), and contains three interbeds of coastal clay, which have been numbered Batu Gajah Clay 1 to 3 (BGC1-3). The unit contains several paleosols and channeled erosion surfaces, the latter generally covered with a thin lag deposit, representing hiatuses in the depositional record.

6.3.2 Former practice

Duyfjes (1936) attributed the breccias of Trinil to the Pucangan Formation, based on a correlation with the deltaic series of the Jombang area. This correlation is unfounded. The deltaic sandstones of the eastern Kendeng Hills and the breccias of Trinil represent different depositional settings and their age relation is unknown.

6.4 Trinil Formation (revised unit)

6.4.1 Definition

We propose to return to Dubois' original name, the Trinil Formation, for the bedded tuffs with clayey interbeds. The redefined unit explicitly excludes the terrace deposits. The unit overlies a channeled erosion surface over the Vertisol developed in BGC-3, covered with a lag deposit rich in reworked calcareous concretions. The erosion surface locally cuts through the Vertisol and BGC-3, reaching down into the underlying breccia (BGL-5). We define the contact between this lag deposit and the overlying aggradational series of bedded, fluvial tuffs as the lower boundary of the Trinil Formation. The tuffs reach a thickness of ca. 50 m. A four to six m thick layer of lacustrine clays and diatom-rich ash forms a prominent marker bed about halfway within the tuff series. We refer to this level as Main Lacustrine Bed. The tuff series below this marker bed is referred to as Trinil Member 1, the overlying tuffs as Trinil Member 2.

6.4.2 Former practice

Duyfjes (1936) renamed Dubois' Trinil Beds the Kabuh Formation, correlating the deposits with fluvial sands and conglomerates that form the top of the deltaic series of Jombang. This correlation is unfounded: both fluvial series have a different composition, represent a different depositional setting and may very well have a different age. Duyfjes proceeded to define the fossils of Trinil as a distinguishing feature of the Kabuh Formation, which is circular reasoning. Moreover, Duyfjes did not recognize the T2 and T4 terrace deposits and added these strata to the Kabuh Formation, which makes this formation, at least in Trinil, a mixed and invalid unit.

6.5 Trinil Member 3

6.5.1 Definition

We add the lapilli tuffs at the top of the pre-terrace stratigraphy to the Trinil Formation as a separate member: Trinil Member 3. The deposits form the upward continuation of the fluvial, bedded tuffs. Most of the pyroclastic flows have been fluvially reworked, which compromises an exact definition of the base of this member. We describe the base of the member as a gradational increase of (lithic) pyroclasts, an increase of grey-coloured mono-crystalline grains in the matrix and an increasing occurrence of more prominent channelling and cross-bedding structures. The first preserved pyroclastic flows are found above this transition. Trinil Member 3 has an exposed thickness of ca. 25 m and is covered by younger terrace deposits.

Trinil Member 3 is exposed along the southern margin of the study area. Under the prevailing southward dip, it forms the highest exposed level of the pre-terrace stratigraphy. However, it is possible that the subunit (partly) represents lateral facies change within the Trinil Formation, as the southern exposures may represent the marginal area of the former floodplain, more proximate to the foot slopes of the Lawu.

6.5.2 Former practice

Duyfjes (1936) referred to the lapilli-rich tuffs of the Kali Soko as the Notopuro Formation. For him, the deposits represent a new phase of volcanism-induced deposition, after a long period dominated by fluvial supply of erosion products. This has become an accepted feature within the regional geology (van Bemmelen, 1949). Duyfjes referred to the gravel-bearing terrace deposits of T4 and T2, which he added to the Kabuh Formation. He placed the Kali Soko exposures stratigraphically above the Kabuh Formation and hence noted a change in sediment composition, from abrasion material to pyroclastic material.

6.6 Solo Formation (new unit)

For the deposits of the Solo River, no unit name has been in use. They are generally regarded as alluvium, or locally as terrace deposits. The Solo deposits are of great interest, because of their vertebrate fossils including *Homo erectus*. Moreover, they form an archive of sea-level fluctuations, climate change, tectonism and volcanism, most of which remains unstudied. A separate unit name for these deposits is appropriate. We propose the Solo Formation as a new unit name for all fluvial deposits of the Solo, along the entire river course, either as terraces, valley-fills or floodplain sediments.

6.7 Cross-sections and mapping

The cover of terrace sediments (Solo Formation) complicates geological mapping of the Trinil area. Two stratigraphic sections provide an overview of the occurrence of the newly defined (sub)units in the direct vicinity of Trinil **(Fig. 3A and B)**, illustrating the complex relationship between terrace deposits and pre-terrace strata. The cross-sections partly overlap with the historical cross-sections of Duyfjes (1936) and Carthaus (1911). Supplement 5 provides a geological sketch map of the direct vicinity of Trinil, excluding the terrace-related cover, and party overlaps with the map of Duyfjes (1936).

7. Discussion

Fig. 10 provides a stratigraphic summary and a provisional age framework and relates the Trinil series to local or regional tectonism, volcanism, sea-level fluctuations and climate change.

7.1 Age framework

A published planktonic foraminiferal study, carried out north of Ngawi, ca. 10 km from Trinil, provides a detailed age record of the Kalibeng Formation (Van Gorsel and Troelstra, 1981), showing that the unit covers the Late Miocene and Pliocene. The transition to the overlying lagoonal deposits (Padas Malang Formation) approximates the Pliocene—Pleistocene boundary at 2.6 Ma. The massive mudstones exposed around Trinil form the top of the Kalibeng Formation and hence represent the latest Late Pliocene (~ 3 - 2.6 Ma). Up-section, the biostratigraphic signal becomes disturbed because of shallow depositional depths, influencing the occurrence of planktonic species, and an influx of reworked older species. This means that foraminiferal age markers in the Padas Malang Formation must be interpreted with care. Van Gorsel and Troelstra (1981) reported provisional age markers of around 1.9 Ma within this series.

The Batu Gajah Formation represents a significant time span, characterized by lahar events separated by prolonged periods with limited or no sediment accumulation. The lahars indicate the presence of a nearby volcanic dome, most likely the Old Lawu **(Fig. 1)**. The basal lahar Batu Gajah-1 represents slope failure of weathered dome rock, which indicates that it postdates initial dome build-up. Assuming that dome build-up of Old Lawu dates ~1.9 Ma **(Section 2.1)**, we provisionally assign an age of ~1.8 Ma to the base of the Batu Gajah Formation. This fits well with the reported planktonic age markers of ca. 1.9 Ma within the Padas Malang Formation. Note that this implies that the earliest Old Lawu eruptions were contemporaneous with the latest lagoonal stage, which is confirmed by admixed ash in the top of the Padas Malang Formation. Little age information is available for the individual lahars of the Batu Gajah Formation. In **Section 7.4** we will show that tying the Batu Gajah Formation to the global sea-level curve offers a provisional insight into the age of individual subunits. This points to an age of ~ 600 ka for the Vertisol at the top of the unit, which is in line with a tentative K/Ar age of 0.5 ± 0.3 Ma, reported by Bartstra et al. (1978) for a sample from Batu Gajah Lahar-5. It suggests that the Batu Gajah Formation covers a time span of more than 1 million years.

Joordens et al. (2015) $^{40}Ar/^{39}Ar$-dated detrital hornblende from sediment preserved inside fossil bivalve shells derived from the base of the Trinil Formation, which yielded an age of 0.54 ± 0.10 Ma. OSL measurements on feldspars from the same sediment indicate a burial age of 0.43 ± 0.05 Ma. Together with the constraint provided by the age of ~ 350 ka for the oldest dated Solo terrace sediments, we assume an age range of ca. 550 – 350 ka for the Trinil Formation.

The age range of the terrace sequence (Solo Formation) has been well established at 350 ka – recent **(Section 4.9)**.

7.2 Tectonism

As explained in **Section 2.1**, the former Kendeng Basin had been subject to uplift throughout the Pliocene. Folding and thrusting of the Kendeng Ridge date from the latest Late Pliocene. This is reflected by the onlap of the Trinil series against the Kendeng Hills, which shows that the Kendeng Ridge stood out as a hill range throughout the Pleistocene. During most of the Early and Middle Pleistocene, the tectonic situation around Trinil was relatively stable and Trinil remained proximate to the sea. The thickness of the local series even suggests slight subsidence, possibly as a result of loading by the cone of the Lawu.

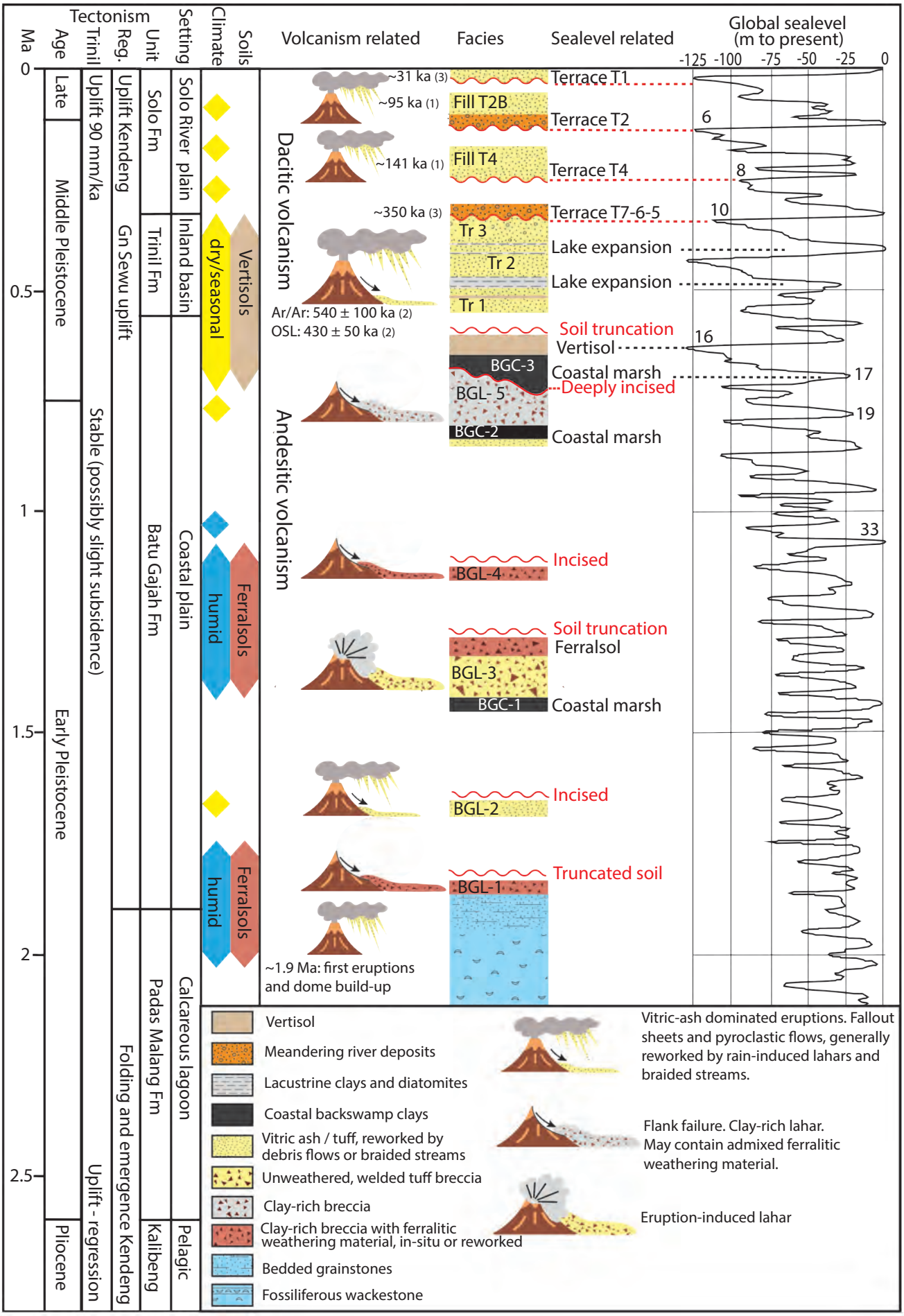


Fig. 10. Stratigraphic summary of the Trinil area in relation to climate, tectonism, volcanism and sea-level fluctuations. Sea-level curve (with Marine Isotope Stages) based on Bintanja and van de Wal (2008). Numerical ages: (1) OSL ages this paper; (2) Ar/Ar and OSL ages from Joordens et al., 2015; (3) OSL ages from Rizal et al., 2020.

The Solo terraces testify to a second phase of folding and uplift, later in the Middle Pleistocene. In **section 4.10** we showed that this uplift stage, which had its focal point in the Kendeng Ridge, dates from the last 350 ka. It can be regarded as a reactivation of the older, Late Pliocene fold zone. The southward dip of the Trinil series, as well as some small-scale thrusts in this series **(Fig. 3A and C)**, must be related to this young tectonic stage.

Duyfjes (1936) and Van Bemmelen (1949) also noted this renewed uplift, but dated it 'early in the Middle Pleistocene', referring to gravelly erosion material in the Middle Pleistocene Kabuh Formation. We showed that these gravels are not part of the tilted substrate, but of the younger terrace deposits.

7.3 Volcanism

Past researchers linked the breccias of Trinil to the volcano Wilis (Carthaus, 1911; Dozy, 1911; Duyfjes, 1936), more than 60 km from Trinil. Lahars travelling such distances are extremely rare and require confined-valley conditions and sufficient gradient (Scott, 1988). We have demonstrated that the lahars of the Batu Gajah Formation were deposited as sheet flows over a wide coastal plain, which points to a more proximal volcanic cone, providing sufficient gradient for a flow to spread out over the adjacent plains. This can only have been the Old Lawu. Wood fragments in lahar Batu Gajah-5, oriented north-south, also point to this volcano as the most likely source.

The volcanic fragments in the lahars of the Batu Gajah Formation indicate andesitic volcanism, which is generally associated with the build-up of high stratovolcanoes with steep slopes. These must have provided the required gradient for the lahars. Most lahars of the Batu Gajah Formation represent slope collapse events of weathered dome-rock. Batu Gajah Lahar-3 is related to primary eruptions and associated explosive dome collapse.

The tuffs of the Trinil Formation mark a drastic change of volcanic style, toward more explosive, gas-rich, dacitic volcanism. The onset of ash deposition over the truncated Vertisol that caps the Batu Gajah Formation, which we have dated to ~ 550 ka, marks the beginning of this new volcanic phase. We postulate that soil truncation is related to these changing volcanic conditions: massive supply of ash over the wide surroundings of Trinil may have caused a dying-off of vegetation, triggering overland flow and soil erosion. The formation of extensive ash sheets is commonly associated with calderas (Fisher and Schmincke, 1984), but an old caldera has not been identified in the vicinity. Probably, it has become buried under the current cone of Lawu.

The oldest terraces T7, T6 and T4 represent incisive, lateral accretion stages under low volcanic supply. The younger terraces reflect alternating stages of abrasion and aggradation, which we linked to intermittent pyroclastic supply **(Section 4.7)**. Again, the nearby Lawu is the most likely source.

7.4 Sea-level fluctuations

Since its emergence in the Early Pleistocene, the Trinil area has been in the proximity of the sea. The local sedimentary series bears witness to multiple base-level changes, which can be related to Quaternary sea-level fluctuations. Referring to the available numerical ages, some elements have been tied to the global sea-level curve (Bintanja and van de Wal, 2008)**(Fig. 10)**.

The fluvial terraces represent alternating stages of incision, reflecting changes in external control, e.g. base level, climate, tectonism and volcanic sediment supply. The ages of the terraces roughly follow the 100 ka glacial cycles, suggesting that eustatic sea-level fluctuations were the decisive mechanism controlling downcutting. We provisionally tied the scour surfaces of the most prominent terraces to the lowstands of the last four major glaciations (MIS10, MIS8, MIS6 and MIS2). The tuffaceous sediments of fill terraces T4, T2B and T1 reflect aggradation stages, which were in the first place a response to an increased sediment input related to volcanic eruptions. The OLS ages of terraces T4 and T2 place these aggradation stages in MIS7 and MIS5.

Proceeding downward in the local stratigraphy to the Trinil Formation, we appear to lose the signal of marine base-level changes. The fluvial beds making up this unit are characterized by a great lateral continuity and occasional channel structures are shallow. This indicates high aggradation rates, but most of all a limited gradient and a stable base level (Miall, 1996, 1977; Hampton and Horton, 2007). The latter is remarkable, knowing that the unit dates from ~550 to 350 ka, a period characterized by high-amplitude sea-level fluctuations. It suggests temporary isolation from the marine base level **(Section 7.6)**.

The underlying Batu Gajah Formation was formed on a coastal plain, after the shallow calcareous lagoon, represented by the Padas Malang Formation, had emerged, presumably around 1.8 Ma. The lahars that dominate this unit represent short depositional events, which were separated by prolonged stable periods. The interface between the individual breccia units contains a record of multiple transgressive and regressive cycles. Tabular interbeds of organic clays represent the formation of a stable or slowly aggrading coastal marsh, reflecting highstands. Weathering profiles or incisions of previously deposited breccias most likely reflect lowstands.

The upper layers of the Batu Gajah Formation contain sufficient age-related clues for a tentative linkage to the global sea-level curve. The Vertisol, forming the top of the unit, represents withdrawal of a coastal marsh (represented by Batu Gajah Clay-3). The paleosol underlies the Trinil Formation, to the base of which we assigned a maximum age of 540 ± 100 ka ($^{40}Ar/^{39}Ar$) and a minimum (OSL) age of 430 ± 50 ka (based on Joordens et al., 2015). Based on the thickness of the truncated paleosol of more than 1 m and an assumed average weathering rate of 1 to 2 cm/ka (Evans et al., 2019), the soil represents a weathering period that may have exceeded 100 ka. This makes it possible to place the onset of well-drained conditions in MIS16, at ~650 ka. MIS16 was an extended glacial, with very low sea levels, marking the end of the Mid-Pleistocene transition, when 41 ky glacial-interglacial cycles shifted to larger amplitude 100 ky cycles (Dean et al., 2015). Counting back from MIS16, we may link the coastal clay in which the paleosol developed (Batu Gajah Clay-3) to the highstand of MIS17. This clay overlies the deeply incised surface of Batu Gajah Lahar-5. These incisions reflect well-drained conditions and a low marine base level, which must have preceded the development of the coastal marsh. We tentatively link these incisions to the lowstand of MIS18.

Further downward, the marine base-level record of the Batu Gajah Formation continues, but lacking numerical ages, it becomes impossible to tie this record to the global sea-level curve. Without doubt the sediment record contains significant hiatuses. Depending on the age of Batu Gajah Lahar-5, the underlying Batu Gajah Clay-2 possibly represents the highstand of MIS19 or MIS21.

The thick, eruption-induced Batu Gajah Lahar-3 contains juvenile volcanic material, which offers good possibilities for radiometric dating. It will present future workers with an interesting age marker to link several stratigraphic elements to the sea-level curve: the underlying coastal clay (Batu Gajah Clay-1) and the thick weathering profile in the top of Batu Gajah Lahar-3. This weathering profile represents a long period (or several intermittent periods) of well-drained conditions, reflecting one or more lowstands. Moreover, it forms an important climatological marker **(Section 7.5)**.

7.5 Climate

The Trinil stratigraphy represents an interesting record of climate change. Batu Gajah Lahars-1 and -4 have a red-colored clayey matrix, indicating ferralitic weathering of rocks along volcanic slopes prior to collapse. The thick in-situ weathering profile that formed in the top of Batu Gajah Lahar-3 represents a 175 – 350 ka timespan of in-situ Ferralsol formation. This shows that humid tropical conditions were dominant during the deposition of the Batu Gajah Formation. Calcareous concretions, found in the top of Batu Gajah Lahar-2, are the only exception to this climatic context and may represent an interval with a dryer, more seasonal climate.

The thick Vertisol that caps the Batu Gajah Formation represents a climate with pronounced wet and dry seasons. We provisionally linked the withdrawal of the coastal marsh and the formation of this soil profile to the lowstand of MIS16. The actual change from humid to dryer climate conditions may predate this Vertisol. Note that the underlying lahar Batu Gajah-5 is the only clay-rich lahar that does not contain admixed red-colored weathering material. The transition from a humid to a dryer climate may therefore predate this lahar. The Trinil Formation (~ 550 – 350 ka) contains abundant indicators of dry and wet seasons, in the form of desiccation cracks, calcareous concretions, horizons with grassy rootlets and interbedded Vertisols.

Our observations are in general agreement with the regional pollen record, which indicates a dominance of tropical forest vegetation throughout the Early Pleistocene (Polhaupessy, 1990; Sémah and Sémah, 2012). The authors noted a transition to more open vegetation types, which they roughly date 'at the end of the Early Pleistocene'. Sémah et al. (2010) noted 'prolonged periods of dry climate' starting around MIS22. Following this conclusion, the thick Ferralsol in Batu Gajah Lahar-3 probably predates MIS22. Open vegetation conditions during the latest Early Pleistocene and the Middle Pleistocene are also inferred from vertebrate fossils, which are dominated by large herbivores (Van den Bergh et al., 1996, 2001) and from oxygen isotope signals in herbivore teeth, indicative of grazing on C_4 vegetation (Janssen et al., 2016; Louys and Roberts, 2020; Puspaningrum et al., 2020). Moreover, on a regional scale, Dennel (2009) noted an increasing length and intensity of dry periods in Asia during the Mid-Pleistocene Transition.

Several authors noted a change to more humid conditions in eastern Java in the Late Pleistocene, probably postdating the formation of the lower terrace of Ngandong (Van den Bergh et al., 1996). This climate change likely affected erosion and sedimentation patterns of the Solo, which may have been recorded in terrace T2 and T1 and forms an interesting subject for future, detailed studies of these terraces.

7.6 Middle Pleistocene isolation: the Ngawi lake basin

The absence of a record of marine base-level changes in the Trinil Formation and the occurrence of lacustrine interbeds point to temporary isolation. The deposition of this unit coincided with a sharp increase of volcanic activity of the Lawu, suggesting that isolation was caused by a volcanic barrier. In **section 5.3** we described the depositional setting of the bedded, predominantly planar laminated tuffs as a wide floodplain with a limited gradient. The climate of dry and wet seasons caused events of peak discharge, supplying abundant unconsolidated fine ash to the floodplain.

Ash-covered surfaces have a poor permeability, favouring flashy sheetflow and unconfined braided flow (Paredes et al., 2007).

Paleocurrent observations in the fluvial tuffs of the Trinil Formation indicate stable, unidirectional flow, directed to the northeast in exposures around Trinil and to the southeast in exposures around Pitu and Sogen. This eastward paleocurrent was also noted by Dubois (1894b, 1908). We postulate the existence of a Middle Pleistocene lake, which must have been located east of Trinil. In this model the lacustrine interbeds as found around Trinil, form a record of lake expansion and retreat, probably representing fluctuations in precipitation rate. On the Sunda Shelf, sea-level highstands are generally related to increased precipitation rates (Heaney, 1991; Van der Kaars et al., 2000; Bird et al., 2005). The Main Lacustrine Bed of the Trinil Formation may relate to the highstands of MIS13 and MIS11.

The eastward paleocurrents point to a hydrological barrier that must have been located west of Trinil**.** Looking at the current landscape, we note that east of Sonde, the lower slopes of Lawu stretch out toward the Kendeng Ridge. This may form a remnant of a Middle Pleistocene barrier, which separated Trinil from the marine base level.

Our study is the first to document the former existence of a lake basin around Trinil (~550 – 350 ka), which we refer to as the Ngawi Lake Basin. This provides a new view on the habitat of *Homo erectus*. During the long dry seasons that characterized eastern Java throughout the Middle Pleistocene, the tree-lined lake must have provided good living conditions for an early human population, yielding molluscs, fish and drinking water, and attracting game.

7.7 A new model for the development of the Solo

The development of the Solo River marks the end of the Ngawi Lake Basin. Several authors have written about the origin of this river and its remarkable course, crossing the island from south to north. Lehman (1936) and Pannekoek (1949) described an abandoned valley through the Gunung Sewu, which they regarded as an old, southward course of the Solo. Further uplift of these hills and associated block-faulting would have caused flow reversal, whereby the river forced its new route through the Kendeng Ridge. This is an unlikely representation of river behavior. Moreover, Rizal et al. (2020) dated Gunung Sewu uplift to ~550 ka, which implies a 200 ka time gap with the development of the oldest Solo terraces, dated to ~350 ka.

We noted in s**ection 7.6** that in the Ngawi Lake Basin an eastward-directed drainage system developed, toward a lake east of Trinil. It is noteworthy that this drainage was parallel to the later Solo. Westward directed, headward erosion of these streams must have gradually cut through the volcanic barrier west of Trinil. We postulate that by ~350 ka, the headwaters of these streams connected to the plains in the west and captured the local southward directed drainage system (the 'Old Solo'), creating a large, eastward-flowing river system. Similar examples of river capture have been described in other volcanic areas, where rivers were temporarily blocked (Maddy et al., 2012; Veldkamp et al., 2012).

This model for the development of the Solo River also sheds a new light on the river's remarkable traversal of the Kendeng Hills. It may have formed as a northward-directed overflow of the former lake. The current transverse valley still reflects its original meandering course. By the time the eastward draining Solo had developed, the former lake overflow had been incorporated in the river's course.

7.8. Landscape reconstructions

The Kalibeng Formation bears witness to the marine Kendeng Basin and records regressive conditions throughout the Pliocene. Ongoing compression of the basin sediments formed east-west directed fold and thrust zones, emerging by the end of the Pliocene. Emergence of the Kendeng Ridge left a sheltered, shallow marine lagoon along its southern slopes. The deposits from this lagoon constitute the Padas Malang Formation.

Lawu developed as an andesitic stratovolcano with steep slopes. The lagoon gradually emerged and a coastal lowland developed, at the foot of Lawu. The plains were occasionally overrun by volcanic debris flows, but such events were separated by prolonged, stable periods. During highstands, muddy, organic-rich coastal marshes developed, which form a contrast with the earlier calcareous lagoons. This reflects an increased supply of acidic river water and fine clastic material to the coastal environment, which points to a larger catchment with weathered soils and / or increasingly humid conditions. During lowstands, the area was subject to incision and weathering. Ferralitic weathering indicates humid tropical climate conditions. A Vertisol at the top of the Batu Gajah Formation indicates that, by this time, the climate had become dryer, with marked dry and wet seasons. The complex of volcanic debris flows, interbedded coastal clays and weathering profiles constitutes the Batu Gajah Formation.

At ca. 550 ka, the Lawu volcanic regime changed from andesitic to dacitic. Explosive volcanism supplied large amounts of vitric ash and fine pumice. A volcanic barrier developed, isolating the plains of Trinil from the marine base level and creating a lake basin. The area became an ash-covered inland plain, with dry, strongly seasonal climate conditions bringing about peak discharges, with sheetflow and shallow braided flow conditions. Drainage was eastward,

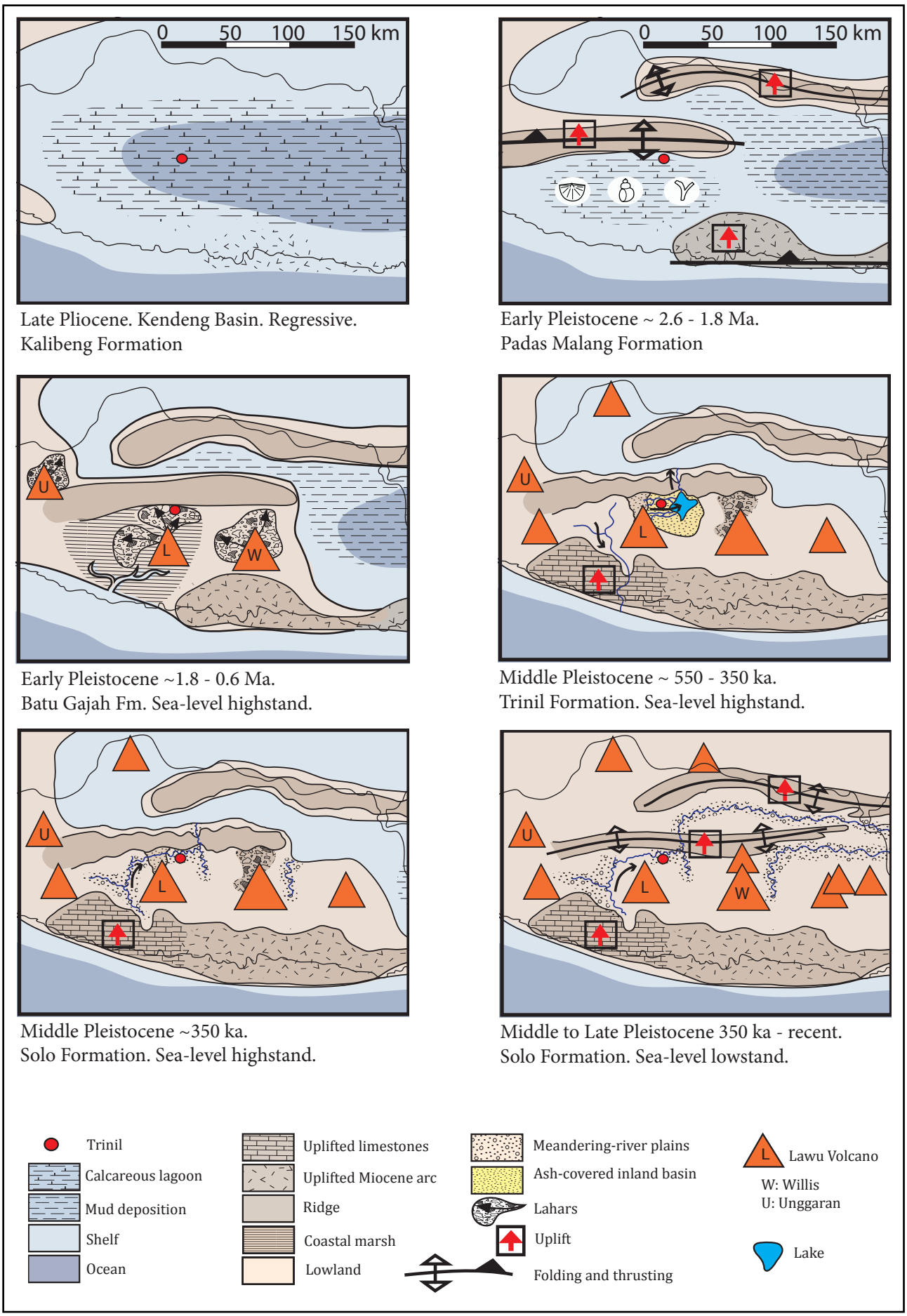


Fig. 11. Plio-Pleistocene paleogeography of Trinil and adjacent parts of eastern Java. Thin black line: outline of present-day eastern Java. Partly based on Huffman et al. (1999), Lunt (2013) and Berghuis et al. (2019).

towards a lake in the lowest part of the plain. The ash-covered plains had a grass-dominated vegetation, but the lake margins were forested. Lake expansion and retreat reflected fluctuations in precipitation rate. Possibly, the lake developed a northern overflow through the eroded remains of the Kendeng Ridge. The ash-dominated fluvial deposits with lacustrine interbeds constitute the Trinil Formation.

Around 350 ka, headward erosion of eastward-flowing streams inside the lake basin connected to the plains west of the volcanic barrier and captured southward-flowing rivers, creating a large, eastward-flowing river system: the Solo. This reconnected the Trinil area to the marine base level, but this time to the north.

The development of the Solo coincided with renewed uplift. Stepwise fluvial downcutting was predominantly controlled by marine base-level changes. This is unsurprising, as the shoreline was in the immediate proximity. The Randublatung Basin, north of the Kendeng Ridge, contains a record of Middle to Late Pleistocene shallow marine clays (Pringgoprawiro and Baharuddin, 1979) and fluvial, Solo-related sediment bodies (Bartstra, 1988), indicating that this lowland was inundated during highstands and formed an extension of the Solo floodplain during lowstands.

8. Retrospective

Our reinterpretations of the Trinil series are primarily based on advances in the field of sedimentology and Quaternary geology and do not disqualify the work of earlier geologists. Although previously regarded as contradictory, many of their interpretations were valid and found their way into our new depositional model of the Trinil Formation, such as fluvial deposition (Dubois, 1907), interbeds of rain-induced volcanic debris flows (Volz, 1907; Dozy, 1911) and shallow lacustrine deposits (Carthaus, 1911; Dozy, 1911). Also Van Es (1931) and Duyfjes (1936) were correct in their interpretation of fluvial conglomerates as erosion products, representing uplift. But they did not note that this material is a younger deposit, related to the terraces. When it comes to the relation between the older tuffs and the overlying terrace deposits, the hypotheses of Elbert (1908) and Bartstra (1982) were surprisingly accurate. Dubois (1908) fiercely rejected Elbert's idea, but his criticism may have been prompted by fear that this would degrade his fossil collection to a mixed assemblage. Lehmann (1936) correctly identified fluvial terraces around Trinil and understood that these are related to the terraces of the Kendeng, but he did not recognize the full terrace sequence and erroneously suggested that his High Terrace (in this paper T7, T6 and T5) is the equivalent of the fossiliferous terrace of Ngandong.

9. Conclusions

The plains of Trinil form the ancient floodplain of the Solo and are shaped as a terraced landscape. During incisive stages, the Solo deepened and widened its valley floor, under gravel-bearing, meandering conditions. Intermittent stages of high pyroclastic supply triggered a change to aggradation and braided flow. Stable uplift and intermittent conditions of incision and aggradation formed a sequence of strath and fill terraces. The terraces range in age from ~350 ka to ~30 ka and correlate with the terraces of the Kendeng Hills, ca. 20 km downstream. The tuffaceous sediment of fill terraces T4 and T2 was previously not recognized as terrace-related and was added to the Kabuh Formation, confounding sedimentological and stratigraphic interpretations. We reject the use of the regional unit Kabuh Formation in the Trinil area, and regard the local tuffs as belonging to either the Trinil Formation (substrate) or the Solo Formation (terrace deposits). This has great consequences for the validity of local fossil assemblages and their ages, as most fossils reportedly derive from the Kabuh Formation.

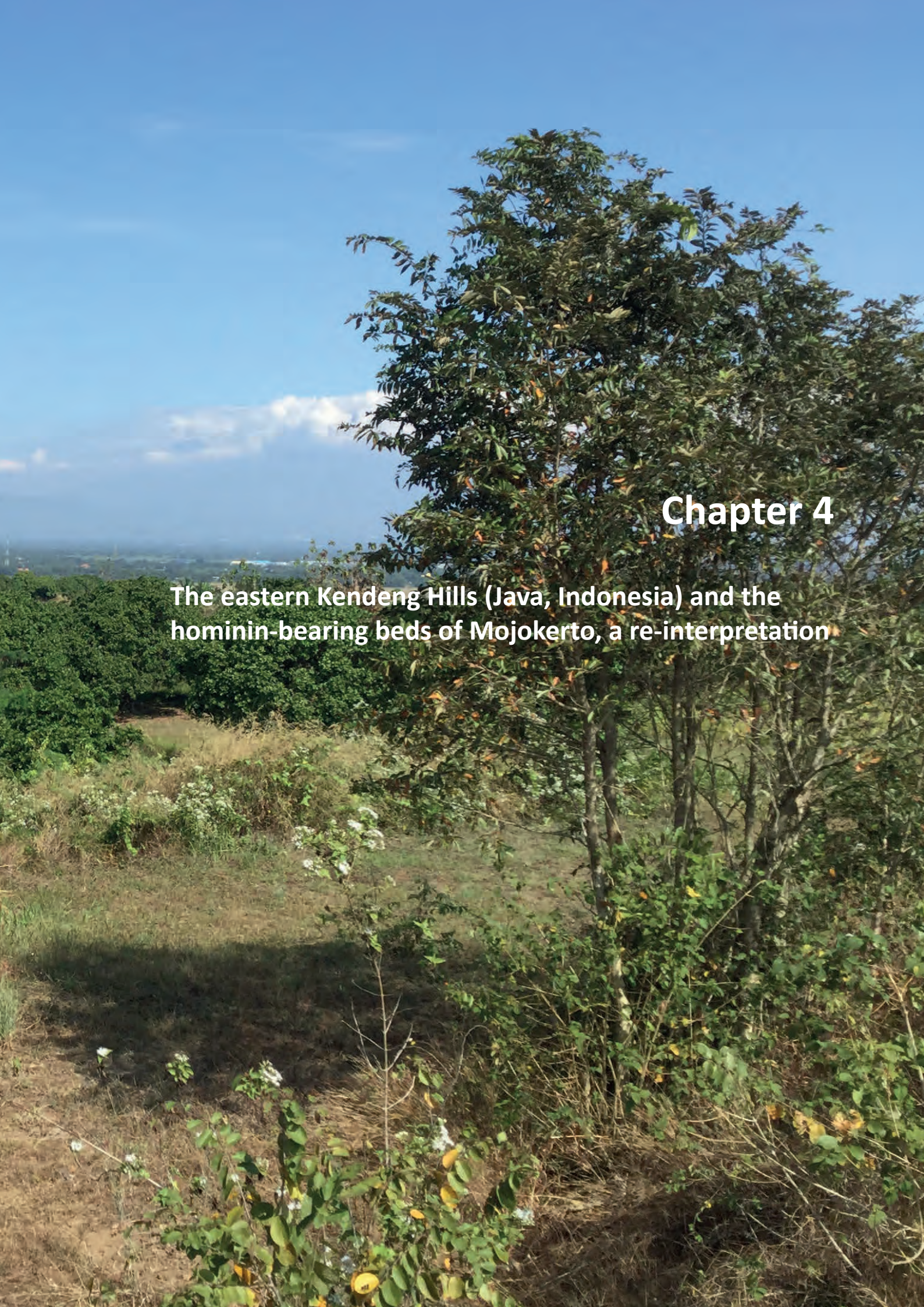
The exposed pre-terrace series has a thickness of 230 m and covers a period from ~3 Ma to ~350 ka. We subdivided the series into four new or revised lithostratigraphic units, representing distinctive depositional landscapes. Our revised stratigraphy forms a local framework and the units should not be synonymized with the existing regional units of Duyfjes (1938a). The (chrono)stratigraphic relation with other famous hominin sites in eastern Java, such as Sangiran and Mojokerto, is complex and awaits further studies.

Our landscape reconstructions provide a new view on the habitat of the Middle Pleistocene *Homo erectus*. A lake basin (~550 – 350 ka) provided the 'fortunate conditions' (Dennell, 2009) required for an enduring presence of *Homo erectus.* In the subsequent stage, this role was taken over by the perennial Solo.

The Trinil depositional series forms an interesting record of Pleistocene tectonism, volcanism, climate change, sea-level fluctuations and fluvial architecture, which gives it regional significance, for Java and maritime Southeast Asia. On a local scale, our stratigraphic revision forms a much-needed basis for a re-evaluation of Dubois' and Selenka's excavation sites and the Trinil fossil assemblages, which will be addressed in a separate publication.



View from the top of the Kedung Waru anticline north of Jetis, looking to the southeast, over the Brantas valley, with Gunung Penanggungan in the distance.



Chapter 4

The eastern Kendeng Hills (Java, Indonesia) and the hominin-bearing beds of Mojokerto, a re-interpretation

CHAPTER 4

The eastern Kendeng Hills (Java, Indonesia) and the hominin-bearing beds of Mojokerto, a re-interpretation

H.W.K. Berghuis, Thijs van Kolfschoten, Shinatria Adhityatama, S.R. Troelstra, Sofwan Noerwidi, Rusyad Adi Suriyanto, Unggul Prasetyo Wibowo, Eduard Pop, Iwan Kurniawan, Sander L. Hilgen, A. Veldkamp, Josephine C.A. Joordens

Published in: *Quaternary Science Reviews* (2022)

Abstract

The eastern Kendeng Hills (Java, Indonesia) expose a 1,000 m thick series that is used as a stratigraphic standard, representing the emergence of eastern Java from the sea. The fluvial top is rich in vertebrate fossils and yielded the Mojokerto (Perning) hominin skullcap, which is regarded as the earliest evidence of *Homo erectus* on Java, with age estimates ranging between 1.9 and 1.49 Ma. The series is commonly regarded as an uninterrupted record of coastal progradation. However, recent studies show that the emergence of eastern Java has been a complex process, under influence of tectonism, volcanism, sea-level fluctuations and fluvial dynamics, leaving a fragmented depositional record that varies from site to site. This is at odds with the prevailing stratigraphic practice of long-distance correlations and questions the existing interpretations of the eastern Kendeng reference sections. Here we present the results of a fieldwork-based re-interpretation of this key stratigraphic record, which we identified as the fill of a previously unrecognized Plio-Pleistocene embayment, surrounded by elongate uplift zones. Clinoform-bedded sandstones relate to a stage of explosive, high-silica volcanism, supplying large volumes of ash. The embayment fill is incised and covered by fluvial deposits, which we relate to the Middle Pleistocene Brantas. The fluvial strata have a cyclic build-up, probably representing sea-level controlled stages of aggradation and degradation. Based on a reconstruction of fluvial cycles, we provisionally link the conglomerate bed in which the Mojokerto *Homo erectus* was found to MIS14 (~550ka). We infer that the published radiometric ages derive from reworked volcanic clasts that make up this incisive fluvial lag and are not representative for the age of deposition. Our study places the eastern Kendeng series in a new landscape context and changes our view of the timing of hominin migration to Java.

1. Introduction

The eastern Kendeng is a gentle fold belt rising up from the alluvial plains of eastern Java **(Fig. 1)**. It exposes a ca. 1,000 m thick regressive series of Pliocene marine mudstones covered by alternating coastal and terrestrial strata of Pleistocene age. The area has special significance, as it holds the reference sections for the regional stratigraphy (Duyfjes, 1938a) and it contains vertebrate fossils, which play a role in the regional biostratigraphy (De Vos et al., 1982; Von Koenigswald, 1935). Moreover, a hominin skullcap, found in 1936 in Perning near Mojokerto (Von Koenigswald, 1936a) is regarded as one of the oldest *Homo erectus* fossils of Java (Huffman, 2001a; Morley et al., 2020; Morwood et al., 2003; Swisher et al., 1994).

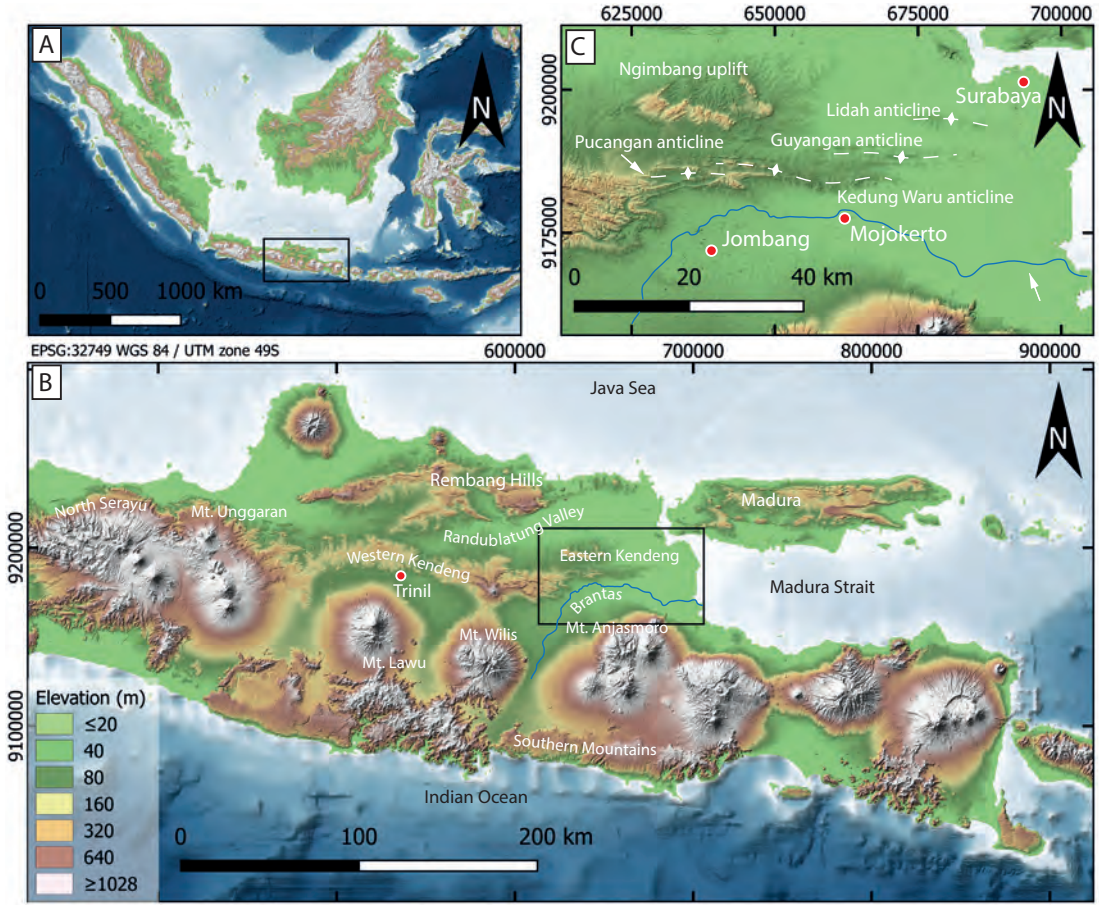


Fig. 1. A: The Indonesian archipelago with the study area on eastern Java. **B:** Eastern Java, the eastern Kendeng Hills and other sites mentioned in the text. **C:** The four anticlines making up the eastern Kendeng Hills. Map data: GEBCO (A, B, C) and ALOS (B, C).

Recent work on the hominin-bearing series of Trinil, ca. 100 km to the west, showed that the local depositional record, previously regarded as uninterrupted and directly related to the eastern Kendeng reference sections, has a complex build-up, of various depositional stages and hiatuses, reflecting the interplay of tectonism, volcanism, sea-level fluctuations and fluvial system dynamics (Berghuis et al., 2021). This complexity is reason to question the validity of the stratigraphic practice proposed by Duyfjes (1938, 1936), which is based on simple, long-distance correlations across eastern Java. This new insight has implications for the eastern Kendeng stratigraphy. If this depositional record can no longer be regarded as the stratigraphic standard of a regional regression, what is its significance on a local scale, in terms of landscapes and depositional processes? And if this record also appears to be more complex than previously thought, how does this affect our ideas on the genesis and age of the Mojokerto hominin find site?

The objectives of our study are:

- To make a fieldwork-based re-inventory of the eastern Kendeng stratigraphic reference sections around Jombang and of the hominin-bearing series of Mojokerto;

- To re-interpret the eastern Kendeng series as a local stratigraphic record, representing local depositional processes and landscapes;

- To link the observed depositional record to published accounts on tectonism, volcanism and climate, and to the Pleistocene sea-level curve;

- To consider the implications of our findings for the age, depositional context and stratigraphic position of the vertebrate-bearing beds of Mojokerto, focussing on the find site of the hominin skullcap.

2. Background

2.1 Geological setting

Java is located along the southern margin of the Sunda Shelf, directly north of the subduction zone where the Indian-Australian oceanic plate subducts under continental Sundaland. In the Early Miocene, most of present-day Java was part of a marine back-arc basin associated with an ancient volcanic arc in the south (Hamilton et al., 1979). In the Late Miocene, volcanism ceased over a length of ca. 200 km, corresponding to present-day eastern Java, probably caused by a buoyant part of oceanic crust that was not able to subduct (Hall and Spakman, 2015). The inactive volcanic arc eroded and changed into a submarine ridge with coral reefs (Smyth et al., 2008). In the adjacent back-arc basin, deposition changed from volcaniclastic turbidity currents to settling of calcareous ooze. In the Late Pliocene, the basin came under compression, possibly as a result of the resumption of active subduction in the south (Smyth et al., 2005). This resulted in uplift and the emergence of elongate hill ranges. The Rembang Hills and the Southern Mountains ridges were uplifted along pre-existing basement faults (Husein et al., 2015; Musliki and Saratman, 1996; Satyana et al., 2004), whereas the western Kendeng formed as a fold-and-thrust belt over the former back-arc basin (Genevraye and Samuel, 1972). In the Early Pleistocene, active volcanism returned, as a late response to resumed subduction, with the Wilis **(Fig. 1B)** as the first major eruption centre (Hartono, 1994).

Besides tectonism along the plate margin, the region has been subject to long-wavelength uplift and subsidence of the Sunda Shelf in relation to patterns of mantle flow (Zahirovic et al., 2016a). Dynamic subsidence of the shelf prevailed during most of the Tertiary and Quaternary, although temporary disturbances of subduction caused intermittent stages of dynamic uplift. Seismic surveys of the submerged shelf revealed the existence of up to five marine sequences, overlying a basal Pleistocene unconformity, which are separated by internal unconformities, representing intermittent stages of fluvial incision (Alqahtani et al., 2015; Darmadi et al., 2007). This reflects a regime of alternating stages of submergence and emergence, following sea-level fluctuations, dating back to MIS11 (Sarr et al., 2019).

2.2 Hominin fossils and Von Koenigswald's vertebrate biostratigraphy

In the late 19th century, Dubois collected vertebrate fossils from fluvial strata along the southern foot slopes of the western Kendeng, notably around the village of Trinil **(Fig. 1B)**. His finds include hominin fossils (Dubois, 1894a), which form the type specimens of *Homo erectus* (Mayr, 1950; Meikle and Parker, 1994). Dubois regarded his vertebrate fossils as one faunal assemblage, which he referred to as the Trinil Fauna (Dubois, 1907). Later, vertebrate-bearing fluvial beds were also found in the eastern Kendeng north of Mojokerto (Cosijn, 1932, 1931). Von Koenigswald (1935, 1934) noted that these fossils differ from the Trinil Fauna and named this new assemblage the Jetis Fauna. According to his observations, the strata that yield the Jetis Fauna form a lower stratigraphic level than the fossil-bearing beds of Trinil. Using faunal characteristics, he assigned the Jetis Fauna to the Early Pleistocene and the Trinil Fauna to the Middle Pleistocene. Besides these two faunal units, Von Koenigswald defined a third: the Ngandong Fauna, referring to the fossil assemblage of a fluvial terrace near the village of Ngandong, discovered a few years earlier (e.g. Oppenoorth, 1932). For this faunal assemblage, Von Koenigswald assumed a Late Pleistocene age.

In 1936 a hominin skullcap was discovered in a conglomerate bed north of Mojokerto, near the village of Perning (Von Koenigswald, 1936a). Its finding spot, within the stratigraphic range of the Jetis Fauna, implied an Early Pleistocene age, older than the hominin fossils from Trinil. The calvaria is regarded as a juvenile specimen (Storm, 1994) and often referred to as the 'Mojokerto child'.

2.3 Stratigraphy

In the 1930's, the Geological Survey of the Dutch East Indies started a geological mapping program of Java, assigning the geologist Duyfjes to map the Kendeng Hills and surroundings (Duyfjes, 1938a). Duyfjes selected his reference sections in the eastern Kendeng north of Jombang **(Fig. 1C)**, which he interpreted as an uninterrupted record of coastal progradation, driven by continuous volcanic supply that exceeded subsidence. The base of the exposed series **(Fig. 2A)** consists of calcareous and diatomaceous mudstones, which he referred to as the Kalibeng Formation. The lower boundary of this material is not exposed, but Duyfjes knew that in the western part of the hill range the calcareous mudstones are underlain by bedded marine claystones with Miocene foraminifera. Consequently, he assigned the Kalibeng Formation to the Pliocene.

The mudstones are overlain by several hundred meters of marine clays, which Duyfjes named the Pucangan Formation, with an assumed Early Pleistocene age. Duyfjes noted that the clays, which are omnipresent in the eastern Kendeng, wedge out toward the west. Around Trinil, they are absent and instead the calcareous Kalibeng Formation is directly overlain by volcanic breccias. Referring to their similar stratigraphic position, and to his model of uninterrupted sedimentation and regional subsidence, Duyfjes correlated the breccias of Trinil with the marine clays of Jombang, naming the breccias of Trinil the volcanic Facies of the Pucangan Formation.

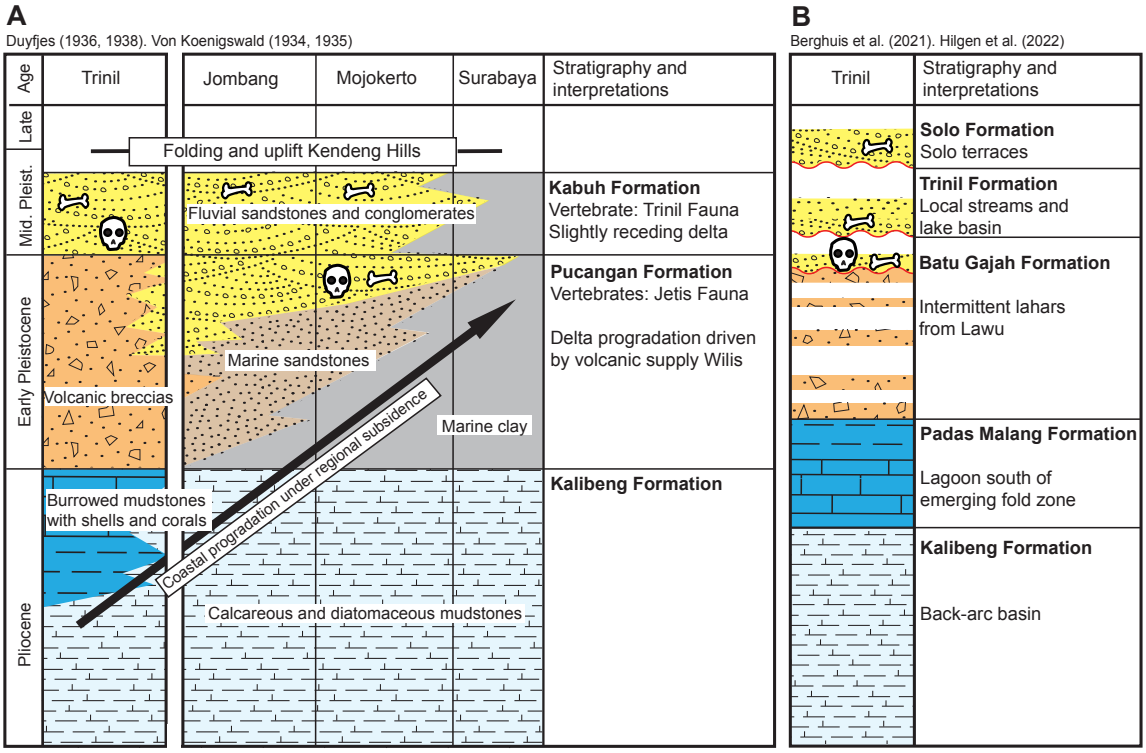


Fig. 2. A: Stratigraphy and correlations of the 1930's. The framework consists of chronostratigraphic units and is based on a landscape model of coastal progradation driven by volcanic supply. **B:** Revised stratigraphy and interpretations of the hominin-bearing series of Trinil. Note: simplified representation, for detailed information on hiatuses, incisions and paleosols refer to the original papers.

Duyfjes observed the marine clays to be overlain by bedded coastal sandstones and fluvial sandstones and conglomerates. He linked these strata to the breccias of Trinil and added them to the Volcanic Facies of the Pucangan Formation, describing a landscape of andesitic lahars and fluvial re-distribution to a muddy coast in the northeast. Referring to Von Koenigswald's (1935, 1934) vertebrate biostratigraphy, Duyfjes drew a unit boundary in the fluvial series. He assigned the lower part of this series, containing the Early Pleistocene Jetis Fauna, to the Pucangan Formation. For the overlying fluvial strata, containing the Middle Pleistocene Trinil Fauna, he defined a separate unit: the Kabuh Formation. This stratigraphic subdivision worked out well for the Trinil area. Here, the volcanic breccias, regarded as the Pucangan Formation, are overlain by fluvial sandstones, which yielded Dubois' Trinil Fauna and therefore 'by definition' form the Middle Pleistocene Kabuh Formation (Duyfjes, 1936).

Duyfjes' stratigraphy (**Fig. 2A)** is essentially a chronostratigraphic framework, combining strata of different facies in stratigraphic units based on assumed age relations. Extrapolations (he spoke of 'parallelization') form a recurrent aspect in his stratigraphy. Even in his reference section, the position of the boundary between the Pucangan and Kabuh Formations is determined by extrapolations with fossil finds from a wide area.

According to Duyfjes' model, the prolonged conditions of regional subsidence finally changed to uplift and folding in the late Middle Pleistocene, after the deposition of the Kabuh Formation, forming the Kendeng Hills.

2.4 Cracks in the stratigraphic model

Recent insight in eastern Java tectonism (**Section 2.1)** indicates that Duyfjes' model of uninterrupted sedimentation under prolonged subsidence, followed by late Middle Pleistocene folding is too simple. The emergence of eastern Java has been influenced by more complex tectonism, forming several elongate uplift zones and leaving intermediate areas as deposition centers. Folding and emergence of the western Kendeng dates from the Late Pliocene and left a shallow basin along its southern flanks. Trinil is located in the marginal area between this uplifted ridge and the adjacent basinal area. Our recent work around Trinil (Berghuis et al., 2021) revealed a complex fill of intermittent lahars, separated by long hiatuses, in which the area was subject to weathering and incision or covered with coastal marshes. The fluvial strata along the top of this series represent several stages of local drainage systems, which were finally captured by the Solo **(Fig. 2B)**.

This shows that the eastern Java depositional record is more complex than previously understood and reflects alternating stages of deposition, non-deposition, erosion and reworking, most of which have local relevance only. This raises questions about the validity of the previous correlations. For Trinil, a local stratigraphic framework has been defined **(Fig. 2B)**. The same has been done earlier in Sangiran (Itihara et al., 1994). However, for the remaining part of eastern Java, Duyjes' units have remained commonly used.

2.5 Revised vertebrate biostratigraphy

Questions have also arisen on the validity of the biostratigraphic framework and its implications for dating and demarcating stratigraphic units. De Vos et al. (1982) re-evaluated the work of Dubois and Von Koenigswald and concluded that their faunal assemblages were made up of mixed finds with poorly documented (stratigraphic) provenance. They proposed a revision of the faunal subdivision, distinguishing between the Trinil HK (= *Hauptknochenschicht* or Main Bone Bed) Fauna, the Kedung Brubus Fauna and the (unchanged) Ngandong Fauna. The Trinil HK Fauna derives from a specific stratigraphic level within the Trinil find site and contains an assemblage that is considered as homogeneous (Van den Bergh, 1999). It is poor in species and may represent an early-stage island setting of eastern Java. The Kedung Brubus Fauna is a richer fauna, pointing to a subsequent influx of species via a land connection with the Asian mainland. De Vos et al. (1982) assigned the fossils from Mojokerto to the Kedung Brubus Fauna, suggesting that the Perning skullcap is younger than the Trinil skullcap.

Van den Bergh et al. (2001) provisionally dated the faunal units to 0.9 Ma (Trinil HK Fauna) and 0.8 – 0.7 Ma (Kedung Brubus Fauna). The revised faunal units and their ages have become generally accepted. Nevertheless, Duyfjes' Pucangan and Kabuh Formations, which were based on the former biostratigraphy, have remained in use, including their assumed (older) ages.

2.6 Recent developments with regard to the vertebrate biostratigraphy

The Ngandong Fauna derives from a single river terrace that has been dated to 140 – 92 ka (Rizal et al., 2020). Recent work in Trinil has shown that that the Hauptknochenschicht or Main Bone bed is made up of two channel fills, which date to 830 – 773 ka and 540 – 380 ka respectively (Hilgen et al., under review; Pop et al., under review). The age of the oldest channel is close to the age as proposed by Van den Bergh et al. (2001). The younger channel incises into the older channel, and its vertebrate fossils may partly or largely be reworked.

Although the age and background of the Ngandong and Trinil HK Faunas are nowadays better understood, this does not account for the Kedung Brubus Fauna. This assemblage derives from a poorly studied fluvial interval of > 200 m thick (Duyfjes, 1936), which may very well have a more complex build-up than commonly assumed.

2.7 Age of the Perning skull

K/Ar and Ar/Ar-dating of pumice from the hominin-bearing bed of Perning (Mojokerto) yielded ages of 1.9 ± 0.5 Ma (Jacob and Curtis, 1971) and 1.81 ± 0.04 Ma (Swisher et al., 1994). These old ages, older than any other known Asian *Homo erectus*, were regarded as evidence of early hominin migration out of Africa. The ages are in line with the former (bio)stratigraphic frameworks Von Koenigswald and Duyfjes and seem to contradict with the revised biostratigraphy of Vos (1982). Morwood et al. (2003) obtained an age of 1.49 ± 0.13 Ma using fission track analyses on multiple zircons from pumice gravel, which still places the fossil among the oldest hominin remains of Java (Matsu'ura et al., 2020), but within the generally accepted age range of Asian of *Homo erectus* (Dennell, 2009). For the interpretations of the available radiometric ages it is noted that the K/Ar and Ar/Ar ages represent crystallization ages of hornblende crystals. This crystallization may already take place in the magma chamber, possibly resulting in a radiometric age that precedes the eruption age. Fission track ages represent the time elapsed since the zircon grains were last exposed to temperatures above 240°C. These ages therefore probably more closely represent the actual eruption age.

The published radiometric ages have been assumed to approximate the age of fluvial deposition, referring to Duyfjes' landscape model of Early Pleistocene volcanic supply and quick eastward fluvial redistribution. De Vos and Sondaar (1994) and Langbroek and Roebroeks (2000) suggested that the sampled pumice consists of reworked volcanic material and that fluvial deposition may be younger. Morwood et al. (2003) provided additional sedimentological justification for their claim of contemporary volcanism, stating the dated material was sampled from a horizon consisting largely of granular pumice, forming a ca. 15 cm thick layer with great lateral continuity.

Paleomagnetic measurements of the depositional record of Mojokerto indicated a dominance of reversed polarities in the basal marine strata, changing to predominantly normal and intermediate polarities around the transition to the terrestrial, fossil-bearing strata (Hyodo et al., 1993; Sartono, 1981). Sartono (1981) related this polarity change to the Brunhes-Matuyama boundary. However, Hyodo et al. (1993) continued their measurements upwards through the stratigraphy and again found predominantly reversed and intermediate polarities. The authors correlated the interval of normal polarities, including the fossiliferous beds, with the Jaramillo Subchron. Swisher et al. (1994) correlated this interval with the Olduvai Subchron, referring to their older radiometric ages, whereas Morwood et al. (2003) correlated it with the Sangiran excursion, a temporary swing of declination between the Olduvai and Jaramillo Subchrons (Hyodo et al., 1992). Huffman (2001) regarded the normal polarities as a result of recent overprint and not indicative of age.

3. Methods

During field campaigns in 2018 and 2019 we studied several river and quarry sections through the anticlines north of Jombang and Mojokerto **(Fig. 1C and 3)**. We followed the routes of the researchers of the 1930's, and added new observations from recent quarries. All sections were measured, described and photographed. Interpretations have been based on published facies models, notably Tucker (1985) for shallow marine carbonates, Elliott (1986) for shallow marine clastic deposits, Bhattacharya (2006) for deltaic and Miall (2014, 1996) for fluvial deposits. The petrography of sand and conglomerate beds was determined in the field by hand lens and described semi-quantitatively. Special attention has been paid to unconformities in the form of (subaqueous) scour surfaces, fluvial incisions or paleosols, representing hiatuses in the depositional record. The successions between such unconformities are referred to as depositional sequences.

Fossil molluscs and corals were collected, described and photographed in the field. Identification has been carried out at Naturalis Biodiversity Center, based on descriptions and photographs, mostly up to genus level. Vertebrate fossils have not been excavated.

For the lower part of the studied section, published foraminiferal analyses are available (Berghuis et al., 2019). For the upper part of the section, additional samples were prepared and investigated for microfossils at the Vrije Universiteit, Amsterdam. To retrieve the foraminifera, the samples were placed in a cup with hot water and a detergent. After soaking for some hours, the samples were washed over a >63µm sieve and dried on a hotplate. Subsequently, the dry residues were studied under a binocular microscope. Total occurrences of planktonic and benthic foraminifera were listed as poor, moderately rich or rich. The faunal analysis was carried out semi-quantitatively, with occurrences per species listed as scattered, common or abundant. Diatoms, mainly occurring in the unstudied < 63µm fraction, were not included in our study.

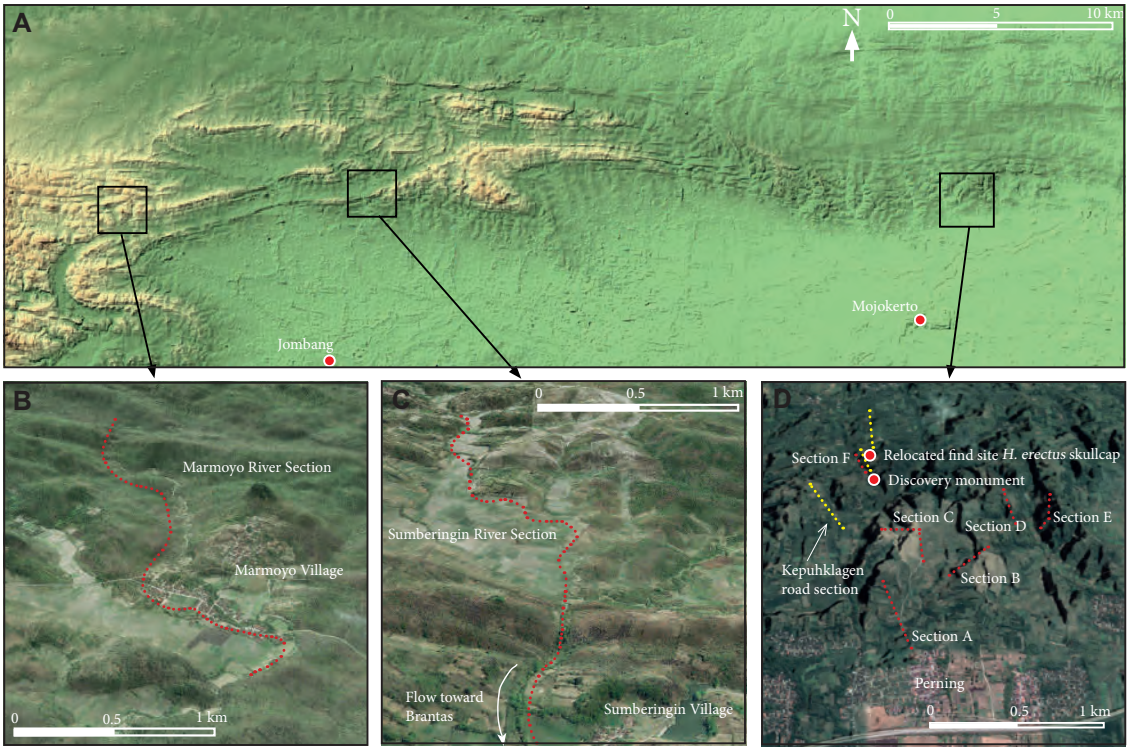


Fig. 3. A: The eastern Kendeng and the studied sections north of Jombang and Mojokerto. **B:** Marmoyo River Section (Jombang area). **C:** Sumberingin River Section (Jombang area). **D:** Kepuhklagen Road Section near Perning, quarry sections and Homo erectus find site (Mojokerto area).

4. Sedimentology

Six genetically significant facies associations (FA) were identified, based on texture, composition, sedimentary structures, (micro)fauna and stratigraphic position. The six FA represent depositional settings ranging from open marine to coastal and terrestrial.

4.1 FA1: Open marine, bathyal depths

4.1.1 Description:

White, planar laminated or platy diatomaceous mudstones **(Fig. 4, photo 1)** alternating with white, massive calcareous mudstones **(Fig. 4, photo 2)**. The massive calcareous facies contains varying amounts of admixed detrital clay and

may locally be referred to as calcareous-argillaceous mudstones, with a light grey color **(Fig. 4, photo 3)**.

The diatomaceous facies is poor in foraminifera, with a planktonic/benthic-ratio > 99% (=P/B-ratio). Planktonic foraminifera are represented by scattered occurrences of *Globorotalia tumida*, *Globigerinoides trilobus, Globigerinoides ruber* and *Sphaeroidinella dehiscens.* Benthic foraminifera are extremely scarce or absent. For diatoms, reference is made to Reinhold (1937), who referred to the diatomaceous strata of the eastern Kendeng as the Pengampon Formation.

The massive calcareous facies is rich in well-preserved foraminifera, with a P/B-ratio of ~99%. Planktonic foraminifera are dominated by *Globorotalia menardii* (dex.), *Neogloboquadrina pseudopima, G. trilobus, Globigerina bulloides, G. tumida* and *G. ruber.* Scattered benthic foraminifera consist of *Gyroidina* sp., *Uvigerina peregrina, Pullenia bulloides, Bulimina marginata* and *Cibicidoides wuellerstorfii*.

4.1.2 Interpretation:

The mudstones of FA1 represent open marine conditions. Benthic foraminiferal species, as well as the P/B-ratio of over 99%, point to bathyal depths. The laminated diatomaceous facies represents stages of eutrophication, blooming phytoplankton and reduced oxygen conditions, which Berghuis et al. (2019) relate to upwelling. The massive calcareous mudstones represent intervening stages of reduced phytoplankton growth, normal oxygen conditions and a rich planktonic foraminiferal fauna, dominated by tropical species. Admixed argillaceous material reflects a low supply of fine terrestrial detritus.

4.2 FA2: Mud-dominated outer shelf

4.2.1 Description

Dark grey, slightly bluish, massive clay **(Fig. 4, photo 4)**. The material is moderately rich in fine organic matter and practically devoid of admixed sand or silt. Carbonate content is very low. Locally the clay contains concentric calcareous concretions (diameter up to ~10 cm).

The clay is moderately rich in foraminifera, with a P/B-ratio of ~ 95%. Planktonic foraminifera consist primarily of *G. menardii* (sin. and dex.), *N. pseudopima*, *Neogloboquadrina humerosa*, *G. trilobus*, *G. tumida* and *G. ruber*. The benthic assemblage is represented by scattered occurrences of *Lenticulina* sp., *Ammonia supera*, *Eponides* sp., *Pseudorotalia gaimardii, B. marginata, Hoeglundia elegans, Uvigerina* sp., *Laticarinina pauperata* and *Gyroidina* sp.

4.2.2 Interpretation

This FA is regarded as extensively bioturbated marine mud. The composition of the material points to a rich supply of terrestrial weathering products and a setting in the proximity of an emerged landmass. The benthic assemblage is dominated by shelf species, but also contains deeper water species such as *Uvigerina* sp., *L. pauperata*, *Gyroidina* sp. and *B. marginata*, suggesting upper bathyal to outer shelf depth conditions. Benthic species as *Ammonia supera* and *Pseudorotalia gaimardii* point to low dissolved oxygen concentrations at the seabed, which probably relate to microbial respiration of accumulated organic matter. Microbial respiration probably also caused the slightly bluish color of the clays and the occurrence of concentric calcareous concretions (e.g. Sellés-Martínez, 1996) The concretions occur on distinct levels and probably reflect episodes of reduced sedimentation, allowing for concretion growth over a longer period. The moderately rich occurrence of planktonic foraminifera shows that normal oxygen conditions prevailed in the water column.

4.3 FA3 Mud-dominated shallow marine

4.3.1 Description

Light grey, bedded marine clay with sandy laminae and thinly interlayered clay-sand alternations, moderately rich in organic matter **(Fig. 4, photo 7)**. Sandy laminae and thicker sand beds are fine-grained and dominated by fine shell debris, admixed with lithic grains (andesite and pumice) and occasional glauconite. The material contains sparse vertical burrows. Sand beds may have wavy or lenticular bedding structures. Locally, channelled sand beds occur, with a fill of coarse shell fragments, fine gravel (mainly moderately rounded andesite clasts) and clay pebbles. Occasional interbeds are found of massive, blocky-structured, dark grey clays, which may contain fine root traces and dispersed fine pyrite crystals.

The sediment is moderately rich in foraminifera, with a P/B-ratio of ~ 75%. Planktonic foraminifera are poorly preserved and often have broken or iron-stained tests. *G. trilobus, Dentoglobigerina altispira, G. menardii* (dex.), *Pullenia-atina obliquilocuta, G. ruber*, *G. tumida* and *Sphaeroidinella subdehiscens* are among the most common species. Benthic foraminifera are represented by rich occurrences of *Pseudorotalia coinoides, Asterorotalia trispinosa, Elphidium* sp. and the larger species *Amphistegina lessonii* and *Gypsina* sp.



Fig. 4. Selected photographs of the Jombang section. **(1)** Diatomaceous mudstones (FA1). **(2)** Calcareous mudstones (FA1). **(3)** Argillaceous-calcareous mudstones (FA1). **(4)** Massive marine clays (FA2). **(5)** Paleosol capping the massive marine clays. **(6)** Transgressive lag over the paleosol, with shell fragments and andesite gravel. **(7)** Shallow marine clay-sand alternations (FA3). **(8)** Shell beds capping coastal progradation cycles (FA3). **(9)** Idem, close up. **(10)** Clinoform-bedded tuffaceous sand alternating with laminated mud (FA4). **(11)** Clinoform-bedded tuffaceous sand (FA4), overview of sets separated by internal unconformities (Kabuh quarry).

The material contains cemented sand beds (up to 15 cm thick) rich in bivalve fragments (**Fig. 4, photo 8 -9)**, consisting of Pectinidae indet, Carditidae indet., *Ostrea* sp., and *Timoclea* sp. The fragments have rounded edges and are arranged in laminae, with the shells mostly in a convex-upwards position.

4.3.2 Interpretation

FA3 is indicative of shallow marine conditions under a rich supply of fine clastic material. The preservation of bedding structures is indicative of a relatively high sedimentation rate. Clays with fine sandy laminae represent inner shelf, subtidal depths, with sandy laminae reflecting storms or episodes of high fluvial discharge. Wavy and lenticular-bedded clay-sand alternations point to tidal currents. Channelled incisions with coarse fills rich in shell fragments represent tidal or estuarine channels. Interbeds of massive organic clays with fine pyrite crystals are indicative of coastal marshes, with thorough bioturbation and intermittent flooding (Pons et al., 1982).

The bivalve species are indicative of relatively turbulent conditions. The rounded shell fragments point to transport. Their occurrence as laminae with a convex-upward orientation reflects winnowing, either under shallow subtidal conditions or under intertidal conditions. The calcite-cementation of some of the shell beds may relate to early diagenesis by intermittent subaerial exposure, pointing to an origin as intertidal bars.

The benthic foraminiferal assemblage is characteristic of coastal or estuarine conditions. The planktonic foraminifera represent open water conditions and must have been transported to the coast by waves and tidal currents. An abundance of broken and iron-stained planktonic tests indicates that the assemblage contains reworked specimens, probably supplied as a terrestrial weathering product.

4.4 FA4 Ash-dominated deltas

4.4.1 Description

Yellowish grey, fine-grained tuffaceous sandstones, forming dm-scale bedding structures separated by mud drapes or thicker, laminated mud layers **(Fig. 4, photo 10)**. The beds are normal graded and have an indistinct, parallel stratification. Grains consist of monocrystalline feldspars, vitric grains, lithic pumice and scarce fine shell fragments. Thicker sand beds often have a composite build-up of several amalgamated, graded sand layers.

The sandstone beds may be horizontally bedded, but more often form clinoforms with a depositional dip of 5 to 15°, locally reaching even steeper inclinations of up to 25° **(Fig. 4, photo 11; Fig. 5, photos 9 and 11)**. Dipping beds often have a slightly incisive base, covered with a veneer of coarse tuffaceous sand with fine pumice gravel and clayey rip-up clasts, quickly grading upwards into fine tuff. The bedding planes are often distorted by soft sediment deformation or slumping. Horizontally-bedded sandstones are dominated by fine tuff and have more prominent clayey interbeds **(Fig. 5, photo 1)**.

The material is poor in foraminifera, mostly with abraded and poorly preserved tests. Benthic species include *B. marginata*, *A. supera*, *Cibicides* sp., *Amphistegina* sp. Among the fragmented planktonic tests are *Neogloboquadrina* sp. and *Sphaeroidinella* sp.

4.4.2 Interpretation

FA4 represents deltaic depositional conditions under a high supply of volcanic ash, pointing to explosive volcanism in the hinterland. Clinoform-bedded sands with thin clayey interbeds were deposited on the dipping delta slope. Tuffaceous sand beds with thicker clayey interbeds and a low or indistinct depositional dip may represent a pro-delta setting or a setting along a shallow, low-gradient coast.

The normal grading and slightly incisive base of the foresets reflect delta progradation by intermittent turbidity currents. The dominance of silt and fine-grained sand and the scarcity of well-rounded, coarser material points to supply by sediment-laden rivers, with a high suspension load and relatively low bed-load transport. Possibly, the sand beds represent short episodes of extreme run-off, which caused incoming high-density river water to plunge beneath the seawater, flowing over the delta slope as turbidity currents (e.g. Mulder and Syvitski, 1995; Zavala, 2020). Such situations may be related to flash floods in the upstream reach of the river and may have been amplified by ebb currents in the river mouth. Also, soft sediment deformation and slumps hint at episodes of high sediment supply and destabilization of the delta slope. Clay laminae, alternating with fine-sandy foresets, represent settling from a buoyant plume in front of the river mouth during intervening stages. The rhythmic build-up of fine sandy foresets and mud drapes may reflect seasonal variation in river discharge.

The scarce, abraded and broken foraminifera are regarded as reworked tests and must have been supplied to the delta by the river. Note that the benthic species form an unusual assemblage of bathyal and coastal species, which also points to reworking.

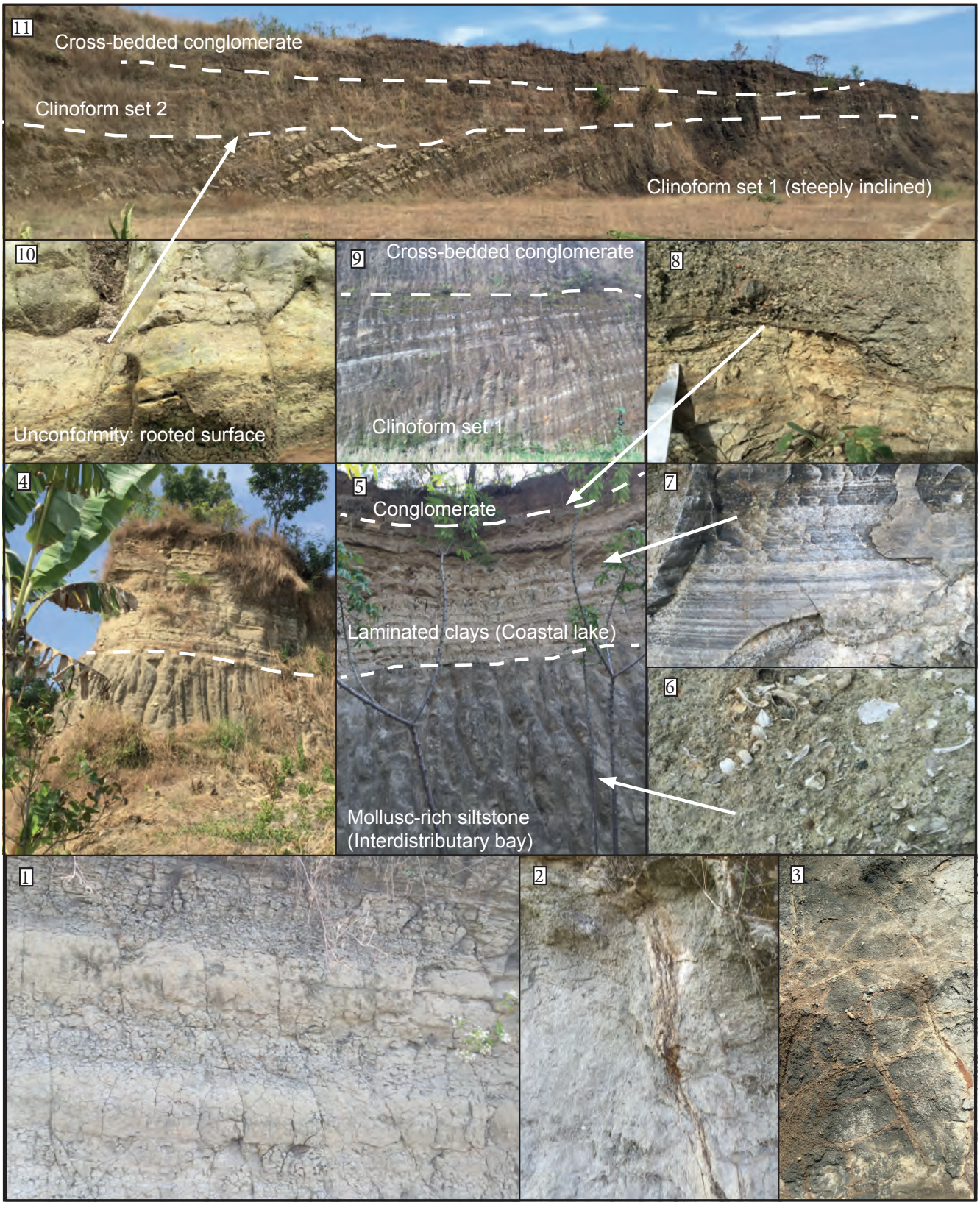


Fig. 5. Selected photographs of the Mojokerto section. **(1)** Bedded tuffaceous sand and laminated mud (FA4) forming base of the exposed section. **(2)** Tree root, paleosol overlying basal series of bedded tuffaceous sand. **(3)** Mud cracks, same level as photo 2. **(4)** Mollusc-rich siltstones (interdistributary bay) sharply overlain by laminated clays (coastal-lake facies) (FA5). **(5)** Idem, laminated clays (FA5) are incised and overlain by cross-bedded conglomerate bed (FA6). **(6)** Close-up mollusc-rich siltstones (FA5). **(7)** Close-up laminated clays (FA5). **(8)** Close-up incisive contact between laminated clays (FA5) and cross-bedded conglomerate (FA6). **(9)** Clinoform-bedded sandstones (FA4), incised and overlain by cross-bedded conglomerates (FA6). **10:** Horizon with fine root traces marking unconformity between clinoform-bedded sets. **(11)** Two clinoform-bedded sets separated by unconformity, set 2 is incised and overlain by cross-bedded conglomerates.

4.5 FA5 Sheltered interdistributary bays and coastal lakes

4.5.1 Description

Greenish grey, massive, siltstones with marine molluscs **(Fig. 5, photo 6)**. The sediment is thoroughly bioturbated, locally preserving vertical burrows. The material consists of tuffaceous grains (vitric particles and monocrystalline feldspars), fine shell debris and calcareous grains and is admixed with calcareous mud. The material is rich in gastropods (*Turitella* sp., *Architectonica* sp., Tonnidae indet., *Strombus* sp., *Oliva* sp., *Ficus* sp., *Natica* sp.) and bivalves (Veneridae indet, Pectenidae indet., *Anadara* sp., *Ostrea* sp.). The shells are found either fragmented or in-situ. Fragmented shells have sharp edges and occur dispersed through the sediment. The material contains scattered free-living corals *Goniopora stokesi*.

The material is poor in foraminifera, dominated by benthic species as *Amphistegina* sp. and *Ammonia* sp. Planktonic foraminifera are scarce and are represented by unidentifiable, abraded and broken specimens.

Loacally, the mollusc-rich siltstones are sharply overlain by finely laminated clays **(Fig. 5, photos 4, 5 and 7)**, without traces of incision or weathering that might point to a depositional hiatus. The clay is made up of light and dark grey laminae, forming distinct and laterally continuous couplets. The dark laminae have a thickness of 2-3 mm and consist of clay with fine decomposed plant fragments and may contain imprints of leave fragments. The light laminae range in thickness between 1 and 4 mm and are composed of clay with admixed fine ash. Remarkably, the laminated clays are devoid of marine molluscs, which forms a great contrast with the underlying mollusc-bearing siltstones. Except for extremely scarce occurrences of broken foraminiferal tests, the material is also devoid of foraminifera.

4.5.2 Interpretation

The burrowed, mollusc-rich mudstones represent a sheltered, shallow marine setting. In **Section 6.5** we will see that this sheltered environment is closely related to the landscape of ash-dominated deltas as described in section 4.4, suggesting a background as interdistributary bays.

The rich mollusc assemblage, dominated by gastropods, represents a low-energy and clear-water habitat, with a depth range of 5 to 20 m. Also the benthic fauna dominated by *Amphistegina* sp. and the scattered free-living corals point to shallow, clear-water conditions. Scarce abraded tests of planktonic foraminifera are regarded as reworked specimens, probably supplied by rivers.

Dispersed shell fragments with sharp edges do not show signs of significant transport or wave action. Fragmentation is probably related to predation and compaction. In-situ molluscs point to episodic rapid burial. The ash-dominated composition of the sediment points to terrestrial supply from a volcanic hinterland.

The sharp transition to laminated clays represents an abrupt change to stagnant-water conditions. The sudden disappearance of marine molluscs and foraminifera suggests that the former lagoon has become isolated from the sea, changing the area into a coastal lake. The preservation of fine laminae suggests anoxic bottom conditions. Anoxic conditions in coastal lakes are often related to salt bottom waters, leading to stratification and inefficient mixing of the water column (Zolitschka et al., 2015).

4.6 FA6 Meandering and anastomosing rivers

4.6.1 Description

Reddish-brown conglomerates, yellowish-grey cross-bedded and planar bedded sandstones and dark grey organc clays, forming fining-upward sequences with a preserved thickness of up to 8 m. A sequence has a channelled or planar erosive base, covered with ca. 1.5 m of trough cross-bedded conglomerate **(Fig. 6 photos 1-3 and 8-9)**. The conglomerate has a matrix of cemented coarse sand (feldspars, pyroxenes, hornblendes, lithic pumice and andesite) and contains moderately to well-rounded gravel (2-5 cm), with a polymict composition of pumice, dacite and andesite. Clayey rip-up clasts (up to 10 cm) are common. The conglomerate contains scattered, well-mineralized, disarticulated and often fragmented vertebrate bones. This basal lag is overlain by several meters of medium to fine-grained sandstones. Trough cross-bedding structures may be found in the lower few meters **(Fig. 6, photo 10)**, but more often the sand is planar bedded and alternates with thin clay layers with fine root traces or thin paleosols with a blocky texture, root traces and fine carbonate concretions **(Fig. 6, photos 5 and 7)**. Frequently, thicker (~1 m) interbeds occur of massive, dark grey clay rich in organic matter (**Fig. 6, photo 6)**, containing in-situ molluscs (*Corbicula* sp., *Geloina* sp.).

4.6.2 Interpretation

The erosive lower boundary of a fluvial sequence, overlain by a gravelly lag, points to incision by a laterally mobile gravel-bed river, suggesting meandering conditions. The polymict gravel derives from the foot of the Wilis and Anjasmoro volcanoes and the rounding reflects stable bed-load transport. The overlying fining-upward sequence generally

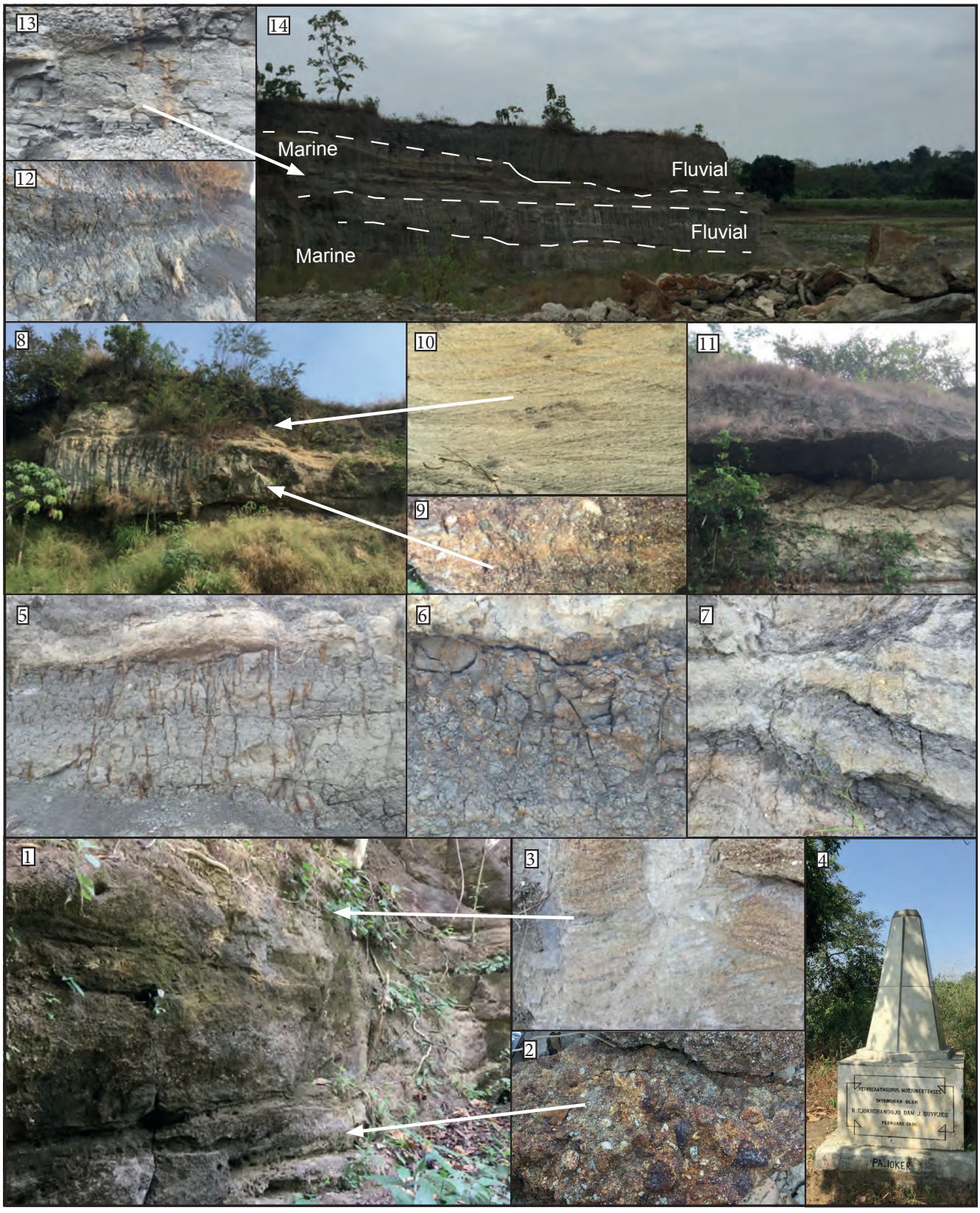


Fig. 6. Selected photographs of the Mojokerto section (continued). **(1)** First conglomerate lag, base of the fluvial series (FA6), oldest preserved stage of the ancient Brantas. **(2)** Idem, close-up. **(3)** Idem. **(4)** Monument commemorating Homo erectus find, placed on basal conglomerate bed. Later reconstructions indicated that the actual find site is the second conglomerate bed. **(5)** Stacked floodplain deposits with root traces (FA6). **(6)** Vertisol in floodplain series (FA6). **(7)** Stacked floodplain soils, covered with overbank deposits (FA6). **(8)** Incision covered with second conglomerate lag (FA6). **(9)** Close-up second conglomerate lag. **(10)** Cross-bedded sand overlying second conglomerate lag (FA6). **(11)** Incision and third conglomerate lag. **(12)** Bedded organic clays and transition to marine interval. **(13)** Bedded marine claystones and sand with sparse burrows and mollusc fragments (FA3). **(14)** Alternating marine claystones and incisive fluvial sandstones, top of the section (FA3 and FA6).

represents meandering conditions, with trough cross-bedded point-bar deposits overlain by floodplain soils. However, stacking of planar-bedded fine-grained sand and interbedded floodplain soils forms a distinctive feature of the fluvial sequences, pointing to repeated burial of the floodplain by wash-overs or avulsions from the main channel. Overbank deposition and high floodplain sedimentation rates are indicative of anastomosing conditions and are generally associated with rapid base-level rise (Makaske, 2001). Also the occurrence of thicker clayey interbeds points to this direction, as anastomosed rivers have low-lying, saucer-shaped floodplains, which frequently develop into wetlands. The in-situ molluscs in these clay layers represent a fresh or brackish water habitat. Probably, the fluvial fining upward cycles reflect an initial erosive stage, under meandering conditions, followed by an aggradational stage, under (partly) anastomosing conditions.

5. The depositional records of Jombang and Mojokerto

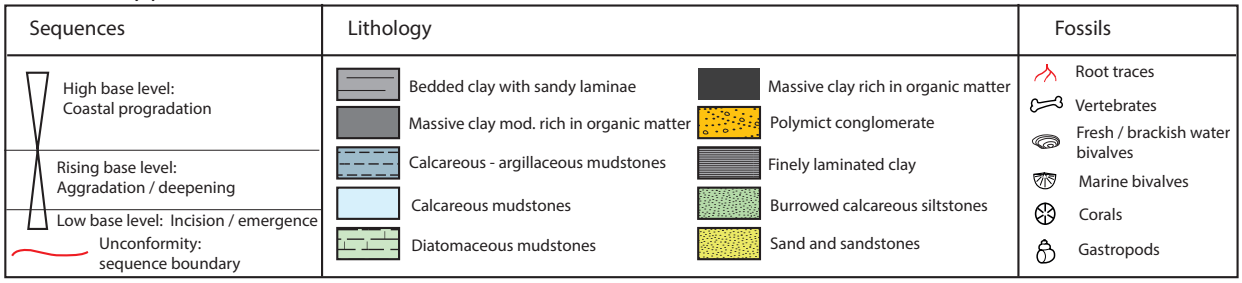
5.1 Jombang

North of Jombang, the Pucangan anticline rises up from the Brantas floodplain **(Fig. 1)**. Duyfjes (1938) selected river sections through the south flank of this anticline, as a reference for his Kendeng stratigraphy. We focussed on the Marmoyo and Sumberingin Sections **(Fig. 3)**, as these two sections cover the entire depositional series that makes up this flank of the anticline. Moreover, a published foraminiferal biostratigraphy provides detailed age control of the marine strata making up the base of these sections (Berghuis et al., 2019). The Marmoyo and Sumberingin Sections reach a total thickness of ca. 1,000 m **(Fig. 7 and 8)**.

The base of the series, exposed in the core of the anticline, consists of calcareous and diatomaceous mudstones (FA1), dating from the Early Pliocene. The material is generally very low in admixed detrital clay, but around 290 m above the base of the section, clay content increases, changing the sediment into calcareous-argillaceous mudstones. Foraminiferal age markers indicate that this facies change dates to ~ 3.8 Ma. Ca. 430 m above the base of the section this material quickly grades into plastic marine clays (FA2). An array of planktonic age markers provides good age control over this part of the section (**Fig. 7)**, indicating that this prominent facies change dates to 3.0 Ma.

The massive clays reach a thickness of 250 m. The base of the clays still contains a characteristic tropical planktonic foraminiferal assemblage. However, higher up a strong decline of *G. tumida*, a coiling change from dextral to sinistral in *G. menardii* and the appearance of *Neogloboquadrina* cf. *pachyderma* point to slightly cooler water conditions. These fauna changes are regionally used to mark the Plio-Pleistocene boundary (Blow, 1969; Bolli et al., 1989). The massive clays are capped with a ca. 1.5 m thick weathering profile of stiff, crumbly, red-coloured clay with fine iron concretions **(Fig. 4, photo 5)**. This layer is truncated and covered with a lag of coarse sand with shell fragments and fine andesitic gravel **(Fig. 4, photo 6).** The lag is overlain by shallow marine clay-sand alternations with shell fragments (FA3), reaching a thickness of 120 m. This shallow marine series can be roughly subdivided in three superimposed coarsening upwards sequences, grading from clay with fine sandy laminae to clay-sand alternations with wavy and lenticular bedding structures. Toward the top of these sequences, calcite-cemented shell lags occur **(Fig. 4, photos 7-9)**, as well as dark grey organic clay layers with fine pyrite crystals. Planktonic age control is lost, as most age-relevant species are thermocline-dwelling and require sufficient water depth. Moreover, the material contains abundant red-stained planktonic foraminifera with eroded tests, which probably derive from eroded older strata, further complicating age determinations. For example, *D. altispira, S. subdehiscens* and dextrally coiled *G. menardii,* all present in the shallow marine strata, are Pliocene species for which extinctions were found lower in the depositional record **(Fig. 7)**.

At ~ 810 m above the base of the section, the shallow marine clays quickly grade into fine-grained, bedded tuffaceous sandstones (FA4). Today the sand quarry of Kabuh, ca. 1.5 km west of the Sumberingin Section, provides excellent exposures of this material **(Fig. 4, photo 10-11)**. The bedding planes dip ca. 40° (N145S). Reducing this value with the tectonic dip, which is ca. 30° (N170E), leaves an eastward-directed dip of 10 to 15°, which we regard as a sedimentary, clinoform-related dip. The series reaches a total thickness of ca. 150 m and is built up of superimposed deltaic progradation sequences, forming sets of clinoforms with a thickness ranging between 10 and 50 m. Sets of clinoforms are separated by unconformities marked with burrows or fine root traces, often covered with a lag of fine shell fragments and clay pebbles.



Legend to **Fig. 7 and 9.**

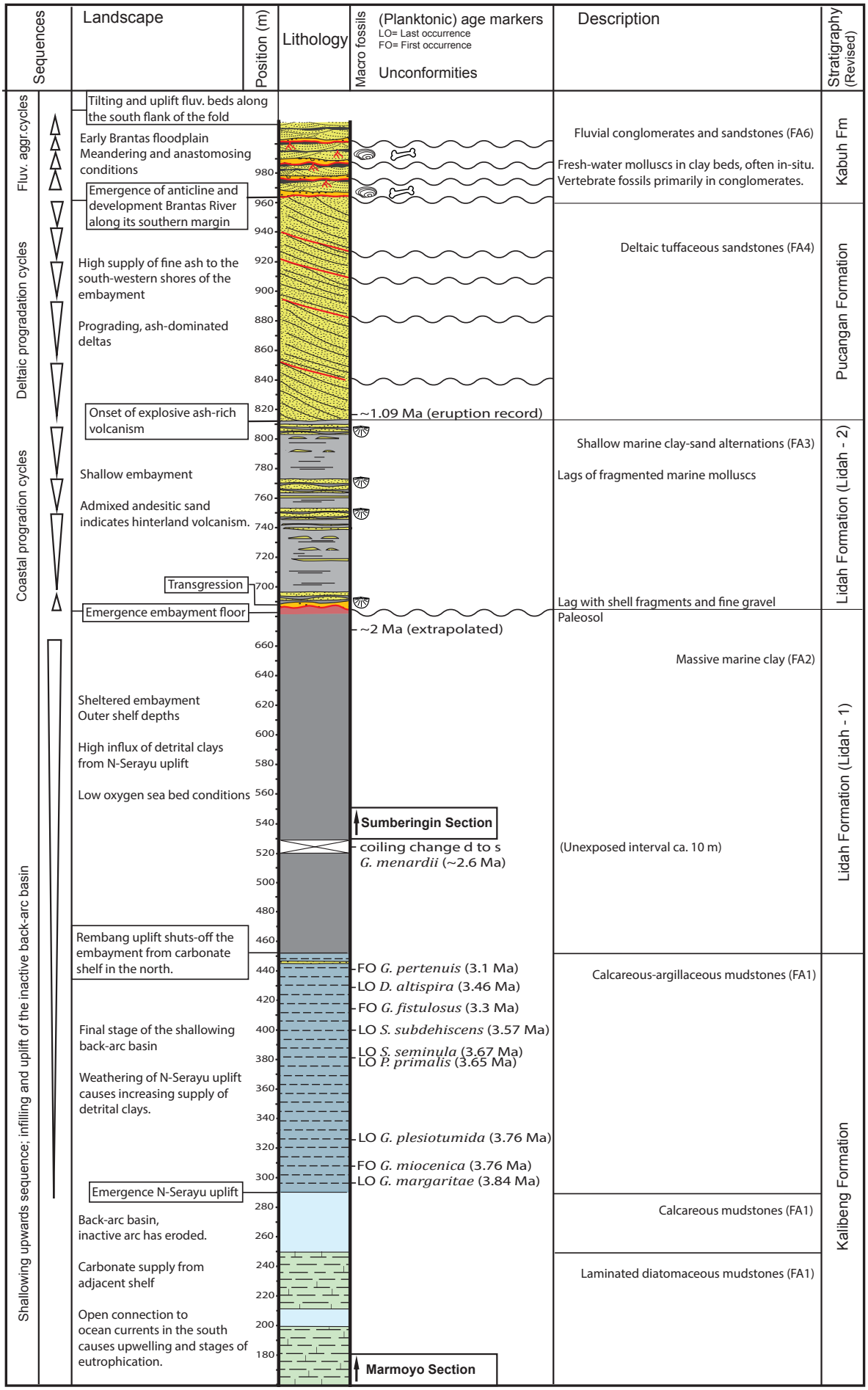


Fig. 7. Composite stratigraphic column of the Pucangan anticline north of Jombang, based on the Marmoyo and Sumberingin River Sections. See separate legend. Planktonic foraminiferal age markers are based on Berghuis et al. (2019). Age estimate of ~1.09 Ma is based on a provisional link with the Wilis eruption record (Hartono, 1999). FA = Facies Association, see **Section 4**. Revised unit definitions based on this paper.

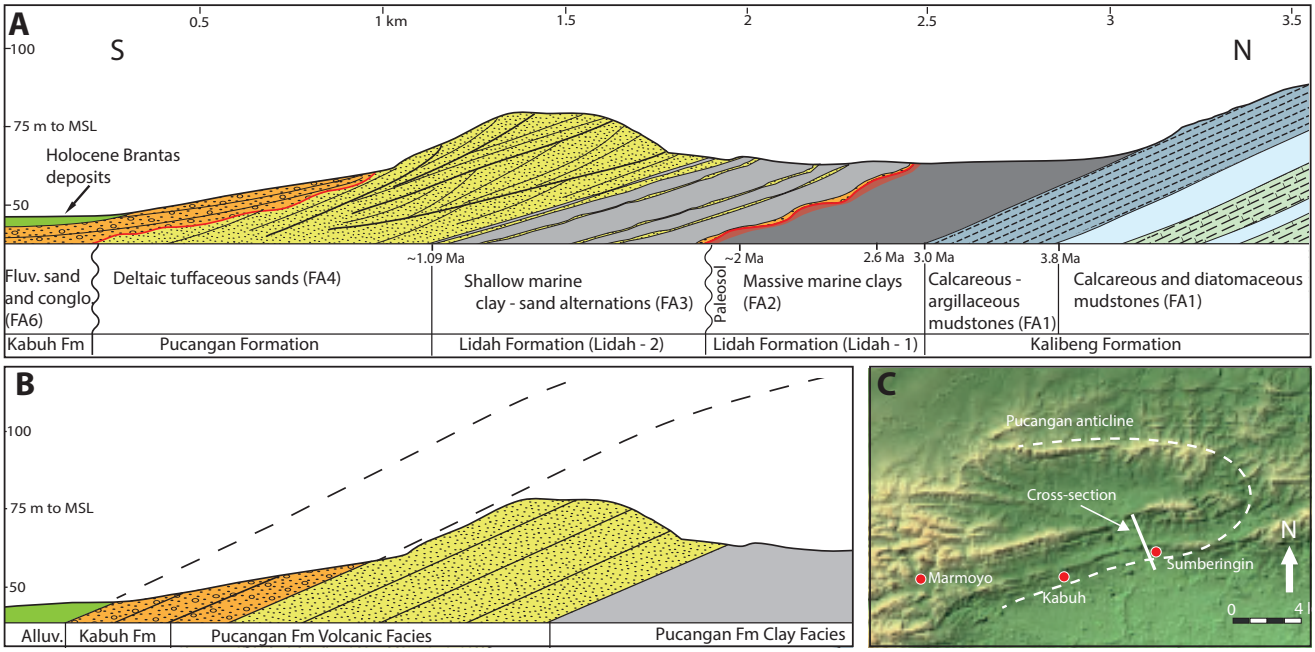


Fig. 8. A: Schematic cross-section over the south flank of the Pucangan anticline north of Jombang. FA = Facies Association, see section 4. The fluvial strata making up the southern foot slopes of the anticline postdate initial folding. They are part of a younger fluvial valley fill and have become tilted and uplifted along the margin of the anticline by continued folding. **B:** Previous interpretation and unit definition (Duyfjes, 1938), in which the series forms an uninterrupted record of coastal progradation and pre-dates folding. Fluvial strata along the southern flank do no re-appear along the northern flank, but were correlated with marine deposits which were regarded of equal age and which were referred to as the marine facies of the Kabuh Formation. **C:** Location of the cross-section.

The Kabuh quarry does not expose the top of the clinoform-bedded series, but in the Sumberingin River Section, the series can be traced southwards toward the footslopes of the hill range **(Fig. 8A)**. Here, the tuffaceous clinoform-bedded series is truncated by a channelled erosion surface, covered with a trough-crossbedded, reddish-brown conglomerate lag. This basal lag is overlain by a ~ 25 m thick, poorly exposed fluvial series (FA6), made up of three or four stacked fining-upward sequences, each with an incisive base covered with a conglomerate lag.

5.2 Mojokerto

The succession as exposed around Jombang can be traced eastward toward the Kedung Waru anticline north of Mojokerto **(Fig. 1)**. This low and smooth fold contains the bone-bearing fluvial strata that form the type locality of Von Koenigswald's Jetis Fauna and yielded the Perning skullcap. Duyfjes (1938), Huffman and Zaim (2003) and Morley et al. (2020) described a section through the anticline along Kepuhklagen Road. We restudied this section by combining detailed sections of the sand quarries north of the village of Perning, directly east of the Kepuhklagen Road, offering an unprecedented insight into the geological build-up of the anticline **(Fig. 3D)**. Six quarry sections (sections A to F) were studied, representing a combined thickness of 54 m **(Fig. 9 and 10)**.

The strata as exposed in the Kedung Waru anticline form the stratigraphic equivalent of the top of the Jombang section. Shallow marine clays (FA3) make up the core of the Kedung Waru anticline. The material is exposed several kilometers east of the Kepuhklagen Road Section. Duyfjes (1938) also reported the material in exposures along Kepuhklagen Road, but this could not be confirmed during our field studies.

In the studied quarry sections of Perning - Kepuhklagen, the lowest exposed stratigraphic level consists of the bedded, fine-grained tuffaceous sandstones (FA4). The material makes up the base of quarry sections A and E **(Fig. 10)** and reaches a maximum exposed thickness of 5 m. The tuffaceous beds have prominent clayey interbeds **(Fig. 5, photo 1)** and do not have a significant clinoform-related dip. The strata are capped with a thin weathering profile, with shrinkage cracks and root traces **(Fig. 5, photos 2-3)**. In quarry section A, two paleosols are found at this level, separated by several meters of shallow marine sands and clays with shell fragments and interbedded organic clays with fine root traces and pyrite crystals, with a facies similar to FA3, but with a more tuffaceous composition of the sand grains.

The paleosol is overlain by ca. 8 m of burrowed, ash-rich siltstone, rich in marine molluscs (FA5), which is sharply overlain by ca. 5 m of finely laminated clays (FA5) **(Fig. 5, photos 4-7)**. In quarry section A, several meters of organic clays with root traces are found between the mollusc-rich siltstones and the laminated clays.

The laminated clays become slightly sandier toward the top and are overlain by fine-grained bedded tuffaceous sandstones (FA4), with a prominent depositional dip of ca. 25° (N40E), corrected for tectonic dip **(Fig. 5, photos 9 and 11)**. Moreover, the steeply dipping clinoforms have a parallel, mostly undistorted bedding structure. Remarkably, the

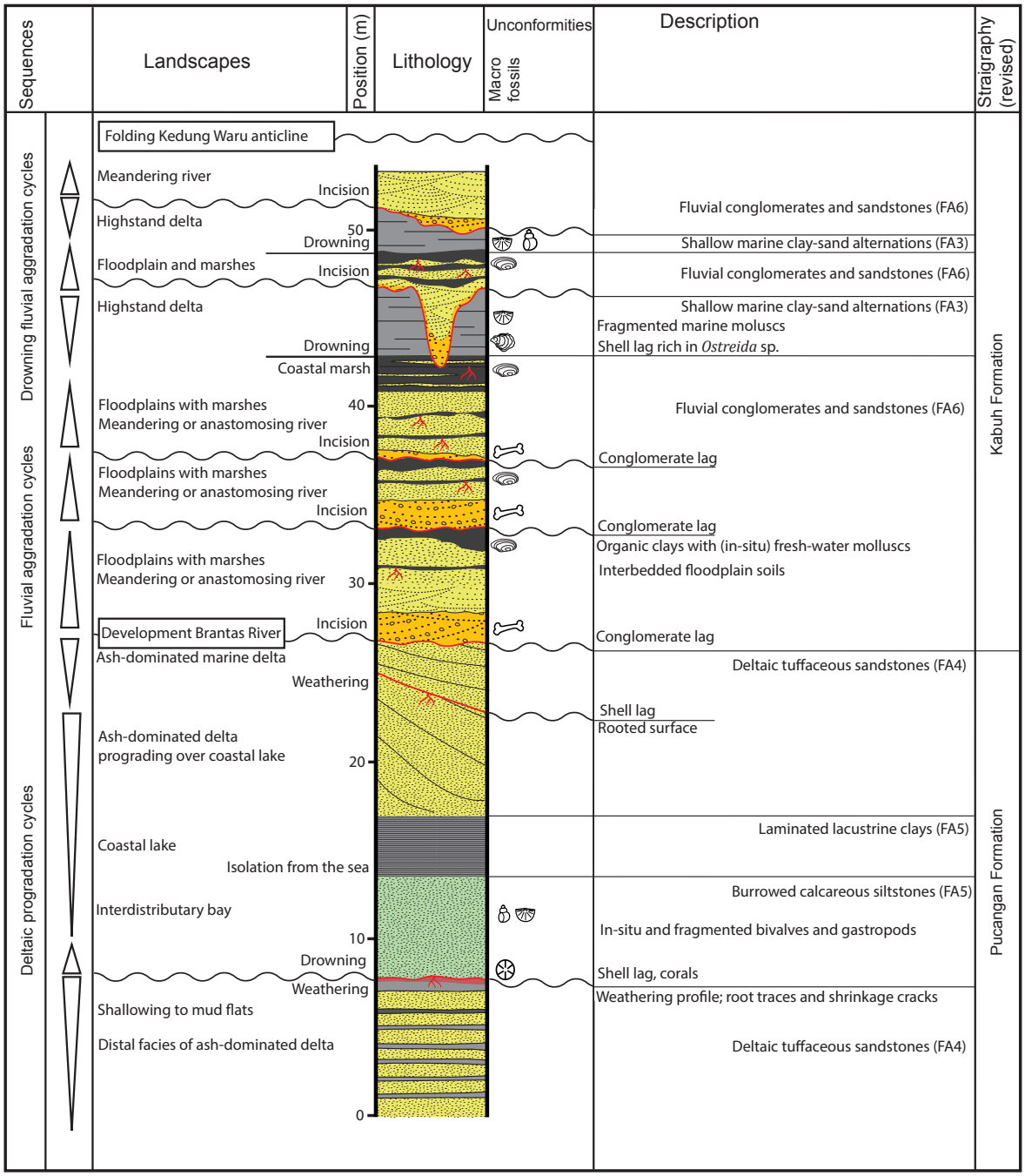


Fig. 9. Composite stratigraphic column of the Kedung Waru anticline north of Mojokerto, based on quarry sections east of Kepuhklagen Road. FA = Facies Association. Revised unit definitions based on this paper. Legend: See Fig. 7.

tuffaceous beds in this part of the section are devoid of shell fragments or foraminifera, a feature that was also noted by Huffman and Zaim (2003). The steeply dipping clinoforms form one single set. In some of the larger quarries, a second set can be observed, separated from the underlying set by an unconformity with fine, red-colored grass-root traces **(Fig. 5, photos 10 and 11)**. The clinoforms in the overlying set have a depositional dip of ca. 15° (N35E) and contain low quantities of shell debris and scarce foraminifera, mostly as abraded or broken tests. The clinoforms can be traced along the quarry sides for hundreds of meters and locally wedge out into the surrounding laminated clays **(Fig. 10)**.

The tuffaceous clinoforms are truncated by a channelled erosion surface **(Fig. 5, photos 9 and 11)**, locally leaving only several meters of the clinoform-bedded sands or even cutting down into the underlying laminated clays. Where the deltaic sands wedge out, the erosive surface incises the laminated clay **(Fig. 5, photos 5 and 8)**. The erosion surface is covered with a cross-bedded, cemented conglomerate bed **(Fig. 6, photos 1-3)**, which is overlain by (planar) bedded, medium to fine-grained sand with interbedded paleosols and clays (FA6). Several meters higher a new erosion surface is found, which is slightly channelled but in general forms a planar erosion surface that can be traced over long distances. It is covered with a cemented conglomerate lag, forming a plateau at ca. 59 m +MSL along the southern and central part of the hill range, which is around the axis of the anticline **(Fig. 11A)**. The erosion surface truncates the

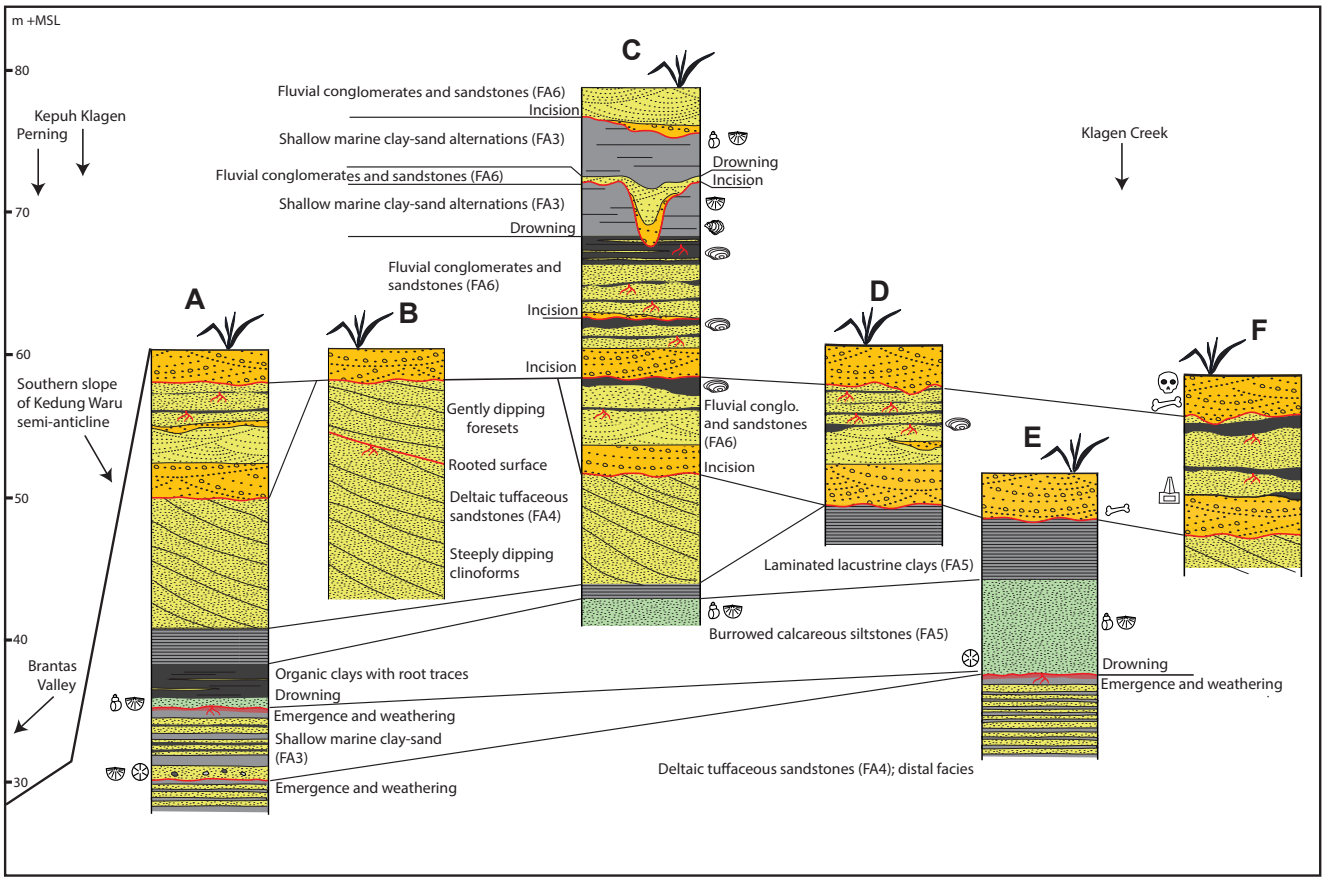


Fig. 10. Quarry sections of the Kedung Waru anticline north of Jombang, east of Kepuhklagen Road. FA = Facies Association, see **Section 4**. For details, see composite stratigraphic column **(Fig. 9)**. Location of the quarry sections is indicated in **Fig. 3D**. Legend: see **Fig. 7**.

underlying fluvial sequence with its more irregular erosive base. Locally, the younger erosion surface directly truncates the deltaic beds **(Fig. 10, section B)**. Although the 59 m +MSL plateau resembles a fluvial terrace, remnants of overlying deposits indicate that it has formed by erosion of overlying, less consolidated material. This material again consists of bedded fluvial sand with interbedded floodplain soils and organic clays (FA6). It is exposed in isolated hills along the core of the anticline, reaching ca. 79 m +MSL. Moreover, it forms elongate crests of northward-dipping strata along the north flank of the anticline. Another prominent abrasion surface, again with a lag of cross-bedded conglomerate, marks the base of a third fining-upward sequence. This sequence grades into bedded organic clays **(Fig. 6, photo 12)**, which are sharply overlain by an unstructured lag of rounded shell fragments, dominated by *Ostrea* sp. It marks the transition to bedded claystones, with thin sandy interbeds and sparse marine molluscs (FA3) **(Fig. 6, photo 13)**. The marine interval, which reaches a thickness of ca. 5 m, is deeply incised by channels with a fill of (cross-)bedded conglomerates and sandstones (FA6), which is again overlain by shallow marine clay-sand alternations (FA3). This marine interval is once again fluvially incised and the moderately cemented fluvial fill of this incision (FA6) caps the isolated hilltops **(Fig. 6, photo 14)**.

Upon comparing our field descriptions with the published studies of this site, we found that the internal structure of the Kedung Waru anticline is different than previously thought. Its south flank is largely missing, probably due to faulting, which changes the perspective of the local stratigraphy **(Fig. 11C)**. Fortunately, it is possible to trace back most of the previous field observations. Von Koenigswald (1935, 1934) and Duyfjes (1938, 1936) used two mollusc-bearing intervals as field markers, which the latter referred to as mollusc beds 2 and 3 **(Fig. 11B)**. Mollusc bed 2 is the burrowed siltstone interval (FA5) within the ash-dominated deltaic series (FA4). Mollusc bed 3 is the shallow marine interval (FA3) near the top of the section, interbedded between fluvial strata. Von Koenigswald based his Jetis Fauna on vertebrate fossils collected from bone-bearing gravelly beds between the two mollusc beds. This suggests that the bones derive from the conglomerate lags of the three fluvial sequences that overlie the deltaic series. A monument commemorating the find of the *Homo erectus* skullcap was placed on top of the lowest conglomerate bed, at a site north of Klagen Creek. However a later study indicated a higher conglomerate bed, exposed slightly further to the north, as the find spot (Huffman et al., 2005). Most likely, this is the conglomerate bed that forms the base of the second fluvial sequence **(Fig. 10F)**.

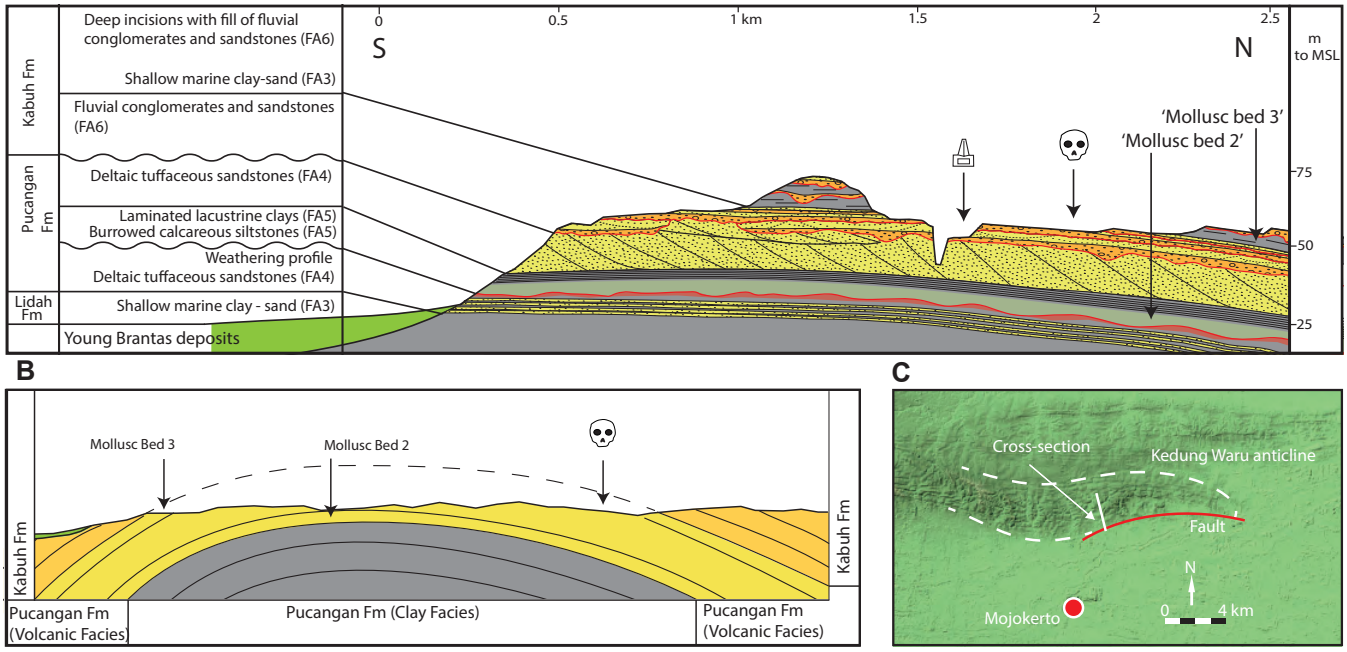


Fig. 11. A: Schematic cross-section over the Kedung Waru anticline north of Mojokerto. South flank of the anticline is missing, probably due to faulting. Fluvial strata covering the anticline erosively overlie the Early Pleistocene marine series and represent the ancient Brantas floodplain, which has been warped up and included in the fold. Cemented conglomerate lags have been prepared by erosion and form plateaus along the axis of the anticline and form cuesta-like ridges along the north flank of the anticline. **B:** Previous interpretation and unit definition (Duyfjes, 1936), in which the series forms an uninterrupted record. Missing south flank of the anticline was not noted. Reconstruction of historic observations is aided by the use of two prominent mollusc-bearing levels as marker beds. Mollusc bed 2 is the mollusc-bearing siltstone interval below the steeply inclined clinoforms; mollusc bed 3 is the marine interval at the top of the fluvial series. **C:** Location of the cross-section. Note the missing south flank of the anticline, probably by faulting.

6. Discussion

6.1 From back-arc basin to sheltered embayment

The calcareous and diatomaceous mudstones (FA1) that form the base of the eastern Kendeng depositional record are part of a well-studied, regional series that is recognized as the fill of the ancient back-arc basin (Lunt, 2013; Van Gorsel and Troelstra, 1981). The material dates from the Late Miocene to Pliocene and represents the final stage of the basin, in which the Miocene volcanic arc was no longer active and the influx of clastic material had largely stopped.

Planktonic foraminiferal age markers **(Fig. 7)** indicate that the depositional record of the Marmoyo Section dates back to the Early Pliocene. The scarce benthic foraminifera point to bathyal depth conditions**,** roughly estimated to 800 m. Moving upwards through the mudstone series of the Marmoyo Section, the introduction of benthic species such as *Bolivina robusta* points to gradual shallowing to upper bathyal depths.

The calcareous-argillaceous mudstones that form the upper part of the mudstone series reflect an increasing supply of fine terrestrial weathering products, pointing to emerging land surfaces in the vicinity. It forms the prelude of the subsequent transition to massive, plastic clays rich in fine terrestrial organic material (FA2). The geographic distribution of the clays in the subsoil of eastern Java provides an interesting insight into the depositional landscape. The material can be traced eastwards to the mostly unfolded coastal plains of Surabaya, whereas to the north and the west, the material can be traced into the Randublatung Valley **(Fig. 1)**. Here, the clays wedge out against the southern foot slopes of the Rembang Hills and the northern foot slopes of the western Kendeng. This gives an image of a narrow, muddy marine embayment between elongate emerged ridges. We refer to this previously unrecognized Plio-Pleistocene landscape, along the western edge of the ancient Madura Strait, as the Surabaya Embayment **(Fig. 12A)**.

There must have been a rich supply of terrestrial weathering products to the embayment, which cannot have been provided by the low-altitude ridges that formed the embayment margins, which were largely made up of calcareous strata. Sediment supply from the Sunda Shelf in north is also unlikely, as Late Pliocene carbonates below the Java Sea indicate that this area remained submerged (Lunt, 2013; Morley et al., 2016). In **Section 6.3** we will see that widespread emergence of this part of the Sunda Shelf occurred later, in the Early Pleistocene. But even if some areas of this carbonate platform already emerged in the Late Pliocene, they cannot have formed a significant clastic source.

A more likely source area for the clayey fill of the Surabaya Embayment is found in the west. Here, the North Serayu Mountains form an impressive mountain range, today reaching altitudes of over 2,000 m +MSL. Similar to the western Kendeng, the North Serayu were formed by folding and thrusting of the fill of the Mio-Pliocene back-arc basin,

during the Late Pliocene compressive stage (Satyana and Armandita, 2004). But in this area, the uplifted strata consist of turbidite claystones (Satyana, 2007), which must have made the uplift zone a massive source of easily-weatherable clastic material.

Returning to the well-dated marine series of the eastern Kendeng, we can now make an interesting reconstruction of Plio-Pleistocene landscapes in relation to tectonism and emerging surfaces. The Pliocene mudstones series was deposited in the shallowing back-arc basin, with an open connection to the Indian Ocean in the south and the submerged Sunda Shelf in the north. The increasing admixture of argillaceous material in the top of this mudstone series, which dates back to 3.8 Ma, reflects the early emergence of the North Serayu Mountains. The predominantly calcareous composition of the sediment shows that the connection with the carbonate shelf in the north was still open. The subsequent transition to plastic clays, dated to 3.0 Ma, indicates that the area became cut-off from the supply of calcareous mud, which can be explained by the emergence of the Rembang Ridge. The change in sediment composition thus signals the birth of the sheltered Surabaya Embayment **(Fig. 12A)**.

6.2 The Pliocene regression as a function of uplift and deposition

The succession of marine mudstones and massive clays, which makes up the lower part of the Marmoyo-Sumberingin Section of Jombang up to the paleosol at 680 m, exhibits a distinctive shallowing-upward trend. A reconstruction of depositional depths **(Fig. 13)** indicates that the Pliocene regression was not merely an effect of sedimentary infilling of the inactive back-arc basin, but also involved uplift of around 0.5 mm/a. This uplift may have been related to isostatic rebound by the disapearance of the Miocene volcanic arc, Late Pliocene compression, or regional long-wavelength uplift.

The benthic foraminiferal assemblage of the base of the massive clays, consisting of upper bathyal species as *B. marginata* and shelf species as *A. supera* and *P. gaimardii*, suggests outer shelf depths of around 200 m. However, moving up-section through the clays, reduced occurrences of shelf species and re-appearance of bathyal species as *Uvigerina* sp., *L. pauperata* and *Gyroidina* sp. reflect deepening to upper bathyal depths, which may be roughly estimated to ~ 300 m, suggesting subsidence of the embayment between 3 and 2 Ma. This temporary subsidence, which also explains the great thickness of the clays, is remarkable, referring to the paleogeographic setting of an enclosed embayment surrounded by emerging ridges, under a predominantly compressive regime. Corrected for on-going sedimentation, total subsidence in this period may have amounted to ~250 m **(Fig. 13)**. This local subsidence may have been related to complex movements along pre-existing basement faults, which are omnipresent in eastern Java, and relate to a Paleogene rift system (Husein et al., 2015). Uplift of the Rembang Hills, as well as several isolated uplift zones within the Randublatung Valley, also relate to vertical movement along basements faults.

6.3 Emergence and subsequent development of a shallow embayment

The paleosol that caps the massive clays represents emergence of the embayment floor. The clays directly below the paleosol bear no evidence of gradual shallowing, in the form of sedimentary structures or increasing occurrences of shallow-water benthic foraminifera. This suggests that emergence was caused by resumed uplift rather than by gradual depositional in-filling of the embayment **(Fig. 13)**. Based on scarce planktonic age markers and an assumed sedimentation rate of 18 cm/ka, the age of the massive clays directly below the paleosol has been estimated to ~2 Ma (Berghuis et al., 2019). It is interesting that this age roughly corresponds with the estimated age of regional emergence of the Sunda Shelf (Lunt, 2013; Morley et al., 2016), which is generally linked to long-wavelength uplift of the larger Sunda Shelf. This suggests that emergence of the Surabaya Embayment was, at least partly, related to regional uplift. The estimated age of ~2 Ma for the top of the massive clays can be regarded as the maximum age of emergence of the embayment floor. The red-colored weathering profile with iron concretions testifies to a humid tropical climate, which is in line with the Early Pleistocene pollen record of eastern Java (Polhaupessy, 1990; Sémah and Sémah, 2012. Assuming a weathering rate of 1-2 cm / ka (Evans et al., 2019) and a preserved thickness of 1.5 m, the paleosol equals a minimum weathering period of 75 to 150 ka.

The overlying marine clay-sand alternations (FA3) reflects the development of a shallow sea. Referring to the maximum age of the paleosol and its weathering period, the maximum age of this re-submergence may be estimated to 1.9 or 1.8 Ma. Interestingly, this rough age estimate is supported by the occurrence of andesitic sand and fine gravel, at the transgression surface and in the overlying shallow marine sediment. This granular volcanic material, which is absent in the massive clays below the paleosol, indicates that re-submergence postdates the earliest Wilis eruptions of ~1.9 Ma, which are regarded as the oldest Pleistocene andesitic eruptions of this part of Java **(Section 6.4)**.

The (temporary) re-submergence of this part of eastern Java is remarkable, as around 1.8 Ma Sundaland is generally characterized by widespread subaerial exposure. The shallow sea may have been connected to ocean waters in the east through the ancient Madura Strait **(Fig. 12B)**, or to the Indian Ocean in the south through a tectonic gap in the Southern Mountains, forming a shallow embayment.

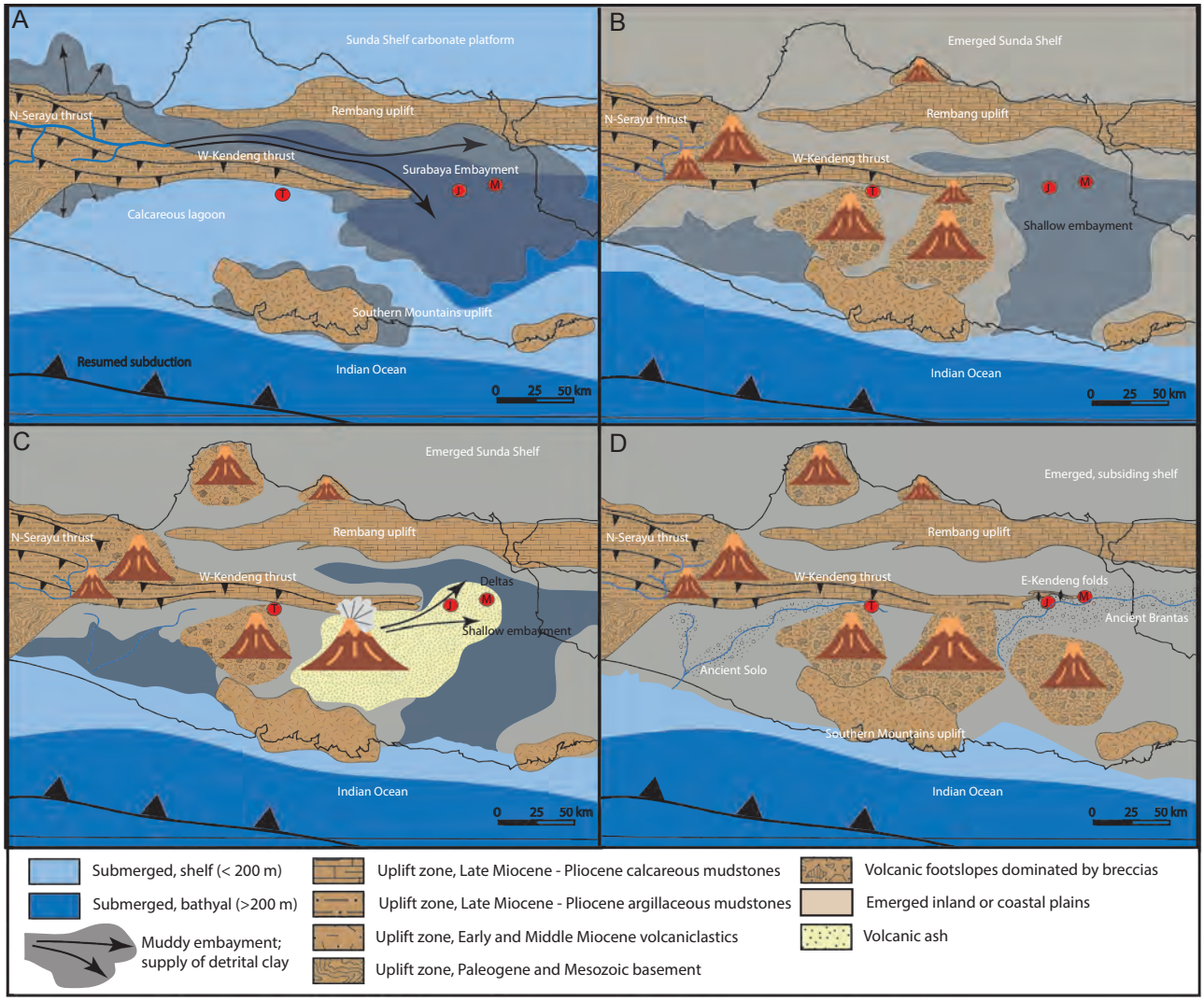


Fig. 12. Paleogeography of eastern Java. **A:** Late Pliocene – Early Pleistocene, ~ 3 Ma to 2 Ma. Narrow embayment between elongate uplift zones (Surabaya Embayment). Upper-bathyal to outer-shelf depth conditions. Sediment supply from North Serayu uplift. **B:** Early Pleistocene ~2 – 1 Ma. Embayment is uplifted, along with the greater Sunda Shelf region. After a stage of emergence, a shallow embayment develops. **C:** Early Pleistocene ~ 1 Ma: Explosive, high-silica eruptions of the Wilis. High supply of unconsolidated ash to the shallow embayment, development of quickly prograding deltas. **D:** Middle Pleistocene: Uplift and incision. Development of Brantas drainage system over the emerged shelf of the current Madura Strait.

The preservation of ca. 125 m of sandy clays, deposited under subtidal and intertidal conditions, points to renewed, gradual subsidence **(Fig. 13)**. The build-up of three superimposed coastal progradation sequences may relate to Early Pleistocene, low-amplitude sea-level fluctuations with a 41-ka cyclicity. Depending on the preservation of successive sea-level cycles, the shallow marine strata may cover several hundred thousand years. Unfortunately, planktonic foraminiferal age control is lost in these shallow marine strata (**Section 5.1**). However, an age anchor is provided the transition to the overlying deltaic series **(Section 6.4)**.

6.4 Explosive volcanism and the development of ash-dominated deltas

The transition to clinoform-bedded tuffaceous sandstones (FA4) represents a drastic landscape change, toward a setting dominated by ash-laden rivers, supplying their sediment load to the shallow embayment. This points to a stage of explosive volcanism in the hinterland, with voluminous ash falls and pyroclastic flows. The Early Pleistocene eruptive stages of the Wilis and Anjasmoro were dominated by intermediary to mafic rocks. The only recorded stage of Early Pleistocene, explosive, high-silica magmatism is associated with remnants of calderas found in the larger Wilis area. This stage is undated, but Hartono (1994) K/Ar-dated pre- and post-caldera andesite rocks, which gives a rough insight into the age the caldera stage. The early, pre-caldera eruptive stages of the Wilis are characterized by basalts, basaltic andesites and andesites with K/Ar-ages between 1.99 and 1.09 Ma. Two samples from a younger eruptive stage, post-dating the caldera, were dated to 0.81 and 0.57 Ma. Although the used bulk-dating technique is probably not very accurate, the data roughly indicate the period between 1.09 and 0.81 Ma as a time window for the caldera stage.

Assuming a causal link between this stage of explosive volcanism and the rapidly prograding deltas **(Fig. 12C)**, the deltaic sandstones may date to ~ 1 Ma. Paleo-climate indicators support this age estimate: The rhythmic build-up of

ashy foresets and clayey interbeds reflects episodes of peak fluvial discharge separated by longer stages of reduced discharge, which points to a strong seasonality. Eastern Java pollen records reflect a change from humid tropical conditions toward more arid conditions with a pronounced rainy season during the Mid Pleistocene Transition (Sémah et al., 2010). Moreover, Morley et al. (2020) described pollen assemblages from the deltaic beds of Mojokerto that point to a mainland vegetation dominated by grasslands.

The ash-rich deltaic series is well traceable over the folds of the eastern Kendeng and probably represents multiple, rapidly prograding deltas along a coastal plain. Seasonal discharge conditions, a thin vegetation cover and abundant fine granular volcanic material may have caused braided fluvial conditions on the plains (Ashworth et al., 1994), with frequently shifting channel patterns and river mouths.

The deltaic series gives an impression of rapid deposition and may very well cover a relatively short time period, possibly of around 100 ka. Unconformities, separating sequences of delta progradation, possibly reflect high-frequency sea-level oscillations, which may roughly be linked to lowstands in the range between MIS32 and MIS26. However, there may also be other factors involved, such as shifts of the river mouth and stages of reduced volcanic supply. A relatively short stage of deltaic progradation, and a preserved thickness of ca. 150 m, point to considerable subsidence, which may have been partly caused by loading of the quickly accumulating sediment body and compaction of the underlying clays **(Fig. 13)**.

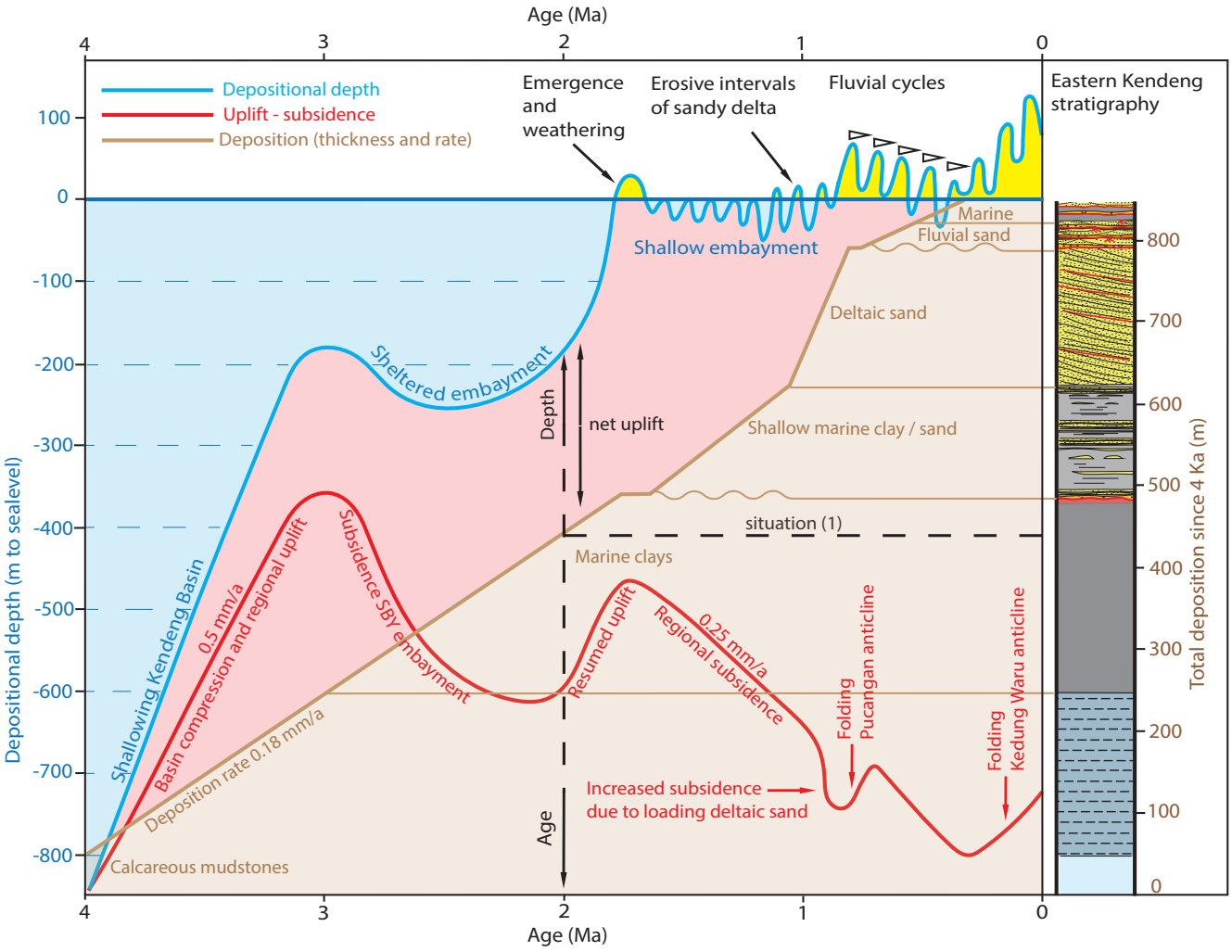


Fig. 13. Model of deposition, uplift and subsidence of the eastern Kendeng for the last 4 Ma. Depositional depth estimates have been based on benthic foraminiferal assemblages and depositional facies. Deposition rate of 0.18 mm/a has been based on planktonic foraminiferal age markers in the upper part of the calcareous mudstone series and has provisionally been extrapolated through the overlying clays. For details, see Berghuis et al. (2019). The pink area represents the difference between total deposition since T0 (4 Ma) and depositional depth, which provides insight into the vertical movement (net uplift) since T0. The red line is the resulting uplift-subsidence curve. How to read: Situation 1 (example). Age: 2 Ma; sediment: massive marine clays; deposition rate: 0.18 mm/a; depositional depth 200 m; vertical movement: uplift rate ca. 0.5 mm/a. The graph gives a general insight into the tectonic history of the eastern Kendeng. From 4 – 3 Ma the area was subject to uplift, probably representing compression of the former back-arc basin. Around 3 Ma the Surabaya Embayment developed between emerging ridges and became subject to temporary subsidence, which we relate to vertical movements along older basement faults. Uplift resumed around 2 Ma. After a stage of subaerial exposure, the area became subject to subsidence, with a rate of ~ 0.25 mm/a, which is within the range of regional shelf subsidence as determined by Sarr et al. (2019). Around 300 ka, the Kedung Waru fold developed, leading to local uplift.

6.5 The deltaic landscape of Mojokerto

The bedded tuffaceous sandstones that form the base of the Mojokerto Section have relatively thick clayey interbeds and lack a prominent depositional dip, pointing to a more distal deltaic setting. The overlying rooted weathering profile reflects sea-level lowering and temporary subaerial exposure of the delta body. Organic clays with pyrite crystals, locally preserved at this level, represent coastal marsh conditions.

The overlying interval of mollusc-rich calcareous siltstones (FA5) points to re-submergence. The ash-dominated composition of the material and its position interbedded between the clinoform-bedded series, links it to the deltaic depositional landscape. We regard the sheltered, shallow marine setting as an interdistributary bay between elongate delta lobes. We infer that the volcanic ash, dominating the sediment of this facies association, was supplied to these bays during episodes of extreme run-off and flooding of the main channels on the delta plain. During subsequent, prolonged calmer stages, clear-water conditions returned and the volcanic ash became thoroughly mixed with calcareous sediment by bioturbation.

The sharp transition to laminated, lacustrine clays (FA5) points to isolation of the former bay, by delta-lobe progradation or by sea-level lowering, forming a coastal lake. The couplets of light and dark laminae probably represent seasonal variation, the lighter-colored laminae reflecting increased supply of detrital clay and fine volcanic ash during the rainy season, probably by flooding stages of the main fluvial channel. The dark laminae reflect intervening calmer periods, characterized by settling of fine organic material. The laminae may be regarded as varve couplets, representing yearly cycles of rainy and dry seasons. With an average thickness of such couplets of 3 or 4 mm, 1 meter of laminated clays may represent a deposition time of ~ 300 years, which agrees with varve-counted sedimentation rates in similar eutrophic lakes in coastal settings (i.e. Kelsey et al., 2005). With a maximum thickness of several meters, the laminated clays represent short-lived coastal lakes.

The overlying series of tuffaceous deltaic sandstones (FA4) represents renewed delta progradation, probably caused by a shift of the river mouth. The stratigraphic position of these clinoforms suggests that the delta partly developed inside the coastal lake. This may explain the relatively steep inclination of the foresets, as fresh-water conditions of the receiving basin must have caused rapid mixing and abrupt sedimentation near the river mouth, forming a Gilbert-type delta (Postma et al., 1990). The preservation of steep foresets must have been aided by the stagnant water conditions, which prevented the delta front from frequent slumping (Nemec, 1990). Moreover, the setting as a stagnant coastal lake with anoxic bottom waters explains the absence of marine fossils in the deltaic beds.

The unconformity that subdivides the inclined strata in two deltaic sets reflects a stage of subaerial exposure and the development of a grassy vegetation cover. The overlying clinoforms reflect re-submergence and continued deltaic progradation, with the flatter foresets and low quantities of admixed shell fragments pointing to a marine setting.

6.6 Fluvial incision of the delta surface

The sandy clinoforms and overlying fluvial strata have since decades been regarded as foresets and topsets (Duyfjes, 1938a; Huffman and Zaim, 2003; Kumai, 1985; Morley et al., 2020). However, the clinoforms (FA4) are made up of fine-grained volcanic ash, with scarce fine pumice gravel, whereas the overlying fluvial sediment (FA6) contains polymict volcanic conglomerates rich in rounded andesite clasts. This great difference in sediment composition and texture indicates that the foresets and the overlying fluvial strata do not represent one and the same depositional system. Instead, the sharp contact between the foresets and the fluvial strata represents younger fluvial incision and forms a hiatus of unknown duration. The conglomerate bed overlying this erosive contact is a lag deposit associated with this incisive stage.

The exposures of Mojokerto provide additional evidence for this younger fluvial truncation of the deltaic series. The fluvial strata overlie the clinoforms without a trace of a sigmoidal transition. Within a deltaic setting, a sharp, planar fluvial truncation surface may be indicative of a stagnant or falling base level. However, tracing the truncation level along the Mojokerto quarries reveals an irregular erosion surface, reflecting a paleo-landscape of incised valleys, much unlike a sea-level controlled delta plain. Moreover, in areas where the delta lobes wedge out, the erosion surface continues and incises the laminated lacustrine clays, again demonstrating that fluvial truncation is unrelated to the prograding delta.

The position of the fluvial strata along the Pucangan anticline north of Jombang suggests that fluvial truncation of the deltaic sands is related to folding and uplift **(Fig. 8A)**. The strata make up the southern footslopes of the anticline, but do not re-appear along the opposite flank. Thus far, this has been explained by lateral facies change **(Fig. 8B)**: shallow marine clays exposed along the north flank were interpreted as the chronostratigraphic equivalent of the fluvial strata along the south flank (Duyfjes, 1938, pp. 48). This stratigraphic approach is based on the assumption that (1) we are looking at an uninterrupted series and (2) folding postdates deposition of the entire series. However, the erosive base of the fluvial strata shows that the assumption of uninterrupted sedimentation is incorrect. The occurrence of the

fluvial strata along the south flank of the anticline indicates that the material was deposited alongside the emerging fold, which suggests that the incisive lower boundary of the strata is linked to fold-related uplift. Differences in tectonic dip support this landscape model. The deltaic sandstones underlying the fluvial strata have an average southward tectonic dip of 30°, whereas the fluvial strata dip only 10° to 15°, suggesting that fluvial deposition postdates initial folding and uplift of the anticline. We conclude that the fluvial strata are part of a fluvial fill that formed in the lowlands south of the upcoming anticline **(Fig. 12D)** and that the erosive base reflects fold-related uplift. The current position of the fluvial strata, uplifted and slightly tilted along the southern foot slopes of the Pucangan anticline, must be a result of later or continued folding.

In the Kedung Waru anticline of Mojokerto, we find the same fluvial series, but here it is included in the fold **(Fig. 11A)**. This illustrates the younger age of the anticline, which is also apparent from its gently dipping flanks and lower altitude. The fluvial strata have a similar incisive lower boundary over the underlying deltaic strata as in the Jombang area, but at this site without a noticeable angular disconformity, as incision predates folding. It is tempting to regard the incision surfaces over the deltaic series of Jombang and Mojokerto as isochronous. Possibly, folding of the Pucangan anticline was accompanied by uplift of a wider area, causing fluvial incision around Jombang and Mojokerto. However, the erosion surface may just as well have a more complex background, reflecting advancing uplift and sea-level cycles.

6.7 Aggradation and degradation of the Middle Pleistocene Brantas

The fluvial series of Jombang and Mojokerto marks the development of a drainage system with its headwaters in the volcanic highland of Mounts Wilis and Anjasmoro and with wide floodplains south of the upcoming eastern Kendeng anticlines **(Fig. 12D)**. This fluvial system was highly similar to the current Brantas and can be regarded as the river's earliest stage.

On seismic profiles of the Madura Strait, the Middle Pleistocene fluvial system can be traced eastwards toward the shelf edge, suggesting a position of Mojokerto ~200 km inland from the coastline (Susilohadi, 1995). The seismic profiles show a prominent erosive surface over the Pliocene marine substrate, testifying to prolonged Madura Strait exposure. This basal erosion surface is currently found ca. 200 m below sea level and is covered with ~ 150 m of marine sediment, consisting of several sequences, each with an incisive base, reflecting intermittent submergence and drainage of the shelf **(Fig. 14A)**. A similar build-up of the seabed has been reported from seismic profiles of the Java Sea (Darmadi et al., 2007). Sarr et al. (2019) and (Husson et al., 2020) linked this to regional, long-wavelength subsidence of the shelf, with the marine sequences overlying the basal unconformity representing an intermittent regime of transgressions dating back to MIS11.

A graphical representation of the subsiding Madura Strait shelf, against the background of the Pleistocene sea-level curve (Bintanja and van de Wal, 2008), provides insight into this process of progressive submergence **(Fig. 14C)**. The black line represents the subsiding shelf edge (current depth 175 – 200 m) under a regional shelf subsidence rate of 0.2 mm/ka (Sarr et al., 2019). This indicates that the subaerially exposed Madura Strait area may have experienced minor overflows of the shelf edge during the highstands of MIS15 and MIS13, but only from MIS11 onwards it fully submerged during highstand conditions.

This landscape model of a gradually subsiding shelf provides a mechanism to explain the aggradation-degradation cycles as recorded by the Mojokerto fluvial series. The cyclic build-up of the fluvial series probably has a complex background, related to sea-level fluctuations, tectonism, climate change and varying volcanic supply. However, Veldkamp and Tebbens (2001) indicated that in the subsiding lower reaches of large Pleistocene rivers, sea-level fluctuations are often the dominant mechanism controlling aggradation and degradation cycles, filtering out the impact of other factors controlling river behavior. We therefore provisionally regard the fluvial cycles of the Mojokerto record as responses to intermittent, sea-level controlled drowning of the floodplain downstream of Mojokerto.

For a reconstruction of aggradation-degradation cycles, we simulated the equilibrium profile of the Middle Pleistocene Brantas, referring to the similarly dimensioned and well-studied longitudinal profile of the Meuse (Tebbens et al., 1999). Like the ancient Brantas, this river has a ca. 200 km long lower reach of coastal lowlands, and a slightly uplifted middle reach. Middle Pleistocene Mojokerto was part of the subsiding lower reach of the river, with a setting similar to the present-day coastal plains of Surabaya and Mojokerto. Referring to the gravelly texture of the channel deposits and a position adjacent to the Kendeng uplift, we projected the position of Middle Pleistocene Mojokerto close to the hinge line that marks the transition toward the uplifted middle reach, with an estimated riverbed height of ~70 m above base level in equilibrium conditions **(Fig. 14B)**.

Our reconstructions suggest that before MIS19, sea level probably remained below the edge of the subsiding shelf and sea-level fluctuations did not have a notable impact on river behaviour. The MIS19 and MIS17 highstands may have caused minor flooding of the river-mouth area, but we assume that the Brantas profile remained in its equilibrium state, with around Mojokerto a stable altitude of ~70 m above the shelf edge **(Fig. 14B)**. MIS15 caused the

first stage of more significant flooding of the shelf edge, forcing the river to readjust its longitudinal profile by gradient backfilling in its downstream reach. We provisionally regard the first aggradational fluvial sequence of Mojokerto, overlying the basal conglomerate bed, as this MIS15-related fluvial depositional wedge.

The overlying erosion surface, marked by the second conglomerate lag, is tied to the MIS14 lowstand. Likewise, the subsequent aggradational sequence and the overlying incisive conglomerate bed may be tied to MIS13 and MIS12.

During the two intervening lowstands (MIS14 and MIS12), sea levels dropped below the shelf edge and the river may have degraded its valley back to its equilibrium state 70 m above the shelf edge. The fact that around Mojokerto, fluvial aggradation sequences are partly preserved suggests that valley-degradation stages were not long or intense enough to re-establish the river's equilibrium profile. But the partial preservation of aggradation sequences may also have had other causes, such as a local subsidence rate that slightly exceeded regional subsidence. In **Fig. 14B**, we projected the base of each consecutive incision stage at the assumed equilibrium position of 70 m above base level, which results in an (apparent) local subsidence rate of 0.25 mm/a.

MIS11 is characterized by an extreme sea-level rise, reaching a level that slightly exceeds present-day sea level. In combination with continued shelf subsidence, this resulted in widespread submergence of the shelf. Our river profile reconstructions suggest that the Brantas valley drowned beyond Mojokerto, setting the floodplain of Mojokerto ca. 25 m below sea level. This would explain the build-up of the third aggradational sequence of Mojokerto, which grades upwards into this first marine interval. The subsequent MIS10 lowstand resulted in a rapid base-level fall of more than 100 m. We relate the deep, channelled incisions into the marine interval of Mojokerto to this stage of intense fluvial downcutting. During the subsequent highstand of MIS9, this incised landscape again drowned, forming the second marine interval, which again became incised during the subsequent lowstand of MIS8.

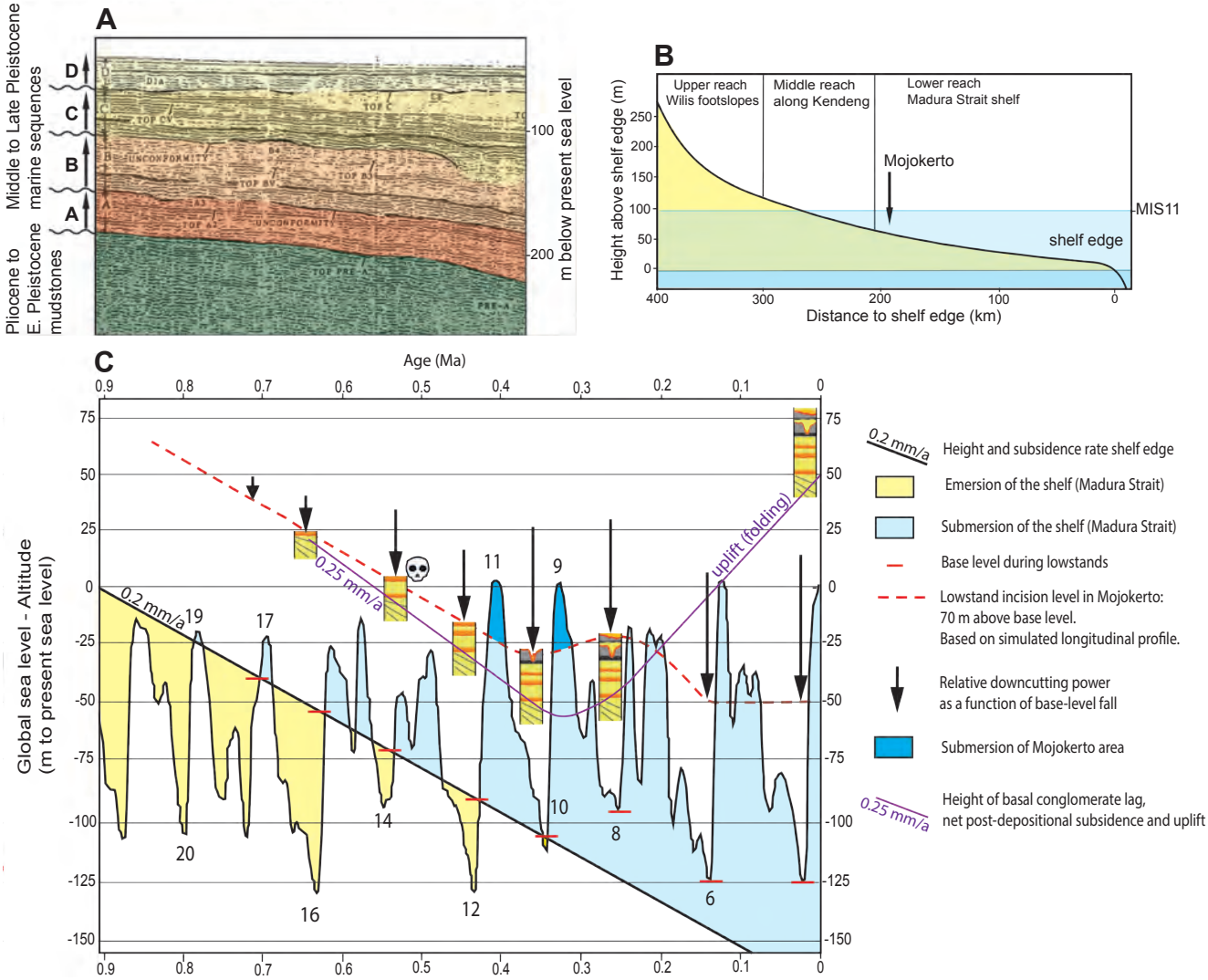


Fig. 14. A: Seismic profile over the Madura Strait (Susilohadi, 1995). Basal unconformity represents prolonged Early Pleistocene subaerial exposure. Overlying marine sequences with incised top represent intermittent re-submergence of the shelf during highstands, under regional subsidence. First large-scale submergence is linked to MIS 11 (Sarr et al, 2019). **B:** Simulated longitudinal equilibrium profile of the Middle Pleistocene Brantas during sea-level lowstand, with water level below the shelf edge. Subsidence resulted in overflows of the shelf edge during highstands, reaching increasingly further inland. During MIS11, flooding of the Brantas drainage system reached beyond Mojokerto. **C:** Reconstruction of successive fluvial cycles in relation to sea-level fluctuations and subsidence. The Perning skullcap was found in the conglomerate lag that forms the base of the second fluvial sequence, suggesting an MIS14 age. Sea-level curve based on Bintanja and Van de Wal, 2008.

From MIS8 onwards, lowstand sea levels remained above the shelf edge and consequently the Brantas base level was determined solely by global sea level. Assuming that MIS8 degradation reached the river's equilibrium profile, with a local erosion base 70 m above lowstand sea level, suggests a change in local tectonic conditions toward uplift **(Fig. 14B)**. This is not surprising, as currently the fluvial series forms the top of the Kedung Waru anticline. Apparently, Kedung Waru folding dates back to ca. 300 ka, pushing up the valley floor and forming an anticline alongside the Brantas. Younger sea-level cycles must have continued to cause valley degradation and aggradation, but only in the active floodplain south of the anticline. The MIS6 and MIS4 degradation stages must have incised the valley floor down to ~ 50 m below present-day sea level. The gravelly lags of these incision stages are buried under the Holocene fill that constitutes the current Brantas floodplain.

6.8 Age of the fossil-bearing fluvial strata of Mojokerto

Our study suggests that the bone-bearing fluvial strata of Mojokerto are significantly younger than previously thought. Whereas commonly regarded as Early Pleistocene, we propose a Middle Pleistocene age, roughly ranging between MIS16 and MIS11. This new age estimate solves an important biostratigraphic inconsistency, as the vertebrate fossil assemblage of Mojokerto is commonly recognized as the Middle Pleistocene Kedung Brubus Fauna. Moreover, it is in line with the climate record of eastern Java. Several authors reported humid tropical conditions during most of the Early Pleistocene, changing toward more arid conditions with a pronounced rainy season during the Mid Pleistocene Transition, referring to pollen records (Sémah et al., 2010), paleosols (Berghuis et al., 2021; Brasseur et al., 2011) and isotope ratios in herbivore molars (Janssen et al., 2016; Puspaningrum et al., 2020). The previous, Early Pleistocene age estimates of the fluvial, fossil-bearing strata therefore imply that they were formed under humid tropical conditions, however floodplain soils with carbonate concretions and grassy rootlets, as well as a grass-dominated pollen record, point to a relatively dry climate and open vegetation.

However, a Middle Pleistocene age is in conflict with the published paleomagnetic measurements of Mojokerto (Hyodo et al., 1993). Our new age model suggests that the transition from predominantly reversed polarities in the deltaic beds to predominantly normal or intermediate polarities in the overlying fluvial beds represents the Brunhes-Matuyama polarity change, however this is incompatible with the reported reversed polarities higher in the stratigraphy. Magnetic overprint of the primary signal cannot explain this discrepancy, as after the Brunhes-Matuyama transition, no significant polarity changes have occurred. The discrepancy may be related to Middle Pleistocene geomagnetic excursions (Laj and Channell, 2007) or to different stratigraphic interpretations. With respect to the latter, we note that Hyodo et al. (1993) described a 200 m thick depositional record along Kepuhklagen Road, with long unexposed intervals and undetailed facies descriptions, based on earlier work of Kumai (1985). Sampling was carried out along the roadside section over a distance of more than 2 km, extrapolating the sample positions to their 200 m long stratigraphic column. Our stratigraphic section **(Fig. 9)**, based on carefully measured quarry sections directly east of the road, covers a total exposed thickness of only 53 m, leaving virtually no unexposed intervals. Kumai (1985) and Hyodo et al. (1993) based their stratigraphic interpretations on Duyfjes' (1938) cross-section over the area, which is, as we showed in **Section 5.2** and **Fig. 11**, an incorrect representation of the Kedung Waru fold.

Our revised age estimate for the fluvial strata of Mojokerto also conflicts with the published radiometric ages of 1.81 ± 0.04 Ma (Swisher et al., 1994) and 1.49 ± 0.13 Ma (Morwood et al., 2003). These ages, either crystallization or eruption ages, have been accepted to approximate the age of deposition, based on the assumption that pumice-bearing conglomerate beds represent 'short influxes of coarse volcanic material to the delta plain, triggered by distant volcanism' (Huffman, 2001a; Huffman and Zaim, 2003). For the conglomerate beds this is highly unlikely, considering the vast surface of the floodplain and the great distance to the volcanoes. Moreover, it is in contradiction with the polymict composition and moderate to well rounding of the material, and with the incisive base of the beds. These conglomerate beds are clearly lags associated with fluvial incision stages and are made up of reworked material, which readily explains the old radiometric ages. Morwood et al. (2003) reportedly sampled the dated pumice from a 15 cm thick interbed dominated by pumice gravel, which the authors relate to contemporary eruptions. This may indeed be a valid argumentation. But on the other hand, pumice gravel is one of the most common components of the polymict conglomerates. Local and hinterland incision must therefore have involved remobilization of older, loose pumice, which may occasionally have become concentrated in fluvial sediment by selective sorting.

6.9 Age and habitat of the Mojokerto *Homo erectus*

Our reconstructions of fluvial incision and aggradation cycles indicate that the conglomerate bed that yielded the Mojokerto skullcap may be linked to the MIS14 lowstand, which dates to ~ 550 ka (Railsback et al., 2015). The vertebrate fossils in the incisive conglomerate beds were found as single bones and bone fragments. Locally, these conglomerates are particularly rich in fossils, pointing to hydraulic accumulation, possibly in the inside bend of the meandering channel. The bones may represent a contemporaneous fauna, deriving from carcasses on the floodplain, which were picked up during flooding stages and re-deposited in the channel. However, considering the incisive background of the conglomerate beds, bones may also have been reworked from underlying aggradational fluvial sequences. Fluvial

incision may have preferentially removed fine sediment, leaving a lag of skeletal material, exhumed from the previous fluvial sequence (Rogers and Kidwell, 2007). This implies that the hominin skullcap may either be contemporaneous with the MIS14 conglomerate bed in which the fossil was found, or may have been reworked from the underlying MIS15 aggradational sequence, implying a possible age range of ~ 600 – 550 ka. It cannot be ruled out that the fossil was reworked from even older strata, eroded upstream. However, referring to the fragile nature of the skullcap and the absence of abrasion marks, such a background is considered unlikely.

Our re-interpretations also imply a revision of the habitat of the Mojokerto *Homo erectus*. Previously regarded as a coastal environment, based on an assumed topset relation with the underlying deltaic series (Huffman, 2001a; Huffman and Zaim, 2003; Morley et al., 2020), we replace this image for the inland floodplain of the ancient Brantas. Floodplain soils with carbonate concretions and grassy rootlets point to a relatively dry climate and open vegetation. A published record of pollen and spores from the fluvial series of Mojokerto reflects a vegetation dominated by grasses with few trees, with local swamp forests dominated by marsh ferns (Morley et al., 2020). The swamp forests are probably related to the low-lying, frequently inundated floodplains of the anastomosed river. Mangrove pollen are scarce or absent in the fluvial series, confirming a setting that was, at least most of the time, at considerable distance from the coast. Scattered mangrove pollen were found shortly below the hominin bed, pointing to an approaching coastline at the top of the underlying fluvial sequence. The hominin-bearing conglomerate bed, probably representing a subsequent lowstand, is devoid of mangrove pollen. Scattered mangrove pollen were also reported higher-up in the fluvial series, below the marine interval, again heralding the approaching coastline. Scarce occurrences of pollen from montane trees must have been transported from the forested slopes of Mounts Wilis and Anjasmoro.

Although climate conditions may have been dryer than today, the large and forested hinterland probably secured perennial discharge of the river. This year-round availability of water, and the presence of herds of grazers, which dominate the local vertebrate-fossil assemblage, must have made the Middle Pleistocene Brantas valley and the surrounding grass-covered plains a suitable area for enduring hominin presence.

6.10 Validating the revised age model of the Mojokerto fossiliferous beds

To test our age estimate for the fossiliferous fluvial deposits, single-grain Ar/Ar dating may be carried out on multiple volcanic hornblende and potassium feldspar crystals, following the approach of Hilgen et al. (under review). In order to get insight into a possible difference between hornblende crystallization ages and eruption ages, additional fission-track dating may be carried out, preferably on minerals from the same pumice as sampled for the Ar/Ar dating. We postulate that this will yield a wide range of ages, representing the complex incisive origin of the sediment. The age range will provide insight into the maximum age of a layer, with the youngest age of the range ideally being a maximum age close to the depositional age. Our age framework suggests that the fluvial sequences at the top of the Mojokerto series, overlying the first marine incursion, relate to stages of rising sea level after the lowstands of MIS10 and MIS8 **(Fig. 14)**. This implies that ages may fall within the range of optical dating methods, which can be tested by OSL-dating.

The fossiliferous strata of Mojokerto consist of superimposed fluvial sequences separated by erosion surfaces. This asks for a sampling and dating strategy that aims for dating individual sequences. The numerical ages can then be used to validate or adjust our correlations with the Pleistocene sea-level curve.

Renewed paleomagnetic measurements, in combination with multiple Ar/Ar dating, will also be of great value. Sampling can be carried out in open quarry sections, to make sure that there is no uncertainty over stratigraphic position. And again, sampling and interpretation should bear in mind the build-up of stacked depositional sequences.

A significant age difference is expected between the sediment on either side of the basal fluvial erosion surface, i.e. between the top of the deltaic series and the lowest fluvial sequence. As we relate the stage of delta progradation to explosive volcanism, this sediment may offer good possibilities to find contemporaneous eruption products, providing an important age constraint for the overlying fluvial strata that likely have a more mixed composition.

7. Implications for the eastern Java stratigraphy

Our re-interpretation of the eastern Kendeng reference sections sheds a new light over the significance of Duyfjes' (1938) stratigraphy. We identified most of the sedimentary record as the fill of a local embayment. Extrapolation of these units to areas such as Trinil, located outside this former embayment, has little lithological or paleo-environmental significance and merely suggests age relations, most of which are unproven. The only exception is the Kalibeng Formation, which is a regional unit that predates the embayment.

Duyfjes indicated the marine clays, overlying the Kalibeng Formation, as the Clay Facies of the Pucangan Formation. The clays represent the most prominent facies of the embayment fill and are also found in the subsoil of the Randublatung Valley and around Surabaya. The eastern Kendeng Hills are in fact a series of young folds over the former

embayment area, offering a unique insight into the embayment fill. Unfortunately, early researchers describing wells in the adjacent plains were not fully aware of this situation and gave these clays different names, such as Mergel Ton (Trooster, 1937), Blue Clays (van Bemmelen, 1949) or Lidah Formation (Brouwer, 1966). Lately, there is a tendency to expand the name Lidah Formation to the clays exposed in the eastern Kendeng (Pringgoprawiro, 1983), which is a stratigraphic improvement that we follow in this paper.

We found the clays of the eastern Kendeng to be made up of two series, separated by a paleosol. The lower series, consisting of massive clays with a shelfal and upper bathyal benthic foraminiferal fauna (FA2), represents the early, deep-water stage of the Surabaya Embayment. The overlying series consist of shallow marine clay-sand alternations with a neritic benthic foraminiferal fauna and shell fragments (FA3) and represent a later marine incursion, in the form of a shallow embayment. We propose to assign these series to separate members, Lidah-1 and Lidah-2. Wells in the nearby plains (Bolli, 1966) indicate a similar build-up, of massive clays that may be referred to as Lidah-1 overlain by sandy clays that may be referred to as Lidah-2. However, we note that the chronological and paleogeographic significance of the two clay-series may differ from site to site and needs further investigation. For example, in the coastal plains, the top of the clays is probably of Middle Pleistocene age, representing intermittent transgressions dating back to MIS11.

In the eastern Kendeng, the shallow marine clays are capped with tuffaceous deltaic sands (FA4), which we linked to a short stage of explosive volcanism. Similar strata have not been reported from wells in the nearby Randublatung Valley, suggesting that the material wedges out to the north and east, or that the shallow marine inlet that was filled by the delta did not cover the entire area of the previous deep-water embayment **(Fig. 12C)**. Duyfjes regarded this material as the Volcanic Facies of the Pucangan Formation. We propose to hold on to this well-known unit name, but restrict its use to the tuffaceous deltaic series of the eastern Kendeng. Extrapolations to other areas and to strata with different facies suggest unfounded age relations and should be avoided.

The fluvial top of the eastern Kendeng series (FA6) is not part of the actual embayment fill, but relates to the Brantas drainage system that developed later. This readily explains the problems involved with the historic correlations, for example to the Trinil area **(Fig. 2)**. Although ages may partly overlap, the fluvial strata of the eastern Kendeng and Trinil represent different drainage systems, with other source areas of their sediment load and a different tectonic and volcanic control of incision and aggradation. The fluvial strata of the ancient Brantas system may be referred to as the Kabuh Formation, holding on to Duyfjes' unit name. Note that Duyfjes placed the lower boundary of the Kabuh Formation ca. 20 m higher, adding the base of the fluvial strata to the Pucangan Formation, based on an assumed difference in vertebrate fossil assemblages within the fluvial series. After the faunal revision by De Vos et al., (1982), this practice has lost its significance. We propose to place the boundary between the Pucangan and Kabuh Formations at the erosive base of the fluvial series.

8. CONCLUSIONS

The regressive series of the eastern Kendeng represents the fill of a relatively deep Plio-Pleistocene embayment, situated between emerging uplift zones, which we refer to as the Surabaya Embayment. The eastern Kendeng stratigraphic units, defined in the 1930's and until today regarded as a regional standard, have local significance only.

The embayment formed ~3 Ma, as the emerging Rembang Ridge shut-off the area from the calcareous shelf in the north. Around 2 Ma the embayment emerged, along with the greater Sunda Shelf, which left a paleosol on the >200 m thick clayey embayment fill. Shallow marine clays overlying the paleosol reflect renewed submergence and the development of a shallow embayment.

A transition to deltaic sandstones indicates a sharply increased supply of volcanic ash, which we relate to a stage of explosive, high-silica volcanism of the Wilis and which probably dates from the period between ~1.09 and 0.81 Ma. The Mojokerto delta, with its steeply inclined foresets, was part of this larger delta landscape and formed in an interdistributary bay and associated coastal lake.

The top of the eastern Kendeng series consists of fluvial strata, which have an incisive base and are unrelated to the underlying deltaic deposits. We link this fluvial cover to the early Brantas, which had a similar position as the present-day Brantas, but continued over the emerged Madura Strait toward the shelf edge, ~ 200 km to the east. Shelf subsidence in combination with sea-level fluctuations caused intermittent flooding of the shelf edge.

The fluvial, vertebrate-bearing strata have a cyclic build-up, representing alternating aggradation and degradation stages, which we provisionally link to sea-level fluctuations. Our reconstruction of these aggradation and degradation stages provides a new age framework. Previously regarded as Early Pleistocene, we propose a Middle Pleistocene age for the fluvial strata. This solves an important biostratigraphic inconsistency, as the vertebrate fossil assemblage of the material is commonly recognized as the Middle Pleistocene Kedung Brubus Fauna.

We link the conglomerate bed that yielded the Mojokerto skullcap to lowstand MIS14, with an age of ~ 550 ka. The fossil may be contemporaneous to this conglomerate bed, but considering the incisive background of the bed, it may also have been reworked from the previous aggradational sequence linked to MIS15, dating to ~600 ka.

Our age estimate of the hominin-bearing conglomerate bed of Mojokerto is significantly younger than the published Ar/Ar-age of 1.81 ± 0.04 Ma (Swisher et al., 1994) and fission track-age of 1.49 ± 0.13 Ma (Morwood et al., 2003). These authors linked the conglomerates to volcanic events, assuming that the obtained numerical ages approximate the age of deposition. However, our re-interpretation of the conglomerate beds as fluvial lags associated with incisive stages of the Brantas, implies that the material probably derived from an incised volcanic hinterland. To test our age estimates, a combination of multiple single-grain Ar/Ar and fission-track dating may be carried out. We expect that this will yield a wide range of ages, with the youngest age of the range ideally being a maximum age close to the depositional age. The youngest strata of the fluvial series may fall into the age range for OSL-dating.

A Middle Pleistocene age of the fossiliferous strata of Mojokerto is supported by normal paleomagnetic polarities. However, Hyodo et al. (1993) reported a return to reversed polarities higher in the stratigraphy, which conflicts with our age interpretation. We infer that this discrepancy is related to a Middle Pleistocene magnetic excursion or to the previous, incorrect interpretation of the local stratigraphy, which was based on roadside observations with thick unexposed intervals. Our interpretations have been based on a study of recent sand quarries, which provide a full exposure of the strata that make up the anticline. A renewed paleomagnetic study, based on samples from open quarry sections, may provide a final answer on this matter.

Finally, our re-interpretations involve a revision of the habitat of the Mojokerto *Homo erectus*. The previous claims of a coastal habitat were based on an assumed foreset- topset-relation with the underlying deltaic series. We replace this for the inland fluvial plains of the perennial Brantas, surrounded by savannah-like plains.



The deltaic sandstones of the Mojokerto area, quarry of Kepuh Klagen.



Chapter 5

Response the comment by Huffman and Zaim

CHAPTER 5

Response to the comment by Huffman and Zaim

H.W.K. Berghuis, Thijs van Kolfschoten, Shinatria Adhityatama, S.R. Troelstra, Sofwan Noerwidi, Rusyad Adi Suriyanto, Unggul Prasetyo Wibowo, Eduard Pop, Iwan Kurniawan, Sander L. Hilgen, A. Veldkamp, Josephine C.A. Joordens

Published in: *Quaternary Science Reviews* (2023)

Huffman and Zaim (2023) published a comment in Quaternary Science Reviews:

Geological age estimate for the Mojokerto child's skull Homo erectus; comment on Berghuis et al. "The eastern Kendeng Hills (Java, Indonesia) and the hominin-bearing beds of Mojokerto, a reinterpretation"

We gratefully accepted the offer by the journal to write a response. This became an interesting and valuable debate. For a full understanding and appreciation, the reader may have to refer to the published comment by Huffman and Zaim (2023).

Response to the comment by Huffman and Zaim

Huffman and Zaim criticize our analysis of the stratigraphic context and age of the *Homo erectus* child skull from Mojokerto. The disagreement stems from our different points of departure. Huffman and Zaim base their analysis and conclusions on sedimentological interpretations and stratigraphic models of the 1930's, wherein strata and their assumed ages are correlated over large distances across eastern Java (Duyfjes, 1936, 1938a).

In contrast, our recent studies in the Trinil (Berghuis et al., 2021) and Mojokerto areas (Berghuis et al., 2022) have revealed an area-specific intricate build-up of shallow marine and fluvial sequences, often separated by irregular incisive contacts, testifying of highly dynamic Pleistocene landscapes subject to volcanism, tectonism and sea-level fluctuations. For Trinil, our findings have in the meantime been confirmed by a detailed dating study (Hilgen et al., 2023). This underlines the need for a local instead of a regional sedimentological approach. We are aware that our observations and interpretations are often in sharp contrast with almost 100 years of geological and paleontological literature and it is understandable that this arouses confusion or disbelief. We are therefore pleased with the comments by Huffman and Zaim and with the opportunity given by QSR to respond.

Huffman and Zaim put forward several substantive matters that are interesting to discuss. For our response, we frequently refer to illustrations in our 2022 publication. For convenient reading, we added the composite stratigraphic column of the Mojokerto area (Fig. 9 of Berghuis et al., 2022) to this article as **Fig. 1A**. This may be held next to the stratigraphic column (Fig. 1C) of the comments by Huffman and Zaim.

The basis of their comment is that the authors insist that the hominin-bearing bed is part of a deltaic sequence. *The hominin-bearing lens occurs in deltaic strata … (which) we informally refer to as the Klagen beds (Lines 41-43).* While understandable, this interpretation is incorrect and can easily be refuted. Indeed, the exposures are dominated by a conspicuous clinoform-bedded unit, consisting of fine tuffaceous sand with clayey interbeds, reflecting shallow-water deltaic progradation. We described this material in Section 4 of Berghuis et al. (2022) as Facies Association 4.

The material is nicely shown in the quarry photograph of Huffman and Zaim (Fig. 1D of their comment). The authors regard this photograph, which was first published in Huffman and Zaim (2003), as a textbook example of delta progradation, with foresets (indicated as B) overlain by topsets (indicated as A). The authors further state: *The A/B relationship and bed sets … are pertinent to determining the geological age of the discovery area succession (Lines 64 – 65).* However, as the two insets of their picture show, there is no sedimentological or lithological difference between B and A, except for a difference in clinoform dip. This is a very common feature within the deltaic series of this area. The strata form sets, representing superimposed deltaic progradation sequences. See for good examples Fig. 4 (photo 11) and Fig. 5 (photo 11) of Berghuis et al. (2022). The contact between these bed sets are internal unconformities, which may have different backgrounds, such as a shifted position of the distributary channel, a short pause in the supply of fresh volcanic ash, or a sea-level change. Individual deltaic sets may have a somewhat different clinoform dip (value and direction). Indeed, one of the interesting features of the deltaic strata of Mojokerto is the relatively steep dip of the lowest clinoform set. This probably relates to deltaic progradation under sheltered conditions, which may have been an interdistributary lagoon or a coastal lake (see section 6.5 of Berghuis et al., 2022). In any case, the B-A contact, by Huffman and Zaim indicated as an important (*pertinent*) boundary between foresets and topsets is in fact 'only' a boundary between two clinoform sets. Bed set A has a lower dip, which gives an appearance of a foreset-topset relation. Note that the quarry photograph (Fig. 1D of the comments) only offers a single perspective and that Huffman and Zaim do not specify the view direction or any measured clinoform dip. Note also that we indicated a similar (possibly the same) build-up of two superimposed clinoform sets in our composite stratigraphic section (**Fig. 1A of this article)**.

Thus, having misidentified foresets for topsets, Huffman and Zaim proceed by stating that the fluvial conglomerates overlying the deltaic series (in their Fig. 1C indicated as MS or monument sandstone) are part of this 'topset association'. In their text: … *the marine topsets that concordantly underlie the MS (Line 83)*. However, the conglomerate bed has a sharp lower boundary, truncating the underlying deltaic strata, certainly not concordantly, which would also be highly unusual for a fluvial channel lag. The authors probably intend to say that they regard the conglomerate bed to be part of their 'topset association'. Indeed, the deltaic beds and the overlying horizontal fluvial bed have the appearance of a foreset-topset relation. The fact that the contact between these elements is erosive (instead of more gradual or sigmaoid) is not in conflict with such an interpretation, but would merely indicate a stagnant or falling baselevel during delta progradation.

However, a great difference in texture and sediment composition shows that the deltaic beds (all of which are foresets) and the overlying conglomerates cannot represent one and the same system of deltaic progradation. The deltaic strata are made up of fine-grained volcanic ash with scarce fine, angular pumice gravel. The overlying fluvial bed is a polymict conglomerate with medium to coarse, well-rounded andesite clasts. Whereas the deltaic series represents a coastal landscape-setting under an extremely high supply of suspended fine-grained volcanic matter by ash-choked

rivers, the conglomerate reflects a large and stable river landscape, with long-distance bedload transport of erosion material from the volcanic hinterland. The lower boundary of the conglomerate must therefore be a younger fluvial truncation of the delta body, representing a hiatus in the depositional record, which makes this contact the real *pertinent* stratigraphic boundary of the Mojokerto section.

Huffman and Zaim proceed to add all overlying fluvial strata to the delta sequence: *The Klagen beds are best interpreted as the product of a prograding, river-dominated, sand rich marine delta lobe (Line 92).* This is a peculiar interpretation, which implies that this deltaic sequence is made up of ~15 m of foresets overlain by ~ 40 m of topsets (thicknesses based on the stratigraphic column of Huffman and Zaim, Fig. 1C). It is hard to imagine a landscape background for such a sequence. The deposition and preservation of this thick, uninterrupted topset series would have required a situation of considerable sea-level rise, whereas at the same time deltaic progradation continued and the delta plain did not drown. Note also that according to the landscape sketches of for example Huffman et al. (2007) the coastline was always in the immediate vicinity. This is a very unlikely representation of the coastal landscape. Remarkably, the authors suggested in Huffman and Zaim (2003) that this thick 'topset series' may relate to a glacio-eustatic drop in sea level, a statement that was repeated in Morley et al. (2020), to which Huffman and Zaim contributed as co-author. This is a puzzling statement. A lowstand would cause emergence and incision of the coastal delta and not the accumulation of a 40 m thick 'topset' series.

In Berghuis et al. (2022) we presented a new landscape model, in which the fluvial series is unrelated to the underlying deltaic series. We showed that the fluvial series has a cyclic build-up of three stacked fluvial sequences **(Fig. 1A of this article)**, each with an erosive base marked by a conglomerate bed, which we regard as fluvial aggradation - degradation cycles on a subsiding floodplain. They relate to a large river system, which may be the early Brantas. We tentatively linked the fluvial sequences to Middle Pleistocene sea-level fluctuations (**Fig. 1B of this article**. See for a detailed explanation Section 6.7 of Berghuis et al., 2022). The vertebrate fossils are concentrated in the conglomerate beds marking the base of the fluvial sequences. The third fluvial cycle grades into marine clays, which shows that eventually the floodplain drowned, a transgression which we tentatively linked to MIS11.

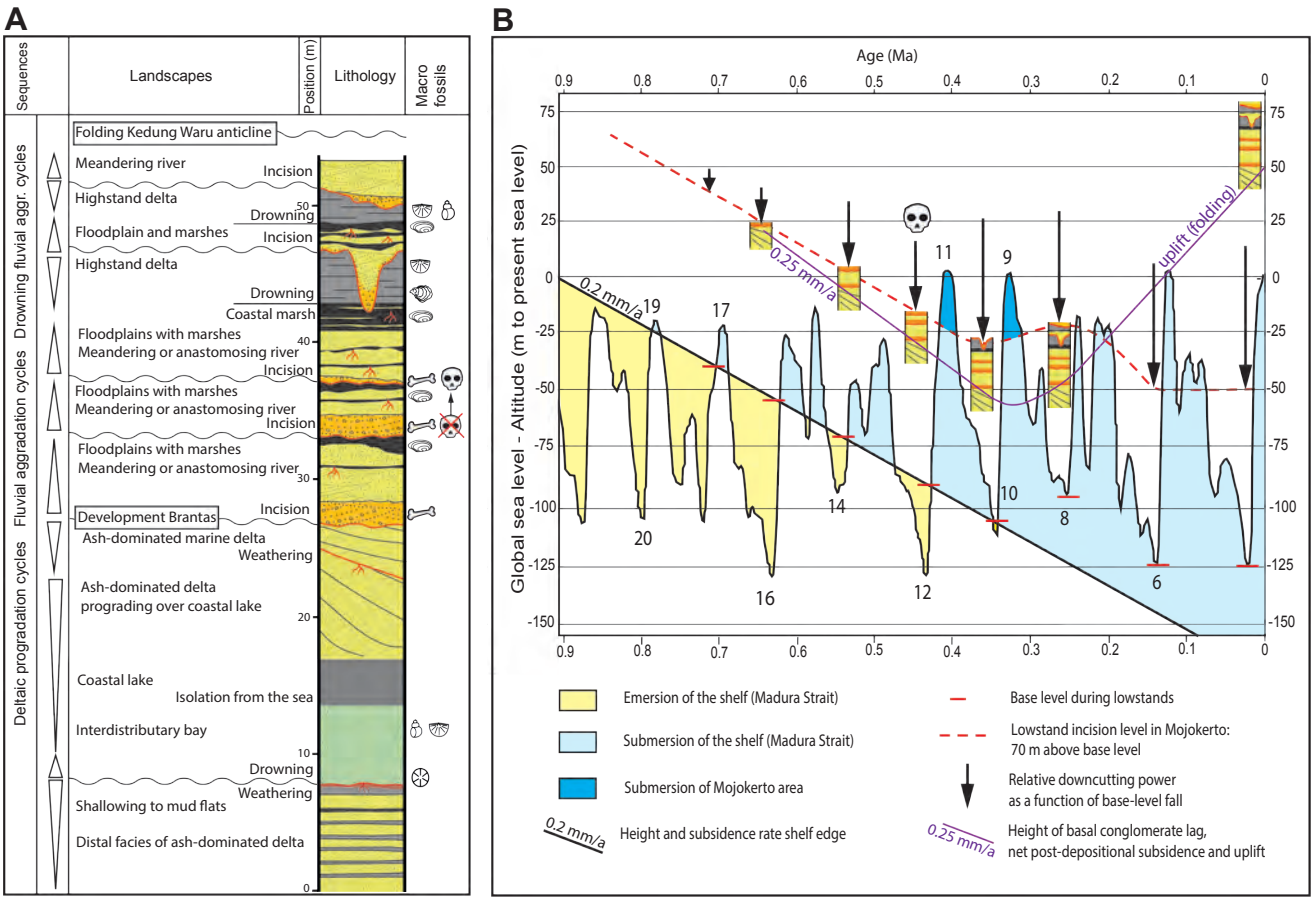


Fig. 1. A: Composite stratigraphic column of the Kedung Waru anticline north of Mojokerto, based on quarry sections east of Kepuhklagen Road. From: Berghuis et al. (2022). Please refer to this paper for detailed facies descriptions. Note the revised stratigraphic level of the Perning Homo erectus skull. **B:** Reconstruction of successive fluvial cycles in relation to sea-level fluctuations and subsidence. From: Berghuis et al. (2022). Please refer to this paper for more information. Based on the comment by Huffman and Zaim we changed the correlation of the 1936 find level of the Perning skull to the conglomerate lag that forms the base of the third fluvial sequence, suggesting an MIS12 age for the hominin-bearing layer. Sea-level curve based on Bintanja and van de Wal (2008).

With respect to the position of the hominin-bearing bed within these fluvial sequences, Huffman and Zaim bring in an important observation. The authors state: … *mudstone with paleosol development overlies the PB* (Perning Bone bed) *and the burrowed sandstone marking the subsequent marine flooding (Line 77).* The authors base this observation on their excellent study to relocate the 1936 find site of the *Homo erectus* skull, which included site clearance and test excavations and yielded a detailed stratigraphy of the skull discovery site (Huffman et al., 2006). The find site lies just outside the large new quarries and is today fully overgrown. In the field, we correlated the 1936 find site with the conglomerate bed that marks the base of the second fluvial sequence. However, the observation of Huffman and Zaim indicates that our correlation is incorrect and that the hominin skull actually derives from the overlying conglomerate bed, which marks the incisive base of the third fluvial sequence **(Fig. 1A of this response to comment)**. Referring to our correlations with the sea-level curve **(Fig. 1B)**, this ties the hominin-bearing conglomerate to MIS12 (instead of MIS14, as was suggested in Berghuis et al., 2022), giving a revised age estimate of ~450 ka.

We hope that we have been able to clarify our interpretations, and we are grateful to Huffman and Zaim for pointing out their detailed observations of the sediments at the *Homo erectus* find site, thus allowing us to further refine our correlation with the sea-level curve.



The BMS land reclamation shortly after its completion in 2015. View to the east.
On the background, ships are passing by, on their way to the port of Tanjung Perak (Surabaya).



Chapter 6

A late Middle Pleistocene lowstand valley of the Solo River on the Madura Strait seabed, geology and age of the first hominin locality of submerged Sundaland

CHAPTER 6

A late Middle Pleistocene lowstand valley of the Solo River on the Madura Strait seabed, geology and age of the first hominin locality of submerged Sundaland

H.W.K. Berghuis, A. Veldkamp, Shinatria Adhityatama, Tony Reimann, Alice Versendaal, Iwan Kurniawan, Eduard Pop, Thijs van Kolfschoten, Josephine C.A. Joordens

Published in: *Quaternary Environments and Humans* (2025)

Abstract

The island of Java (Indonesia) is renowned for its Pleistocene hominin-bearing vertebrate fossil sites. Recently, a marine sand extraction work in the Madura Strait, off the coast of Surabaya, hit upon vertebrate-rich sandstones. More than 6,000 vertebrate fossils have been retrieved from the dredged sand, amongst which are two skull fragments ascribed to *Homo erectus*. The fossils form the first vertebrate record from submerged Sundaland, the lowland plains that connected the great islands of western Indonesia to the Asian mainland during Middle and Late Pleistocene lowstands. Here we present the results of a comprehensive study of the age, depositional background and landscape setting of the subsea fossil locality. The fossiliferous sandstones form the fill of a lowstand valley of the Solo River. The material was OSL-dated to 162 +/- 31 and 119 +/- 27 ka, which links the valley to the lowstand of MIS6. Fluvial backfilling was probably related to the stage of rising sea in the run-up to MIS5. The top of the valley fill consists of marine sandstones, pointing to valley drowning and a change to estuarine conditions, probably during peak highstand conditions of MIS5e. The Madura Strait submerged valley is of similar age as the Solo terrace of Ngandong, one of the richest *Homo erectus* sites of Java and regarded as yielding the youngest record of this species.

1. Introduction and aims

In 2014 and 2015, a total volume of >5 million m3 of sand was extracted from the Madura Strait seabed north of Surabaya (Indonesia) and used for the development of a land reclamation along the coast of Gresik **(Fig. 1B and C).** The extracted sand appeared to be rich in vertebrate fossils. Over 6,000 specimens were collected from the surface of the reclamation site, representing a diverse vertebrate fauna of fish, reptiles and mammals (Berghuis et al., 2025b), including two *Homo erectus* skull fragments (Berghuis et al., 2025d).

The fossils provide a rare and unprecedented insight into the Pleistocene vertebrate fauna of submerged Sundaland **(Fig. 1A)**. This area, the largest drowned shelf of the world, was widely exposed during Pleistocene glaciations, connecting Borneo, Sumatra and Java to the Asian mainland (Voris, 2000). It formed an important habitat for Pleistocene species (Louys and Turner, 2012) and provided a pathway for faunal dispersal to Java (Salles et al., 2021; Van den Bergh et al., 2001; Van Den Bergh, 1999; De Vos et al., 1982), which included *Homo erectus* (Louys and Kealy, 2024; Kaifu et al., 2008; Antón, 2003).

Recent insights emphasize the evolutionary complexity of the Pleistocene hominin fossil record of eastern Asia (Kaifu and Athreya, in press), which besides *Homo erectus* includes several forms of 'post-*erectus* grade' archaic *Homo* such as Neanderthals and 'Denisovans' (Liu and Wu, 2022; Athreya and Hopkins, 2021; Athreya and Wu, 2017; Reich et al., 2010) and the diminutive *Homo luzonensis* and *Homo floresiensis* (Détroit et al., 2019; Brown et al., 2004). Sundaland must have played a central role in this complex evolutionary pathway and insight into its fossil record is essential.

This paper presents the results of our study of the geological setting of the subsea site. The study aimed for an analysis of the depositional conditions and age of the fossil-bearing strata. Moreover, the study aimed to place the Madura Strait subsea site in a wider landscape framework, by correlations with the on-shore geology of Java and with the off-shore geology of submerged Sundaland, as known from seismic data.

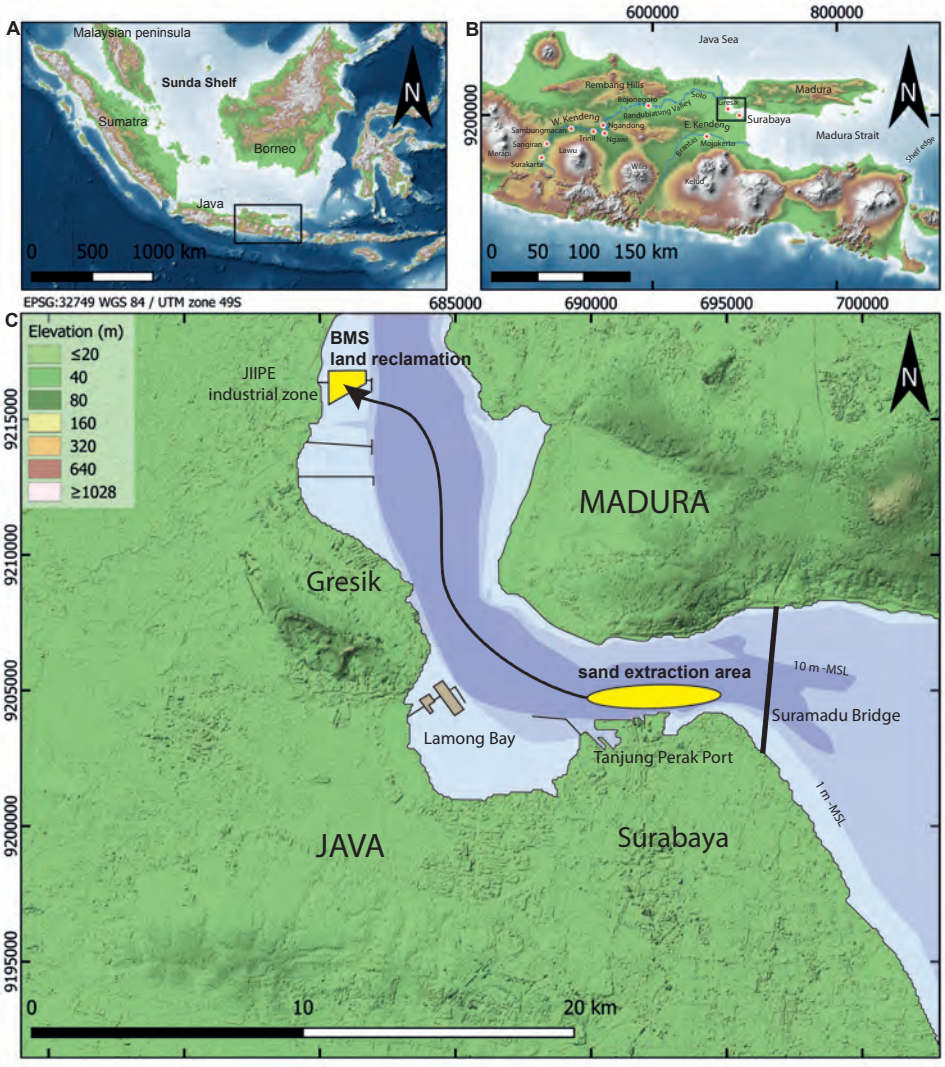


Fig. 1. A: The Sunda Shelf of Southeast Asia, with the Indonesian archipelago. Box indicates the position of map B. **B:** Eastern Java, the Madura Strait, the Solo River, Surabaya and other sites mentioned in the text. Box indicates position of map C. **C:** The Madura Strait north of Surabaya, with the sand extraction area and the BMS land reclamation. Map data: GEBCO and ALOS.

2. Sand extraction and land reclamation

The Madura Strait shores around Surabaya form a mud-dominated coastal lowland, with wide intertidal mudflats. In the Surabaya port, nautical depth is provided by a tidal channel running through the sea strait between the islands of Java and Madura. During earlier marine construction activities, patches of sandstones and conglomerates were found below the seabed of this tidal channel. Sand is a much sought-after resource in this urbanized region and is used for land reclamations along the shallow coast. In 2013, it was decided to use the material for the development of an artificial island along the coast of Gresik, west of Surabaya **(Fig. 1C).** The work was assigned by Berlian Manyar Sejahtera (BMS), a local port company that today uses the island as a port logistics site. The work was carried out in 2014 and 2015 by the marine contractor Van Oord Indonesia and involved the extraction of >5 million m3 of sand and sandstones. Use was made of a trailing suction hopper dredger, a vessel that collects bottom sediment by dragging a suction pipe over the seabed **(Fig. 2A)**. The suction pipe was mounted with a drag head, penetrating and loosening the sandstones and mixing the loosened material with water. The drag head included a 30 by 30 cm grid that prevented the uptake of larger rock fragments. The loosened and water-saturated material was sucked up and stored in the vessel's hopper **(Fig. 2B)**. When fully loaded, the vessel sailed to the land reclamation site and connected with a floating pipeline to discharge the sand to the site **(Fig. 2C)**, where the material was redistributed by shovels **(Fig. 2D)**.

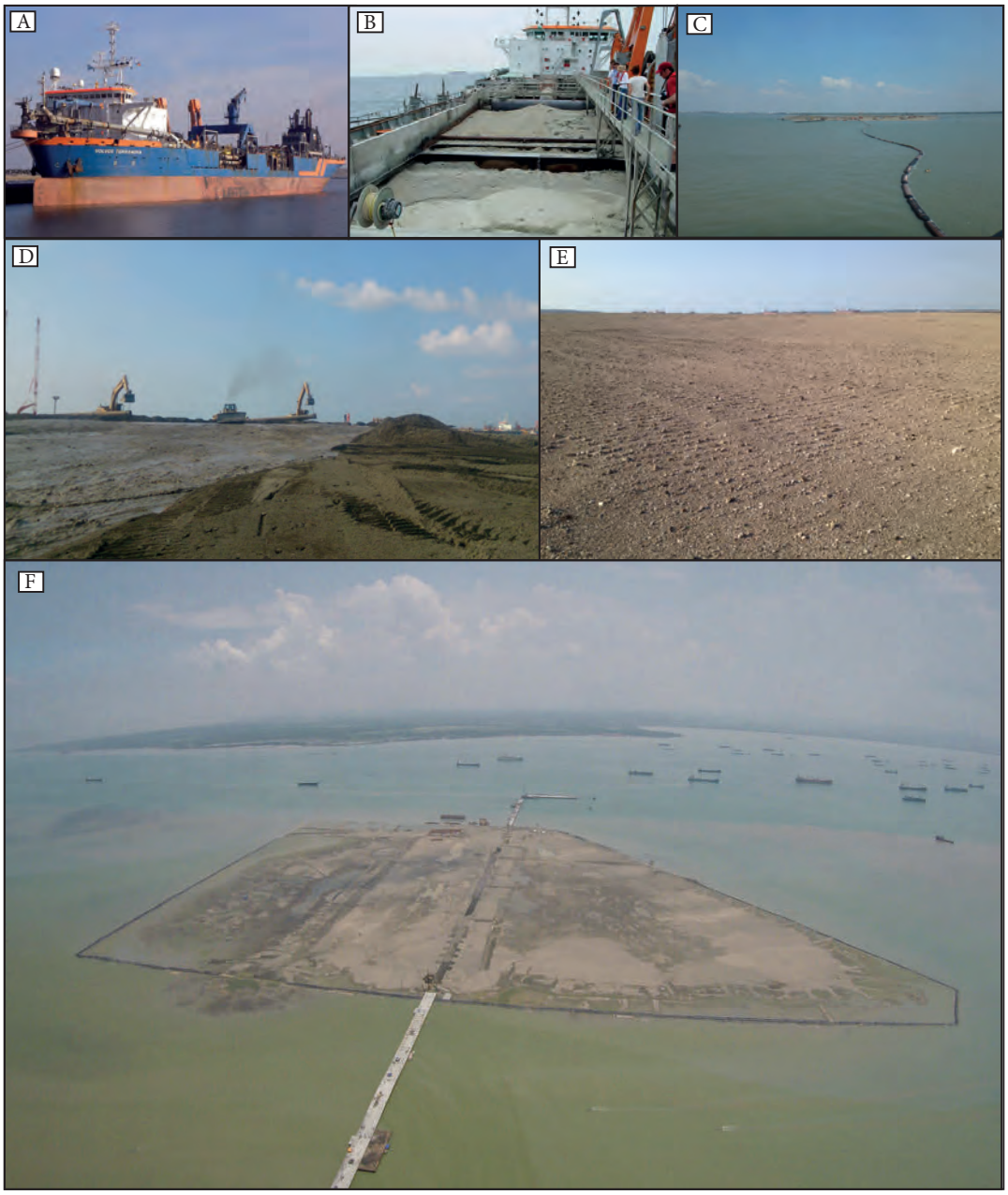


Fig. 2. Selected photographs of the 2014-2015 sand extraction and land reclamation work. **A:** The Trailing Suction Hopper Dredger Volvox Terranova. **B:** Fully loaded hopper of the Volvox Terranova. **C:** Floating pipeline for discharging the hopper load to the BMS reclamation site. **D:** Pipeline handling and sand redistribution at the reclamation site. **E:** Surface of the reclamation site after dewatering. **F:** Aerial view of the BMS land reclamation after completion. View to the east. All pictures: courtesy of Van Oord Indonesia, BMS, Sealand Coastal Consultancy and Pelindo III.

Prior to the work, average water depth at the dredging site was ~20 m -MSL (local reference level, see **Section 4**). Dredging was carried out in east-west trails and proceeded down to a depth of 32 m –MSL, not reaching the base of the sandstone body. By April 2015, the artificial island was completed **(Fig. 2E and F)**, with a total surface of ~100 ha and a height of over 4 m +MSL. The island was left for dewatering and compaction and was safely accessible by July 2015.

3. Geological setting

Java lies along the southern margin of the Sunda Shelf **(Fig. 1A)**, directly north of the line where the Indian-Australian oceanic plate subducts under continental Sundaland. A volcanic arc forms the mountainous core of the island. To the north, the foot of the volcanoes gradually changes into a lowland plain, which stretches out to the Java Sea coast. In eastern Java, this lowland has been subject to Pliocene compression, which formed east-west trending uplift zones, the Kendeng and Rembang Hills (**Fig. 1B**), both of which are made up of folded Miocene to Pliocene marine strata.

The Rembang Hills continue to the east as the island of Madura, leaving the Madura Strait as a semi-enclosed shelf sea. The southwestern shore of the Madura Strait, around the city of Surabaya, is a subsiding coastal plain. Fine terrestrial sediment is supplied by tidal currents and by the Brantas River. The build-up of the subsoil of Surabaya is roughly known from penetration tests related to construction works (Satrya, 2014). It consists of an unconsolidated muddy surface layer with a thickness of ca. 20 m, overlying more consolidated marine clays. Analogous to similar mud-dominated subsiding shorelines worldwide (Zagwijn, 1989), the unconsolidated surface layer probably represents Holocene coastal progradation. At a depth of around 200 m there is a transition to Pliocene calcareous mudstones.

A more detailed insight into the geological build-up of this lowland zone is provided by several gentle anticlines rising up from the coastal plains west of Surabaya, known as the eastern Kendeng Hills **(Fig. 3A)**. Folding reflects local compression and dates back to the Middle Pleistocene (Genevraye and Samuel, 1972). From west to east, the anticlines become lower and younger, and consequently incorporate younger material. Duyfjes (1938a and b) studied outcrops in these anticlines, which he presented as a several hundred meters thick stratigraphic section, of calcareous mudstones, overlain by marine clays, deltaic sandstones and fluvial sandstones. He interpreted this section as an uninterrupted record of coastal progradation. Moving eastward along the anticlines, toward Surabaya, he noted that the deltaic and fluvial sandstones wedge out in the marine clays, which according to him demarcated the maximum reach of Pleistocene coastal progradation.

Until recently, Duyfjes' interpretations remained uncontested. However, there is a substantial problem involved in his model of uninterrupted coastal progradation, namely that it does not take into account Pleistocene sea-level fluctuations. Sarr et al. (2019) demonstrated that the Sunda Shelf was widely exposed during most of the Early Pleistocene. The shelf became subject to regional subsidence in the Middle Pleistocene (Husson et al., 2020), which gradually brought its surface within the range of sea-level highstands, causing intermittent and progressive stages of submergence. Seismic profiles of the central zones of the Madura Strait show a stacking of four to five marine sequences, overlying a basal unconformity (Susilohadi, 1995), indicating that the Madura Strait Shelf followed the same tectonic trend as the larger Sunda Shelf (Berghuis et al., 2022).

Clearly, the sub-seabed stratigraphy of the central Madura Strait is inconsistent with Duyfjes' (1938a) model of uninterrupted sedimentation and coastal progradation. In the past years, we re-investigated the eastern Kendeng exposures, paying special attention to sea-level-related cyclicity (Berghuis et al., 2022, 2019). This resulted in a revised stratigraphy **(Fig. 3B)** and a new model of the Pliocene and Pleistocene development of this coastal area. The transition from calcareous mudstones to marine clays is gradual and could be dated to ~3 Ma by planktonic foraminiferal markers. The facies change probably relates to the emergence of the Rembang Ridge, which created a sheltered embayment along its southern border, cut-off from the supply of calcareous matter from the north. The clays that were deposited in this embayment have a characteristic, massive facies and contain benthic foraminifera that reflect water depths of around 200 m. A thick, red-colored weathering profile overlies these marine clays, showing that the embayment eventually emerged. Referring to planktonic markers and an estimate of sedimentation rates, emergence may roughly be dated to ~1.8 Ma. The weathering profile is overlain by bedded clay-sand alternations rich in shell fragments with shallow-water benthic foraminifera, representing a new transgression, presumably still during the Early Pleistocene. This series has a cyclic build-up of stacked coastal progradation sequences, reflecting sea-level fluctuations. The preservation of these sequences indicates that the area must have been subject to subsidence. The material is conformably overlain by clinoform-bedded ash layers, representing a stage of explosive volcanism, during which the coastal area was overrun by ash-rich deltas. The clinoforms are sharply overlain by fluvial conglomerates and sandstones, which, in contrast to earlier interpretations (Huffman et al., 2005; Duyfjes, 1938a) are not part of the underlying record of deltaic progradation, but form a younger unit that erosively overlies the older clinoform-bedded series (Berghuis et al., 2023, 2022, but see Huffman and Zaim, 2023 for a different interpretation). Well-rounded

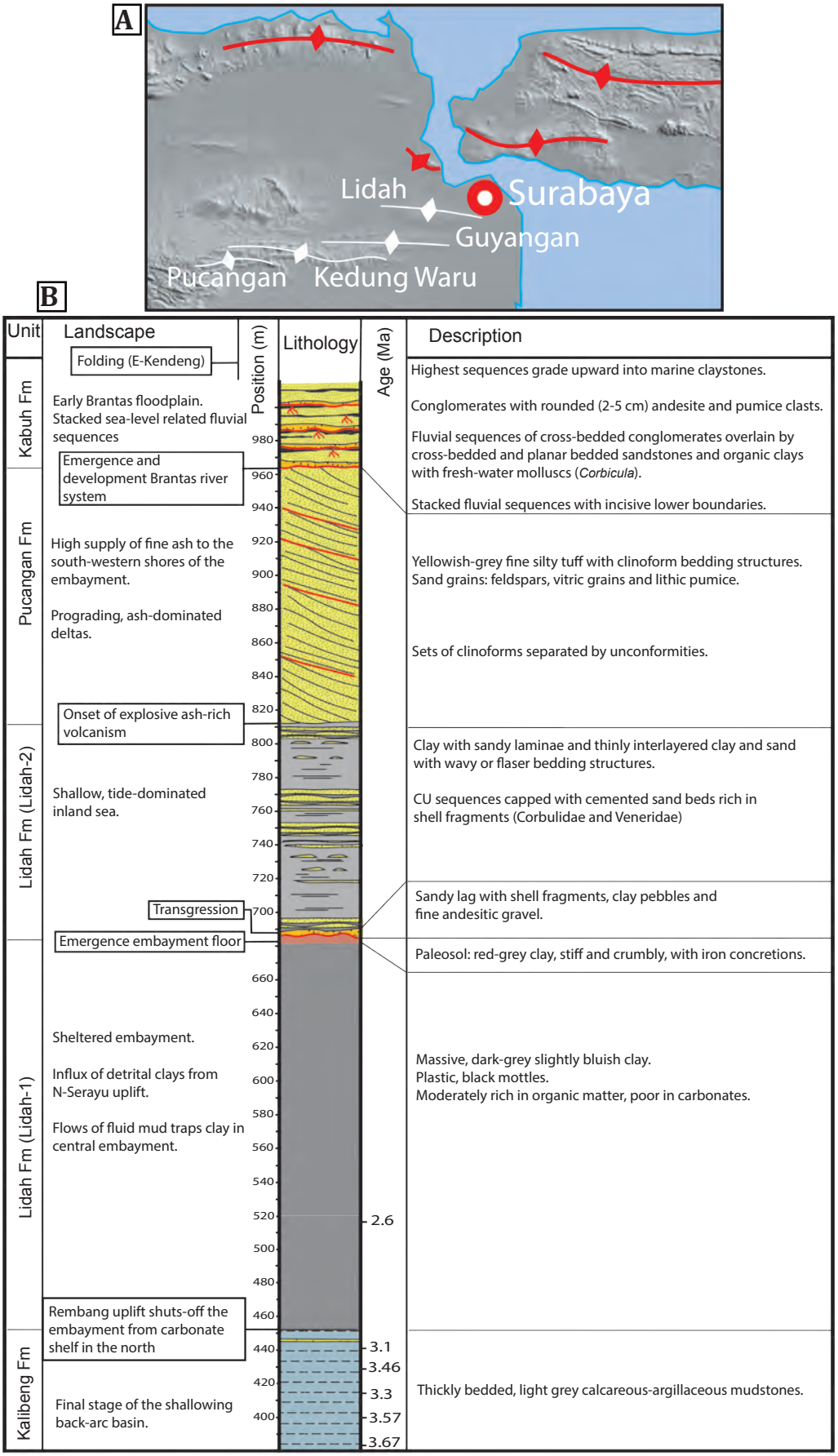


Fig. 3. A: Fold zones eastern Java. In white: the Middle Pleistocene to recent anticlines of the eastern Kendeng in the coastal zone of Surabaya. In red: the Pliocene anticlines of the Rembang Hills. **B:** Stratigraphic section of the Pucangan anticline (from: Berghuis et al., 2022; 2019). Stratigraphic units have local significance only. Ages based on planktonic foraminiferal markers. See mentioned papers for details.

andesite pebbles link these younger fluvial strata to a large and stable river system, which is regarded as the ancient Brantas. The strata form several stacked fluvial sequences, each with an erosive base. The repeated incision and aggradation cycles probably primarily reflect sea-level fluctuations in the river's lower reach. Several of the higher fluvial sequences grade upward into marine claystones and sandstones with shell fragments, reflecting drowning of the river valley during peak highstands.

In Berghuis et al. (2022) we proposed a revised stratigraphy for the eastern Kendeng Hills, based on Duyfjes (1938a), but with local significance only **(Fig. 3B)**. In this revised stratigraphy, the marine clays are subdivided into two members: Lidah-1 consists of the basal, massive marine clays, deposited in the relatively deep Late Pliocene embayment. Lidah-2 consists of the overlying shallow marine clay-sand alternations, which we associated with local subsidence, probably also dating from the Early Pleistocene. The conformably overlying clinoform-bedded ash is referred to as the Pucangan Formation. The fluvial sequences that unconformably overlie the marine strata at the top of the eastern Kendeng section form the Kabuh Formation, a unit which is linked to the Middle Pleistocene Brantas drainage system.

4. Material and methods

Our study of the geological build-up of the seabed of the Madura Strait north of Surabaya has been based on available research data, deriving from various construction projects in the port area.

A relevant data source is the pre-dredge survey, carried out in 2013 by Van Oord Indonesia as a preparation for the sand extraction work. During this study, the seabed was surveyed by sub-bottom profiling, using a Parametric Sediment Echo-Sounder (SES-2000 standard, Innomar), and by placing 48 shallow penetration (max. 5 m) vibro-cores. Penetration depth of the sub-bottom profiler depends on sediment texture and may reach 10 to 20 m in clay-dominated subsoils. The interpretation of sub-bottom profiles has been based on Damuth (1980).

Other relevant data sources are core logs of deep drillings, which provide insight into the sub-seabed geology down to depths of 60 to 100 m. The core logs derive from three infrastructure works: the Suramadu Bridge construction (2003-2009), the construction of jetties and bridges in Lamong Bay (2013-2016), and the Maspion jetty expansion (2012). The Suramadu Bridge connects Java to Madura and the deep drillings related to its construction form a unique cross-section over the sea strait.

The reclamation material was only partly crushed during the dredging process, leaving abundant intact sediment blocks and chunks on the reclamation site, which were studied with a hand-held lens and photographed at the site. Representative samples were collected and stored at the Geological Museum Bandung. Based on a comparison with the core logs of the Suramadu Section, it was possible to reconstruct the original position of individual facies in the sub-seabed stratigraphy.

Three sediment samples were selected for Optically Stimulated Luminescence (OSL) dating. Sample preparation and dating was carried out at the Netherlands Center for Luminescence Dating and at the Cologne Luminescence Laboratory (Germany). Based on previous experiences with OSL-dating of similar sandstones from Java (Hilgen et al., 2023; Berghuis et al., 2021; Rizal et al., 2020; Joordens et al., 2015), we applied the elevated temperature post-IR IRSL measurement protocol $pIRIR_{290}$ (Joordens et al., 2015; Buylaert et al., 2012) for sand-sized, potassium-rich feldspar extracts. Each sample was crushed and sieved. K-rich feldspars were extracted and purified from the samples using the preparation procedure as described in Kars et al. (2014).

All used geotechnical reports have kindly been made available by PT Pelindo III, the operator of the port of Surabaya, and by Van Oord Indonesia, the contractor of the sand extraction work. All studies on the reclamation site have been carried out under kind permission by BMS, owner and operator of the site.

Depths have been presented in meters below mean sea-level (MSL), which is the average sea level in the Surabaya port over a 14-days tidal cycle, regardless of wind or swell. Maximum tidal amplitude in Surabaya is 1.8 m.

5. Results

5.1 Sub-bottom profiling

Section A (locations: see **Fig. 4**) is a north-south profile over the Madura Strait, right in front of the Surabaya port **(Fig. 5A)**. The northern half of the profile, toward the Madura coast, shows a deep penetration of the acoustic signal, pointing to clay-dominated sediment. The top layer, from the seabed down to a depth of ca. 18 m -MSL, shows parallel bedding structures, pointing to interbedded layers of higher reflection, probably sandy laminae. Toward the axis of the sea strait, these bedding structures become oblique, which suggests slumping of large clayey blocks. This area has been subject to nautical deepening, which may have caused the slumps. Below 18 m -MSL, the sedimentary structures disappear, while the acoustic signal still has a reasonable penetrating capacity, pointing to a fine-textured, more massive subsoil, which may be either fine sand or clay. In the southern half of the section, toward the Java coast,

penetration is very low, pointing to a coarse-textured subsoil. This is confirmed by three shallow test-drillings, which contain cemented, medium to coarse sand and conglomerate. Section B **(Fig. 5B)** is an east-west profile of the sea-bed in front of the port. In the eastern part of the section, penetration is moderate to low, with dispersed reflection, indicative of fine or medium sand. Again, this is confirmed by test-drillings. Note that the structures deeper in the profiles are harmonic reflections of the seabed. Toward the western part of the section, the sandy material becomes covered by several meters of bedded clays. Section C **(Fig. 5C)**, located in front of Lamong Bay, shows again a top layer of several meters of clay-dominated sediment with horizontal bedding structures. At a depth of ca. 25 m -MSL this material is underlain by more massive sediment with moderate penetration, which may be either fine sand or clay. In the eastern part of the section, the bedded top layer appears to thin abruptly. A test drilling shows that the top layer continues to consist of marine mud with sandy laminae. Possibly the signal is blurred by gasses in the muddy topsoil (gas blanking).

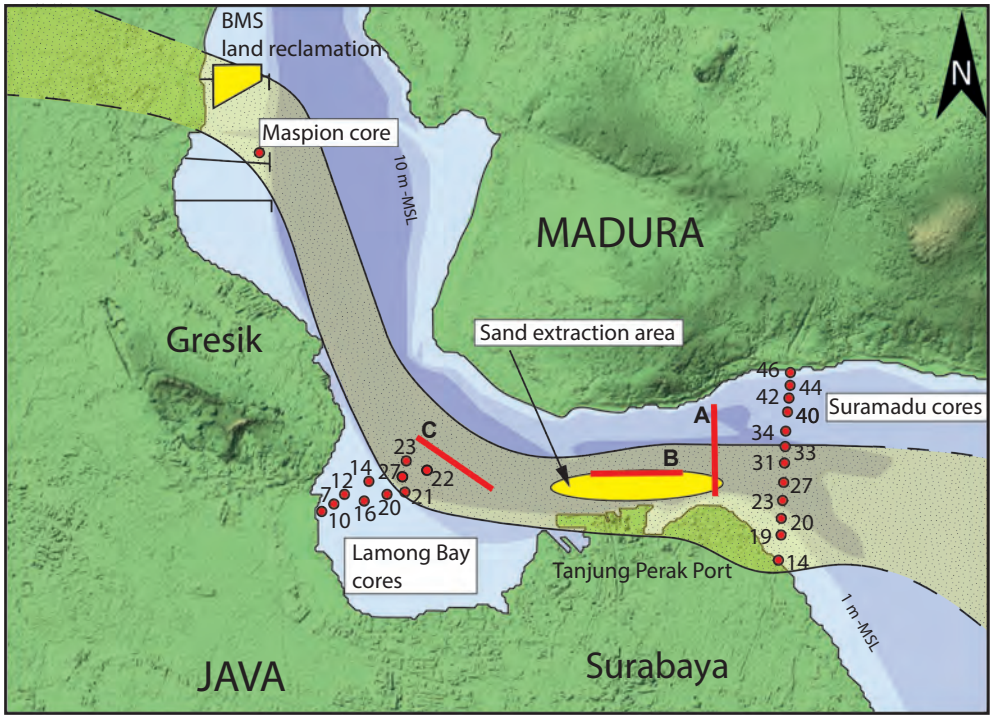


Fig. 4. The Madura Strait north of Surabaya, with positions of the sub-bottom profiling sections (red lines, A-C) and the deep drillings (red circles) as used for this study. Dotted zone: Inferred position of the sand-filled paleovalley.

5.2 Deep drillings of the Suramadu Bridge

Description

The Suramadu cores form a cross-section over the Madura Strait, only a few hundred meters east of seismic profile A **(Fig. 4)**. The cores show a deeper subsoil made up of grey, massive and firm clays **(Fig. 6A)**. The material is poor in admixed fine sand and forms a uniform and, as it appears from the core logs, uninterrupted unit. Along the Madura shore, these clays continue upward to ca. ~20 m -MSL, with at the top several interbeds of cemented, clayey sand with shell debris.

The series is capped by a ca. 5 m thick weathering profile of stiff, reddish-brown, sandy clay with iron concretions. The weathering profile is sharply overlain by grey, unconsolidated mud with interbeds of loose fine sand with shell fragments, which continues upwards to the intertidal zone and makes up the mudflats along the Madura shore. This part of the Suramadu Section correlates well with the northern part of sub-bottom profile A **(Fig. 5A)**. The bedded top layer of this acoustic section can be tied to the unconsolidated top layer of coastal mud. The underlying material with the dispersed acoustic signal is the massive clayey subsoil.

Moving toward the axial part of the sea strait, the clay series with its weathered top becomes steeply incised by a large, sand-filled channel structure, cutting down to a depth of ~ 50 m –MSL. The base of this channel is covered by several meters of brown, cemented conglomerate. This conglomerate grades upward into yellowish-grey sandstones with occasional thin conglomerate interbeds. Upward, at a depth of around 30 m -MSL, the sediment changes into grey, cemented sandstones with shell fragments, containing interbeds of grey, sandy claystones, also containing shell debris. In most of the cores, the transition to shell-bearing sandstones is marked by a well-cemented conglomerate bed with coarse shell fragments. The shell-bearing sandstones continue upward to the present seabed, which in the axial part of the sea strait is blanketed by 1 or 2 m of unconsolidated sand with shells and city waste, forming mobile

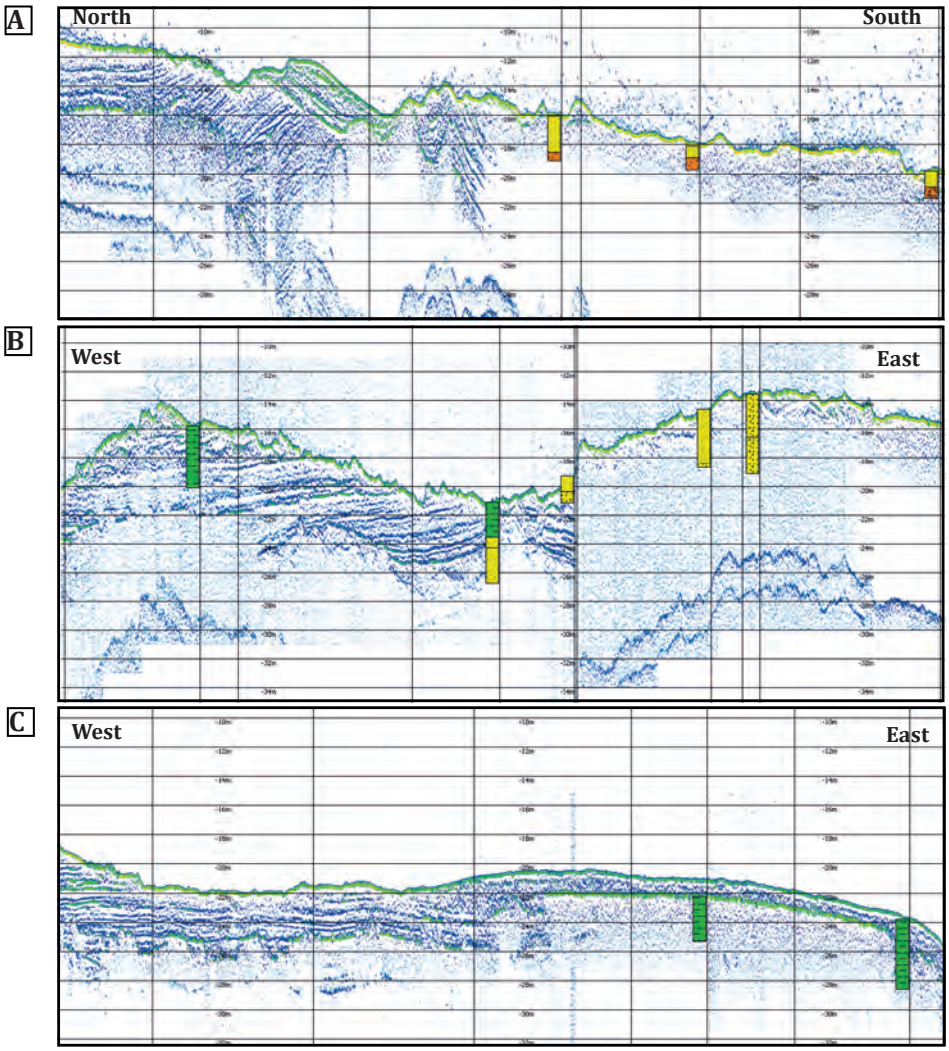


Fig. 5. A-C: Sub-bottom profiling sections over the Madura Strait seabed North of Surabaya. Locations of the sections indicated on **Fig. 4.** Color code test drillings: Green = clay or mud; yellow = sandstone or loose sand; orange = conglomerate. Data: courtesy of Van Oord Indonesia.

tidal bars. Further toward the Java coast, the cemented sandstones are covered with mud and loose fine sand with shell debris, forming a similar tidal mudflat as along the Madura coast. Again, this part of the Suramadu Section compares well with the corresponding part of sub-bottom profile A **(Fig. 5A)**, which also shows the presence of sandy material directly below the seabed.

Interpretation

The Suramadu cores show the extracted sandstone body at the Madura Strait seabed as a large sand-filled channel, deeply cut into the clayey substrate. We regard this incision as a Pleistocene river-valley, related to a past sea-level lowstand. Molengraaff and Weber (1921) already pointed at the presence of such ancient river courses on the Sunda Shelf. More recently, stacked lowstand channels were described from seismic profiles of the Java Sea (Albab and Aryanto, 2017). The sandy fill of the incision follows the standard sequence of transgressively-filled valleys (Bowen and Weimer, 2003). The basal conglomerate, currently at a depth of 50 m -MSL, forms a fluvial lag that probably relates to the incision of the valley, during a stage of falling sea level. The overlying sandstones represent fluvial back-filling during the subsequent stage of rising sea level. Occasional conglomerate interbeds reflect a stacking of flow channels during this aggradation stage. The upward change to shell-bearing marine sandstones and clays indicates that eventually the valley drowned and changed into an estuary. Marine conglomerates, found at the transition from fluvial to marine shell-bearing sandstones, reflect increased energy conditions during this change to estuarine conditions, as a result of tidal currents.

A relation with Pleistocene sea-level fluctuations suggests that the area may have been subject to repetitive fluvial incision and aggradation cycles. An indication for the presence of stacked incised valleys is found in the base of cores 19 and 23, where sandstones rich in shell fragments are found below the incisive base of the large paleovalley. The facies of this material contrasts with the surrounding massive marine clays and also with the overlying fluvial sandstones and conglomerates. Possibly, this material represents the estuarine top of an older valley fill.

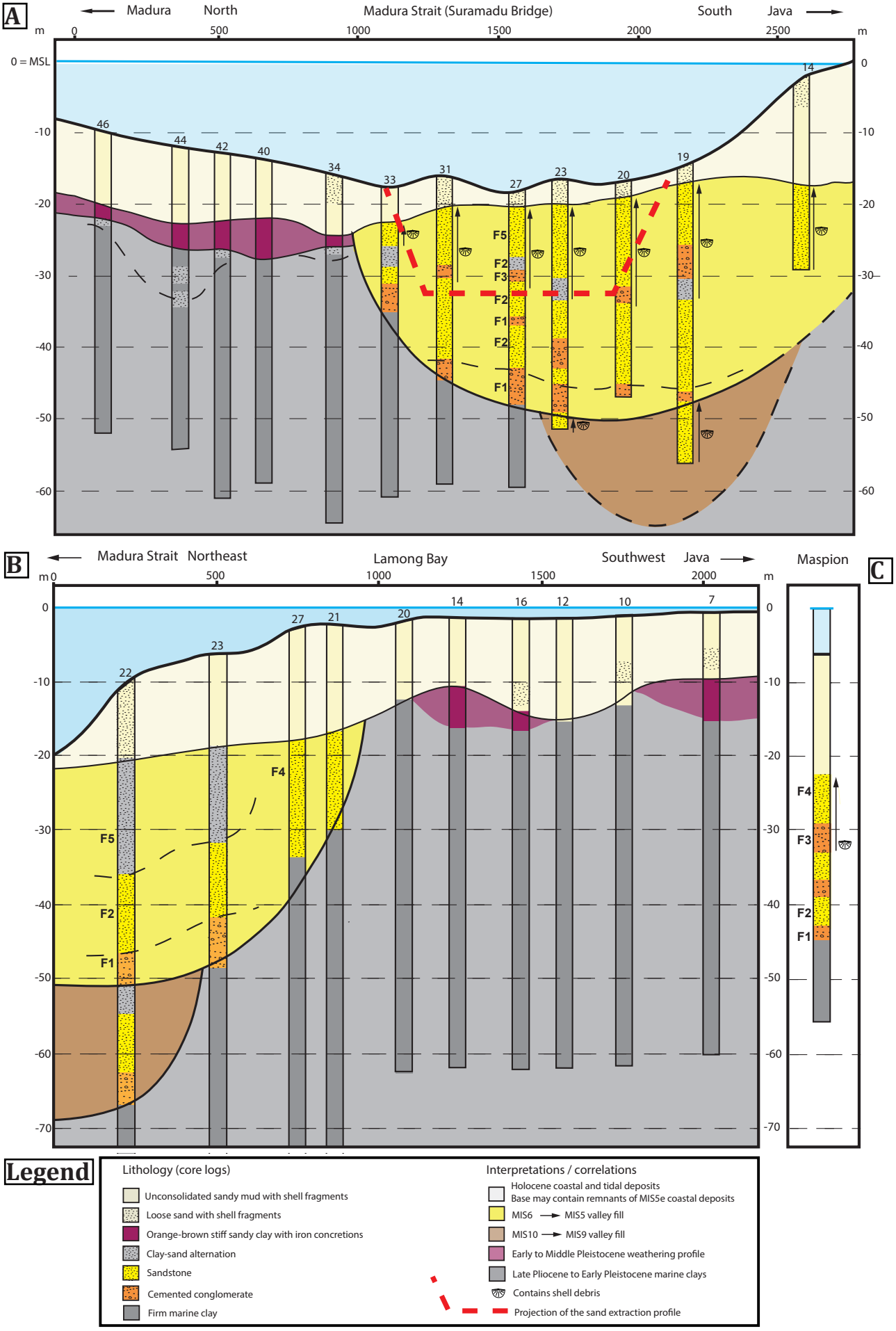


Fig. 6. Deep drillings in Madura Strait north of Surabaya, with correlations and interpretations. Drilling locations indicated on Fig. 4. **A:** Suramadu cores and section. **B:** Lamong Bay cores and section. **C:** Maspion core. Data: courtesy of Pelindo III.

Although the sand-filled valley is the focal point of this study, it is valuable to have a closer look at the clayey substrate in which the valley was cut. The massive and uniform facies of these clays suggests a relation with the Late Pliocene to Early Pleistocene marine clays from the base of the eastern Kendeng exposures **(Fig. 3B)**. The occurrence of this material so close to the surface is unexpected, as in the eastern Kendeng anticlines it is covered by more than 200 m of shallow marine clays and deltaic sands. Conclusive evidence for this relatively old age of the clayey subsoil north of Surabaya can only be based on an analysis of its foraminiferal fauna, which could not be carried out in absence of samples. However, the correlation is confirmed by the weathering profile capping the massive clays in the Madura Strait cores, which was found at the same stratigraphic position in the eastern Kendeng Section **(Fig. 3B)**. Its red color and abundant iron concretions are indicative of ferralitic weathering processes under humid tropical conditions. On eastern Java, humid conditions prevailed during the Early Pleistocene, whereas the Middle Pleistocene climate was relatively dry (Sémah and Sémah, 2012; Sémah et al., 2010; Polhaupessy, 1990). Middle Pleistocene paleosols on eastern Java are therefore usually vertisols, whereas ferralitic paleosols are only known from the Early Pleistocene and are usually older than ~1 Ma (Berghuis et al., 2021; Brasseur et al., 2011). This points to an Early Pleistocene age of the thick weathering profile in the Suramadu cores and a correlation with the Early Pleistocene paleosol of the eastern Kendeng Section.

5.3 Deep drillings of Lamong Bay and Maspion

The Lamong Bay cores derive from the south coast of the Madura Strait, directly west of Surabaya **(Fig. 4).** Again, the cores show a deeper subsoil of firm, massive clays **(Fig. 6B)**, which can be traced down to a depth of at least 100 m -MSL (maximum penetration). Upward, these massive clays continue to ca. 15 m -MSL, where we see again the red weathering profile and a top layer of unconsolidated coastal mud. Moving off the coast, the firm clays become steeply incised by a large channel structure with a fill of cemented sandstones. The base of this incision lies ~ 50 m -MSL, similar to the base of the large paleovalley of the Suramadu cores, strongly suggesting that we are looking at the same valley system. Also the valley fill is similar, with a base of fluvial conglomerates and sandstones and a marine top of shell-bearing sandstones and claystones. In core 23, the paleovalley was cut directly into the massive clayey subsoil. However, in core 22 sandy clays and sandstones continue below the valley base. This material grades downward into a cemented conglomerate bed, which sharply overlies the firm clayey subsoil at a depth of 68 m -MSL. We regard this as an erosion remnant of an older incised valley, preserved below the 50 m -MSL paleovalley. Probably, the sandstones that were found in the base of cores 19 and 23 of the Suramadu Section represent the top of the fill of this same valley system. The shell-bearing sandstones and claystones that form the top of this older valley fill show that also this lowstand valley eventually drowned and changed into an estuary.

The cores of Lamong Bay only hit upon the southern margin of the large 50 m -MSL paleovalley. The remaining part of the paleovalley must be located below the seabed of the deeper sea strait, north of Lamong Bay. The clayey top layer of sub-bottom profile C **(Fig. 5C)** may be a layer of younger mud covering the valley fill, or it may be the claystone facies of the marine top of the valley-fill.

The Maspion core **(Fig. 6C)** shows again the incised valley, cut into the deeper subsoil made up of massive clays. The base of incised valley was found at a depth of 45 m MSL. The height difference with the valley base in the Suramadu Section may reflect the ancient river-gradient, suggesting eastward flow. However, care must be taken with this interpretation, as deformation and compaction of the clayey subsoil may have affected the vertical position of valley base.

5.4 Extraction profile

The sand extraction was carried out directly north of the port of Surabaya. The work followed the trace of the large paleovalley **(Fig. 4)** in an area where the targeted material is found directly at the seabed. The dredging work proceeded to a depth of 32 m -MSL, removing a sand-dominated top layer with a thickness of ~12 m. The extraction profile has been projected against the Suramadu Section **(Fig. 6A)**, which lies directly east of the extraction zone. This shows that the extracted material consists mostly of the marine sandstones that make up the top of the valley fill. Excavation also penetrated several meters into the underlying fluvial sandstones and conglomerates.

5.5 Facies of the extracted material

The uncrushed sediment blocks on the reclamation site (BMS-island) have been subdivided into five genetically significant facies **(Table 1 and Fig. 7)**. A comparison with the core logs of the Suramadu Section provides a valuable insight into the original stratigraphic context of these facies.

The fluvial conglomerate (Facies 1) forms a fluvial channel deposit. The sand extraction work did not reach down to the basal channel lag of the paleovalley at ca. 50 m -MSL. Therefore, the conglomerates at the reclamation site must derive from interbedded channel deposits within the overlying sandy valley fill, representing aggradation and stacking of flow channels. The fluvial sandstones (Facies 2) also derive from this same part of the valley fill, shortly below the transition to marine strata. The material was probably deposited as a stacking of channel bars during fluvial aggrada-

tion. The marine conglomerates (Facies 3) are regarded as a tidal lag deposit. In the Suramadu Section, this facies occurs at the transition from fluvial to estuarine deposits and forms a transgressive lag. The gravel clasts may represent direct fluvial supply to the estuary, or they may have been reworked from the underlying fluvial beds by tidal scour. The shell fragments represent taxa that are common in shallow coastal waters and estuaries. The marine sandstones (Facies 4) derive from the upper part of the valley fill and represent estuarine depositional conditions. The material was deposited as bars in aggrading, laterally mobile tidal channels. The marine sandy clays (Facies 5) represent tidal depositional conditions and were probably deposited in shallow tidal channels or on subtidal flats between the main tidal flow paths. In the Suramadu cores, such sandy clays form interbeds within the marine sandstones.

Description	*Interpretation*
Facies 1. Calcite-cemented, massive or coarsely bedded conglomerate with moderately to well-rounded gravel (diameter 2-6 cm). Coarse sandy matrix made up of monocrystalline (feldspars, pyroxenes, hornblendes) and lithic (pumice, andesite) grains. Gravel consists of andesite, dacite and pumice, with scarce non-volcanic clasts (sandstones or mudstones).	Fluvial channel deposit
Facies 2. Calcite-cemented, medium to fine-grained sandstone with planar laminae or cross-bedding structures. Sand made up of monocrystalline (feldspars, pyroxenes, hornblendes) and lithic (pumice) grains.	Fluvial channel fill
Facies 3. Calcite-cemented, massive, poorly sorted conglomerate with moderately to well-rounded gravel (diameter 2-6 cm) and shell fragments. Sandy matrix made up of shell debris and volcanic grains. Gravel composition as in facies 1. Rich in shell fragments (Pectenidae, Verenidae, Gastropoda and Balanidae).	Tidal lag
Facies 4. Calcite-cemented, medium to fine-grained sandstone with planar laminae or cross-bedding structures. Sand made up of shell debris and volcanic grains. Veneers of larger shell fragments.	Estuarine channel fill
Facies 5. Firm clay or claystone with sandy laminae. The sandy laminae are parallel or wavy and may form lenticular and flaser bedding structures. Sand is fine to medium-grained and rich in shell debris.	Estuarine inter-channel deposit

Table 1. The five facies of the extracted material, based on uncrushed sediment blocks from the BMS reclamation site; descriptions and interpretations. For photos see **Fig. 7**.

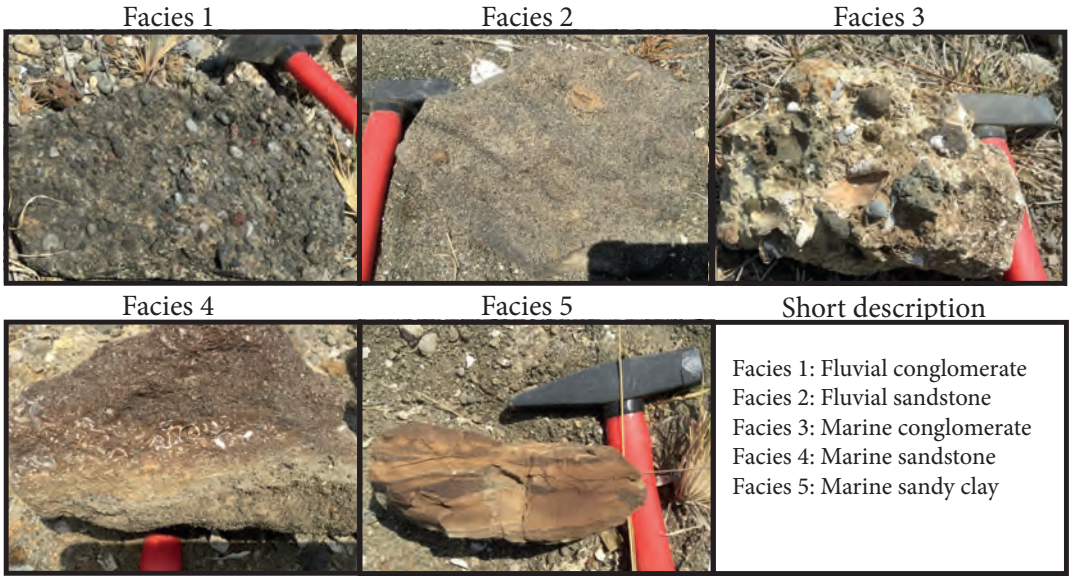


Fig. 7. The five facies of the extracted material, based on uncrushed sediment blocks from the BMS reclamation site; selected photographs. For detailed descriptions see **Table 1**.

5.6 Provenance of the vertebrate fossils

Bone fragments are frequently found in Facies 1 (fluvial conglomerates), Facies 2 (fluvial sandstones) and Facies 3 (marine conglomerates), but not in Facies 4 and 5. Interestingly, the marine conglomerates form the most fossil-rich facies. Almost all blocks of this material contain fine bone debris and larger bone or tooth fragments. This makes Facies 3 a rather exotic mixture of volcanic and marine sand, rounded andesite gravel, large fragments of marine shells and fragmented fossils of terrestrial vertebrates.

5.7 OSL-dating

Three sediment samples from the reclamation site were selected for OSL-dating **(Table 2)**. Unfortunately, no suitable sample could be obtained from the marine conglomerates with its abundant fossil fragments, due to a dominance of shell fragments and low feldspar content. However, a more feldspar-rich sample (Sample 1, CLL-Sura1) was taken from a block of uncrushed, medium-grained marine sandstones (Facies 4), which presumably derives from the same estuarine sequence. Sample 2 (CLL-Sura 2) derives from a block of fine-grained fluvial sandstone (Facies 2), which

contained an unidentified fragment of mineralized bone. Sample 3 (NCL-1320099) was prepared from the sandstone fill of the neural arch of a fossil cervid vertebra. The material consists of fine-grained, cemented sandstone lacking shell fragments and is regarded as Facies 2 (fluvial sandstones).

Test measurements showed that the natural $pIRIR_{290}$ OSL signal of sample 1 is in saturation. Therefore, for this sample only an estimate of the minimum palaeodose could be determined, based on the 2*D0 threshold (Wintle and Murray, 2006). The natural signals of samples 2 and 3 are well below the onset of OSL signal saturation. To test the performance of the $pIRIR_{290}$ protocol for these samples, we carried out dose recovery tests. Dose recovery ratios, corrected for residual doses, were 1.00±0.10 (n = 4) and 1.03 ± 0.09 (n = 2), respectively, confirming the suitability of the $pIRIR_{290}$ protocol for the samples. For the two samples, $pIRIR_{290}$ equivalent doses were measured on 18 and 5 aliquots respectively. The corresponding palaeodose was calculated as the arithmetic mean and the 1-sigma standard error of the equivalent dose distributions. Finally, the palaeodoses were corrected for a remnant dose of 30±15 Gy, as proposed by Joordens et al. (2015) for comparable deposits measured with the feldspar $pIRIR_{290}$ protocol.

For determining the dose rates, the activity concentrations of Uranium, Thorium and ^{40}K were measured by high-resolution gamma spectrometry. For sample 3, which is the sandstone fill of the cervid vertebra, it was not possible to retrieve sufficient material for gamma spectrometry. As this sample has a similar composition as sample 2 and probably represents the same vertebrate-bearing fluvial sandstone unit, we assumed that the gamma spectrometry measurements of sample 2 are also applicable for sample 3. The conversion from activity concentrations to dose rates has been carried out with the dose rate calculator DRAC (Durcan et al., 2015). For the water content attenuation, we assumed a gravimetric moisture content of 15 ± 5 % for all samples. For the internal dose rate we assumed an effective K-content of our K-rich feldspar of 12.5 ± 0.5 % (Huntley and Baril, 1997). The cosmic dose rate was calculated in DRAG, based on geographic latitude and altitude of the sampled units, as well as a reconstruction of the thickness and density of the overburden. The latter must have varied over time, mostly in relation to sea-level changes. Referring to sampling depth (excavation depth) and sea-level reconstructions, we estimated the average thickness of the overburden to ~35 m.

With the obtained dose rates, the paleodoses could be converted to OSL-ages, which yielded OSL ages of 162±31 and 119±27 for samples 2 and 3 (fluvial sandstones). For sample 1 (marine sandstone), only a minimum age (≥462±71 ka) could be given. Laboratory fading tests have been conducted on aliquots of samples 1 and 2, following the approach of Auclair et al. (2003). No significant fading trend was observed for the $pIRIR_{290}$ signal of both samples and thus no fading correction was applied to the final ages.

Sample	Lab-ID	Description	Palaeodose (Gy)	Uranium (ppm)	Thorium (ppm)	Potassium (%)	Total dose rate (Gy)	Age (ka)
1	CLL-Sura 1	Marine sandstone	>1390±73[a]	9.38±0.64	1.49±0.14	0.34±0.01	3.01±0.34	≥462±71
2	CLL-Sura 2	Fluvial sandstone	216±31[b]	1.08±0.08	1.91±0.16	0.61±0.02	1.33±0.16	162±31
3	NCL-1320099	Fluvial sandstone *	158±31[b]	n/a	n/a	n/a	1.33±0.16[c]	119±27[c]

* Sandstone fill of fossil vertebral centre.
[a] Minimum dose estimate based on the 2*D0 threshold.
[b] Palaeodose is corrected for a remnant dose of 30±15 Gy according to Joordens et al. (2015).
[c] Too little material for gamma spectrometry. Dose rate estimate taken from lithologically similar sample 2.

Table 2. OSL dating of 3 sandstone samples, Madura Strait subsea site. Summary of results.

6. Discussion

6.1 Age of the paleovalley, its sandy fill and its vertebrate fossils

The OSL-ages of the two fluvial sandstone samples (samples 2 and 3), of 162±31 and 119±27 ka, provide an age frame for the stage of fluvial backfilling of the submerged valley. It links fluvial aggradation to the lowstand of MIS6 and the subsequent stage of rising sea level toward the highstand of MIS5e. Consequently, the valley was probably cut during the preceding stage of falling sea level, in the run-up to the lowstand of MIS6. The overlapping interval of the two OSL-ages (and their margins) is 146 – 131 ka, which we regard as the 'most likely age range'. This range fits well with the proposed model of valley-aggradation and drowning, as it covers the stage of rising sea-level in the run-up to MIS5. The estuarine strata that form the top of the valley fill in that case represent peak MIS5e highstand-conditions, which implies an age of around 123 ka. Unfortunately, the latter could not be confirmed by OSL-dating. The sampled marine sandstone (sample 1), which was expected to be representative of this estuarine top of the valley fill, has a minimum OSL-age of 462±71 ka. Possibly, the sample derives from a block of older sediment which was hit upon by the sand excavation work, or which had become reworked in the valley fill. It may for example derive from the marine sandstones of the older channel system, that was found underlying the large MIS6 paleovalley in drillings 23 and 19 of the Suramadu Section and drilling 22 of Lamong Bay **(Fig. 6)**.

Fluvial fossil localities often have a complex accumulation history, which may include exhumation and reworking of fossils from older accumulative cycles (Rogers et al., 2010). However, if we consider the valley fill as a single, un-

interrupted aggradational sequence, the vertebrate fossils may very well be contemporaneous to the surrounding sediment. Reworking of older fossil material may rather be associated with incisive conditions. During the MIS6 downcutting stage, fossils may have been exhumed from older fluvial cycles. Such reworked fossils would in that case be expected in the basal lag deposit of the MIS6 paleovalley. This basal channel lag lies ca. 20 m below the depth reached by the sand extraction work **(Fig. 6)**. In the top of the valley fill, the occurrence of reworked older fossil is unlikely. We therefore provisionally regard the 'most likely age range' of the excavated fluvial sandstones, of 146-131 ka, to be representative for the vertebrate fossils. Note however that the occurrence of older marine sandstones among the reclamation material (sample 1) shows that the situation may be more complex. In a taphonomic study of the Madura Strait assemblage (Berghuis et al., 2025c) we will go deeper into the process of fossil accumulation and into the age and homogeneity of the Madura Strait fossil assemblage.

6.2 The paleovalley as an ancient course of the Solo

Based on the available drilling data and sub-bottom profiles, the position of the MIS6 paleovalley can be traced from the Suramadu Bridge, along the sand extraction area to the northern margin of Lamong Bay and subsequently to the Maspion core in Gresik **(Fig. 4)**. West of Lamong Bay, south of Gresik, uplifted Pliocene limestones form an isolated hill, which was formed during the same Late Pliocene compression stage that uplifted the Rembang ridge. The position of this bedrock outcrop, as well as the absence of the paleovalley in the southern cores of Lamong Bay, indicates that the MIS6 paleovalley must have had a more northern course, roughly following the current sea strait between Surabaya and Gresik. This gives an impression of an ancient river draining the Java Sea Shelf and flowing eastward to the Madura Strait Shelf, or vice versa. This, however, is an unlikely drainage pattern, connecting two subsiding shelfs. More importantly, a river draining one of these vast subsiding alluvial plains cannot have supplied the volcanic sand and andesite gravel that make up the valley fill. The composition and texture of the valley fill points to a large river with its origins in the central volcanic highland of Java. Today, there are two of such rivers in proximity of Surabaya **(Fig. 1B)**. The Brantas reaches the Madura Strait south of Surabaya, whereas the Solo flows to the Java Sea, north of Surabaya. The present course of the Solo is the result of canalization in the early 20th century. Originally the river debouched in the Madura Strait directly north of Gresik. The paleovalley at the Madura Strait seabed lies in the direct extension of this original course of the Solo, strongly suggesting that it is a Pleistocene lowstand valley of this river. This points to an eastward flow direction, which is in line with the gradient of the valley base between the Maspion and Suramadu cores. A relation with the Solo is interesting, as it connects the Madura Strait subsea locality with the on-land hominin sites of the Solo valley, such as Trinil and Ngandong **(Fig. 1B)**.

6.3 Reconstructing Solo incision and aggradation cycles on the Madura Strait Shelf

The origin and Pleistocene development of the Solo is well-known from studies of its fossil-bearing terraces (Berghuis et al., 2021; Lehmann, 1936). The river system originated in the Middle Pleistocene, when headward erosion cut a passage through the western Kendeng Hills, draining a previous lake basin south of this hill range and eventually capturing a pre-existing southward-directed drainage system **(Fig. 8A and B)**. The oldest terraces of this newly formed river system were OSL-dated to ~350 ka (Rizal et al., 2020), which suggests that the transverse valley through the Kendeng was cut during the lowstand of MIS10. If this is correct, lowstand paleovalleys of the Solo on the Madura Strait Shelf cannot be older than MIS10.

The incision and aggradation cycles of the Pleistocene Solo on the shelf surface, such as recorded in the Madura Strait north of Surabaya, may be regarded as responses to alternating stages of emergence and submergence in the river's lower reach. Referring to Sarr et al. (2019) and Husson et al. (2020), the regime of intermittent and progressive shelf submergence goes back to the Middle Pleistocene. Seismic profiles of the central zones of the Madura Strait show a sub-seabed stratigraphy consisting of four to five stacked marine sequences (**Fig. 9A)**, overlying a basal unconformity (Susilohadi, 1995). This basal unconformity currently lies at a depth of ca. 200 m –MSL and may be regarded as the Early Pleistocene land surface of Sundaland. A graphic representation of the subsiding Madura Strait Shelf against the sea-level curve (Bintanja and van de Wal, 2008) illustrates the process of progressive shelf submergence during Middle Pleistocene highstands **(Fig. 9C)**. Under a regional subsidence rate of 0.2 mm/a (Sarr et al., 2019), the first Middle Pleistocene stage of extensive Madura Strait submergence probably relates to MIS11. The graph also shows that, after this first large-scale flooding stage, there was a dramatic base-level fall of > 100 m in the period toward MIS10. Possibly, this quick regression initiated the strong wave of headward erosion that cut the traverse valley through the Kendeng, marking the origin of the Solo drainage system.

In order to reconstruct the incision and aggradation cycles of the Pleistocene Solo, we simulated the river's equilibrium profile **(Fig. 9B)**, referring to the similarly-dimensioned longitudinal profile of the Meuse (Tebbens et al., 1999). The inland plains of Surakarta and Ngawi form the river's uplifted middle reach. The northern margin of the Kendeng traverse valley forms a hinge line, marking the transition to the river's subsiding lower reach, which during lowstands extended eastward to the shelf edge, ca. 200 km east of Surabaya.

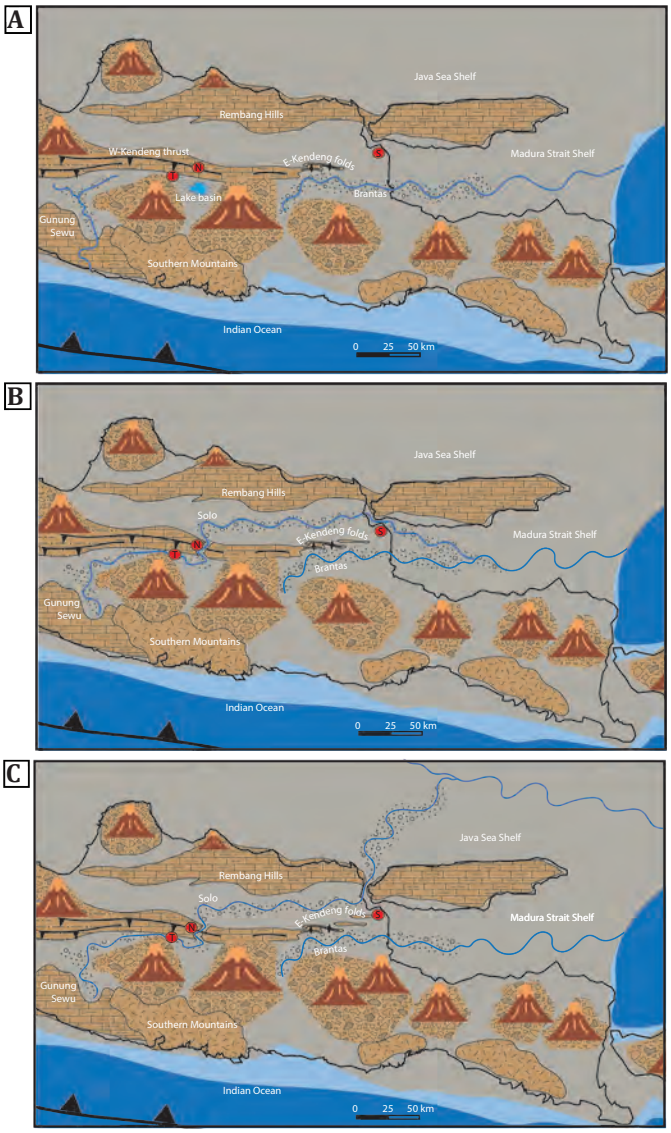


Fig. 8. Pleistocene paleogeography of eastern Java, the Madura Strait and Java Sea shelf area (part of the Sunda Shelf) and the Solo drainage system. Sea-level lowstand situations. Red circles indicate locations of Trinil (T), Ngandong (N) and Surabaya (S). **A:** Middle Pleistocene around 400 ka (MIS12?). The Brantas river system has already developed. The inland plain around Trinil, between the volcanoes Wilis and Lawu is a poorly drained lake basin. More to the west, a southward-directed drainage system exists. **B:** Middle Pleistocene between 350 and 140 ka (MIS10, MIS8, MIS6). Strong headwards erosion, presumably during MIS10, cut the Kendeng traverse valley and drained the lake basin south of the Kendeng. Eventually, also the existing drainage more to the west was captured, forming the large, eastward-directed Solo drainage system. The Madura Strait shelf area, exposed during lowstands, now holds two large perennial rivers, which possibly merge in their downstream reaches. **C:** Late Pleistocene (MIS4, MIS2). Headward erosion of northern rivers may have created a passage through the Rembang Ridge, possibly after MIS5, capturing the Solo and forcing a new course of the Solo towards the Java Sea shelf area.

Projecting the Madura Strait vertebrate site on this simulated equilibrium profile gives an altitude of around 60 m above base level. This makes it possible to estimate local incision levels, assuming that that during each lowstand, Solo downcutting reached the equilibrium state of 60 m above base level. As base level we used the altitude of the subsiding shelf edge or, when sea level did not drop below the shelf edge, lowstand sea-level. This effective lowstand base-level has been indicated by red bars in **Fig. 9C**. For each lowstand, the corresponding valley incision around present-day Surabaya, has been indicated. We tied the incision of the vertebrate-rich paleovalley to MIS6, referring to the OSL-age of the valley fill. The graph nicely illustrates the process of valley-filling during the subsequent stage of rising sea-level towards MIS5 and shows that eventually the valley drowned. The graph also shows that, under a subsidence rate of 0.2 mm/a, the base of the MIS10 incision is preserved below the MIS6 incision, while the MIS8 incision is overprinted by the deeper-reaching incision of MIS6. The remains of an older valley system, locally found below the base of the MIS6 paleovalley, therefore probably relate to MIS10, reflecting the earliest stage of the river's existence. An MIS8 paleovalley has probably not been preserved in this area. OSL-sample 1, with an age of ≥462±71 ka, possibly derives from the sandy fill of this MIS10 channel.

The position of the paleosol, which we regard as the ancient land surface in which the Solo incised, has been added to **Fig. 9C** (purple line) by taking the vertical distance of 35 m between the base of the MIS6 incision and the top of the paleosol. In section 4.2 we noted that the paleosol may reflect prolonged subaerial exposure, dating back to the Early Pleistocene. This implies that it may be the equivalent of the basal erosion surface of the seismic profiles of the deeper Madura Strait. **Fig. 9C** shows that the peak highstand conditions of MIS5e not only drowned the Surabaya

paleovalley, but also the surrounding plains, represented by the paleosol. The unconsolidated sediment that in the present situation covers the paleosol is therefore not necessarily only of Holocene age, but may contain remnants of coastal sediment from this earlier flooding stage.

It is remarkable that we found a prominent MIS6 paleovalley north of Surabaya, whereas there appears to be no trace of Solo valleys related to MIS4 and MIS2. **Fig. 9C** gives a predicted incision depth of 65 m -MSL of the MIS2 paleovalley near Surabaya. Under an unchanged course, MIS2 Solo incision would therefore have removed most of the previous lowstand valleys and their sandy fills. Possibly, the river took a more southern course during MIS4 and MIS2, which implies that the remains of these younger paleovalleys must lie below the city of Surabaya. We have no detailed core data of metropolitan Surabaya, however, available soil charts and foundation reports from the city area point to a clay-dominated subsoil and do not mention the presence of a significant sand body (Satrya, 2014). Therefore, in case the subsoil of Surabaya contains the traces of MSI4 or MIS2 paleovalleys, their valley fill must be dominated by clays. Clayey valley fills may relate to the more humid climate conditions that have prevailed on Java since the Late Pleistocene (Van der Kaars and Dam, 1995).

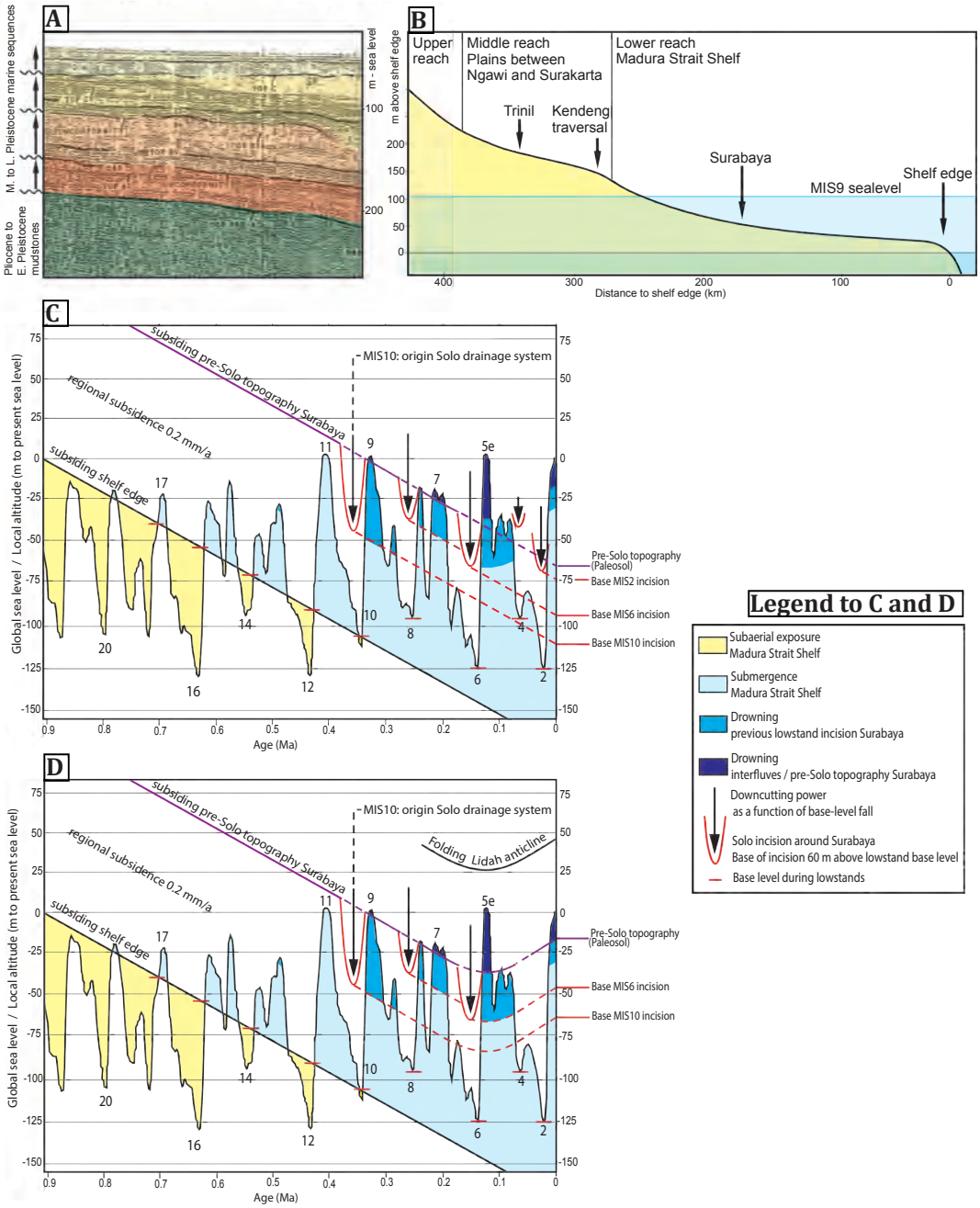


Fig. 9. A: Seismic profile over the Madura Strait (Susilohadi, 1995). Basal unconformity represents prolonged Early Pleistocene subaerial exposure. Overlying marine sequences with incised top represent intermittent submergence of the shelf during Middle Pleistocene highstands, under regional subsidence. First stage of large-scale submergence probably relates to MIS 11. **B:** Simulated longitudinal equilibrium profile of the Solo. Situation during sea-level lowstands, with sea level below the shelf edge. Position of present-day Surabaya is ~ 60 m above lowstand base-level. During highstands such as MIS9, flooding of the Solo valley reached beyond Surabaya. **C:** Reconstruction of the subsiding shelf edge in relation to sea-level fluctuations and subsidence and reconstruction of successive fluvial cycles of the Solo around present-day Surabaya. Sea-level curve based on Bintanja and van de Wal (2008), regional subsidence based on Sarr et al. (2019). **D:** Idem, but with the addition of local, fold-related uplift as a result of local compression and folding of the Lidah anticline. This provides an explanation for the current depths of the MIS10 and MIS6 incisions in the subsoil. MIS4 and MIS2 incisions were not found and have been left out.

Another and possibly more plausible explanation for the absence of MIS4 and MIS2 paleovalleys of the Solo around Surabaya is the development of a northern passage through the Rembang Ridge. Today, this opening in the hill range forms the connection between the Java Sea and the Madura Strait **(Fig. 1B)**, but it may very well have an origin as a fluvial valley. Similar to the earlier development of the Kendeng traverse valley, the stage of rapid sea-level fall associated with MIS4 may have initiated strong headward erosion of local rivers along the margin of the Java Sea Shelf, eventually cutting a passage through the Rembang Ridge and capturing the Solo around present-day Gresik. Moreover, it is possible that during peak MIS5e highstand conditions, the local saddle in the hill range became drowned. This might have generated strong tidal currents, widening and deepening the sadle, paving the way for the development of a new, northward directed river course over the Java Sea Shelf during MIS4 **(Fig. 8C)**.

6.4 Recent upwarping

The graphic representation of incision and aggradation cycles of the Solo, under a regime of sea-level fluctuations and shelf subsidence **(Fig. 9C)**, nicely explains the occurrence of the two superimposed paleovalleys at the Madura Strait seabed north of Surabaya. However, under a continued regional subsidence of 0.2 mm/a (red dotted lines in **Fig. 9C**), these incisions project at depths below their actual depths. The current vertical position of the ancient valleys may relate to recent upwarping. As explained in **Section 3**, the coastal zone is subject to compression, which is expressed by the eastern Kendeng folds southwest of Surabaya. From west to east, the folds become progressively younger. Folding of the Kedung Waru anticline **(Fig. 3A)** probably dates back to ~350 ka (Berghuis et al., 2022) and involved a change from regional 0.2 mm/a subsidence to local uplift of around 0.3 mm/a. The Lidah anticline, which continues eastward into urban Surabaya, is the youngest and most eastern fold, pushing up the surface to an altitude of ~25 m +MSL. The Surabaya coastline lies on the northern flank of this anticline and must have been affected by this uplift. In **Fig. 9D**, we added local warping-up of the clayey subsoil to our graph, assuming fold-related uplift of 0.3 mm/a, similar to the Kedung Waru anticline. With respect to the timing of this uplift, we applied a 'best fit scenario', using the current position of the MIS6 incision and the paleosol as a reference. This suggests a gradual change from regional subsidence to local, fold-related uplift at ~125 ka.

6.5 Correlations with the Solo terraces

In the Kendeng traverse valley, at least 4 terraces have been distinguished **(Fig. 10)** which were dated by Rizal et al. (2020). A correlation with the Madura Strait paleovalleys is interesting, but it is important to note that the upstream terraces and downstream paleovalleys are not necessarily direct and contemporaneous landscape equivalents. There may for example have been differences in timing of the response to degradation or aggradation events along the longitudinal river profile (Bull, 1990). Moreover, degradation and aggradation on different river stretches may have been regulated by different processes. On the Madura Strait Shelf, this fluvial behaviour was probably primarily a response to sea-level fluctuations, but higher-up along the longitudinal river profile, factors such as varying volcanic supply and local uplift may have been more important.

Nevertheless, a provisional correlation has been made, in the first place based on the available dating results **(Fig. 10)**. Comparing the ages of the Kendeng terraces to the sea-level curve **(Fig. 9)**, it seems that also in this area the main downcutting stages may have been responses to sea-level fall. Note that with the exception of the higher terrace, which is a gravelly strath terrace, the OSL-ages of the Kendeng terraces refer to the terrace fill, which overlies the basal erosion surface and postdates downcutting.

The upper terrace contains the oldest known Solo deposits and probably represents the earliest stage of the river system, shortly after the development of the Kendeng traverse valley. Erosion remnants of this oldest terrace can also be found south of the Kendeng (Berghuis et al., 2021). This earliest incisive stage of the Solo, which we linked to MIS10, is probably the equivalent of the lowest, partly preserved paleovalley of the Madura Strait north of Surabaya.

The middle and lower terrace of the Kendeng traverse valley have OSL-ages that overlap with the valley-fill of the large, fossiliferous paleovalley of the Madura Strait, but the lower terrace clearly gives the best age fit. The terrace sediment was dated by a combination of OSL, Ar/Ar and U-series techniques, yielding a Bayesian-modelled age of 140 – 92 ka (Rizal et al., 2020). We provisionally linked downcutting of this terrace and incision of the largest Madura Strait paleovalley to the stage of falling sea-level related to MIS6. The middle terrace of the Kendeng traverse valley is older and its downcutting is possibly related to MIS8.

6.6 Relation between the Madura Strait subsea site and the upstream hominin sites along the Solo

The proposed correlation between the fossiliferous valley fill of the Madura Strait and the lower terrace of the Kendeng traverse valley is of great interest, as this terrace yielded the rich vertebrate fossil assemblage of Ngandong, including 11 partial skulls and 2 tibiae assigned to *Homo erectus* (Huffman et al., 2010; Weidenreich, 1951; Oppenoorth, 1932), which is regarded as the youngest record of this hominin species on Java (Rizal et al., 2020).

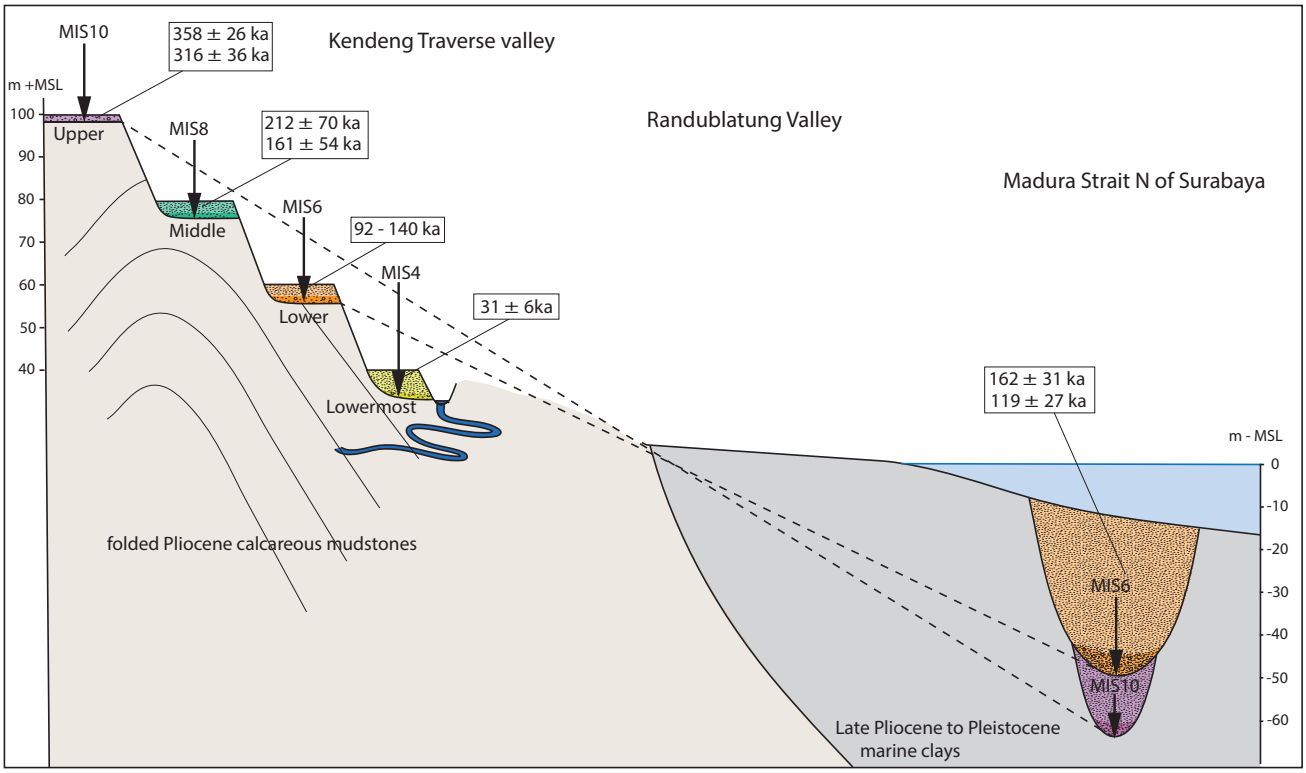


Fig. 10. Provisional correlation between the Solo terraces of the Kendeng traverse valley and the incised valleys of the Madura Strait north of Surabaya. Terrace ages from Rizal et al., 2020. These ages are OSL-ages or, for the lower terrace, Bayesian-modelled of OSL, U-series and Ar/Ar ages. Dated material of the upper terrace is a lag that probably relates to downcutting. For the other terraces, the dated material is probably the terrace fill, postdating downcutting. The proposed correlations are the downcutting stages and their inferred relation to sea-level lowstands. The lower terrace of the Kendeng traverse valley is the hominin-bearing Ngandong terrace.

Not only are the Ngandong and Madura Strait sites of similar age, they are also tied to the same river valley. Yet, there may have been relevant landscape differences. Ngandong represents a setting along the uplifted middle reach of the Solo, whereas the Madura Strait site represents a setting along the river's lower reach, surrounded by lowland plains **(Fig. 10)**. Stream velocities around Ngandong were probably higher. Moreover, Ngandong was probably not invaded by the sea during peak-highstand conditions of MIS5e, although the shoreline may have come close to the Kendeng traverse valley and a salt-water wedge may have reached further upstream, especially during periods of low discharge. Another important difference is that the highland of Java probably had more rain than the lowland plains, which must have had an effect on vegetation types and faunal communities. An analysis of the Madura Strait assemblage and a comparison with the Ngandong assemblage may shed a better light on these matters (Berghuis et al., 2025b).

Further upstream, south of the Kendeng traverse valley, the Solo terrace landscape continues. Lower uplift rates make that individual terrace levels are more difficult to recognize. Moreover, fluvial behaviour of the Solo has been strongly influenced by sediment supply, with ash-rich fill-terraces reflecting eruptive stages of the nearby Lawu (Berghuis et al., 2021). The hominin skulls Ngawi 1 and Sambungmacan 1-3 were found in this area and may very well derive from the Solo terraces. Unfortunately, details on their age and stratigraphic provenance are not available (Kaifu et al., 2015; Delson et al., 2001). The skulls may also derive from the Trinil Formation, which forms the local substrate and consists of fluvially reworked ash, deposited in a local lake basin shortly before the development of the Solo drainage system **(Fig. 9A)**. This unit, which is highly fossiliferous, is often difficult to distinguish from ash-dominated fill terraces in isolated outcrops (Pop et al., 2023b).

The skullcap from Trinil (Dubois, 1896), today regarded as the type specimen of *Homo erectus* (Pop et al., 2024; Mayr, 1950), was also excavated in the Solo valley south of the Kendeng, but certainly predates the origin of this river. At the find site, there are two superimposed bone beds, which were dated to 830 – 773 ka and around 450 ka respectively (Hilgen et al., 2023). Referring to the ancient morphology of the skullcap, it probably derives from the oldest bone bed, and may even have been reworked from older layers. Interestingly, also an intact hominin femur was discovered in Trinil. It was originally associated with the skull cap (Dubois, 1896), but is today commonly regarded as a younger specimen, deriving from the Solo terrace deposits that erosively overlie the older deposits (Pop et al., 2023a; Ruff et al., 2022). This terrace, locally referred to as T2 (Berghuis et al., 2021), is probably the equivalent of the vertebrate-rich terrace of Ngandong and thus may be of similar age as the Madura Strait site. Further upstream along the present Solo valley, Sangiran is the richest *Homo erectus* site of Java. The local fossils are probably of late Early to early Middle Pleistocene age and predate the origin of the Solo (Matsu'ura et al., 2020; Kaifu et al., 2008).

6.7 Correlation with the eastern Kendeng stratigraphy

In **Section 5.2** we correlated the massive clays that make up the deeper subsoil of coastal Surabaya with the Late Pliocene to Early Pleistocene massive marine clays (Lidah-1) of the eastern Kendeng section **(Fig. 3B)**. The transgressively-filled incised valleys of the Madura Strait are comparable to the fluvial incision and aggradation cycles that make up the top of the eastern Kendeng section, both forming a record of fluvial response to Middle Pleistocene sea-level fluctuations and progressive submergence of the Madura Strait Shelf. However, the fluvial records represent two different river systems. The fluvial to estuarine top of the eastern Kendeng section relates to the Brantas drainage system and is referred to as the Kabuh Formation. The valley-fill sequences of the Madura Strait relate to the Solo drainage system. In Berghuis et al. (2021) we proposed to refer to all (terrace-related) deposits of this river system as the Solo Formation.

The ca. 260 m thick series of coastal, partly deltaic deposits (Lidah-2 and Pucangan Formation), which in the eastern Kendeng section lies between the massive marine clays and the fluvial top, is absent in the coastal area around Surabaya. The accumulation and preservation of this shallow marine series in the eastern Kendeng area point to significant, local subsidence, and to a connection with the sea. Possibly, the occurrence of local subsidence zones relates to vertical movement along basement faults, a process that was described by Lunt (2013) for the wider eastern Java area.

6.8 Landscape setting of the Madura Strait paleovalleys

The Madura Strait paleovalleys north of Surabaya are lowstand valleys of the Solo, cut in an ancient land surface that had been stably exposed since the Early Pleistocene. Valley incision in this area probably dates back to MIS10, when the Solo developed as a large eastward-directed drainage system. If we regard the paleosol of the Madura Strait stratigraphy as the ancient land surface in which the valleys incised, then the MIS10 valley of the Solo had a depth of 50 m compared to the surrounding lowland. MIS6 incision was less pronounced, cutting a valley of around 30 m. During intermittent highstands, the valleys drowned and changed into estuaries. During peak highstand-conditions of MIS5e also the surrounding plains submerged.

The ferralitic paleosol in which the valleys were cut, had originally formed under humid conditions. However, by the time the surface was incised, climate conditions had changed to more arid, leaving the ferralitic soil properties as a relic of passed climate conditions. This is confirmed by the valley fill of monocrystalline sand and rounded andesite gravel, which points to sediment supply from a hinterland subject to physical abrasion under arid or semi-arid climate conditions rather than chemical weathering under humid, densely vegetated conditions.

7. Conclusions

The subsea vertebrate locality of the Madura Strait north of Surabaya is a submerged lowstand valley of the Solo. Valley incision relates to MIS6. Two samples from the fluvial valley fill were OSL-dated to 163+/- 31 ka and 129 +/- 27 ka, which links fluvial aggradation to the stage of rising sea-level between MIS6 and MIS5. The top of the valley fill consists of shell-bearing marine sandstones, reflecting drowning of the river valley and a change to estuarine conditions during peak MIS5e highstand conditions.

Vertebrate fossils of the valley fill are associated with fluvial sandstones and conglomerates, and with a marine conglomerate bed that marks the transition between fluvial and estuarine sandstones. Most of the available fossils derive from this transitional bed, which is regarded as a tidal or transgressive lag.

The late Middle Pleistocene age of the site is of great interest in terms of hominin evolution, as this period is characterized by a great morphological diversity and mobility of hominin populations in the region (Kaifu and Athreya, in press). The subsea site is of similar age as the Ngandong terrace of the Kendeng Hills and terrace T2 of Trinil, both of which yielded hominin fossils, which are generally regarded as the last occurrence of a long-standing, isolated *Homo erectus* population. Although of similar age and tied to the same river, the landscape context of these find sites was probably different. The Trinil T2 terrace and the Ngandong terrace were formed along the river's middle reach, at the foot of the volcanic highland of Java. The Madura Strait submerged valley represents a lowland setting. The lowland plains probably had a lower precipitation rate, which may have affected vegetation and faunal communities.

Under the relatively dry Middle Pleistocene climate of eastern Java, herds of herbivores and groups of hominins on the lowland plains were probably dependent on large perennial rivers, providing drinking water and terrestrial as well as aquatic food sources. These drainage systems may very well have formed important dispersal routes for hominins and other species. The Middle Pleistocene Madura Strait Shelf had two of these rivers, the Brantas and the Solo, which must have made the area an attractive habitat.



The Geological Museum in Bandung, built in 1929 as Geologisch Laboratorium.



Chapter 7

First vertebrate faunal record from submerged Sundaland, the late Middle Pleistocene hominin-bearing fauna of the Madura Strait

CHAPTER 7

First vertebrate faunal record from submerged Sundaland: the late Middle Pleistocene, hominin-bearing fauna of the Madura Strait

H.W.K. Berghuis, Gert Van den Bergh, Thijs Van Kolfschoten, Unggul Prasetyo Wibowo, Iwan Kurniawan, Shinatria Adhityatama, Indra Sutisna, Ivo Verheijen, Eduard Pop, A. Veldkamp, Josephine C.A. Joordens

Published in: *Quaternary Environments and Humans* (2025)

Abstract

The Sunda Shelf currently holds the world's largest shelf sea. During Pleistocene sea-level lowstands the area emerged, forming a vast landmass called Sundaland. Intermittently exposed Sundaland played an important role in the regional vertebrate biogeography and evolution of species including *Homo erectus* and, in the Late Pleistocene, *Homo sapiens*. So far, our models of the Pleistocene biogeography of Sundaland were based on the distribution of extant species and on island fossil assemblages, notably from Java (Indonesia). Here we present the first vertebrate fossil record from subsea Sundaland. The fossils derive from the sandy fill of a lowstand valley of the Solo River in the Madura Strait, which was OSL-dated to 162±31 and 119±27 ka. The cemented sand was recently extracted and used for a landfill in the port of Surabaya. The assemblage consists of at least 36 species and provides a unique insight into the lowland fauna of emerged Sundaland, during the late Middle Pleistocene. The lowland river had a rich reptile community, consisting of various turtle species, crocodilians, varanids, and pythons. The nearby estuary was frequented by several shark species, including the extinct *Hemipristis serra,* as well as several species of stingrays. Some of these also ascended the river. The lowland plains surrounding the river were populated by herbivores such as Hippopotamidae and several species of Bovidae, Cervidae, and Proboscidea. The terrestrial community represents a grass-dominated environment and is similar to the contemporaneous fossil assemblage of Ngandong (Java). However, on a detailed level, there are conspicuous differences. For example, *Duboisia santeng, Axis lydekkeri,* and *Epileptobos groeneveldtii* are absent in Ngandong and were generally believed to have become extinct by the end of the Middle Pleistocene. Their presence in the Madura Strait assemblage shows that the species persisted on the lowland plains. Interesting is also the presence of more rarely encountered species such as *Varanus komodoensis*, *Macaca* sp. and *Homo erectus* on the lowland plains. Metrically, *Elephas* sp. molars from the Madura Strait site are relatively high-crowned, whereas *Bos palaeosondaicus* is relatively small-statured compared to its Middle Pleistocene relatives from Java. The fossil fauna from the Madura Strait reflects a thus far unknown vertebrate coastal lowland community that lived in and around the lower reaches of the Middle Pleistocene Solo River.

1. Introduction

In 2014 and 2015, sand was dredged from the seabed of the Madura Strait **(Fig. 1A-B)**, in front of the port of Surabaya (Java, Indonesia), and used for the development of a land reclamation west of the city **(Fig. 1C).** The work was assigned by a local port company, Berlian Manyar Sejahtera (BMS), and involved the construction of an artificial island along the coast. Upon completion, the reclamation site turned out to be strewn with vertebrate fossils. Sealand Coastal Consultancy, at this time the engineering consultant of the Surabaya port-operator Pelindo III, recognized the scientific interest of the fossils. After consultation with BMS, Pelindo III, and officials of the Geological Museum Bandung, it was decided to collect and secure the fossils from the site before the construction of port-handling infra-structure. The fossils were stored in the Geological Museum Bandung. In 2017, it was decided to integrate the study of the assemblage in the Indonesian-Dutch research program 'Studying Human Origin in East Java'.

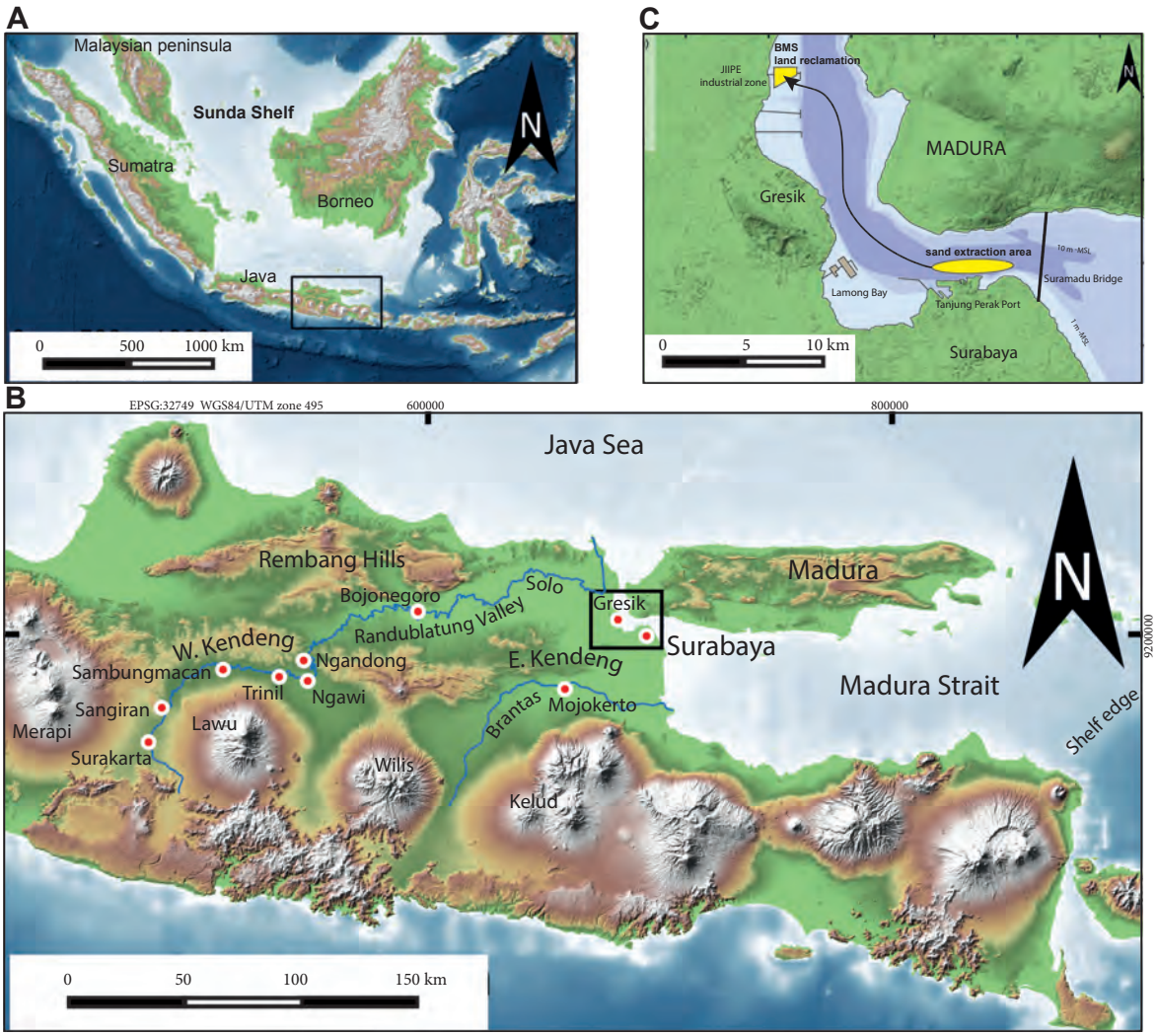


Fig. 1. A: The Sunda Shelf of Southeast Asia, with the Indonesian archipelago. Box indicates the position of map B. **B:** Eastern Java, the Madura Strait, Surabaya, the Solo River, and other sites mentioned in the text. Box indicates the position of map C. **C:** The Madura Strait north of Surabaya, with the sand extraction area and the location of the BMS land-reclamation. Map data: GEBCO and ALOS.

What makes the Madura Strait fossil assemblage special? In the first place, it is one of the largest and most complete vertebrate fossil assemblages collected from this region since the great excavations on Java of the late 19th and early 20th century (Selenka and Blanckenhorn, 1911b; Dubois, 1908). These historic excavations yielded fossil assemblages that, up to today, form the basis of the regional Pleistocene vertebrate taxonomy and shaped our interpretations of the regional biogeography and vertebrate evolution (Hooijer, 1958a, 1955; Janensch, 1911b; Stremme, 1911; Dubois, 1908, 1907). The occurrence of *Homo erectus* in these fossil assemblages makes the region of particular interest for hominin evolution and dispersal (Antón, 2003; Kaifu, 2017). Up to today, palaeontological research teams are working on Java and frequently find new material. However, except for occasional new hominin finds (Widianto et al., 2023; Noerwidi et al., 2021; Zaim et al., 2011), detailed descriptions and measurements of the non-hominin vertebrate fossils are usually not provided. This implies that potentially valuable material remains unrecognized, and that opportunities are missed to build up new comparative data sets and local reference collections. Note in this respect that over the past century, vertebrate taxonomies have been revised and species definitions updated. As a consequence, the existing reference collections and taxonomic literature, although generally of outstanding quality, may be outdated or

confusing. The Madura Strait assemblage offers a unique opportunity for a detailed descriptive and metric study, using updated taxonomies and measurement protocols, which may serve as a reference for future finds in the region.

In the second place, the interest of the Madura Strait assemblage lies in its underwater provenance and its relation with the biogeographic region known as Sundaland. Already since the first discovery of vertebrate fossils on Java, the Pleistocene migration of species to the island has been subject of discussion. Initially, it was hypothesized that the dispersal of land vertebrates to Java had taken place via a land bridge over the Andaman and Nicobar Islands. Later, the discovery of ancient drainage systems on the bottom of the Java Sea (Molengraaff and Weber, 1921) showed that this shelf sea must have once been exposed, forming a large landmass that connected Java, Sumatra and Borneo to the Asian mainland. Van Bemmelen (1949) proposed to refer to this Pleistocene landmass as Sundaland, and to the present-day shelf sea as the Sunda Shelf **(Fig. 1A)**. This extensive shelf sea, the largest drowned shelf of the world, was probably widely exposed during most of the Early Pleistocene (Husson et al., 2020). Regional subsidence brought the area into the range of sea-level fluctuations during the Middle Pleistocene, causing intermittent stages of submergence during interglacials (Sarr et al., 2019). During Middle and Late Pleistocene glaciations, Sundaland was exposed (Voris, 2000), providing a pathway for faunal dispersal to Java (Van den Bergh et al., 2001; Van Den Bergh, 1999; De Vos et al., 1982). Meijaard (2003) and Heaney (1991) noted that during glaciations, this exposed land surface may not have been an area over which species could freely pass. The central lowland of the exposed landmass was probably associated with dry climate conditions and open, savannah-like vegetation, forming a barrier for forest-dependent species. However, for open habitat-dwelling herbivores and early hominins, the lowland plains may have formed a corridor for dispersal to Java (Louys and Kealy, 2024; Husson et al., 2022; Louys and Meijaard, 2010; Antón, 2002). The central savannah of emerged Sundaland may even have been a refugium for open-habitat species, in periods when the adjacent Asian mainland became too dry (Louys and Turner, 2012).

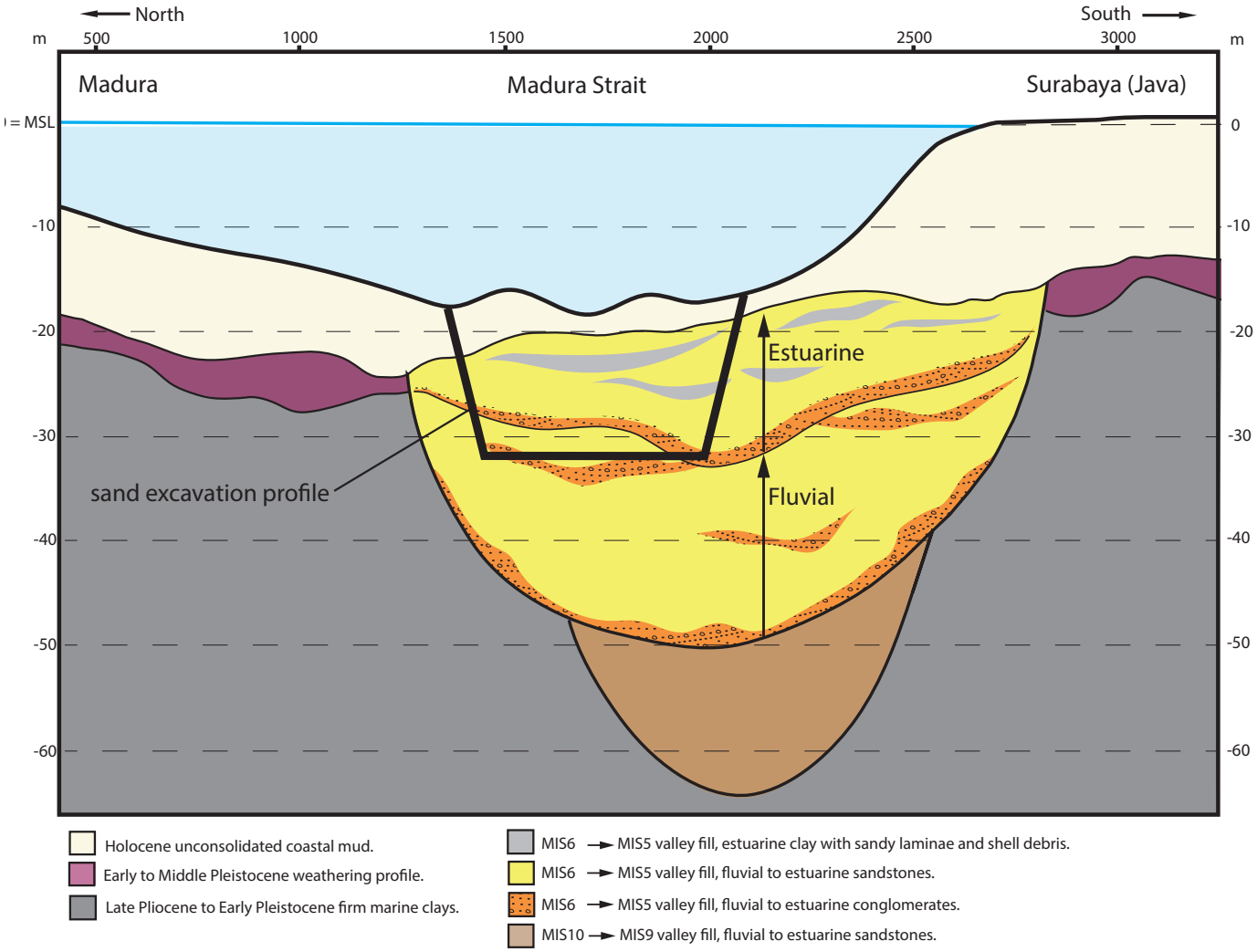


Fig. 2. Schematic cross-section over the Madura Strait north of Surabaya, with a projection of the sand-extraction profile. The local subsoil contains the remnants of two superimposed paleovalleys of the Solo. The extracted material is the sandy fill of the highest paleovalley. Incision of the two paleovalleys has been tied to the lowstands of MIS10 and MIS6 respectively. The valley-fill sequences relate to subsequent transgressive stages. For details, see Berghuis et al. (2025a; 2025c).

Thus far, the models of the Pleistocene biogeography of Sundaland and species dispersal have primarily been based on the distribution of extant species on the islands of Southeast Asia and on the Pleistocene fossil assemblages from Java. Sumatra and Borneo yielded interesting Late Pleistocene cave faunas (De Vos et al., 1982) but relevant older fossil assemblages from open-air sites from these islands are rare. Moreover, there have thus far been no fossil finds from the seabed (Adhityatama and Yarista, 2019). This is remarkable and in great contrast with other shallow shelf seas in the world, such as the North Sea, where seabed dredging and trawling yielded abundant vertebrate fossils (Mol and Bakker, 2022; Kolfschoten and Essen, 2004) including hominin fossils and arftefacts (Niekus et al., 2019; Hublin et al., 2009). The absence of similar finds from the Java Sea or South China Sea may be due to the high fluvial supply of fine terrestrial detritus, blanketing the seabed with Holocene mud. But it is probably also related to a lack of awareness. Note in this respect that large-scale seabed dredging has been carried out in this area, in relation to land reclamation works in Singapore and Jakarta, and that trawling fishing is common in the region.

The Madura Strait assemblage is the first vertebrate faunal record from submerged Sundaland. It offers a unique insight into the fauna of the lowland plains that must have formed the dominant Pleistocene landscape element of Sundaland and therefore forms an important contribution to our understanding of the regional biogeography. In a previous publication (Berghuis et al., 2025a) we described the subsea vertebrate locality as the sandy fill of a submerged lowstand valley of the Solo **(Fig. 2)**. Off the coast of Surabaya, the base of the incised valley lies at a depth of 50 m below mean sea level (MSL). The valley fill has a thickness of ca. 30 m and consists of fluvial sandstones and conglomerates, which change upwards into marine sandstones and marine clay-sand alternations. Two fluvial sandstone samples yielded OSL-ages of 162±31 and 119±27 ka, indicating that the valley fill is associated with MIS6 and with the subsequent transgressive stage in the run-up to MIS5. Consequently, the valley was probably cut during the preceding stage of falling sea-level in the run-up to MIS6. The upwards change to marine strata indicates that the valley was eventually invaded by the sea, changing the valley into an estuary.

The study aimed to provide:

1: a detailed metric and morphological description of the Madura Strait assemblage, which may serve as a reference for future comparative studies of fossil finds in the region.

2: insight into the vertebrate fauna of the lowland plains of Sundaland during the late Middle Pleistocene and into its implications for regional biogeography and faunal dispersal.

This publication presents the results of the palaeontological analysis of the entire Madura Strait assemblage, with the exception of two hominin skull fragments, which are presented separately (Berghuis et al., 2025d).

2. Methods

The first fossil-collecting campaign was carried out between July and September 2015. The entire surface of the site was explored on hands and knees (by H.B.), collecting all vertebrate fossils visible to the naked eye. The work did not include digging trenches or sieving of sediment. Additional searches took place in 2016, 2017, and 2018, collecting in areas that had been subject to erosion by run-off, or where construction-related ground works had exposed new material.

The collected fossils were transported to the Geological Museum Bandung, where the material was cleaned, provisionally ordered, labelled and stored. The total number of collected specimens is 6,372. Most specimens received a separate collection number. In other cases, a collection number was given to a group of related fossils or fossil fragments, which were referred to as specimen A, B, etc. The fossil remains are heavily mineralized and strongly fragmented. A systematic taphonomic analysis has been carried out and is presented separately (Berghuis et al., 2025c).

Morphological description and taxonomical identification of the material was carried out at the Geological Museum Bandung. Measurements were taken with a digital calliper following the guidelines of Von den Driesch (1976). The dental nomenclature is based on Herman (1994) for batoid fish, Cappetta (1987) for sharks, Van den Bergh (1999) for proboscideans and Hillson (2005) for other (mammalian) species. The osteological nomenclature is based on Williston (1925) for reptiles and on Pales et al. (1971) for mammals. Dextral and sinistral positions are indicated as (d), (s) or when unknown as (d/s).

For direct morphological comparison, extensive use has been made of the collection of the Geological Museum Bandung. Other institutes that have been visited for comparative studies are the Trinil Museum (Indonesia), Naturalis Biodiversity Center (the Netherlands), the Zoological Laboratories of Leiden University (the Netherlands) and Tübingen University (Germany) and the Museum für Naturkunde of Berlin (Germany). Identifications have been based on recent and commonly accepted taxonomies of extant and extinct species, with references to relevant publications. For Java, with its long history of palaeontological research, this is not always an easy task, as the taxonomies have been subject to repeated revisions, while abandoned species names are still frequently used.

We followed the hierarchy and taxonomic subdivision of Nelson et al. (2016) for fishes, Pincheira-Donoso et al. (2013) for reptiles and Wilson and Reeder (2005) for mammals. The even-toed ungulates, represented by a large number of taxa within the Madura Strait assemblage, have been referred to as the Order Artiodactyla, thus not following Montgelard et al. (1997) who proposed to revise this order into Cetartiodactyla, a revision which is debated (Prothero et al., 2022).

3. Systematic palaeontology

The Madura Strait assemblage has a high species diversity, representing four taxonomical Classes and eleven Orders **(Table 1)**. In the next sections, the identified species will be discussed per taxonomical Order. The species represent different ecosystems, ranging from terrestrial to fluvial and estuarine. In **Section 4** we will go deeper into the background of the assemblage in terms of vertebrate communities and Sundaland biogeography.

Class Chondrichthyes (Huxley, 1880) - cartilaginous fish
Superorder Galeomorphii Compagno, 1973 - galean sharks
Order Carcharhiniformes (Compagno, 1977) - ground sharks
Superorder Batoidea (Compagno, 1973) - rays
Order Myliobatiformes (Compagno, 1973) - stingrays
Class Actinopterygii (Klein, 1885) - ray-finned fish
Order Siluriformes Cuvier, 1817 - catfish
Class Reptilia Laurenti, 1768 - reptiles
Superorder Lepidosauria (Haeckel, 1866) - lepidosaurs
Order Squamata (Oppel, 1811) - scaled reptiles
Order Testudines (Batsch, 1788) - turtles
Order Crocodilia (Owen, 1842) - crocodilians
Class Mammalia Linnaeus, 1758 - mammals
Order Proboscidea (Illiger, 1811) - elephantoids
Order Primates (Linnaeus, 1758) - primates
Order Carnivora (Bowdich, 1821) - carnivores
Order Perissodactyla (Owen, 1848) - odd-toed ungulates
Order Artiodactyla (Owen, 1848) - even-toed ungulates

Table 1. The vertebrate fauna (Phylum Chordata) of the Madura Strait: subdivision in taxonomic Classes and Orders.

3.1 Order Carcharhiniformes (Compagno, 1973) – ground sharks

Pleistocene shark teeth from Java were first described by Dubois (1907) and Hennig (1911). These teeth were excavated from fluvial strata in Trinil and ascribed to the freshwater shark *Carcharias gangeticus*, a species today referred to as *Glyphis gangeticus* (Nelson et al., 2016). Two morphologically deviant teeth from Trinil were ascribed to *Carcharias taurus* (Joordens et al., 2009; Koumans, 1949), which is an extant coastal species. Yudha et al. (2018) described fossil shark teeth from museum collections in Java, mostly of unknown age or stratigraphic provenience.

Family: Hemigaleidae Hasse, 1878 – weasel sharks
Genus: *Hemipristis* Agassiz, 1843
***Hemipristis serra* Agassiz, 1843**

Available material (N=5). Upper teeth: SBY5050, SBY646. **Lower teeth:** SBY7129A-C.

Description and identification: SBY5050 **(Fig. 3)** is an eye-catching specimen among the shark teeth from the Madura Strait, because of its large size and conspicuous coarse serrations along the cutting edges. The crown is triangular and slightly distally inclined, with a convex mesial cutting edge and a concave distal cutting edge. The labial face of the crown is flat, but the lingual face is arched, which gives it a robust appearance. Also, the root is arched at the lingual side, with a prominent protuberance. The root is bilobate, with a nutritive groove at the lingual side and a prominent concavity between the lobes.

The convex and concave cutting edges with coarse serrations are highly similar to the upper teeth of *Hemipristis elongata,* the extant snaggletooth shark of the Indian Ocean and the western Pacific. However, the size of SBY5050 **(Table 2)** exceeds the range of this species and links it to the extinct sister species *Hemipristis serra* (Kent, 2018). *Hemipristis serra* is known from numerous Miocene to Pleistocene localities worldwide and inhabited shallow tropical seas (Cappetta, 1987). Four other specimens have been assigned to this species. SBY7129B **(Fig. 3)** has a morphology that is highly similar to SBY5050, but is smaller and more inclined. It is slightly weathered, but remnants of the coarse serrations are visible along the concave distal cutting edge. Its size and morphology fall within the range of this species' lower lateral teeth. SBY7129A **(Fig. 3)** is a lower anterior tooth, recognizable by its pointed, unserrated, and hooked morphology**.** They are differentiated from *Glyphis gangeticus* lower anterior teeth (see below) by their larger size, as well as the thicker, strongly bilobate root, with at the lingual face a characteristic rounded protuberance and nutritive groove.

Family: Carcharhinidae Jordan and Evermann, 1896
Genus: *Glyphis* Agassiz, 1843
***Glyphis gangeticus* (Müller & Henle, 1839) – Ganges shark**

Synonyms: *Prionodon gangeticus*, *Eulamia gangetica*; *Carcharias gangeticus*; *Carcharhinus gangeticus*

Available material (N=51). Upper teeth: SBY640A-D, SBY641A-E, SBY5048A-E, SBY5049A-C, SBY7122A-H, SBY7133A-I. **Lower teeth:** SBY654A-E, SBY5047A-F, SBY7123A-F.

Description and identification: The upper teeth have flat, broad, triangular, blade-like cusps with finely serrated cutting edges. Their root is thin and flat, only slightly arched at the lingual side, and lacks a prominent neck, which gives the teeth a tall and slender appearance. We pictured two representative specimens **(Fig. 3)**. SBY5048A is an anterior tooth, with an erect, symmetrical shape. SBY5048B is a lateral tooth, characterized by a semi-oblique, backward-pointing blade, a straight mesial cutting edge, and a slightly notched distal cutting edge. The lower teeth of this species have a different morphology, with a long and pointed crown and unserrated cutting edges. The pictured specimen SBY5047A **(Fig. 3)** has downward projecting, bilobate and rounded roots. This, in combination with its significant length and inward-hooked shape, identifies the specimen as an anterior tooth.

The slender, triangular crowns with finely serrated cutting edges and thin roots are characteristics of the upper teeth of the genus *Glyphis* (Compagno, 2001). *Glyphis* species live in the tidal or freshwater zone of large muddy rivers and occur in an area stretching from the Indian peninsula to northern Australia. The genus holds a number of species, including *Glyphis gangeticus*, *Glyphis glyphis* and *Glyphis garricki* (Compagno, 2001). The latter two species occur in the lowland rivers of Borneo and New Guinea. These two species have a spear-like thickening at the top of the lower anterior teeth, which appears to be absent in the specimens from the Madura Strait. In this respect, the Madura Strait teeth correspond with the extant *G. gangeticus* of India.

Genus: *Carcharhinus* Blainville, 1816
C*archarhinus* cf. *leucas,* Valenciennes, 1839 – bull shark

Available material (N=20). Teeth: SBY7124A-C, SBY7125A-F, SBY7126A-B, SBY7132A-I.

Description and identification: The teeth have triangular cusps with finely serrated cutting edges. The crown and the root are relatively thick and rounded, especially at the lingual face. The root is slightly bilobate, with a nutritive groove at the lingual face. There is a prominent neck between the crown and the root at the lingual face, and a prominent distal heel, resulting in a relatively great basal crown width. We pictured two representative specimens: SBY7124A and B **(Fig. 3).**

The teeth may, at first glance, appear similar to those of *G. gangeticus*. However, they differ from this species by their lower crown height **(Table 2)** and rounded lingual face. The specimens correspond well with the teeth of *Carcharhinus leucas* and *Carcharhinus amboinensis* (Compagno, 2001), two species with morphologically identical teeth. Both species are extant in Indonesian waters. We ascribe the specimens to *C.* cf. *leucas* because of their size **(Table 2)**, which is slightly above the reported size range of *C. amboinensis* (Lin et al., 2022; Kocsis et al., 2019). *Carcharhinus leucas* has a coastal habitat, enters shallow bays and estuaries and may ascend rivers. The upper and lower teeth of this species are morphologically similar. We loosely subdivided the Madura Strait specimens into upper and lower teeth by the criteria that the species' upper teeth are slightly larger and thicker, whereas the lower teeth have a slightly more pronounced bilobate root (Compagno, 2001).

Specimen	*Taxonomy*	*Tooth position*	*Crown height (mm)*	*Mesial crown edge length (mm)*	*Basal crown width (mm)*
SBY5048A	*Glyphis gangeticus*	Upper anterior	19.2	21.5	18.1
SBY5048B	*Glyphis gangeticus*	Upper lateral	12.7	18.6	17.7
SBY5047A	*Glyphis gangeticus*	Lower anterior	17.1	18.4	8.9
SBY7124A	*Carcharhinus* cf. *leucas*	Upper lateral	13.9	20.1	18.2
SBY7124B	*Carcharhinus* cf. *leucas*	Lower lateral	12.1	19.4	19.5
SBY5051	*Galeocerdo cuvier*	Upper lateral	16.0	25.1	28.1**
SBY5050	*Hemipristis serra*	Upper lateral	27.3*	31.3*	23.1
SBY7129A	*Hemipristis serra*	Lower anterior	28.4	32.1	15.2
SBY7129B	*Hemipristis serra*	Lower lateral	19.1	21.9	15.7

Table 2. Measurements (mm) Carcharhiniformes teeth (specimens pictured in **Fig. 3**).
* Small part of crown tip broken off, given value is estimate of unbroken state. ** Measurement includes distal cusplet.

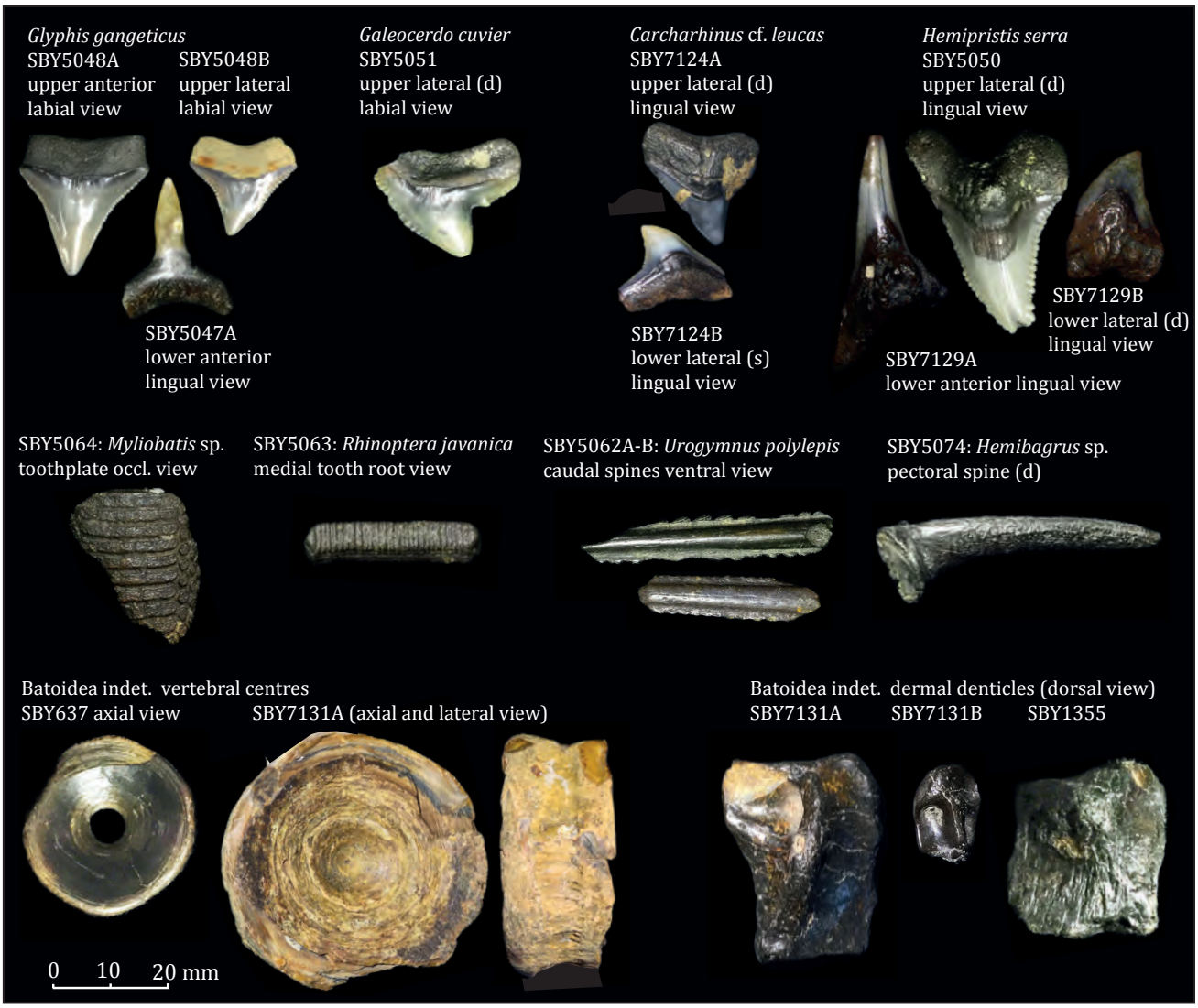


Fig. 3. Fish remains (Myliobatiformes, Carcharhiniformes, Siluriformes) from the Madura Strait assemblage. Selected photographs. For measurements see **Tables 2** and **3**.

Genus: *Galeocerdo* Müller and Henle, 1837
Galeocerdo cuvier (Péron & Lesueur, 1822) – tiger shark

Available material (N=3). Upper teeth: SBY5051, SBY7134A-B.

Description and identification: SBY5051 **(Fig. 3)** is a tooth with a backward-curved crown with a distal cusplet, forming a prominent distal heel. It has coarse serrations along the mesial cutting edge of the main cusp and the distal cusplet. The posterior cutting edge of the main cusp has finer serrations. The root is robust and arcuate. The anterior part of the root is broken off.

The backward-curved crown with the serrated distal cusplet is characteristic of *Galeocerdo cuvier*. The species has similar-shaped upper and lower teeth. However, Compagno (2001) noted that in the upper teeth, the serration pattern on the distal heel increases in height anteriorly toward the notch, a feature which we also observe in SBY5051. *Galeocerdo cuvier* is a common tropical to warm-temperate species with a preference for turbid continental waters and often enters into estuaries.

Specimen	*Taxonomy*	*Tooth position*	*w (mm)*	*l (mm)*	*w/l-ratio*	*h-crown*	*h-root*
SBY5064	*Myliobatis* sp.	medial	17.5	2.3	7.6	0.99	0.71
SBY5063	*Rhinoptera javanica*	medial	29.80	5.71	5.23	1.73	1.39
SBY7121A	*Rhinoptera javanica*	medial	>27.45*	6.84	> 4.01	1.80	1.51
SBY7121B	*Rhinoptera javanica*	medial or 3rd lateral	>13.78*	8.40	--	3.85	2.45

Table 3. Measurements (mm) Myliobatiformes teeth. * Incomplete specimens. Given values are measured (minimum) widths.

3.2 Order Myliobatiformes (Compagno, 1973)

There are no previous records of Pleistocene Myliobatiformes from Java, except for two spine fragments collected in Trinil in the 1890s, which had earlier been referred to as Siluroidea indet. (Koumans, 1949; Dubois, 1908). Joordens et al. (2009) re-interpreted the specimens as caudal spines of the giant freshwater stingray *Himantura chaophraya*, a species nowadays referred to as *Urogymnus polylepis* (Nelson et al., 2016).

Suborder: Myliobatoidei - stingrays
Family: Myliobatidae (Bonaparte, 1838)
Genus: *Myliobatis* Cuvier, 1816
***Myliobatis* sp.**

Available material (N=1). Dental plate fragment: SBY5064.

Description and identification: SBY5064 **(Fig. 3)** is a fragment of a dental plate made up of at least nine teeth rows, each consisting of one laterally enlarged medial (symphysial) tooth and three lateral teeth along both buccal sides. The medial teeth are six-sided, straight, and extremely buccolingually enlarged **(Table 3)**, without significant size variation between the tooth rows. The lateral teeth are not buccolingually enlarged, but square-shaped and placed in an imbricated position, shifted half of a tooth length over the neighbouring rows. The teeth have a smooth occlusal surface. The opposite surface (root view) has a fine pattern of narrow plate elements, directed mesiodistally over the dental plate, separated by grooves.

Pavement-like dental plates are found in Myliobatinae and Rhinopterinae, two subfamilies of Myliobatidae. The described plate architecture, with rows consisting of one laterally enlarged medial tooth sided by three not enlarged lateral teeth, is characteristic of Myliobatinae. The straight, extremely enlarged medial teeth, with little width variation of these medial teeth over the consecutive rows, are indicative of the genus *Myliobatis* (Herman et al., 1994).

The size of the fossil dental plate is indicative of a stingray with a disk width of around 50 cm. Currently, two *Myliobatis* species of this size occur in the Indonesian seas: *M. tobijei* and *M. hamlyni*. However, both are deep-water species, which makes their occurrence in the Madura Strait assemblage unlikely. The fragment is therefore referred to as *Myliobatis* sp.

Family: Rhinopteridae Jordan & Evermann, 1896
Genus: *Rhinoptera* Cuvier, 1829
***Rhinoptera javanica* (Müller & Henle, 1841) – flapnose ray**

Available material (N=3). Teeth: SBY5063, SBY7118A-B.

Description and identification: SBY5063 **(Fig. 3)** is a six-sided, straight, buccolingually enlarged tooth, deriving from a disarticulated dental plate of a stingray. The tooth is larger and more robust than the medial teeth of the articulated dental plate SBY5064 that we ascribed to *Myliobatis* sp., but it has a lower width/length-ratio **(Table 3)**. It has a smooth occlusal surface and a comb-like base (root view), consisting of fine mesiodistally oriented ribs. The position of the root is shifted several mm posteriorly from the crown, which is an interlocking mechanism that makes that crowns partly rest on the root of the adjacent teeth row.

The robustness and relatively low w/l-ratio of the tooth are characteristic of Rhinopterinae dental plates, which are made up of only ca. ten rows of relatively large teeth (Herman et al., 1994). As for Myliobatinae, the teeth rows consist of a medial tooth flanked along both sides by lateral teeth, which are placed in an imbricated pattern. However, in contrast to Myliobatinae, the lateral teeth are hexagonal. Moreover, the lateral teeth are not of uniform size, but become increasingly enlarged toward the medial tooth. The latter is still the widest tooth of the row, but with an enlargement that is not as extreme as in Myliobatinae.

Another difference is that Rhinopterinae dental plates are not as tightly interlocked, which makes that single teeth are found more often (Claeson et al., 2010). There are two extant *Rhinoptera* species in Indonesian waters: *Rhinoptera jayakari* and *Rhinoptera javanica.* The former has highly robust medial teeth, with a w/l-ratio that hardly exceeds 3 (Pradeep et al., 2018). Moreover, it is a deep-water species, which makes its occurrence in the Madura Strait assemblage unlikely. The latter species lives in coastal and estuarine waters and has a dentition that closely matches the Madura Strait specimens, with respect to morphology and size range (Herman et al., 1994). With a width of ~30 mm and a w/l-ratio of ~5, SBY5063 is identified as a medial tooth **(Table 3)**. We therefore ascribe the specimens to *R. javanica*.

Family: Dasyatidae (Jordan, 1888)
Genus: *Urogymnus* (Müller & Henle, 1837)
***Urogymnus polylepis* (Bleeker, 1852) – giant freshwater stingray**

Synonyms: *Himantura polylepis*, *Himantura chaophraya*

Available material (N=3). Caudal spine fragments: SBY 5062A-C.

Description and identification: The specimens **(Fig. 3**) are fragments of straight caudal spines, with symmetrical serrations along both lateral margins and a frequency of nine or ten serrations per cm. The dorsal side of the spines is smooth and convex, whereas the ventral side has a rounded axial rib. In SBY5062A this axial rib is slightly tapering, indicating a position toward the distal end of the spine. With a width between 7 and 8 mm, the fragments must derive from large and robust spines, with an estimated length of around 15 cm, which clearly exceeds the size range of *Myliobatis*. Spines with a length up to ~10 cm are known from *R. javanica* (Schwartz, 2007). Concerning size and morphology, the spine fragments from the Madura Strait compare well with the spines of the giant freshwater stingray *Urogymnus polylepis* (Cuny and Piyapong, 2007), an extant species, living in large lowland rivers and estuaries of Southeast Asia, including Sumatra and Borneo and until recently on Java (Iqbal et al., 2020). The fossils are also highly similar to the Pleistocene specimens from Trinil, ascribed to this species by Joordens et al. (2009).

3.3 Superorder Batoidea, Compagno, 1973

Batoidea indet. - rays

Available material (N=18). Vertebral centra: SBY7130A-G, SBY637, SBY642, SBY662, SBY666 and SBY7130A, SBY7127. **Dermal denticles:** SBY1355, SBY7131A-C, SBY7183.

Description and identification: The vertebral centra are cylindrical and biconcave and have concentric growth bands, which associate them with cartilaginous or bony fish. Compared to their diameter, they have a short anteroposterior length. For example, the pictured specimens SBY637 and SBY7130A **(Fig. 3)** have a diameter of 28 and 40 mm and an anteroposterior length of ~12 and 16 mm respectively. This short anteroposterior length (less than 50% of the radius) is characteristic of Batoidea (Kozuch and Fitzgerald, 1989). Another morphological trait that points to Batoidea is the absence of clear dorsal and ventral foramina along the sides of the vertebral centrum. Because of a lack of diagnostic features and in the absence of useful reference collections or ichthyological descriptions, the specimens have been assigned to Batoidea indet. Referring to their size and to the fluvial to estuarine depositional conditions of the site, the specimens may represent Pristidae (saw fishes), but may also very well derive from the giant stingray *Urogymnus polylepis*.

The Madura Strait assemblage contains several rectangular, flat bony elements with a concave base. SBY1355 **(Fig. 3)** measures 34 mm anteroposteriorly and mediolaterally. Its dorsal surface is ornamented with fine striations that radiate outward from a rounded central keel. Its ventral surface is smooth and slightly convex. SBY7131A and B **(Fig. 3)** have a more elongated outline and a smooth upper surface, with a longitudinal keel that is slightly inclined to one side, running diagonally over the dorsal surface. The specimens have the appearance of crocodilian osteoderms, but they differ from such elements by the absence of a pitted ornamentation on the dorsal surface. We refer to the specimens as Batoidea indet., because of the similarity with the batoid dermal denticles described by Lopes et al. (2016) and Bourbon (2011). Detailed ichthyological descriptions of batoid dermal denticles are unfortunately not available.

3.4 Order Siluriformes (Cuvier, 1817) - catfish

Pleistocene remains of Siluriformes from Java are scarce. Dubois (1908, 1907) mentioned the occurrence of *Clarias magur* among the fossils from Trinil. Hennig (1911) described several pectoral spines and cranium fragments from Trinil as *Clarias* sp. and Siluridae indet. Koumans (1949) re-analysed the material collected by Dubois and recognized three species: *Hemibagrus nemurus*, *Clarias batrachus* and *Clarias leiacanthus,* which was confirmed by Joordens et al. (2009). Yudha et al. (2020) studied museum specimens from of Java, mostly of unknown age and stratigraphic provenience, and recognized several additional species.

Family: Bagridae Bleeker, 1858
Genus: *Hemibagrus* Bleeker, 1862
***Hemibagrus* sp.**

Available material (N=1). Pectoral spine (d): SBY5074.

Description and identification: SBY5074 **(Fig. 3)** is an intact pectoral spine with a length of 53 mm. The specimen is slightly worn and the serrations on the lateral surfaces have largely vanished. The spine has a relatively straight shaft. It slightly bends inwards at the proximal side, which shows that it is a dextral spine. The shaft widens toward the articulation, leaving a prominent and elongated notch (the basal recess) along its posterior face. Its size and morphology

are similar to other Pleistocene spines from Java, identified as *Hemibagrus* cf. *nemurus* by Yudha et al. (2020) and Koumans (1949). However, nowadays around 40 extant species are recognized within the genus *Hemibagrus*, most of which live in Southeast Asian drainage systems (Ng and Kottelat, 2013). Lacking clear osteological descriptions, it is not realistic to determine a single fossil spine to species level. SBY5074 is therefore assigned to *Hemibagrus* sp.

3.5 Order Squamata Oppel, 1811 – scaled reptiles

Records of Pleistocene Squamata from Java are scarce. Several dorsal vertebrae of Varanidae were found in Trinil and one in Kedung Brubus (Janensch, 1911a; Dubois, 1908). Hooijer (1972) ascribed most of these to *Varanus salvator*, the Asian water monitor, which is still extant on Java. He ascribed several larger specimens to *Varanus komodoensis*, suggesting that the current occurrences of this species on the islands of Komodo, Rinca, and Flores are relicts of a wider distribution during the Pleistocene.

There is one record of Early to Middle Pleistocene Serpentes, which is a single vertebra from Trinil (Janensch, 1911a). This specimen was only mentioned in the find list, without further details or determination. In the 1990's, a complete skeleton of a Late Pleistocene snake was found in Ciharuman, West-Java, which was ascribed to *Malayopython reticulatus* (Aziz and de Vos, 1999).

Suborder: Lacertilia Günther, 1867
Family: Varanidae Merrem, 1820
Genus: *Varanus* Merrem, 1820
***Varanus komodoensis* Ouwens, 1912 – Komodo dragon**

Available material (N=2). Dorsal vertebrae: SBY533 and SBY7137.

Description and identification: The two vertebrae **(Fig. 4)** have a procoelous centrum and prominent outwards projecting zygapophyses. In both specimens, the posterior part of the centrum and the neural spine are missing. Pre- and postzygapophyses are preserved, although small fragments of the tips are missing. Zygapophysal dimensions could be estimated, using intact varanid vertebrae as a morphological reference **(Table 4)**. Morphologically, the specimens closely match with dorsal vertebrae of recent varanids curated at Naturalis Biodiversity Center and Tübingen University, as well as with the Pleistocene *Varanus* vertebrae from Java presented by Hooijer (1972).

Hocknull et al. (2009) measured a large sample of recent *V. komodoensis* and *V. salvator* vertebrae and provided species-specific size ranges. The measurements of the Madura Strait specimens **(Table 4)** follow the methods of these authors. A bivariate plot **(Fig. 5)** of pre-prezygapophysal width and pre-postzygapophysal length places the two specimens from the Madura Strait in the size range of *V. komodoensis*.

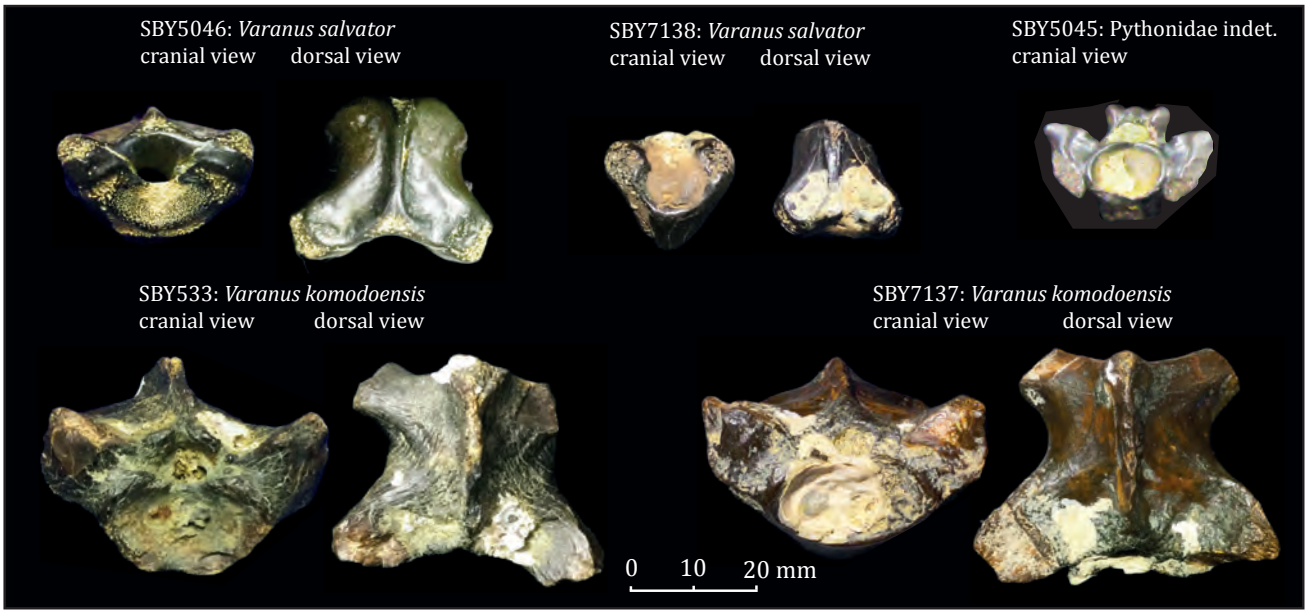


Fig. 4. Dorsal vertebrae of Squamata (Varanidae, Pythonidae) from the Madura Strait assemblage. Selected photographs. For measurements see **Table 4**.

Varanus salvator (Laurenti, 1768) – Asian water monitor

Available material N=2. Dorsal vertebrae: SBY5046, SBY7137.

Description and identification: Morphologically, the two specimens **(Fig. 4)** are similar to the two vertebrae ascribed to *Varanus komodoensis*. Also their state of preservation is similar, with the posterior part of the centrum and the

neural arches broken off. SBY5046 has almost complete zygapophyses. In SBY7137, the postzygapophyses are missing. Metrically, the two specimens are significantly smaller **(Table 4).** Note that the postzygapophysal sizes of SBY7137 are estimates. Both specimens plot below the size range of *V. komodoensis* and fall in the range of *V. salvator* **(Fig. 5)**.

Specimen	*Taxonomy*	*Cotylar width (CW) (mm)*	*Pre-pre (mm)*	*Post-post (mm)*	*Pre-post (mm)*	*Zygosphene width (mm)*
SBY533	*Varanus komodoensis*	20.9	48	37	38	
SBY7137	*Varanus komodoensis*	22.4	50	40	41	
SBY5046	*Varanus salvator*	15.1	31	29	28	
SBY7138	*Varanus salvator*	10.0	22		21	
SBY5045	Pythonidae indet.	10.3	25.8			10.4
	*Malayopython reticulatus**	16.2	46.3			16.2

Table 4. Measurements of Varanidae and Pythonidae vertebrae (mm), methods based on Hocknull et al. (2009). Pre-pre = pre-prezygapophysis width; post-post = post-postzygapophysis width; pre-post = pre-postzygapophysis length. Centrum lengths could not be taken, as centra are incomplete. All zygapophysal measurements involve reconstructions of broken tips.
*: Measurements taken from a central trunk vertebra of the Late Pleistocene *Malayopython reticulatus* of West-Java stored in the Geological Museum Bandung.

Suborder: Serpentes Linnaeus, 1758 - snakes

Family Pythonidae Fitzinger, 1826 - pythons

Pythonidae indet.

Available material (N=1). Trunk vertebra: SBY5045.

Description and identification: SBY5045 **(Fig. 4)** is a procoelous vertebra with a prominent zygosphene, which links the specimen to the suborder Serpentes (Holman, 2000). The posterior part of the centrum is broken off and also the postzygapophysis is largely missing. The prezygapophysis is intact, except for a small part of the dextral tip. Both diapophyses have been broken off. Along the dorsal side, the neural spine is broken off. The cotyle is laterally expanded. From an anterior view, the zygosphene has a trapezoid shape and a convex roof, with its lateral edges upturned dorsally. The centrum has a preserved ventral length of 10.6 mm and has a massive, triangular shape, widening anteriorly.

The sizes of the centrum, the cotyle, and the zygosphene **(Table 4)** point to a large snake. The wide, triangular shape of the centrum is characteristic of Boidae and Pythonidae (Ikeda, 2007). Giant Boidae are absent in Southeast Asia and unknown from the regional fossil record. Two large Pythonidae: *Malayopython reticulatus* and *Python bivittatus*, are extant on Java, living in grasslands, marshes and forests. Both are also good swimmers. In the absence of relevant comparison collections or published osteological descriptions, we refer to the specimen as Pythonidae indet.

Morphologically, SBY5045 compares well with the Late Pleistocene *Malayopython reticulatus* of West-Java, which is stored at the Geological Museum Bandung. We took reference measurements of the central trunk vertebrae of this complete skeleton **(Table 4)**, which are above the size of the single vertebra from the Madura Strait.

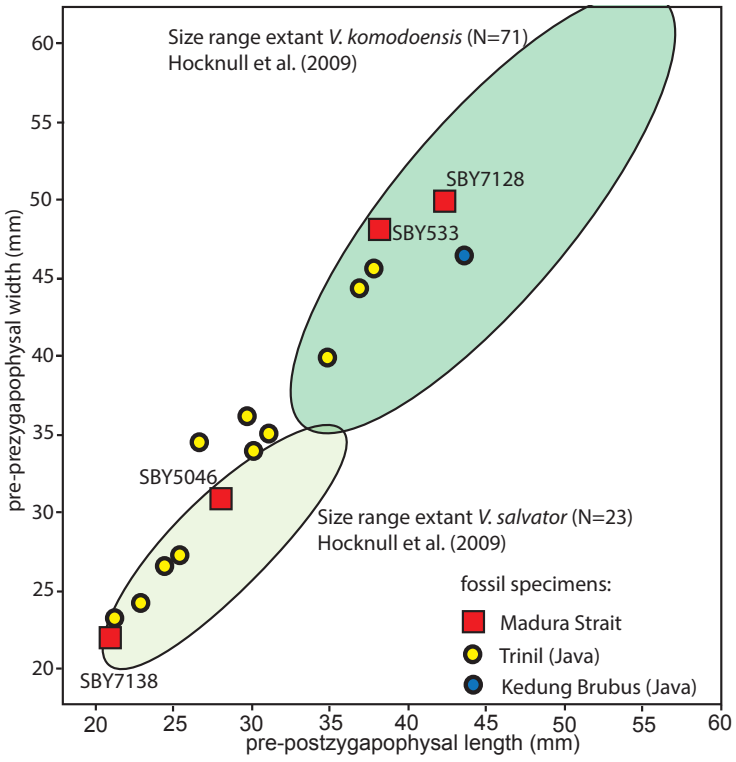


Fig. 5. Bivariate plot of the Varanidae dorsal vertebrae from the Madura Strait (pre-prezygapophysal width and pre-postzygapophysal length) in relation to size ranges of extant *V. salvator* and *V. komodoensis* and sizes of fossil specimens from Trinil and Kedung Brubus. All reference sizes from Hocknull et al. (2009).

3.6 Order Testudines (Batsch, 1788) - turtles

Fossil shell fragments of freshwater turtles are common finds on Java, but they are generally left unidentified. Jaeckel (1911) introduced five new Pleistocene species, based on mostly fragmented material from Trinil. The species were rejected by Karl (1987) and synonymized with extant species. An interesting review of these earlier fossil finds from Java is given by Claude et al. (2024). There are around fifteen extant species of medium to large freshwater turtles in western Indonesia and more in Southeast Asia (Rhodin et al., 2015). For our comparisons, we focussed on the extant, lowland-river turtles of Java, Sumatra, and Borneo.

Family: Geoemydidae (Theobald, 1868) – hard-shelled turtles
Geoemydidae indet.

Available material (N=102). Neural plate fragments (21): SBY5031. **Costal plate fragments (42):** SBY5032, SBY7165. **Peripheral plate fragments (17):** SBY5033, SBY7141. **Plastron fragments (22):** SBY5034.

Description and identification: The shell fragments are smooth-surfaced and have a thickness ranging between several mm and 16 mm. Sutures marking the boundary between the individual plate fragments are not observable and the break surfaces appear to be random, bearing no relation with the original plate boundaries. This points to an advanced state of ossification and fusing of plate elements. The plate fragments have been ordered and grouped by their position in the original shell, distinguishing between neural fragments (with fused vertebrae at the ventral side), costal fragments (with fused ribs), peripheral fragments (preserving parts of the carapace margin) and unarched plastron fragments. Some fragments preserve sulci, which are imprints of seams between the epidermal scutes that covered the ossified plates. In some cases, the sulci provide insight into the original position of the fragment in the turtle shell. For example **(Fig. 6)**: SBY5033A is a peripheral plate fragment preserving the sulci between two marginal scutes and a costal scute. SBY5032A is a fragment of the first sinistral costal plate, preserving the sulci between the first costal scute and the first two vertebral scutes. SBY5033B is a peripheral plate fragment, preserving a sulcus between two marginal scutes and a small part of the sulcus that marks the boundary with the adjacent costal scute. This specimen is special, as it also preserves a fine imprint of the scute's reticulated micro-ornamentation (annuli).

All smooth-plated freshwater turtles of western Indonesia belong to the family of Geoemydidae (Rhodin et al., 2015). Among the Geoemydidae species, there are notable morphological differences of the individual plate elements. However, the strongly ossified and randomly broken fragments offer little clues for species identification based on plate morphology. Nevertheless, some useful taxonomic information can be extracted from the fragmented material. For example, all neural plate fragments have a smooth dorsal surface, which points to the absence of species such as *Siebenrockiella crassicollis*, which have a dorsal keel. Likewise, all peripheral plate fragments have smooth margins, excluding species with serrated carapace margins such as *Heosemys grandis* (Rhodin et al., 2015).

The plate fragments are referred to as Geoemydidae indet. Based on the size and thickness of the plates, we assume that the plate fragments derive from medium to large freshwater species such as *Batagur affinis* and *Orlitia borneensis*, both of which are extant in western Indonesia.

Genus: *Batagur* Gray, 1856
***Batagur affinis* (Cantor, 1847)**

Synonym: *Batagur siebenrocki*

Available material (N=1). Hypoplastron fragment: SBY7139.

Description and identification: SBY7139 **(Fig. 6)** is a lateral fragment of a dextral hypoplastron, preserving the rounded inguinal notch and the transition toward the bridge. Sulci demarcate the margins between the femoral, abdominal, inguinal, and lateral scutes Yudha et al. (2020a, Fig. 8) provided drawings of plastron morphology and sulci patterns for several Geoemydidae. The broad and rounded inguinal notch of SBY7139 links the fragment to the genus *Batagur*. Moreover, the two smoothly curved sulci and their approach to the inguinal notch, as well as the sulci demarcating the inguinal scute, which form an elongated triangle anterior of the inguinal notch, are characteristic of this genus.

The fragment is highly similar to the plate of the southern river terrapin *Batagur affinis,* the extant *Batagur* of Sumatra and Borneo, living in lowland rivers and tidal zones. *B. affinis* is closely related to *Batagur baska* of mainland Asia and has recently been indicated as a separate species (Moll et al., 2021). A carapace from Trinil, described by Jaeckel (1911) as *Batagur siebenrocki*, was re-interpreted by Karl (1987) as *B. baska.* Referring to the geographic proximity of their extant population, *Batagur affinis* is a more appropriate name. Note that there is no osteological difference between both species.



Fig. 6. Geoemydidae and Trionychidae remains from the Madura Strait assemblage. Selected photographs of shell fragments. Carapace fragments in dorsal view and plastron fragments in ventral view.

Genus: *Orlitia* (Gray, 1873)
***Orlitia borneensis* (Gray, 1873) – Bornean river turtle**

Synonym: *Batagur signatus*

Available material (N=1). Xiphiplastron fragment: SBY5031.

Description and identification: SBY5031 **(Fig. 6)** is a fragment of a dextral xiphiplastron with a narrow and triangular shape, pointing posteriorly. Its medial margin is rounded and demarcates a pronounced, semi-circular anal notch. The posterior tip has broken off. Pritchard et al. (2009) provided images of the plastron of relevant turtle species, showing conspicuous morphological differences. A posteriorly pointing xiphiplastron with a large, semi-circular anal notch is characteristic of *Orlitia borneensis*.

Orlitia borneensis is a giant freshwater species of Borneo and Sumatra, with carapaces reaching a length of ~ 80 cm (Rhodin et al., 2015). Probably, the thickest unidentifiable plate fragments from the Madura Strait assemblage also derive from this species. There are two earlier records of this species from the Pleistocene of Java: two small plate fragments from Trinil were described as *Batagur signatus* by Jaeckel (1911) and provisionally re-interpreted by Karl (1987) as *O. borneensis.* Moreover, Setiyabudi et al. (2016) assigned a costal plate from Sambungmacan to this species.

Family: Trionychidae Fitzinger, 1826 – soft-shelled turtles
Genus: *Chitra* Gray, 1844
***Chitra chitra* Nutaphand, 1986 – Asian narrow-headed softshell turtle**

Synonym: *Chitra selenkae*

Available material (N=29). Neural plate fragments (7): SBY5004. **Costal plate fragments (16):** SBY5005. **Plastron fragments (4):** SBY5006.

Description: The plate fragments are relatively thick (5 – 12 mm) and have an ornamentation of thick, vermiform ridges and broad valleys. Three examples are pictured in **Fig. 6.** SBY5005A is an 11 mm thick costal fragment including a section of the lateral margin of the carapace. Note that peripheral plates are absent in Trionychidae. The plate margin is slightly undulating and preserves a small part of the exposed rib tip. The dorsal surface of the plate has an ornamentation of elongate ridges and valleys running parallel to the plate margin. The ridges are coarse and rounded, with a ridge height of ~ 2 mm and an interval of 5 to 10 mm between the ridge crests. SBY5005B is a costal fragment with a similar ornamentation, but on this fragment, it forms a more irregular pattern of open, semi-circular valleys and ridges. SBY5006A is a plastron fragment preserving a lateral margin with three prongs. At its ventral face it has a similar coarse vermiform surface sculpturing, forming parallel and semi-circular ridges and valleys.

The surface ornamentation of thick vermiform ridges and broad valleys is characteristic of *Chitra chitra* (Pritchard et al., 2009). Useful pictures of museum specimens are provided by Gemel and Haring (2011), showing that carapace sculpturing patterns change from irregular and semi-circular ridges on the neural plates and medial zones of the costal plates to parallel ridges and valleys along the plate margins. The undulating outer margin of SBY5005A is characteristic of the anterior two costals. Comparison with the pictured specimens indicates that the fragment derives from the second dextral costal plate. Although surface sculpturing is generally described as a trait of carapaces, the descriptions and pictures of Gemel and Haring (2011) show that the plastron of *C. chitra* has a similar ornamentation. The morphology of the SBY5006A, with its three spiky projections, compares well with the dextral hypoplastron of the museum specimens presented by these authors.

Chitra chitra is a giant freshwater turtle living in large lowland-rivers of Southeast Asia, with a carapace length reaching ~100 cm (McCord and Pritchard, 2002). Pleistocene remains from Java were recorded by Jaeckel (1911), who originally assigned the material to *Chitra selenkae*.

Genus: *Pelochelys* Gray, 1864
***Pelochelys cantorii* Gray, 1864 – Cantor's giant softshell turtle**

Synonym: *Chitra minor*

Available material (N=7). Carapace (5) and plastron fragments (2): SBY5087A-G.

Description and identification: The plate fragments have a thickness of 6 – 10 mm and have a vermiform ornamentation of coarse and rounded ridges. This ornamentation differs from *C. chitra* by the occurrence of irregular ridges with frequent gaps and cross-connections. Pictured examples are costal fragments SBY5087A and B **(Fig. 6)**, the latter preserving a part of the plate margin with an exposed rib tip. As a result of the irregular ridges, the intermediate depressions form wells rather than valleys. These wells have a diameter of around 6 mm and a rounded morphology,

with gently sloping walls that grade into the well bottoms.

The surface ornamentation of irregular ridges surrounding rounded wells is characteristic of *Pelochelys cantorii* (Pritchard et al., 2009). Useful descriptions and photographs of museum specimens are provided by Gemel and Haring (2011). *P. cantorii* is a giant freshwater turtle living in lowland rivers and estuaries of Southeast Asia and is extant on Java. There have been no reported finds of this species from Java except for one or two plastron fragments from Trinil that were described as *Chitra minor* by Jaeckel (1911). McCord and Pritchard (2002) suggested that these fragments may represent *P. cantorii*.

Genus: *Amyda* Saint-Hilaire, 1809
***Amyda cartilaginea* (Boddaert, 1770) – black-rayed softshell turtle**

Synonyms: *Trionyx trinilensis*; *Trionyx cartilagineus*

Available material (N=5). Carapace fragments: SBY5000

Description and identification: SBY5000A **(Fig. 6)** is a 6 mm thick costal plate fragment, ornamented with fine, well-defined and vertically oriented ridges, extending ~0.8 mm above the surface of the plate. The ridges form an irregular, angular pattern, leaving flat-bottomed wells with a quasi-hexagonal shape and a diameter of around 3 mm. Discontinuities in the ridges are rare and virtually all wells are closed.

The surface ornamentation of angular, flat-bottomed wells surrounded by thin vertical ridges is characteristic of *Amyda cartilaginea* (Pritchard et al., 2009). Note the great difference with the coarser and rounded ridges of *C. chitra* and *P. cantorii.*

A. cartilaginea is a large Southeast Asian species with a preference for lowland rivers and marshes and is extant on Java. So far, only two other plate fragments of this species are known from the Pleistocene of Java. These are plastral fragments from Trinil, described by Jaeckel (1911) as *Trionyx trinilensis* and re-interpreted by Karl (1987) as *A. cartilaginea*.

Genus: *Dogania* Gray, 1844
***Dogania subplana* (Saint-Hilaire, 1809) – Malayan softshell turtle**

Available material (N=6). Carapace fragments (5): SBY5001. **Hypoplastron fragment:** SBY5002.

Description and identification: SBY5001A-B **(Fig. 6)** are costal plate fragments with a thickness of app. 4 mm. Their dorsal surface is covered with a fine latticework of closely spaced, rounded, punctuate wells with a diameter of around 1.5 mm. This fine, orange- skin-like surface ornamentation of the carapace is characteristic of *Dogania subplana* and compares well with museum specimens described and pictured by Pritchard et al. (2009).

Dogania subplana is a medium-sized freshwater turtle of Southeast Asia, with a carapace length reaching around 35 cm. The species is still present on Java and has a preference for rivers with a gravelly riverbed.

Testudines indet.

Available material (N=24). Ribs: SBY650, SBY1560, SBY1561, SBY1476. **Scapula,** distal fragment: SBY517 (s). **Humerus,** proximal fragment: SBY2122. **Radius**, proximal fragment: SBY1484 (s). **Ulna,** distal fragments: SBY492, SBY497. **Pelvis,** fragment: SBY509, SBY1035, SBY3000. **Femur,** shaft fragments: SBY708, SBY1530. **Metapodial:** SBY1477. **Unidentified limb bones fragments:** SBY506, SBY926, SBY1607, SBY1759, SBY1779, SBY3018, SBY5043A-C.

The identified ribs are the characteristic cone-shaped ribs of the sacral zone. Due to the unavailability of pertinent anatomical descriptions or museum specimens of the relevant turtle species, the anatomical position of smaller limb bone fragments could not always be determined with certainty.

3.7 Order Crocodilia Owen, 1842 - crocodilians

Dubois (1908, 1907) excavated crocodilian skulls from Trinil, which he ascribed to two new species: *Crocodylus ossifragus* and *Gavialis bengawanicus*. Müller (1923) concluded that *C. ossifragus* is synonymous to *Crocodylus siamensis*, the extant freshwater crocodile of Southeast Asia and only recently extinct on Java. Delfino and de Vos (2010) concluded that *G. bengawanicus* is a valid Pleistocene species, differing from the extant *Gavialis gangeticus* by skull morphology and tooth positions.

Family: Crocodylidae Cuvier, 1807
Genus: Crocodylus Laurent, 1768
***Crocodylus siamensis* Schneider, 1801 – Siamese crocodile**

Synonym: *Crocodylus ossifragus*

Available material (N = 24). Teeth: SBY319, SBY328, SBY5068A-F, SBY5069A-G, SBY5081A-B, SBY5071C, SBY7135A-B. **Osteoderms:** SBY1170, SBY5041A-B, SBY5042.

Description and identification: The teeth **(Fig. 7)** are robust and conical and have a relatively blunt tip. Maximum crown height is ~ 45 mm. The teeth have a semi-round cross-section, with faint mesial and distal keels and a maximum (mesiodistal) diameter of ~ 28 mm. They are slightly curved (toward the lingual side). The cones have a thin enamel cover with fine longitudinal striations. The teeth were generally found as loose crowns, only SBY5069A has a significant piece of the root attached. The teeth are identical to the dentition of a recent skull of *C. siamensis* and to a set of Pleistocene teeth from Java, all of which are kept in the Geological Museum Bandung. Moreover, they compare well with the descriptions by Janensch (1911a) and Müller (1923) of *C. siamensis* teeth.

The difference in size of the teeth relates to their position in the tooth row and to growing stage in the tooth-regeneration process. The species develops its largest teeth in the fourth mandibular, fourth premaxillary, and fifth maxillary alveoli. The largest teeth of the Madura Strait assemblage, such as SBY7135A **(Fig. 7)**, probably derive from one of these tooth positions.

SBY5042 **(Fig. 7)** is a fragment of a large rectangular osteoderm with fibrous margins. The lateral or medial half of the osteoderm is missing. It has an anteroposterior length of 39 mm, a mediolateral width of 85 mm (estimated width of complete specimen), and a thickness of 11 mm. It is flat to slightly convex, with a rounded, ca. 8 mm high central keel at the posterior side of the dorsal surface. Its dorsal surface has a pitted ornamentation, whereas its ventral surface is smooth, with fine crisscross striae. Its morphology and measurements compare well with Pleistocene *C. siamensis* osteoderms from Java described and pictured by Delfino and de Vos (2010).



Fig. 7. Crocodilia remains (*Crocodylus*, *Gavialis*) from the Madura Strait assemblage. Selected photographs. Teeth in mesial or distal view. Osteoderms in dorsal view. Vertebrae in lateral view. For measurements of vertebrae see **Table 5**.

Family: Gavialidae Adams, 1854
Genus: *Gavialis* Oppel, 1811 - charial
***Gavialis bengawanicus* Dubois, 1908**

Available material (N=4). Teeth: SBY645, SBY5071A-B. **Osteoderm:** SBY5044.

Description and identification: SBY5071A-B **(Fig. 7)** are slender, pointed teeth with a conical shape. The crowns are labiolingually compressed and strongly curved inwards (lingually). The thin enamel layer is covered with fine striations. Both teeth have a crown height of ~25 mm. The basal crown diameter is 6 mm labiolingually and 8 mm me-

siodistally. SBY5044 **(Fig. 7)** is a complete osteoderm with a mediolateral width of 63 mm, an anteroposterior length of 54 mm, and a thickness of around 8 mm. Its dorsal surface is ornamented with large pits, whereas its smooth ventral surface is marked with fine crisscross striae. The osteoderm is slightly convex and has a fine median keel with a height of ca. 3 mm at the posterior side of the dorsal face.

The teeth and the osteoderm match the descriptions of *G. bengawanicus* remains by Janensch (1911a), Delfino and de Vos (2010), and Martin et al. (2012). These authors described teeth with cone heights up to ~30 mm. The osteoderms of this species differ from *C. siamensis* by their lighter build, few but proportionally larger pits, and a thinner medial keel. Based on a comparison with extant *Gavialis* skins, we assume that SBY5044 is a nuchal or mid-dorsal osteoderm.

Crocodilia indet.

Available material (N=4). Vertebral centra: SBY474, SBY511, SBY514, SBY7136.

Description and identification: The vertebral centra are recognized as crocodilian by their cylindrical, elongate corpora and their strongly procoelous morphology, with prominent sub-round condyles and cotyles. Zygopophyses and neural spines have mostly broken off. SBY7136 **(Fig. 7)** has a ventral keel and, based on the fracture surfaces along the side of the corpus, must have had prominent parapophyses, which indicates that the specimen is a cervical vertebra. SBY474 **(Fig. 7)** preserves part of the neural arch. Diapophyses are partly preserved and the fracture surfaces indicate that in a complete state, these must have formed prominent transverse processes. The corpus lacks a ventral keel, but it has small, rounded parapophyses along its sides, which identifies the specimen as one of the anterior dorsal vertebrae. Measurements of the pictured specimens are given in **Table 5**.

The vertebrae compare well with isolated Pleistocene crocodilian vertebrae in the Geological Museum Bandung, both in size and morphology. Chamero et al. (2014) carried out a detailed analysis of crocodilian vertebrae and found no significant morphometric differences between *Crocodylus* and *Gavialis*. Also with respect to body weight and length, there are no significant differences between the extant Southeast Asian populations. We therefore refer to the specimens as Crocodilia indet.

Specimen	*Taxonomy*	*Vertebra*	*Corpus length (mm)*	*Cotylar diameter (mm)*
SBY7136	Crocodilia indet.	Cervical	39	27
SBY474	Crocodilia indet.	Dorsal	40	28

Table 5. Measurements (mm) crocodilian vertebrae pictured in **Fig. 7.**

3.8 Order Proboscidea Illiger, 1811

Proboscidean fossils have been recognized on Java for more than 150 years (Saléh, 1867). This material is dominated by the extinct genus *Stegodon*. Martin (1886) described two species: *Stegodon trigonocephalus* and *Stegodon airawana*. Von Koenigswald (1933) and Hooijer (1955) attributed all Javanese *Stegodon* remains to a single species: *S. trigonocephalus*. Besides *Stegodon*, there are proboscidean remains of the genus *Elephas*. Dubois (1908) ascribed the material to an extinct species, *Elephas hysudrindicus*. It differs from *Elephas maximus,* the extant Asian elephant, by its skull morphology and molar sizes.

For the descriptions and measurements of proboscidean dentition we followed Van den Bergh (1999). Ridges or lamellae are counted in Arabian numbers (anterior to posterior) or Roman numbers (posterior to anterior). Anterior and posterior talons are labelled as 'x'. The lamellar frequency (LF) refers to the number of ridges (for *Stegodon*) or lamellae or plates (for *Elephas*) over a longitudinal distance of 10 cm, measured at the base of a crown. Because of differences in lamellar spacing along the lingual and buccal side of molars, the LF was measured at both sides and the given value is the average.

Family: Stegodontidae (Osborn, 1911)
Genus: *Stegodon* Falconer, 1847
***Stegodon trigonocephalus* Martin, 1887**

Synonyms: *Stegodon airawana* (Martin, 1887; Stremme, 1911); *Stegodon ganesa* var. *javanicus* (Dubois, 1908)

Available material (N= 31). M^1, posterior fragment: SBY83 (d). **M_1,** posterior fragment: SBY81 (d), **M2,** posterior fragment: SBY84, **M2 or M3,** central fragment: SBY82. **Tooth fragments,** unknown position: SBY87, SBY88, SBY89, SBY90, SBY93A-E, SBY95A-G, SBY96A-E, SBY97, SBY98, SBY100, SBY103, SBY2001, SBY3164.

Description and identification: Fragments of *Stegodon* dentition are recognized by their lophodont build of widely spaced, wedge-shaped ridges with a relatively thick, wrinkled enamel cover, each loph terminating in 6 to 15 conelets. For four relatively large specimens **(Fig. 8)**, the tooth position could be determined**.** The relevant measurements

of these molars have been listed in **Table 6**.

SBY83 is a fragment of an upper molar, preserving the posterior talon and four intact ridges, none of which are worn. Ridge III has the greatest width, measuring 64.5 mm. This size falls in the range of *S. trigonocephalus* M^1 specimens from Trinil, which have a maximum width of 59 to 66 mm (N=3) (Hooijer, 1955; Janensch, 1911b). SBY81 is a tooth fragment preserving the posterior talon and six and a half ridges. The posterior two ridges are unworn, the other ridges are slightly worn. The slightly concave wear surface in combination with the concave upward crown base identifies the specimen as a lower cheek tooth. The buccally-concave curvature of the crown (in occlusal view) shows that it derives from the right mandible. The widest ridge is number IV and measures 60.4 mm buccolingually. This modest width suggests that the fragment derives from a dP_4 or an M_1. **Fig. 9** shows the width of the individual ridges of SBY81 compared to the measured ridge widths of fossil *Stegodon* dP_4 and M_1 from Trinil and Flores, referring to our measurements of specimens available in Naturalis Biodiversity Center and the Geological Museum Bandung. Note that the dP_4 specimens are not only smaller, but also have a different crown morphology, reaching their maximum width at the posterior or penultimate ridge, whereas the M_1 specimens reach their greatest width further anteriorly. For this feature, SBY81 falls in the M_1 category. The width of SBY81 compares well with the width of the fossil M_1 of *S. trigonocephalus* from Trinil (width range 58.3-66.0 mm, N=4) and exceeds the size range for dP_4 (width range 42.5-54.0 mm, N=7).

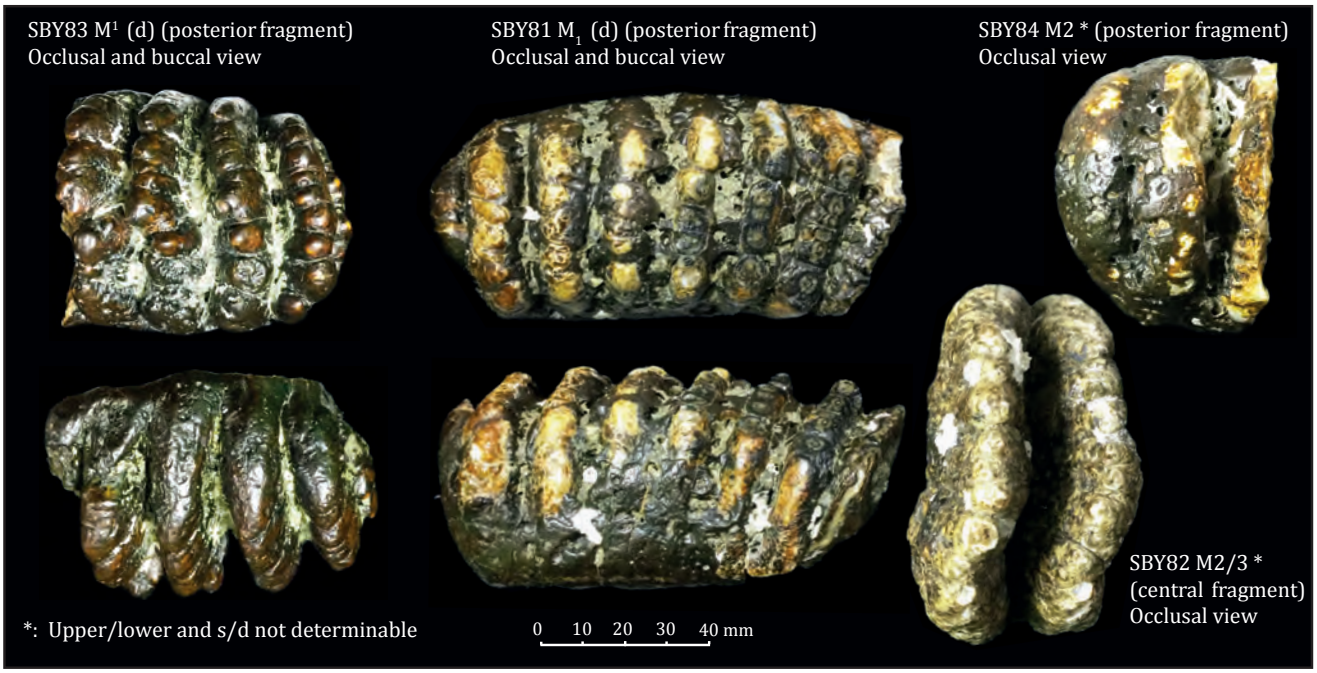


Fig. 8. *Stegodon trigonocephalus* molar fragments from the Madura Strait. Selected photographs. For measurements see **Table 6.**

SBY84 preserves only the posterior talon and 1½ ridges. Ridge II has a width of 74.9 mm; the maximum width of the molar must have been slightly larger. This value falls in the range of second molars, either from the upper or lower teeth row. Hooijer (1954) found a maximum ridge width of 76-94 mm for the M^2 (N=11) and 68–85 mm for the M_2 (N=11), based on molars from various find sites on Java. SBY82 preserves only two unworn ridges from the middle portion of a molar. The cement between the ridges is largely dissolved, leaving the enamel-covered ridges exposed. Small damaged surfaces show an enamel thickness reaching over 6 mm. The ridges have a width of over 94 mm and a height of 60 mm. The fragment may again derive from an (upper) second molar, but a third molar is more likely. Hooijer (1955) provided width ranges of 76–107 (N=19) for the M^3 and 68–98 for the M_3 (N=17).

Specimen	*Element*	*Ridges*	*w (mm)*	*h (mm)*	*h/w-index*	*LF*	*ET (mm)*
SBY83	M^1 (d)	-4x	64.5	41.7	64	6.8	3.1-4.5
SBY81	M_1 (d)	-⅙6x	60.4	>42	70	7.2	3.7
SBY84	M2	-½1x	74.9	57.0	73	6.2	3.5-4.6
SBY82	M2/M3	-2-	94.3	60.3	64	4.3	4.0-6.4

Table 6. *Stegodon trigonocephalus* molar fragments, measurements of specimens pictured in **Fig. 8**. Ridges: number of preserved ridges, talon is indicated as x. w and h: width and height of largest preserved ridge; if worn the minimum height is indicated as >x. h/w-index: measured or estimated for widest preserved, unworn ridge. LF: ridge or lamellar frequency (average of buccal and lingual values measured at the base of the crown). ET: enamel thickness.

Although all *Stegodon* remains from Java are nowadays referred to as a single species, there are minor differences between the molars of various find sites. Von Koenigswald (1934) and Van den Bergh (1999) proposed a subdivision in subspecies. The specimens from Trinil and Kedung Brubus, forming the largest sample of *Stegodon* molars from Java, are regarded as *S. trigonocephalus trigonocephalus*. For the Madura Strait find site, the youngest subspecies *S.*

trigonocephalus ngandongensis is relevant. This subspecies was defined based on molars from the Solo terrace of Ngandong, with an age that is similar to the fossil fauna of the Madura Strait. The *Stegodon* molars from Ngandong are relatively large, falling in the upper part of the size range of *S. trigonocephalus trigonocephalus*. Moreover, the molars often have one ridge more per homologue element, and tend to have a median cleft.

With respect to crown width, SBY83, SBY84, and SBY82 fall in the size ranges of *S. trigonocephalus trigonocephalus* from Trinil, but for all three specimens, the crown heights are slightly above the recorded ranges. Unfortunately, no homologue elements are available from Ngandong for direct comparison. Looking at SBY81, we find again that the molar width is well within the range of the M_1 of *S. trigonocephalus trigonocephalus*. Hooijer (1955) found an LF of 6 and 7.25 for the Trinil specimens. Upon re-measurement and calculating the measured results to the average of the lingual and buccal values, we found that these values are slightly lower, ranging between 6.0 and 7.0. With an LF of 7.2, SBY81 is slightly above this range. Two complete M_1 specimens of *S. trigonocephalus* from Trinil have x8x ridges while one M_1 from the same locality has a ridge formula of x9x. The comparatively high LF of SBY81 suggests that this specimen may originally have had a ridge formula of x9x or even x10x.

We conclude that the dimensions of the fragmentary Madura Strait molars are in the upper size range of *S. trigonocephalus*, mainly with respect to ridge height. This relatively large height, together with the high ridge frequency of SBY81, links the material from the Madura Strait to the *Stegodon* molars from Ngandong. We tentatively ascribe the material from the Madura Strait to the subspecies *S. trigonocephalus ngandongensis*.

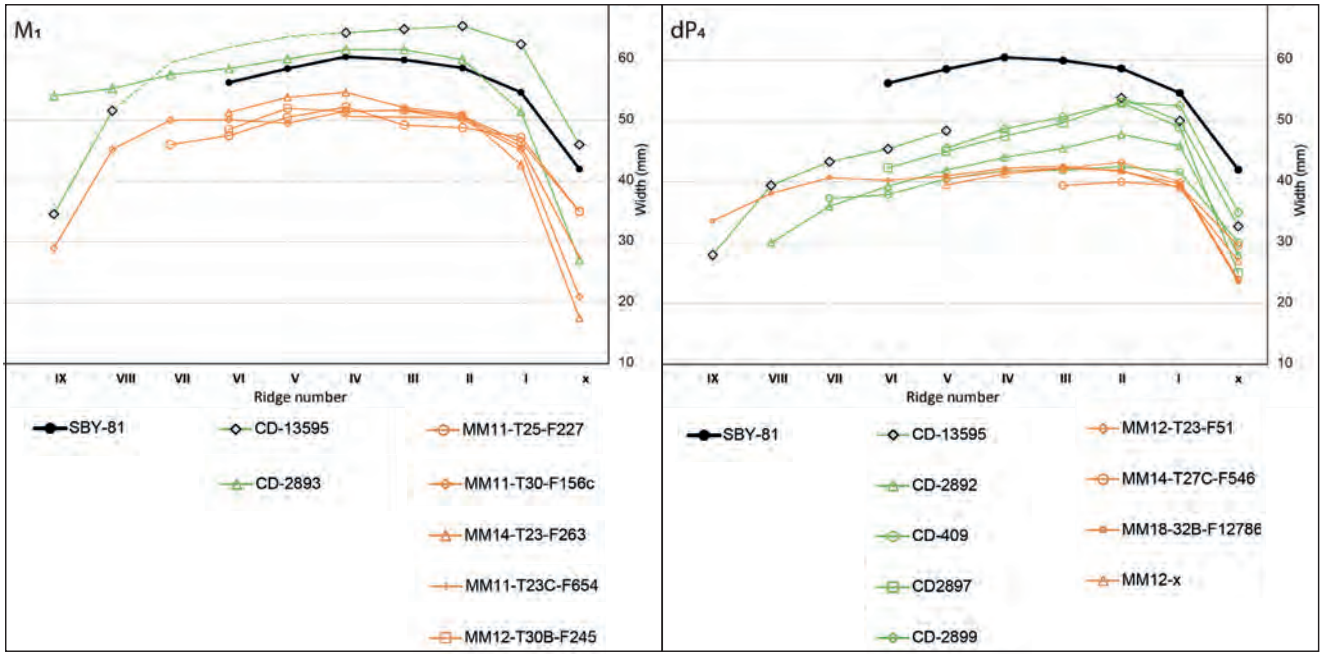


Fig. 9. Ridge-width plot of SBY81 (posterior molar fragment of *Stegodon trigonocephalus*) in comparison with various reference specimens of *Stegodon* dP4 and M1. Orange and yellow plots: *Stegodon florensis* from Flores. Green and grey plots: *Stegodon trigonocephalus* from Trinil. References based on our new measurements of specimens in the Geological Museum Bandung and Naturalis Biodiversity Center. dP4 and M1 CD-13595 derive from a single maxilla.

Family: Elephantidae Gray, 1821
Genus: *Elephas* Linnaeus, 1758
***Elephas* sp.**

Available material (N=15). dM^4, fragment: SBY85 (s/d). **M^3,** posterior fragments: SBY77 (s), SBY7039 (d). **M_2 or M_3,** anterior fragment: SBY79 (s). **Tooth fragments,** unknown position: SBY78, SBY80, SBY86A-E, SBY91, SBY94, SBY99, SBY104.

Description and identification: Fragments of *Elephas* cheek teeth can be recognized by their transverse lophs, which form platy, parallel lamellae with a relatively thin, delicately folded enamel layer, features that clearly differ from the thick and wrinkled ridges of *Stegodon* cheek teeth. Moreover, the lamellae (or plates) reach significantly greater heights than the ridges of *Stegodon.* For four relatively large fragments **(Fig. 10)**, the tooth position could be determined.

SBY77 is a fragment of a high-crowned, rather slender molar, preserving eight lamellae, the anterior two of which are incomplete. Most of the cement has disappeared, leaving the enamel of the lamellae exposed. The width and height of the lamellae decrease posteriorly. Along the tapering posterior end of the molar, only the posterior talon is missing. The posterior tapering identifies the specimen as a third molar. Only the anterior three preserved lamellae are worn, with a plane wear surface forming an angle of ~45 degrees with the lamellae, which is indicative of a third molar from the upper tooth row. From a lateral view, the lamellae are slightly folded, forming a weak S-shape with

the apices pointing anteriorly, but they lack the sharp basal bend characteristic of lower third molars. In occlusal view the right side of the crown is convex and the left side slightly concave. In upper molars the convex side is the buccal side, identifying this specimen as an M^3 of the left side. The preserved lamellae are regarded as lamellae I to VIII. The greatest measured width of 61 mm corresponds with plate VI, while plates VII and VIII are too damaged to take width measurements. Plates IV and V have estimated heights of ~140 mm (the tips of the digitations are broken), against a width of 55.2 and 57.7 mm, respectively. This results in H/W-indices of 253 at plate IV and 243 at plate V. The wear figures of the worn plates VI-VII are tripartite and lack pronounced median expansions. The broken digitations of plate V also show a tripartite division, while the most posterior plates have a single median cleft. Enamel thickness varies between 3.27 and 3.79 mm. The enamel is double-layered, with the outer layer occupying approximately 1/3 of the total thickness.

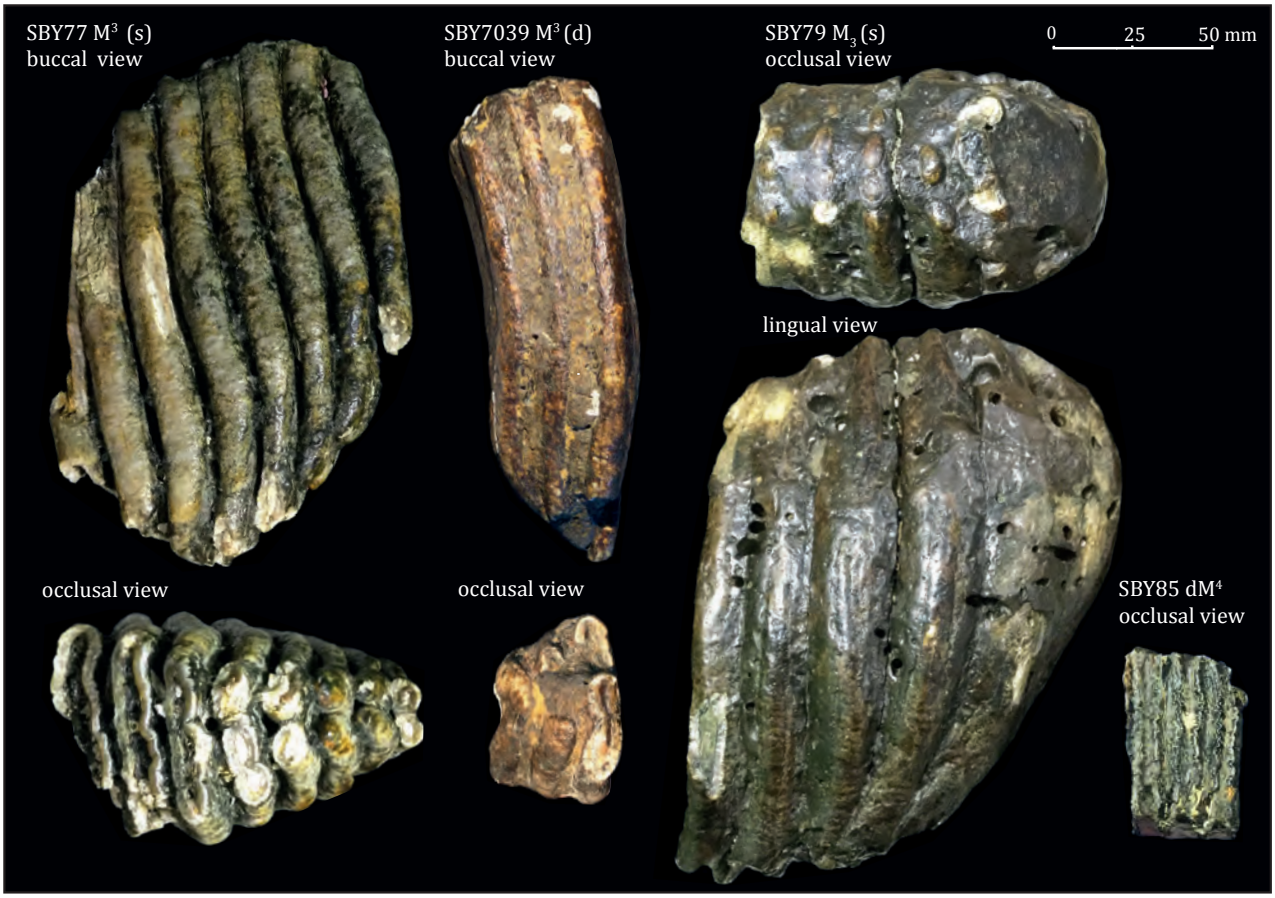


Fig. 10. *Elephas* sp. cheek teeth from the Madura Strait assemblage. Selected photographs. For measurements see **Table 7**.

Specimens and reference	*Element*	*Plates*	*w (mm)*	*h (mm)*	*h/w-index*	*LF*	*ET (mm)*
SBY77	M^3 (s)	8(x)	61.0 (VI)	140 (V)	~253 (IV)	8.1	3.5
SBY7039	M^3 (d)	-3-	62.9 (IV)	136 (III)	~242 (III)	8.4	3.2
E. hysudrindicus#	M^3 (N=9)		80-95	170-180	183-209	6-7 (4.6‡)	(2.4-3.0‡)
E. maximus#	M^3 (N=11)		74-85	165-210	215-269	6-8	--
*E. maximus**	M^3 (N=11)		63-98*	170-260*	--	--	(1.8-2.7‡)
SBY85	dM^4	-3-	48	> 57-63	>134	10.1	2.0
E. hysudrindicus#	dM^4 (N=3)		54-58			8-9.5	
E. hysudrindicus#	M^1 (N=1)		58			--	
E. maximus##	dM^4 (N=18)		41-57			8.5-10# (N=4)	
E. maximus##	M^1 (N=13)		53-79			7-7.5# (N=2)	
SBY79	M_2 or M_3 (s)	x5-	81.2 (V)	176 (III)	218 (IV -V)	5.3	2.6-3.0
E. hysudrindicus#	M_2 (N=4)		67-69	124-145		5-7.5	
E. hysudrindicus#	M_3 (N=15)		70-87	115-150	155-201	5-9# (4.7‡)	2.6† (3.1-4.55‡)
E. maximus##	M_2 (N=20)		58-87	155-245	177-209‡	5-8#	2.0-2.3‡
E. maximus##	M_3 (N=25)		66-100	170-260	153-217#	5-7# (4.5‡)	1.8-3.2‡

Table 7. *Elephas* sp. molar fragments: measurements of specimens pictured in **Fig. 10** (blue rows) in comparison with published size ranges of *Elephas hysudrindicus* and *Elephas maximus*. Clarification of abbreviations and symbols:

P: Number of preserved plates or lamellae (Given only for the Madura Strait specimens).

w and h: width and height of largest preserved ridge, if worn h = indicated as >x.

h/w-index: measured or estimated for widest preserved ridge. LF: lamellar frequency (average of buccal and lingual values, measured at the crown base).

ET: enamel thickness. * Data from Roth and Shoshani (1988). # Data From Hooijer (1954). ‡ Own measurements. † Data from Maglio (1973).

SBY7039 is a posterior molar fragment consisting of three lamellae. Like in SBY77, the lamellae gradually decrease posteriorly in width and height. The preserved plates are regarded as plates II, III, and IV. The talon and posterior plate (I) are missing. In lateral view the lamellae are very weakly S-shaped, almost straight, and together with the tapering this indicates that we are again dealing with the posterior portion of an M^3. Only plate IV is worn. Plates II and III are unworn and have a medial cleft, while plate IV has a tripartite division. On what is believed to represent the convex buccal side of plates IV and III, the conule is broken. The greatest width (62.9 mm) of the fragment is measured at plate IV. The greatest unworn plate height is measured at plate II and reaches 136 mm. The H/W indices of the unworn lamellae III and II are 242 and 255.

Although Middle Pleistocene *Elephas* material from Java is commonly referred to as *E. hysudrindicus*, the high-crowned and relatively slender appearance of the two M^3 fragments from the Madura Strait is remarkable and resembles the dentition of the extant *E. maximus*. **Table 7** shows the measurements of the two M^3 fragments from the Madura Strait in relation to published size ranges of the same tooth element for the Pleistocene *E. hysudrindicus* from Java and extant Southeast Asian *E. maximus* (data from Roth and Shoshani, 1988; Maglio, 1973; Hooijer, 1955).

As the specimens from the Madura Strait only preserve the tapering posterior plates, a direct comparison of width and height with published size ranges of intact molars is impossible. Looking at the H/W-index and the lamellar frequency, both specimens fall above the range of *E. hysudrindicus* and within the range of *E. maximus*. However, the difficulty with this comparison is that the published species-specific ranges of the H/W-index and lamellar frequency are based on measurements of largely intact molars and were taken at the central zone of the crown, whereas SBY77 and SBY7038 only preserve the posterior zone of the crown. For the lamellar frequency this is probably no problem, as plate thickness usually does not show significant variation within a crown (Van Den Bergh, 1999). But whether an H/W-index measured at posterior fragments is also valid for the central zone of the crown is not clear.

Therefore, for a more profound judgement of the molars, we need to compare the M^3 specimens from the Madura Strait with the posterior zone of relevant reference specimens. Hooijer (1955, table 59) measured the individual plates of four M^3 specimens of *E. maximus*, each with complete and unworn posterior zones. For *E. hysudrindicus* such record was not available. For this reason, we selected and measured five suitable M^3 specimens of *E. hysudrindicus* in Naturalis Biodiversity Center, deriving from various find sites on eastern Java, all with intact and unworn posterior plates (collection numbers CD11656, CD2352, CD2030, CD2501 and CD2359). We also measured the M^3 of the Menden *E. hysudrindicus*, of which a (replica) mounted skeleton is exhibited in the central hall of the Geological Museum Bandung. Its intact M^3 molars are partly concealed in the maxilla, which makes that the given sizes involve minor estimates. Moreover, the posterior plates of the M^3 have not emerged. However, the measurements are particularly valuable, as they derive from a molar that can be ascribed to *E. hysudrindicus* with certainty, based on skull morphology (Rizal et al., 2020).

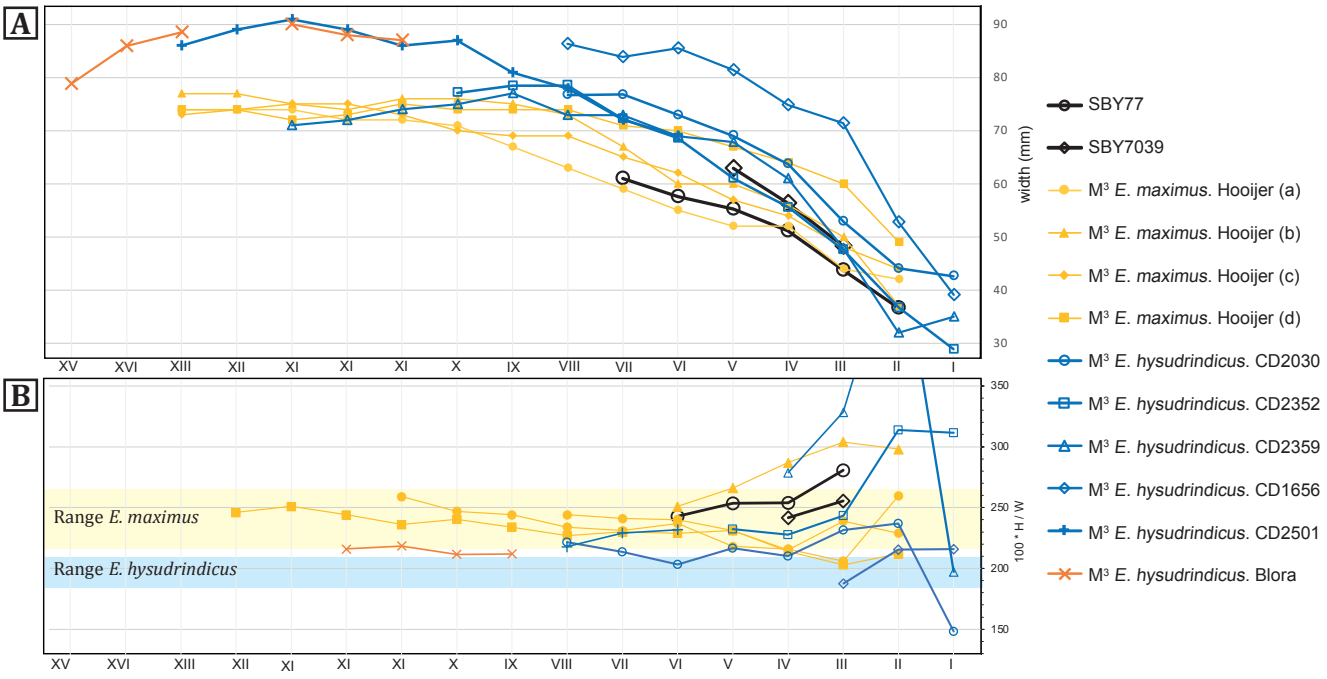


Fig. 11. SBY77 and SBY7039 (posterior fragments of *Elephas* M3) compared to relevant M3 specimens with intact posterior zones. Reference measurements of *Elephas maximus* from Hooijer (1955), indicated as a,b,c,d by this author. Reference measurements of *Elephas hysudrindicus* based on our own new measurements of specimens from Naturalis Biodiversity Center and the Geological Museum Bandung (the Blora specimen).
A: Plate width plot. **B:** H/W-index plot. Indicated H/W-ranges from Hooijer (1955).

Fig. 11A plots the posterior plate widths of the reference M^3 specimens of *E. maximus* and *E. hysudrindicus* in relation to the two specimens from the Madura Strait. The *E. maximus* molars have a uniform build-up, with plate widths of ~ 45 mm in plate II, gradually increasing in anterior direction and reaching their maximum width of 70 to 75 mm around plate IX. The *E. hysudrindicus* upper third molars however show more variation in posterior plate widths. The Menden *Elephas* and two of the molars from Naturalis (CD2501 and CD11656) follow a trend that may be expected from *E. hysudrindicus*, with plate widths plotting above the range of *E. maximus*, reaching a maximum plate width of around 90 mm in plate X or XI. However, the other three specimens, also labelled as *E. hysudrindicus*, have lower plate widths and plot along the upper range of the M^3 of *E. maximus*. The two M^3 fragments from the Madura Strait follow a plate width trend that has most affinity with the *E. maximus* reference specimens.

In **Fig. 11B** we plotted the H/W-indices of the individual (unworn) posterior plates of the same reference specimens in relation to the specimens from the Madura Strait. The yellow and blue bands are the ranges given by Hooijer (1955). The M^3 specimens of *E. maximus* plot close together, with H/W-values ranging between 229 and 259 in the central molar area and with a bit more variation in the posterior four lamellae. As expected, the *E. hysudrindicus* reference specimens have lower H/W-indices in the central molar area, with values ranging between 195 and 232, according to our measurements. Note that the found values are slightly above the range in H/W-indices as reported by Hooijer (1955). However, in their four posterior plates, the *E. hysudrindicus* reference specimens show an extreme variation in the H/W-values. This variation indeed makes it difficult to draw taxonomic conclusions from the H/W-values of the isolated posterior fragments from the Madura Strait. However, looking at the graph, we may still conclude that the two M^3 fragments from the Madura Strait have most affinity with the *E. maximus* reference specimens.

Another interesting molar fragment is SBY85 **(Fig. 10).** It consists of three lamellae, with lamellae missing on both sides. All lamellae have a similar width of 48 mm and an enamel thickness of 2 mm. The wear surface is slightly convex, indicating that the fragment derives from an upper molar. The lamellae are worn and have a height ranging between 57 and 63 mm, giving a H/W-index of >134. The plate widths indicate that the fragment derives from either a dM^4 or an M^1. **Table 7** compares the measurements of the specimen with published size ranges of the dM^4 and M^1 of *E. maximus* and *E. hysudrindicus.* With a width of 48 mm and a laminar frequency of 10.1, the specimen falls in the range of a dM^4 of *E. maximus.* Note, however, the small sample size of the *E. hysudrindicus* comparative specimens, which inhibits firm taxonomic conclusions.

The fourth specimen that is worth discussing is SBY79 **(Fig. 10).** It is an anterior fragment of a high-crowned lower molar, preserving five unworn lamellae and the anterior talon. From a lateral view, the lamellae are weakly curved, with their tips pointing backward. The curvature is most prominent in the talon and anterior two lamellae. Cement covers most of the upper part of the crown, but the tips of the conules are free from cement. The anterior part of the crown bears a flat, steeply inclined oval contact facet developed on the cement surface, where the tooth was in contact with its precursor. The relatively large width of 84.1 mm (at plate 5 from the front), with a slight increase of lamellar width from front to back, indicates that the specimen is the anterior portion of either an M_2 or M_3. The lamellae reach their maximum width at about 1/3 of their height (from the crown base). The slightly curved outline of the crown in occlusal view indicates that the molar derives from the sinistral mandible. The basal lamellar frequency is 5.3. **Table 7** compares the plate dimension of SBY79 with the published size ranges for the M_2 and M_3 of *E. hysudrindicus* and *E. maximus*. Plate width, lamellar frequency, and enamel thickness of SBY79 fall within the overlapping ranges of M_3 of *E. hysudrindicus* and M_2 and M_3 of *E. maximus.* The plate height and H/W-index are slightly above the range of *E. hysudrindicus*. The specimen has therefore most affinity with the M_2 or M_3 of *E. maximus*.

For over a century, it has been the taxonomic practice to regard all Middle Pleistocene *Elephas* remains as *E. hysudrindicus*. A major problem is that the diagnostic criteria for distinguishing between *E. hysudrindicus* and *E. maximus* are based on skull morphology. There are also metric differences between the dentition of both species, but with overlapping ranges. Metrically, the Madura Strait material is closer to the recent *E. maximus* than to most of the Middle Pleistocene material referred to as *E. hysudrindicus.* However, our re-measurements of museum specimens showed that this also applies to some of the Pleistocene molars thus far attributed to *E. hysudrindicus*, and of which the detailed stratigraphic provenance is unknown. To avoid confusion about species identifications, we refer to the material from the Madura Strait as *Elephas* sp.

Proboscidea indet.

Available material (N=54): dI (deciduous tusk): SBY161. **I (tusk fragments):** SBY293A-D, SBY294-300, SBY303, SBY314-318, SBY320, SBY322–227, SBY329–334, SBY343, SBY7050, SBY7051, SBY7190. **Vertebrae:** SBY10, SBY49, SBY57, SBY343, SBY1242, SBY3676. **Rib:** SBY1, SBY2294. **Humerus,** distal fragment: SBY1703 (s/d). **Radius,** distal fragment: SBY344 (s/d). **Lunatum:** SBY578 (s). **Femur,** caput: SBY38, SBY3677. **Patella:** SBY50. **Astragalus,** fragment: SBY7030 (s/d). **Metatarsal 2,** proximal fragment: SBY7199. **Metapodial,** proximal fragments: SBY1069, SBY1601, distal fragment: SBY13.

Description and identification: Proboscidean tusk fragments are recognized by the absence of an enamel layer and the presence of a characteristic pattern of crossing lines (Schreger Pattern) in the dentine. Differences in this dentine

pattern have been used to distinguish between the ivory of mammoth and modern elephants (Espinoza and Mann, 1993), but to date there are no publications on Schreger patterns in *Stegodon*. The tusk fragments from the Madura Strait have therefore been left as Proboscidea indet.

The fragmented postcranial remains have been recognized as proboscidean by direct comparison with (mounted) reference specimens in the Geological Museum Bandung. For this material, there are so far no morphological criteria to distinguish between *Elephas* and *Stegodon*.

3.9 Order Primates Linnaeus, 1758 (non-hominin)

The first recorded non-hominin primate fossil from an open-air site on Java is an isolated molar from Trinil, described by Stremme (Stremme, 1911) as *Macacus* sp. Dubois' earlier excavations had also yielded scarce non-hominin primate remains, but the material remained undescribed for several decades. Hooijer (1962) studied this material and assigned several isolated teeth from Trinil as well as a maxilla fragment from Bangle to the genus *Macaca*. Moreover, he assigned a skull from Teguan and a partial palate from Bangle to the genus *Trachypithecus* and a partial palate from Sumber Kepuh to the genus *Presbytis,* both of which are colobine monkeys belonging to the langur group. Recently, a partial femur was described from the Dubois collection, which may be assigned to the Family Hylobatidae (Ingicco et al., 2014).

While primate fossils from the Early to Middle Pleistocene open-air sites of Java are rare, they have been found more frequently at Late Pleistocene to Holocene cave sites on Java and Sumatra. This material, consisting of isolated teeth and occasional mandible or maxilla fragments, has been assigned to the genera *Macaca*, *Trachypithecus, Hylobates, Symphalangus, Nasalis* and *Pongo* (Smith et al., 2021; De Vos et al., 1982; Hooijer, 1962a; Badoux, 1959).

Note that this publication only discusses the non-hominin primates. The taxonomy of two hominin skull fragments from the Madura Strait (attributed to *Homo erectus)* and their relation to the available hominin material from the region, are presented in a separate publication (Berghuis et al., 2025d).

Family: Cercopithecidae Gray, 1821 – Old world monkeys
Tribe: Papionini Burnet, 1828
Genus: *Macaca* Lacépède 1799 - macaque
***Macaca* sp.**

Synonym: *Macacus*

Available material (N=1). Ulna fragment: SBY7174 (d).

Description and identification:

SBY7174 **(Fig. 12)** is a proximal fragment of a dextral ulna, with a total length of 37 mm. The olecranon, trochlear notch and the radial notch are well-preserved. The olecranon is 8.8 mm high. Its proximal surface, where the triceps muscles attach, is rugose and has a prominent groove. Moreover, this proximal surface is slightly inclined, the medial margin being higher than the lateral margin and the anterior margin being higher than the posterior margin.

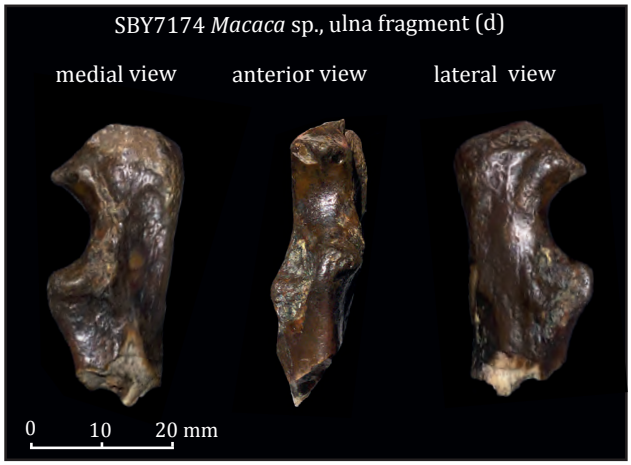


Fig. 12. *Macaca* sp. proximal ulna fragment (d) from the Madura Strait assemblage.

The proximal anteroposterior length of the olecranon is 11.4 mm, but the olecranon projects anteriorly toward the anconeal process, reaching a maximum anteroposterior length of 17.8 mm at the olecranon beak. The opening of the trochlear notch is semi-circular in lateral and medial view and has a proximal-distal length of 11.6 mm, measured from the beak to the coronoid process. The coronoid process is robust and protrudes anteriorly to a similar extent as the olecranon beak, which makes that the opening of the trochlear notch projects anteriorly. The radial notch is well-developed and slightly concave. The preserved part of the shaft is straight, while the posterior side of the olecranon is tilted posteriorly ca. 5 degrees.

The morphology and size of the ulna point to a medium-sized primate. A relation with Hylobatidae (gibbons) can be excluded, as the taxa of this family have a different ulnar morphology, with a strongly reduced height of the olecranon and an upwards-directed opening of the trochlear notch (Nishimura et al., 2022; Harrison, 1989). Referring to the extant and recorded Pleistocene species of Java, a relation with *Macaca*, *Trachypithecus* or *Presbytis* is likely. The relatively great height of the olecranon process compared to the size of the trochlear notch points to *Macaca* rather than *Trachypithecus* and *Presbytis* (Harrison, 1989, 1982). Most of all, the slightly backward tilt of the olecranon is characteristic of *Macaca* and other Papionini taxa. In Colobinae such as the langurs *Trachypithecus* and *Presbytis*, the olecranon is tilted anteriorly relative to the shaft (Milne and Granatosky, 2021; Egi et al., 2007).

There are two extant macaque species of Southeast Asia: *Macaca fascicularis*, occurring on Java and Bali, and the slightly larger *Macaca nemestrina* of Sumatra, Borneo and Malaysia. Hooijer (1962) found that all Pleistocene *Macaca* molars from Java fall in the size range of *M. fascicularis*. For postcranial material, relevant comparison material is not available. We therefore refer to SBY7174 as *Macaca* sp. Extant *Macaca* are quadrupedal, mixed arboreal and semi-terrestrial, with a habitat ranging from forest to scrubland and coastlines.

3.10 Order Carnivora (Bowdich, 1821) - carnivores

Carnivora are scarce in the Pleistocene fossil record of Java (Volmer et al., 2016; Louys, 2014; Brongersma, 1935). The rare finds are dominated by felids such as *Panthera tigris* and *Panthera pardus.* The former only recently became extinct on Java, whereas the latter is still extant on the island. Pleistocene canids are the extant dhole *Cuon alpinus* and the extinct *Cuon trinilensis.* Besides these species, there are extremely rare records of machairodont cats (Kurtén, 1962) and hyenas (Geraads, 1979).

Family: Felidae Fisher von Waldheim, 1817
Genus: *Panthera* Oken, 1816
***Panthera pardus* (Linnaeus, 1758) - leopard**

Available material (N=1). Scapula fragment: SBY1544 (s).

Description and identification: SBY1544 **(Fig. 13)** is a distal fragment of a sinistral scapula with an oval glenoid cavity. The supraglenoid tubercle is well developed and largely intact, only a flake of the facet and the margin with the glenoid cavity is missing**.** The transition toward the supraglenoid tubercle forms a distinct notch along the upper margin of the glenoid cavity. Although the tip of the coracoid process is broken off, it is still recognizable as a slender and downward projecting process. The acromion is broken off, but a small part of its base remains. It is placed centrally on the dorsal surface of the scapula, at a distance of 12 mm from the margin of the glenoid cavity.

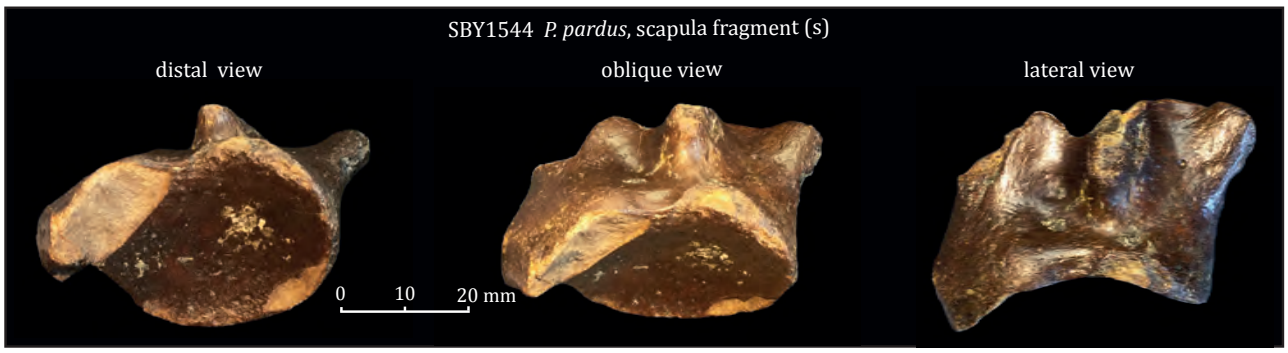


Fig. 13. *Panthera pardus* distal scapula fragment (s) from the Madura Strait assemblage. For measurements see **Table 8.**

The short distance between the base of the acromion and the glenoid cavity, its central position on the scapula surface, and the well-developed supraglenoid tubercle are characteristic features of a carnivore scapula. The morphology and position of the supraglenoid tubercle, forming a notch along the margin of the glenoid cavity and the downward projecting coracoid process, point to a felid rather than to a canid. **Table 8** lists the measurements of the glenoid

cavity of SBY1544, compared to the size ranges of *P. tigris* and *P. pardus*. Note that the size ranges are based on measurements of extant adult tigers and leopards from India. SBY1544 is clearly below the size range of *P. tigris* and near the upper margin of the size range of *P. pardus*. A relevant measurement is the distance between the base of the acromion and the margin of the glenoid cavity. This distance is significantly shorter in *P. pardus* than in *P. tigris* and is one of the characteristic traits of this species (Podhade et al., 2019). In SBY1544, this distance is within the range of *P. pardus* and far below the range of *P. tigris*.

Specimen and reference	Sample	*Gleonoid cavity length (mm)*	*Glenoid cavity width (mm)*	*Glenoid cavity to acromion distance (mm)*
SBY1544		38.4	32.8	13
*Panthera tigris**	N=5	55-60	37-40	31-35
*Panthera pardus***	N=4	33-36	23-27	6-21

Table 8. Measurements (mm) of scapula fragment SBY1544 (**Fig. 13)** in comparison with published size ranges of *Panthera tigris* and *Panthera pardus*.
* Tomar et al. (2018). ** Podhade et al. (2019)

3.11: Order Perissodactyla Owen, 1848 – odd-toed ungulates

The Pleistocene Perissodactyla fauna of Java consists of Rhinocerotidae and Tapiridae. Tapir remains are rare finds and mainly associated with forest faunas. *Rhinoceros* remains are more common. Dubois (1907) described two new Pleistocene species: *Rhinoceros sivasondaicus* and *Rhinoceros kendengindicus*. Hooijer (1946) synonymized the former with the extant *Rhinoceros sondaicus* of Java. The latter relates to the extant *Rhinoceros unicornis* of India (Antoine et al., 2022; Antoine, 2012). A third extant species of Southeast Asia is *Dicerorhinus sumatrensis*, the two-horned rhinoceros of Sumatra and Borneo. The species is unknown from the fossil record of Java.

Family: Rhinocerotidae Owen, 1845
Genus: *Rhinoceros* Linnaeus, 1758
***Rhinoceros sondaicus* (Desmarest, 1822) – Javan rhinoceros**

Synonym: *Rhinoceros sivasondaicus*

Available material (N=27). Dentition, dP^3: SBY5076 (d). **P^2:** SBY5075A (d). **M^1:** SBY5073 (d). **M^2:** SBY5077 (s), SBY7142 (d). **M^1 or M^2**, fragment: SBY7181 (d). **P_3:** SBY142 (d). **M_1:** SBY141 (s), SBY147 (s). **M_2:** SBY146 (d). **Tooth fragments,** unknown position: SBY152A-C, SBY7056. **Vertebrae:** SBY7109, SBY463. **Scapula,** distal fragments: SBY7180 (s), SBY7193 (d). **Radius,** proximal fragments: SBY7046 (d), SBY7047 (s/d). **Trapezium:** SBY1313 (d). **Femur,** shaft fragment: SBY33 (d). **Tibia,** shaft fragment: SBY11 (d). Distal fragment: SBY231 (s). **Astragalus,** fragment: SBY251 **Phalanx 3**: SBY7007A-B.

Description and identification: SBY5073 **(Fig. 14)** is a large fragment of a Rhinocerotidae upper molar, showing its characteristic rectangular outline and thick enamel. The crown is broken anteroposteriorly and only the buccal part, with the prominent ectoloph, is preserved. The protolophs and metalophs, making up the mesial and distal parts of the crown, are partly preserved. The preserved buccal face of the crown is smooth and uninterrupted and has an enamel thickness of 0.95 mm. The positions of the paracone fold and parastyle show that the molar derives from the dextral maxilla. The two lingual infoldings, the medisinus and postsinus, are partly preserved. They form smooth, U-shaped valleys with rounded valley-heads and lack a crista.

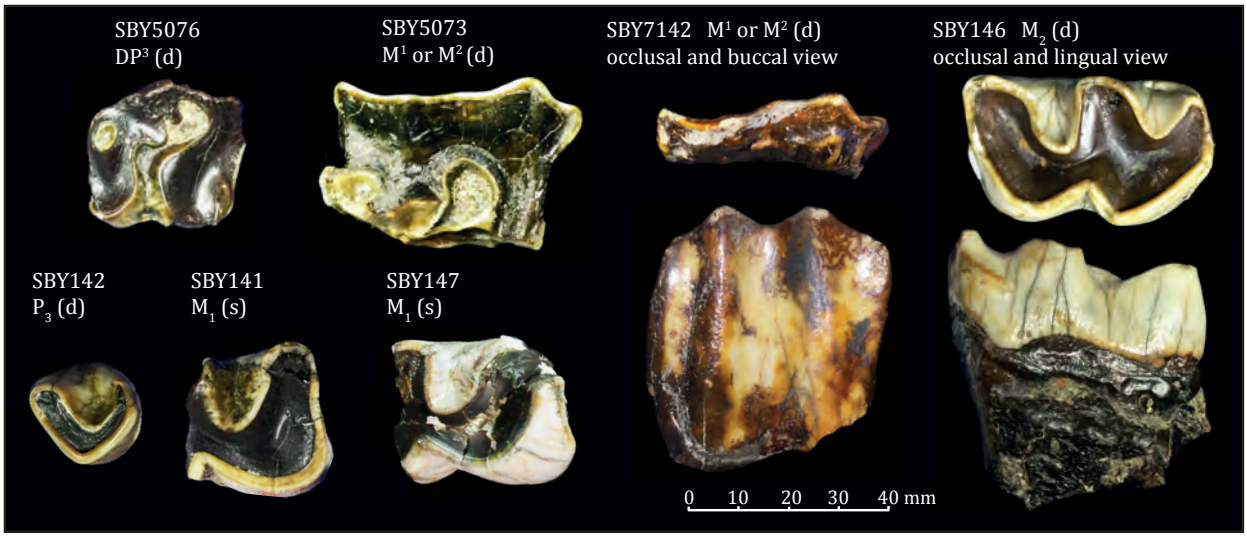


Fig. 14: *Rhinoceros sondaicus* cheek teeth from the Madura Strait assemblage. Selected photographs. For measurements see **Table 9**.

The buccal outline of the crown, with the prominent parastyle is characteristic for both *R. sondaicus* and *D. sumatrensis*. In *R. unicornis*, the parastyle is insignificant (Guérin, 1980). Moreover, the latter species has V-shaped sinuses with cristas at the valley head, both of which are absent in SBY5073. Hooijer (1946) observed that in *D. sumatrensis* upper molars, the postsinus is deeper than the medisinus, whereas in *R. sondaicus* the medisinus is deeper. In SBY5073, the medisinus is clearly deeper than the postsinus, indicating that we are dealing with *R. sondaicus*. Morphologically, there are no notable differences between the last premolar and the first two molars of *R. sondaicus.* Referring to size ranges (Guérin, 1980), SBY5073 derives either from an M^1 or an M^2 **(Table 9)**.

Molar fragment SBY7142 **(Fig. 14)** is highly similar to SBY5073, but preserves only the buccal face of the crown. Referring to its mesiodistal length, it is again an M^1 or an M^2. The fragment is only slightly worn and has a crown height of 50 mm. An interesting specimen is SBY5076 **(Fig. 14)**. It is a strongly worn, almost intact crown with a similar morphology as SBY5073, but with a fine build, a deeply-protruding medisinus and a curved buccal face. It corresponds in size, morphology, and enamel thickness with the dentition of a juvenile maxilla pictured by Guérin (1980) and is probably a dP^3.

Specimens and reference	*Element*	*l (mm)*	*w (mm)*
SBY5076	DP^3 (d)	38.3	35.4
SBY5073	M^1 or M^2 (d)	47.8	--
SBY7142	M^1 or M^2 (d)	46.5	--
D. sumatrensis	M^1	46-51.5	46.6-54
	M^2	47.5-55	48-57
R. sondaicus	**M^1**	46-51	52.6-60
	M^2	44.5-55	53-62.5
R. unicornis	M^1	48-58	62-72
	M^2	53-62	64.5-76
SBY142	P_3	--	23.3
SBY141	M_1 or M_2 (s)	--	29.5
SBY147	M_1 or M_2 (s)	--	29.9
SBY146	M_2 (d)	50.4	32.1
D. sumatrensis	M_1	31-40.5	23-27.5
	M_2	39-47.5	23.5-28
R. sondaicus	**M_1**	41-46.5	26-32
	M_2	40.5-51	27-32.5
R. unicornis	M_1	46-48	28-32.5
	M_2	52-56.5	31-36

Table 9. *Rhinoceros sondaicus* cheek teeth. Measurements of specimens pictured in **Fig. 14** (blue rows) in comparison with published size ranges of relevant Rhinocerotidae. Size ranges from Guérin (1980) based on extant populations, with sample sizes ranging between 4 and 26. In bold: matching size ranges.

SBY146 **(Fig. 14)** is an intact lower molar, with a characteristic morphology of paired, U-shaped lophs, referred to as the trigonid (anterior loph) and talonid (posterior loph). It has a well-developed anterior cingulum and a smaller posterior cingulum. The crown is moderately worn and has a height of 25 mm (buccal) or 18 mm (lingual). The enamel thickness is 1.9 mm. The two valleys at the lingual face of the crown are rounded. Guérin (1980) noted that in *R. unicornis,* both valleys are V-shaped, whereas in *R. sondaicus* and *D. sumatrensis* the valleys are either U- or V-shaped. Therefore, SBY146 belongs to one of the latter species. Guérin (1980) also noted that in *R. sondaicus*, the depth of the two valleys is of similar magnitude, whereas in *D. sumatrensis* there is a great difference in depth. In SBY146, the posterior valley is only slightly deeper than the anterior valley, which again points to *R. sondaicus* as the most likely species. This is confirmed by the size of the crown, which is above the range of *D. sumatrensis* lower molars **(Table 9)**. With a crown length of 50.4 mm, it is probably an M_2 of *R. sondaicus.*

SBY141 and SBY147 are posterior fragments (talonids) of crowns with a morphology that is similar to SBY146. Both fragments have a crown width that is above the size range of *D. sumatrensis* and within the range of the M_1 or M_2 of *R. sondaicus* **(Table 9)**. SBY142 is a single trigonid, which, based on its size, probably derives from a P_3.

3.12 Order Artiodactyla Owen, 1817 – even-toed ungulates

Family Hippopotamidae Gray, 1821

The fossil Hippopotamidae of Southeast Asia belong to the extinct genus *Hexaprotodon,* characterized by six incisors. The genus was first described by Falconer and Cautley (1836), based on a skull from India, which they referred to as *Hexaprotodon sivalensis.* The first record of similar material from Java is by Dubois (1908), who described a calvarium from Kedung Brubus as *Hexaprotodon sivajavanicus*. Von Koenigswald (1933) proposed a taxonomic subdivision of the material from Java in several species. Hooijer (1950) assigned all Pleistocene remains from Java to *Hippopotamus* (*Hexaprotodon*) *sivalensis*. However, De Visser (2008) carried out a biometric study of the Asian fossil material and proposed to maintain the separate species name *Hexaprotodon sivajavanicus* for all Javanese material, which differs from the Asian mainland material by its smaller size.

Genus: Hexaprotodon Falconer and Cautley, 1836

***Hexaprotodon sivajavanicus* Dubois, 1908**

Synonyms: *Hexaprotodon namadicus*, *Hippopotamus* sp., *Hippopotamus simplex*, *Hippopotamus antiquus*, *Hippopotamus sivalensis*

Available material (N=30). Incisors, I_1 or I_3, fragments**:** SBY130A-B, SBY7171. **Canines**, **lower C,** fragments**:** SBY149 (d), SBY7170 (d). **Upper cheek teeth: M^1 or M^2:** SBY145 (d), SBY156 (s). **Tooth fragments**, unknown position: SBY92A-B, SBY110, SBY131, SBY5055, SBY5056, SBY7182. **Mandibula,** fragment with roots of M_3: SYB108 (s). **Vertebrae:** SBY455, SBY463, SBY465. **Scapula,** distal fragments: SBY4 (d), SBY1689 (s). **Hamatum:** SBY705 (s). **Capitatotrapezoid,** distal fragment: SBY7200 (d). **Metacarpus,** fragment of MC-II: SBY681 (d). **Femur,** shaft fragment: SBY12 (s). **Tibia,** distal fragments: SBY231 (s), SBY1172 (d). **Astragalus:** SBY5089 (s). **Cuneiform:** SBY566 (d). **Metatarsus,** proximal fragment of MTII: SBY1138 (s), proximal fragment of MTIII: SBY551 (s).

Description and identification: SBY7171 and SBY130A **(Fig. 15)** are fragments of incisors with a rounded, slightly laterally-compressed cross-section. Although not well visible, the enamel coating seems to have been present all around the crown. The enamel layer, with a thickness of 1.1 mm, is white and smooth. Within the Pleistocene fauna of Java, only Hippopotamidae have such large, enamel-covered incisors. In the genus *Hexaprotodon*, upper incisors have a circular section, whereas lower incisors are slightly mediolaterally compressed, which indicates that SBY7171 and SBY130A are fragments of lower incisors. Also their size suggests that both specimens derive from the lower tooth row: The two specimens have an estimated anteroposterior diameter of 28 and 26 mm, whereas the maximum recorded diameter of upper incisors of the Javanese *H. sivajavanicus* is 15 mm (de Visser, 2008). Referring to measurements of lower incisors by Hooijer (1950), the fragments probably derive from either an I_1 of I_3, falling in the upper size ranges for these two elements **(Table 10)**.

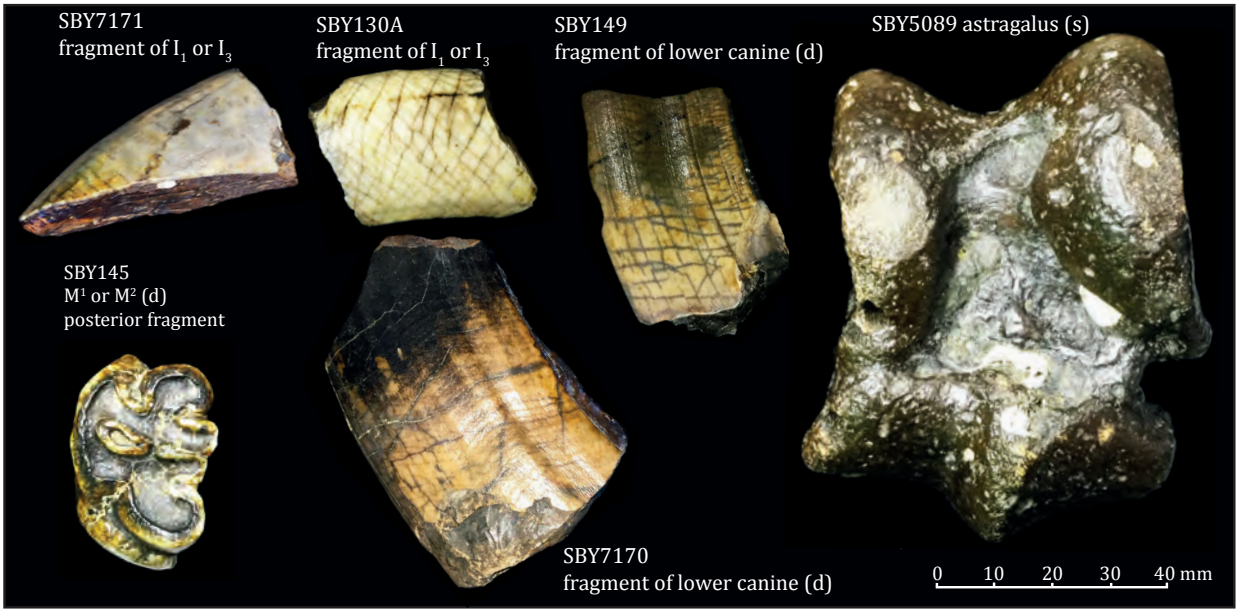


Fig. 15. *Hexaprotodon sivajavanicus* remains from the Madura Strait assemblage. Selected photographs. For measurements see **Tables 10** and **11.**

SBY149 and SBY7170 **(Fig. 15)** are fragments of large canines. They are laterally compressed and have a rounded anterior face and a flat posterior face. SBY7170 preserves a central cavity. The anterior face as well as the lateral faces are covered with enamel, but along the posterior face, in the inside bend of the tooth, enamel is absent and the dentine is exposed. The enamel layer has a thickness of 1.1 mm and has fine longitudinal striations. The large, curved teeth with a U-shaped cross-section, striated enamel and a lack of enamel at the posterior face are characteristic of Hippopotamidae lower canines. A superimposed, smooth longitudinal valley marks the medial face of the tooth, which makes both specimens fragments of dextral canines. The specimens have an anteroposterior diameter of 35 and 44 mm respectively, which corresponds to the size range provided by Hooijer (1950) for *H. sivajavanicus* from Java **(Table 10)**.

SBY145 **(Fig. 15)** is recognized as a Hippopotamidae cheek tooth by its characteristic trefoil-wear pattern and thick and smooth enamel layer, reaching a thickness of ~3 mm. Hippopotamidae molars consist of four relatively high, bunodont cusps. SBY145 is broken buccolingually and only preserves two cusps with an intermediate infundibulum. The fragment is identical to the posterior part of Dub2318a, an isolated upper molar labelled as M^2 by Hooijer (1950, plate VIII-9). The preserved cusps are probably the hypocone and metacone. The specimen has an articular facet along the posterior face and a prominent cingulum at what must be the lingual face, which indicates that the molar derives from the dextral maxilla. In Hippopotamidae, there is considerable overlap between the M^1 and M^2, both in

size and morphology. The crown width of 38.7 mm falls in the size range of both tooth positions for *H. sivajavanicus* (**Table 10**), referring to crown measurements of intact fossil maxillae (Hooijer, 1950; Van der Maarel, 1932; Stremme, 1911).

Specimen (SBY) and published size ranges	*Element*	*Diameter (mm) max. (ant-post)*	*l (mm)*	w (mm)
SBY7171	I_1 or I_3	28 (estimate)		
SBY130	I_1 or I_3	26 (estimate)		
I_1 (N=14)*		23-27		
I_2 (N=14)*		16-25		
I_3 (N=14)*		17-26		
SBY149	C lower	35		
SBY7170	C lower	44		
C lower (N=15)*		37-54		
SBY145	M^1 or M^2		--	38.7
M^1 (N=13)#			34-41	31-41
M^2 (N=15)#			38-50	36-48

Table 10: *Hexaprotodon sivajavanicus* incisor, canine and molar fragments. Measurements of specimens pictured in **Fig. 15** (blue rows) in comparison with published size ranges of reference specimens from the Pleistocene of Java.
* From: Hooijer (1950). #: From: Stremme (1911), Van der Maarel (1931) and Hooijer (1950).

An interesting postcranial specimen is the astragalus SBY5089 **(Fig. 15)**. It differs from similar-sized bovid astragali **(Fig. 27)** by its rounded, robust body and its great width compared to its height. It has a distinct Hippopotamidae morphology of the distal articulation, which consists of two rounded facets separated by an obliquely oriented median ridge. Note that in bovid astragali the two condyles are separated by a median groove. Only five other *Hexaprotodon* astragali have been recorded from the Pleistocene of Java. See for reference the pictured specimens in Stremme (1911, Taf. XIX-6) and Hooijer (1950, Plate XX). SBY5089 falls in the size range of these earlier finds, except for a slightly larger lateral height **(Table 11)**.

Specimen (SBY) and published size ranges	*Element*	Lat. h GLl	Mid. h	Med. h GLm	Dist. w Bd	Max. thickness Dl (ant-post)
SBY5089	Astragalus	89.1	77.0	73.0	61.8	48.5
Astragali Java (N=5)		77-85	69-80	--	60-64	--

Table 11: *Hexaprotodon sivajavanicus* astragalus. Measurement of SBY5089 **(Fig. 15)** in comparison with published size range of all known reference specimens from the Pleistocene of Java. Reference measurements from Stremme (1911), Stromer (1914), Hooijer (1950). Measurements methods and codes: Von den Driesch (1976).

Family: Suidae Gray, 1821

Dubois (1908) described two Pleistocene suids from Java: *Sus brachygnathus* and the larger *Sus macrognathus*. Detailed descriptions of skulls and dentition were provided by Stremme (1911), Von Koenigswald (1933), and Hardjasasmita (1987). According to Von Koenigswald (1933), the Pleistocene species may be related to the extant *Sus verrucosus* of Java and to *Sus celebensis* of Sulawesi. *Sus scrofa vittatus*, nowadays the most common species on Java, probably arrived during the Late Pleistocene (Van den Bergh et al., 2001).

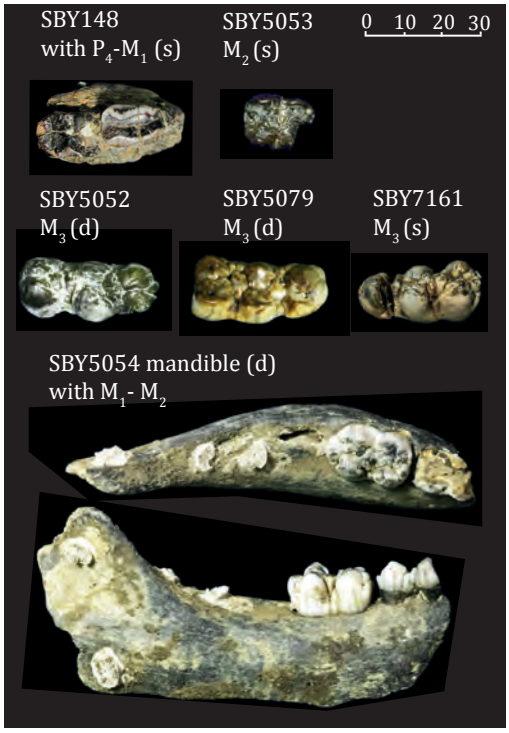
Genus: Sus Linnaeus, 1758
***Sus brachygnathus* Dubois, 1908**

Synonyms: *Sus hysudricus, Sus vatualangensis*

Available material (N=14). Mandibula, fragment with P_2-P_3-P_4: SBY132 (s), fragment with P_4-M_1: SBY148 (s), fragment with M_1-M_2–M_3: SBY5054 (d), fragment with M_3: SBY336 (s), fragment with root of M_3: SBY102 (d). **Lower dentition, M_2:** SBY5053 (s). **M_3:** SBY5052 (d), SBY5079 (d), SBY7161 (s), SBY7162 (d). **Scapula,** distal fragment: SBY7020 (s). **Humerus,** distal fragment: SBY1519 (d). **Radius,** distal fragment: SBY691 (s). **Metatarsus,** MT2: SBY7023 (s).

Description and identification: SBY148 **(Fig. 16)** is a mandible fragment with a heavily worn P_4 and M_1. The P_4 has a characteristic elongate, tricuspid suid morphology. The M_1 preserves the outlines of four bunodont cusps and a median subsidiary cusp, as well as a hypoconulid cusplet. SBY5053 **(Fig. 16)** is an isolated, heavily worn M_2. The wear surface shows the outlines of the four cusps and the median subsidiary cusp. Most of the anterior cingulum and the metaconid are missing.

SBY5054 **(Fig. 16)** is a mandible fragment, preserving a large part of the body and the ramus. It has two unworn molars, a broken M_1 and a complete M_2. The M_2 has a characteristic morphology of 4 bunodont cusps, a median subsidiary cusp, and a strongly developed hypoconulid at the posterior side. The M_3 has not yet emerged, which indicates that the mandible belonged to a juvenile individual. The mandible is broken at the base, which offers a view of the base of the unerupted M_3 and even allows measurement of the crown.



The collection contains three unworn, isolated M_3 specimens, with three rows of bunodont cusps and intermediate subsidiary cusps **(Fig. 16)**. SBY7161 has a pronounced anterior cingulum and anterior subsidiary cusp, both of which are largely absent in SBY5079 and SBY5052. Along the posterior face, all specimens have a well-developed talonid. Note the absence of enamel in SBY5052, which is indicative of a molar that passed the digestive tracts of a crocodilian or another predator (Fisher, 1995).

Metrically, all crowns plot in the size ranges of the Pleistocene *S. brachygnathus* from various Javanese localities as given by Hardjasasmita (1987), Von Koenigswald (1933), and Stremme (1911) and below the size range of *S. macrognathus* **(Fig. 17)**. Most M_3 specimens from the Madura Strait plot close together and have, compared to the reference sample, relatively long and slender crowns. Only SBY7161 is somewhat smaller, plotting along the lower margin of the size range of *S. brachygnathus* M_3.

Fig. 16. *Sus brachygnathus* dental remains from the Madura Strait assemblage. Selected photographs. All molars in occlusal view. SBY5054 in occlusal and buccal view.

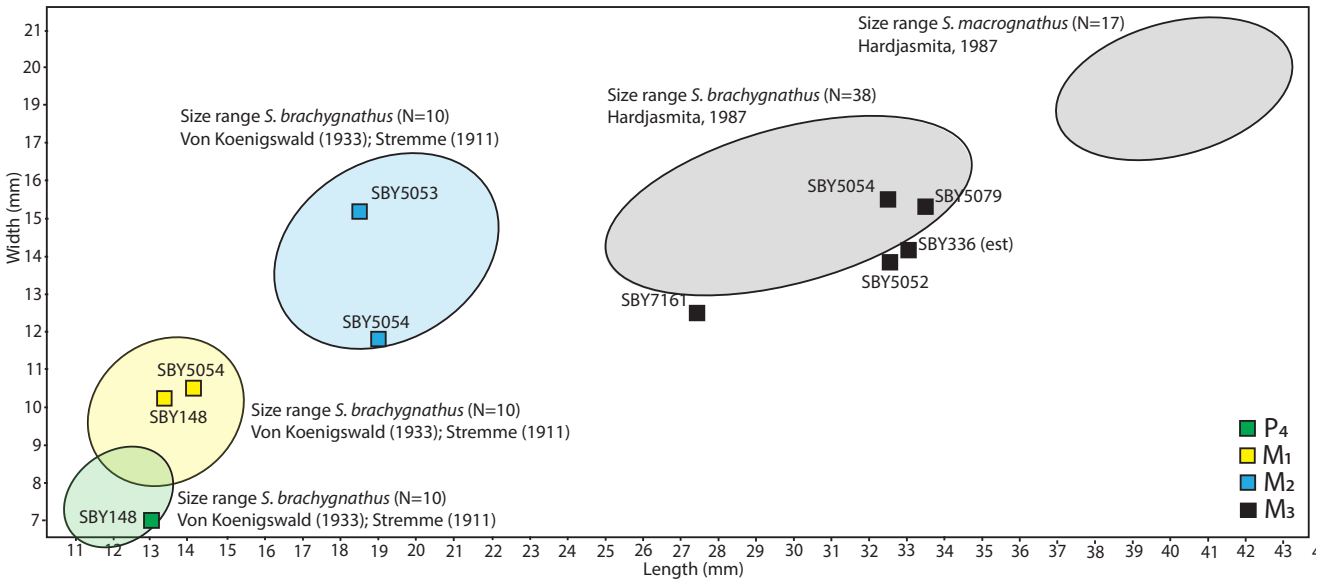


Fig. 17. *Sus brachygnathus* dental remains from the Madura Strait assemblage. Bivariate plot of crown length and width, with published size ranges for *S. brachygnathus* and (for the M_3 only) *S. macrognathus*, based on fossils from various Pleistocene sites on eastern Java.

Sus cf. *macrognathus* Dubois, 1908

Synonym: *Sus terhaari*

Available material (N=2). Phalanx 1: SBY186, SBY193.

Description and identification: Among the sample of Artiodactyla first phalanges, SBY186 and SBY193 stand out by their deviant morphology **(Fig. 28A)**. In comparison to their length, they have a robust shaft with a conspicuous supra-articular inflation directly above the distal articulation. Moreover, they have an asymmetrical, anteriorly-pointing morphology of the proximal articular surface. Both traits are characteristics of suids (Schmid and Garraux, 1972). The size of the proximal articular surface plots in the range of *Bos palaeosondaicus* **(Fig. 28B)**. However, the two specimens have a shorter and comparatively robust shaft. In the bivariate plot of shaft length and width **(Fig. 28C)**, both specimens are easily differentiated from bovid phalanges.

The phalanges, with an articular face that equals those of Bovini, point to a particularly large-bodied suid. Within the Pleistocene fauna of Java, the only candidate species is *Sus macrognathus*. This is an interesting finding, as

recorded fossils of this species are rare and only consist of fragmented maxillae, mandibles, and isolated cheek teeth. Postcranial material of this species has never been found or recognized. The two first phalanges from the Madura Strait may therefore be the first postcranial elements to be assigned this species. In the absence of dental material to support the presence of this species within the assemblage, we refer to the specimens as *Sus* cf. *macrognathus.*

Family: Cervidae Goldfuss, 1820

Cervids are common within the Pleistocene fossil assemblages of Java. Species definitions have primarily been based on antler morphology, which resulted in a complex taxonomy with over a dozen species (Von Koenigswald, 1933). A recent morphometric comparison of molars paved the way for a taxonomic simplification (Gruwier et al., 2015). The small Pleistocene species *Axis lydekkeri* (Martin, 1886) is related to the extant *Axis (Hyelaphus) porcinus* of mainland Southeast Asia and *Axis (Hyelaphus) kuhlii* of Bawean Island (Gruwier et al., 2015). The modest-statured *Axis javanicus* (Von Koenigswald, 1933) is not part of the *Hyelaphus* subgenus and probably relates to the extant *Axis axis* of mainland Asia (Meijaard and Groves, 2004). There are also remains of larger deer in the fossil assemblages of Java. Dubois (1908) assigned this material to a new species, *Cervus kendengensis.* In most literature, this large-statured Pleistocene cervid of Java is nowadays referred to as Cervus (*Rusa*) sp. Grubb (2005) raised *Rusa* to genus level, which makes *Rusa* sp. a more appropriate attribution for the fossil material from Java, which is morphologically similar to the extant *Rusa timorensis* of Java and *Rusa unicolo*r of the Asian mainland, Sumatra and Borneo (Gruwier et al., 2015; Meijaard and Groves, 2004).

Genus: *Axis* Smith, 1827
***Axis lydekkeri* (Martin, 1886)**

Synonyms: *Cervus zwaani*, *Cervus oppenoorthi*

Available material (N=36). Antler, antler base with burr and pedicle: SBY7177 (s). Antler base with burr: SBY347 (d), SBY381 (d) SBY387 (d), SBY448 (d), SBY718 (d), SBY721 (d), SBY358 (s), SBY377 (s), SBY446 (s), SBY557 (s), SBY715 (s), SBY791 (s), SBY799 (s), SBY809 (s), SBY857 (s), SBY892 (s), SBY2665 (s), SBY441 (s/d), SBY763 (s/d), SBY888 (s/d), SBY7201 (d). **Mandibula,** fragment with P_3: SBY7172 (d), fragment with M_1 and M_2: SBY7116 (s). **Lower dentition, M_3:** SBY5080 (d). **Radius,** proximal fragment: SBY254 (d). **Os malleolus:** SBY6013 (s). **Astragalus:** SBY182 (d), SBY5099 (d), SBY6008 (s), SBY183 (s), SBY7043 (d). **Scapho-cuboid:** SBY7042 (s). **Phalanx 1**: SBY198, SBY6006. **Phalanx 2:** SBY197.

Description and identification: SBY448 and SBY721 **(Fig. 18)** are antler bases, preserving the burr (coronet), the base of the main beam, and the base of the brow tine. The burr is slightly pearled and the antler base is finely ribbed. The antler base has a diameter of ~30 mm and a height of ~35 mm, measured from the burr to the angle between the brow tine and the main beam. The backward-directed main beam and the forward-directed brow tine both make an angle of ~ 45 degrees with the burr. The preserved lower part of the main beam has a diameter of ~ 20 mm. The antler bases are identical to several complete antlers of *A. lydekkeri* stored in the Geological Museum Bandung (collection nrs. K98 and K105) and correspond with the dimensions and morphological descriptions provided by Stremme (1911) and Von Koenigswald (1933) for this species. Besides the small size (complete specimens have a total beam length of 30 to 35 cm), the antlers of this species are characterized by their fine-ribbed surface and an internal angle of ~90 degrees between the main beam and the brow tine.

SBY7116 **(Fig. 19)** is a fragment of a sinistral mandible with the M_1 and M_2. The mandible is slender, with a height of ca. 24 mm and a thickness of 12.8 mm (measured below the M_2). The molars have a dull, rugose enamel. Both molars are slightly worn and, with a worn height of 14 mm, relatively low-crowned. The crowns have a modest lingual cingulum and narrow toward the apex. The occlusal face has a characteristic cervid morphology of isolated conids and open infundibula. Along the lingual face, the molars have well-developed entostylids and mesostylids, which run obliquely along the crowns. Near the apex of the crown, there is a small metastylid. Along the buccal face, the molars have a small and low ectostylid near the base of the crown. SBY5080 **(Fig. 19)** is an unworn M_3 with a small bone fragment surrounding the root. It has a similar rugose enamel structure as the molars of SBY7116 and shows a similar widening of the crown toward the base. The unworn crown height is ~ 18 mm. It has a prominent metastylid and a small, low ectostylid, but lacks a posterior ectostylid.

Size ranges of *A. lydekkeri* lower molars were provided by Stremme (1911), referring to 12 complete mandibles from Trinil **(Fig. 20)**. The M_1 of mandible fragment SBY7116 plots along the species' upper size margin, whereas the M_2 plots slightly above the size range of the Trinil specimens. Their size is comparable to molars found in Ngebung, which were assigned to the subspecies *A. lydekkeri ngebungensi* based on their relatively large size (Moigne et al., 2004). The M_3 SBY5080 plots well within the size range of *A. lydekkeri* as provided by Stremme (1911).

Limb bones have been assigned to *A. lydekkeri* based on a morphological and metric analysis of ruminant skeletal remains. Relevant, pictured specimens are SBY254, a proximal half of a dextral radius **(Fig. 24)**, SBY183, a sinistral astragalus **(Fig. 27)**, SBY198 and SBY197, first and second phalanges **(Figs. 29 and 30)**.



Fig. 18. Cervidae antler bases from the Madura Strait assemblage. Selected photographs.

Genus: *Axis* Smith, 1827

Axis javanicus Von Koenigswald, 1933

Available material (N=17). Antler, antler base with burr and pedicle: SBY427 (d). Antler base with burr: SBY435 (d), SBY864 (d), SBY368 (s), SBY420 (s), SBY880 (s). **Lower dentition, M_2:** SBY127 (s). **M_3**: SBY7114 (s). **Metacarpus**, proximal fragment: SBY73 (d). Distal fragment: 7153 (d). **Astragalus:** SBY178 (d), SBY7164 (s), SBY179 (s), SBY180 (s). **Calcaneum,** fragment: SBY7052 (s). **Phalanx 1:** SBY7154, SBY201.

Description and identification: SBY427 and SBY435 **(Fig. 18)** are antler bases, preserving the burr, the base of the main beam and the base of the brow tine. SBY427 also preserves a pedicle. The burr is weakly pearled and the surface of the main beam is weakly ribbed. The main beam is directed sharply to the back and has a diameter of 25 - 30 mm. The specimens match the descriptions of *A. javanicus* by Von Koenigswald (1933), who defined the species by its antlers, which are slightly larger than those of *Axis lydekkeri,* have a weak surface ornamentation and have an internal angle between the main beam and the brow tine of more than 90 degrees. The Madura Strait specimens also compare well with several intact antlers assigned to *A. javanicus* stored in the Geological Museum Bandung. The relatively thick, backward-directed main beam of these complete antlers has a strong curvature, curving forward as well as outward, and reaches a length of ~ 50 cm.

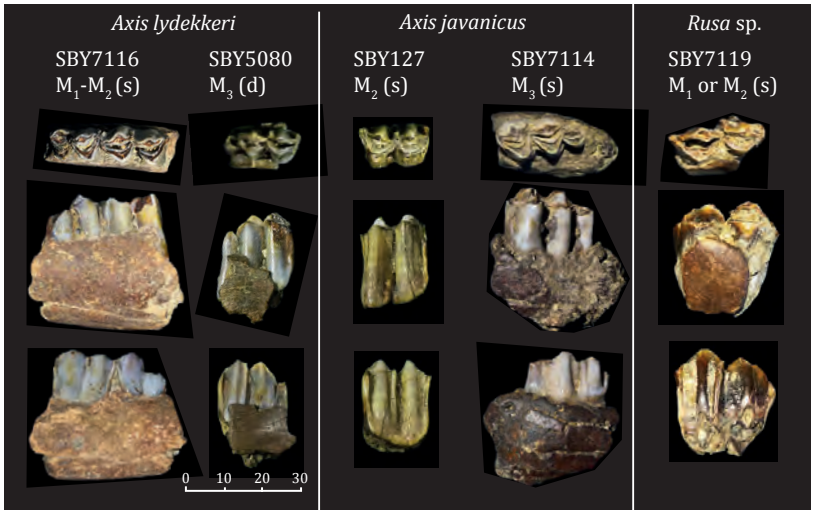


Fig. 19. Cervidae lower molars from the Madura Strait assemblage. Selected photographs in (from top to bottom) occlusal, buccal and lingual view. For crown measurements see **Fig. 20**.

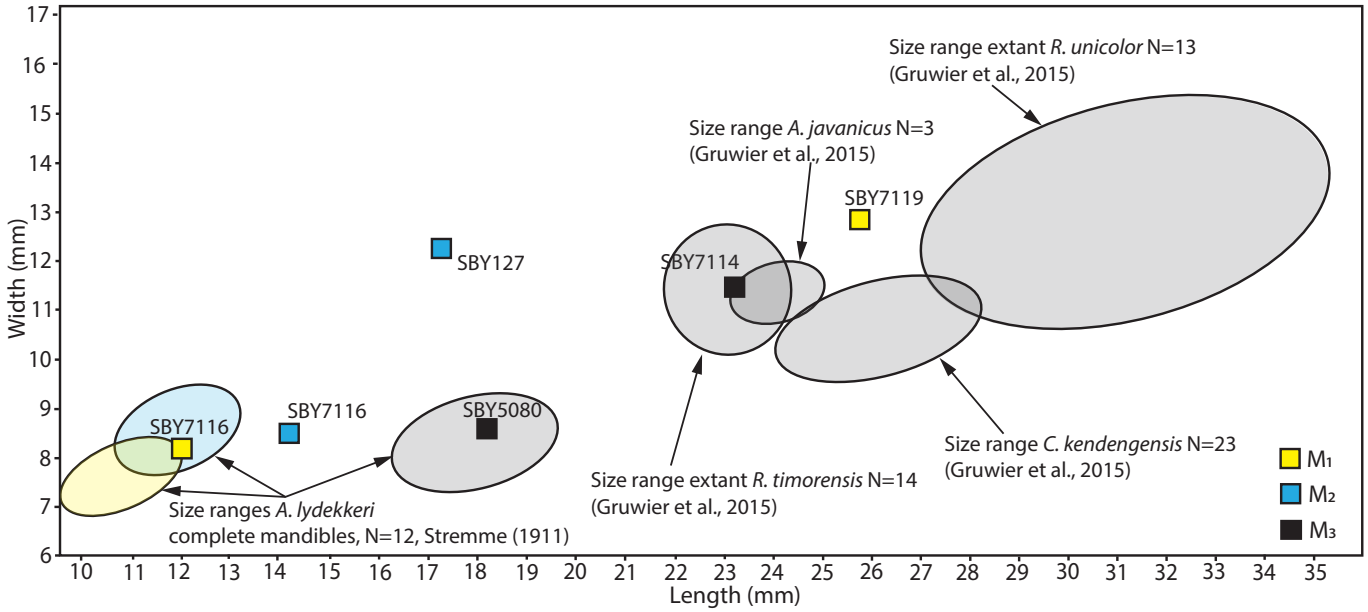


Fig. 20. Cervidae lower molars from the Madura Strait assemblage. Bivariate plot of crown length and width, with published size ranges of extant and fossil species. Note that SBY7119 may also be an M_2.

SBY7114 **(Fig. 19)** is a small fragment of a sinistral mandible with a slightly worn M_3. Below the M_3, the mandible has a thickness of 18.5 mm. The crown has a strongly rugose enamel and thickens toward the base. Its occlusal surface has a cervid morphology of isolated conids and partly connected infundibula. It has a well-developed metastylid and an obliquely, outward-directed mesostylid. An ectostylid is absent or has not yet emerged.

SBY127 is an isolated sinistral M_2 with a similar rugose enamel structure, basal thickening, and an occlusal face of isolated conids. The crown is only slightly worn and has a height of 26 mm. It has a low ectostylid, only present along the crown base. In the bivariate plot of crown length and width, both specimens plot above the range of *A. lydekkeri* **(Fig. 20)**. The M_3 SBY7114 falls in the overlapping size ranges of the fossil *A. javanicus* and the extant *Rusa timorensis*. Gruwier et al. (2015) found that the Pleistocene *Rusa* sp. molars exceed the molars of the extant *R. timorensis* in size. SBY7114 is therefore regarded as *A. javanicus* rather than *Rusa* sp. SBY127 has a similar crown width and is assigned to the same species. Unfortunately, no published size ranges are available for the M_2 of *A. javanicus*.

Two metacarpal fragments SBY73 and SBY7153 have been assigned to *A. javanicus*, based on a morphological and metric analysis **(Fig. 25)**. The specimens represent a medium-sized cervid, plotting above the size range of *A. lydekkeri* and below the range of *Rusa unicolor*. The same applies to several cervid astragali, such as SBY180 **(Fig. 27)**. For the cervid first phalanges only two size groups were found. We tentatively assigned the specimens of the larger size group to *A. javanicus,* as they plot relatively close to *A. lydekkeri* phalanges and appear to be too small to be assigned to *Rusa* sp. **(Fig. 28)**.

Note that the species *A. javanicus* has thus far only been identified by its antlers and isolated dentition. The postcranial bones from the Madura Strait are the first postcranial elements to be ascribed to this species.

***Axis* sp.**

Available material (N=241). Antler: 193 beam fragments labelled as SBY370, SBY441, and SBY7206 and 27 small tines labelled as SBY371 and SBY7203. **Cervical vertebrae:** SBY461, SBY475, SBY476, SBY482, SBY504, SBY513, SBY525, SBY537, SBY7105**. Thoracic vertebrae:** SBY478, SBY488, SBY7103, SBY7106, SBY7107. **Lumbar vertebrae:** SBY185, SBY491, SBY535, SBY538**. Scapula,** distal fragments: SBY682, SBY1641, SBY2111.

Description and identification: The beam fragments are assigned to the genus *Axis* because of their smooth to finely-ribbed surface and small to modest size, with diameters ranging between 10 and 30 mm. The fragments may loosely be assigned to either *A. lydekkeri* or *A. javanicus* based on beam thickness and surface ornamentation. However, as beam diameter and surface ornamentation decrease distally, species allocation becomes more uncertain with decreasing diameter of the fragments. The same applies to the small (up to ~ 50 mm long) tines, which may be brow tines, bez tines or crowns of the main beam.

Scapula fragments and vertebrae have been left out of comparative analyses. All small scapulae and vertebrae with a cervid morphology have been listed as *Axis* sp.

Genus: *Rusa* (Smith, 1827)
***Rusa* sp.**

Synonyms: *Cervus kendengensis, Cervus* (*Rusa*) sp.

Available material (N=95). Antler, antler base with burr and pedicle: SBY367 (s), SBY431 (s/d). Antler base with burr: SBY361 (d), SBY418 (s), SBY422 (d), SBY428 (d), SBY429 (d), SBY433 (d), SBY436 (s), SBY440 (s), SBY443 (s), SBY444 (d), SBY845 (d), SBY7178 (d). 43 beam fragments labelled as SBY372 and 7 tines labelled as SBY373. **Lower dentition, M_1 or M_2:** SBY7119 (s) **Cervical vertebrae:** SBY7187, SBY7188. **Thoracic vertebrae:** SBY1758. **Lumbar vertebrae:** SBY496, SBY505, SBY507, SBY510, SBY519, SBY526, SBY536, SBY7189. **Metacarpus,** proximal fragment: SBY7184 (s). Shaft fragment: SBY58 (s). Distal fragment: SBY5091 (d). **Scaphoid:** SBY1516 (s). **Femur,** proximal fragment: SBY29 (d), SBY30 (s). Caput: SBY3481 (s/d). Distal fragment: SBY221 (d). **Tibia:** Distal fragments: SBY226 (s/d), SBY1600 (s), SBY7204 (d). **Cuneiform:** SBY7202 (d). **Astragalus:** SBY174 (s), SBY176 (s), SBY173 (s), SBY177 (s), SBY7043 (d). **Calcaneum:** SBY7197 (d). **Phalanx 2:** SBY7169.

Description and identification: SBY433 and SBY444 **(Fig. 18)** are bases of large antlers with a pearled burr and a rugged surface ornamentation of longitudinal ribs. The base of the antler, between the burr and the internal angle between the main beam and the brow tine, has a height of 50-60 mm. The main beam is slightly backward-directed and has a basal diameter of 40–45 mm. The forward projecting brown tine has broken off in both specimens. SBY431 derives from a similar, large and strongly ornamented antler and preserves a ca. 55 mm long pedicle. The antler fragments compare well with the antlers of the extant *Rusa timorensis* and *Rusa unicolor* and with several mounted Pleistocene antlers kept in the Geological Museum Bandung, most of which are labelled as *Cervus kendengensis*. Due to a lack of diagnostic features to differentiate between these species based on fragmented antler remains, and following the current taxonomical practice for the Pleistocene cervids of Java, the material is assigned to as *Rusa* sp.

SBY7119 **(Fig. 19)** is a worn sinistral M_1 or M_2 preserving some of the surrounding bone. It has rugose enamel and a cervid morphology, with an occlusal surface characterized by isolated conids and open or connected infundibula. Along the lingual face, it has an oblique, outward-directed mesostylid and entostylid and a well-developed metastylid. Along the buccal face, it has straight and well-defined ribs, lacking a visible ectostylid. Its crown size plots far above the size ranges of *Axis lydekkeri* and also above the sizes of the two molars from the Madura Strait that we assigned to *Axis javanicus* **(Fig. 20)**. For the extant or fossil species of *Rusa*, reference size ranges are only available for the M_3. SBY7119 has a higher crown width than the Pleistocene M_3 specimens that were assigned to C*ervus kendengensis*. Its crown width is more comparable to the M_3 of the extant *Rusa unicolor*. We therefore assign SBY7119 to *Rusa* sp., noting that it is relatively large compared to the available Pleistocene *Rusa* molars from Java. Lacking useful references, it is impossible to make out whether the specimen is an M_1 or an M_2.

Postcranial remains have been assigned to *Rusa* sp. based on a morphological and metric analysis of ruminant material. An interesting specimen is the distal metacarpal fragment SBY5091 **(Fig. 25)**. From an anterior view, its median groove continues distally along the shaft until ca. 20 mm above the distal condyle, which identifies the specimen as a cervid (Heintz, 1970). With a distal width of 49 mm, the specimen is remarkably large, approaching the size of bovid species such as *Bos palaeosondaicus*, which shows that the *Rusa* sp. of the Madura Strait must have been particularly large-statured. *Rusa* sp. astragali are well-represented in the assemblage **(Fig. 27)**. Metrically, these astragali are comparable to two fossil astragali from Sangiran attributed to *Rusa* sp. (Moigne et al., 2004). SBY7169 **(Fig. 29)** is a cervid second phalanx that plots slightly below the size range of *B. palaeosondaicus,* again pointing to a particularly large posture.

Family: Bovidae Gray, 1821

Dubois (1908) distinguished three large bovid species from the Pleistocene of Java: *Bos (Bibos) palaeosondaicus, Bubalus palaeokerabau* and *Leptobos groeneveldtii.* The former two are common Pleistocene species and related to the extant *Bos javanicus* and *Bubalus bubalis* of Southeast Asia. *Leptobos groeneveldtii,* later revised to *Epileptobos groeneveldtii* (Hooijer, 1958a) is a rare Pleistocene species, only recorded by two skulls and scarce horncore fragments. Besides these three species, all of which are Bovini, Dubois recognized a small bovid, which he named *Anoa santeng* (Dubois, 1891). The species, which was renamed *Duboisia santeng* (Brongersma, 1937; Stremme, 1911), belongs to the Boselaphini and relates to the extant *Tetracerus quadricornis* and *Boselaphus tragocamelus* of India (Rozzi et al., 2013). There are also scarce fossil records of *Capricornis sumatraensis,* the extant serow of Sumatra and mainland Southeast Asia. This material, consisting of isolated teeth, derives from Late Pleistocene caves of Sumatra and Java (Badoux, 1959; Hooijer, 1958a).

Species definitions have primarily been based on the morphology of skulls and horncores. Metric details were provided by Hooijer (1958) and Stremme (1911). With respect to the dentition, these authors found no morphological or metric differences between the two most common bovid species *B. palaeokerabau* and *B. palaeosondaicus*, except for a slight size reduction of the P_2 in *B. palaeosondaicus.* Isolated cheek teeth from the Javanese find sites are therefore generally referred to as Bovidea indet. With respect to limb bones, the authors concluded that *B. palaeokerabau* and *B. palaeosondaicus* exceeded their extant descendants in size. Moreover, the authors noted that in the extant as well as fossil species, *Bubalus* differs from *Bos* by having more expanded articular facets in the limb bones. Yet mea-

surement data are scarce and bovid postcranial material from Java has mostly been identified as Bovidae indet.

The Madura Strait assemblage is rich in bovid remains and forms an interesting sample for a comparative study. For molars and limb bones, an extensive morphological and metric comparison has been carried out.

Tribe: Bovini Gray, 1821
Genus: *Bubalus* Smith, 1827
***Bubalus palaeokerabau* Dubois, 1908**

Synonyms: *Bubalus buffelus*, *Buffelus palaeokerabau*

Available material (N=101). Horncore fragments: SBY301 (d), SBY304 (s/d), SBY348 (d), SBY558 (s/d), SBY369 (d), SBY564 (s/d), SBY5084 (d), SBY5085 (d), SBY5093 (s), SBY7045 (s/d), SBY7195 (s), SBY7198 (s/d). **Upper dentition, M^1**: SBY117A, SBY117E, SBY126A, SBY126D, SBY126F, SBY7143A, SBY7143B. **M^2:** SBY126C, SBY3402. **M^3:** SBY124D, SBY124G, SBY125A, SBY137A, SBY137C, SBY137E, SBY137F, SBY7145A, SBY7145E. **Lower dentition, M_1:** SBY135A, SBY135C, SBY135E. SBY7147A. **M_2:** SBY116B, SBY118, SBY123B, SBY123F, SBY124A, SBY124C, SBY124D, SBY124G, SBY125B, SBY125C, SBY129B. **M_3:** SBY122A, SBY122B, SBY122C, SBY122D, SBY7149A-B, SBY7151. **Humerus,** distal fragments: SBY2 (s), SBY7 (s/d), SBY221 (s/d), SBY468 (s/d), SBY577 (s/d), SBY680 (s/d), SBY7014 (d). **Radius,** proximal fragments: SBY17 (s), SBY28 (s). Distal fragments: SBY227 (s), SBY1201 (s). **Scaphoid:** SBY520 (s). **Lunatum:** SBY203 (s). **Pyramidal:** SBY7001 (d). **Hamatum:** SBY1633 (d). **Metacarpus,** proximal fragment: SBY19 (s/d). Shaft fragment: SBY22 (s). Distal fragments: SBY53 (d/s), SBY5090 (d). **Femur,** shaft fragment: SBY18 (s). **Tibia,** distal fragments: SBY15 (d), SBY16 (d), SBY45 (d), SBY7035 (d). **Os malleolus:** SBY3440 (d), SBY6009 (d), SBY6011 (d), SBY7185. **Astragalus:** SBY163 (s), SBY164 (s), SBY165 (d), SBY169 (d), SBY170 (d), SBY464 (d), SBY5094 (s), SBY5096 (s), SBY7156 (d). **Naviculo-cuboid:** SBY456 (d). **Metatarsus,** proximal fragments: SBY20 (s), SBY 51 (s/d). Distal fragments: SBY222 (s/d), SBY225 (d). **Phalanx 1**: SBY62, SBY6004. **Phalanx 2:** SBY190, SBY1571, SBY7158, SBY7175.

Description and identification: In the absence of complete crania, species identification has in the first place been based on horncore morphology. Horncores of *B. palaeokerabau* have a smooth outer surface and a characteristic subtriangular cross-section, with one flat face and two more rounded faces (Hooijer, 1958a). Even in a fragmented state, such horn cores can easily be recognized. A good specimen is SBY5084 **(Fig. 21)**. The fragment has a maximum diameter of 69 mm and derives from the central part of a dextral horn core. The flat side is the superior face of the horn core, with a sharp angle at its anterior edge.

Upper and lower molars have provisionally been assigned to *B. palaeokerabau* based on a metric and morphological analysis of all isolated bovid molars and a comparison with museum specimens **(Fig. 22 and 23,** further explanation on the figures). Note that the taxonomic conclusions are indicative only. Overlap between the large bovid species is significant, both in crown size and morphology. Together with Khurniawan (2019), our work forms a first attempt for a systematic analysis of isolated bovid molars from the Pleistocene of Java or surrounding submerged Sundaland.

For the identification of bovid long bones, a similar strategy was followed, using a metric analysis in combination with scarce morphological evidence and comparisons with published size ranges of extant and fossil species (**Fig. 24-26,** further explanation on the figures). Ordering of long bone fragments with intact articulations provides distinct size groups. The specimens of the largest size group, with pronounced laterally-expanded articular facets, have been assigned to *B. palaeokerabau*, which is confirmed by reference measurements of extant and fossil *Bubulus*.

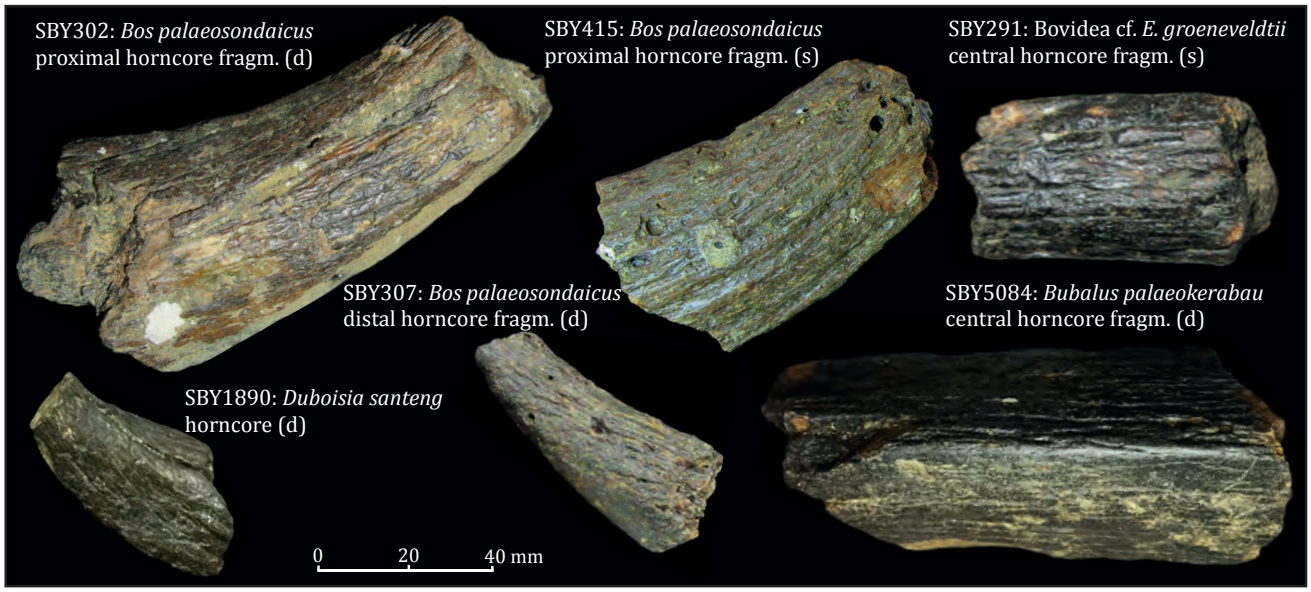


Fig. 21. Bovidae horn cores from the Madura Strait assemblage. Selected photographs. SBY302 in posterior view. SBY307, SBY415, and SBY5084 in anterior view. SBY1890 in lateral view. SBY291: view direction not determinable.

Small and massive bone elements, such as astragali and phalanges, have been found in relatively large numbers and are often intact. Hooijer (1958) noted that the size differences between *Bubalus* and *Bos* are most pronounced in the distal zones of the extremities, which makes these elements an interesting subject for size analyses. The astragali from the Madura Strait cluster in distinct size groups **(Fig. 27**, further explanation on the figure). Published size ranges for fossil or extant *Bubalus* are not available. The largest astragali from the Madura Strait roughly correspond in size with the largest astragali of Kedung Brubus (Weinand, 2005) and are provisionally assigned to *B. palaeokerabau*. The specimens articulate well with the largest tibiae, assigned to the same species.

For the first and second phalanges, similar size analyses have been carried out **(Fig. 28 and 29,** further explanation on the figures). Again, the largest specimens form a distinct size group, with robust shafts and proportionally wide articulations. Reference measurements in related extant species are not available, but the specimens significantly exceed the extant *Bos taurus* in size (Ocal et al., 2004). We tentatively assigned the specimens of this size group to *B. palaeokerabau.* First phalanx SBY6004 articulates well with the largest metacarpals and metatarsals of the assemblage, which were assigned to the same species.

Genus: *Bos* Linnaeus, 1758
***Bos (Bibos) palaeosondaicus* Dubois, 1908**

Synonyms: *Bison sivalensis*, *Bibos banteng*, *Bibos protocavifrons*

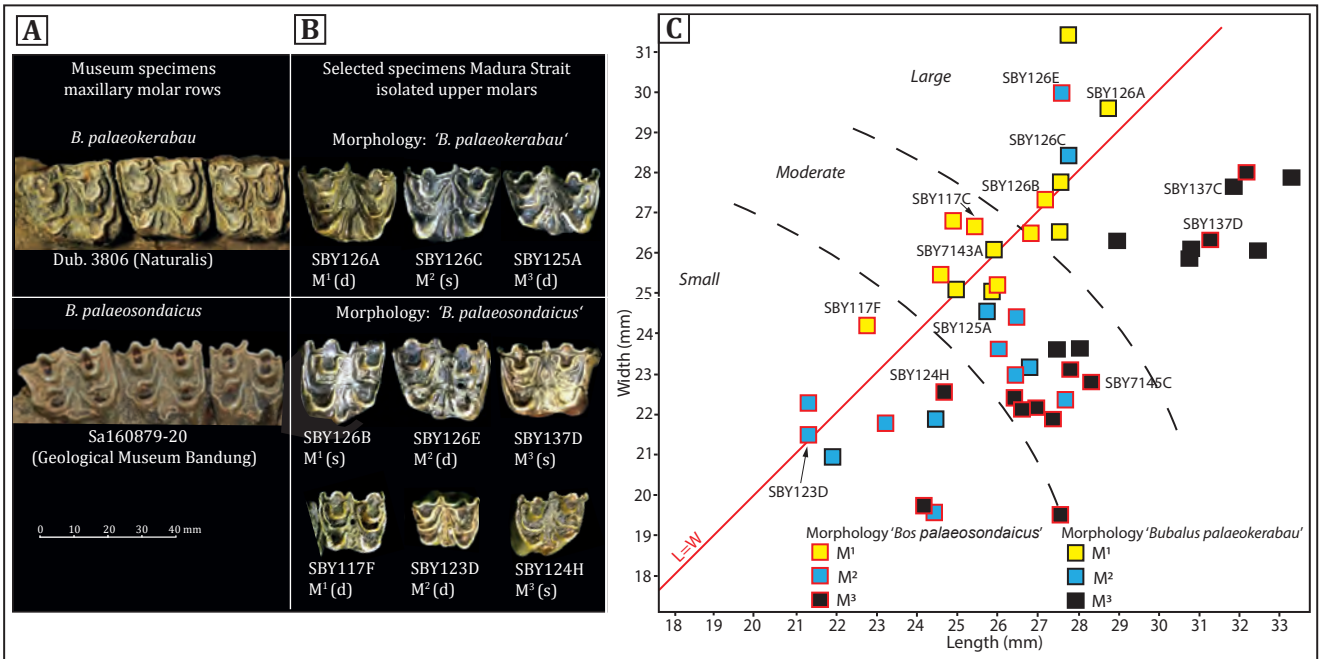
Available material (N=129). Horncore fragments: SBY302 (d), SBY307 (d), SBY308 (s/d), SBY310 (d), SBY311 (s), SBY312 (s/d), SBY313 (s/d), SBY415 (s), SBY7194 (s/d). **Upper dentition**, **M^1:** SBY116A, SBY116C, SBY117B, SBY117C, SBY117D, SBY117F, SBY126B. **M^2:** SBY121, SBY124B, SBY126E, SBY129A. **M^3:** SBY124A, SBY124C, SBY124E, SBY124F, SBY124H, SBY137B, SBY137D, SBY7145B, SBY7145C. **Lower dentition, M_1:** SBY120, SBY135B, SBY135D, SBY155, SBY7160. **M_2:** SBY115A, SBY115B, SBY115C, SBY115D, SBY123D, SBY123E, SBY124B, SBY7148B, SBY7148C. **M_3:** SBY119, SBY122E-G, SBY125C, SBY139, SBY157A, SBY157B, SBY157C, SBY157D. **Humerus,** distal fragments: SBY3 (s), SBY23 (d), SBY1272 (d). **Radius,** proximal fragments: SBY37 (d), SBY1205 (d), SBY7152 (s), SBY7159 (s). Shaft fragments: SBY34 (d), SBY68 (s/d). Distal fragments: SBY483 (d), SBY42 (s/d), SBY48 (s), SBY7024 (s), SBY7025 (s). **Ulna,** shaft fragment: SBY534 (s/d). **Scaphoid:** SBY208 (d), SBY210 (d). **Lunatum:** SBY205 (d), SBY206 (d), SBY207 (d), SBY212 (d), SBY211 (s), SBY215 (s), SBY7186 (d). **Capitato-trapezoid:** SBY1728 (d). **Hamatum:** SBY209 (d), SBY2159 (s). **Metacarpus,** proximal fragments: SBY21 (s), SBY24 (d), SBY53 (s). Distal fragments: SBY220 (s), SBY223 (s/d). **Femur,** proximal fragment: SBY5072 (d). Shaft fragment: SBY31 (s). Distal fragment: SBY686 (s/d). **Tibia,** distal fragments: SBY26 (d), SBY25 (s), SBY226 (s), SBY229 (d), SBY230 (d). **Os malleolus:** SBY6010 (d), SBY6012 (d). **Astragalus:** SBY166 (d), SBY167 (s), SBY171 (d), SBY172 (s), SBY5095 (d), SBY5097 (s), SBY7155 (s). **Calcaneum:** SBY27 (s), SBY1200 (d), SBY7021 (d), SBY7196 (s). **Naviculo-cuboid:** SBY218 (s), SBY224 (d). **Cuneiform:** SBY1461 (s), SBY1790 (d). **Metatarsal,** shaft fragment: SBY59 (d). Distal fragment: SBY6002 (s/d). **Phalanx 1**: SBY187, SBY188, SBY189, SBY191, SBY192, SBY194, SBY672, SBY7155. **Phalanx 2**: SBY195, SBY200, SBY202, SBY204, SBY1575, SBY6005, SBY7053, SBY7192. **Phalanx 3:** SBY7169.

Description and identification: Just as for the other bovid species, the identification of *B. palaeosondaicus* among the fragmented material from the Madura Strait has in the first place been based on horncores. SBY302 and SBY415 **(Fig. 21)** are large fragments of relatively thick horncores with a rugged outer surface. The fragments closely match the taxonomical descriptions by Hooijer (1958), by their oval cross-section, strong curvature, and rough longitudinal grooves. The latter are slightly twisted in a spirally pattern. The fragments have a maximum diameter of 67 and 58 mm respectively and show a strong distal tapering. The longitudinal grooves are twisted posteriorly, which indicates that SBY302 derives from a dextral and SBY415 from a sinistral horn core. SBY307 **(Fig. 21)** is the distal tip of a dextral horn core, with a similar oval cross-section and twisted longitudinal grooves. It has a faintly flattened surface on the inside of the curvature, which is also recognized in the distal-most zones of the horn cores of the available museum specimens.

Isolated molars have been assigned to *B. palaeosondaicus* based on an analysis of size ranges and morphology and our comparison of museum specimens **(Fig. 22 and 23,** further explanation on the figures). As noted earlier for the molars assigned to *B. palaeokerabau*, the taxonomic conclusions are indicative only.

Bovid long bones assigned to *B. palaeosondaicus* are large and robust, but lack the extreme lateral inflation of the articular facets that is characteristic for *B. palaeokerabau* **(Fig. 24-26)**. Based on an analysis of bovid material, most of which derives from Trinil and Kedung Brubus, Hooijer (1958) and Stremme (1911) found that *B. palaeosondaicus* limb bones slightly exceed those of the extant *Bos javanicus* in size. For the Madura Strait assemblage this could not be confirmed. The limb bones assigned to *B. palaeosondaicus* are similar in size to those from the extant *Bos javanicus*. Note that morphologically, the Pleistocene and extant species are identical (Hooijer, 1958a; Von Koenigswald, 1933). The taxonomic subdivision between the Pleistocene species *Bos palaeosondaicus* and the recent or Holocene species *B. javanicus* is based on palaeontological tradition rather than on morphological or metric distinction. We therefore prefer to use the species name *Bos palaeosondaicus* for the late Middle Pleistocene material from the Madura Strait.

Within the sample of Bovini astragali **(Fig. 27)** there is a distinct cluster of medium-sized specimens, which has tentatively been assigned to *B. palaeosondaicus.* The size group overlaps with the medium-sized bovid astragali from Kedung Brubus (Weinand, 2005)*,* which probably also represents this species. Reference measurements of the extant *B. javanicus* are not available*.* Note that the size group falls apart into two sub-clusters, which may reflect sexual dimorphism within the species*.* Also within the sample of first and second phalanges **(Fig. 28 and 29)**, there is a distinct



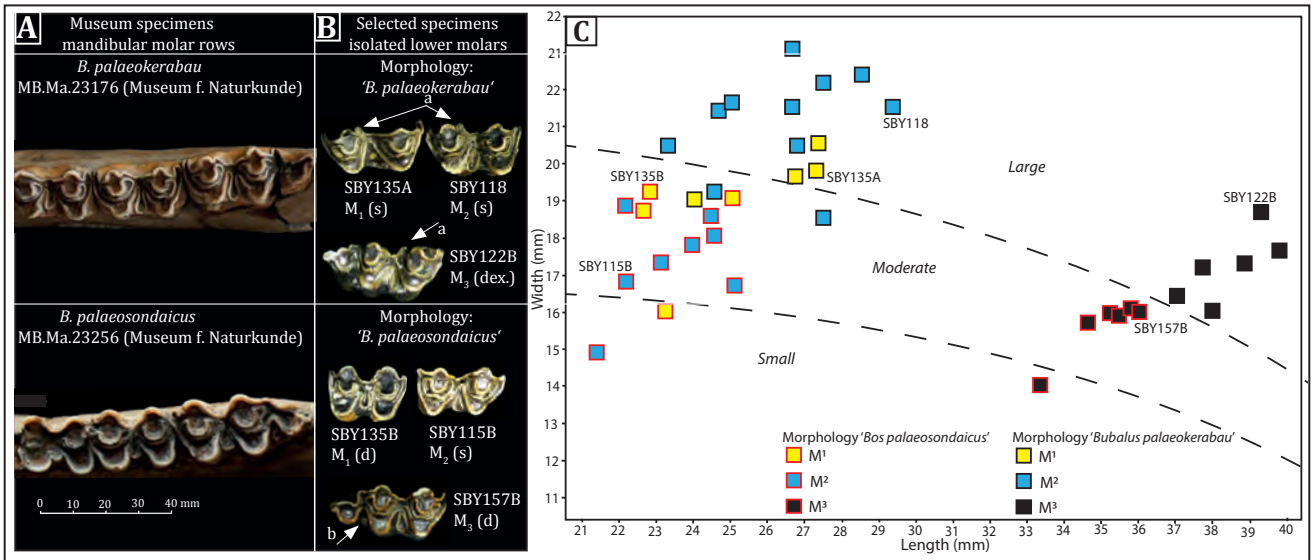
The bovid (Bovini) upper molars from the Madura Strait roughly plot in three size groups (large, moderate and small). Direct metric comparison with museum specimens is difficult, because upper molars with an undisputed taxonomy are as a rule concealed in intact maxillae. Measurements of concealed molars are taken higher up the crown and are dependent on wear stage. However, a rough metric inquiry of museum specimens indicates that the molars of size groups 'large' and 'moderate' are similar to the dentition of *B. palaeokerabau* and *B. palaeosondaicus*. *B. palaeokerabau* molars seem to reach slightly larger sizes, but size ranges overlap. Intra-species size variation may relate to sexual dimorphism. Reliable distinction between the two species based on size is therefore not possible.

With respect to crown morphology, Stremme (1911) and Hooijer (1958) found no reliable morphological differences between *B. palaeokerabau* and *B. palaeosondaicus,* or on a more basic level between the genera *Bos* and *Bubalus.* Bacon et al. (2011), working on fossil assemblages from Thailand, noted more complex folds of the infundibula and more voluminous cones and conids in *Bubalus* than in *Bos*. We carefully checked these traits in the available museum collections from Java. With respect to the infundibula, the morphological differences are not convincing. The anterior infundibulum can be U-shaped or Y-shaped, whereas the posterior infundibulum has a twisted Y- or X-shape. The occlusal morphology of the infundibula varies with wear, which makes it a difficult basis for species identification. However, with respect to cone size and morphology there indeed appears to be a difference between the two species. In *B. palaeosondaicus*, the protocone and hypocone tend to form rounded, wide ribs, whereas in *B. palaeokerabau* the ribs are often thinner. Sukiato (2019) found that these thinner ribs are visible on the occlusal face as narrow, U-shaped lobes, especially in the protocone (see **A:** reference specimens). Ordering the Madura Strait molars based on protocone morphology, we noted another morphological difference: the crowns with the more voluminous protocones, presumably representing *B. palaeosondaicus*, have prominent and often bilobed entostyles, which fill up most of the area between the protocone and hypocone ribs. The crowns with the narrow protocones, presumably representing *B. palaeokerabau*, generally have a thinner and unbilobed entostyle, leaving a larger open area between the protocone and hypocone, which is mostly filled with cement (see **B**: selected Madura Strait specimens). We used these morphological traits to subdivide the crowns from the Madura Strait in two groups. The size plot **(C)** shows that the molars of both morphological groups are distributed over the size ranges 'large' and 'moderate', with a slight overrepresentation of the molars assigned to *B. palaeokerabau* in the size group 'large'.

The molars of the size group 'small' are slightly below the size ranges of the available museum specimens of *B. palaeokerabau* and *B. palaeosondaicus*. Morphologically, they are similar to the crowns that we assigned to *B. palaeosondaicus,* i.e. with rounded protocone and hypocone ribs. Possibly the specimens derive from small females of this species. It is also possible that there are *Epileptobos groeneveldtii* molars among the size group 'small'. As was noted by Hooijer (1958), the molars of this rare species are relatively small and morphologically similar to *B. palaeosondaicus*.

Fig. 22. Bovidae (Bovini) upper molars from the Madura Strait assemblage. **A:** Reference maxillary molar rows in occlusal view. **B:** Selected specimens from the Madura Strait in occlusal view. **C:** Metric and morphological analysis. Crown measurements were taken 10 mm above the crown base. Numbered specimens are pictured in B.

size group of medium-sized Bovini. Reference measurements of relevant extant or fossil Bovini are not available. The specimens are similar in size to the phalanges of the extant *Bos taurus* (Ocal et al., 2004). We tentatively assigned the phalanges to *B. palaeosondaicus*.



The bovid (Bovini) lower molars from the Madura Strait roughly plot in 3 size groups (large, moderate and small). As noted for bovid upper molars **(Fig. 22)**, direct metric comparison with reference material is difficult, because all taxonomically identified museum specimens are intact mandibular molar rows. A metric inquiry of museum specimens indicates that *B. palaeokerabau* and *B. palaeosondaicus* crowns are similar to the size groups large and moderate of the Madura Strait.

Looking at the available reference mandibles of these two species, we found no significant difference in volume or roundness of the conids that might serve as a similar taxonomical marker, such as used for bovid upper molars. Suraprasit et al. (2016), working on a Middle Pleistocene assemblage from Thailand, noted that *Bubalus* lower molars generally have a distinct metastylid, whereas in *Bos* this stylid is absent or only developed near the apex of the crown. Moreover, the authors noted a posterior ectostylid in the M_3 of the genus *Bos*, while this stylid is generally absent in *Bubalus*. The latter was noted earlier by Colbert and Hooijer (1953), who found this trait not sufficiently reliable to serve as a taxonomic marker. Upon comparison with reference mandibles, we conclude that the observations by Suraprasit et al. (2016) are mostly valid for the Middle Pleistocene species of Java and may be used as indicative taxonomic markers to distinguish between *B. palaeokerabau* and *B. palaeosondaicus*, at least within a larger sample of isolated molars (see **A**: reference specimens and **B**: selected specimens from the Madura Strait. a = metastylid in *B. palaeokerabau*. b = posterior ectostylid in the M_3 of *B. palaeosondaicus*.

We subdivided the lower molars from the Madura Strait using these tentative morphological criteria, assigning the crowns with a metastylid to *B. palaeokerabau* and the crowns lacking a clear metastylid to *B. palaeosondaicus*. As expected, none of the M_3's with a metastylid has a posterior ectostylid. In a few M_3's, both the metastylid and the posterior ectostylid appeared to be absent or not observable. These specimens have provisionally been assigned to *B. palaeosondaicus*, thus giving priority to the absence of the metastylid as taxonomic marker. Within the size plot **(C),** the size groups 'large'and 'moderate' largely overlap with this tentative morphological distinction: most crowns with a *B. palaeokerabau* morphology fall in the size group 'large'; most crowns with a *B. palaeosondaicus* morphology fall in the size group 'moderate'.

Fig. 23. Bovidae (Bovini) lower molars from the Madura Strait assemblage. **A:** Reference mandibular molar rows in occlusal view. **B:** Selected specimens from the Madura Strait in occlusal view. **C:** Metric and morphological analysis. Crown measurements were taken 10 mm above the crown base. Numbered specimens are pictured in B.

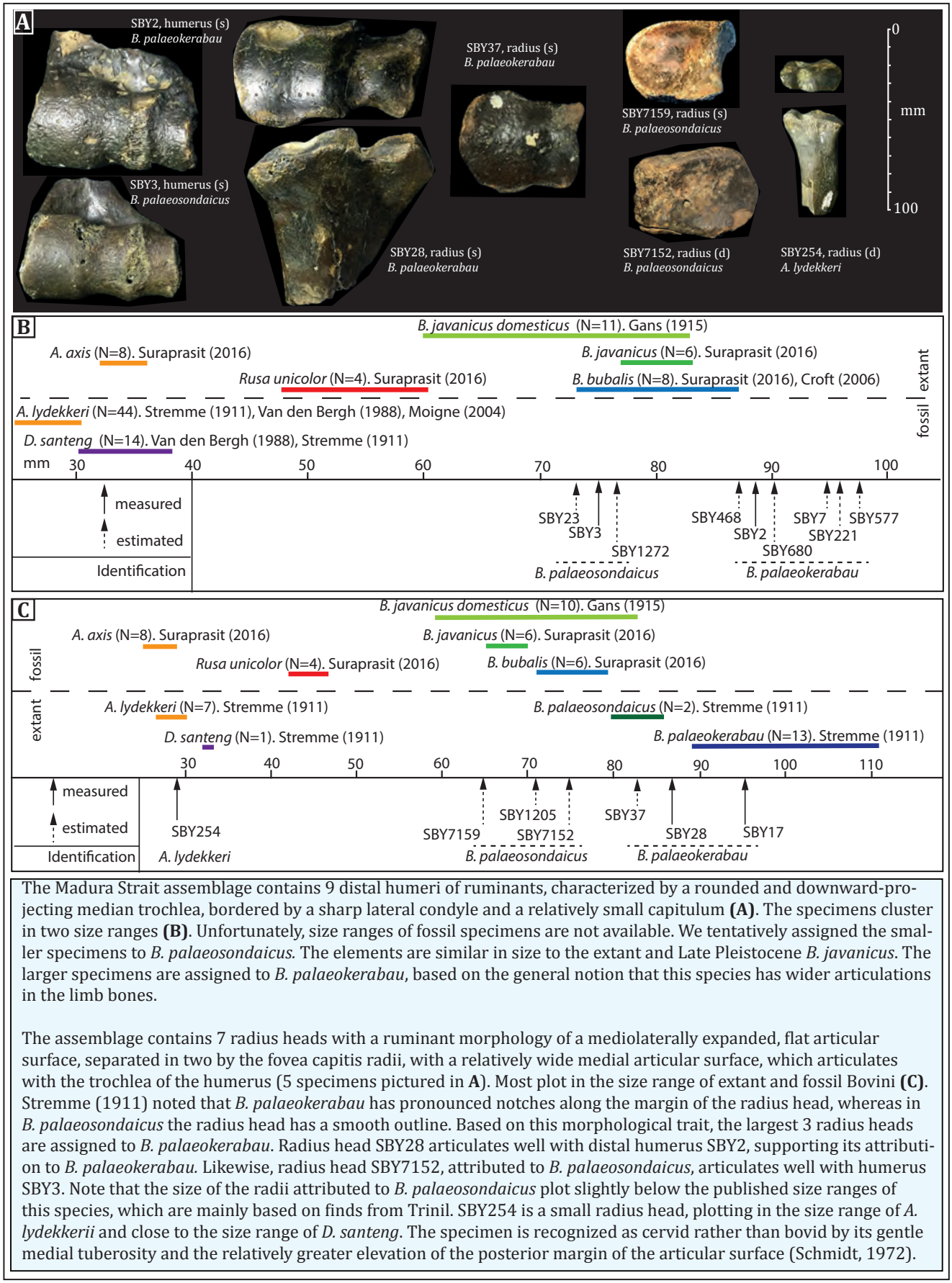
Genus: *Epileptobos* Hooijer, 1956
Epileptobos groeneveldtii (Dubois, 1908)

Synonyms: *Leptobos groeneveldtii*, *Leptobos cosijni*

Available material (N=4). Horncore fragments: SBY291 (s/d), SBY305 (s/d), SBY306 (s/d), SBY7038 (s/d).

Description and identification: Among the horncore fragments from the Madura Strait, four specimens have a slightly deviant morphology. Their ribbed surface is similar to *B. palaeosondaicus,* but the fragments lack the robust, oval-shaped cross-section, the strong distal-tapering, and the strong curvature. SBY291 **(Fig. 21)** is a fragment of a ribbed horncore with a circular cross-section and a diameter of ~50 mm at both sides. Its curvature is insignificant, and this absence of curvature is accentuated by the straight, untwisted longitudinal grooves. SBY7038 is a larger fragment, with a preserved length of 17 cm. The fragment has break surfaces at both sides, with a diameter of 44 mm at the proximal side and 37 mm at the distal site.

The fragments resemble the descriptions of *E. groeneveldtii* horn cores by Hooijer (1958) and fit well with the relatively long and only gently curved horn cores of the two crania of this species that are stored at Naturalis Biodiversity Center (collection numbers Dub. 2765 and 2766). SBY291 is probably the central portion of a horncore, SBY7038 represents a more distal zone, with the tip broken off. In the absence of curvature, tapering or twisted grooves, it is

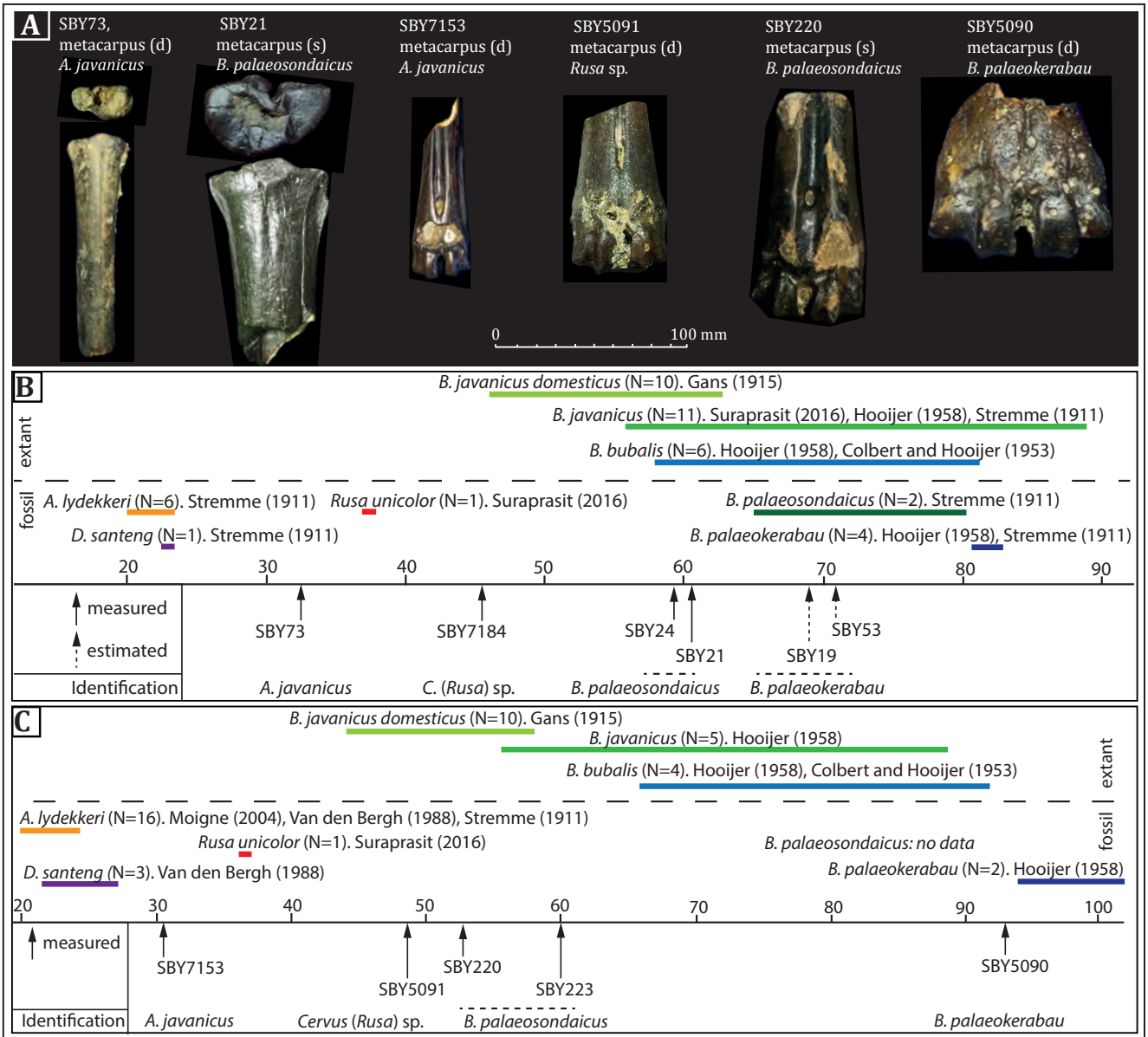


The Madura Strait assemblage contains 9 distal humeri of ruminants, characterized by a rounded and downward-projecting median trochlea, bordered by a sharp lateral condyle and a relatively small capitulum **(A)**. The specimens cluster in two size ranges **(B)**. Unfortunately, size ranges of fossil specimens are not available. We tentatively assigned the smaller specimens to *B. palaeosondaicus.* The elements are similar in size to the extant and Late Pleistocene *B. javanicus*. The larger specimens are assigned to *B. palaeokerabau*, based on the general notion that this species has wider articulations in the limb bones.

The assemblage contains 7 radius heads with a ruminant morphology of a mediolaterally expanded, flat articular surface, separated in two by the fovea capitis radii, with a relatively wide medial articular surface, which articulates with the trochlea of the humerus (5 specimens pictured in **A**). Most plot in the size range of extant and fossil Bovini **(C)**. Stremme (1911) noted that *B. palaeokerabau* has pronounced notches along the margin of the radius head, whereas in *B. palaeosondaicus* the radius head has a smooth outline. Based on this morphological trait, the largest 3 radius heads are assigned to *B. palaeokerabau*. Radius head SBY28 articulates well with distal humerus SBY2, supporting its attribution to *B. palaeokerabau.* Likewise, radius head SBY7152, attributed to *B. palaeosondaicus*, articulates well with humerus SBY3. Note that the size of the radii attributed to *B. palaeosondaicus* plot slightly below the published size ranges of this species, which are mainly based on finds from Trinil. SBY254 is a small radius head, plotting in the size range of *A. lydekkerii* and close to the size range of *D. santeng*. The specimen is recognized as cervid rather than bovid by its gentle medial tuberosity and the relatively greater elevation of the posterior margin of the articular surface (Schmidt, 1972).

Fig. 24. Ruminant humeri and radii from the Madura Strait assemblage. Morphological and metric analysis. **A:** Selected photographs in frontal view (humeri) and proximal view (radii). Radii SBY2 and SBY254 also in anterior view. **B:** Metric analysis humeri: width of distal articulation (BT) and published size ranges (mm). C: Metric analysis radii: width of proximal articulation (Bfp) and published size ranges (mm). Measurements and codes based on Von den Driesch (1976).

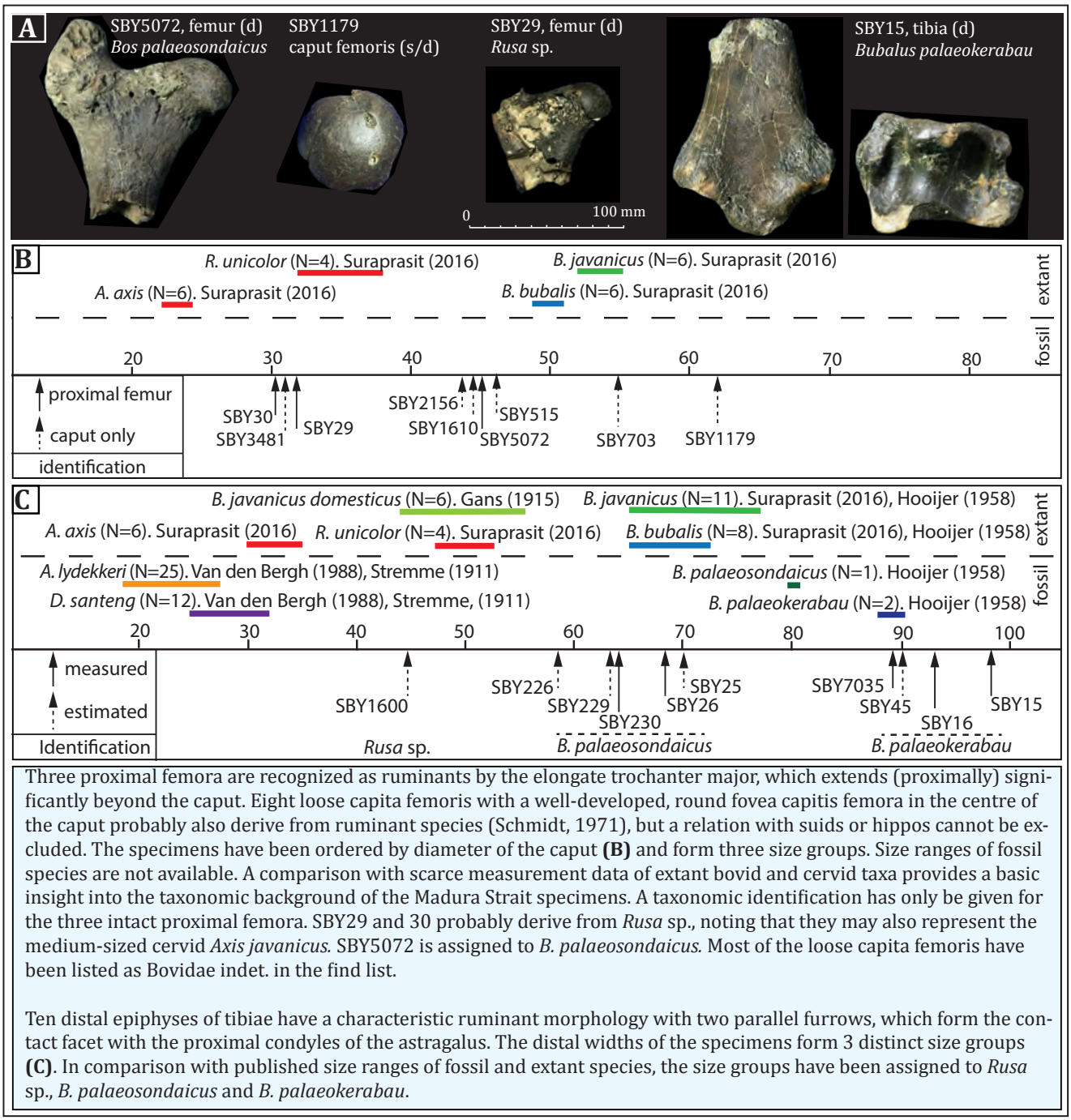
impossible to decide whether the specimens derive from sinistral or dextral horncores. The other two specimens, SBY305 and SBY306, are distal tips of slender horncores with a round cross-section.



In absence of *Equus* in the Pleistocene of Java, all fused metacarpals derive from ruminants. Among the proximal fragments **(A)**, SBY73 stands out by its small size. It is recognized as a cervid rather than the small bovid *D. santeng* by the course of the median ridge at the articular surface, which is interrupted by the central cavity (Van den Bergh, 1988). Its size is intermediate to reference specimens of *A. lydekkeri* and *Rusa* sp. **(B)**. We therefore assigned the specimen to the medium-sized cervid *A. javanicus*. The other proximal fragments fall in the size range of Bovini. All have a well-preserved articular surface of two facets separated by a ridge. The medial facet, articulating with the unciform, continues further anteriorly than the lateral facet. Stremme (1911) noted that in *Bos*, this medial facet is significantly larger, whereas in *Bubalus* both facets are of similar size. Based on this morphological marker, we assigned SBY21 and SBY24 to *B. palaeosondaicus.* SBY19 and SBY53 have a wider proximal articulation. Their facets are damaged, but appear to be of similar size. The specimens have provisionally been assigned to *B. palaeokerabau*. All proximal fragments plot slightly below the published size ranges of the fossil species, which are primarily based on specimens from Trinil.

Among the distal fragments, only SBY7153 is small-sized. It is recognized as a cervid by the median groove along the anterior face of the shaft, which ends ca. 2 cm proximal of the distal epiphysis, whereas in bovids it continues to the epiphysis (Heinz, 1971). The specimen plots above the published size range of *A. lydekkeri* and is assigned to *A. javanicus* **(C)**. Remarkably, also SBY5091 has this cervid morphology of the median groove. The specimen, which comes close to the size range of Bovini, must be assigned to *Rusa* sp. and is illustrative of this species' large size. SBY220 and SBY223 have a median groove continuing to the distal epiphysis. They are assigned to the Middle Pleistocene *B. palaeosondaicus*, noting that again the specimens appear to be relatively small. Reference sizes from the Pleistocene of Java are not available, but the Madura Strait specimens plot in the lower size range of the extant *B. javanicus.* SBY5090 is laterally expanded, characteristic of *Bubalus*, and similar-sized as two reference specimens of *B. palaeokerabau* from Trinil.

Fig. 25. Ruminant metacarpalia from the Madura Strait assemblage. Morphological and metric analysis. **A:** Selected photographs in anterior view. Proximal fragments also in proximal view. **B:** Metric analysis proximal fragments: width of proximal epiphysis (Bp) and published size ranges (mm). **C:** Metric analysis distal fragments: width of distal articulation (Bd) and published size ranges (mm). Measurements and codes based on Von den Driesch (1976).



Three proximal femora are recognized as ruminants by the elongate trochanter major, which extends (proximally) significantly beyond the caput. Eight loose capita femoris with a well-developed, round fovea capitis femora in the centre of the caput probably also derive from ruminant species (Schmidt, 1971), but a relation with suids or hippos cannot be excluded. The specimens have been ordered by diameter of the caput **(B)** and form three size groups. Size ranges of fossil species are not available. A comparison with scarce measurement data of extant bovid and cervid taxa provides a basic insight into the taxonomic background of the Madura Strait specimens. A taxonomic identification has only be given for the three intact proximal femora. SBY29 and 30 probably derive from *Rusa* sp., noting that they may also represent the medium-sized cervid *Axis javanicus.* SBY5072 is assigned to *B. palaeosondaicus.* Most of the loose capita femoris have been listed as Bovidae indet. in the find list.

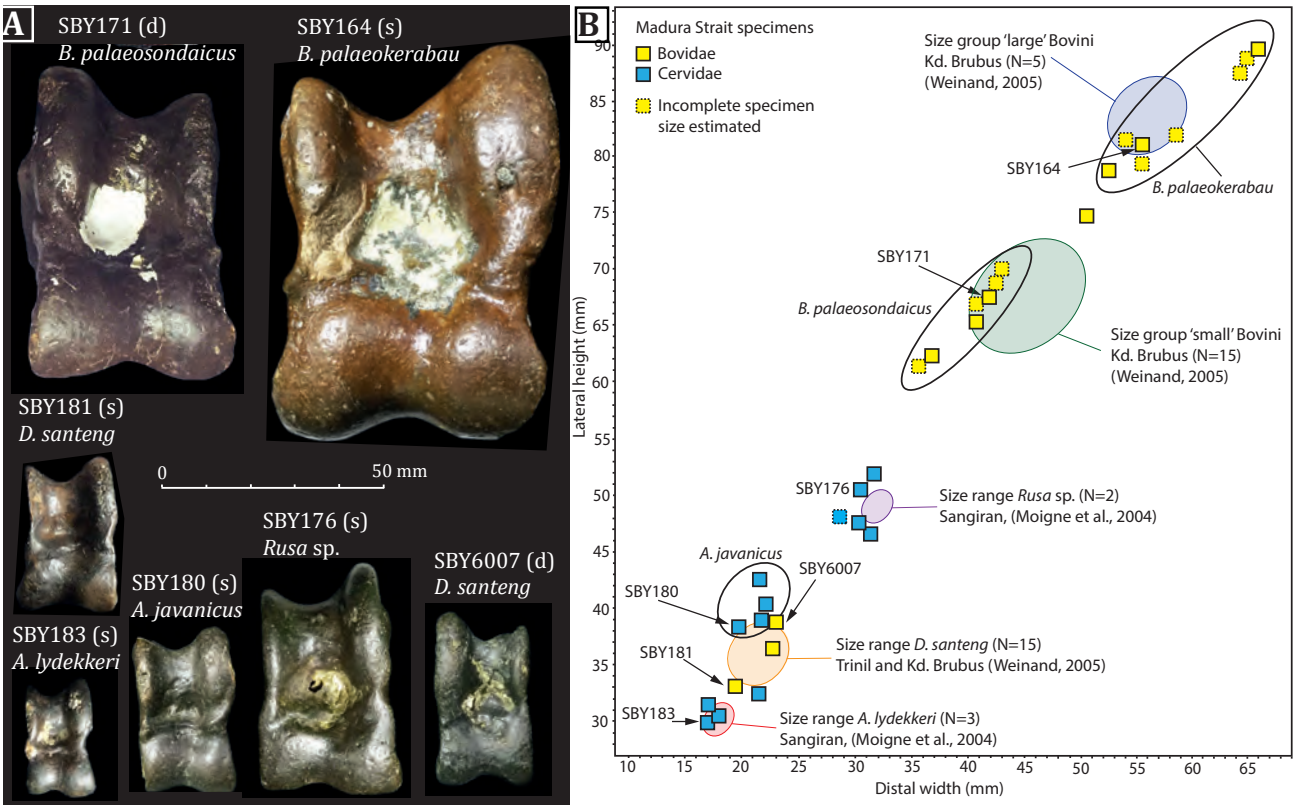
Ten distal epiphyses of tibiae have a characteristic ruminant morphology with two parallel furrows, which form the contact facet with the proximal condyles of the astragalus. The distal widths of the specimens form 3 distinct size groups **(C)**. In comparison with published size ranges of fossil and extant species, the size groups have been assigned to *Rusa* sp., *B. palaeosondaicus* and *B. palaeokerabau*.

Fig. 26. Ruminant femora and tibiae from the Madura Strait assemblage. Morphological and metric analysis. **A:** Selected photographs. Femora SBY29 and SBY5072 in frontal view. Caput femoris SBY1179 in articular view. Tibia SBY15 in frontal and distal view. **B:** Metric analysis femora: diameter (depth) caput femoris (DC) and published size ranges (mm). **C:** Metric analysis tibiae: width of distal epiphysis (Bd) and published size ranges. Measurements and codes based on Von den Driesch (1976).

Bovini indet.

Available material (N=88). Palladium, fragment: SBY7002. **Maxilla,** fragment with DP^4: SBY7160 (d). **Mandibula,** fragment with dP_4-M_1: SBY7149 (d), fragment with dP_4: 7150 (s), fragment with P_3 –P_4: SBY133 (d), fragment with M_2 and M_3: SBY5067 (s). **Deciduous dentition, dP^3:** SBY120. **dP^4:** SBY123A and C. **dP_3:** SBY5059. **dP_4:** SBY5057. **Incisor:** SBY162. **Premolars, P^2:** SBY153A, SBY153B, SBY5078. **P^3:** SBY144A-B, SBY3403A-C. **P^4:** SBY128A-F, SBY144C. **P_2:** SBY158A. **P_3:** SBY138A-B, SBY158B-C, SBY5061, SBY7167. **P_4:** SBY3401. **Cervical vertebrae:** SBY498, SBY451, SBY457, SBY461, SBY470, SBY1204, SBY1208, SBY7012, SBY7031, SBY7032, SBY7102. **Thoracic vertebrae:** SBY451, SBY454, SBY458, SBY460, SBY467, SBY479, SBY7034, SBY7015, SBY7033, SBY7036, SBY7101, SBY7111. **Lumbar vertebrae:** SBY459, SBY466, SBY472, SBY473, SBY481, SBY495, SBY508, SBY522, SBY528, SBY529, SBY534, SBY7027. **Caudal vertebra:** SBY216. **Scapula,** distal fragments: SBY9 (d), SBY56 (d), SBY1532 (d), SBY7057 (s), SBY7179 (s). **Humerus,** distal fragments: SBY7011A-B (s/d). **Radius:** shaft fragment: SBY7006 (s). **Femur,** caput (s/d) small: SBY703, SBY1610, SBY2156, SBY5125, caput (s/d) large: SBY1179 (s/d), SBY7044 (s/d), SBY7110. **Tibia,** proximal fragment: SBY7005 (s). Distal fragment (juvenile): SBY7013 (d).

Description and identification: The Madura Strait assemblage contains several deciduous premolars, one incisor, and a large number of (fragmented) premolars of Bovini. Published accounts on the metrics or morphology of this mate-



The Madura Strait assemblage contains 31 (mostly) complete ruminant astragali. Cervid and bovid astragali can be separated by the morphology of the distal condyles (Heintz, 1971). In cervids, the lateral condyle is larger than the medial condyle and the median valley separating the two condyles is slightly off-centre, shifted medially. In bovids both condyles are almost equal in size, with a smooth median valley in the centre. This trait is important to separate *D. santeng* from similarly-sized cervids.

The astragali fall apart in several well-marked size groups **(B)**. The smaller size groups can be linked with published size ranges of *A. lydekkeri*, *D. santeng* and *Rusa* sp. Four specimens with a cervid morphology plot slightly above the size range of *D. santeng.* We assign these to *A. javanicus,* as we know from the molar analysis that this cervid species must have been intermediate in size between *A. lydekkeri* and *Rusa* sp.

The larger bovid astragali from the Madura Strait roughly plot in two size ranges. Previous researchers did not differentiate such large astragali into separate species. Weinand (2005) measured large bovid astragali from Trinil and Kedung Brubus available in Naturalis Biodiversity Center. For the specimens from Kedung Brubus, he found two size ranges, which compare well with the two size ranges from the Madura Strait. Among the specimens from Trinil he found a dominance of larger astragali, comparable to the largest specimens from Kedung Brubus.

Referring to the repeatedly found pattern of more robust limb bones in *Bubalus* compared to *Bos*, both in fossil and in extant species, we provisionally separated the bovid astragali in *B. palaeosondaicus* and *B. palaeokerabau* based on size groups. The size differences within these groups may reflect sexual dimorphism.

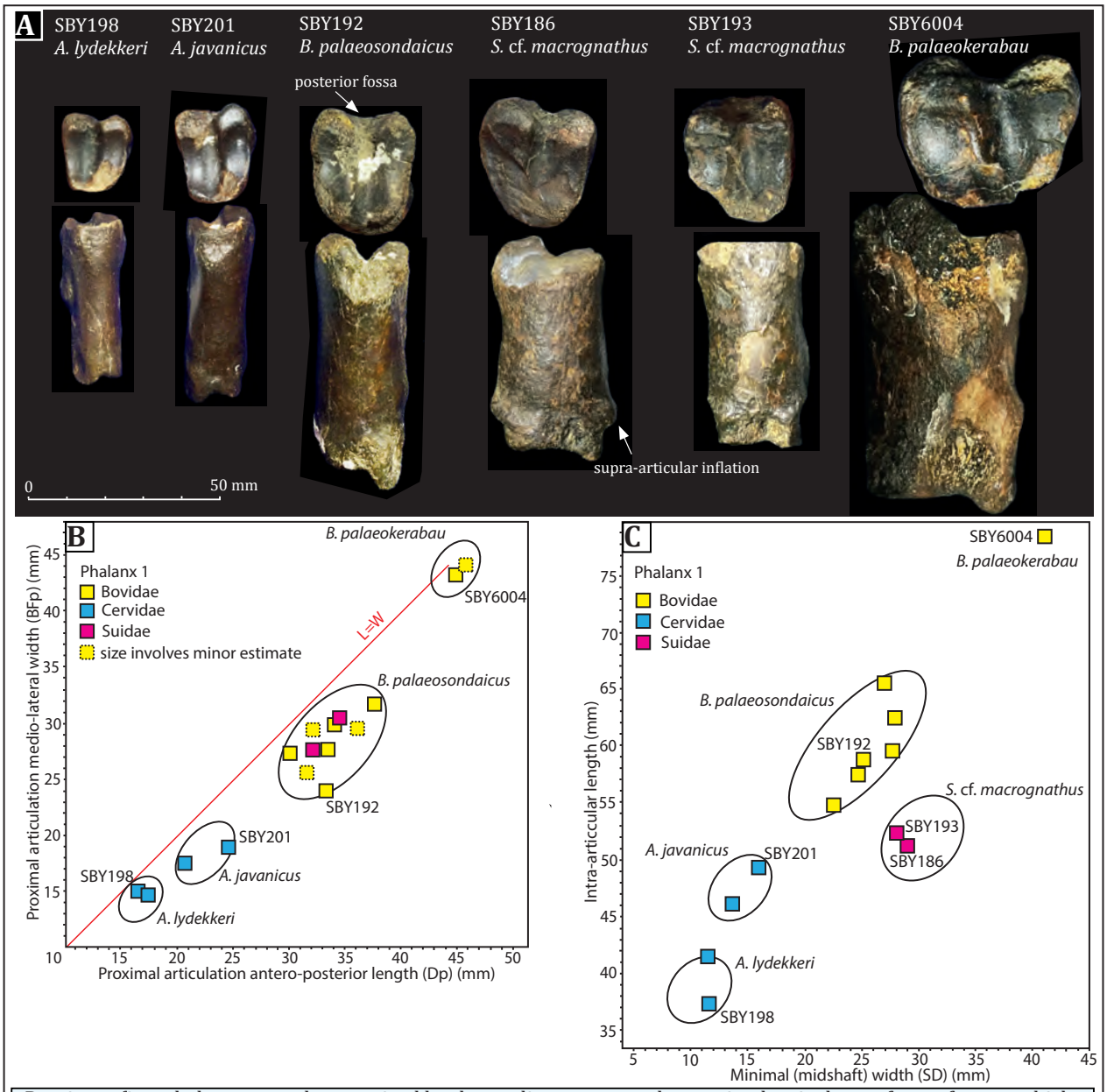
Fig. 27. Ruminant astragali from the Madura Strait assemblage. Morphological and metric analysis. **A:** Selected photographs in anterior view. **B:** Metric analysis: bivariate plot of distal width DW) and lateral height (LH) and published size ranges. Measurements and codes based on Von den Driesch (1976).

rial are scarce. Colbert and Hooijer (1953) noted a reduced size of the P_2 in *Bos* compared to *Bubalus.* However, there is no intact bovid P_2 in the collection. The sample size of intact specimens is not sufficient to carry out a meaningful metric or morphological comparison of premolars. Bovid scapulae and vertebrae have been left out of the comparative analysis of the larger bovid postcranial material. All these elements have been referred to as Bovini indet.

Tribe: Boselaphini Knottnerus-Meyer, 1907
Genus: *Duboisia* Stremme, 1911
***Duboisia santeng* (Dubois, 1891)**

Synonyms: *Anoa santeng*, *Tetracerus kroesenii*, *Duboisia kroesenii*, *Antilope mojokertensis*

Available material (N=7). Horncore: SBY1890 (d). **Mandibula,** fragment with M_1, M_2 and M_3: SBY105 (d). **Lower dentition:** M_2: SBY101 (d). **Astragalus:** SBY181 (s), SBY5098 (d), SBY6007 (d). **Phalanx 2**: SBY7041.



Ruminant first phalanges are characterized by the median groove at the proximal articular surface, a feature which they share with suids. In cervids, the posterior fossa only affects the outlines of the articular face, but in bovids it continues proximally into the articular surface, where it forms a notch between the two sesamoid facets (Heintz, 1971). See for example in **(A)** the well-developed posterior fossa in SBY192 and SBY6004. Based on this morphological trait, all smaller specimens of the assemblage are cervid rather than bovid, which implies that *D. santeng* is probably not represented among the first phalanges.

SBY186 and SBY193 have a different outline of the proximal surface, which is slightly asymmetrical and pointed anteriorly. Their deviant morphology among the sample of first phalanges is more pronounced in the shaft, which is relatively wide and has an inflation directly above the distal articulation. This is a characteristic trait of suids (Schmidt, 1974). The only large suid known from the Pleistocene of Java is *Sus macrognathus*. The specimens are tentatively referred to as *Sus* cf. *macrognathus.*

Metrically, the phalanges plot in distinct size ranges. Published size ranges of relevant fossil and extant species are not available. The size groups have been assigned to species based on direct comparison with museum specimens and articulation with metapodials. With respect to the size of the proximal articular face **(B)**, the 2 suid phalanges fall in the size range of *B. palaeosondaicus*. However, looking at the metrics of the shaft **(C)**, they form a distinct group, with a shorter length and a relatively great width.

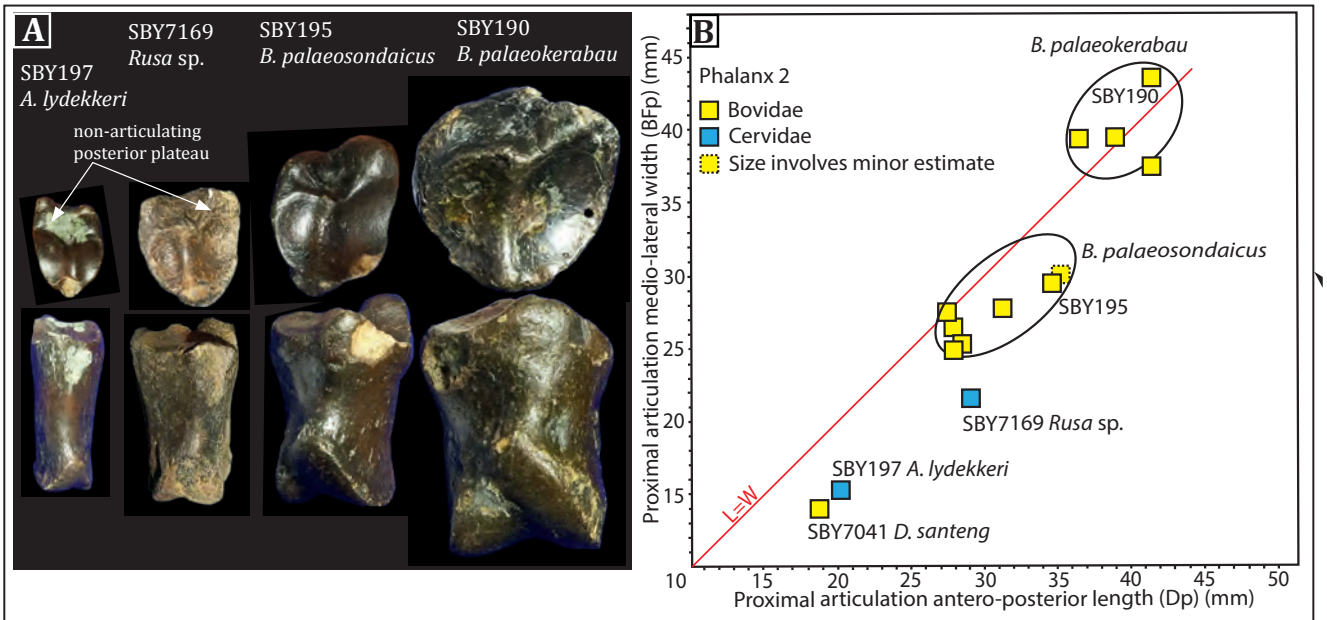
Fig. 28. Ruminant and suid first phalanges from the Madura Strait assemblage. Morphological and metric analysis. **A:** Selected photographs in proximal and anterior view. **B:** Metric analysis; bivariate plot of length (Dp) and width (BFp) of the proximal articular face. **C:** Metric analysis; bivariate plot of shaft width (SD) and length. No distinction has been made between phalanges from the forelimb and hindlimb. Measurements and codes based on Von den Driesch (1976) except for intra-articular shaft length: callipers placed in median groove.

Description and identification: SBY1890 **(Fig. 21)** is an almost complete dextral horncore, only missing the distal tip. It is slightly antero-posteriorly compressed, with a trapezium-shaped cross-section. Its anterior face is flattened, whereas its wider posterior face is rounded. Also the lateral face is flattened, forming a keel at the transition to the anterior face. The horncore has a maximum (proximal) diameter of 30 mm and tapers over a short distance. The horncore is strongly curved upward and forward. Total preserved length is 45 mm. The horncore compares well with several intact skulls in the Geological Museum Bandung and Naturalis Biodiversity Center (collection nrs. Dub. 2037-2039.) The base of the specimen from the Madura Strait must have broken off close to the skull. Total missing length of the horn core tip is 15 to 20 mm, which gives an estimated complete length of the horn core of around 65 mm.

SBY105 **(Fig. 30A)** is a fragment of a dextral mandibular ramus. The lower margin of the ramus is damaged, but the molar row is intact, preserving the M_1, M_2 and M_3. Below the M_2, the mandible has a height of 29.0 mm and a thickness of 14.2 mm. The molars are slender and relatively high-crowned. The enamel is smooth, white and shiny and lacks a cement cover. In buccal view, the protoconids and hypoconids form prominent, straight ribs.

The M_2 has a low basal pillar (ectostylid). The molars are slightly worn and have an occlusal morphology with merged conids and two isolated, U-shaped infundibula. SBY101 **(Fig. 30A)** is an isolated, unworn lower molar with a slender crown morphology lacking a cingulum or basal thickening. It has shiny white enamel and straight ribs, highly similar to the molars of mandible fragment SBY105 and a size comparable to the M_2 of this specimen.

Although the crown sizes are similar to cervids, the crown morphology is indicative of a bovid. Note in this respect the absence of basal thickening, the straight protoconid and hypoconid ribs, the smooth and shiny enamel, and the isolated infundibula. See **Fig. 19** for a direct comparison with cervid lower molars. The only small-sized Pleistocene bovid species of Java are *Duboisia santeng* and *Capricornis sumatrensis*. Metrically, SBY105 is below the size range of *C. sumatrensis,* but it compares well with several mandibles of *D. santeng* stored at the Trinil Museum, the Geological Museum Bandung, and Naturalis Biodiversity Center (collection nrs. Dub. 2053 and 2068d), with respect to mandibu-



Ruminant (and suid) second phalanges are characterized by a median ridge at the proximal articular surface and a groove at the distal articulation. Heintz (1971) noted two morphological markers at the proximal articulation surface that may be used for differentiation between relevant genera. 1) The articulation consists of two facets, of which the lateral facet is slightly longer (anteroposteriorly). In bovids, this size difference between the two facets is significant, whereas in cervids there is a modest size difference. In the Madura Strait assemblage, this morphological difference is not always easy to recognize. Based on its similar-sized facets, SBY7169 is regarded as a cervid, whereas the larger phalanges SBY195 and SBY190 are clearly bovid. 2) Cervids have a non-articulating plateau along the posterior margin of the proximal face, whereas in bovids the corresponding zone is an irregularly sloping transitional surface towards the posterior face. This plateau is well-developed in SBY197 and SBY7169, identifying the specimens as cervids. Metrically, the second phalanges fall apart in distinct size groups **(B)**. The two cervid phalanges have been assigned to *A. lydekkeri* and *Rusa* sp. based on size comparison and articulation with available metapodials, which for example indicates that SBY7169 is too large for *A. javanicus*. Among the bovid specimens, *B. palaeokerabau* stands out by its larger size and considerable lateral expansion. Size differences within the bovid size groups may represent sexual dimorphism as well as differences between forelimb and hindlimb.

Fig. 29. Ruminant second phalanges from the Madura Strait assemblage. Morphological and metric analysis. **A:** Selected photographs in proximal and anterior view. **B:** Metric analysis; bivariate plot of length (Dp) and width (BFp) proximal articular face. Measurements and codes based on Von den Driesch (1976).

lar size, molar morphology, and molar sizes. The smooth and shiny enamel is a characteristic trait of the species, a feature which it shares with other Boselaphini (Moigne et al., 2016). The molar sizes plot within the published size ranges of *D. santeng*, which are mostly based on specimens from Trinil **(Fig. 30B)**.

The unworn M_2 SBY101 has a crown height of 25.2 mm and a H/W-index of 2.80. There is only one record of an unworn lower molar of *D. santeng*, found in Trinil and stored in Naturalis Biodiversity Center (numbered Dub. 2509A). Hooijer (1958) described it as an M_1, but we note that it may also be an M_2. With a crown width of 10 mm and a crown height of 26.5 mm, it has a H/W-index of 2.65, similar to the specimen from the Madura Strait.

We carefully examined all small-sized ruminant postcranial material for the presence of *D. santeng* remains, using the morphological criteria provided by Van den Bergh (1988) and Heintz (1970). The only postcranial elements that could be assigned to this species are three astragali: SBY181, SBY5098, SBY6007 **(Fig. 27A)**. They are distinguished from cervid astragali by their similar-sized distal condyles, separated by a smooth median valley. The attribution of the three astragali to *D. santeng* is supported by their sizes, plotting in the size range of this species as provided by Weinand (2005) **(Fig. 27B)**. The astragalus sizes are intermediate between *A. lydekkeri* and *A. javanicus*, the two small cervids of the Madura Strait assemblage.

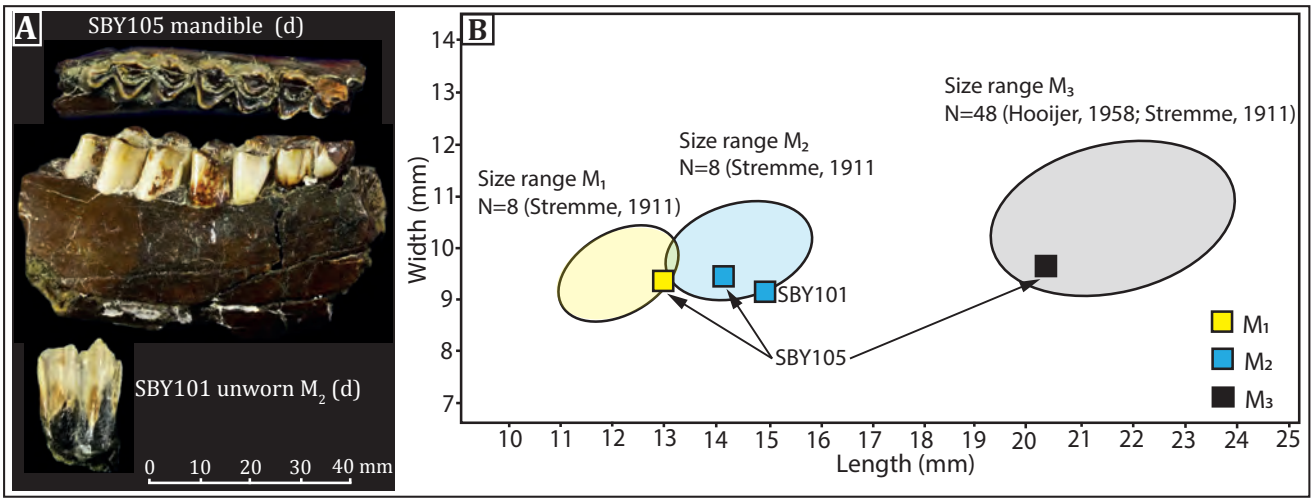


Fig. 30. *Duboisia santeng* lower molars from the Madura Strait assemblage. **A:** SBY105 in occlusal view and buccal view and SBY101 in lingual view. **B:** Bivariate plot of crown lengths and widths with published size ranges.

4. Discussion

4.1 The Madura Strait assemblage as a reference for regional palaeontological studies

4.1.1 First records and rare specimens

The Madura Strait assemblage yielded several vertebrate species that were thus far unknown from the Middle Pleistocene fossil record of Java or the Sundaland region. Moreover, it contains rare specimens, most of which were thus far not available in Indonesian museum collections.

The shark *Carcharhinus* cf. *leucas* was previously unknown from the Pleistocene of the Sundaland region. Recently, several teeth from the museum collection of Naturalis Biodiversity Center, excavated in Sangiran in the 1930s, were ascribed to this species (Kocsis, 2024). Another shark, *Galeocerdo cuvier*, was only known from rare teeth in Late Pliocene marine strata near Sangiran (Yudha et al., 2018). Interesting is also the occurrence of *Hemipristis serra,* an extinct species known from various Late Oligocene to Pleistocene sites worldwide (Cappetta, 1987). We could find no fossil records of this species from the Sundaland region, except for several teeth pictured by Yudha et al. (2018) and assigned to *Hemipristis* sp., which possibly represent this same extinct species. Relevant Southeast Asian records come from Taiwan (Lin et al., 2022) and Sulawesi (Hooijer, 1958b, 1954), both probably dating from the Early Pleistocene. The late Middle Pleistocene *H. serra* teeth from the Madura Strait may very well be the youngest recorded occurrence worldwide of this extinct species.

Two stingrays, *Rhinoptera javanica* and *Myliobatis* sp., were previously unknown from the Pleistocene of Sundaland, although the former was recently also reported in the museum collection of Naturalis (Kocsis, 2024), again deriving from a 1930s excavation in Sangiran. Three spine fragments of the giant stingray *U. polylepis* are very rare specimens. There are two similar specimens from the Pleistocene of Java, both excavated in Trinil in the 1890s and today housed at Naturalis Biodiversity Center (Joordens et al., 2009).

Other highly rare Pleistocene specimens are varanid and snake vertebrae. There are several specimens from Trinil

and Kedung Brubus (Hooijer, 1972; Janensch, 1911a; Dubois, 1908), all of which are stored in Naturalis Biodiversity Center or the Museum für Naturkunde Berlin. Two of the Madura Strait specimens fall in the size range of *Varanus komodoensis.* There is one record of an Early to Middle Pleistocene snake vertebra from Java, found in Trinil (Janensch, 1911a). The specimen, which was never described or pictured, is probably housed in the Museum für Naturkunde Berlin. The Madura Strait assemblage contains one Pythonidae trunk vertebra, which is the first described Middle Pleistocene snake fossil from Java.

A new record for the Pleistocene of Indonesia is the freshwater turtle *Dogania subplana*. The species is extant in Southeast Asian rivers and was recorded in the Late Pleistocene fossil record of Sarawak, Malaysian Borneo (Pritchard et al., 2009). Highly rare is the *Macaca* ulna fragment from the Madura Strait. There are only a few records of non-hominin primate remains from the Middle Pleistocene of Java, most of which are dental elements. Thus far, only one postcranial fossil had been described. This is a femur from Trinil assigned to Hylobatidae (Ingicco et al., 2014), which is kept at Naturalis Biodiversity Center. Another rare specimen is the astragalus of *Hexaprotodon sivalensis*. There are five earlier records of similar specimens from Java, all of which are housed in Naturalis Biodiversity Center or the Museum für Naturkunde Berlin.

4.1.2 Species-specific morphological traits

Our morphological analyses of the Madura Strait assemblage provided new insights into species-specific morphological traits, which may also be of use for the identification of other, fragmentary fossil remains from the region. The most important contributions relate to turtle plate fragments and bovid molars.

Morphological distinction between Geoemydidae (hard-shelled turtles) is difficult, due to a scarcity of diagnostic features. The plates are often fused and the breaks are random. However, we showed that it is possible to get a general insight into the species composition of an assemblage. For the Madura Strait assemblage, several potential species could be discarded by the absence of serrated margins or crested cervical plate fragments. Moreover, we could find species-specific matches for a limited number of plate fragments, referring to sulci patterns and the morphology of plate margins, which in the case of the Madura Strait assemblage point to the presence of *Orlitia borneensis* and *Batagur* sp. Our identification procedure is therefore useful for large samples of fragmented Geoemydidae shells and gives a general indication of represented species. For Tryonychidae (soft-shelled turtles), identification of plate fragments has been based on plate ornamentation, following the morphological subdivision of Pritchard et al. (2009). It appeared to be relatively straightforward to organize the fragments into four morphological groups, representing *Chitra chitra*, *Pelochelys cantorii*, *Amyda cartilaginea* and *Dogania subplana*.

For our study of bovid molars, we compared the dentition of *Bubalus* and *Bos*, both in extant and fossil species. Despite morphological overlap, it proved to be possible to make a tentative subdivision between *Bubalus palaeokerabau* and *Bos palaeosondaicus***,** based on morphological traits. The identifications are supported by metric control: the crowns with a *Bubalus* morphology are overall slightly larger than the crowns with a *Bos* morphology. Moreover, the ratio *Bubulus* to *Bos* within the molar sample is similar to the ratio among horn core fragments or postcranial fragments. We conclude that our morphological identification procedure is a valuable tool in large samples of bovid molars and gives a reasonable insight into the composition of the fossil bovid fauna. Note that for the molar analysis, we left the rare and extinct taxon *Epileptobos* out of consideration, due to a scarcity of reference specimens.

4.1.3 Species-specific size ranges

A large fossil sample such as the Madura Strait assemblage offers opportunities for metric analyses. We measured dental and postcranial elements of various genera and species, and compared the measurement results to published size ranges or new reference measurements of museum specimens. The metric data have been combined in tables and graphs, forming an easy reference for future palaeontological studies in the region. For *Elephas* cheek teeth and Artiodactyla postcranial elements, our metric analyses provided new insights into species-specific size ranges or local evolutionary trends.

The *Elephas* teeth from the Madura Strait are relatively slender, high-crowned, and metrically closer to the extant *Elephas maximus* than to the Middle Pleistocene *E. hysudrindicus.* The difficulty is that the diagnostic criteria for distinguishing the extinct *E. hysudrindicus* from the extant *E. maximus* are primarily based on skull morphology. Hooijer (1955) also found metric differences between the dentition of the two species, but with overlapping ranges. We measured several Middle Pleistocene museum specimens attributed to *E. hysudrindicus* from various sites on Java and found that also among this material there are slender and high-crowned specimens, with plate sizes similar to *E. maximus.* The taxonomic implications of this finding are unclear (see also **Section 4.4**).

The fragmented limb bones from the Madura Strait are dominated by Artiodactyla. Within comparable fossil assemblages from Java, this material is generally left unidentified, or identified up to genus only. We selected cervid and bovid specimens based on the morphological criteria provided by Schmid and Garroux (1972), Heintz (1970) and

Van den Bergh (1988) and measured the sizes of the articular surfaces. The elements fall apart in distinct size ranges, which compare well with published size ranges of relevant extant and Pleistocene species. Interestingly, the limb bones of the intermediate-sized cervid *Axis javanicus* form a distinct, well-defined size range. This is the first time that postcranial material of this species, formerly only known from antlers (Von Koenigswald, 1933) and molars (Gruwier et al., 2015) has been identified. The larger bovid material forms at least two size groups, which could be assigned to *Bos palaeosondaicus* and *Bubalus palaeokerabau* based on a greater medio-lateral width of the articulations in the genus *Bubalus*. The limb bones assigned to *Bos palaeosondaicus* are small compared to fossil reference specimens from Java. The material falls in the size range of the extant *Bos javanicus*, which is on the average slightly smaller than its Pleistocene ancestor (see also **Section 4.4**).

4.2 Fauna list and translation to vertebrate communities

The total find list consists of 6,372 specimens, from which 19% could be identified **(Table 12**). We recognized a total of 36 vertebrate species, divided over 11 orders. One of the most conspicuous characteristics of the assemblage is its ecological mixture. In order to get a better idea of the ecological context of the species, the assemblage has been subdivided into three vertebrate communities or habitats: estuarine, fluvial and terrestrial. For each habitat, we provided relative abundances of the available taxa. To this end, we equated the number of specimens with the number of individuals per taxon, which is an appropriate method for highly dispersed fossil assemblages (Badgley, 1986).

Order	*Family*	*Species*	*NISP*	*%*
Carcharhiniformes	Hemigaleidae	*Hemipristis serra*	5	0.08
	Carcharhinidae	*Glyphis gangeticus*	51	0.8
		Carcharhinus cf. *leucas*	20	0.31
		Galeocerdo cuvier	3	0.05
Myliobatiformes	Myliobatidae	*Myliobatis* sp.	1	0.02
		Rhinoptera javanica	3	0.05
	Dasyatidae	*Urogymnus polylepis*	3	0.05
Batoidea (Superorder)*	Indet.		18	0.28
Siluriformes	Bagridae	*Hemibagrus* sp.	1	0.02
Squamata	Varanidae	*Varanus komodoensis*	2	0.03
		Varanus salvator	2	0.03
	Pythonidae	indet.	1	0.02
Testudines	Geoemydidae	Geoemydidae indet.	102	1.6
		Batagur affinis	1	0.02
		Orlitia borneensis	1	0.02
	Tryonychidae	*Chitra chitra*	29	0.46
		Pelochelys cantorii	7	0.11
		Amyda cartilaginea	5	0.08
		Dogania subplana	6	0.09
	indet.		24	0.38
Crocodilia	Crocodylidae	*Crocodylus siamensis*	24	0.38
	Gavialidae	*Gavialis bengawanicus*	4	0.06
	indet.		4	0.06
Proboscidea	Stegodontidae	*Stegodon trigonocephalus*	31	0.49
	Elephantidae	*Elephas* sp.	15	0.24
	indet.		54	0.85
Primates	Hominidae	*Homo erectus*	2	0.03
	Cercopithecidae	*Macaca* sp.	1	0.02
Carnivora	Felidae	*Panthera pardus*	1	0.02
Perissodactyla	Rhinocerotidae	*Rhinoceros sondaicus*	27	0.42
Artiodactyla	Hippopotamidae	*Hexaprotodon sivajavanicus*	30	0.47
	Suidae	*Sus brachygnathus*	14	0.22
		Sus cf. *macrognathus*	2	0.03
	Cervidae	*Axis lydekkeri*	36	0.56
		Axis javanicus	17	0.27
		Axis indet.	241	3.78
		Rusa sp.	95	1.49
	Bovidae	*Bubalus palaeokerabau*	101	1.59
		Bos palaeosondaicus	129	2.02
		Epileptobos groeneveldtii	4	0.06
		Bovini indet.	88	1.38
		Duboisia santeng	7	0.11
Total determined			1212	19.02
Total indetermined			5160	80.98
TOTAL			6372	100

Table 12: Vertebrate taxonomy, identified and unidentified specimens; Madura Strait assemblage. Specimen counts and percentages (rounded to two decima-places) of the entire assemblage.* The specimens listed as Batoidea indet. may (partly) be Myliobatiformes.

The estuarine community **(Table 13)** consists of large fish species, which is obviously a sampling bias. The estuaries of Southeast Asia are rich in smaller fish (Kottelat, 2013). Finding remnants of these species, if preserved, requires sediment sieving and microscope analysis, which was outside the scope of this study. The abundance of shark teeth relates to their excellent preservation potential, but also to their frequent shedding, which may reach several thousand teeth in a lifetime. Any assessment of species abundances based on shark teeth must therefore be made with caution and merely has significance in comparison with other shark species. Most of this fossil material probably derives from the estuarine deposits that form the top of the valley fill. A few species, such as the river shark *Glyphis gangeticus,* the giant stingray *Urogymnus polylepis*, and the catfish *Hemibagrus* sp. have an estuarine to lowland-river habitat. This implies that their remains may also have been part of the fluvial sandstones that form the basal part of the valley fill. In the case of *G. gangeticus*, this probably contributed to the high abundance of its fossil remains in the assemblage.

Order	*Species*	*%*
Carcharhiniformes	*Hemipristis serra*	4.8
	Glyphis gangeticus	48.6
	Carcharhinus cf. *leucas*	19
	Galeocerdo cuvier	2.9
Batoidea (superorder)	Batoidea indet.	17.1
Myliobatiformes	*Myliobatis* sp.	1
	Rhinoptera javanica	2.9
	Urogymnus polylepis	2.9
Siluriformes	*Hemibagrus* sp.	1
TOTAL		100

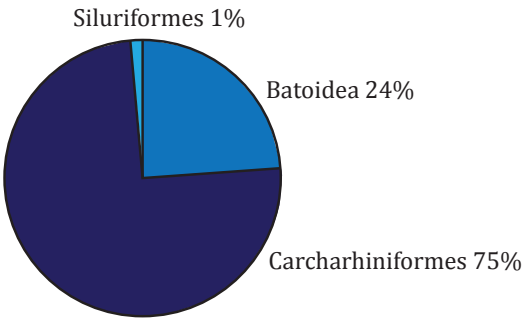


Table 13. The estuarine community: estuarine and lowland-river fishes. Madura Strait assemblage. Percentages (rounded to one decimal place) of total identified specimens for this community. Pie diagram shows the community per taxonomical order or (for Batoidea) superorder.

The fluvial community **(Table 14)** consists of reptiles and mammals tied to the river as their main habitat. Besides one caudal spine attributed to *Hemibagrus* sp. (added to the estuarine community), we found no remnants of fluvial fish, which relates to the applied sampling methods. The abundance of turtles partly relates to the high preservation potential of turtle shells and to their fragmentation, causing sample inflation. The crocodilians are mainly represented by teeth. Just as we noted for sharks, this may lead to an overestimate of crocodilian abundances, caused by shedding of teeth. On the other hand, crocodilian postcranial material is probably underrepresented in the find list, as we did not have access to a collection of relevant comparative skeletal material.

Order	*Species*	*%*
Squamata	*Varanus salvator*	0.8
	Pythonidae sp.	0.4
Testudines	Testudines indet.	10
	Geoemydidae indet.	42.5
	Batagur affinis	0.4
	Orlitia borneensis	0.4
	Chitra chitra	12.1
	Pelochelys cantorii	2.9
	Amyda cartilaginea	2.1
	Dogania subplana	2.5
Crocodilia	Crocodilia indet.	1.7
	Crocodylus siamensis	10
	Gavialis bengawanicus	1.7
Artiodactyla	*Hexaprotodon sivajavanicus*	12.5
TOTAL		100

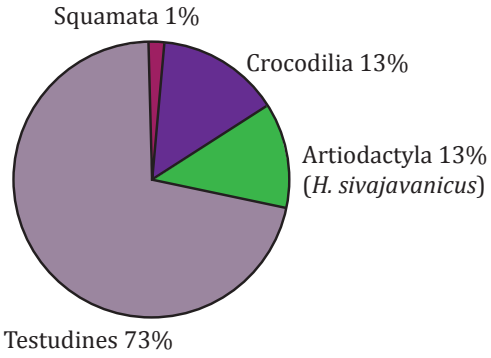


Table 14. The fluvial community: reptiles and mammals tied to the river. Madura Strait assemblage. Percentages (rounded to one decimal place) of total identified specimens for this community. Pie diagram shows the community per taxonomical order.

The terrestrial community **(Table 15)** is dominated by mammals, most of which are herbivores. There is probably a bias against small- to medium-sized animals, which again relates to not-implementing sediment sieving, but also to the higher susceptibility of small bones to carnivore mastication and chemical or physical destructions (Behrensmeyer et al., 1979). Small animals like rodents were not found. Medium-sized animals, with body weights of around 60 kg, are scarce and their abundances are probably underestimated. This concerns species such as *Sus brachygnathus, Duboisia santeng* and *Axis lydekkeri.*

Order	*species*	*%*
Squamata	*Varanus komodoensis*	0.2
Proboscidea	*Stegodon trigonocephalus*	3.6
	Elephas sp.	1.7
	Proboscidea indet.	6.2
Primates	*Homo erectus*	0.2
	Macaca sp.	0.1
Carnivora	*Panthera pardus*	0.1
Perissodactyla	*Rhinoceros sondaicus*	3.1
Artiodactyla	*Sus brachygnathus*	1.6
	Sus cf. *macrognathus*	0.2
	Axis lydekkeri	4.2
	Axis javanicus	2
	Axis sp.	27.8
	Rusa sp.	11
	Bubalus palaeokerabau	11.6
	Bos palaeosondaicus	14.8
	Epileptobos groeneveldtii	0.5
	Bovini indet.	10.1
	Duboisia santeng	0.8
TOTAL		100

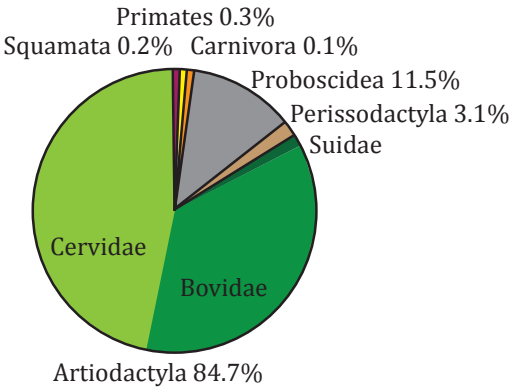


Table 15. The terrestrial community: mammals and reptiles of the lowland plains. Madura Strait assemblage. Percentages (rounded to one decimal place) of total identified specimens for this community. Pie diagram shows the community per taxonomical order, with Artiodactyla subdivided in families.

Cervidae make up 45% of the terrestrial assemblage, however, their great representation is primarily accounted for by antler fragments. If we focus only on other elements such as molars, astragali, or phalanges, the representation of cervids is much lower and bovids are always in the majority. Taking a closer look at the material, we found most antlers to be shed antlers. Out of 13 antler bases of the genus *Rusa,* only 2 preserve a pedicle. For the genus *Axis* this is even more extreme: out of 26 antler bases, only 1 preserves a pedicle. This great dominance of shed antlers results in an overestimate of cervid presence. We therefore recalculated the occurrence of cervids within the population by only including antler bases with a pedicle, which are in fact frontal fragments. This changes the relative abundances of all terrestrial species and brings up a dominance of bovids **(Table 16)**. The occurrence of proboscideans within the terrestrial community is probably somewhat underestimated. Proboscideans were mainly recorded by their dentition, including fragmented tusks. Remnants of limb bones are scarce, which is probably also a taphonomic bias, as fragments of such large bones often do not preserve recognizable articulations, complicating their determination.

4.3 The vertebrate biostratigraphy of Java and age overlap with the Ngandong Fauna

The Pleistocene terrestrial vertebrate assemblages of Java are generally discussed in terms of faunal units, which were defined by Von Koenigswald (1934, 1933) and later revised by de Vos et al. (1982). The units are regarded as records of intermittent dispersal waves of new species to Java, and as records of local evolution and extinction (Van den Bergh et al., 2001, 1996; Leinders, 1985; Sondaar, 1984). Moreover, the faunal units have commonly been used as chronostratigraphic markers (Zaim, 2010; Duyfjes, 1938a). Relevant Pleistocene faunal units are the Trinil HK Fauna, Kedung Brubus Fauna, Ngandong Fauna, and Punung Fauna.

Recent studies provided new insights into the age and (lack of) homogeneity of the faunal units. The Trinil HK Fauna primarily derives from two stacked fluvial channels, dated to 830-773 ka and 540–380 ka respectively, but probably also contains fossils from the younger Solo terrace deposits (Hilgen et al., 2023; Pop et al., 2023a). The younger channel may contain fossils that were locally reworked from the older channel, and both channels may contain fossil mate-

Order	species	%
Squamata	*Varanus komodoensis*	0.4
Proboscidea	*Stegodon trigonocephalus*	5.5
	Elephas sp.	2.7
	Proboscidea indet.	9.7
Primates	*Homo erectus*	0.4
	Macaca sp.	0.2
Carnivora	*Panthera pardus*	0.2
Perissodactyla	*Rhinoceros sondaicus*	4.8
Artiodactyla	*Sus brachygnathus*	2.5
	Sus cf. *macrognathus*	0.4
	Axis lydekkeri	2.7
	Axis javanicus	2.1
	Axis sp.	3.8
	Rusa sp.	5.9
	Bubalus palaeokerabau	18.1
	Bos palaeosondaicus	23.1
	Epileptobos groeneveldtii	0.7
	Bovini indet.	15.7
	Duboisia santeng	1.3
TOTAL		100

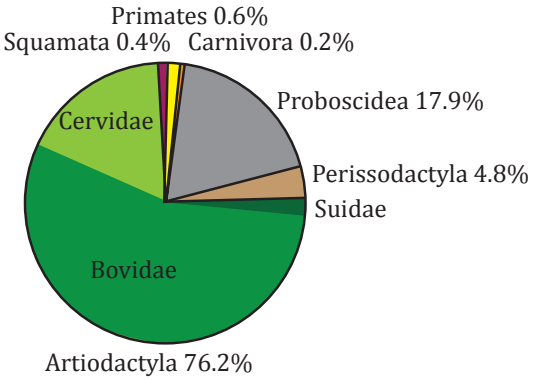


Table 16. The terrestrial community: mammals and reptiles of the lowland plains. Madura Strait assemblage. Similar to **Table 15**, but with a correction for shed antlers. Percentages (rounded to one decimal place) of total identified specimens for this community. Pie diagram shows the community per taxonomical order, with Artiodactyla subdivided in families.

rial reworked from the underlying older strata. The Ngandong Fauna derives from a fluvial terrace that has been dated to 140 – 92 ka (Rizal et al., 2020). The age and stratigraphic background of the Kedung Brubus Fauna is not fully understood, but is generally assumed to be intermediate to the Trinil HK and Ngandong Faunas. However, it may very well have a complex depositional background and a temporally mixed composition. The Punung Fauna derives from cave breccias that have been dated to 128 – 115 ka (Westaway et al., 2007). Kaifu et al. (2022) provided an updated stratigraphy and updated species list for the Punung Fauna.

With an OSL age of 162±31 and 119±27 ka, and a most likely age range of 146 – 131 ka (Berghuis et al., 2025a), the Madura Strait fossiliferous valley fill overlaps in age with the Ngandong terrace and with the Punung cave breccias. Looking at the composition of the fossil faunas from these three sites, there is a great similarity between the Madura Strait assemblage and the Ngandong Fauna. Both are dominated by open-grassland herbivores and both contain the archaic mammal species that characterize the Early and Middle Pleistocene of Java, such as *Stegodon* and *Homo erectus.* The Punung Fauna is a different fauna, which includes modern and rainforest-dependent taxa such as *Pongo* sp. (orang-utan). Note, however, that the rainforest dependency of the latter species has recently been questioned (Louys et al., 2022; Spehar et al., 2018). The transition to the Punung Fauna is regarded as a major faunal turn-over, representing a change from dry and open conditions to humid and forested conditions during MIS5 (Van den Bergh et al., 2001). The Ngandong Fauna, as well as the Madura Strait assemblage, predates this faunal turnover and may be tied to MIS6.

The Ngandong assemblage was excavated between 1931 and 1934, unearthing ~25,000 fossils including twelve hominin calvaria and two hominin tibia (Huffman et al., 2010; Weidenreich, 1951; Oppenoorth, 1932). The non-hominin collection was never investigated in detail. Von Koenigswald (1933) provided a list of species, which has become the basis of the Ngandong Fauna. In later years, the species list was updated, following taxonomical revisions and brief inquiries of the stored material (Van den Bergh et al., 2001; Van Den Bergh, 1999; De Vos et al., 1982). Unfortunately, detailed specimen counts and metric data of the Ngandong assemblage are not available. Moreover, the non-hominin collection is poorly catalogued and possibly partly lost, which makes it difficult to carry out re-investigations or to take new measurements.

4.4 The faunal records of Ngandong and Madura Strait compared: implications for the late Middle Pleistocene vertebrate biogeography of Sundaland

Not only are the assemblages from Ngandong and the Madura Strait of similar age, they also have a shared relation

with the Pleistocene Solo River. However, there may have been a relevant difference in landscape setting. Ngandong lies along the uplifted middle reach of the Solo, bordering the volcanic highland of Java, whereas the Madura Strait site represents the lower reach of this river, in the lowland plains of Sundaland that had become emerged during MIS6. It is interesting to see whether there are faunal differences between the two fossil assemblages that may be linked to this difference in landscape setting.

A conspicuous difference between the two fossil assemblages is the wealth of shark and stingray remains among the fossils from the Madura Strait, none of which were recorded in Ngandong. It shows that the river shark *Glyphis gangeticus* was a common species in the lower reach of the late Middle Pleistocene Solo. Other sharks such as *Carcharias leucas*, *Galeocerdo cuvier*, and *Hemipristis serra* roamed the estuary. The former two species are still extant in Indonesian coastal waters and are known to occasionally ascend lowland rivers. Another fish of the lowland Solo was the giant stingray *Urogymnus polylepis*. Today, this species is extant in lowland rivers of Southeast Asia, but extinct on Java. Two other stingrays, *Rhinoptera javanica* and *Myliobatis* sp. were present in the estuary. The former is still extant in Indonesian coastal waters. The latter is unknown from present-day Indonesian coasts. It may have been related to the extant *Myliobatis aquila* of the western Indian Ocean or *Myliobatis australis* of Australia, both of which are modest-sized stingrays with a coastal habitat. This suggests a wider geographic range of the ancestors of either of these species in the late Middle Pleistocene.

The absence of such shark and stingray remains in Ngandong suggests that these species did not ascend the Solo this far inland. However, it is very well possible that occasional shark teeth in the Ngandong terrace deposits have remained unnoticed or undocumented. Note in this respect that Dubois found 16 *G. gangeticus* teeth as well as two *U. polylepis* stingrays in Trinil. Later, Selenka discovered another 12 shark teeth in Trinil (Joordens et al., 2009). Their exact stratigraphic provenance is unknown. It is possible that these species occurred naturally in the Trinil area at certain times, but it is also possible that all or some of these specimens were actually brought to the site by *Homo erectus* for use as tools (Gilson et al., 2021; Joordens et al., 2015).

Another faunal difference between the assemblages is the richness of river-related reptiles in the Madura Strait assemblage and their scarcity in the assemblage from Ngandong. Von Koenigswald (1933) noted rare remains of *Crocodylus siamensis* among the fossils from Ngandong, but none of *Gavialis bengawanicus*. He also briefly mentioned the occurrence of turtle shell fragments, including 'rare Trionychidae'. The Madura Strait assemblage is extremely rich in turtle shell fragments, moreover, it contains teeth and osteoderms of *Crocodylus siamensis* and *Gavialis bengawanicus* and vertebrae of *Varanus salvatori* and Pythonidae. Just as we noted for sharks and stingrays, the abundance of river-related reptiles in the Madura Strait assemblage must be related to lowland conditions, with a wide and slowly moving river. The species diversity among the fresh water turtles from the Madura Strait is unique compared to other regional Pleistocene sites and is similar to the turtle community in Southeast Asian lowland rivers that have not been affected by environmental degradation.

When it comes to large terrestrial herbivores, there are important similarities between the assemblages from Ngandong and the Madura Strait. Both assemblages are dominated by the large bovids *Bos palaeosondaicus* and *Bubalus palaeokerabau*. In the Madura Strait assemblage, we noted a reduced body size of *B. palaeosondaicus* compared to the older assemblages of Trinil and Kedung Brubus. Whether this reflects a late Middle Pleistocene evolutionary trend towards reduced body size or dispersal of new bovid groups across Sundaland is unknown. Unfortunately, me- tric data of *B. palaeosondaicus* remains from Ngandong are not available. The presence of *Epileptobos groeneveldtii* in the Madura Strait assemblage is interesting, as this species is absent in Ngandong and was thus far regarded to have gone extinct in the course of the Middle Pleistocene. It may reflect a slightly older age of the Madura Strait assemblage, or an enduring presence of *E. groeneveldtii* on the lowland plains of Sundaland in the late Middle Pleistocene.

Also with respect to proboscideans, the Ngandong and Madura Strait assemblages appear to be similar. *Stegodon trigonocephalus* is the most common proboscidean species on both sites. We also noted a metric similarity of the dentition of this species from both sites, pointing to the same subspecies: *S. trigonocephalus ngandongensis.* The genus *Elephas* is also part of both assemblages, although the genus appears to be rare in Ngandong. Von Koenigswald (1933) mentioned only one incomplete cheek tooth from Ngandong and Rizal et al. (2020) reported two additional *Elephas* tooth fragments from the original fossil assemblage. In the Madura Strait assemblage, the genus is represented by a much larger number of tooth fragments. This different abundance of *Elephas* remains probably reflects a difference in geographic distribution, but it is difficult to say whether this can be explained by a preference of *Elephas* for the lowland plains. Note that *Stegodon* and *Elephas* must have been competing for grassy resources and probably avoided habitat overlap (Puspaningrum et al., 2020). The fact that the two proboscidean taxa are both well-represented in the Madura Strait assemblage may relate to migration of herds of proboscideans from different grazing areas to the river during dry seasons, or it may reflect time-averaging of the assemblage. The late Middle Pleistocene *Elephas* of the Madura Strait has, on average, more slender and high-crowned cheek teeth than the Middle Pleistocene *E. hysudrindicus* from Trinil and Kedung Brubus. Whether this also accounts for the scarce *Elephas* teeth from Ngandong is unknown. Metrically, the teeth from the Madura Strait are similar to the extant *E. maximus*. It is gen-

erally thought that the dispersal of *E. maximus* from the Asian mainland to the Sundaland area occurred in the Late Pleistocene, with a find near Cipeundeuy (West-Java) as the oldest known occurrence on Java, bracketed by radiocarbon ages of 35.5 ka and 29.6 ka (Van Den Bergh, 1999; Dam, 1994). The taxonomical significance of the high-crowned *Elephas* molars of the Madura Strait is unknown. It may for example reflect a late Middle Pleistocene evolutionary trend within *Elephas hysudrindicus* towards greater hypsodonty, or an early dispersal wave of *Elephas maximus* across the plains of Sundaland. Taxonomical interpretation can only be based on metric analyses of intact skulls, which are not available among the assemblages from Ngandong and the Madura Strait. To avoid confusion about species identifications, we referred to the material from the Madura Strait as *Elephas* sp.

In general, we may conclude that the large bovid and proboscidean taxa that dominated the hills of Middle Pleistocene Java also dispersed over the emerging plains during sea-level lowstands, at least during MIS6. The same accounts for other large species such as *Rhinoceros sondaicus*, *Hexaprotodon sivajavanicus*, all of which are part of the fossil assemblages of Ngandong and the Madura Strait. However, there are some interesting differences among the smaller terrestrial species, which probably have biogeographic significance. One of these relates to the small bovid *Duboisia santeng.* This species is represented in the Madura Strait assemblage by a horn core, a mandible, an isolated molar, and several astragali. The species is commonly regarded as endemic to Java, with a small body size that reflects insular isolation (Rozzi et al., 2013). Its fossil remains are abundant in the older faunal assemblages from Trinil and Kedung Brubus, but absent in Ngandong, which has thus far been regarded as evidence of its extinction in the course of the Middle Pleistocene. The occurrence of this species in the Madura Strait assemblage is surprising and points to an enduring presence of *D. santeng* during the late Middle Pleistocene. Moreover, it shows that the species dispersed over the exposed Sundaland plains during lowstands, which seems to contradict its assumed prolonged isolation. The occurrence of *D. santeng* on the lowland plains of Sundaland also sheds a new light over possible fossil finds of this species in Thailand (Nishioka and Vidthayanon, 2018) and mainland Malaysia (Hooijer, 1962b).

Another interesting difference between the assemblages from Ngandong and the Madura Strait relates to the genus *Axis.* The small-bodied *Axis lydekkeri* is a common species in the older faunal assemblages from Trinil and Kedung Brubus, but there is confusion over its presence in the assemblage from Ngandong. Note in this respect the differences between the faunal descriptions of De Vos et al. (1982), Van den Bergh et al. (2001), and Gruwier et al. (2015). In his original descriptions, Von Koenigswald (1933) noted an absence of *Axis lydekkeri* in the assemblage from Ngandong, and the presence of a new, medium-sized species, which he named *Axis javanicus.* The taxonomic confusion partly relates to the fact that later authors did not regard *Axis javanicus* as a valid species. However, Gruwier et al. (2015) confirmed the validity of the species by a comparative study of molars. Interestingly, both *A. lydekkeri* and *A. javanicus* are common in the Madura Strait assemblage. For *A. lydekkeri* this implies a continued presence up to the latest Middle Pleistocene and dispersal over the exposed Sundaland plains. The species is probably ancestral to the extant *Axis kuhli*, a species only found on the small island of Bawean in the Java Sea. In this respect, the dispersal and survival of herds of *A. lydekkeri* on the lowland plains of Sundaland is not surprising. The presence of *Axis javanicus* in the Madura Strait assemblage confirms the age overlap with the Ngandong Fauna. According to Gruwier et al. (2015), the species is related to the extant *A. axis* of the Indian mainland. Its presence in the fossil assemblages of Ngandong and the Madura Strait reflects a period of great geographic dispersal of this medium-sized *Axis* species over Sundaland during the lowstand of MIS6.

The large-statured *Rusa* sp. is common in the assemblages from Ngandong and the Madura Strait. In the Madura Strait assemblage, we found particularly large sizes of postcranial elements. Whether this also accounts for the fossil remains from Ngandong is unknown. There is uncertainty over the ancestral relation between the Middle Pleistocene *Rusa* sp. and the two extant species *Rusa timorensis* of Java and *Rusa unicolor* of Sumatra. Gruwier et al. (2015) noted that the fossil molars from Java are metrically similar to the extant *R. timorensis.* However, the postcranial remains from the Madura Strait fall in the size range of the larger *R. unicolor.* The implications of this finding with respect to evolutionary lineages and dispersal of *Rusa* deer over Sundaland are unknown.

Also among the predators, there are some noteworthy differences between the assemblages from Ngandong and the Madura Strait. The Madura Strait assemblage is extremely poor in mammalian carnivores, with only one specimen attributed to *Panthera pardus.* The Ngandong assemblage is richer in carnivore remains, which have been ascribed to three species: *Megacyon merriami*, *Panthera pardus* and *Panthera tigris* (Volmer et al., 2016). Especially *P. tigris* is well-represented in this fossil assemblage, by a complete skull, diverse skull fragments, isolated teeth, and several postcranial elements (Brongersma, 1935; Von Koenigswald, 1933). Surely, the greater abundance of carnivore remains partly relates to a larger sample size (the original Ngandong assemblage consisted of around 25,000 fossil specimens), but also in relative terms, the difference in representation of carnivores is remarkable. A possible explanation for the scarcity of carnivore remains in the Madura Strait might be that the death assemblage relates to stages of drought. Ferreira and Viljoen (2022) noted that in such assemblages, carnivore remains may be scarce, as these species have high survival rates under drought conditions, profiting from an abundance of weakened herbivores.

The scarcity of carnivore fossils within the Madura Strait assemblage may also be an actual reflection of the ancient faunal community. There may for example be a relation with the presence of the predatory reptile *Varanus komodoensis* in the Madura Strait assemblage. In its current territories, such as the island of Flores, this species is the only large predator of the terrestrial food chain, but on Middle Pleistocene Sundaland there must have been a niche overlap with felid and canid carnivores. Possibly, the predator community of the upland region was dominated by carnivores, whereas *V. komodoensis* was dominant on the lowland plains. In this respect, it is interesting that Volmer et al. (2016) and Hertler and Volmer (2008) noted a sharply increased body mass of the tigers from Ngandong compared to earlier tigers from Java. The authors related this to niche overlap and 'unusually intense competition among carnivores'. Possibly, this was not (only) an inter-carnivore competition, but also a competition between tigers and Komodo dragons. Unfortunately, the limited availability of fossil material from carnivores and Komodo dragons makes it impossible to draw detailed conclusions on this subject.

Finally, the presence of *Homo erectus* in Madura Strait assemblage has interesting implications for hominin dispersal over Sundaland in the late Middle Pleistocene (Berghuis et al., 2025d).

4.5 Climate, vegetation and biogeography

The Middle Pleistocene of Java is characterized by a climate of long and intense dry seasons and a grass-dominated vegetation (Sémah et al., 2010). This probably accounted also for the greater Sundaland region, especially during glacial stages (Dennell, 2009). A pollen study of a lacustrine core in West-Java revealed exceptionally dry conditions during the latest Middle Pleistocene (Van der Kaars and Dam, 1995).

We have no direct data on the climate or vegetation of the exposed Madura Strait shelf area during the late Middle Pleistocene lowstand of MIS6. However, analogous to the current situation, in which eastern Java is significantly dryer than western Java, climate conditions in this part of the Sundaland region may have been particularly dry. The herbivore-dominated assemblage of the Madura Strait indeed suggests open vegetation conditions. Possibly, remnant forests or swamp forests remained along the course of the perennial rivers. In Berghuis et al. (2024a) we showed that the late Middle Pleistocene Madura Strait Shelf had two of such large rivers: the Solo and the Brantas. During the long dry seasons, the swampy riversides may have attracted herds of herbivores from the surrounding plains.

Compared to the lowland plains, the volcanic highland of present-day Java probably had a higher precipitation rate and slightly cooler conditions. There is evidence that patches of remnant forests remained on the hills of Java throughout the Middle Pleistocene (Morley et al., 2020; Sémah and Sémah, 2012; Polhaupessy, 1990). Clear evidence for anthropic impact and clearance of the forest does not occur until late in the Holocene, after the rise of the ancient kingdoms on Java at the end of 1st millennium A.D.

The history of landscape change in Java over the last 2.5 million years appears to have been highly complex and may be described as a repeated expansion and fragmentation of the rain forest. The extent of rain forest throughout the Holocene appears to have been quite sensitive to small perturbations, making it somewhat difficult to reconstruct, especially for relatively ancient Holocene forest recessions. This distribution of climate and vegetation over Java and the surrounding Sundaland plains must have played an essential role in the geographic distribution of species. *Varanus komodoensis* may for example have preferred the hot and dry lowland plains. On the other hand, the occurrence of *Duboisia santeng* on the lowland plains is unexpected, as this species is thought to have preferred forests over grassland (Rozzi et al., 2013). Possibly, the species dispersed over lowland Sundaland through remnant forests along the main rivers, or through mangrove forests along the coast.

5. Conclusions

The Madura Strait assemblage provides a unique insight into the late Middle Pleistocene vertebrate fauna of the lowland plains of Sundaland. The fossils derive from the fill of a large paleovalley of the Solo River, the incision of which relates to the lowstand of MIS6. The lowland river was rich in fluvial reptiles, such as various turtle and crocodilian species. Herds of large herbivores roamed the surrounding plains, pointing to a grass-dominated vegetation. Among these were *Stegodon trigonocephalus* and *Elephas* sp., as well as the bovids *Bubalus palaeokerabau, Bos palaeosondaiucus* and *Epileptobos groeneveldtii.* Other species, such as the smaller bovid *Duboisia santeng*, *Rhinoceros sondaicus* and *Macaca* sp. point to the presence of patches of forest or open woodland, possibly along the river course. Among the predators of the lowland plains was *Varanus komodoensis*. The only carnivore of the assemblage is *Panthera pardus*. The nearby estuary was rich in sharks and stingrays, some of which also ascended the lowland river.

The terrestrial species composition is highly similar to the contemporary Ngandong Fauna of Java, and differs markedly from the slightly younger Punung Fauna, which represents a more humid, forested habitat. The Ngandong assemblage derives from an upstream terrace of the Solo River and therefore forms an upland equivalent of the Madura Strait assemblage. As may be expected, the lowland fauna of the Madura Strait is richer in fluvial reptiles and estuarine fish than the Ngandong assemblage. Among the terrestrial herbivores, the presence of *Duboisia santeng,*

Epileptobos groeneveldtii and *Axis lydekkeri* in the lowland fauna of the Madura Strait is interesting. These species are absent in the Ngandong assemblage and were thus far regarded to have gone extinct on Java in the second half of the Middle Pleistocene. Their occurrence in the Madura Strait assemblage shows that the species persisted on the lowland plains, up to the latest Middle Pleistocene. Another interesting difference with the Ngandong assemblage is the scarcity of carnivores in the lowland fauna of the Madura Strait and the absence of *Panthera tigris*. A possibility is that in the lowland plains, the tigers were outcompeted by *Varanus komodoensis*.

The Madura Strait assemblage is among the richest Pleistocene vertebrate assemblages of the region. It contains several species thus far unrecorded for the Pleistocene of Java or Indonesia. Moreover, it contains rare specimens, thus far not available in Indonesian museum collections. Our morphometric analyses provided valuable new insights into species-specific morphological features and size ranges. For example, the *Elephas* sp. cheekteeth of the Madura Strait are relatively slender and high-crowned compared to the cheekteeth of the Middle Pleistocene *Elephas hysudrindicus* from Java. And the common bovid *Bos palaeosondaicus* is on the average slightly smaller-statured than its Middle Pleistocene relatives from Java. In both cases, these metric differences may represent a regional evolutionary trend or geographical variation. Our metric analysis of cervid postcranial bones made it possible to demonstrate the presence of the intermediate-sized species *Axis javanicus,* a species thus far only known from dentition or antlers. The species probably relates to the *Axis axis* of India, and its presence in the assemblages from the Madura Strait and Ngandong probably represents a short dispersal wave over Sundaland during the late Middle Pleistocene.

In general, the results of our taxonomical analyses underline the importance of studying complete fossil assemblages (rather than 'cherry-picking') and building up local reference collections from various Pleistocene sites in the region. Such 'complete-assemblage' studies can be carried out for newly excavated material. Also, an inquiry of thus far undescribed fossil material from previous excavations, abundantly available in Indonesian museums, is highly promising.



Sorting a random subsample of fragmented fossils from the Madura Strait site, preliminary analyses in Surabaya, August 2015. Picture by Odile van den Heuvel.



Chapter 8

The taphonomy of the Madura Strait fossil assemblage, a record of selective hunting and marrow processing by late Middle Pleistocene Sundaland hominins

CHAPTER 8

The taphonomy of the Madura Strait fossil assemblage, a record of selective hunting and marrow processing by late Middle Pleistocene Sundaland hominins

H.W.K. Berghuis, Thijs Van Kolfschoten, Unggul Prasetyo Wibowo, Iwan Kurniawan, Shinatria Adhityatama, Indra Sutisna, Eduard Pop, A. Veldkamp, Josephine C.A. Joordens

Published in: *Quaternary Environments and Humans* (2025)

Abstract

The Madura Strait assemblage is the first vertebrate faunal record of submerged Sundaland. The material derives from an ancient valley of the Solo River, which was cut during the lowstand of MIS6. The geological background of the site and the taxonomy of the fossils have been described in previous publications. However, the significance of the assemblage within the Pleistocene biogeography of Southeast Asia can only be understood if we have insight into its accumulation history and homogeneity, and into the representativeness of the OSL-dated sediment for the fossils it contains. Moreover, the presence of hominin fossils raises questions on hominin subsistence strategies, which may have left traces in the fossil record. Over the past decades, similar questions have successfully been addressed by systematic taphonomic studies of fossil assemblages, notably from Africa and Europe. However, such studies are rare in Southeast Asia. Moreover, taphonomic studies of assemblages from subsea sites lag behind. Here we describe the results of a systematic taphonomic study of the Madura Strait assemblage. The fossils of terrestrial species form a homogenous assemblage, representing a steady supply of skeletal elements to the river, presumably during yearly flooding stages. OSL-dated fluvial sandstone samples point to a most likely age range of 146-131 ka. The material has been subject to fluvial size-sorting, but the absence of significant rounding points to short transportation distances and a local provenance. The skeletal remains accumulated in the fluvial valley fill or became concentrated in an overlying marine lag, as a result of tidal scour during the subsequent transition to estuarine conditions. Fossils of estuarine species derive from the estuarine sediment overlying this basal marine lag and are linked to peak-highstand conditions around MIS5e (~123 ka). The bone remains of terrestrial species have been subject to two fracturing stages: a green-state fracturing stage prior to fluvial uptake and a sub-fossil-state fracturing stage during later marine reworking. Extensive green-state fragmentation of ruminant limb bones points to hominin bone battering and marrow processing. The age-at-death frequency distribution of bovids is indicative of selective hunting of prime adult prey. Cut marks on turtle bones show that hominins also fed on these aquatic species.

1. Introduction

Since the classic taphonomic publications of the late 20th century (Lyman, 1994; Behrensmeyer, 1984; Binford, 1981) and the 'hunting or scavenging' discussions of the eastern African hominin sites (Domínguez-Rodrigo et al., 2021; Egeland et al., 2007; Domínguez-Rodrigo, 2002; Blumenschine, 1995, 1986; Selvaggio, 1998; Bunn et al., 1986), systematic taphonomic studies have become an essential part of zoo-archeological research (Sala et al., 2024; Wang et al., 2022; Stewart et al., 2020; Fourvel et al., 2018). This research has strongly improved our understanding of past ecosystems and the role of hominin populations therein. Remarkably, systematic taphonomic studies have never been carried out for the assemblages from Java.

Another area where taphonomic research lags behind is submarine zoo-archeology (Louys, 2018). Flooded continental shelfs may contain valuable faunal and archaeological records of past terrestrial vertebrate faunas (Bailey and Cawthra, 2023; Flemming, 2021; Kolfschoten and Laban, 1995). Shelfs that have been subject to subsidence may even preserve a stacking of buried landscapes, representing subsequent Pleistocene sea-level cycles, potentially holding multiple faunal or archaeological records (Hijma et al., 2012). However, despite the relevance of these submerged landscapes, systematic taphonomic studies of fossil assemblages from subsea sites are rare (Smith and Smith, 2003). This is a missed opportunity: submarine sites are difficult to access and their detailed stratigraphic and sedimentary background can often not be studied by direct observations, which leaves taphonomy as an important tool for studying past ecological and geographical conditions.

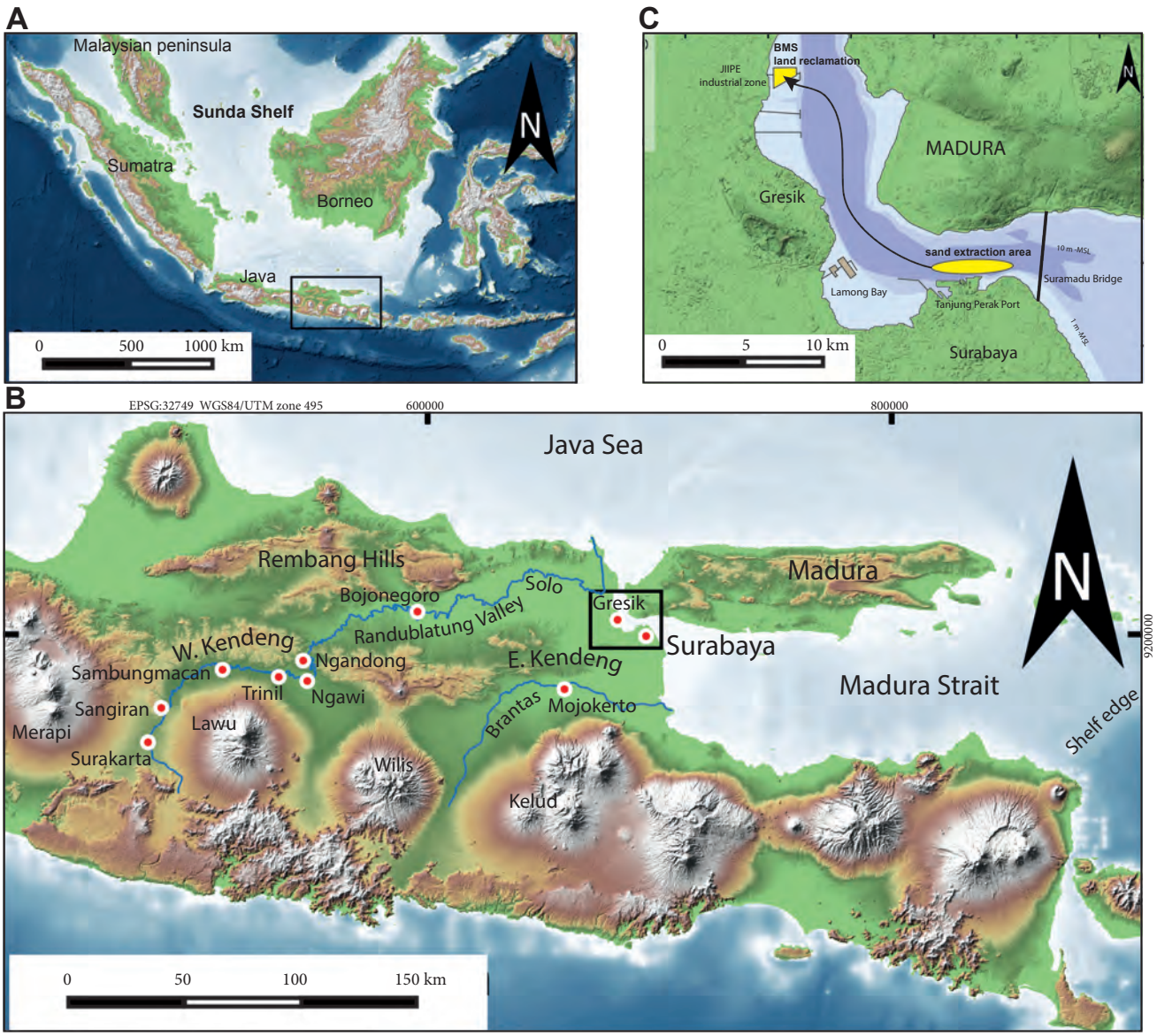


Fig. 1. A: The Sunda Shelf of Southeast Asia, with the Indonesian archipelago. Box indicates the position of map B. **B:** Eastern Java, the Madura Strait, Surabaya, the Solo River, and other sites mentioned in the text. Box indicates the position of map C. **C:** The Madura Strait north of Surabaya, with the sand extraction area and the location of the BMS land-reclamation. Map data: GEBCO and ALOS.

The Sunda Shelf **(Fig. 1A)** is the world's largest shelf sea. During the Pleistocene, the shelf was intermittently exposed, forming a wide continental area known as Sundaland (van Bemmelen, 1949), connecting the current islands of western Indonesia with the Asian mainland. This regime of intermittent shelf-exposure played an important role in the regional evolution and dispersal of vertebrate species (Louys and Meijaard, 2010; Van den Bergh et al., 2001), which included *Homo erectus* and, from the Late Pleistocene onward, *Homo sapiens* (Louys and Kealy, 2024; Husson et al., 2022; Antón, 2003).

Early and Middle Pleistocene vertebrate and archaeological records from this region are primarily known from Java (Indonesia). Localities as Sangiran, Trinil, Mojokerto and Ngandong yielded rich fossil assemblages (Von Koenigswald, 1935, 1933; Oppenoorth, 1932; Selenka and Blanckenhorn, 1911b; Dubois, 1908, 1907), which reflect a long and complex history of local evolution and regional dispersal of species (Van Den Bergh, 1999; De Vos et al., 1982). *Homo erectus* presence on Java probably goes back to at least 1.3 Ma (Matsu'ura et al., 2020). The skulls from Ngandong, dated to 140-92 ka (Rizal et al., 2020) are the youngest known fossil remains assigned to this hominin species.

The Sunda Shelf is a subsiding shelf (Husson et al., 2020; Sarr et al., 2019) with a great and thus far unexplored potential for faunal and archaeological records (Adhityatama and Yarista, 2019). Recently, a large vertebrate fossil assemblage was dredged from the Madura Strait, the sea strait between Java and Madura, along the southeastern margin of the Sunda Shelf **(Fig. 1B)**. It consists of 6,372 specimens and is the first faunal record from submerged Sundaland, consisting of estuarine fishes, river-related reptiles and terrestrial, mostly mammalian species (Berghuis et al., 2025b), which include ancient hominins (Berghuis et al., 2025d). The material derives from the sandstone fill of a lowstand valley of the Solo River, which was excavated during a submarine sand-extraction work and used for the reclamation of an artificial island in the port area of Surabaya. Two samples of the fluvial sandstones in which the fossils were embedded were OSL-dated to 162±31 and 119±27 ka (Berghuis et al., 2025a).

The Madura Strait assemblage offers an unprecedented insight into the vertebrate fauna of late Middle Pleistocene Sundaland. The geological background of the fossil-bearing strata is well-understood, thanks to a wealth of deep-drilling data from construction works in the adjacent port of Surabaya (Berghuis et al., 2025a). Nevertheless, several important questions have remained unaddressed. For example, has there been extensive hydraulic transport? How did the skeletal remains from terrestrial vertebrates become mixed with the remains of fluvial and estuarine vertebrates? Does the assemblage represent a single accumulation event or a longer period of accumulation? Are the OSL-ages of the sediment representative for the fossils it contains? These questions, which relate to the accumulation history and homogeneity of the assemblage, cannot be addressed by direct geological observations of the submarine excavation site. However, a systematic taphonomic study, in combination with the available geological data, may offer important new insights. Besides these accumulation-related aspects, a systematic taphonomic study may also provide relevant insights into the past ecosystem, and into the role that hominins played in this ecosystem.

This study, therefore, aims for a detailed reconstruction of the taphonomic pathways that the Madura Strait vertebrate fossils have been through, from mortality and disarticulation to accumulation, preservation and sampling. More specifically, the study aims to address three main research questions:

1. What is the history of accumulation, ecological mixing and sampling of the fossil remains and to what extent are the OSL-ages of the sediment representative of the ages of the fossil remains?

2. To what extent does the assemblage represent living populations and what does it tell us of past ecosystems and landscapes?

3. Can we find indications of hominin behavior, such as foraging and food processing behavior?

2. Geological background of the site and fossil excavation

At the sandstone extraction site, the Madura Strait has a depth of ca. 20 m. The seabed is made up of firm, massive marine clays of Pliocene to Early Pleistocene age. North of the Surabaya port area, a submerged valley of the Solo can be traced over the seabed for several kilometres. It was cut into the clayey subsoil, down to a depth of ca. 50 m –MSL (= local mean sea level) and has a fill of fluvial sandstones with lenses of fine conglomerate, which change upwards into marine clay-sand alternations with fine shell debris **(Fig. 2)**. For more geological details, reference is made to Berghuis et al. (2025a).

In 2014-2015, sand was extracted from the valley fill by submarine dredging and used for the reclamation of an artificial island in the Gresik, in the Surabaya port area **(Fig. 1C)**. The work was commissioned by Berlian Manyar Sejahtera (BMS), a local port company, which today operates the reclamation site for port logistics. For the sand extraction, use was made of a trailing suction hopper dredger, a vessel that collects bottom sediment by dragging a suction pipe over the seabed. The suction pipe was mounted with a drag head, penetrating and loosening the sandstones and mixing the loosened material with water. The loosened and water-saturated material was sucked up and stored in the ves-

sel's hopper. A 30/30 cm grid at the dredge head prevented the uptake of larger fragments. When fully loaded, the vessel sailed to the land reclamation site, where it was connected to a floating pipeline for discharge. Dredging was carried out in east-west trails and proceeded down to a depth of 32 m –MSL. A projection of the dredging profile is shown in the geological cross-section **(Fig. 2)**, indicating that most of the extracted sand derives from the upper part of the fill, which consists of estuarine sandstones and claystones. Sand extraction only penetrated several meters into the underlying fluvial strata.

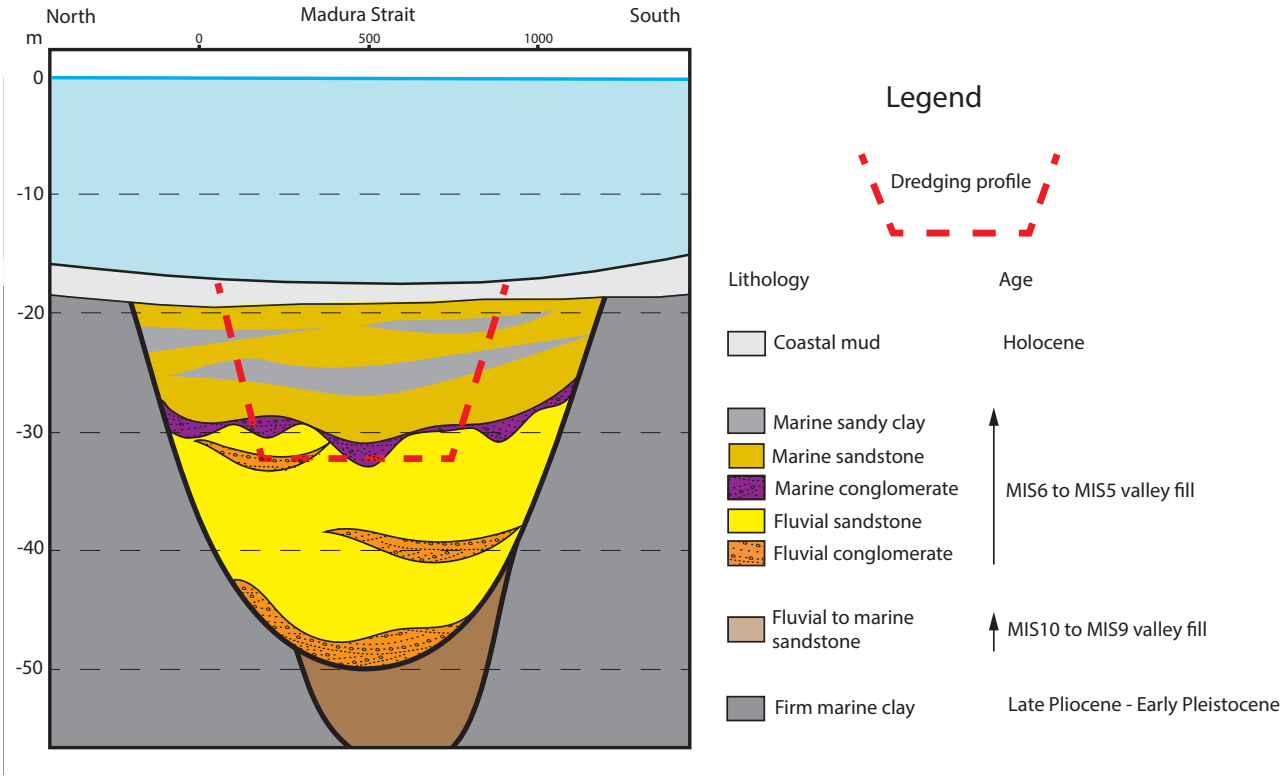


Fig. 2. Schematic cross-section of the Madura Strait paleovalley north of Surabaya. Based on deep drilling data of the Suramadu Bridge. For details, see Berghuis et al. (2025a).

The reclamation material of the BMS-island is a poorly sorted mixture of sand, shell fragments and dispersed fine gravel. Fossils were mostly found as isolated specimens on the surface. The more than 100 ha wide reclamation area was meticulously searched on hands and knees (by H.B.), collecting vertebrate remains visible to the naked eye. Sediment sieving or trenching was not carried out.

Of interest is the occurrence of sediment blocks at the reclamation site, which passed the dredging process intact, and which provide a semi-direct insight into the sedimentological background of the site and into the distribution of fossils in their original sedimentological context. The blocks have a maximum size of ca. 30/30 cm, which relates to the grid on the dredge head. In Berghuis et al. (2025a) we subdivided these sediment blocks into five genetically significant facies **(Fig. 3)**. The original stratigraphic position of these facies could be reconstructed through a comparison with the deep-drilling-based cross-section over the excavation site **(Fig. 2)**. The two fluvial facies represent the basal part of the valley fill. The marine sandstones and claystones represent the estuarine top of the valley fill and mark the drowning of the valley, during peak highstand-conditions. The marine conglomerates derive from a ca. 1 m thick bed at the boundary between fluvial and estuarine parts of the valley fill. In Berghuis et al. (2025a) we described the bed as a tidal lag deposit, mantling the transgressive surface. Vertebrate fossils were found to be associated with fluvial sandstones and conglomerates and with the marine conglomerate.

OSL-ages are available from two samples of the excavated fluvial sandstones. One sample was taken from a block of uncrushed fluvial sandstone found on the reclamation site. Another sample was taken from the fluvial sandstone fill of the neural canal of a cervid vertebra found on the reclamation site. The found OSL-ages, of 162±31 and 119±27 ka, suggest that fluvial backfilling relates to the lowstand of MIS6 and the subsequent transgression in the run-up to MIS5. Valley incision probably relates to the preceding stage of falling sea-level, prior to peak lowstand conditions of MIS6 (Berghuis et al., 2025a). The change from fluvial to estuarine strata shows that, in the course of the transgression, the valley was invaded by the sea. A marine sandstone sample from the reclamation site, which was expected to be representative of this estuarine top of the valley fill, was OSL-dated to ≥462±71 ka. This old and unexpected OSL-age suggests that the sample derives from a block of older sediment, which was hit upon by the dredger, or which had become reworked in the valley fill. It may for example originate from the marine sandstone top layer of the MIS10 valley fill that underlies the large MIS6 paleovalley **(Fig. 2)**.

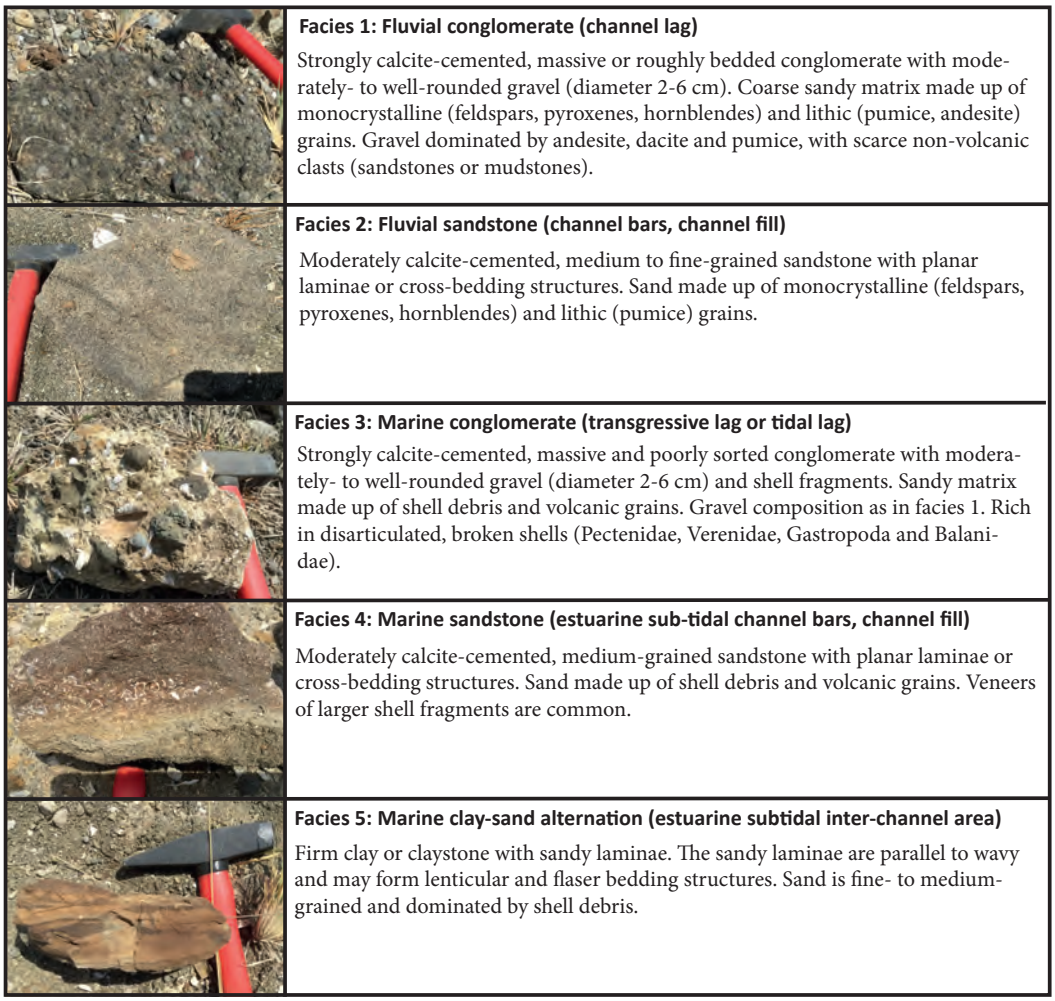


Fig. 3. The five facies of the extracted material, based on uncrushed sediment blocks on the BMS reclamation site (From: Berghuis et al., 2025a).

3. Methods

The quantification of taxa and skeletal elements, as well as the analysis of post- and perimortem bone modification, were carried out in the Geological Museum Bandung, which houses the assemblage. Whenever possible, we used published and commonly accepted procedures, classes and terminology, with references added. Quantifications have been expressed as NISP (number of identified specimens), MNI (minimum number of individuals) or MAU (minimum animal units), following the definitions of Binford (1981) and Lyman (1994).

Observations were made by the naked eye or by using a hand-held lens. Microscope or stereomicroscope analyses have, at this stage, not been conducted, as we aimed for the analysis of large numbers of specimens rather than a detailed inquiry of specific specimens.

Specimen sizes have been based on the measurement protocol provided by Von den Driesch (1976). Fragment sizes (mm) are the largest linear size of a specimen, measured in any direction. The size distribution analysis of the assemblage is based on a random subsample (N=500).

The weathering analysis follows the guidelines of Behrensmeyer (1978). The subdivision in 'weathering stages' has been based on an analysis of the cortical surface of long-bone shafts. Bone weathering rates differ among taxa, with the bones of smaller taxa being more susceptible to weathering. In our analysis, we only included bones of medium to large species. As weathering stages are indicative of surface exposure prior to fluvial uptake and deposition, we only included bone remains of terrestrial species. A difficulty is that the available shaft remains are strongly fragmented and that it is not always clear whether the fragments derive from a fluvial reptile or a terrestrial mammal. We randomly selected 100 shaft fragments from the assemblage, omitting material that has a reptilian morphology. We regard this as a representative sample of long-bone shaft fragments of medium to large terrestrial species. Note in this respect that among the entire assemblage, there is a dominance of skeletal remains of terrestrial mammals, whereas the remains of fluvial reptiles, other than turtle shells, are relatively scarce. Looking only at postcranial bone remains, excluding dentition, horns, antlers or turtle shell, the ratio between the number of identified specimens of fluvial and terrestrial species is ca. 1:10.

Fracturing, fragment types and fracture morphology have been analyzed for long-bone remains from medium to large ruminants, which in the Madura Strait assemblage are mostly Bovidae or Cervidae. The analyses have been based on the criteria of Johnson (1985) and Villa and Mahieu (1991), distinguishing between spiral fractures, straight transverse fractures, straight diagonal fractures, longitudinal fractures and jagged fractures. The analyses of cylindrical shaft fragments and epiphyseal fragments have been based on all available specimens within the assemblage. Cylindrical fragments have two fracture faces, which have been counted separately. For the analysis of non-cylindrical shaft fragments, we selected a random subsample (N=100). Following Villa and Mahieu (1991), only the proximal and distal sides of these non-cylindrical fragments were considered, thus giving two counts per specimen. Note that for these latter fragments, the assignment to ruminants has been based on cortical thickness, estimated shaft circumference and the presence of a well-developed medullar cavity. Undoubtedly, this sample is somewhat commingled with, for example, similar-sized hippopotamid or suid bone remains. However, referring to teeth and identified post-cranial remains, these taxa are much less common and it may confidently be assumed that they only form a minor part of the sample of the non-cylindrical shaft fragments.

The analysis of bone surface marks has been based on an inquiry of the entire assemblage, excluding the dental elements. The same applies for the analysis of marine bioerosion and encrustation.

A skeletal part analysis has been conducted for large Bovidae (Bovini) and Cervidae. For this purpose, the skeletal parts of individual species within these families have been lumped together. This is necessary, as not all skeletal parts were determined up to the same level of detail (Berghuis et al., 2025b). For example, bovid and cervid limb bones could often be identified to species or genus level based on metric analyses, but vertebrae were mostly assigned to Bovidea or Cervidae indet. Moreover, lumping skeletal parts in larger taxonomic groups creates more adequate sample sizes. Obviously, this obscures potential differences among the individual species in terms of biogeographic ranges, differential survivorship of skeletal parts or hunting / predation pressure. On the other hand, the composite samples are useful for exploring differential hydraulic transport of skeletal parts, or potential transport decisions of body parts by hominins.

An age-mortality profile could only be made for large bovids, as this is the taxon from which dental elements are available in sufficient numbers to allow for this analysis. Just as for the skeletal part frequency analysis, we lumped together all available dental remains of Bovini. This creates a larger sample and makes it possible to include deciduous dentition, which could only be identified to family level. This procedure provisionally assumes that the individual bovid species were subject to similar mortality and that the timing of teeth eruption and wear was similar among the species. Our analysis has been based on four mandibular dental elements: DP_4, M_1, M_2 and M_3. We focused on crown height, which forms the most practical and reliable basis for age estimates (Klein and Cruz-Uribe, 1983; Voorhies, 1969; Kurtén, 1953). Given crown heights (CH) represent the distance between the base of the enamel and the occlusal face, measured at the anterior lobe along the buccal face. For mandible fragments with molars in place, crown heights were estimated.

4. Results

4.1 Assemblage description

The Madura Strait assemblage consists of 6,372 specimens. It is dominated by small skeletal remains with linear sizes up to 80 mm **(Fig. 4)**. As the specimens were hand-picked from the reclamation site (Berghuis et al., 2025b), without sieving or microscope analyses, the lower size limit of the available specimens is around 5 mm. In the size classes above 80 mm, abundances quickly reduce. Maximum specimen size is ca. 20 cm. This is below the grid size of 30/30 cm as used on the dredging head during sand excavation, which indicates that the maximum specimen size is not a sampling bias caused by the dredging process.

	Nr	*%*
Total specimens	6372	100
Total identified (NISP)	1212	19.02
Total unidentified	5160	80.98

Table 1: The Madura Strait assemblage, total specimens and total identified specimens (NISP).

The fossils have been through strong diagenetic alteration. Bone remains have a dark brown to black colour and are heavily mineralized. The open spaces of cancellous bone are mostly filled with calcite. The fossils lack attached ferrous or calcareous concretions. The bone fragments from the Madura Strait subsea site have a smoothly polished surface, which, in combination with their mineralized state, gives the material a shiny appearance. All-sided polishing of a fossil bone is generally associated with smooth abrasion by fine, moving sediment particles in flowing water (Behrensmeyer, 1988; Shipman and Rose, 1988). Note, however, that this abrasion must have been modest. None of the specimens may be referred to as rounded and the bone contours are always sharp, with well-recognizable articulations and protuberances.

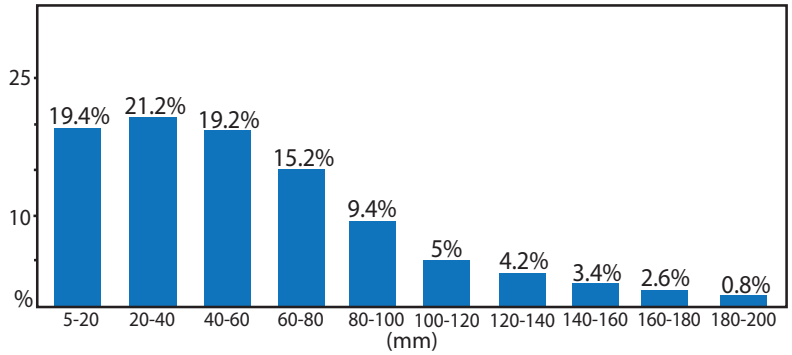


Fig. 4. Size distribution of the Madura Strait assemblage. Shown sizes (in mm) are the largest linear size of a specimen, measured in any direction. Analysis based on a random subsample (N=500) from the entire assemblage.

Order	*Family*	*Species*	*NISP*	*%*	*Community*
Carcharhiniformes	Hemigaleidae	*Hemipristis serra*	5	0.41	Estuarine
	Carcharhinidae	*Glyphis gangeticus*	51	4.21	Estuarine
		Carcharhinus cf. *leucas*	20	1.65	Estuarine
		Galeocerdo cuvier	3	0.25	Estuarine
Myliobatiformes	Myliobatidae	*Myliobatis* sp.	1	0.08	Estuarine
		Rhinoptera javanica	3	0.25	Estuarine
	Dasyatidae	*Urogymnus polylepis*	3	0.25	Estuarine
Batoidea *	Indet.		18	1.49	Estuarine
Siluriformes	Bagridae	*Hemibagrus* sp.	1	0.08	Estuarine
Squamata	Varanidae	*Varanus komodoensis*	2	0.17	Terrestrial
		Varanus salvator	2	0.17	Fluvial
	Pythonidae	indet.	1	0.08	Fluvial
Testudines	Geoemydidae	Geoemydidae indet.	102	8.42	Fluvial
		Batagur affinis	1	0.08	Fluvial
		Orlitia borneensis	1	0.08	Fluvial
	Tryonychidae	*Chitra chitra*	29	2.39	Fluvial
		Pelochelys cantorii	7	0.58	Fluvial
		Amyda cartilaginea	5	0.41	Fluvial
		Dogania subplana	6	0.50	Fluvial
	indet.		24	1.98	Fluvial
Crocodilia	Crocodylidae	*Crocodylus siamensis*	24	1.98	Fluvial
	Gavialidae	*Gavialis bengawanicus*	4	0.33	Fluvial
	indet.		4	0.33	Fluvial
Proboscidea	Stegodontidae	*Stegodon trigonocephalus*	31	2.56	Terrestrial
	Elephantidae	*Elephas* sp.	15	1.24	Terrestrial
	indet.		54	4.46	Terrestrial
Primates	Hominidae	*Homo erectus*	2	0.17	Terrestrial
	Cercopithecidae	*Macaca* sp.	1	0.08	Terrestrial
Carnivora	Felidae	*Panthera pardus*	1	0.08	Terrestrial
Perissodactyla	Rhinocerotidae	*Rhinoceros sondaicus*	27	2.23	Terrestrial
Artiodactyla	Hippopotamidae	*Hexaprotodon sivajavanicus*	30	2.48	Fluvial
	Suidae	*Sus brachygnathus*	14	1.16	Terrestrial
		Sus cf. *macrognathus*	2	0.17	Terrestrial
	Cervidae	*Axis lydekkeri*	36	2.97	Terrestrial
		Axis javanicus	17	1.40	Terrestrial
		Axis sp.	241	19.88	Terrestrial
		Rusa sp.	95	7.84	Terrestrial
	Bovidae	*Bubalus palaeokerabau*	101	8.33	Terrestrial
		Bos palaeosondaicus	129	10.64	Terrestrial
		Epileptobos groeneveldtii	4	0.33	Terrestrial
		Bovini indet.	88	7.26	Terrestrial
		Duboisia santeng	7	0.58	Terrestrial
Total			1212	100	

Table 2. Vertebrate taxonomy Madura Strait assemblage, from: Berghuis et al., 2025b. Percentages are rounded to two decimal places.
*: = Superorder. The specimens are possibly Myliobatiformes. Note: the allocation to vertebrate communities is slightly arbitrary (see text).

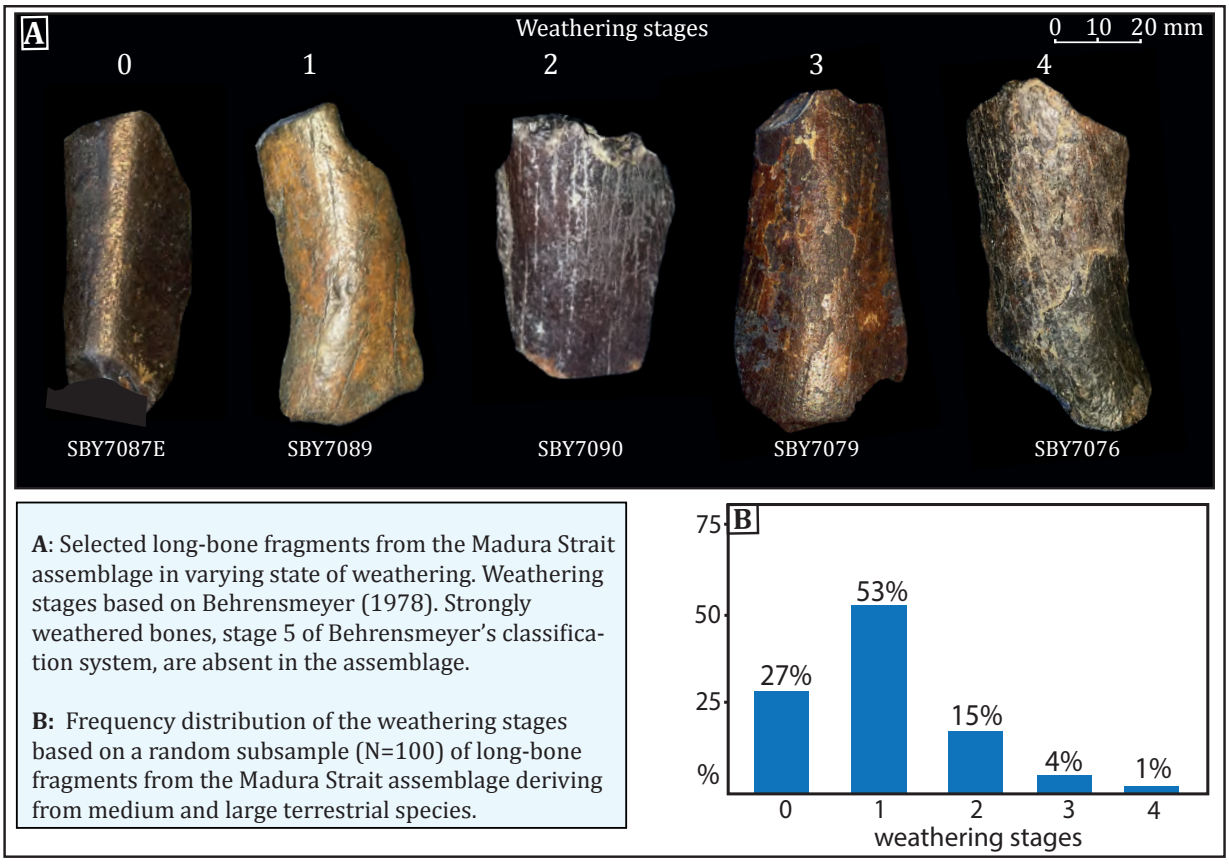
Only around 4% of the specimens is more or less intact. These are mostly dental elements or small and robust post-cranial bones such as vertebrae, carpalia, tarsalia or phalanges. The other 96% of the assemblage consists of fragmented skeletal material, mostly with multiple break surfaces. Approximately 19% of the specimens could be identified to skeletal element and taxon, mostly to species or genus level **(Table 1)**.

A total of 36 vertebrate species was recognized, divided over 11 orders **(Table 2)**. One of the conspicuous characteristics of the assemblage is its ecological mixture. In Berghuis et al. (2025b), we subdivided the species into three vertebrate communities: estuarine, fluvial and terrestrial. The allocation of species to these vertebrate communities is, in some cases, slightly arbitrary. Estuarine fish ascend rivers, whereas the fluvial reptiles also occur along the estuary. Likewise, terrestrial species come to the riverbank for water and food resources, while hippopotamids, added to the fluvial community, come on land at night for grazing.

4.2 Weathering

Weathering of bones gives an indication of their post-mortem surface exposure prior to burial. For the Madura Strait assemblage, this post-mortem weathering history varies between the species from different ecosystems. Skeletal remains from the estuarine community consist of shark and ray teeth and vertebrae of batoid fish. As may be expected from the aquatic living conditions, their fossil remains are always unweathered. Remains from the fluvial community consist of turtle shell fragments, crocodilian teeth and postcranial remains of fluvial reptiles and hippopotamids. The material is generally unweathered, although some specimens do bear traces of weathering. Such specimens may have become stranded on the riverbank, or they may derive from body parts that were taken ashore by predators (including hominins).

The analysed shaft fragments of medium to large terrestrial mammals are mostly unweathered or slightly weathered, most specimens falling in weathering stages 0 or 1 **(Fig. 5).** These are specimens with a smooth cortical surface or with few fine surface cracks. Ca. 20% of the specimens show more drying cracks and exfoliation of outer bone layers and fall in weathering stages 2, 3 and 4.



A: Selected long-bone fragments from the Madura Strait assemblage in varying state of weathering. Weathering stages based on Behrensmeyer (1978). Strongly weathered bones, stage 5 of Behrensmeyer's classification system, are absent in the assemblage.

B: Frequency distribution of the weathering stages based on a random subsample (N=100) of long-bone fragments from the Madura Strait assemblage deriving from medium and large terrestrial species.

Fig. 5. Weathering analysis of long-bone fragments of terrestrial species, Madura Strait assemblage. See **Section 3** (Methods) for sample selection procedure. Weathering stages based on Behrensmeyer, (1978).

4.3 Fracturing

The skeletal remains from the Madura Strait assemblage are highly fragmented. The vast majority of the fracture surfaces on the bone remains has the same dark colour and shiny, mineralized appearance as the bone's unbroken cortical surface, showing that breakage predates bone diagenesis. Recent fractures, related to the dredging process, are easily recognized by their light brown colour. Such recent fractures generally form minor damage only, such as broken tips or edges **(Fig. 6)**.

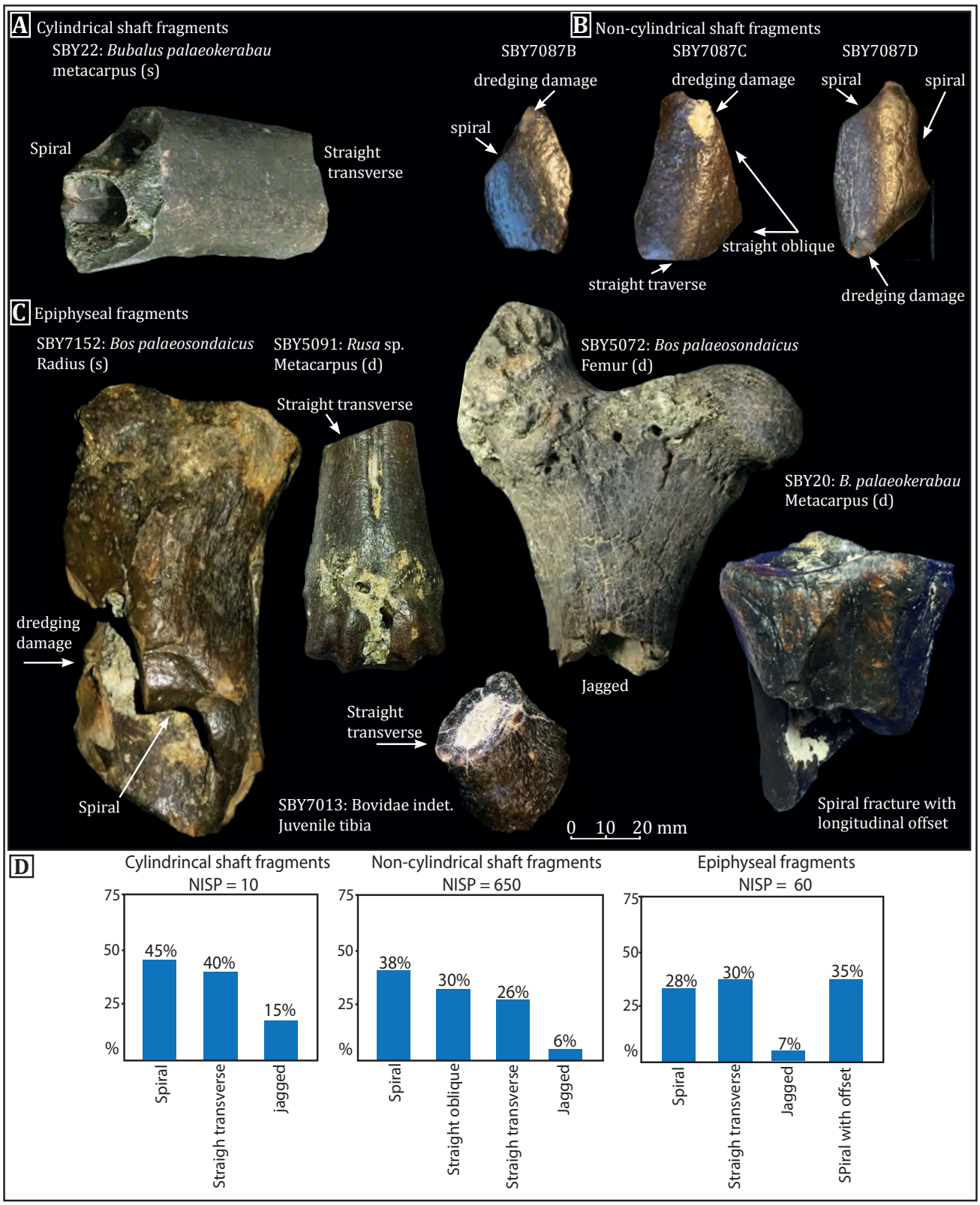


Fig. 6. Fracturing of long bones of medium to large ruminants, Madura Strait assemblage. **A-C:** Selected photographs of cylindrical shaft fragments, non-cylindrical shaft fragments and epiphyseal fragments. **D:** Fracture types for each of these fragment types. Fracture analyses based on all identified specimens (for cylindrical and epiphyseal fragments) and on random subsample of 100 specimens (for the non-cylindrical specimens).

Among the available long-bone fragments of medium to large ruminants, cylindrical shaft fragments are extremely scarce, only represented by 10 specimens, with preserved lengths of 3 to 14 cm. Epiphyseal fragments are much more common and represented by 60 specimens. These generally preserve a few centimeters of the adjacent shaft. Non-cylindrical shaft fragments are abundant, with a total of ~650 specimens. They generally preserve < 25% of the shaft diameter and are elongated in outline, with a common W/L-ratio of ~0.4.

We analyzed the fracture morphology based on the criteria of Johnson (1985) and Villa and Mahieu (1991), distinguishing between spiral fractures, straight transverse fractures, straight diagonal fractures, longitudinal fractures and jagged fractures **(Fig. 6)**. Spiral fractures have a concave or convex outline and cut through the shaft with an angle of ~45 degrees with the axis of the shaft. Straight transverse fractures cut perpendicularly through the shaft. Straight diagonal fractures cut through the shaft with an angle of < 45 degrees with the axis of the shaft. Zooming in on the fracture, spiral and diagonal fracture faces run obliquely from the cortical surface to the medullar cavity, forming an acute or obtuse angle with the cortical surface. Straight transverse fractures run straight to the medullar cavity and form a right angle with the cortical surface. Fracture surfaces are smooth for spiral and straight diagonal fractures, smooth and sharp for straight transverse fractures, and rough for jagged fractures.

Among the cylindrical fragments, there is a dominance of spiral and straight transverse fracture faces **(Fig. 6D)**. Jagged fracture faces are uncommon. Fragments may have different fracture morphologies at either side. For example, bovid metacarpal fragment SBY22 **(Fig. 6A)** has a spiral fracture at the distal side and a straight transverse fracture at the proximal side. Also, among the epiphyseal fragments, spiral and straight transverse fractures are most common. Jagged fractures, with small right-angle offsets along the fracture face, are scarce and only observed in strongly weathered specimens such as the proximal bovid femur SBY5072 **(Fig. 6C)**. A few specimens, such as the proximal bovid metacarpal SBY20 **(Fig. 6C)**, have an intermediate fracture morphology, consisting of a spiral face with a longitudinal offset. The smaller shaft fragments have multiple fracture faces. Among the non-cylindrical shaft fragments, there is a dominance of spiral and straight oblique fractures.

The dominance of spiral and diagonal fractures points to breakage in a fresh (green) state, while the bones were still moist, rich in collagen and contained marrow in the medullary cavity (Lyman, 1994; Villa and Mahieu, 1991; Johnson, 1985). The intermediate fractures, consisting of a spiral fracture face with a longitudinal offset, may be indicative of breakage after some drying had taken place, with a spiral fracture front hitting an incipient drying crack. However, it is also possible that breakage took place in a green state, with the longitudinal offset following the internal bone structure, as was noted specifically in metapodials by Blumenshine (1988). The rare occurrence of jagged fractures is in line with the low degree of weathering. Only rare, weathered bone elements may have stepped fracture faces, pointing to breakage of dry bone.

The frequent occurrence of straight transverse break surfaces does not comply with this model of fresh-bone breakage. Straight transverse fractures are sometimes associated with breakage of dry bone, but this is, in this case, not very likely, considering the fact that straight transverse breaks are observed in unweathered bone. They are, however, also common in bones that experienced incipient mineralization (Lyman, 1994; Johnson, 1985; Morlan, 1980). Note in this respect the sharp fracture face of SBY7013 **(Fig. 6)**, which resembles broken glass rather than broken bone tissue.

4.4 Bone surface marks

Gnawing and chewing marks

Traces of gnawing by carnivores or rodents are rare. Among the sample of ruminant cylindrical shaft fragments, carnivore-gnawed edges are absent. Small-scale gnawing marks are observed on ca. 5% of the limb-bone epiphyses, such as distal scapula SBY9 **(Fig. 7)**. There are only two examples of more intense gnawing in the assemblage, which is the distal bovid femur SBY31 **(Fig. 7)**, from which the epiphysis is gnawed off, with characteristic ragged edges along the distal margins (Jalvo and Andrews, 2016; Binford, 1981). Also the adjacent shaft of this specimen shows irregular scores. Several circular perforations resemble tooth punctures, but are recognized as *Gastrochaenolites* borings by their downward-increasing diameter **(Section 4.5)**.

The other bone fragment with intense gnawing traces is SBY7013 **(Fig. 7)**, a juvenile bovid tibia from which most of the distal end has been gnawed off. This specimen also has some poorly preserved, rather coarse marks at the adjacent shaft, which may be carnivore or crocodile tooth pits but may also be hominin chop marks or percussion pits. Among the hundreds of smaller shaft fragments, we found no evidence of significant gnawing.

Curved marks

SBY7075 is a small rib fragment of unknown taxonomical origin. It has three shallow striations with a curved outline and a similar orientation, roughly parallel to the bone axis, and a length of around 20 mm **(Fig. 7)**. Two scores have a width of ca. 1.5 mm, the third one (lowest on the picture) is slightly wider, but possibly consists of two superimposed scores. Curved striations are uncommon for human butchery or carnivore tooth dragging. However, they have been described from carcasses foraged by *Varanus komodoensis* (D'Amore and Blumenschine, 2009), crocodilians (Njau and Gilbert, 2016) and vultures (Fisher, 1995), all of which use repetitive, side-wards-directed strokes of the head when defleshing carcasses, which may produce curved marks.



Fig. 7. Surface marks on bone fragments. Madura Strait assemblage.

Linear marks

Linear marks have been found on three specimens. SBY5067 is a sinistral mandible fragment assigned to *Bos palaeosondaicus*, which has fine, parallel linear marks running obliquely over the medial surface below the M_2 **(Fig. 7)**. They have similar lengths of around 11 mm and a cross-sectional width of 1 mm. The marks have a V-shaped section, which is most clearly observed on the lowest mark on the mandible. Micromorphological details such as Hertzian cones or fine striations, within or directly beside the main cuts, are absent or not preserved. SBY517 is a sinistral scapula of a large turtle, with fine linear marks at its dorsal side, running parallel to the bone axis **(Fig. 7)**. They have a length of 10 mm and a cross-sectional width of < 1 mm. SBY650 is a rib from the sacral zone of a turtle. It has parallel linear marks at its ventral side, running parallel to the bone axis **(Fig. 7)**. The marks are relatively short (4-8 mm) and wide (> 1 mm).

Linear marks may be associated with trampling, carnivore tooth-dragging or hominin butchery (Jalvo and Andrews, 2016; Andrews and Jalvo, 1997; Fisher, 1995; Lyman, 1994). For the described specimens, a relation with trampling is unlikely, as these trampling-related marks generally occur in greater numbers, as irregular scratches with varying ori-

entations and lengths (Behrensmeyer et al., 1986). The V-shaped section of the marks, as well as their isolated occurrence lacking surrounding traces of carnivore gnawing or gripping, points to hominin butchery rather than carnivore foraging (Costamagno et al., 2019; Lyman, 1994; Shipman and Rose, 1988; Bunn et al., 1986; Binford, 1981). For the two turtle bones with linear marks, no direct equivalents are known from hominin butchery sites. However, their fine, V-shaped outline, parallel position and the absence of surrounding tooth scores are indicative of hominin butchery rather than trampling or carnivore-tooth dragging. Their longitudinal orientation probably reflects defleshing activity (Costamagno et al., 2019).

Predator ingestion

SBY5052 **(Fig. 7)** is a lower third molar of *Sus brachygnathus.* The molar is unworn and its occlusal morphology is well-preserved. However, it completely lacks its enamel cover. Note the difference with SB5079, a highly similar specimen but with enamel. The complete dissolution of enamel is indicative of a molar that passed the digestive tract of a predator, most likely a crocodilian (Fisher, 1995). SBY7080 **(Fig. 7)** is a shaft fragment, probably deriving from a small herbivore. It has rounded edges and a strongly polished surface that might relate to digestive etching by a carnivore or crocodilian (Andrews and Jalvo, 1997).

Percussion marks

The spiral and oblique fractures, as described for ruminant long bone fragments, point to intense, green-state fragmentation. This makes it relevant to search for indications of hominin battering, in the form of percussion pits, percussion notches with negative flake scars or impact flakes (Blumenschine and Selvaggio, 1988). Such features, however, appear to be scarce or disputable. A number of small shaft fragments, such as SBY7074 **(Fig. 7)**, have small pits along the fracture edges, which might be regarded as impact pits. Note however that similar pits along fracture edges were attributed to trampling by Blasco et al. (2008) and to hyena mastication by Coil et al. (2020). Larger pits that may relate to percussion were only found on the bovid tibia SBY7013 **(Fig. 7)**.

Some of the turtle shell fragments show semi-circular notches (indentations) along the fracture edges. Note, for example, SBY7165A and B, both being Geoemydidae carapace fragments **(Fig. 7)**. They have semi-circular notches with diameters of 15 and 19 mm, which may relate to hammerstone breakage. However, they lack other characteristic features of hammerstone impact, such as a negative flake scar, or impact pits surrounding the notch. Another possibility is that the notches are crocodilian tooth punctures (Njau and Gilbert, 2016; Milan et al., 2011). Specimen is SBY7210 **(Fig. 7)** is a Geoemydidae carapace fragment with ca. 3 mm wide, irregular grooves and scratches. These may be crocodilian tooth scores, but the marks may also have been caused by slippage of the turtle shell over a stone anvil during battering (Blumenschine and Selvaggio, 1988; Fisher, 1995).

4.5 Marine bioerosion and encrustation

A conspicuous taphonomic feature of the assemblage is the rich occurrence of small sub-circular boreholes of the trace fossil *Gastrochaenolites* (Leynerie, 1842). Among the bone remains with linear sizes over 30 mm, ca. 80% of the specimens has been affected by this type of marine bioerosion. Dental elements and smaller bone specimens are mostly unaffected. The boreholes have an aperture of 2 to 4 mm and are oriented perpendicular to the bone surface. They continue downward into a circular or oval chamber, which is slightly wider than the aperture **(Fig. 8).** The trace fossil is associated with rock-boring bivalves, mostly of the genera *Lithophaga* Röding, 1798 and *Gastrochaena* Spengler, 1783 (Kleemann, 1980). Both are common in Southeast Asian coastal waters and occur in the intertidal and subtidal zone. They make their borings in hard substrates, which may be rocky shorelines, coral, other shells and in rare cases fossil bones (Lopes, 2012). In several bone specimens from the Madura Strait assemblage, shell fragments of the boring bivalve have remained in the chamber.

The boreholes are generally found on all sides of the specimens, which shows that the specimens have been subject to rolling and reorientation by waves or tidal currents. The internal walls of the bored chambers are strongly mineralized and have the same dark color as the bone surface surrounding the boreholes, indicating that marine exposure and bioerosion predate diagenesis. Break surfaces, especially those exposing cancellous bone, are often particularly rich in boreholes, which shows that, at least in these cases, fragmentation preceded bioerosion.

Besides bioerosion, the Madura Strait bone remains show scarce traces of encrusting Ostreida Fërussac, 1822 and Cirripedia Burmeister, 1834 **(Fig. 8)**. The ostreid and cirriped crusts are mainly found in sheltered cavities along the bone surface and along break surfaces. The thin and scarce shell crusts on the bones suggest that conditions at the sea bed did not allow for prolonged encrustation. This may relate to frequent remobilization of the bone fragments at the seabed (Taylor and Wilson, 2003). Cirriped shells are often damaged and partly eroded. Their shells have a calcite fill, indicating that marine encrustation predated diagenesis.

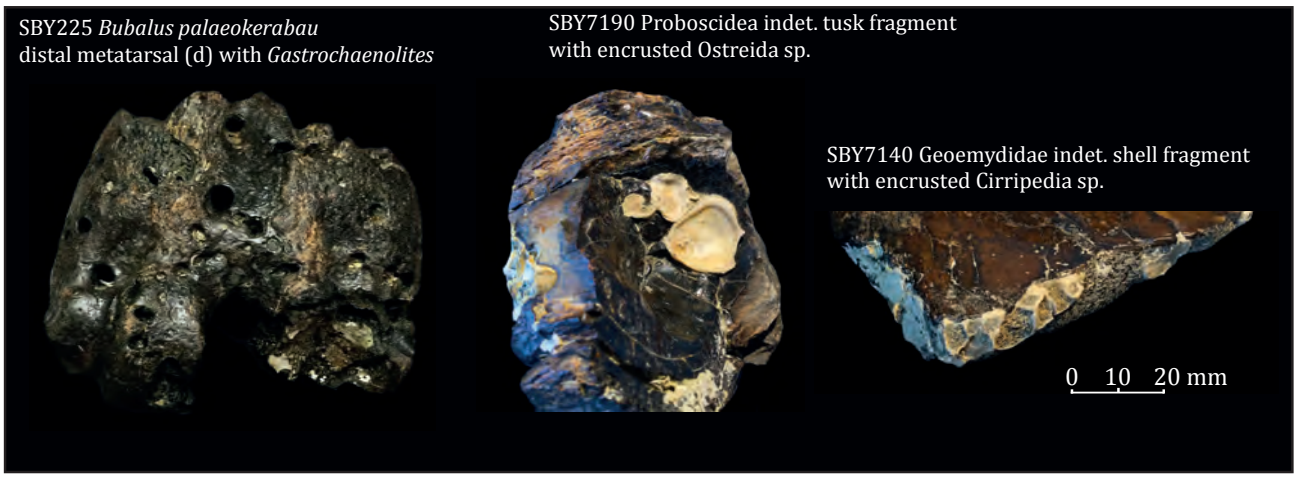


Fig. 8. Marine bioerosion and bioencrustation, selected photographs. Madura Strait assemblage.

4.6 Skeletal part frequency

A skeletal part analysis has been conducted for large Bovidae (Bovini) and Cervidae. Skeletal parts have been expressed as NISP and, if possible, as MAU (minimal animal units), which is the minimum number of individuals (MNI) represented by specimens per skeletal part, without taking into account left or right position. For extensively mixed assemblages, MAU is a more useful unit than MNI. The use of MAU also has the advantage that it makes it possible to include elements for which the sidedness could not be determined. Moreover, for analysing the survival rates or susceptibility to hydraulic transport of individual skeletal elements, sidedness is not relevant.

Among the remains of Cervidae **(Table 3)** there is a dominance of antler fragments. Their abundance among the identified specimens is caused by fragmentation in combination with a characteristic morphology, which makes the material easy to recognize even in a fragmented state. Moreover, most of the antlers are shed antlers. From all available antler bases (N=42), only 3 preserve a pedicle, indicating that these actually derive from dead individuals. This gives an MAU of only two, based on antlers with a pedicle.

Also for other cervid body parts, the representation as MAU is very low. Note the extreme scarcity of dental elements. Clearly, cervids only form a modest part of the death assemblage, an aspect that is masked by the great abundance of antler fragments. In this context, the high NISP of cervid astragali forms an anomaly.

Antler, skull, dentition, vertebrae	*NISP*	*MAU*	*Forelimb*	*NISP*	*MAU*	*Hindlimb*	*NISP*	*MAU*	*Foot*	*NISP*	*MAU*
Antler base	*38*	19	Scapula distal	3	2				Phalanx 1	4	1
Antler shaft fr. / tine	*270*		Humerus prox.	-		Femur prox.	2	1	Phalanx 2	3	1
Antler with pedicle	*4*	2	Humerus shaft	-		Femur shaft	-		Phalanx 3	-	
Maxilla fr.	-		Humerus dist.	-		Femur distal	1	1			
Mandibula fr.	*2*		Radius prox.	1	1	Tibia prox.	-				
Deciduous dentition	-		Radius shaft	-		Tibia shaft	-				
Premolars	-		Radius dist.	-		Tibia dist.	3	2			
Molars	4	1	Ulna fragm.	-		Astragalus	14	7			
Cervical vertebrae	*11*	2	Carpalia	1	1	Other tarsalia	4	2			
Thoracic vertebrae	*6*	1	Metacarpus prox.	2	1	Metatarsus prox.	-				
Lumbar vertebrae	*12*	2	Metacarpus shaft	1	1	Metatarsus shaft	-				
Caudal vertebrae	-		Metacarpus dist.	2	1	Metatarsus dist.	-				

Table 3: Cervidae specimen counts per skeletal element, Madura Strait assemblage.

Compared to Cervidae, the skeletal part frequency distribution of Bovidae fossil remains **(Table 4)** is more proportional to their anatomical distribution. Nevertheless, there are some relevant differences among the different body parts. Elements with high structural densities and low surface-to-volume ratios, such as molars, carpalia and tarsalia are dominant. Among the long bones, cylindrical shaft fragments are very scarce, whereas epiphyseal fragments are common. The survivorship of individual epiphyseal parts is proportional to bone density, with the distal humerus, proximal radius and distal tibia being the epiphyseal areas of highest structural density in bovids (Kreutzer, 1988). Phalanges are common within the assemblage, but expressed as MAU, their occurrence is low. The same accounts for vertebrae. For example, a total of 12 thoracic vertebrae only represents an MAU of 1.

Horn core, skull, dentition, vertebrae	*NISP*	*MAU*	*Forelimb*	*NISP*	*MAU*	*Hindlimb*	*NISP*	*MAU*	*Phalanx*	*NISP*	*MAU*
Horn core fr.	*25*		Scapula distal	5	3				Phalanx 1	10	2
Cranium fr.	*1*		Humerus prox.	-		Femur prox.	1	1	Phalanx 2	12	2
Maxilla fr.	*1*		Humerus shaft	-		Femur shaft	2	1	Phalanx 3	1	1
Mandibula fr.	*4*		Humerus dist.	12	6	Femur dist.	1	1			
Deciduous teeth	*4*		Radius prox.	6	3	Tibia prox.	1	1			
Premolar	23	4	Radius shaft	3	2	Tibia shaft	-				
Molar	82	6*	Radius dist.	7	4	Tibia dist.	10	5			
Cervical vertebra	*11*	2	Ulna fragm.	1	1	Astragalus	16	8			
Thoracic vertebra	*12*	1	Carpalia	16	4	Other tarsalia	9	3			
Lumbar vertebra	*12*	2	Metacarpus prox.	5	3	Metatarsus prox.	2	1			
Caudal vertebra	*1*	1	Metacarpus shaft	1	1	Metatarsus shaft	1	1			
			Metacarpus dist.	4	2	Metatarsus dist.	3	2			

Table 4: Bovini specimen counts per skeletal element, Madura Strait assemblage. *: Based on all 6 molar positions combined. Looking at individual molars, MAU = 10, based on 20 M_2 specimens.

4.7 Mortality profile of Bovini

An age-mortality profile could only be made for large bovids, as this is the taxon from which dental elements are available in sufficient numbers to allow for such analysis **(Table 4)**. **Fig. 9B** plots the measured crown heights of all measured specimens. The DP_4 is only represented by 3 specimens, each in different wear stages. Their low occurrence compared to permanent lower molars reflects a scarcity of young individuals among the death assemblage.

The available M_1 specimens occur in various wear stages, with a slight dominance of half-worn crowns. Among the M_2 and M_3, there is a clear dominance of unworn or slightly worn specimens, with rare occurrences of half-worn or strongly worn specimens. The M_3 erupts around the beginning of sexual maturity. Therefore, the large numbers of unworn or slightly worn M_3 specimens point to a dominance of prime-age (or young adult) individuals within the death assemblage.

To get an indicative insight into the age-at-death distribution, we converted the measured crown heights to age estimates, using the equation by Spinage (1973):

$$Age_{death} = Age_{max} - 2(Age_{max} - Age_e)\,(CH/CH_0) + (Age_{max} - Age_e)\,(CH^2/CH_0^2),$$

in which:

Age_{max} is the potential ecological longevity or maximum ecological age;

Age_e is the eruption age of the measured molar;

CH is the measured crown height;

CH_0 is the unworn crown height.

The eruption ages and maximum ecological age have been estimated based on observations in domestic cattle (Silver, 1963), extant wild American buffaloes (Frison and Reher, 1970) and captive and wild *Bos javanicus* (Chaiyarat et al., 2023):

Estimated eruption ages:

M_1: 6 months. M_2: 18 months. M_3: 30 months. Maximum ecological age: 15 years

The unworn crown height has been set at 40 mm for the DP_4 and 70 mm for the three permanent lower molars, which is the average height of the available unworn crowns within the assemblage.

Fig. 9C plots the calculated ages at death for the individual dental elements. For the few DP_4 specimens in the assemblage, the converted ages are straightforward and similar to the age estimating practice in extant domestic cattle. The unworn DP_4 **(Fig. 9A)** derives from a calf of less than 6 months. Mandible fragment SBY7149 **(Fig. 9A)**, with a moderately worn DP_4 and an upcoming M_1, represents an age of ~ 6 months. The sample of M_2 and M_3 specimens, dominated by unworn or slightly worn specimens, reflects an age of death shortly after their eruption. Among the sample of lower molars, only a few specimens are strongly worn, which reflects a scarcity of mature individuals among the death assemblage. SBY157D, a strongly worn M_3 from which the posterior lobe has broken off **(Fig. 9A),** represents the oldest age-at-death of all analyzed teeth, with an estimated age of over 10 years.

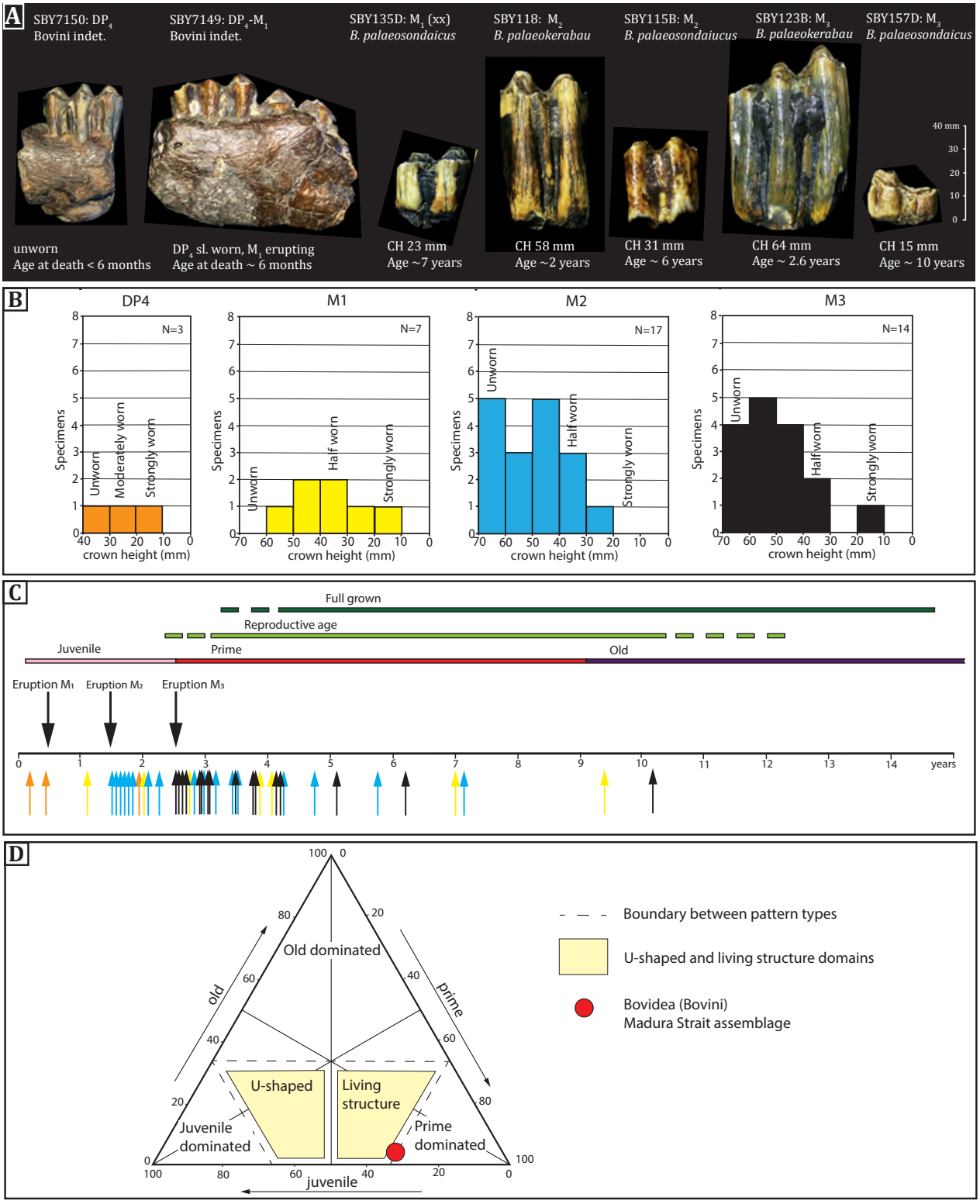


Fig. 9. Mortality profile of Bovini. Madura Strait assemblage. **A:** Selected mandibular dental elements in various wear stages, with age estimates. **B:** Crown height plots for the four investigated tooth positions. **C:** Plotted calculated ages for the individual mandibular dental elements. Colors of the arrows refer to the colors used for the individual dental positions as used in the crown height plots (B). **D:** Triangular graph of Bovini mortality, graph based on Stiner (1990).

The ages-at-death have been subdivided into three age groups, following the criteria of Stiner (1990). In this framework, juveniles are defined by the presence of deciduous dentition. Prime adults have fully developed permanent cheekteeth and are at the height of their reproductive stage. The old adults are characterized by a reproductive decline. The transition to old individuals has been set at 61% of the estimated maximum ecological age, which is ~ 9 years (for an average maximum ecological age of 15 years).

The individual ages-at-death for each of these age groups have been converted into percentages, which for the Bovini of the Madura Strait gives 30% juveniles, 65% prime adults and 5% old adults. These values have been plotted on a triangular graph **(Fig. 9D)**, again based on the methods of Stiner (1990) and with revisions by Bunn and Pickering

(2010) and Discamps and Costamagno (2015). The corners of this graph correspond to strong biases toward each of the three age groups. The yellow zones in the central lower part of the graph demarcate the expected ranges of 'U-shaped' and 'living-structure' domains. The U-shaped domain represents attritional or natural mortality due to disease, malnutrition, accidents or predation focusing on the most vulnerable prey. The living-structure domain represents mass or catastrophic mortality. The Madura Strait Bovini form a prime-dominated death assemblage, plotting along the margin toward the living-structure mortality domain.

5. Discussion

5.1 Vertebrate communities, stratigraphic distribution and taphonomy

The subdivision of the fossil assemblage into three vertebrate communities **(Table 2)** not only provides insight into past ecosystems, but is also relevant from a stratigraphic and taphonomic point of view. Skeletal remains from the three communities may have had a different distribution in their original stratigraphic context and may have been through different taphonomic pathways.

With respect to the stratigraphic distribution, it may be expected that the remains of terrestrial and fluvial species derive from the fluvial base of the valley fill, whereas the remains of estuarine species derive from the marine or estuarine sediment forming the top of the valley fill **(Fig. 2)**. Ecological mixing would then have been caused by the dredging process. This, however, is clearly not the case. Fossils found as isolated specimens on the surface of the reclamation site often carry adhered sediment or have cavities filled with sediment, providing insight into their original sedimentary context. For most of the fossils of terrestrial or fluvial species, this adhered cemented sand contains shell debris, indicating that the specimens derive from marine or estuarine sediment. Relatively few fossils of terrestrial or fluvial species have adhered cemented sand made up entirely of volcanic grains, indicating that these derive from the fluvial lower part of the valley fill.

A better insight into the original stratigraphic distribution of the fossils is offered by the blocks of uncrushed sediment on the reclamation site. These show that vertebrate fossils are associated with fluvial sandstones, fluvial conglomerates and marine conglomerates (Facies 1-3, **Fig. 3**). Each of these three fossil-bearing facies contains disarticulated and mostly fragmented remains of terrestrial and fluvial species. The marine conglomerate clearly forms the richest fossil-bearing facies. Almost all observed blocks of this material contain fragmented vertebrate skeletal elements, which are randomly dispersed through the sediment, with no preferred orientation.

There is, however, an obvious but highly relevant taphonomic difference between the vertebrate remains embedded in the different facies: most bone remains in the marine conglomerate are affected by marine bioerosion, whereas this is never the case for material embedded in the fluvial sandstone or conglomerate. This makes marine bioerosion an important and easy-to-observe taphonomic signature of material deriving from the marine conglomerates. Around 80% of the larger bone remains that were found as loose specimens on the reclamation site bear traces of marine bioerosion, indicating that this material derives from the marine conglomerate. Dental elements and smaller bone fragments are mostly free of marine bioerosion, but this relates to their unsuitability as a substrate for bivalve boring or encrusting. It may therefore be assumed that around 80% of all fossils from terrestrial and fluvial species derives from the marine conglomerate and only 20% from the underlying fluvial sandstones and conglomerates.

It is obvious to assume that the fossil remains of estuarine species derive from the estuarine deposits that form the top of the valley fill. However, this could not be confirmed at the reclamation site, as no fossil remains were observed in blocks of estuarine sandstones and clays (Facies 4 and 5, **Fig. 3**). This sediment is, on average, less cemented than the marine conglomerate and the underlying fluvial sandstones and conglomerates, and consequently was more thoroughly crushed during dredging. Unexpectedly, the fossil remains of estuarine species are free of marine bioerosion, which at least partly may be explained by the teeth-dominated composition of this material.

5.2 Transport, accumulation and concentration

5.2.1 Terrestrial and fluvial species

Based on the observations mentioned above, we infer that the collected fossils of terrestrial and fluvial species derive from the top of the fluvial valley fill, just below the transition to estuarine deposits, and from the overlying marine conglomerate bed, which marks the transition between fluvial and estuarine deposits **(Fig. 2)**. We estimated that ca. 80% of the specimens derive from the marine conglomerate bed. In both stratigraphic levels, fossils are disarticulated, fragmented and polished. Break patterns point to a dominance of green-state fragmentation.

Fresh bones do not easily break during hydraulic transport (Behrensmeyer et al., 1979), which indicates that green-state fragmentation predates hydraulic transport. The skeletal material must, therefore, have already been fragmented and disarticulated, when it was taken up by the river. The material was probably washed into the river from the floodplain. During subsequent hydraulic transport, the material must have become subject to size sorting, explaining

the modest size of the available fossil material, dominated by specimens with linear diameters < 100 mm **(Fig. 3)** (Pante and Blumenschine, 2010).

The skeletal remains probably stranded on river banks or bars, or became trapped in channel lags, and were subsequently buried by fluvial sediment under conditions of late Middle Pleistocene base-level rise. The skeletal remains in the marine conglomerate may have a similar background of fluvial transport into the estuary and accumulation in tidal channels. However, effective transport of gravel and bones is unlikely in a lowland river, in its slow-moving transitional reach toward the estuary. Transport of skeletal remains in this river reach may have occurred during a catastrophic high-discharge event. But under such conditions, we would expect floating carcasses to be swept to the estuary (Mallon et al., 2018; Brongersma-Sanders, 1957), which contrasts with the fragmented state of the skeletal remains in the marine conglomerate. There is, however, a more likely mechanism for the concentration of vertebrate fossils in the marine conglomerate. In Berghuis et al. (2025a) we identified the bed as a lag deposit, mantling a transgressive surface. Transgression surfaces are often associated with scour by waves and tidal currents, leaving a transgressive surface mantled with a coarse lag of fragmented shells and locally eroded material. In case of a transgression into an incompletely filled incised channel, such transgression-related scour is mainly caused by tidal currents, which are amplified as they become compressed in the drowned valley. Estuarine scour during this initial stage of valley drowning is sometimes amplified by the inability of fluvially supplied sediment to keep pace with the rising sea level: as more sediment is trapped in the lower reaches of the drowning river, sediment input into the estuary is reduced, which may lead to abrasion of previously deposited material (Cattaneo and Steel, 2003; Dalrymple, 1992). Marine abrasion surfaces with fossil-rich lags eroded from the underlying strata have been described from various sites worldwide (Rogers and Kidwell, 2000; Smith and Kitching, 1997; Wells, 1944; Krumbein, 1942). Among such marine fossiliferous lags, tidal scour surfaces over previous fluvial strata have been described as the most productive bone beds (Rogers and Kidwell, 2007).

Our interpretation of the marine conglomerate as a lag deposit covering a tidal scour surface readily explains its high fossil concentration, as well as its exotic facies, as a mixture of fluvial gravel, terrestrial vertebrate fossils and marine shell fragments. It also explains the common occurrence of bivalve borings in the bone remains of the marine conglomerate bed, as this turbulent reworking stage must have been a stage of non-deposition, in which the exhumed skeletal remains were exposed at the sea bed and became colonized by boring and encrusting bivalves.

This taphonomic pathway of temporary burial in fluvial deposits, followed by exhumation and concentration in a tidal lag deposit, also provides an explanation for two other taphonomic features of the Madura Strait assemblage: the polished appearance of the bone remains and the occurrence of straight transverse breaks. Although polishing of bones may relate to fresh-state hydraulic transport, it has often been associated with abrasion of bones in a pre-mineralized state (Rogers et al., 2010; Andrews and Jalvo, 1997; Behrensmeyer, 1988; Morlan, 1980). A similar thing applies to straight transverse breaks. These are highly uncommon in bones fractured in a fresh state. They are sometimes found in bones broken in a weathered state, but are most common in bones broken in a state of incipient fossilization (Lyman, 1994; Johnson, 1985; Morlan, 1980).

5.2.2 Estuarine species

The fossil remains of estuarine species must have gone through a different process of accumulation. The fossils, consisting of shark teeth, stingray teeth and batoid vertebrate centra, probably occurred as occasional, isolated elements dispersed through the estuarine deposits and may be regarded as an autochtonous, attritional accumulation of fish remains, which Kidwell (1986) referred to as the 'normal rain of body parts on the seafloor'. This accumulative background also explains the absence of bioerosion, as boring or encrusting bivalves require turbulent bottom conditions, in order to prevent the bored substrate from becoming buried. This attritional accumulation model is supported by two other observations: the fossil remains of estuarine species are mostly unfragmented and unpolished. These relevant taphonomic features are somewhat obscured by the dominance of small, robust and shiny elements as shark teeth, but looking only at batoid vertebral centra, their intact and mostly unpolished state, together with the already mentioned absence of marine bioerosion, forms a relevant contrast with the available bone remains of fluvial and terrestrial species.

Attritional accumulation of fish body parts in the estuary implies that these remains may also occur in the transgressive lag, in which case these are elements that were added to the lag during the reworking stage. Moreover, some species of the estuarine community actually have a mixed estuarine and fluvial habitat. For example, the Ganges shark *Glyphis gangeticus* and the giant stingray *Urugymnus polylepis,* spend most of their life in lowland rivers. Their remains may, therefore, also be expected in the fluvial strata, and may also have been subject to reworking during the transition to estuarine conditions. This potentially long stratigraphic range probably (partly) explains the large numbers of *Glyphis gangeticus* teeth in the assemblage.

5.3 Age and homogeneity of the assemblage

A relevant question is, how does this complex taphonomic pathway affect the age and homogeneity of the assemblage? The two OSL-dated sandstone samples were collected on the reclamation site. Referring to the dredging profile, they must derive from the top of the fluvial series, directly below the transgressive lag **(Fig. 2)**. Within the proposed model of fossil accumulation and enrichment, all fossil remains of terrestrial and fluvial species in the assemblage were initially buried in this fluvial sediment, although most of the fossils were subsequently reworked in the marine lag. One of the dated sandstone samples derives from the sandstone fill of the neural canal of a cervid vertebra, directly linking the sampled material to fossil embedding. The obtained OSL-ages, of 162±31 and 119±27 ka, are therefore representative for the age of initial burial, at least for the skeletal remains of terrestrial and fluvial species.

This does not necessarily imply that the OSL-ages are also representative of the ancient environment in which the species lived. In previous papers (Pop et al., 2023a; Hilgen et al., 2023; Berghuis et al., 2023, 2022, 2021), we noted that the on-land vertebrate fossil sites of Java, such as Trinil, bear evidence of multiple cycles of fluvial erosion and sedimentation, resulting in complex and often mixed-age fossil assemblages, either as a result of reworking or uncontrolled fossil collecting. However, these Javanese sites represent upstream fluvial settings, which were characterized by variable and often short-duration fluvial responses, not only to sea-level fluctuations but also to uplift, volcanism, sediment availability and changing local drainage systems. It is reasonable to assume that the Sundaland plains offered more stable conditions, with large lowland rivers that responded primarily to sea-level fluctuations.

The OSL- ages link the fluvial sediment in which the fossils were embedded to the lowstand of MIS6 and the subsequent stage of rising sea-level in the run-up to MIS5 **(Fig. 10A)**. The preceding incision of the valley is probably related to the stage of falling sea-level prior to MIS6 **(Fig. 10B, situation 1)**. This incision is partly nested in the fill of an older incised valley **(Fig. 2)**. Reworking of fossil material from this older valley fill cannot be excluded, however, such reworked older fossils may be expected in the basal lag of the MIS6 paleovalley, which lies at 50 m -MSL, almost 20 meters below the maximum depth reached by the dredging work. It is not very likely that reworked fossils from this older valley fill have become mixed in these higher fluvial layers. Assuming that the stage of rising sea-level offered stable conditions of fluvial backfilling, the skeletal remains in the fluvial sediment may be regarded as a homogeneous fauna, with an age that is contemporary to the age of burial.

The OSL-age of the fluvial strata, and thus the age of the environment in which the species lived, may be narrowed to 146 – 131 ka, which is the overlapping interval of the two OSL-ages and their margins **(Fig. 10A)**. This 'most likely age range' fits well with the proposed model of valley-aggradation and valley drowning, as it overlaps with the stage of rising sea-level between MIS6 and MIS5 **(Fig. 10B, situation 2)**.

The fossils occur dispersed through the top of the fluvial series. In theory, it is possible that the fossils derive from a single death event and that stratigraphic dispersal is a result of diffusion during fluvial transport. But it is more likely that the stratigraphic dispersal reflects a steady or intermittent supply of skeletal remains to the river over a longer period, with a most likely age range of 146 – 131 ka. In **sections 5.5 and 5.6** we will go deeper into this subject, with a discussion of mortality patterns.

Exhumation and concentration of fossils in the marine lag are associated with subsequent valley drowning, which changed the valley into an estuary. Fluvial aggradation and valley drowning were part of the same transgression, which implies that the period of initial burial, prior to marine reworking, must have been short. In any case, drowning of the valley and the associated stage of marine reworking must have predated peak highstand conditions of MIS5e, which implies that the marine conglomerate is slightly older than 123 ka **(Fig. 10B, situation 3)**. Its vertebrate content of terrestrial and fluvial species, which was reworked from the underlying fluvial strata, may still be regarded as homogeneous, within the most likely age range of 146 – 131 ka.

The fossil remains of estuarine species must be slightly younger. This material derives from the estuarine sand and clay that make up the top of the valley fill and which are associated with peak MIS5e highstand conditions, dating to around 123 ka **(Fig. 10B, situation 4)**. As we regard these fossils as an attritional accumulation of fish remains on the sea bed, their age must be equal to the age of the surrounding estuarine sediment.

5.4 Bone diagenesis

The bone remains are evenly mineralized on all sides, without observable colour differences between the bone's cortical surface, break surfaces and the internal walls of marine borings. Bone diagenesis must, therefore, relate to final burial, which for the material from the marine conglomerate implies after the reworking stage.

It is interesting to look in more detail at the strong mineralization of the fossil material. Bone diagenesis involves recrystallization of calcium phosphates into a more stable mineral phase, replacing phosphates by carbonates, fluorides and chlorides. Additionally, Ca^{2+} may be substituted by Fe^{2+}, U^{4+}, Zn^{2+} or Mn^{2} (Keenan, 2016; Pfretzschner, 2004). The

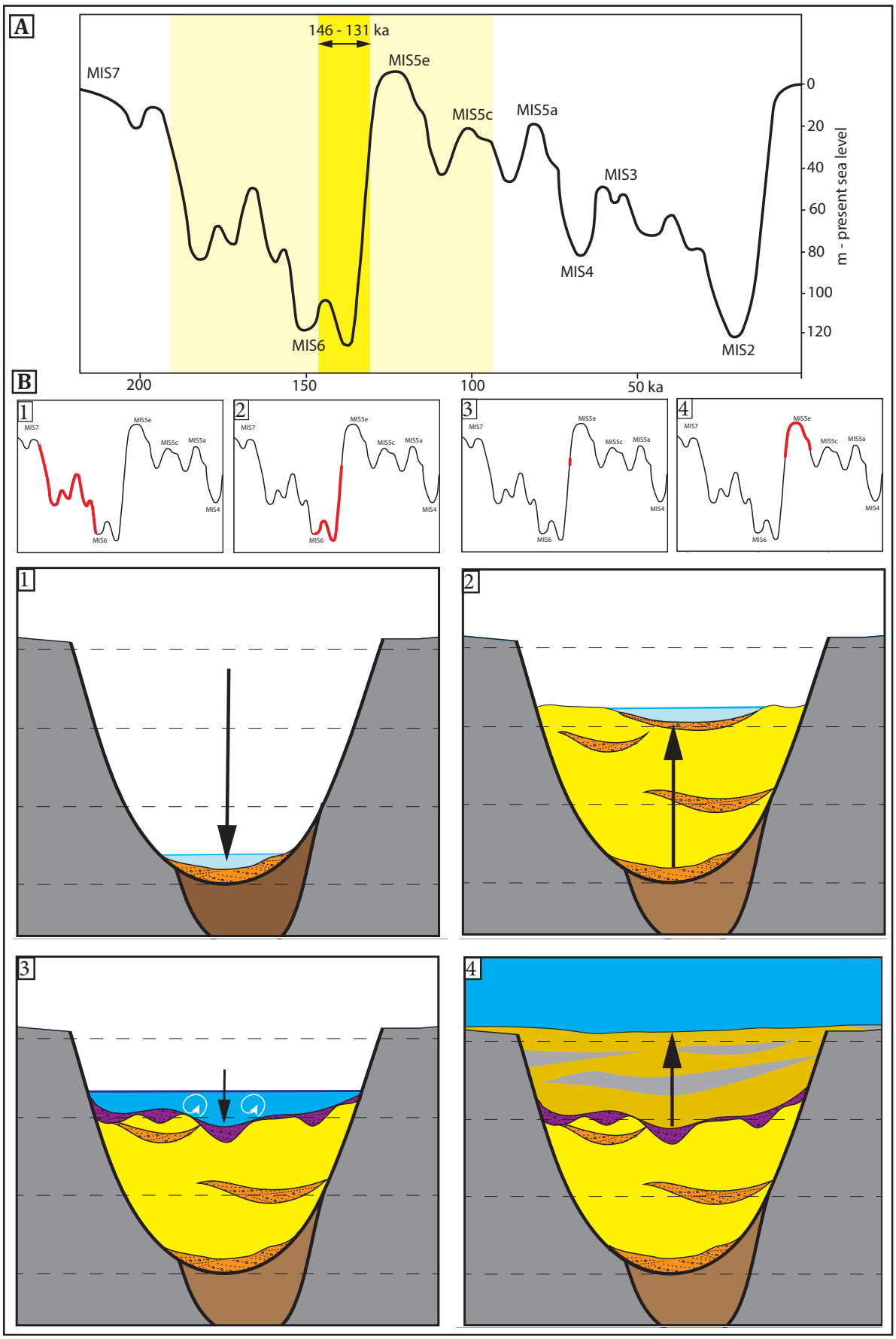


Fig. 10. Development of the Madura Strait paleovalley in relation to the sea-level curve. **A:** The late Middle Pleistocene and Late Pleistocene sea-level curve (from: Bintanja and Van der Wal, 2008) with projected range of the two available OSL-ages of the fluvial sandstones, including their error margins. OSL-ages are 162±31 and 119±27 ka (Berghuis et al., 2024a). The overlapping age (146 – 131 ka) is the most likely age range of fluvial back-filling. **B:** Four stages of valley incision and backfilling and their relation to the sea-level curve. For legend: see **Fig. 2**. **(1)** Valley incision under conditions of falling valley sea-level preceding MIS6. Note nesting in older valley fill. **(2)** Fluvial backfilling under conditions of rising sea-level preceding MIS5, accumulation of vertebrate fossils from terrestrial and fluvial species. **(3)** Drowning of the valley and temporary tidal scour. Fossils embedded in the fluvial sandstones become concentrated in a marine lag. **(4)** Estuarine deposition during MIS5e highstand conditions. Attritional accumulation of skeletal remains of estuarine fish.

good preservation of Pleistocene bones from the Javanese sites probably relates to their embedding granular volcanic material, which provided ion-rich diagenetic fluids.

The embedding in granular sediment of volcanic origin must also have contributed to the strong mineralization of the Madura Strait fossils. Moreover, the sub-marine setting of the site (at least during MIS1 and MIS5) and the embedding of the fossils in or directly below marine sediment may have further increased the availability of dissolved minerals in the circulating porewater. Another relevant difference with most of the on-land sites of Java is that the Madura Strait site has probably been under continuous water-saturated conditions, whereas most of the on-land sites of Java have been under intermittent water-saturated and dry conditions. These intermittent oxidizing conditions frequently left coatings or concretions on the fossils from the Javanese sites, which are absent on the fossils from the Madura Strait.

5.5 Weathering and fluvial uptake

The scarcely weathered state of the bone remains of terrestrial species shows that the material was taken up by the river shortly after the animals' death. Most bone remains fall in weathering stages 0 and 1. Behrensmeyer (1978) estimated that weathering stage 0 reflects a surface exposure time of less than one year, whereas weathering stage 1 may represent one to three years of surface exposure. Her estimates were based on African savanna conditions, which may have been similar to the savanna-dominated Middle Pleistocene plains of Sundaland.

Behrensmeyer (1978) also noted that long-term attritional accumulations are usually mixtures of variably weathered material, whereas a dominance of a single weathering stage is indicative of increased or catastrophic mortality. The dominance of unweathered bones in the Madura Strait assemblage may, in that respect, be regarded as an indication of increased or catastrophic mortality. However, as noted in **Section 5.3**, the dispersal of fossils through the fluvial valley fill rather points to a steady or intermittent supply of skeletal remains to the river during a longer period. This may be explained by a steady supply of skeletal remains in relation to cyclic stages of climate-induced mortality and fluvial uptake. The regional late Middle Pleistocene climate was characterized by a long dry season and a short rainy season, with a high variation in river discharge (Sémah et al., 2010). At the end of a long dry season, animals must have congregated along the river as the last resource for food and water. Under such conditions, we may expect an increased, drought-related mortality, resulting in a high accumulation rate of bones on the floodplain. These could readily be taken up by the river during the subsequent rainy season, supplying a new load of scarcely weathered bones to the river system.

5.6 Mortality and evidence of selective hunting

The model of increased, drought-related mortality at the end of dry seasons, followed by fluvial uptake in the rainy season adequately explains the steady accumulation of scarcely weathered bones in the fluvial valley fill. However, this is not in line with the age-at-death frequency distribution of the available bovid molars. Under conditions of drought, a U-shaped age distribution is expected, with an overrepresentation of very young and very old individuals, being the age classes most susceptible to ecological mortality, and an underrepresentation of reproductively active adults. The age-frequency distribution of large bovids from the Madura Strait assemblage is not U-shaped, but prime-dominated **(Fig. 9C and D)**. Prime-dominated mortality patterns are uncommon under natural conditions, because they are in contrast with the structure of a living population and with age-specific vulnerability among such populations. Humans appear to be the only species to regularly produce prime-based mortality in prey (Marin et al., 2017; Driver and Maxwell, 2013; Stiner, 2013, 2009, 1990; Speth and Clark, 2006; Gaudzinski and Roebroeks, 2000; Steele, 2003). As such, prime-dominated mortality is a strong indicator for selective hunting.

However, care must be taken with this interpretation. The mortality signal may for example have been biased by taphonomic factors, such as a low preservation of deciduous dentition (Munson and Garniewicz, 2003) or differential transport of dental elements of different size, shape or weight (Bunn and Pickering, 2010). Indeed, we showed that Madura Strait assemblage probably represents a period of several thousand years and has been subject to fluvial and dredging-related mixing. Moreover, the bovid dental elements probably do not represent a single kill, but may rather represent a longer period, with repeated hunting and butchery events. Under such conditions of time averaging, the signal of repeated prime-dominated kills is likely to have become overprinted by a normal, ecological mortality signal, which makes the persistence of a prime-dominated signal even more relevant. The Madura Strait age-at-death distribution of bovids, which is prime-dominated, but plotting toward the living structure domain **(Fig. 9D)**, may very well be explained by this overprint of ecological mortality.

There is, however, another strong argument in favor of a hunting-related mortality, and against a drought-related catastrophic mortality, which is the intensely green-state fragmented state of ruminant limb-bone shafts, together with the high representation of intact, ungnawed epiphyses **(Section 5.7)**.

5.7 Marrow processing

The fracture patterns in the limb bones of cervids and bovids testify to two fracturing stages: a first stage shortly after death, when the bones were still fresh and rich in collagen, and a second stage during marine reworking, when the bones were in a pre-mineralized state. Referring to the morphology of small shaft fragments, with a dominance of oblique and spiral fracture faces, the extensive fragmentation of ruminant long-bone shafts is linked to the first fracturing stage. As explained in **Section 5.2.1**, this fresh-state fragmentation must have taken place before fluvial uptake. Potential breaking agents are trampling, predator mastication or hominin battering. With the congregation of herds of large herbivores along the river during the dry season, it is well-imaginable that skeletal remains have become subject to trampling. Trampling is generally associated with randomly oriented scratch marks (Andrews and Jalvo, 1997; Fisher, 1995). These have not been observed. Their absence is not a strong argument against trampling as a breaking agent, as surface marks have been poorly preserved on the polished Madura Strait bones. A more relevant argument that speaks against trampling is that robust bovid limb bones are only vulnerable to trampling in a weathered state (Lyman, 1994). Fresh, collagen-rich bovid bones may occasionally have been broken by trampling, for example by passing herds of proboscideans, but it is unlikely that this caused green-state fragmentation of virtually all limb bone shafts.

Looking at predator mastication, only hyenids are capable of large-scale fragmentation of bovid long bones (Palmqvist et al., 2011; Diedrich, 2012). They feed on the spongy, fat-containing cancellous bone of epiphyses and may crack long-bone shafts to consume marrow. Hyenids were common on the Asian mainland during most of the Pleistocene. Among these was the giant hyena *Pachycrocuta brevirostris* (Dennell, 2008; Boaz et al., 2004; Turner and Antón, 1996). The species went extinct in Asia in the course of the Middle Pleistocene and was gradually replaced by the extant spotted hyena *Crocuta crocuta* (Kurtén, 1956). In the late Middle Pleistocene, this new species also inhabited the southern part of the Asian mainland, with reported fossil finds from southern China (Defen and Chunhua, 2016), Thailand (Suraprasit et al., 2016) and the Taiwan Strait (Tseng and Chang, 2007). However, hyenids are extremely rare in the fossil assemblages from Java. There are few reported finds of *Pachycrocuta brevirostris* (Geraads, 1979; Hooijer, 1964; Brongersma, 1937), which are probably of early Middle Pleistocene age. Its successor *Crocuta crocuta* is unknown from Java. Among the rich late Middle Pleistocene faunal assemblage from Ngandong, hyenid material was not found (Volmer et al., 2016; Von Koenigswald, 1935), which suggests that *C. crocuta* did not disperse this far southwards and may even have been absent on Sundaland (Louys, 2014). Also in the Madura Strait assemblage, which is of similar age as the assemblage from Ngandong, hyenid remains were not found.

Carnivores, however, are elusive species in fossil faunas and it is difficult to be sure that their absence in a fossil record implies a genuine absence in the past ecosystem. It is, therefore, relevant to also look for taphonomic indications of hyenid presence or absence. Typical hyena damages to ruminant long bones are gnawed epiphyses and crushed shafts, associated with scoring and pitting of the cortical surface of the shaft fragments (Lyman, 1994; Johnson, 1985; Binford, 1981). Hyenid bone destruction starts with epiphyseal gnawing, with means that hyenid bone accumulations are characterized by low epiphysis-to-shaft ratios (Marean and Spencer, 1991). This is, however, opposite to what we see in the Madura Strait assemblage, which shows an overrepresentation of epiphyses and an underrepresentation of cylindrical shaft fragments, at least among the ruminant species. Moreover, the abundantly available epiphyseal fragments show no or only modest gnawing damage. Also, the cortical surface of shaft fragments has no convincing hyenid teeth marks. Despite the later polishing, hyena bone crushing would expectedly have left intense gnawing marks and tooth punctures. Therefore, referring to the absence of hyenas in the Madura Strait assemblage and in similar-aged assemblages from Java, and referring to the absence of convincing evidence of hyena-inflicted bone modification, we may confidently conclude that hyenas were not part of the local ecosystem and cannot have been responsible for the fragmentation of ruminant long bones.

This leaves the hominin population as the main suspect of long-bone fragmentation. The medullar cavities of limb bones are filled with fat- and nutrient-rich marrow, which has been an essential and reliable part of the hominin diet for most of our evolutionary history (Speth, 2010a; Cordain et al., 2001). In eastern Africa, evidence of hominins breaking up limb bones for marrow extraction goes back more than 2 million years (Pobiner, 2007; Pickering and Egeland, 2006; Heinzelin et al., 1999). Intensely fragmented shafts of ruminant limb bones, with green-state fracture patterns, along with a high representation of intact and ungnawed epiphyses, are characteristic of hominin marrow exploitation. Other evidence for hominin-induced breakage of long bone shafts are percussion pits (Blumenschine and Selvaggio, 1988), percussion notches (Capaldo and Blumenschine, 1994) and percussion-induced conchoidal flake scars on the medullary surfaces of shaft fragments (Binford, 1981). Such more direct indications of hammerstone-percussion are scarce among the Madura Strait material, which may relate to the obliterating effect of polishing. However, with trampling as an unlikely breaking agent and an absence of hyenas in the ecosystem, hominin bone-battering appears to be the most plausible explanation for the intense fresh-state fragmentation of the bovid limb bones from the Madura Strait.

5.8 Hominin foraging strategies

Discussions on hominin foraging strategies have revolved around the debate over hunting or scavenging (Pobiner, 2020, 2007; Plummer and Bishop, 2016; Egeland et al., 2007; Domínguez-Rodrigo and Pickering, 2003; Domínguez-Rodrigo, 2002; Blumenschine and Cavallo, 1992). Much of this work focused on the analysis of carnivore teeth marks and hominin butchery marks on bones and their order in time. A relevant ecological characteristic of the late Middle Pleistocene Madura Strait fauna, which sets it apart from most Pleistocene ecosystems in Eurasia and Africa, is the absence of hyenas. The Madura Strait hominins must have been the only species in the ecosystem that could gain access to marrow from the medullar cavities of large mammalian limb bones. This may have favored a scavenging strategy, in which the hominins could simply collect limb bones from carcasses left by flesh-specialist predators such as felids, Komodo dragons or crocodiles. However, recent studies of Pleistocene hominin sites in Africa mostly point to early access to carcasses, suggesting active scavenging of felid kills rather than passive scavenging (Domínguez-Rodrigo et al., 2022). Felid carnivores, as well as crocodilians or Komodo dragons, preferentially prey upon the most vulnerable members of the herds, in most cases young individuals. This is not what we see from the age frequency distribution of bovids, with its overrepresentation of prime adults **(Fig. 9D)**. As explained in **Section 5.6**, we regard this as evidence of selective hunting by the Madura Strait hominins. Selective hunting of prime adult prey was most likely related to their higher fat content. Prime adults accumulate much larger amounts of fat in the medullar cavities of limb bones than juveniles. Juveniles, even when easily accessible in the form of scavengeable carcasses, may, therefore, have been low-ranked resources in comparison to prime adults.

The transition toward selective hunting is regarded as an important evolutionary shift in hominin subsistence strategy (D'Errico, 2003). Selective hunting is associated with modern behavior and requires technological developments such as long-range weapons or cooperative ambush strategies. The timing of the change from non-selective hunting or active scavenging to selective hunting may have varied in different geographical reaches. Prime-dominated patterns are common among Late Pleistocene archaeological faunal assemblages worldwide, but have also been described for Middle Pleistocene assemblages in Europe and the Middle East (Stiner et al., 2009; D'Errico, 2003) and even for Early Pleistocene sites in southern and eastern Africa (Bunn, 2019; Bunn and Gurtov, 2014). In Middle or Late Pleistocene sites of Europe and the Middle East, selective hunting is commonly associated with Neanderthals or other archaic, post-erectus humans (Langdon, 2022; Speth, 2013, 2010b; Stiner, 2009; Domínguez-Rodrigo et al., 2007; Speth and Clark, 2006). In China, a prime-dominated assemblage has been described from the late Middle to early Late Pleistocene site of Xuchang-Lingjing (Wang et al., 2022; Zhang et al., 2009). Here, selective hunting of prime-aged bovids and marrow processing is associated with post-erectus archaic hominins, possibly Denisovans (Li et al., 2017; Trinkaus and Wu, 2017).

Our finding that the late Middle Pleistocene hominins of the Madura Strait were engaged in selective hunting of prime adult prey and marrow processing fits, timing-wise, in a worldwide trend. Of great interest though is that the Madura Strait hominins were probably part of the Ngandong population (Berghuis et al., 2025d), commonly regarded as *Homo erectus* and as the descendants of a long-standing, isolated lineage (Kaifu et al., 2008; Antón, 2003). Relevant question are: did this population develop this modern subsistence strategy autonomously? Or was it introduced by contact with more advanced populations?

Selective hunting and marrow processing by the Madura Strait hominins reflect the important role of animal fat in their diet. Several researchers pointed at the importance of animal fat to our hominin ancestors, who appear to have preferred fatty tissue such as brains, tongue and marrow over lean meat (Ben-Dor et al., 2011; Speth, 2010b; Speth and Clark, 2006; O'Connell et al., 1988). In this respect, it is interesting that the only convincing cutmarks found on the bovid bone remains from the Madura Strait are linear marks on mandible SBY5067 **(Fig. 7)**. Besides their morphological characteristics, their anatomical position and orientation point to butchery. Ruminant mandibles with obliquely oriented cutmarks on the medial face, positioned below the M_2, have been described from various Early to Middle Pleistocene butchery sites, such as Koobi Fora, Kenia (Pobiner et al., 2008) and Combe Grenal, France (Binford, 1981, pp. 99-100) and also from Late Pleistocene or Holocene butchery sites (Bourgeon et al., 2017; Fisher, 1995). The marks are commonly associated with severing the mylohyoid muscle for tongue removal. Apparently, the Madura Strait hominins not only aimed for bone marrow, but also for the fat-rich tongue of their prey.

Our finding that the Madura Strait hominins were engaged in hunting, marrow processing and tongue removal do not necessarily imply that hunting large game was the primary part of the local subsistence strategy. It is well conceivable that the Madura Strait hominins also relied on edible plants, seeds and fruits or insects, and may have turned to animal fat during the dry season, when there was a lower availability of these alternative nutrients (Speth and Clark, 2006). Moreover, cutmarks found on two turtle bones as well as scratch marks and potential percussion notches on turtle shell fragments show that river turtles were also part of the local diet. These marks are the earliest evidence of turtle consumption by hominins in Southeast Asia. Butchery marks on turtle bones have been described for Early Pleistocene assemblages from Kenya (Braun et al., 2010) and Spain (Espigares et al., 2019) and for a Middle Pleistocene assemblage from Israel (Blasco et al., 2016). On Java, butchery marks have been described on turtle bones of

Late Pleistocene (ca. 30 ka) age, which must have been associated with anatomical modern humans (Setiyabudi et al., 2021). Earlier, Joordens et al. (2009) already pointed at the likelihood that the ancient hominins of Java foraged on aquatic, river-related species. In a subsequent paper, Joordens et al. (2015) demonstrated that the Javanese *Homo erectus* collected and consumed river mollusks in the Middle Pleistocene, around 500 ka.

5.9 Differential representation of body parts

A disproportional representation of individual body parts was noted among the bovid and cervid remains. Most of these may be related to differences in structural density or differential hydraulic transport. For example, the high representation of small and robust body parts such as molars, carpalia and tarsalia relates both to differential transport of these small elements and to their relatively high structural density, favoring their survival. The importance of structural density for the survivorship of individual skeletal parts is also illustrated by the disproportional representation of individual epiphyseal parts. The dominance of distal humeri, proximal radii and distal tibiae correlates with their relatively high structural density (Kreutzer, 1988), which makes these parts more resistant to destruction, either as a result of hominin battering or post-discard destruction by for example foraging canids or rodents or during hydraulic transport.

Among the skeletal parts of cervids, there is an extreme overrepresentation of antlers and a remarkable scarcity of dental elements and bone remains. In Berghuis et al. (2025b) we related the high representation of antler fragments in the assemblage to antler shedding and to their strong fragmentation, in combination with a well-recognizable morphology. However, there may very well have been other factors involved, such as differential hydraulic transport or ethological factors. The extant cervid species of Indonesia, such as *Rusa timorensis* and *Axis kuhli*, are mostly solitary or live in small groups. They are not dependent on open water, but live from the moisture offered by plants (Ali et al., 2021). They probably did not congregate along the river and may even have avoided these areas, where they may have been subject to intense predator or hunting pressure, which explains the scarcity of cervid skeletal remains in the assemblage. The abundance of shed antlers may relate to shedding behavior. Possibly, solitary bucks left their territory to cast their antlers at sites closer to the river.

An interesting aspect of the frequency distribution of bovid skeletal parts is the low representation of vertebrae compared to long-bone epiphyses. This may very well again relate to differential fluvial transport or differences in susceptibility to post-discard destruction. Within the scheme of Voorhies (1969), vertebrae are more susceptible to hydraulic transport than limb bones. Considering the fact that we regard the assemblage as a downstream accumulation, this would expectedly have resulted in an overrepresentation of these elements and not in an underrepresentation. Note, however, that the Voorhies groups of differential hydraulic transport are based on intact bones. The lower susceptibility to hydraulic transport of long bones relates, within this scheme, to the high structural density of long-bone shafts. Isolated epiphyses and vertebrae have overlapping structural densities (Kreutzer, 1988), both being elements with thin cortical walls and significant grease-rich cancellous portions (Cleghorn and Marean, 2007). This would make these body parts equally susceptible to post-discard destruction and hydraulic transport.

A possibility is that the low representation of vertebrae relates to hominin carcass processing. *Homo erectus* may have crushed limb bones at the kill site, but they may also have transported body parts to a convenient location for processing and consumption, for example to escape competition with other predators (Domínguez-Rodrigo et al., 2007; Oliver, 1994; Potts et al., 1988). Although highly hypothetical, selective transport of bovid limb bones to a riverside camp for marrow processing may provide an explanation for the high representation of long-bone epiphyses compared to vertebrae. And it explains the abundance of long-bone fragments in the assemblage.

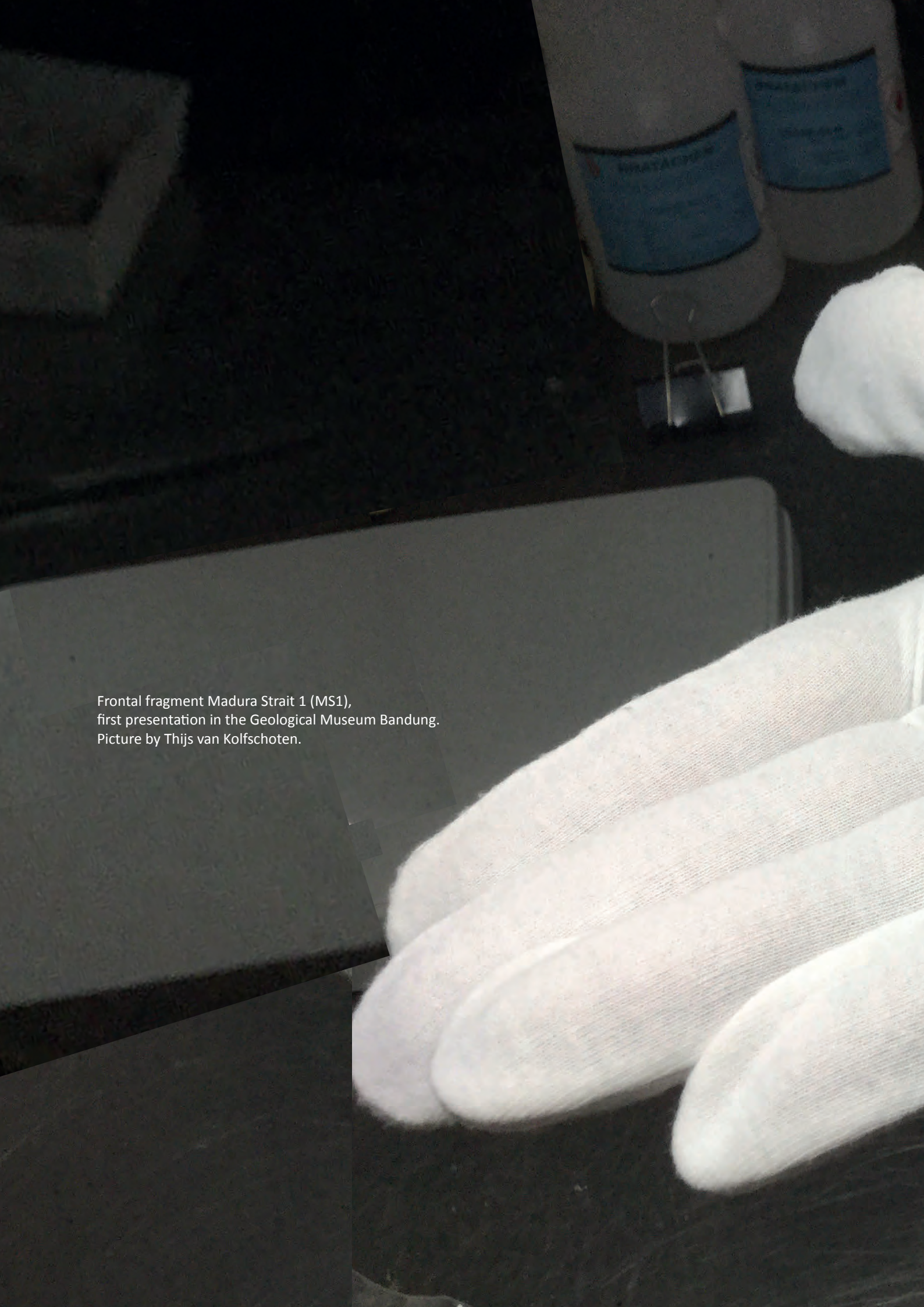
6. Conclusions

The fossil remains of terrestrial and fluvial species derive from the fluvial fill of paleovalley of the Solo associated with the lowstand of MIS6. Part of the fossil material became concentrated in an overlying marine lag deposit, which relates to the subsequent transgression. The fossil remains of the terrestrial species are regarded as homogeneous within a most likely age range of 146-131 ka.

The age-at-death frequency distribution of bovids points to selective hunting, aiming for fat-rich prime adult prey. Extensive green-state fragmentation of ruminant limb bones points to hominin bone battering and marrow processing. Hunting and marrow processing probably took place on the floodplain, where herds of herbivores gathered during the dry season. Cut marks on a bovid mandible show that the hunters not only aimed for bone marrow, but also for other fat-rich body parts such as the tongue. Cut marks on turtle bones show that the Madura Strait hominins also foraged on turtles.

The skeletal remains, deriving from hunts, but also from natural, ecology-related mortality, were taken up from the floodplain during flooding stages in the rainy season, and accumulated on the valley fill.

Remarkably, there have thus far been no systematic taphonomic studies of the fossil assemblages of Java. As we have shown here, it is expected that such studies will provide essential insights into dietary breadth, prey acquisition and carcass processing by hominins on Java in the Pleistocene.



Frontal fragment Madura Strait 1 (MS1),
first presentation in the Geological Museum Bandung.
Picture by Thijs van Kolfschoten.

Chapter 9

The late Middle Pleistocene *Homo erectus* of the Madura Strait, first hominin fossils from submerged Sundaland



CHAPTER 9

The late Middle Pleistocene *Homo erectus* of the Madura Strait, first hominin fossils from submerged Sundaland

H.W.K. Berghuis, Yousuke Kaifu, Unggul Prasetyo Wibowo, Thijs Van Kolfschoten, Indra Sutisna, Sofwan Noerwidi, Shinatria Adhityatama, Gert Van den Bergh, Eduard Pop, Rusyad Adi Suriyanto, A. Veldkamp, Josephine C.A. Joordens, Iwan Kurniawan

Published in: *Quaternary Environments and Humans* (2025)

Abstract

Eastern Asia yielded a rich fossil record of Pleistocene hominins, ranging from *Homo erectus* and the diminutive island species *Homo floresiensis* and *Homo luzonensis*, to post-*erectus* grade late archaic *Homo* (including Denisovans), and finally to anatomically modern humans. The Sunda Shelf played an important role in the dispersal and evolution of hominin populations. The shelf has been widely exposed during most of the Pleistocene, forming a landmass known as Sundaland. Today, the area holds the world's largest shelf sea. Thus far, hominin fossils from submerged Sundaland were not available. Here we report on the finding of two hominin cranial fragments from the submerged Sunda Shelf, retrieved during a dredging work in the Madura Strait, off the Java coast. The specimens derive from the sandy fill of a late Middle Pleistocene submerged valley of the Solo River and consist of a frontal fragment and a parietal fragment. Metric and morphological comparisons with Pleistocene skulls from the Asian mainland, Java and Flores point to a relation with the late *Homo erectus* of Java, in particular with the crania from Sambungmacan. The Madura Strait hominins were probably part of an MIS6 population that lived along the Solo, which in this period continued eastward over the exposed shelf area of the Madura Strait. Probably, the large perennial rivers of Sundaland offered good living conditions for *Homo erectus*, in a late Middle Pleistocene climate setting that was relatively dry.

1. Introduction

Hominin diversity and evolutionary complexity in eastern Asia are among the recent foci of paleoanthropological research (Kaifu and Athreya, in press; Bae and Wu, 2024; Liu et al., 2022; Ni et al., 2021). *Homo erectus* appeared in the region during the Early Pleistocene, as shown by fossil remains from China and Java. The late Middle Pleistocene populations of the eastern Asian mainland consist of multiple forms of 'post-*erectus* grade' archaic *Homo* including Neanderthals and an enigmatic group called 'Denisovans' (Liu and Wu, 2022; Athreya and Hopkins, 2021; Athreya and Wu, 2017; Reich et al., 2010). In contrast, the hominin fossil record of Java suggests a persistence of *H. erectus* throughout the Middle Pleistocene (Baab, 2011; Kaifu et al., 2008; Kidder and Durband, 2004; Schwartz and Tattersall, 2003; Antón, 2003) and possibly into the Late Pleistocene (Rizal et al., 2020).

The Sunda Shelf **(Fig. 1A)** must have played an important role in regional patterns of hominin dispersal, isolation and evolution (Louys and Turner, 2012; Dennell, 2008). The shelf was probably widely exposed during most of the Early and Middle Pleistocene (Husson et al., 2022, 2020), forming an important habitat for vertebrate species and providing a pathway for *Homo erectus* dispersal to Java. Regional subsidence brought the shelf surface within the range of sea-level fluctuations in the course of the Middle Pleistocene, causing intermittent flooding stages during interglacials (Berghuis et al., 2022; Sarr et al., 2019). The persistence of the Javanese *Homo erectus* lineage throughout the Middle Pleistocene, and possibly into the Late Pleistocene, may relate to this regime of intermittent shelf-submergence, in combination with the remote geographic setting of Java, on the southeastern edge of the Sunda Shelf.

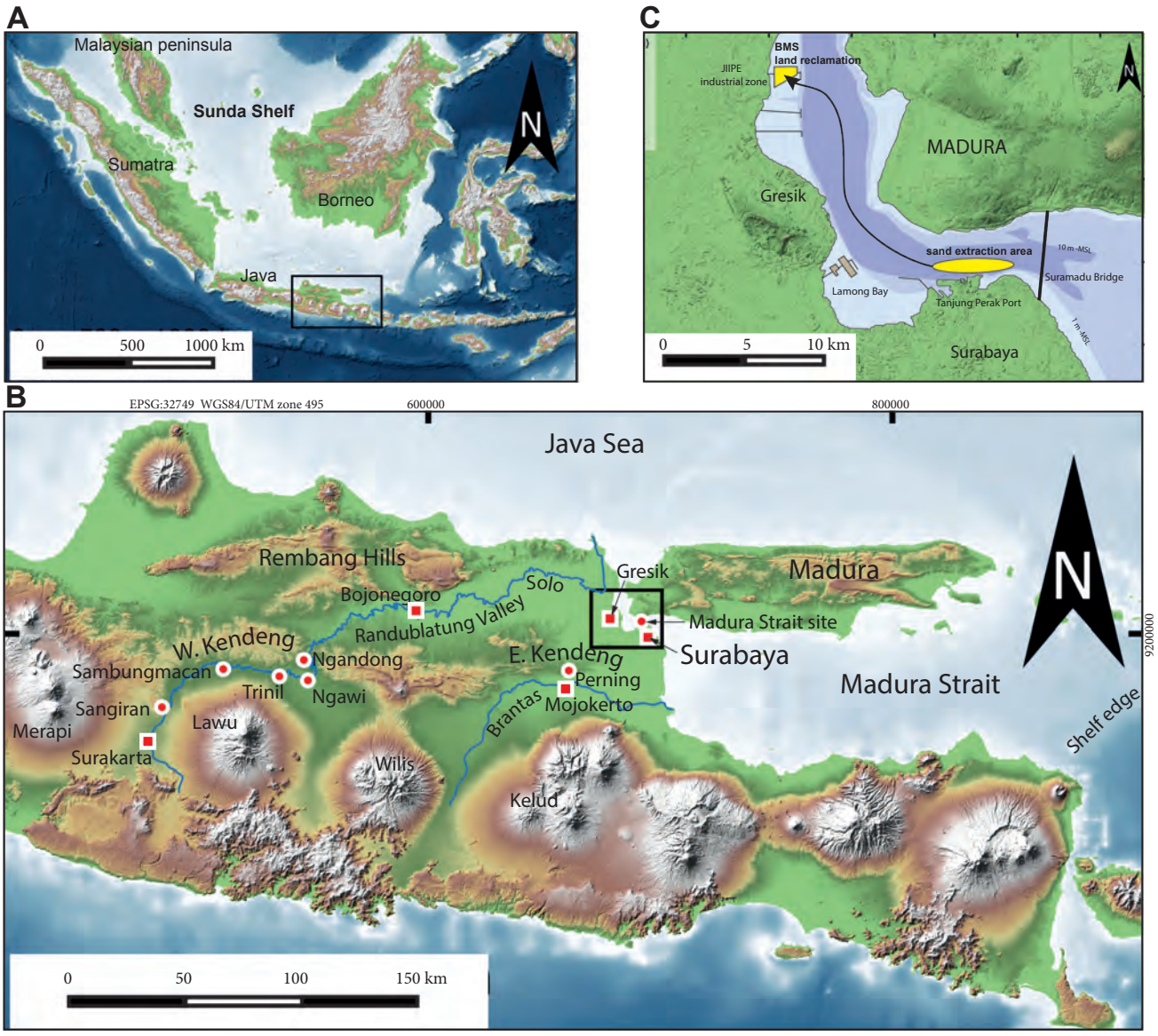


Fig. 1. A: The Sunda Shelf of Southeast Asia, with the Indonesian archipelago. Box indicates the position of map B. **B:** Eastern Java, the Madura Strait, the Solo River, Ngandong, Sambungmacan, and other hominin sites. Box indicates the position of map C. **C:** The Madura Strait north of Surabaya, with the sand extraction area and the location of the BMS land-reclamation. Map data: GEBCO and ALOS.

Recent discoveries have brought to light the existence of diminutive Pleistocene hominins on the islands of Luzon and Flores, off the Sunda Shelf, referred to as *Homo luzonensis* and *Homo floresiensis* (Kaifu et al., 2024; Détroit et al., 2019; Brown et al., 2004). Probably, these populations descended from groups of *Homo erectus* who became isolated on these islands and experienced endemic speciation (Kaifu et al., 2024, 2011b; Zanolli et al., 2022).

Meanwhile, genomic studies on extant human populations suggest that there may have been a Late Pleistocene Denisovan population in the Sundaland region, or on Wallacea islands off the Sunda Shelf, prior to the arrival of anatomically modern humans around ~ 50 Ma (Teixeira et al., 2021; Jacobs et al., 2019; Cooper and Stringer, 2013). Thus far, fossil evidence of this population is lacking.

Clearly, our understanding of hominin dispersal and evolution in this region is hampered by the absence of fossils from the submerged Sunda Shelf. In Berghuis et al. (2025a, 2025b) we presented the first subsea vertebrate-fossil assemblage from this area, retrieved during a dredging work in the Madura Strait, close to the Java coast. The fossils date from the late Middle Pleistocene, an age roughly coinciding with the last recorded presence of *Homo erectus* on Java. Hominin presence at the site was inferred from cut-marks and battered ruminant long bones (Berghuis et al., 2025c). Among the Madura Strait fossils are two hominin skull fragments. In this publication, we present a metric and morphological description of the two specimens and compare them with contemporaneous hominin remains from the region.

2. The Madura Strait site

2.1 Dredging and fossil collecting

In 2014 and 2015, around five million m3 of sand was dredged from the Madura Strait seabed and used for the development of an artificial island along the coast of Gresik, west of Surabaya **(Fig. 1B and C).** The work was assigned by Berlian Manyar Sejahtera (BMS), a local port company that today uses the island for cargo handling. The work was carried out with a trailing suction hopper dredger. The suction pipe was mounted with a drag head, penetrating and loosening the cemented seabed material. When fully loaded, the vessel sailed to the reclamation site and connected to a floating pipeline to discharge its load.

By April 2015 the artificial island had reached its final surface of ~100 ha **(Fig. 2)** and was left for dewatering. Upon inspection, the site appeared to be strewn with vertebrate fossils. In the following months, the surface of the site was meticulously searched for fossils, collecting a total of 6,732 specimens. The fossils were stored in the Geological Museum, Bandung.



Fig. 2. The BMS island in the Madura Strait shortly after reclamation, June 2015. View to the east, toward Madura. Courtesy of Pelindo III.

2.2 Geology, age of the subsea site and age of the fossils

The subsea sand-extraction area lies in the port of Surabaya. Over the past decades, the port has been subject to geotechnical studies in relation to port construction works. These data, which include a large number of deep drillings, made it possible to reconstruct the geological setting of the underwater sand extraction site (Berghuis et al.,

2025a). The seabed in this part of the Madura Strait is dominated by a thick unit of firm marine clay, dating from the Late Pliocene to Early Pleistocene. In the central part of the sea strait, this material is incised by tidal currents. Locally, patches of cemented sand and conglomerates have become exposed, reflecting the position of an ancient valley of the Solo. The valley was cut into the clayey subsoil, down to a depth of ca. 50 m –MSL (= local mean sea level) and has a fill of fluvial sandstones with lenses of fine conglomerate, which change upwards into marine clay-sand alternations with fine shell debris **(Fig. 3)**. The sandy fill follows the standard sequence of transgressively-filled valleys (Bowen and Weimer, 2003). The basal conglomerate forms a fluvial lag that relates to the incision of the valley, during a stage of falling sea level. The overlying sandstones represent fluvial back-filling during the subsequent stage of rising sea level. Occasional conglomerate interbeds reflect a stacking of flow channels during this aggradation stage. The upward change to marine sandstones and clays indicates that eventually the valley drowned and changed into an estuary. Sand excavation proceeded down to a depth of 32 m –MSL, cutting through the marine top of the valley fill and several meters into the underlying fluvial sandstones with occasional conglomerate beds.

On the BMS reclamation site, the facies of the excavated material can be recognized in blocks of uncrushed sediment. These consist of laminated marine sandstone and clay with fine shell debris, or cross-bedded fluvial sandstones and conglomerates. The latter two contain dispersed, fragmented skeletal remains. Two fluvial sandstones samples, collected from the reclamation site, have been OSL-dated. One sample derives from a block of uncrushed fluvial sandstone with adhered vertebrate fossils. The second sample was taken from the sandstone fill of the neural canal of a cervid vertebra. The found OSL-ages, of 162±31 and 119±27 ka, link fluvial backfilling of the paleovalley to the lowstand of MIS6 and the subsequent transgression in the run-up to MIS5 (Berghuis et al., 2025a). Valley incision probably relates to the preceding stage of falling sea-level, prior to peak lowstand conditions of MIS6.

On the reclamation site, occasional blocks can be observed of a marine conglomerate, consisting of rounded gravel and broken shells in a calcite-cemented matrix of volcanic sand and shell debris. Remarkably, this material is exceptionally rich in fragmented skeletal remains. On the core logs of the deep drillings, this marine conglomerate forms a ca. 1 m thick interbed at the boundary between the fluvial and marine valley fill. The material is regarded as a tidal lag deposit, reflecting increased energy conditions during the early drowning stage of the river mouth. The gravel and fossils were probably reworked from the underlying fluvial sediment.

The on-land vertebrate fossil sites of Java often bear evidence of multiple cycles of fluvial erosion and sedimentation, resulting in complex and often mixed-age fossil assemblages, either as a result of reworking or uncontrolled fossil collecting (Pop et al., 2023a; Hilgen et al., 2023; Berghuis et al., 2023, 2022, 2021). However, these sites represent upstream fluvial settings, which have been subject to variable and often short-duration fluvial responses to sea-level fluctuations, tectonism or volcanism. It is reasonable to assume that the Sundaland plains offered more stable conditions, with large lowland rivers that responded primarily to sea-level fluctuations.

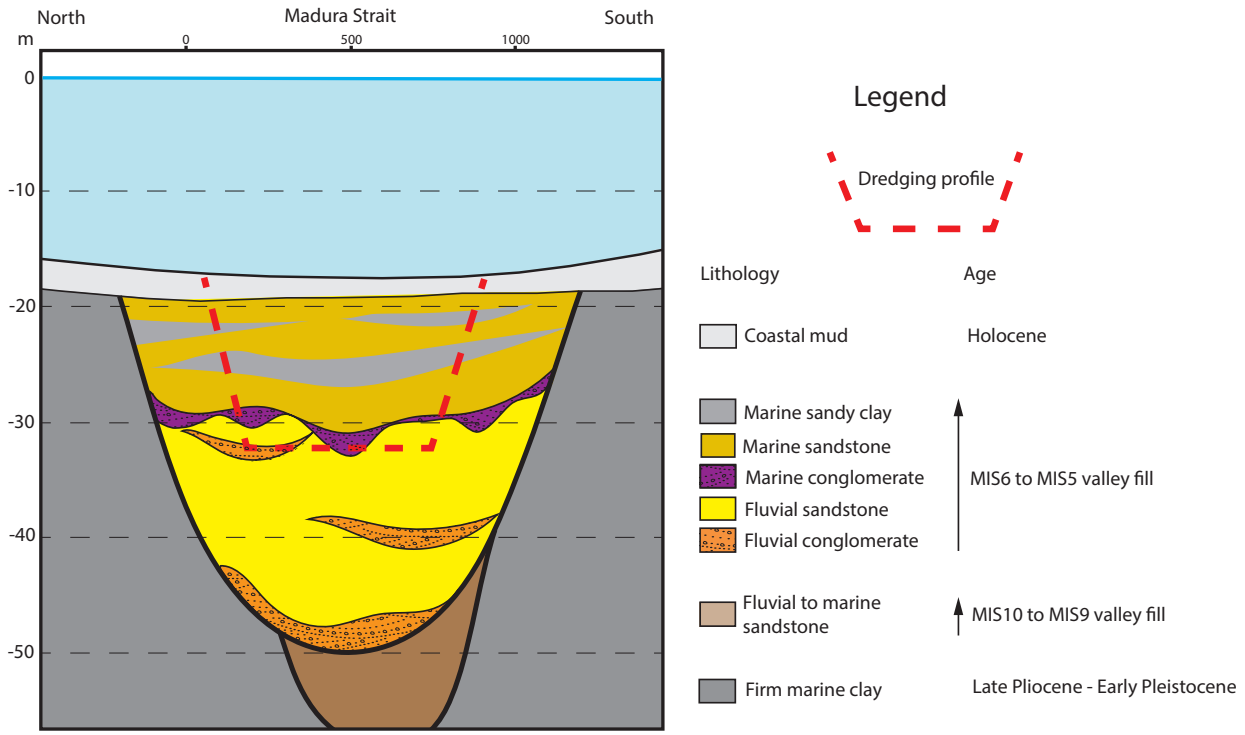


Fig. 3. Schematic cross-section of the Madura Strait paleovalley north of Surabaya and depth profile of the dredging work. Cross-section is based on deep drilling data of the Suramadu Bridge. For details, see Berghuis et al. (2025a and c).

Assuming that the MIS6 to MIS5 stage of rising sea-level offered stable conditions of fluvial backfilling, the skeletal remains in the fluvial sediment may be regarded as a homogeneous fauna, with an age that is contemporary to the age of burial. The age may be narrowed to 146 – 131 ka, which is the overlapping interval of the two OSL-ages and their margins. This 'most likely age range' fits well with the proposed model of valley-aggradation and valley drowning, as it overlaps with the stage of rising sea-level between MIS6 and MIS5 (Berghuis et al., 2025c). Concentration of fossils in the marine lag is associated with the subsequent drowning of the valley, which must have slightly predated peak MIS5e highstand conditions of 123 ka. The overlying marine sandstones and clays may be tied to MIS5e.

2.3 The fossil fauna

The vertebrate assemblage from the Madura Strait site covers 36 species, divided over 11 orders (Berghuis et al., 2025b). The assemblage is dominated by remains of large bovids *Bos palaeosondaicus* and *Bubalus palaeokerabau*, as well as the elephantoids *Stegodon trigonocepohalus* and *Elephas* sp. This herbivore-dominated community points to open vegetation conditions and a relatively dry climate, which is in line with the Middle Pleistocene pollen record of Java (Sémah et al., 2010; Van der Kaars and Dam, 1995). This was probably also the case for the greater Sundaland region, especially during glacial stages (McGrath et al., 2023; Louys and Roberts, 2020; Louys and Meijaard, 2010; Bird et al., 2005). The fossil fauna roughly overlaps with the contemporaneous assemblage of Ngandong (Java). Nevertheless, there are some noteworthy differences. Among the terrestrial herbivores of the Madura Strait, the presence of *Duboisia santeng*, *Epileptobos groeneveldtii* and *Axis lydekkeri* is interesting. These species are unknown from Ngandong and were previously regarded to have gone extinct on Java in the second half of the Middle Pleistocene. Their presence in the Madura Strait indicates that the species persisted on the emerged lowland plains. Another difference is that the Madura Strait assemblage is richer in fluvial reptiles and estuarine and fluvial fish, which marks the difference between a lowland setting (Madura Strait) and an upland setting (Ngandong). Fossils of estuarine species probably derive from the top of valley fill, which is associated with peak MIS5e highstand conditions.

3. Material and methods

We here report two hominin cranial fragments from the Madura Strait fossil assemblage. Madura Strait 1 (MS1; catalogue no. SBY7120), a right frontal bone fragment, was picked up from the reclamation site in September 2018 by H.B. and was recognized as a hominin frontal fragment at the spot (find coordinates: 7°05'06.82''S / 112° 38'42.63''E). Madura Strait 2 (MS2; catalogue no. SBY7211), a parietal fragment, was picked up from the reclamation site in 2015 by H.B., but was only recognized as a hominin skull fragment during later registration work at the Geological Museum, Bandung. Its exact findspot on the reclamation site is unknown.

High-resolution CT imagery of MS1 was obtained using the microfocal X-ray CT system TX225-ACTIS (Tesco Co.), at The University Museum, University of Tokyo, with the following parameters: 130 kV, 0.24 mA, and 35.18524 microns voxel size. At present, MS2 has not been CT-scanned.

Metric data of MS1 and MS2 were taken with a digital calliper and, for the case of MS1, CT data. The supraorbital torus thickness (SOTT) is the superoinferior thickness measured at the free anterior margin of the brow ridge. The thicknesses were measured at mid-orbit (SOTT mid) and at the lateral corner of the orbit (SOTT lat). Supraorbital torus breadth (SOTB) is the maximum transverse breadth of the frontal across the supraorbital tori. Postorbital breadth (POBB) is the least transverse breadth of the frontal squama measured behind the supraorbital torus, in the concavity of the postorbital constriction. One-sided postorbital constriction (POC 1-sided) is a half of the difference between SOTB and POBB.

The comparative materials are the following *Homo erectus* and post-*erectus* grade archaic *Homo* fossils from Java and other insular (Flores) and continental (China and India) parts of eastern Asia:

The late Early Pleistocene *H. erectus* from Java

This group is represented by the fossils from Sangiran and Trinil. The material may be further divided into two chronological subgroups, referred to as archaic and typical *H. erectus* by Widianto and Noerwidi (2023) or as the Sangiran Lower and Upper paleodemes by Kaifu and Athreya (in press). Referring to the most recent chronologies of Matsu'ura et al. (2020) and Hilgen et al. (2023), the paleodemes date to ~1.1 - 0.9 Ma and 0.9 – 0.773 Ma respectively. The most relevant comparative crania belong to the younger subgroup.

The late Middle Pleistocene *H. erectus* from Java

This group is represented by fossils from Ngandong, Sambungmacan and Ngawi. The material may be referred to as the late Javanese *Homo erectus* (Antón, 2003), or as progressive *Homo erectus* (Widianto and Noerwidi, 2023), or as the Ngandong/Sambungmacan/Ngawi paleodeme (Kaifu and Athreya, in press). The fossils are dominated by cranial remains, found along the middle reach of the Solo. The fossils from Ngandong derive from a fluvial terrace that was dated to 140-92 ka (Rizal et al., 2020), which implies that they may date from the early Late Pleistocene. This, how-

ever, is not very likely. The fossil fauna from Ngandong is the last representant of the Middle Pleistocene grassland or open-woodland vertebrate community of Java and most likely pre-dates the forested conditions of MIS5e (Sondaar, 1984). It is therefore plausible to project the Ngandong skulls in the early part of the age range, roughly between 140 and 130 ka, which links the population to the penultimate glacial period of MIS6. The fossils from Sambungmacan and Ngawi are regarded as roughly contemporaneous with or slightly older than those from Ngandong, based on cranial morphology and limited stratigraphic data (Kaifu et al., 2015; Baba et al., 2003; Antón, 2003).

***Homo floresiensis* from Flores**

This group is represented by early Middle Pleistocene material from Mata Menge and Late Pleistocene material from Liang Bua. From the latter site a relevant comparative skull is available (Kaifu et al., 2011b; Brown et al., 2004).

The early Middle Pleistocene *H. erectus* from northern China

This group is referred to as the Zhoukoudian paleodeme by Howell (1999) and Kaifu and Athreya (in press) and includes fossils from Zhoukoudian Locality 1, and possibly Nanjing (Tangshan) and several other sites (Xing et al., 2018).

The mid-Middle Pleistocene late archaic *Homo* from Hexian, northern China

The skull from this site has a unique morphology (Liu et al., 2017; Kaifu, 2017). Its taxonomic placement is controversial (Kaifu and Athreya, in press), which is why the skull is treated separately within the comparative sample of this study.

The late Middle Pleistocene to early Late Pleistocene late archaic *Homo* from northern and central China

This group, which includes the skulls from Hualongdong, Xuchang, Dali, Jinniushan, and Harbin, may or may not represent multiple species, but we do not separate them because of ongoing controversy (Ni et al, 2021; Liu et al., 2022; Bae and Wu, 2024; Kaifu and Athreya, in press).

The late Middle Pleistocene archaic *Homo* from southern China and India

This group consists of the skulls from Maba (Wu et al., 2011) and Narmada (Cameron et al., 2004). They differ from the northern Chinese archaic *Homo* by their facial morphology (Kaifu and Athreya, in press; Howell, 1999).

4. Results

4.1 Descriptions

4.1.1 Madura Strait 1

Madura Strait 1 **(Fig. 4)** is a frontal fragment, which measures 45 mm mediolaterally and 33 mm anteroposteriorly. It preserves the lateral two-thirds of the dextral supraorbital torus, the supratoral plane, and the basal part of the frontal squama. The specimen is heavily mineralized, exhibits a dark color, and is free from taphonomic distortion. The outer bone surface is well-preserved, except for some minor erosion pits. The inner bone surfaces, i.e. the orbital roof and endocranial surface, are substantially damaged so that much of the cortical bone was lost. Small patches of matrix, almost indistinguishable from the bone in our micro-CT scan, sporadically remain on the bone surfaces. The original orientation of MS1 is difficult to determine, as the orientation of this part of the supraorbital region varies in the comparative sample. In **Fig. 4A and B**, MS1 is oriented with the axis of the torus placed slightly diagonally and in **Fig. 4C** more horizontally.

In the anterior view, the supraorbital torus of MS1 is relatively straight. A weak bulge on the supratoral plane forms the lateral end of the glabellar part of the supraorbital torus (or superciliary arch) **(Fig. 4C)**. The medial aspect the supraorbital margin is accentuated by a gentle, but transversely wide bulge, which probably is a form of the supraorbital process. Medial to this supraorbital process, the superior orbital margin curves gently upward, indicating the presence of a shallow supraorbital notch in the missing medial portion of the frontal. Lateral to this supraorbital process, the vertical thickness of the supraorbital torus remains similar throughout, with no marked lateral thickening at its lateral junction with the temporal line.

Viewed superiorly, the anterior orbital margin is gently curved with no marked development of the supraorbital fissure (frontal incisura) between the glabellar and lateral parts of the supraorbital torus. Postorbital constriction is very weak behind the small zygomatic process. Behind the supratoral plane, the frontal squama is weakly inclined posteriorly, forming a gentle angle with the supratoral plane. Posterior to the lateral part of the supratoral plane and medial to the temporal line that forms the border between the superior and lateral parts of the frontal squama, the anterolateral part of the frontal squama is weakly concave. The CT scan **(Fig. 4D)** indicates that the preserved lateral portion of the supraorbital torus is dense with no lateral development of the frontal sinus.

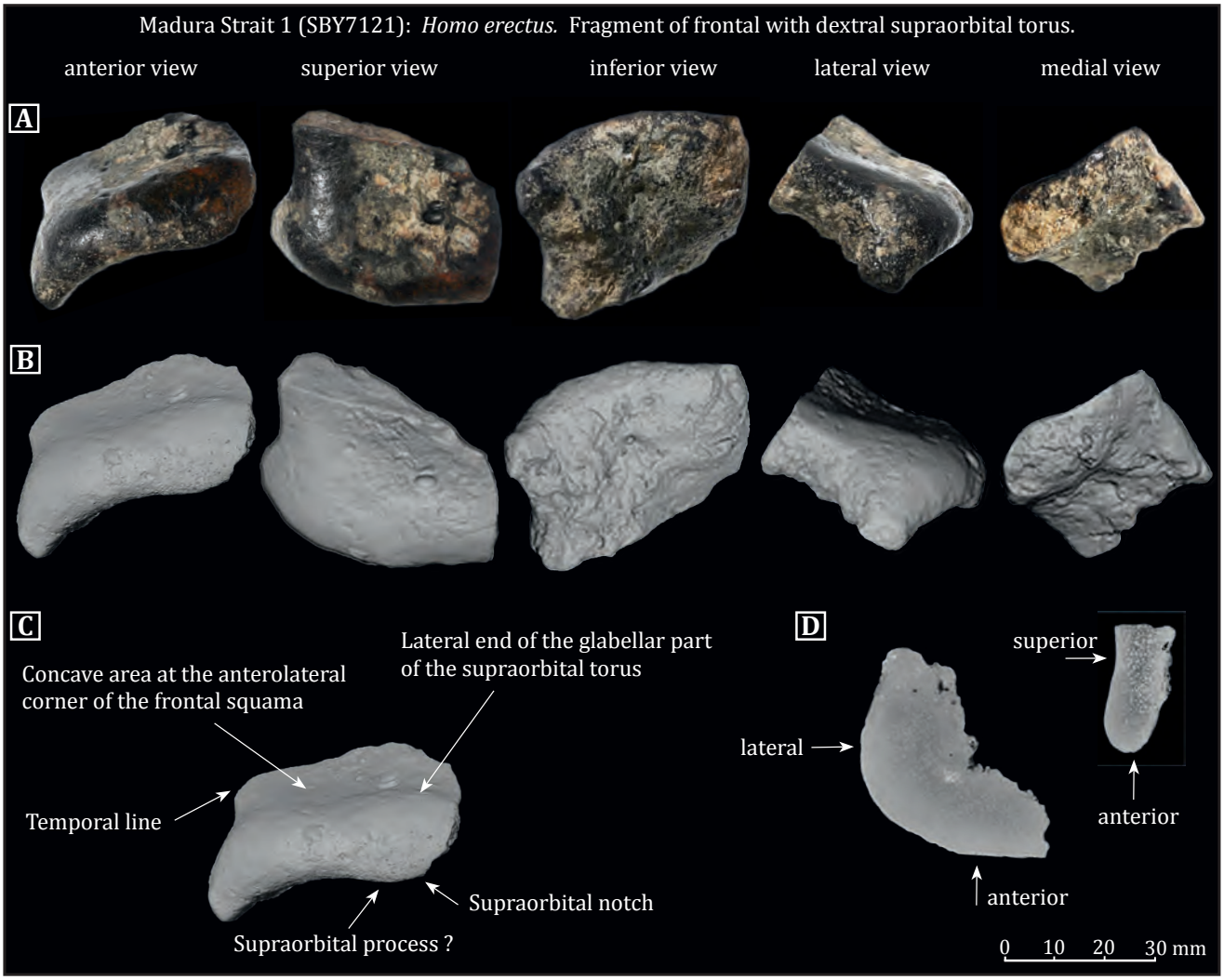


Fig. 4. Madura Strait 1 (MS1): *Homo erectus* frontal fragment with dextral supraorbital torus. **A:** Photographs. **B:** CT-based 3D surface rendered images. Note that the exact orientation of the fragment is unknown. For the anterior view, a slightly diagonal orientation has been assumed. **C:** CT-based 3D surface rendered image of MS1 in a more horizontal orientation, with anatomical indications. **D:** CT-slice.

4.1.2 Madura Strait 2

Madura Strait 2 **(Fig. 5)** is a right or left parietal fragment with the middle part of the sagittal suture. The preserved linear suture length is 39 mm. The maximum preserved anteroposterior length of the specimen is 45 mm and the maximum preserved mediolateral width is 34 mm. The specimen is heavily mineralized, exhibits a dark color, and is free from taphonomic distortion. All bone surfaces are well-preserved.

The preserved suture is moderately serrated on the ectocranial side, but is smooth and straight on the endocranial side, as often seen in the mid-sagittal suture of fossil and extant *Homo*. Granular foveolae (arachnoid fovea) are present as some depressions on the endocranial surface. The cranial thickness is 8.4 mm along the suture and 7.3 mm along the lateral fracture surface. Along this fracture surface, the bone is made up of an outer table of ~2.1 mm, an intermediate diploë layer of ~3.5 mm, and an inner table of ~1.7 mm.

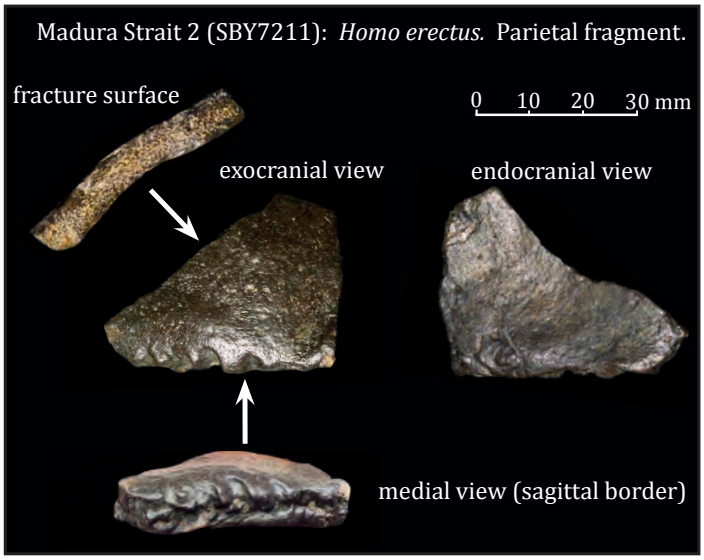


Fig. 5. Madura Strait 2 (MS2): *Homo erectus* parietal fragment with sagittal suture. Photographs. The fragment may either derive from the dextral or sinistral parietal. Orientation (ant-post) of the fragment is unknown.

4.2 Comparisons

4.2.1 Madura Strait 1

Metric comparisons

Table 1 provides metric data of MS1 and crania from the comparative groups. The metric data of comparative skulls derive from previous publications, with the addition of new, unpublished measurements.

In the bivariate plot **(Fig. 6A)** of lateral and midorbit SOT-thicknesses, the late Middle Pleistocene *Homo erectus* from Ngandong stands out by its laterally thickened supraorbital torus, a feature unknown from the earlier *Homo erectus* populations, either from Java or China. The fossils from Sambungmacan and Ngawi exhibit this trend to a lesser extent (together with Ngandong 1). In the late archaic *Homo* from the Asian mainland, the thickness of the supraorbital torus is highly variable. There is some overlap with the Sambungmacan/Ngawi condition, but the lateral thickening such as in the Ngandong crania is absent. MS1 shows a weak lateral thickening of the supraorbital torus, to a condition that is similar to the Sambungmacan/Ngawi crania and Ngandong 1. However, compared to these crania, the torus of MS1 is relatively thin. MS1 also plots relatively close to the Jinnishuan and Xuchang 1 crania, however, as we will see below, these crania strongly differ from MS1 for other metric and morphological aspects.

The bivariate plot of the one-sided postorbital constriction and postorbital breadth **(Fig. 6B)** shows a metric demarcation of the Pleistocene hominin groups from Asia. The early *Homo erectus* from Java and China have a strong postorbital constriction and a relatively small supraorbital breadth, both of which are most pronounced in the late Early Pleistocene crania from Java. The late Middle Pleistocene *Homo erectus* from Java has a low postorbital constriction and modest postorbital breadth. The late Middle Pleistocene late archaic *Homo* crania from northern/central China exhibit a moderate to strong postorbital constriction together with a relatively large postorbital breadth, which reflects the overall large size of these crania.

For the frontal fragment MS1, the full postorbital breadth is unknown. With a preserved postorbital breadth of ~ 40 mm of the right lateral part of the frontal, this value certainly must have exceeded 80 mm. The one-sided postorbital constriction can be measured. Its value, however, depends on the orientation of the frontal fragment, and falls between 5.2 mm (horizontal orientation) and 3.9 mm (diagonal orientation) **(Table 1)**. In the bivariate plot of **Fig. 6B**, MS1 again shows a close affinity with the Sambungmacan crania, which are characterized by a very weak postorbital constriction.

Further comparison with the comparative groups from Java

As demonstrated in the above metric comparisons, the late Early Pleistocene *H. erectus* from Java differs from the late Middle Pleistocene *H. erectus* from Java by its strong postorbital constriction and the absence of lateral thickening of the supraorbital torus, although a weak tendency of the latter is observed in Sangiran 17 (Kaifu et al., 2008; Rightmire, 1990; Santa Luca, 1980; Weidenreich, 1951). For both aspects, MS1 is similar to the younger comparative group.

Another difference is that the supraorbital torus of the late Early Pleistocene *H. erectus* from Java is mostly arched around the orbits, whereas the torus of the late Middle Pleistocene *H. erectus* from Java is relatively straight,with a rather flat supratoral plane. Also for this morphological trait, MS1, with its relatively straight supraorbital torus and flat supratoral plane, has a closer affinity with the younger group. Posterior from the supratoral plane, the angle formed with the root of the frontal squama is variable both in the late Early Pleistocene and late Middle Pleistocene groups of Javanese *H. erectus*, ranging from weak posterior (e.g., Sangiran 17, Ngandong 1 and 6) to more vertical (e.g., Skull IX, Ngandong 7 and Sambungmacan 3) inclinations. The preserved root of the frontal squama of MS1 is weakly inclined. However, looking at the anterolateral part of the frontal squama, lateral to the bulging central zone of the frontal squama and medial to the thick temporal line, we note a distinct concavity, which is a trait of the younger comparative group, the late Middle Pleistocene *H. erectus* from Java **(Figs. 4 and 7)**.

Thus, MS1 fits comfortably in the comparative group of the late Middle Pleistocene Javanese *H. erectus*. Within this group, the frontal fragment shows a closer affinity with the Sambungmacan crania than with the Ngandong crania, referring to its modest lateral thickening of the supraorbital torus and its weak postorbital constriction. However, the torus of MS1 is thinner than the ten adult and one adolescent individuals in this comparative group **(Fig. 6A, Table 1)**. Additionally, the gentle but transversely extensive supraorbital process of MS1 seems to be unique to this specimen **(Fig. 4C)**, although the development of this process is variable in the crania from Ngandong, Sambungmacan and Ngawi, from no development to a small but distinct projection **(Fig. 7)**. Unfortunately, the frontal bone breadth of

MS1 cannot be estimated with confidence, but the transverse breadth of its preserved part is largely comparable to the equivalent portions of the specimens from this comparative group.

Specimen	SOTT (mid)	SOTT (lat)	SOTB	POBB	POC 1-sided	*data sources*
Madura Strait 1	11.5	13			3.9*[a] 5.2*[b]	This study
Sangiran 2	13	12	104	84	10.0	Kaifu et al. (2008)
Sangiran 10	14					Kaifu et al. (2008)
Sangiran 17	16	16	125	101	12.0	Kaifu et al. (2008)
Bukuran	14	12	113	88	12.5	Kaifu et al. (2008)
Sangiran Skull IX	13.8	12.5	111	87	12.0	Kaifu et al. (2011a)
Sambungmacan 1	14	16	118	107	5.5	Kaifu et al. (2008)
Sambungmacan 3	12	15	114	101	6.5	Kaifu et al. (2008)
Sambungmacan 4	14	16	122	116	3.0	Kaifu et al. (2008)
Ngawi 1	13.2	15.9	114	101	6.5	Kaifu et al., 2015
Ngandong 1 (Solo 1)	12	14		(106)	(7.0)*	Kaifu et al. (2008); Kaifu, unpublished data
Ngandong 5 (Solo 4)	12	16	116	103	6.5	Kaifu et al. (2008)
Ngandong 6 (Solo 5)	14	18	122	108	7.0	Kaifu et al. (2008)
Ngandong 7 (Solo 6)	12	18	121	106	7.5	Kaifu et al. (2008)
Ngandong 10 (Solo 9)	12	18	124	110	7.0	Kaifu et al. (2008)
Ngandong 11 (Solo 10)	12	17	132	114	9.0	Kaifu et al. (2008)
Ngandong 12 (Solo 11)	13	19	124	107	8.5	Kaifu et al. (2008)
Liang Bua 1	6.8	8	88	71	8.5	Kaifu et al. (2011b)
Zhoukoudian Skull 3	*10.2*	*9.1*	*108*	88	10.0	Weidenreich (1943); Kaifu, unpublished data
Zhoukoudian Skull 5	11.6	11.7	119	96.6	11.2	Kaifu, unpublished data
Zhoukoudian Skull 10	*13.4*	*13.1*	*119*	98	10.5	Weidenreich (1943); Kaifu, unpublished data
Zhoukoudian Skull 11	*12*		*113*	93	10.0	Weidenreich (1943); Kaifu, unpublished data
Zhoukoudian Skull 12	*14.3*	*12.1*	*118*	95	11.5	Weidenreich (1943); Kaifu, unpublished data
Nangjing	*11*	*9*	*107.4*	*90.2*	8.6	Kaifu, unpublished data
Hexian	17.2	11.8	114	101	6.5	Kaifu (2017)
Dali	*17.1*	*13.6*	125.5	*106.4*	9.6	Liu et al. (2022); Kaifu, unpublished data
Maba	*11.7*	*11.1*	(*119*)	(*102*)	(*8.5*)	Wu and Brauer (1993); Kaifu, unpublished data
Harbin	15	15.5	145.7	125	10.4	Ni et al. (2021); Kaifu and Athreya (in press)
Jinniushan	10.8	13.4	136,5	116	10.3	Ni et al. (2021); Kaifu and Athreya (in press)
Xuchang 1	9.7	12.3	143	125	9.0	Li et al. (2017); Kaifu and Athreya (in press)
Xuchang 4	11.7					Li et al. (2017)
Hualongdong 6	16.5	11,5	(124)	104	10.0	Wu et al. (2021)
Narmada	*14.8*	*15.4*	(*106*)	(*94*)	6.0	Kaifu, unpublished data

Table 1: Measurements (mm) of the brow region of Madura Strait 1 and comparative Pleistocene crania from Asia. Data in italics are measurements taken from casts. Data in parentheses are estimates.

SOTT = Supraorbital torus thickness, measured at midorbit and the lateral corner.

SOTB = Maximum frontal breadth across the supraorbital tori.

POBB = Least frontal breadth measured posterior to the supraorbital torus.

POC 1-sided = One-sided postorbital constriction = (SOTT-POBB)/2. For MS1, two values are shown. a: specimen in diagonal orientation and b: maximum value with specimen in horizontal orientation.

*: Measured as projected breadth between the landmarks of SOTB and POBB using 3D scan data.

Zhoukoudian 3 and Ngandong 5 are adolescents, all other comparative skulls are adults. Developmental age of MS1 is unknown.

Further comparison with the cranium from Flores

The single existing adult *H. floresiensis* cranium, Liang Bua 1 (LB1), has an arched supraorbital torus **(Fig. 7)** and a relatively strong postorbital constriction **(Fig, 6B)**. MS1, with its less arched supraorbital torus and a weaker postorbital constriction, differs from LB1 for both traits. The arched torus and strong postorbital constriction of LB1 resembles more closely the condition of the early Javanese *H. erectus* than the condition of the late Javanese *H. erectus* (Kaifu et al., 2011b).

Most of all, compared to LB1, MS1 has a 60-70% thicker supraorbital torus and a distinctly wider orbit and frontal squama **(Figs. 6 and 7)**. Therefore, the diminutive trend that characterizes *H. floresiensis* is absent in MS1.

Further comparison with the comparative groups from the Asian mainland

As shown in the metric comparisons, the brow region of the early Middle Pleistocene northern Chinese *H. erectus* is characterized by an absence of lateral thickening of the supraorbital torus **(Fig. 6A)** and a strong postorbital constriction **(Fig. 6B)**. Other relevant traits of this comparative group are an arched supraorbital torus, a distinct supratoral sulcus, as well as a relatively vertical frontal squama with a convex (non-concave) anterolateral surface. For illustrations, see Weidenreich (1943), Vialet et al. (2010), Liu et al. (2014, 2005). MS1 differs from this group in all these aspects.

The frontal bone of the Hexian cranium (see Liu et al. (2014) and Cui and Wu (2015) for illustrations) is similar to MS1 in showing a weak postorbital constriction **(Fig. 6B)**. However, it is distinct from MS1 by its supraorbital torus, which is

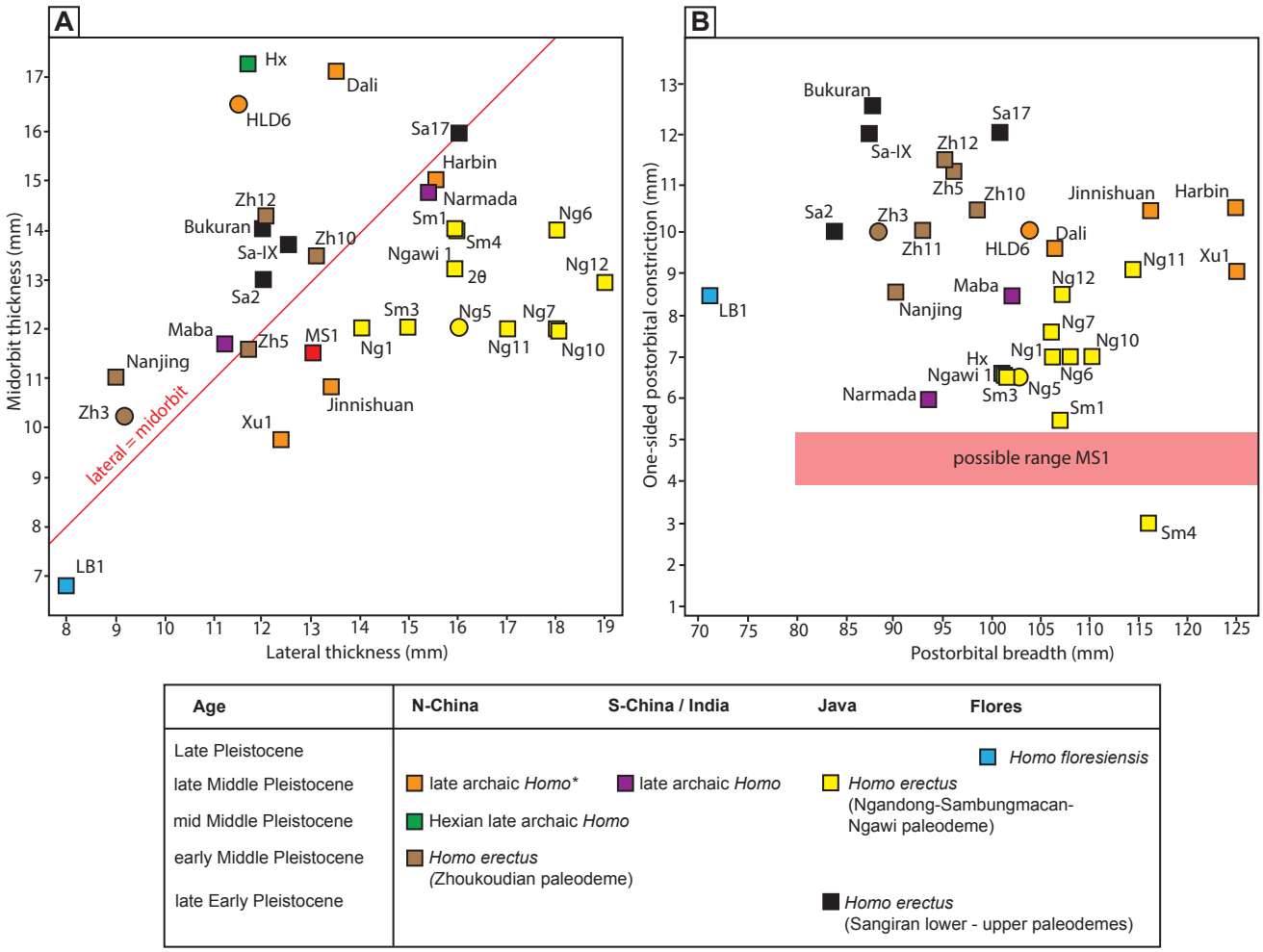


Fig. 6. Bivariate analyses of frontal bone measurements. **A:** Bivariate plot of medial and lateral supraorbital torus thicknesses. **B:** Bivariate plot of one-sided postorbital constriction and postorbital breadth. For details and data sources, see **Table 1**.
*: Xuchang 1 dates from the early Late Pleistocene (Li et al., 2017) or late Middle Pleistocene (Wang et al., 2022).

markedly thickened above the mid-orbit but thin laterally **(Fig. 6A)**. Moreover, the supratoral plane of the Hexian cranium is arched above the orbit and, posterior to this supratoral plane, its frontal squama stands more vertically.

The late Middle and early Late Pleistocene archaic *Homo* crania from northern/central China form a relevant comparative group, by its age overlap with the Madura Strait specimens. For illustrations of these crania, see Ni et al. (2021), Wu et al. (2021, 2019), Li et al. (2017), Liu et al. (2014), and Wu and Athreya (2013). The thickness of the supraorbital torus is variable in this group. In Harbin, Hualongdong 6 and Dali, the torus is rather robust, with the latter two having their greatest thickness above the midorbit. The crania from Xuchang and Jinniushan have more gracile supraorbital tori with a slight lateral thickening, a condition comparable to MS1 **(Fig. 6A)**. However, all crania from this group exhibit a moderate degree of postorbital constriction, which contrasts with the very weak constriction in MS1 **(Fig. 6B)**. Many of the Chinese crania also have very high postorbital breadths, an aspect that unfortunately cannot be compared with the frontal fragment MS1 **(Fig. 6B)**. The late Middle and early Late Pleistocene archaic *Homo* crania from northern/central China are further characterized by a more arched supraorbital torus and a moderately inclined foot of the frontal squama, with a laterally sloping, convex (non-concave) anterolateral part. MS1 differs from these crania for both traits.

The crania from Maba and Narmada (see Liu et al. (2014) and Sonakia (1984) for illustrations) have a variable morphology of the supraorbital torus. Maba does not show a lateral thickening of the torus and exhibits a rather strong postorbital constriction (Wu and Bräuer, 1993). Narmada resembles MS1, in showing a slight lateral thickening of its supraorbital torus, but the entire torus is more robust in Narmada. **(Fig. 6A)**. It also resembles MS1 by its weak postorbital constriction **(Fig. 6B)**. However, both crania differ from MS1 by their arched supraorbital torus and a more vertically oriented frontal squama, with a convex anterolateral part.

The frontal sinus

There is substantial variation in the size and shape of frontal sinuses in fossil and extant hominins (Balzeau et al.,

2022). In general, sinuses appear to be relatively large in the Early Pleistocene *H. erectus* from Java. The late Middle Pleistocene *H. erectus* from Java, represented by the crania from Ngandong and Sambungmacan, tend to have small, centrally restricted frontal sinuses. In this respect, the absence of a frontal sinus in the preserved part of MS1 **(Fig. 4D)** matches with this comparative group.

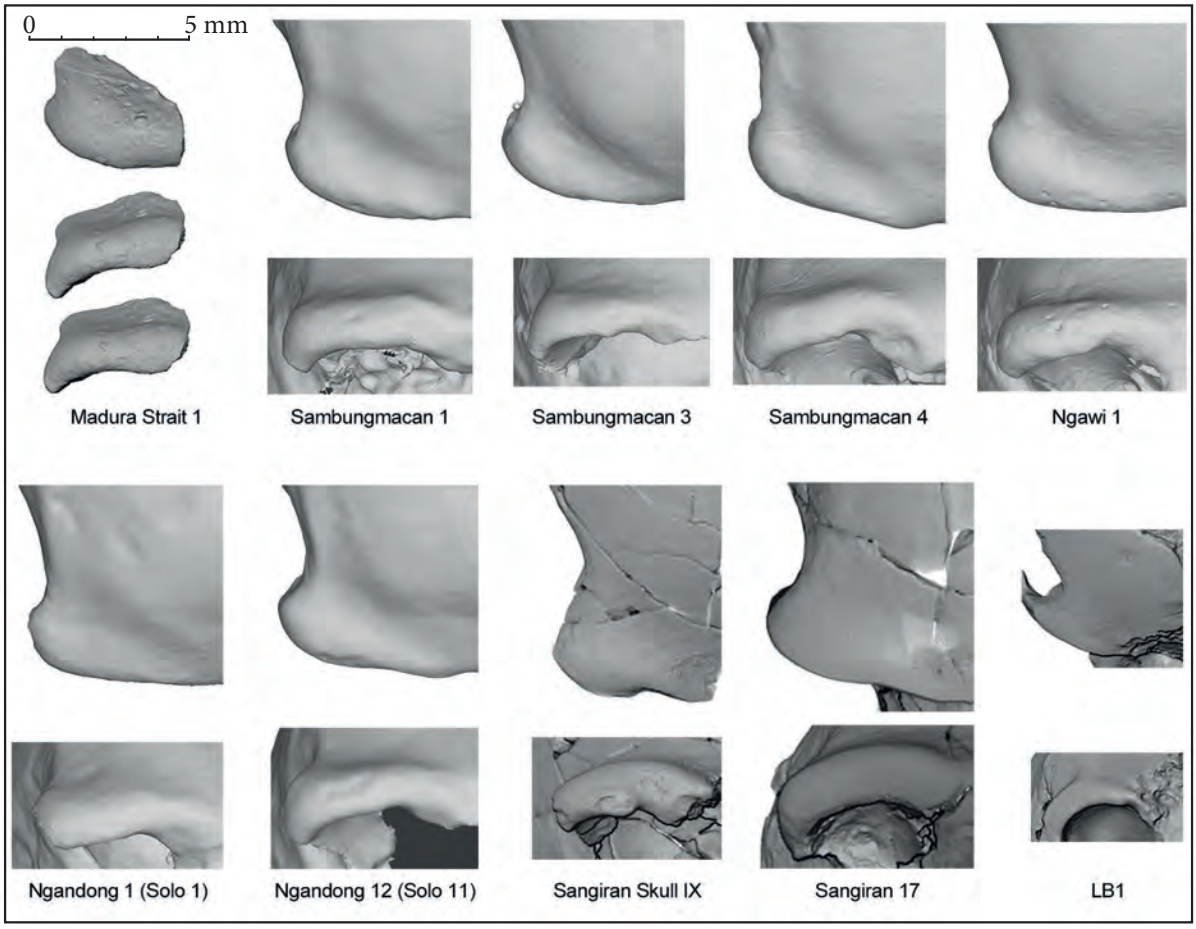


Fig. 7. Frontal and superior views of selected frontal bones from Indonesia. Data obtained from 3D surface scans and CT scans. Two versions of orientation are indicated for the anterior view of MS1 (the upper with reference to Sambungmacan 4 and the lower with reference to Sambungmacan 1, with the superior view based on the former). The left frontals (Sambungmacan 3 and 4) are flipped for ease of comparison.

4.2.1 Madura Strait 2

As a mid-parietal fragment, MS2 lacks the strong sagittal flexion as seen in *Homo sapiens* and may in this respect be regarded as morphologically archaic. The specimen is undiagnostic otherwise. The measured vault thickness along this part of the parietal line falls in the lower range of adult *Homo erectus* as well as modern *Homo sapiens* crania (Balzeau, 2006). The open suture and the modest cranial thicknesses indicate that the specimen derives from an individual that had not reached adulthood at the time of death.

5. Discussion and conclusions

Developmental age

The frontal fragment MS1 has a prominent supraorbital torus and an anteroposteriorly wide supratoral plane, but the torus thickness is slightly below the range of the known adult crania from Java **(Fig. 6A)**. This suggests that MS1 derives from a gracile adult or otherwise from an adolescent. The specimen does not preserve sutures that could have been indicative for developmental age. However, the available adolescent crania in our comparative sample, i.e. Ngandong 5 and Zhoukoudian 3, indicate that except for a slightly smaller size, their morphological differences from adult individuals from the same paleodeme are limited. Therefore, the uncertain developmental age of MS1 probably has limited impact on our morphological interpretations. The open sutures in the parietal fragment MS2 indicate that this specimen derived from a subadult individual.

Geography and chronology

The two hominin cranial specimens derive from the MIS6 (late Middle Pleistocene) valley fill of the Solo, which makes them contemporaneous to the late Javanese *H. erectus*, also referred to as the Ngandong/Sambungmacan/Ngawi pa-

leodeme. All of the reported fossils from this hominin group derive from the Solo Valley, ca. 150 to 200 km upstream of the Madura Strait subsea site. Therefore, in terms of geography and chronology, the two fossils from the Madura Strait may be tied to the Ngandong-Sambungmacan-Ngawi paleodeme.

Taxonomic affinities

Our comparison with various Asian archaic *Homo* crania indicates that the morphology of the frontal fragment MS1 fits comfortably with the sample of the late Javanese *Homo erectus* (the Ngandong/Sambungmacan/Ngawi paleodeme). It exhibits characteristic features of this group, such as a relatively straight supraorbital torus, a flat supratoral plane, a weak postorbital constriction, and a concave anterolateral portion of the frontal squama that slopes gently posteriorly. Within this sample, MS1 is most similar to the Sambungmacan crania, showing a very weak postorbital constriction and modest lateral thickening of the supraorbital torus.

However, MS1 is somewhat unique compared to our sample of the Ngandong/Sambungmacan/Ngawi paleodeme, in displaying a relatively thin supraorbital torus and a considerable supraorbital process. The limited thickness of the supraorbital torus may reflect a not fully matured individual. However, it is also possible that MS1 was an adult individual, in which case the specimen slightly expands the range of variation of supraorbital torus morphology and thickness of this hominin group. MS2, presumably from a subadult individual, shows an archaic character of modest curvature but is otherwise undiagnostic.

Fig. 8 shows MS1 in direct comparison with Sambungmacan 3, the late Middle Pleistocene *H. erectus* cranium from Java that is metrically close to MS1. In this comparative cranium, the supraorbital plane has a rather horizontal orientation. The original orientation of MS1 is unknown.

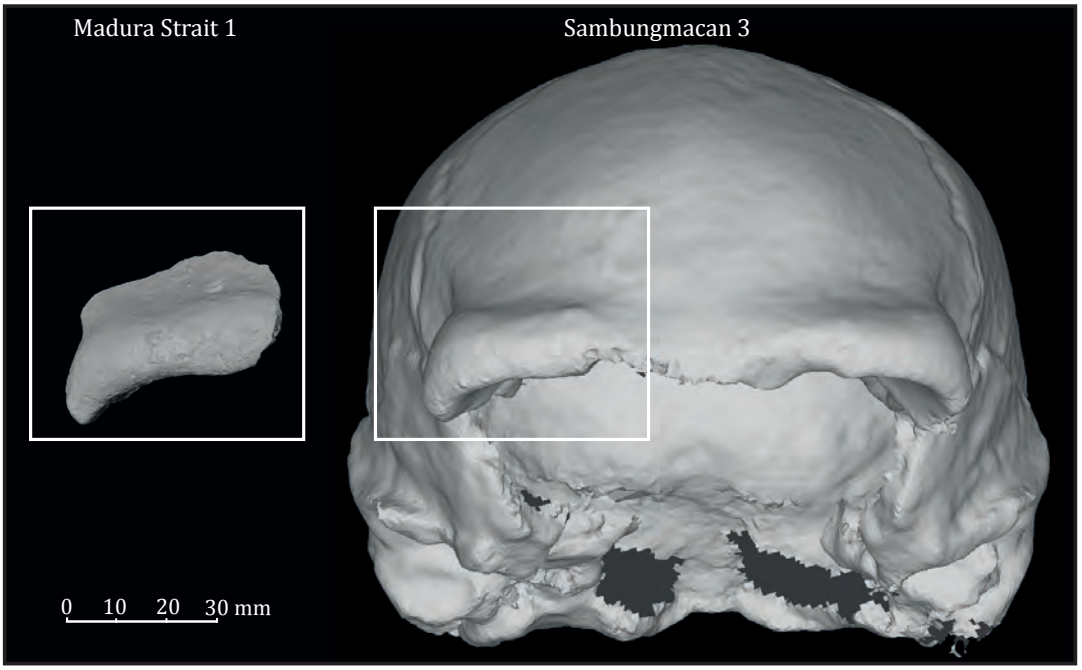


Fig. 8. 3D surface images of MS1 and Sambungmacan 3 (anterior view). This comparative skull has the closest metric and morphological match with MS1.

The MIS6 population of the Solo Valley

The late Javanese *Homo erectus* may be regarded as an MIS6 population living along the banks of the Solo or in the wider catchment area of the Solo. In the Middle Pleistocene climate of Java, characterized by long dry seasons, large perennial rivers such as the Solo probably offered 'fortunate conditions' (Dennell, 2008) for hominin populations, providing drinking water and aquatic food resources and attracting large herbivores. During the MIS6 glacial conditions, the Solo River proceeded eastwards over the exposed shelf of the present-day Madura Strait (Berghuis et al., 2025a, 2022, 2021).

The Madura Strait skull fragments show that the MIS6 *Homo erectus* that we know from Java also dispersed over the surrounding lowland plains, possibly following the course of the Solo. Other groups may very well have populated different areas, following the banks of other lowland rivers on the exposed Sunda Shelf. This lowland habitat places the assumed isolation of the Javanese *Homo erectus* lineage in a different perspective. At least during MIS6, the geographic range of the species exceeded Java and covered a larger area of Sundaland.

The rich vertebrate assemblage from the Madura Strait shows that the same accounted for most other mammalian species that we know from the Javanese fossil localities. This is also in line with the community structure reflected by the Middle Pleistocene vertebrate assemblages from Java, which represent balanced continental conditions, lack evidence of endemism and record the occasional arrival of new herbivore species such as *Elephas hysudrindicus, Rusa* sp., and *Axis javanicus.*

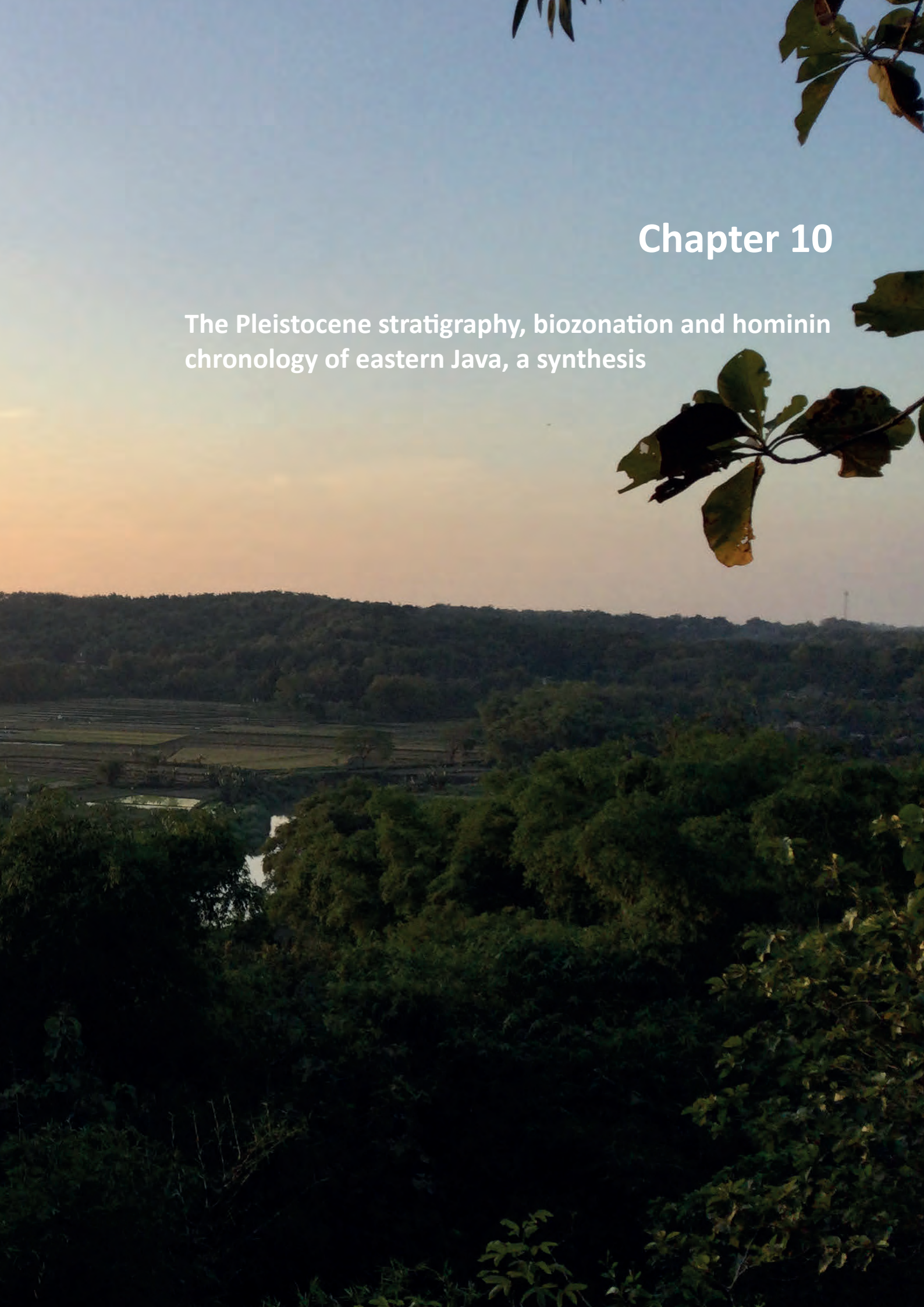
Subsea zooarchaeology

If *Homo erectus* and other Middle Pleistocene vertebrate species were able to disperse over the lowland plains of this part of Sundaland, why wouldn't contemporaneous hominin populations from the Asian mainland have been able to do the same, dispersing southwards over this landmass? Moreover, genomic studies on extant human populations have suggested the existence of Denisovans, a non-*erectus* group of archaic *Homo*, in the Sundaland region in the Late Pleistocene, prior to the arrival of anatomically modern humans (Teixeira et al., 2021; Jacobs et al., 2019; Cooper and Stringer, 2013). This also points to southward migration of post-*erectus* populations, from the mainland to Sundaland, but where is the fossil evidence?

Madura Strait 1, with its morphological and metric affinity with the late *Homo erectus* of Java, does not provide an answer to these questions. However, the two skull fragments do underline the potential of subsea hominin localities on the Sunda Shelf. The answers may very well be at the bottom of the sea.



The Sangiran dome at sunset. View from the southeastern margin of the dome.



Chapter 10

The Pleistocene stratigraphy, biozonation and hominin chronology of eastern Java, a synthesis

CHAPTER 10

From the Solo to the Madura Strait. The Pleistocene stratigraphy, biozonation and hominin chronology of eastern Java; a synthesis

H.W.K. Berghuis, 2026

1. Introduction

This PhD-study aimed for a detailed description of the Madura Strait subsea vertebrate site **(Fig. 1)** and its fossils, and an interpretation against the background of the Pleistocene biogeography of Java and the wider Sunda Shelf. The latter proved to be difficult within the existing framework of the Pleistocene stratigraphy and biozonation of Java. We therefore expanded the research efforts to the onshore vertebrate sites of Java, revising local stratigraphies and re-interpreting available fossil assemblages. The results of these investigations have been presented in **Chapters 2 to 5** of this thesis, focusing on the surroundings of Trinil, Jombang and Mojokerto **(Fig. 1)**. These on-land studies provided us with a much-improved understanding of Pleistocene landscapes and vertebrate communities of Java, against the background of tectonism, volcanism, sea-level fluctuations and climate change, and how these are expressed in the complex geological record of Java and the adjacent shelf. This finally made it possible to describe and interpret the geology and fossil fauna of the Madura Strait subsea site, as presented in **Chapters 6 to 9** of this thesis.

The geology and fossil fauna of individual sites have been described in great detail in the previous chapters and will not be repeated here. In this synthesis, I will shift the focus to the bigger scheme of the stratigraphy and vertebrate biostratigraphy for eastern Java. The stratigraphy of Duyfjes (1938a, 1936) and vertebrate biozonation of Sondaar (1984) have become 'part of the DNA' of all geologists, palaeontologists and archaeologists working on Java. As I will show, these frameworks require an update or revision. In the next sections, I will briefly describe the existing practice, discuss new insights, and present a revised framework.

The stratigraphy and biozonation of eastern and central Java are extremely complex issues, and the available literature on these subjects is enormous. I can only say that the proposed revisions are 'work in progress'. Future research will have to fill in the blanks, refine age ranges, and correct my mistakes.

Understanding hominin dispersal and evolution is the holy grail of geological and palaeontological research of Java. The Madura Strait assemblage, with its hominin skull fragments and traces of hominin subsistence strategies, forms an exciting contribution to our knowledge of the Pleistocene hominins of Java and the adjacent shelf. Also, the proposed revisions of the Pleistocene stratigraphy and biozonation of Java have implications for the interpretation of hominin presence in the region. Therefore, I will conclude this synthesis with a reflection on the chronology of hominin presence on Java and the larger Sunda Shelf, and its implications for hominin evolution and dispersal.

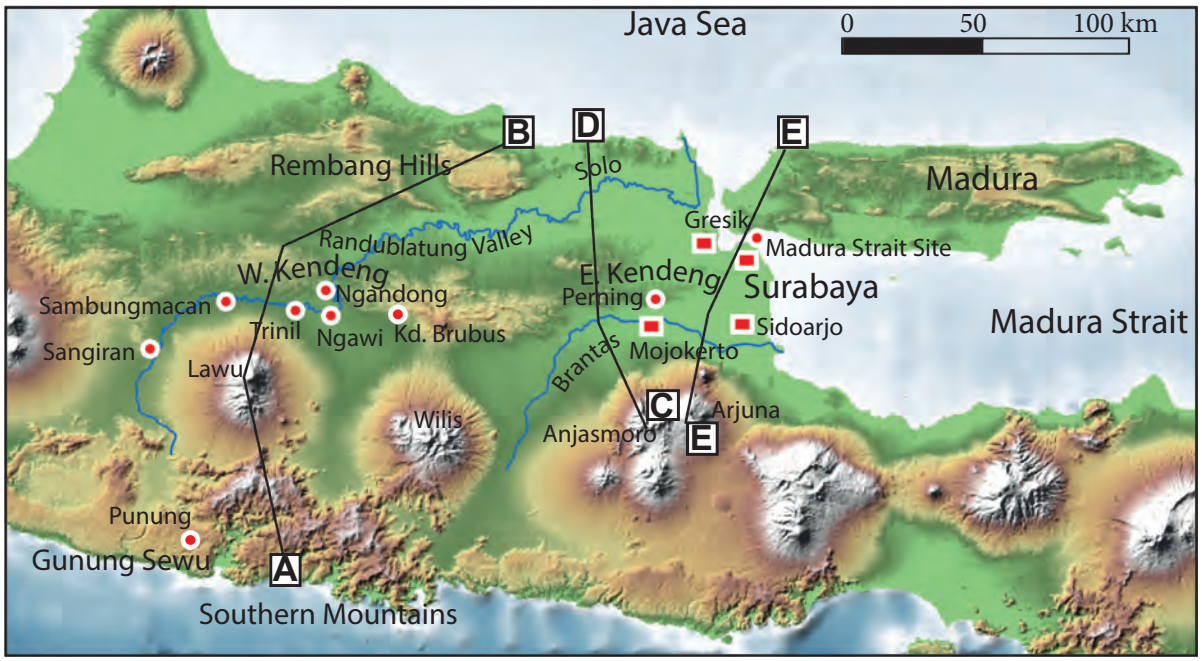


Fig. 1: Eastern Java, the Madura Strait site and other sites mentioned in the text. A-B etc: position of the cross-sections of **Fig. 4**. Map data: GEBCO and ALOS.

2. The shelf and the island

2.1 The shelf

The Sunda Shelf is the world's largest submerged shelf. The island of Java lies along its southern margin, bordering the Indian Ocean in the south, with the subduction zone, where the Australian Plate subducts under the Sunda Plate **(Fig. 2A)**.

Thus far, the Pleistocene stratigraphy of eastern Java has largely ignored its larger landscape context, along the margin of the Sunda Shelf, in a zone of complex subduction-related tectonism. An important question remains un-

answered: how does the Pleistocene stratigraphic record of Java relate to the off-shore stratigraphy of the submerged shelf, and what does this tell us about sea level fluctuations and stages of shelf emergence and submergence? For a shelf island like Java, this must be an essential aspect of its geological history, and one that directly affects our interpretation of the Pleistocene vertebrate communities including the famous *Homo erectus* of Java. Strangely, the Pleistocene vertebrate biozonation of Java is built on a model of such intermittent island stages and land bridges, however, the island stratigraphy does not provide a single clue about this changing landscape.

Since the discovery of ancient drainage systems on the bottom of the Java Sea (Molengraaff and Weber, 1921), it has been known that this wide shelf must have once been exposed. Van Bemmelen (1949) proposed to refer to this Pleistocene landmass as Sundaland. With the recognition of Pleistocene glacio-eustatic cycles, these stages of shelf exposures could be tied to glaciations (Voris, 2000). Sondaar (1984) and Van den Bergh et al. (2001) linked the vertebrate fossil record of Java to this alternation of island stages and land bridges, reflected by either endemism or the arrival of new species.

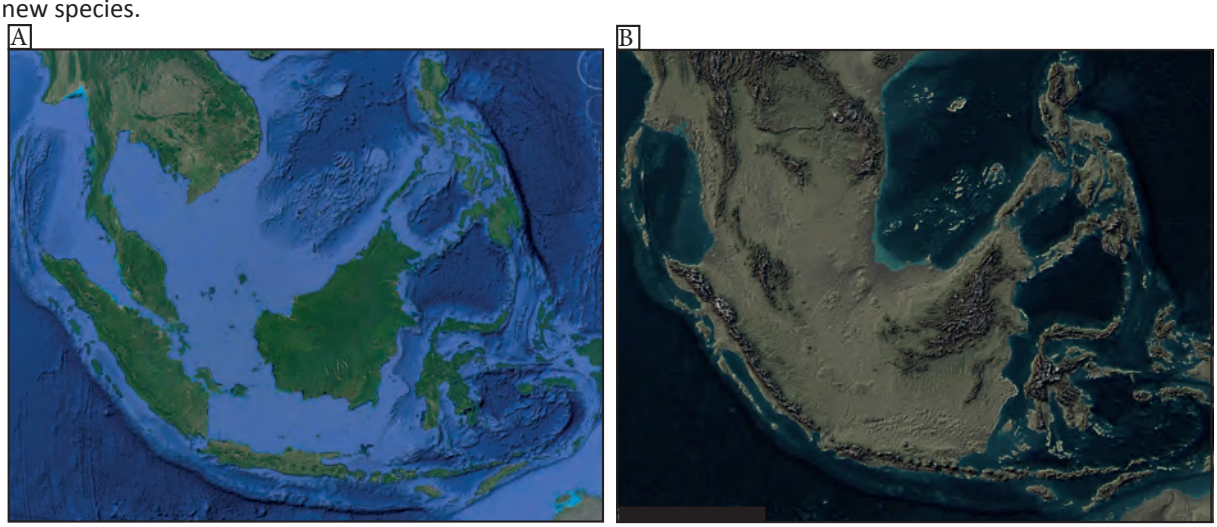


Fig. 2. A: The drowned Sunda Shelf, current situation, with the island of Java centrally in the south and the subduction zone south of the island. **B:** The exposed Sunda Shelf or Sundaland. The shelf was probably widely exposed during the Early and Middel Pleistocene, with intermittent stages of surface contraction during highstands from MIS11 onwards. Map data: Google Earth; Vivid maps, coastlines of the ice age.

Recent insights have completely changed our understanding of the Quaternary paleogeography of the Sunda Shelf. Instead of a stable, largely submerged shelf that was subject to intermittent emergence during sea-level lowstands, Sundaland was probably widely exposed throughout the Early Pleistocene (Louys and Kealy, 2024; Louys and Roberts, 2020; Husson et al., 2022, 2020) **(Fig. 2B)**. Only in the course of the Middle Pleistocene, regional subsidence, with an estimated rate of 0.2 mm/a, gradually brought the shelf surface within the range of sea-level fluctuations (Sarr et al., 2019). A reconstruction of shelf subsidence and Pleistocene sea-level fluctuations indicates that the first stage of large-scale shelf submergence probably dates back to MIS11 **(Fig. 3A)**. On the submerged shelf, this is expressed by a sub-seabed stratigraphy consisting of four to five stacked marine sequences **(Fig. 3B)**, overlying a basal unconformity (Susilohadi, 1995). This basal unconformity may be regarded as the subsided Early Pleistocene land surface of Sundaland, whereas the erosive boundaries between the marine sequences represent Middle Pleistocene, post-MIS11 land surfaces.

This new insight has enormous consequences for our interpretation of the stratigraphy and the vertebrate fossil assemblages of eastern Java, and may rightly be regarded as a paradigm shift. Dhani Irwanto (2016) published an on-line reconstruction of the gradually emerging Sundaland surface under the falling sea-level toward peak MIS2 lowstand conditions. This model can also be used for estimating the highstand Sundaland landscape of the last Middle Pleistocene interglacials, referring to the sea-level curve and the projected subsidence graph of **Fig. 3A**.

For example, during peak MIS11 highstand conditions, the sea-level reached a similar level as today, however, the shelf surface lay ca. 70 m higher than today. This implies that the MIS11 landscape may have been similar to the situation of '70 m below present sea level'. Admittingly, these are generalized reconstructions, suggesting a linear subsidence of the entire Sundaland surface. In reality, there were probably differences in tectonic regime across Sundaland. Nevertheless, the reconstructions give an astonishing image of the Middle Pleistocene highstand landscape **(Fig. 3C)**. During the highstands of MIS11 and 9, Sundaland contracted but remained a contiguous land surface, connected to the Asian mainland. During MIS7, Borneo became separated from the mainland, but Sumatra and Java appear to have remained connected to the Asian mainland as a peninsula, similar to present-day Malaysia, but longer.

Only during MIS5e, and of course during MIS1, a true island landscape developed, with Borneo, Sumatra and Java as islands in a shelf sea. We will see that this new view of Pleistocene Sundaland has significant consequences for our interpretations of the stratigraphy and vertebrate palaeontology of Java.

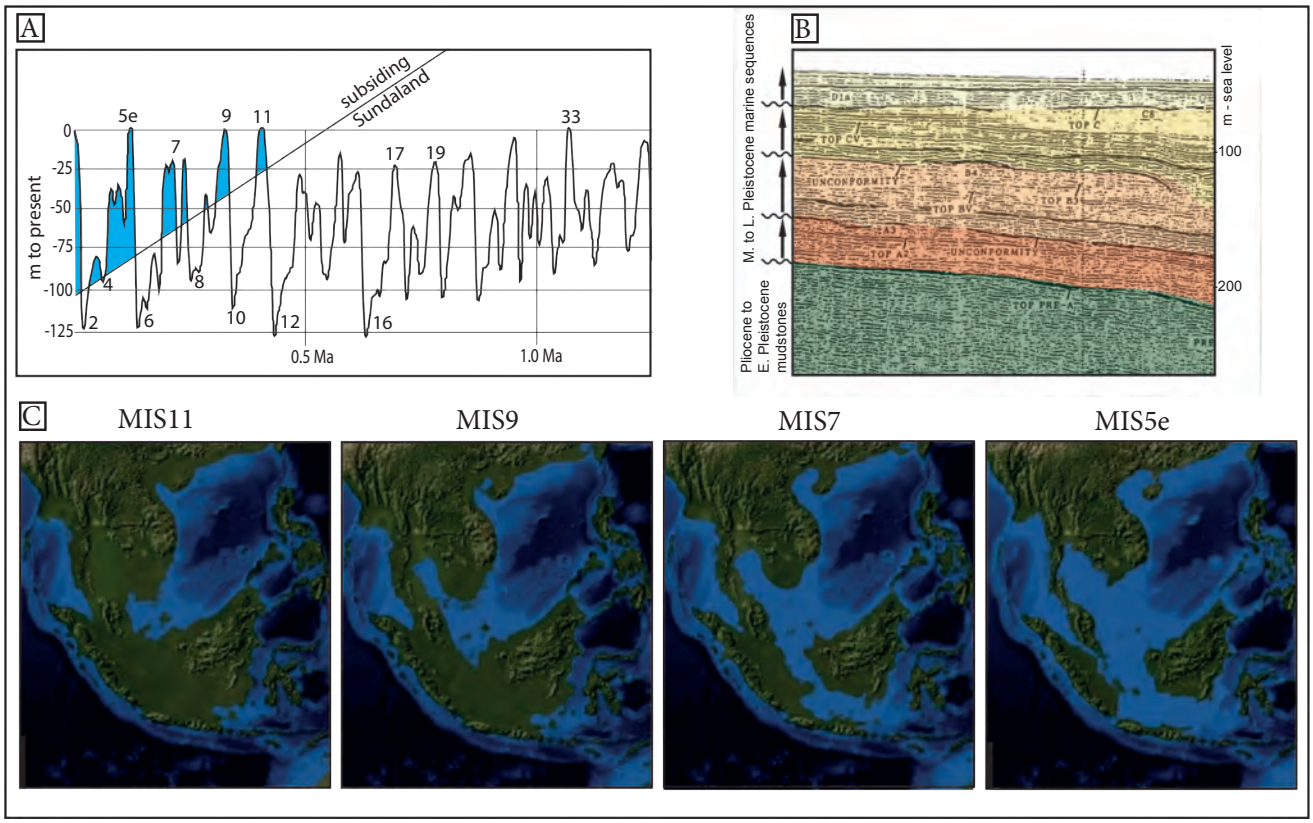


Fig. 3. A: Reconstruction of the subsiding central shelf in relation to sea-level fluctuations and subsidence. Sea-level curve based on Bintanja and van de Wal (2008), regional subsidence of 0.2 mm/a based on Sarr et al. (2019). **B:** Seismic profile over the Madura Strait (Susilohadi, 1995). Basal unconformity represents prolonged Early Pleistocene subaerial exposure. Overlying marine sequences with incised top represent intermittent stages of submergence during Middle Pleistocene highstands, under regional subsidence. First stage of large-scale submergence probably relates to MIS 11. **C:** Reconstructions of the maximum contracted land surface during Middle Pleistocene highstands. Java probably only came under island conditions during MIS5e and MIS1. Map data: Dhani Irwanto (2016).

2.2 The island

Java lies along the dynamic southern margin of the Sunda Shelf, an area shaped by tectonism and vulcanism related to the nearby subduction zone. An array of volcanoes forms the core of the island. However, Java is more than just an island arc. Folded Tertiary strata testify to a long and complex geological past. Three north-south cross-sections of eastern Java **(Fig. 4)** illustrate the geological structures of eastern Java down to a depth of 1,000 m. The sections are based on published studies of oil wells, seismic profiles, and outcrops, summarized by Lunt (2013). It is important to note that simplifications were inevitable. The positions of faults and folds are schematic, and strata have been grouped into composite units. Below, I present a brief discussion of the cross-sections, referring to relevant tectonic and volcanic stages in chronological order.

Paleogene rifting

In the Paleocene and Eocene, active subduction temporarily ceased in the area of present-day eastern Java, and the shelf margin came under an extensional regime (Zahirovic et al., 2016b). A rift system formed, consisting of east-west and southwest-northeast oriented grabens and half-grabens (Lunt, 2013). The basement faults are not shown on the cross-sections, but their presence and continued activity are reflected by folds and faults in the overlying strata. The Paleogene graben-fill makes up the core rocks of the Rembang Hills and Southern Mountains. As we shall see, these hill ranges are inversions of ancient grabens.

The Miocene volcanic arc and its back-arc basin

In the Early Miocene, subduction and volcanism returned to this area (Hall, 2013). A volcanic arc developed in the rift valley that is nowadays prominent as the Southern Mountains. To the north, a back-arc basin formed, which covered most of present-day eastern Java. In the cross-sections, this basin is recognizable by its Mio-Pliocene fill. Along its northern margin, the back-arc basin incorporated the older grabens. In the Late Miocene, active subduction again ceased (Hall and Spakman, 2015). The volcanic arc eroded and was covered with coral reefs (Smyth et al., 2008). The back-arc basin became deprived of clastic supply and the sedimentary regime changed to settling of calcareous ooze, which continued throughout the Pliocene.

Pliocene compression, uplift zones, and the development of an intermediate basin

In the course of the Pliocene, the area came under a northward-directed compressive regime (Hall and Smyth, 2008).

The ancient rift valleys inverted, forming the Southern Mountains and the Rembang Hills, which emerged in the Late Pliocene (Husein et al., 2015; Satyana et al., 2004). Several isolated uplifts, such as the Sekarkurung and Ngimbang Hills, are similar inversions. During this same period, the western Kendeng Hills formed in the axial zone of the back-arc basin. Low-angle, northward-verging folds and thrust faults point to compression of the basin-fill, thin-skinned deformation and detachment of the mudstone-dominated basin-fill from underlying more rigid strata (Genevraye and Samuel, 1972).

The emerging uplift zones changed the adjacent area into a sheltered, shallow-marine basin. It had open connections to the Indian Ocean in the south, through tectonic gaps in the Southern Mountains, and probably also to east, over the Madura Strait shelf. In the northeastern part of this basin, a fill of massive marine clays testifies of a high supply of fine detrital material. The sediment was probably supplied from the North Serayu uplift of Central Java. The clays reach a thickness of several hundred meters, pointing to subsidence. This setting, of a narrow, relatively deep, subsiding embayment between emerging hill ranges, points to ongoing inversion, with the subsiding basin as a paleo-high of the Paleogene rift system.

The area around Sidoarjo serves as a striking example of this inversion-related subsidence. This site is well-studied, due to its reservoir rocks and by the disastrous mudflow that was caused by a test drilling. The area was a horst within the old rift system, which changed into a reef-capped shoal in the Miocene back-arc basin. It inverted under Pliocene compression and became a zone of extreme subsidence (Mazzini et al., 2007; Kusumastuti et al., 2002). The local Late Pliocene to Pleistocene fill reaches a thickness of ~ 1,000 m.

In the basinal area in the southwest, south of the western Kendeng, conditions were completely different. A fill of mollusc-rich calcareous mudstones, with burrows and coral fragments, points to the development of a shallow, clear-water lagoon. The lagoon must have been sheltered from mud supply by the western Kendeng. Moreover, the deeper, subsiding embayment in the northeast must have formed an effecient trap for mud, preventing its further transport. The lagoon was connected to the Indian Ocean in the south through a wide gap in the Southern Mountains. This gap is today recognizable as the Gunung Sewu, a low hill range that only became subject to uplift in the course of the Middle Pleistocene (Rizal et al., 2020).

Emergence of the intermediate basin, volcanism, and local subsidence

Paleosols show that the sheltered basinal area eventually emerged. Scarce planktonic markers, as well as estimates of sedimentation rates, suggest that this emergence dates to ~2 Ma. Around this same time, active volcanism returned to eastern Java, reflecting resumed subduction. The Wilis and Old Lawu are the oldest volcanoes in this area. Both developed in the lowland zone between the Southern Mountains and the western Kendeng. In the cross-sections, I assumed collapse structures below the edifices, reflecting emptying of magma chambers and loading by the cones.

The surrounding lowland was occasionally overrun by volcanic mass flows. Stacked volcanic breccia layers with a great lateral continuity illustrate the enormous scale of these mass flows. The breccia layers are separated by ferralitic paleosols or interbeds of black coastal clays, indicating a setting on a humid, marshy and forested coastal plain that must have been tectonically relatively stable throughout the Early Pleistocene.

The area in the northeast became subject to renewed subsidence and was once again invaded by the sea, forming an embayment that was probably connected to the Indian Ocean in the south. A second unit of marine clays was deposited, with lenticular sandy laminae, pointing to shallow, tide-dominated conditions.

Middle Pleistocene: local uplift, regional subsidence

Around the Early to Middle Pleistocene transition, eastern Java came under renewed or increased compression. The western Kendeng fold zone became re-activated, which also affected the fill of the adjacent basins. In the northeast, the shallow embayment emerged or silted up. This may partly have been triggered by the build-up of the Anjasmoro Volcano, which blocked the connection to the Indian Ocean. With this closing of the southern ocean-connection, the Brantas developed as a large, eastward-directed drainage system. Later, the Solo developed as a second, eastward-directed drainage system.

Around the same time, the wider Sunda Shelf came under a regime of subsidence (Sarr et al., 2019). The lower parts of the shelf became intermittently and progressively submerged during highstands. The Brantas and Solo drainage systems responded to this intermittent drowning of their lower reaches with cycles of incision and deposition, forming incised valleys in their lower reaches that continue below the seabed of the Madura Strait shelf. In the higher reaches, the rivers formed fluvial terraces. The core of eastern Java, however, remained under compression. A series of new anticlines formed, folding the fill of the Plio-Pleistocene, mud-dominated embayment, and shaping the eastern Kendeng Hills.

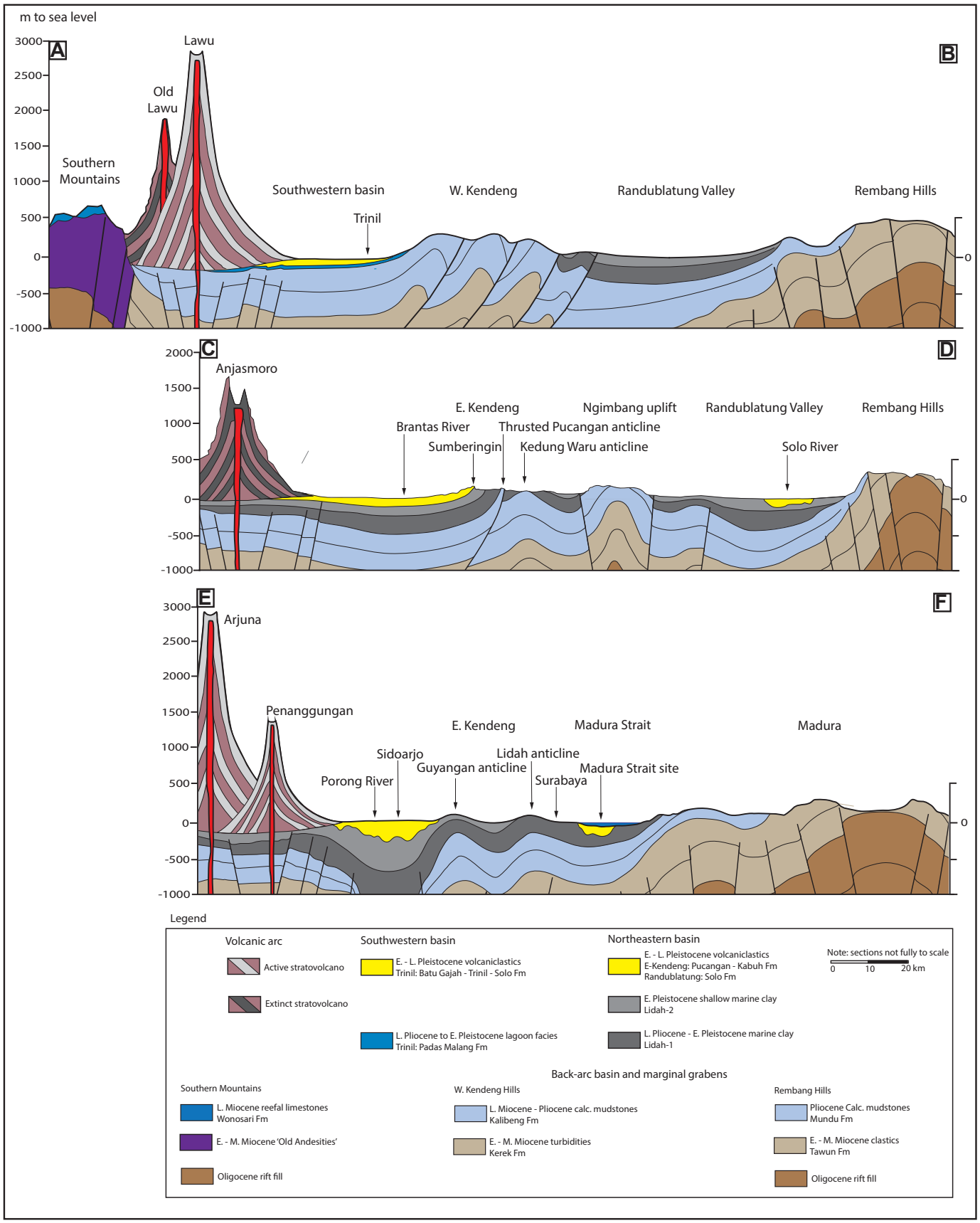


Fig. 4. Schematic cross-sections over eastern Java; structural setting of the relevant depositional basins. Position of the cross-sections indicated on **Fig. 1.**

3. The late Pliocene and Pleistocene stratigraphy of eastern Java

3.1 The stratigraphy of Duyfjes

For almost a century, researchers have based their interpretations of the Pleistocene geology of eastern Java on the stratigraphy of Duyfjes (Duyfjes, 1938a, 1936). This stratigraphy assumes the existence of an uninterrupted and laterally continuous depositional record of marine, deltaic, fluvial and volcanic strata, reflecting the emergence of eastern Java, as a result of volcanic supply and coastal progradation. This long depositional record was subsequently folded and uplifted, forming the Kendeng Hills. As was normal in these days, Duyfjes' units are chronostratigraphic constructs. His model of uninterrupted sedimentation allowed him to correlate his units across the hill range. Correlations were based on thickness measurements and 'parallelization', which implies that he combined different facies in the same unit, assuming that these strata are of similar age and represent lateral variation of the depositional landscape.

In the introduction to this thesis, I provided a graphic overview of Duyfjes stratigraphy and his correlations.

3.2 New insights

Identifying depositional basins

Duyfjes (1938a) referred to his stratigraphy as the 'Kendeng stratigraphy'. This suggested the existence of a large depositional basin, the fill of which had been folded and uplifted as the Kendeng Hills. However, as explained in **Section 2.2**, the structural setting of eastern Java is more complex. The Kendeng Hills are a composite of two tectonic structures. The western Kendeng is the thrusted fill of the Mio-Pliocene back-arc basin. As a result of the uplift of this fold zone, shallow embayments formed in the surrounding area. The eastern Kendeng is younger and is the smoothly folded fill of a Late Pliocene to Pleistocene, mud-dominated embayment. What may have confused Duyfjes is that syntectonic deposition and reactivation of the western and eastern Kendeng affected the fill of the adjacent younger basins. Note the situation along the margins of the western Kendeng thrust zone (cross-section AB, **Fig. 4)**, where the deformation of the younger basin fill gives the impression that these strata are part of a folded 'Kendeng stratigraphy'.

In a complex and composite deformation zone as eastern Java, it is helpful to identify relevant depositional basins and define recognizable lithostratigraphic units that describe the fill of these basins. The most obvious basin is the Mio-Pliocene back-arc basin. In **Fig. 4**, it is recognizable by its fill of Early to Middle Miocene volcaniclastic deposits and Late Miocene to Pliocene calcareous deposits. These roughly correspond with Duyfjes' Kerek and Kalibeng Formations, which are valid and useful stratigraphic units.

After the compression of the Mio-Pliocene back-arc basin and the emergence of uplifted ridges such as the Rembang and western Kendeng Hills, a new landscape formed, with an intermediate, shallow marine basin. It is important to distinguish between a subsiding, mud-dominated embayment in the northeast and a tectonically more stable, initially clear-water basin in the southwest. In the latest Pliocene, these two basins may have been partly connected, but the development of the Wilis caused a complete separation. The fill of the subsiding, mud-dominated basin in the east is exposed in the young folds of the eastern Kendeng, around Jombang and Mojokerto. The fill of the southwestern basin is exposed along the southern footslopes of the western Kendeng and in the Sangiran dome.

3.3 A new stratigraphic framework

From local to regional

In **Chapters 2 to 6** of this thesis, I repeatedly emphasised the difficulties of long-distance correlations and the necessity of working with local stratigraphies. Obviously, this may have obscured the context of the eastern Java stratigraphy and the chronological relations between individual sites. With new numerical ages and an improved understanding of the larger Pleistocene landscapes of eastern Java, it is now possible to place these local stratigraphies in a broader context.

The two Pleistocene basins

Fig. 5 presents an overarching stratigraphic summary for the Late Pliocene and Pleistocene of eastern Java, integrating the stratigraphic records of various sites into a chronological framework. The top of the Kalibeng Formation represents the final stages of the Mio-Pliocene back-arc basin. With the uplift and emergence of the Rembang and western Kendeng, two new basins developed.

The northeastern basin, in the figure represented by the Randublatung Valley, Surabaya and Mojokerto, is marked by its mud-dominated fill. Planktonic foraminiferal markers date the transition from calcareous mudstones to marine clays to 3 Ma, which forms a strong indication of the age of emergence of the fold zones and the development of the intermediate embayment. The fill of the embayment has a relatively uniform build-up, consisting of two marine clay

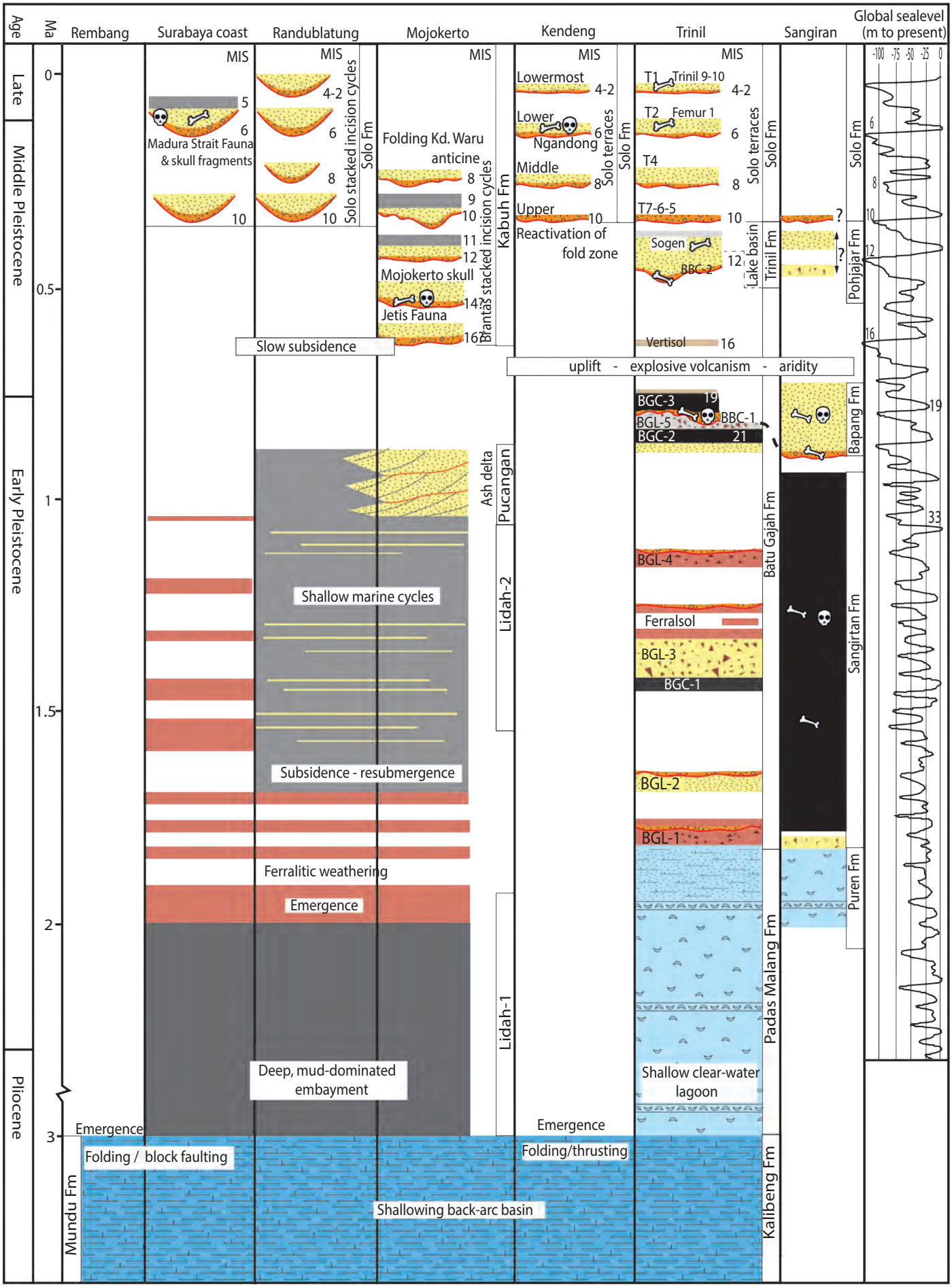


Fig. 5. Stratigraphic summary of eastern Java. Chronological framework of the stratigraphy of various sites and landscape stages. Sea-level curve: Bintanja and Van der Wal (2008). Stratigraphy, ages and correlations based on **Chapters 1-5** of this thesis.

units, referred to as Lidah-1 and 2, representing the early deep-water embayment and the subsequent tide-dominated shallow embayment. The clays are separated by a ferralitic paleosol.

The southwestern basin, in the figure represented by Trinil and Sangiran, is characterized by a basal fill of calcareous sediment with shells and corals. Planktonic markers again show that the transition from open marine to sheltered conditions occurred during the latest Late Pliocene. The calcareous, shell-bearing strata are overlain by coastal black clays and volcanic breccias, and subsequently by fluvial volcaniclastics.

Stratigraphic units

Duyfjes' defined his Pleistocene units in the eastern Kendeng. In the revised stratigraphy, these units have remained mostly in-tact, though with revised unit boundaries, and with a local significance only, for the eastern Kendeng and the adjacent coastal plains of Surabaya and the Randublatung Valley. All marine clays are referred to as the Lidah Formation, as proposed by Brouwer (1966). This is the most prominent unit of the northeastern basin.

The occurrence of Lidah-1, the oldest massive clays, demarcates the position of the embayment that formed between the emerging hill ranges around 3 Ma. Lidah-2 is the fill of the subsequent, shallower embayment. The Pucangan Formation only refers to the ash-dominated deltaic beds, which locally form the top of the fill of the 'Lidah-2-embayment'. The Kabuh Formation refers to the overlying fluvial sequences of the Brantas, which are only exposed in the eastern Kendeng. Note the erosive contact between the Pucangan and the Kabuh Formations. Instead of a prograding deltaic sequence of foresets and topsets, as previously assumed, both units are unrelated and separated by a depositional hiatus.

The stratigraphic units of the southwestern basin have been defined as a new, local stratigraphy for the Trinil area and replace the former units, which were based on correlations with Duyfjes' reference sections in the eastern Kendeng. Note that the new units cannot be compared one-on-one with the former units of Duyfes as used in this area. For example, the Kabuh Formation of Trinil appeared to be an amalgamation of fluvial strata of different ages, including terrace-related deposits of the Solo drainage system.

For the Sangiran area, I used the revised unit names by Itahara et al. (1985), which are a renaming of Duyfjes' units, without further justification.

Chronological ordering

The chronological ordering of the deposits that make up the fill of the two Late Pliocene to Pleistocene basins has been based on the detailed stratigraphic studies, as presented in Chapters 1 – 5 of this thesis. Sea-level calibration is most reliable for the Middle to Late Pleistocene fluvial sequences and terraces of the Solo and the Brantas. For the fluvial cycles of the Solo, this sea-level signal is validated by OSL-datings. The cyclic record of the Brantas and the Solo has also been linked to the Middle Pleistocene marine sequences of the submerged shelf, as shown by seismic profiles **(Fig. 3B)**.

For older strata, the chronological ordering relies largely on occasionally available radiometric dating studies and paleomagnetic profiles. Rough age indications are also inferred from paleoclimate indicators and volcanic markers. There is ample evidence of a climate shift from a humid tropical to a dry climate with a pronounced rainy season, around 1 Ma. Around the same time, there has been a change of volcanic style, from large andesitic strato-volcanoes that occasionally collapsed, to more explosive ash-rich eruptions. For the oldest marine strata, planktonic foraminiferal markers provide insight into age ranges.

One of the interesting features of this (provisional) chronological ordering is that it highlights the fragmented preservation of the Pleistocene depositional record **(Fig. 5)**. The previous, Duyfjes-based stratigraphy of eastern Java has been presented in block-form, suggesting ongoing deposition. This is correct for the marine fill of the Mio-Pliocene back-arc basin, and probably also for the earliest marine stages of the subsequent Plio-Pleistocene basin. However, it certainly does not apply to the overlying coastal and terrestrial strata, which form intricate and laterally variable depositional records, with long hiatuses, that represent either incision or non-deposition.

The bone beds: ages and correlations

Probably the most interesting aspect of the stratigraphic framework is that it places the most important vertebrate-bearing beds of eastern Java in a chronological context. The Sangiran area yields the oldest known vertebrate beds of the eastern part of Java. The fossils are found in a ~ 100 m thick unit of black clays (Sangiran Formation), which was deposited in a coastal marsh. Dated interbeds of volcanic ash and paleomagnetic profiling offer reliable age control over the clay unit (Matsu'ura et al., 2020). The oldest vertebrate fossils are found in its middle part, predating 1.5 Ma. The first hominin fossils are found higher up, at a level that has been dated to ~ 1.1 Ma, or possibly ~1.3 Ma. The black clays of Sangiran form the landscape equivalent of the thinner black-clay interbeds in the brec-

cia-dominated Batu Gajah Formation of Trinil, reflecting a slightly higher topographic setting of Trinil, along the foot of the Old Lawu.

The black clays of Sangiran are sharply overlain by a conglomerate bed (Grenzbank) and subsequently by cross-bedded fluvial sandstones, referred to as the Bapang Formation. Both yielded vertebrate fossils, including hominin remains. The Grenzbank has been dated to ~900 ka. The overlying fluvial sandstones were deposited shortly after. Higher-up in these sandstones, the Brunhes-Matuyama transition (773 ka) forms a reliable age anchor. The hominin fossils of this sandstone unit derive from the stratigraphic range below this polarity reversal.

Since the earliest hominin finds in Sangiran (Von Koenigswald, 1933), the Grenzbank has been correlated with the bonebed of Trinil, traditionally referred to as the Haupt Knochenschicht or HK. Both the Grenzbank and the Haupt Knochenschicht are incisive lags that mark a transition to sandy fluvial deposits. Our re-inventory and dating study of the Trinil excavation site revealed that the Haupt Knochenschicht consists of two superimposed channel lags, which we refer to as Bone Bearing Channel (BBC) 1 and 2 (Hilgen et al., 2023). BBC-1 has an age range of 830 – 773 ka, based on multiple radiometric measurements and its reversed magnetic polarity. BBC-2 is significantly younger and dates to ~450 ka. The correlations between Sangiran and Trinil are of great relevance for our interpretations of fossil faunas and the hominin chronology of eastern Java, which will be further discussed in **Sections 4 and 5**.

Most of the younger bone beds of eastern Java are associated with Middle Pleistocene fluvial sequences of the two large drainage systems. The bone beds of Mojokerto are deposits of the ancient Brantas. In the revised stratigraphy, Duyfjes' Kabuh Formation only refers to these fluvial sequences of the Brantas. This is in line with its vertebrate fossils, forming the Middle Pleistocene Kedung Brubus Fauna. Note that these fossils formed the Early Pleistocene Jetis Fauna of Von Koenigswald (1935), which had made Duyfjes (1938a) decide to regard the material as the Early Pleistocene Pucangan Formation. This inconsistency is resolved in the revised stratigraphy, however note the ongoing discussion on this subject **(Chapter 5)**.

The fluvial sequences of the Solo are represented by fluvial terraces in Sangiran, Trinil and the Kendeng traverse valley. The drainage system probably goes back to MIS10. The lower terrace of Ngandong, one of the richest vertebrate sites of eastern Java, was dated to 140 – 92 ka (Rizal et al., 2020) and can probably be correlated to MIS6. OSL-datings and reconstructions of fluvial incision and aggradation cycles indicate that the T2-terrace of Trinil is the equivalent of the Ngandong terrace. Downstream of the Kendeng traverse valley, the fluvial cycles of the Solo proceed as incised channels in the Randublatung Valley and below the seabed of Madura Strait. The Madura Strait subsea vertebrate site is a transgressively filled incision of MIS6, which links this site to the terrace of Ngandong. Note that MIS4 or MIS2 incisions are absent in the Surabaya coastal area. We assumed that during MIS4, a new transverse valley was cut through the Rembang, leading the river towards the Java Sea shelf in the north.

One vertebrate-bearing level has remained unmentioned. This is a ca. 60 m thick unit of fine, parallel-bedded fluvial tuffs, with paleosols and occasional shallow erosion structures, and with interbedded lacustrine clays, exposed in the Trinil area. This material was previously referred to as the local representative of the 'Kabuh Formation', together with unrecognized terrace deposits and the older fossil-bearing lags deposits. The strata, which we referred to as the Trinil Formation, represent an interesting local landscape stage, when the area around Ngawi was isolated from the marine base level, probably by a volcanic barrier between the Lawu and the western Kendeng. The deposits reflect the existence of a lake, surrounded by a fluvial plain. The material overlies BBC-2, and is incised by the terraces of the Solo, which leaves a short time window of ~ 450 to 375 ka as the likely age range of the Trinil Formation. In **Section 5.2** I will present a detailed profile of Trinil, in relation to its hominin fossils, which provides an interesting image of the setting of this unit.

A Mid-Pleistocene hiatus: Uplift, climate change and volcanic ash

The stratigraphic summary **(Fig. 5)** shows the Early to Middle Pleistocene transition as a poorly represented period in the depositional record. The few preserved records from this period, such as the Grenzbank and Bapang Formation of Sangiran, the bone-bearing channels (BBCs) of Trinil, and the ash-rich delta of the Mojokerto area, testify to significant landscape changes. There were probably three factors involved. One, renewed compression and uplift, which pushed the coastal zone around Sangiran and Trinil above the range of coastal sedimentation. Two, a change of volcanic style, toward more explosive, ash-rich eruptions. And three, a regional change from a humid tropical climate to a much drier climate, with a pronounced rainy season. In eastern Java, these three factors caused a severe landscape change, transforming subsiding coastal forests into dry, grass-covered plains subject to local incision and intermittent ash-falls. In Trinil, this landscape is reflected by local occurrences of fossiliferous channel lags, i.e. the BBCs. The lags are rich in reworked carbonate concretions, pointing to erosion of vertisols. The channel lags also contain ash lenses, probably representing contemporary eruptions. The soil erosion reflects intermittent destruction of the vegetation cover, due to periods of extreme drought and/or events of ash-fall. To the east, the increased ash supply is represented by the development of ash-dominated deltas in the shallow 'Lidah-2'-embayment.

Looking in detail at the Trinil stratigraphy of this period, the relatively young age of the two highest clay beds of the Batu Gajah Fm, BGC-2 and BGC-3, appears to be an anomaly, as they fall in the onset of the period with harsher and drier conditions. Their inferred ages have been based on the numerical ages provided by Hilgen et al. (2023) and the observation that the lahar BGL-5 appears to have overrun the coastal marsh of BGC-2, taking up clay balls from the surface. A slightly older age of the BGC-2, which aligns more closely with the age of the clays of Sangiran, seems logical. The significance of the third clay layer, exposed only on the right river bank in Trinil, may also be reconsidered. This is probably not a coastal clay bed with a wide lateral continuity, like the underlying clay beds, but rather the fill of a local pond.

4. The vertebrate biozonation of central and eastern Java,

4.1 The biozonation of De Vos and Sondaar

Since the 1980s, the vertebrate fossils of eastern Java have been interpreted in terms of faunal stages, based on the work of De Vos et al. (1982) and Sondaar (1984), with an update by Van den Bergh et al. (2001). The authors recognized seven faunal units, which are assumed to reflect the vertebrate community of eastern Java during a specific period (see also the introduction to this thesis). The Satir and Ci Saat Faunas refer to the fossil species excavated from a thick series of fluvial sandstones and interbedded black clays exposed near Bumiayu, in the western part of Central-Java. Note that the stratigraphy and palaeontology of this part of Java falls outside the scope of my studies. However, the two faunal units have become relevant for the eastern part of the island by their correlation to the fossil-bearing series of Sangiran **(Section 4.2)**.

The Trinil-HK Fauna contains the fossil species from the basal bone beds of the Dubois excavation site in Trinil, previously known as the Haupt Knochenschicht (HK) and now identified as BBC-1 and BBC-2. The Kedung Brubus Fauna refers to the vertebrate fossils from Kedung Brubus, ca. 35 km east of Trinil. The site, excavated by Dubois in the late 1890s, consists of a fluvial sandstone series with a reported thickness of ~200 m (Duyfjes, 1936; Van Es, 1931). The Ngandong Fauna contains the fossil species from the lower terrace of the Solo in the Kendeng traverse valley. The Punung and Wajak Faunas are cave faunas from the Southern Mountains.

Order		Proboscidea				Primates						Rodent.		Ph	Carnivora					Perisso.		Artiodactyla													
Species / Unit	*Sinomastodon bumiajuensis*	*Stegodon trigonocephalus*	*Elephas hysudrindicus*	*Elephas* sp.	*Elephas maximus*	*Macaca* sp.	*Trachypithecus* sp.	*Hylobates* sp.	*Pongo* sp.	*Homo erectus*	*Homo sapiens*	*Hystrix* sp.	*Rattus* sp.	*Manis*	*Panthera tigris*	*Panthera pardus*	*Canis* sp. / *cuon* sp.	*Lutrogale* sp.	*Pachycrocuta brevirostris*	*Tapirus indicus*	*Rhinoceros sondaicus*	*Hexaprotodon sivajavanicus*	*Sus brachygnathus*	*Sus macrognathus*	*Sus* sp.	*Axis lydekkeri*	*Axis javanicus*	*Muntiacus muntjak*	*Rusa* sp.	*Cervidae* indet.	*Bubalus palaeokerabau*	*Bubalus arnee*	*Bos palaeojavanicus*	*Bos javanicus*	*Bovidea* indet.	*Duboisia santeng*	*Epileptobos groeneveldtii*
Wajak																																			
Punung																																			?
Ngandong																																			
Kd. Brubus																																			
Trinil HK																																			
Ci Saat																																			
Satir																																			

Table 1. Pleistocene vertebrate (mammalian) biozonation of eastern Java, with updated species lists based on De Vos et al. (1982), Sondaar (1984) and Van den Bergh (2001), Badoux (1959), Storm (2001), Storm et al. (2005), Storm and de Vos (2006), Volmer et al. (2015), Van der Geer et al. (2018) Van den Bergh et al. (2019). Punung and Wajak Fauna includes faunal remains from contemporary caves, following the work of the authors mentioned above. See text for clarifications. Note: species list is not complete. See full lists of above-mentioned works.

The faunal units are commonly presented in the form of a species list. **Table 1** is a new update of this list, with revised taxonomic names, an improved taxonomical ordering, additions of new finds and several taxonomic re-interpretations. New species have for example been added based on finds from the Madura Strait site, which falls under the Ngandong Fauna. Taxonomic re-interpretations have been made for the Punung Fauna. Justifications for the changes are provided in the captions and in this text.

The species composition of successive faunal units has commonly been interpreted in terms of alternating island stages and stages with a continental connection, as a result of Pleistocene glacio-eustatic sea-level fluctuations. The Satir Fauna is regarded as an island fauna. It is very poor in species, all of which are renowned for their ability to cross sea barriers and colonize islands. *Sinomastodon*, an archaic proboscidean taxon of Asia, is the marker species of this fauna. The fauna also contains a giant land tortoise, which is highly characteristic of island communities. The Ci Saat Fauna records new arrivals: *Stegodon trigonocephalus* (replacing *Sinomastodon*), bovids, and *Panthera tigris.* In Sangiran, the Ci Saat Fauna also contains a large canid, as a second carnivore species (Volmer et al., 2016). Moreover, it records

the first hominins on Java. These new arrivals, and the extinction of the large tortoise, point to a mainland connection. Nevertheless, the fauna is commonly still described as 'poor in species' and 'unbalanced', which is explained in terms of marginal isolation, only allowing for corridor dispersal or filter dispersal of vertebrate species (Van der Geer et al., 2018; Van den Bergh et al., 2001).

The subsequent Trinil-HK Fauna again records new species: the small bovid *Duboisia santeng, Sus brachygnathus*, several non-hominin primates and a smaller canid. At the same time, the hippo *Hexaprotodon sivalensis*, common in the two previous faunal units, disappears. Yet, the fauna is commonly still regarded as 'unbalanced'. The subsequent Kedung Brubus Fauna records *Elephas hysudrindicus* and a large-statured cervid of the genus *Rusa* as new arrivals. Moreover, there are scarce records of a new bovid (*Epileptobos groeneveldtii*) and a large suid (*Sus macrognathus*). This fauna is finally regarded as 'balanced', reflecting an open mainland connection, which Van den Bergh et al. (2001) linked to the onset of the Middle Pleistocene glacial-interglacial regime, with large-amplitude sea-level cycles and more pronounced lowstands.

The Ngandong Fauna is similar to the Kedung Brubus Fauna. De Vos et al. (1982) noted that it lacks *D. santeng* and *A. lydekkeri*, suggesting that the species may have become extinct. However, in the Madura Strait assemblage, which is of similar age as the Ngandong Fauna, both species are still present. The Punung Fauna is a cave fauna consisting solely of dental elements brought together by porcupines. The fauna is thought to record a major faunal turnover. Most members of the previous community, including characteristic species such as *S. trigonocephalus,* appear to be absent and may have gone extinct. At the same time, it allegedly records the arrival of modern species, which includes herbivores as well as forest-dependent species such as *Pongo* and *Hylobates*.

4.2 New insights

Correlations to Sangiran and updated age ranges

Thus far, most of the available age ranges for the faunal units have been based on the well-dated depositional record of Sangiran, correlating the faunal units from their key sites to the vertebrate-rich profile of Sangiran (Van den Bergh et al., 2001; Leinders, 1985). According to these correlations, the middle part of the black clays yields the fossil species of the Satir Fauna, including its marker species *Sinomastodon bumiajuensis.* The upper part of the black clays contains the Ci Saat Fauna, with, as mentioned above, the first hominin fossils. Moving upwards, the Grenzbank supposedly contains the 'unbalanced' Trinil-HK Fauna, and the overlying fluvial sandstones, known as the Kabuh or Bapang Formation, contain the 'balanced' Kedung Brubus Fauna.

In the meantime, new numerical ages have become available, for Sangiran, but also for some of the key find sites of the faunal units **(Table 2)**. The new numerical ages contribute greatly to our understanding of the faunal units, but also confront us with an inconsistency between the Sangiran-based age of the Trinil-HK Fauna and the new Trinil chronology of Hilgen et al. (2023). As explained in **Section 3.3**, the Haupt Knochenschicht of Trinil, key level of the Trinil-HK Fauna, is made up of two superimposed channel lags, referred to as BBC-1 and BBC-2, with a significant age difference. Both channel lags are younger than the Grenzbank of Sangiran and overlap with the age range of the overlying Bapang Formation, which according to the commonly accepted biostratigraphic framework contains the Kedung Brubus Fauna. Especially the age of BBC-2 falls well above the expected age range of the Trinil-HK Fauna.

The double-aged Trinil-HK Fauna

Our finding that the Haupt Knochenschicht consists of two channel lags with a significant age difference questions the significance of the Trinil-HK Fauna as an age- specific vertebrate community. Small-scale test excavations during our 2017-2018 field work did not reveal relevant differences between the fossils from BBC-1 and BBC-2, in terms of species composition or preservation state. Both beds contain fragmented fossil remains, with a dominance of *Stegodon trigonocephalus*, large bovids, *Duboisia santeng* and *Axis lydekkeri*. For a more significant comparison between the fossils of both beds we would need much larger numbers of specimens, which is unrealistic, considering that only small remnants of the original bone beds have remained and that the site is protected.

Unit	*Sangiran-based ages*	*Ages of the key sites*
Wajak		> 37.4 – 28.5 ka
Punung		128-118 ka
Ngandong		140 – 92 ka
Kd. Brubus	< 900 ka	
Trinil HK	Grenzbank: 900 ka	BBC-2: ~450 ka BBC-1: 830-773 ka
Ci Saat	1.3 – 0.9 Ma	
Satir	1.9 – 1.5 Ma	

Table 2. Published age ranges of the vertebrate faunal units, based on dating studies in Sangiran and at the key sites of the faunal units. Data from, Sangiran: Matsu'ura et al. (2020). Trinil: Hilgen et al. (2023). Ngandong: Rizal et al. (2020). Punung: Westaway et al. (2007). Wajak: Storm et al. (2013).

Let's assume that the fossil content of BBC-1 and BBC-2 is indeed comparable. An explanation might then be that the fossils in BBC-2 have been reworked from the underlying BBC-1. Both channel lags reflect incision by small rivers. Moderately rounded clasts of locally eroded material point to winnowing rather than significant transport. It is well-imaginable that the BBC-2-river reworked the locally available coarse elements of BBC-1 in its own channel lag. During our 2018 excavations in Trinil, we found a Stegodon tusk embedded in BBC-1, but protruding into the overlying BBC-2. This rather strange position can only be explained by active fluvial incision into an older, bone-bearing channel. We can therefore be sure that reworking did take place, but to which extent BBC-2 also contains younger, contemporary fossils is hard to say. There are some reasons to think that such younger fossils are scarce. Van den Bergh (1999) noted that metrically, the *Stegodon* molars from the 'Haupt Knochenschicht' form a homogenous sample, which speaks against a mixed-age. Moreover, BBC-2 appears to lack characteristic Kedung Brubus species such as *Elephas hysudrindicus* and *Rusa* sp., even though its age falls well into the estimated age range of this faunal unit.

If we assume that most fossils of BBC-2 have been reworked from BBC-1, then the Trinil-HK Fauna, as excavated from its key beds, may still be regarded as 'more or less homogenous', with an age range of 830 - 773 ka, and with an unknown admixture of fossils with an age of ~450 ka. Note that it is of course also possible that the BBCs contain fossils older than 830 ka, reworked from strata underlying BBC-1. Fossils may have been reworked from the black clay bed BGC-3 **(Fig. 5)**, which indeed contains occasional skeletal remains. Likely, this clay bed correlates with the top of the Sangiran black clays, suggesting that its fossils are part of the Ci Saat Fauna.

The 830 – 773 ka age range of BBC-1 comes comfortably close to the 900 ka age of the Grenzbank of Sangiran. Yet, it overlaps with the age of the basal sandstones of the Bapang Formation of Sangiran, which is said to contain the Kedung Brubus Fauna. There is no reason to doubt the available numerical ages, which on both sites are based on multiple measurements and supported by paleomagnetic profiles. A more likely explanation of the conflicting age ranges and fossils faunas lies in the definition and interpretation of species lists.

Significance of species lists

Over the past decades, interpretations of the faunal units and their correlations across find sites have relied on a rather strict interpretation of species lists. My work on the Madura Strait assemblage made me aware of the difficulties of such species lists. A major problem is the significance of rare species in fossil assemblages, such as predators, hominins and arboreal primates. For the identification of the Madura Strait assemblage (N=6372 specimens), I listed the numbers of identified specimens per species and added justifications for the identifications. Several species appeared to be quite rare. For example, only one specimen could be attributed to a carnivore (*Panthera pardus)*, two to a reptilian predator (*Varanus komodoensis*), two to hominins (*Homo erectus*) and one to an arboreal primate (*Macaca* sp.). The occurrence of rare species may be relevant for the interpretation of a vertebrate community. However, their absence is only meaningful if we have insight into the original sample size and the degree of detail of the faunal analyses. Moreover, we need to have insight into the taphonomic background of an assemblage. For most of the assemblages from Java, specimen counts and systematic taphonomic analyses are not available. This reduces the value of species lists and complicates comparisons.

It is not difficult to see the effects of taphonomy, sample size and analytical detail in the species lists. The Trinil-HK and Kedung Brubus Faunas have been based on enormous sample sizes (tens of thousands of specimens). This tells us something about excellent conditions of bone preservation and accumulation. The assemblages derive from beds that were formed under a rather dry climate, which implies low bone-weathering rates, and with a pronounced rainy season, which forms an effective mechanism for the concentration of skeletal elements in fluvial lag deposits. The resulting bone beds attracted palaeontologists like Dubois and Selenka, who collected several ten-thousands of specimens from the sites. Subsequently, the assemblages were studied and documented in detail, thanks to the work of later taxonomists as Hooijer, Janensh and Stremme. If we now look at the assemblages from Bumiayu, as described by van der Maarel (1932), or the corresponding assemblages from the black clays of Sangiran, as described by Aimi and Aziz (1985), it is clear that the species lists of the Satir and Ci Saat Faunas have been based on much smaller samples and less detailed analyses. This, for example, reflects the different conditions for preservation and accumulation in the humid, marshy setting represented by the black clays, which did not result in rich bone beds, but rather in a scattered occurrence of fossils throughout the profile. The lower numbers of fossils, often collected as occasional finds over a longer period, were not studied to the same level of detail as the assemblages from Trinil and Kedung Brubus.

With these taphonomic and analytical differences in mind, it is no wonder that the Trinil-HK Fauna contains more species than the Ci Saat Fauna. Note in this respect that the species list of the Ci Saat Fauna speaks of 'cervids' and bovids', whereas the subsequent Trinil-HK Fauna contains various bovid and cervid species, which clearly reflects the difference in analytical detail. Many of these Pleistocene species were in fact defined based on specimens from the Trinil assemblage. This gives an impression of 'new arrivals' and 'more balanced conditions', but the species may very well have already been present in the Ci Saat Fauna, hidden under the labels 'bovids' and 'cervids'.

Age ranges and stratigraphic ranges

A peculiar aspect of the faunal units is that, with respect to stratigraphic ranges and age ranges, they have much different orders of magnitude **(Fig. 6, left column)**. The Trinil- HK Fauna derives from two bone beds, both representing a short accumulation period. The beds may even represent single events of increased mortality, for example caused by an episode of extreme drought, or by an explosive ash-rich eruption. The same may account for the Grenzbank. In contrast, the poorly studied Kedung Brubus site, with a thickness of > 200 m, may very well have a composite build-up, of stacked fluvial sequences of different ages. Theoretically, this unit covers the ~600 ka between the Trinil-HK and Ngandong Faunas. Also in other areas where the fossils of this this faunal unit are found, such as in the fluvial series around Mojokerto, Jetis, and Perning, the bone-bearing strata appear to represent a long age range, covering most of the Middle Pleistocene **(Chapter 4 of this thesis)**. This places its extensive species list, described as 'balanced', in a completely different perspective. The degree of time-averaging in the Kedung Brubus Fauna must be enormous, certainly in comparison to the Trinil-HK Fauna.

A continental perspective

Our new insight of Pleistocene Sundaland as a stably exposed continental area, only subject to progressive submergence in the course of the Middle Pleistocene, requires a thorough re-interpretation of the faunal stages.

The Satir Fauna, consisting of four pioneer taxa, may rightly be regarded as unbalanced and represents convincing island conditions. Apparently, emerging eastern Java, with its uplifted fold zones and the Wilis and Old Lawu as the earliest eruption centers **(Section 2.2)**, was not yet connected to continental Sundaland during its earliest stages

The Ci Saat Fauna records a large number of immigrant species, including poor swimmers like bovids, *Rhinoceros sondaicus* and *Panthera tigris*, all of which must have arrived via a full land connection. The vertebrate community holds large and medium-sized herbivores, as well as two carnivores, which shows that there must have been considerable predator pressure. A sustainable tiger population requires a wide territory. All this points to a balanced fauna and continental conditions. The label 'unbalanced' was largely based on the relatively low species diversity, but there are important taphonomical and analytical reasons that explain why the Ci Saat Fauna does not contain as many species as subsequent faunal units.

The Trinil-HK Fauna, although commonly still regarded as 'unbalanced', contains a wide range of small- to large-bodied herbivores, as well as secondary consumers of all body sizes, including rats, suids, canids and tigers. It is therefore a rich and highly diverse fauna that bears no evidence of isolation. In fact, the difference with the subsequent Kedung Brubus Fauna, commonly regarded as 'balanced', is insignificant. Yes, the Kedung Brubus Fauna is slightly richer in species, but this is readily explained by the much longer time range represented by this faunal unit compared to the preceding Trinil HK-Fauna.

Endemic species or Sundaland species?

In the previous model of Java as an island with intermittent mainland connections, many of the Pleistocene species from Java have been regarded as endemic or dwarfed. The *Hexaprotodon sivalensis* of the Satir Fauna has a reduced body size compared to its relatives in the younger faunal units (de Visser, 2008), which may indeed very well relate to the island conditions of early-emerging eastern Java. However, for the species of the subsequent Trinik-HK Fauna, the occurrence of island dwarfism is doubtful. Rozzi et al. (2013) and Van der Geer et al. (2011) point at the small-statured *Duboisia santeng* as the best example of an endemic, dwarfed species. Indeed, the species is small compared to mainland *Boselaphus*, its closest relative. However, dwarfed island species generally quickly become extinct when exposed to mainland connections. *Duboisia santeng* has remained a common element of the vertebrate community of this part of Sundaland for at least 700 ka, together with larger-bodied herbivores and carnivores. This does not give an impression of island dwarfism. Note also that the species is part of the Madura Strait assemblage and that it was reported from a fossil assemblage in Thailand (Nishioka and Vidthayanon, 2018), which shows that the species must have had a geographic range that extended far beyond present-day Java.

4.3 A revised biostratigraphy

Climate and landscape

Instead of looking at the Javanese fossil assemblages from an island view point, we need to regard them as records of a continental Sundaland fauna. Changes of the vertebrate community may rather reflect climate change and related shifting of vegetation zones over Sundaland. Pollen records (Sémah and Sémah, 2012; Polhaupessy, 1990) as well as ferralitic weathering profiles (Brasseur et al., 2011) show that present-day eastern Java was under a humid tropical climate throughout most of the Early Pleistocene. The black clays, forming the dominant and characteristic deposits from this period, were deposited in a forested coastal swamp. The first colonizing species of island-stage eastern Java, represented by the Satir Fauna, must have lived in this coastal forest. The same applies for the species of the sub-

sequent Ci Saat Fauna, which I regard as the first continental vertebrate community and which includes the earliest hominins.

The Grenzbank of Sangiran and the BBCs of Trinil represent a drastic landscape change, which, as explained in **Section 3.3,** involved a change from a humid coastal forest to a much drier landscape and a grass-dominated vegetation. In the vertebrate community this is expressed by a shift toward a dominance of grazers such as bovids and the disappearance of *Hexaprotodon*. In essence, it is this climate-related change of the vertebrate community that adequately explains the difference between the Ci Saat and Trinil-HK Faunas.

This new, large-herbivore dominated, grass or open-woodland community, which continues as the rather similar Kedung Brubus Fauna, remained remarkably stable throughout the late Early and Middle Pleistocene. In the course of the Middle Pleistocene, a more pronounced glacio-eustatic cyclicity may have resulted in shifts of climate and vegetation zones over continental Sundaland. Although there is as yet no evidence of significant changes in the vegetation of eastern Java, it is possible that shifting vegetation zones in central Sundaland affected migration patterns of species, possibly explaining the new arrivals of species in the marginal shelf zone of present-day eastern Java. From MIS11 onward, this process may have been amplified by intermittent and progressive contraction of the exposed Sundaland land surface, as shown in **Fig. 3C**. New species recorded by the Kedung Brubus Fauna, such as *Elephas hysudrindicus* and *Rusa* sp., may reflect such migration of species over Sundaland, as a result of shifting vegetation zones and a cyclic contraction of the exposed land surface. However, it is important to note that we have no idea when exactly these species first arrived in this area, within the long time-range covered by the Kedung Brubus Fauna. Note in this respect that a new fossil species is commonly regarded as an 'arrival' on Java, whereas it may very well just represent a brief, possibly climate-related stage, during which the geographic range of a species temporarily covered this part of the Sunda Shelf.

Besides regional climate fluctuations, the gradual development of larger drainage systems, such as the Brantas and the Solo, may have been a relevant factor for the geographic distribution of vertebrate species over Sundaland. The presence of a large river may explain the return of *Hexaprotodon sivalensis* in the Kedung Brubus Fauna. Large drainage systems may also have been of relevance for arboreal primates, migrating along the tree-lined river banks.

MIS6 and MIS5

The Solo terrace of Ngandong was dated to 140 – 92 ka by Rizal et al. (2020). The authors proposed a modelled, most-likely age range for the fossils of 117 – 108 ka. This, however, is not very likely. The fossil fauna is the last representative of the grassland or open-woodland vertebrate community that had existed in this part of Sundaland since ca. 900 ka. As we will see, it definitely pre-dates MIS5e, the first true island stage of Java, represented by the Punung Fauna. Moreover, the fossils derive from the basal conglomerates of the terrace. The fluvial regime must have been determined by various factors, but if we assume that sea-level changes were a decisive factor, then this basal conglomerate may be linked to lowstand-related downcutting rather than highstand-related aggradation. It is plausible to project the Ngandong Fauna in the early part of the age range, for example between 140 and 130 ka, which links the fauna to the penultimate glacial period of MIS6. The fact that the Ngandong Fauna is so similar to the preceding Kedung Brubus Fauna shows that the preceding stages of shelf submergence and Sundaland surface-contraction, linked to the highstands of MIS7, MIS9 and MIS11, left few traces in the local vertebrate community. A new species, only known from the Ngandong Fauna, is *Axis javanicus*. The species is related to *Axis axis* of the Asian mainland and may have reached Java during an MIS6 lowstand dispersal wave.

The Punung Fauna was dated to 128-118 ka (Westaway et al., 2007), which links it to the peak highstand conditions of MIS5e. This makes it a unique faunal record, of what probably was the first island stage of Java. A great faunal difference with the preceding Ngandong Faua is commonly regarded as a faunal turnover, recording the extinction of the preceding grassland community and the arrival or a modern fauna with rain forest-dependent taxa such as *Pongo*. This faunal turnover has commonly been linked to increasing precipitation rates and a change to forested conditions. Looking at the Sundaland charts of **Fig. 3C**, the decisive factor for the disruption of the former, long-standing vertebrate community may very well have been the MIS5 island-setting of Java.

To get an idea of what MIS5 Java may have looked like, it is interesting to refer to the present (Holocene) island situation. Today, the western part of the island is humid and was, up to recently, fully forested. The eastern part of the island is much drier and has a grass-dominated vegetation, such as preserved in Baluran National Park. However, global sea surface temperatures were ca. 1 degree higher during MIS5e than during MIS1 (Wang and Zong, 2020; Hoffman et al., 2017), and it is reasonable to assume a further eastward expansion of the tropical forest over island-stage Java during MIS5e. This may have reduced the available savanna refuge along the eastern edge of the island.

Although this provides a good explanation for the MIS5 extinction of large herbivore taxa such as *Stegodon*, we need to be careful with the concept of a faunal turnover. The idea that the previous, MIS6 vertebrate community was replaced by a new, modern community is difficult to conceive, within the MIS5e island setting of Java. Van den Bergh et

al. (2001) proposed a temporary land bridge during interstadial MIS5d, at ~115 ka, but this does not fit with the age of the Punung Fauna, which predates MIS5d. To understand potential MIS5e species migration, it is good to make a distinction between arboreal primates and herbivores. Under the upcoming MIS5e interglacial conditions, the forest zone shifted eastward, together with the gradual submergence of the shelf, which ultimately brought island conditions to Java. Large herbivores were pushed eastwards to a relict savanna and may eventually have been 'pushed off the island'. At the same time, arboreal primates moved along with the eastward-shifting forested zone. This readily explains the occurrence of arboreal primates as new MIS5 arrivals recorded by the Punung Fauna. However, under these conditions, it is impossible to explain an arrival of new herbivores. Yet, within the commonly accepted species lists, the Punung Fauna is referred to as a 'fully modern fauna' with new herbivores as *Bos palaeojavanicus*, *Bubalus bubalis*, and *Elephas maximus.* I think this is incorrect. It is interesting that the taxonomy of these species has been subject to different interpretations. Von Koenigswald (Von Koenigswald, 1939, 1940) referred to the bovids and cervids of the Punung Fauna under their Middle Pleistocene species names. Badoux (1959), probably the taxonomist who studied the Punung material in most detail, acknowledged that he could not see the difference between the archaic herbivores of the Middle Pleistocene Javanese sites and their extant relatives. Sondaar (1984) still used the Middle Pleistocene taxonomy, but Van den Bergh (2001) and Storm (2001) changed this to the use of modern species names, without further metric or morphological justification.

Now, it is interesting to zoom in on the fossil remains from the Punung caves. The material has been brought to the cave by porcupines, consuming the bone tissue and leaving only crowns. The Punung Fauna taxonomy is thus based solely on isolated crowns. It is, however, rather complicated to distinguish between individual bovid and cervid species based on dental crowns. My work in the Madura Strait assemblage showed that large samples are needed and that taxonomic decisions can only be tentative. More importantly, there is often no clearly described morphological or metric key to distinguish between archaic species and related modern species. In the Madura Strait assemblage, obviously an MIS6 grassland fauna, I frequently found molar sizes of bovids and cervids that overlap with the extant species. Especially for bovids, the distinction between 'archaic' Middle Pleistocene species and modern species is largely a matter of taxonomical tradition.

To a certain extent, this also accounts for the genus *Elephas*. The Middle Pleistocene *Elephas* of Java is traditionally referred to as *Elephas hysudrindicus* and it certainly differs from the extant *Elephas maximus* by skull morphology (Hooijer, 1955). When it comes to isolated cheek teeth, *Elephas maximus* is characterized by a greater hypsodonty, however with overlapping metric ranges. For the Madura Strait assemblage, it proved to be impossible to distinguish between the two species and we decided to refer to the material as *Elephas* sp. The Punung assemblage contains four tooth fragments, which Sondaar (1984) and later authors referred to as *Elephas maximus*. However, as also acknowledged by Van den Bergh et al. (2001), the material is too fragmented for a sound taxonomical interpretation and its allocation to *Elephas maximus* must therefore be questioned.

It thus seems that the 'modern' taxonomical interpretations of the herbivores from the Punung caves have been coloured by the prevailing model of a faunal turnover, However, the scenario of newly arriving herbivores during peak interglacial conditions is extremely unlikely. It is much more likely that the Punung herbivores are survivors of the previous MIS6 community. In that case, a certain size change of their dental elements could have been a result of a changed diet, or may even be regarded as an effect of island conditions. So, yes, the Punung Fauna records a great change of the vertebrate community, with the extinction of *Stegodon trigonocephalus,* newly arriving arboreal primates and an archaic herbivore community under environmental pressure. But, no, the Punung Fauna does not record a turnover in the sense of a largescale replacement of archaic species by a fully modern fauna.

Modern herbivores, including *Elephas maximus*, probably arrived later on Java, during MIS4 and MIS2, when the Sunda Shelf fully re-emerged, the connection with mainland Asia was restored, and grassy plains once again became the dominant Sundaland landscape.

The faunal units of De Vos and Sondaar

The existing vertebrate faunal units of eastern Java form a valuable basic guideline for interpreting the vertebrate communities of the southeastern part of the Sunda Shelf throughout the Pleistocene. The species lists, however, are not 'cast in concrete' and need to be interpreted with care. Comparisons between the faunal units are complicated by great differences in taphonomy, sample sizes, analytical detail and represented age ranges.

It would be ideal to work with more comparable faunal units, with a similar level of detail, preferably representing the vertebrate community during specific marine isotope stages. This level of detail is available for the Ngandong (MIS6), Punung (MIS5e) and Wajak Faunas (MIS4-2), although differences in taphonomy still complicates comparisons between these assemblages. For the older units, especially the long-duration Kedung Brubus Fauna, this level of detail is not available.

A re-interpretation of the existing faunal units is provided in **Fig. 6**. The previous interpretations of the faunal units as a records of intermittent land bridges are largely incorrect. Only the Satir and Punung Faunas represent island stages, though under completely different conditions. There are no significant differences between the Trinil HK-Fauna, Kedung Brubus and Ngandong Faunas. All three units represent a long period of dry climate conditions, a grass-dominated vegetation and a stable continental vertebrate community. The chronostratigraphic significance of the heterogenous Trinil-HK Fauna is unclear, other than that we can say that it probably primarily represents the 'earlier stages' of the dry, grass-dominated landscape stage, which started around 900 ka, possibly with admixed older material (reworked from underlying strata) and younger material (from BBC-2).

There are records of new species in the subsequent Kedung Brubus Fauna, such as *Elephas hysudrindicus*, but these records are undated and stratigraphically not-specified, which makes it impossible to pinpoint a chronological boundary between the Trinil-HK and Kedung Brubus Fauna. Therefore, at this stage, it is appropriate to assume a gradual boundary between the Trinil-HK and Kedung Brubus Fauna. This re-interpretation of the Trinil-HK and Kedung Brubus Faunas makes the apparently contradicting chronologies of Sangiran and Trinil of little significance.

The Ngandong Fauna is very similar to the Kedung Brubus Fauna, but its well-defined age range as an MIS6 lowstand fauna, shortly before the MIS5e island-stage, makes it of great relevance.

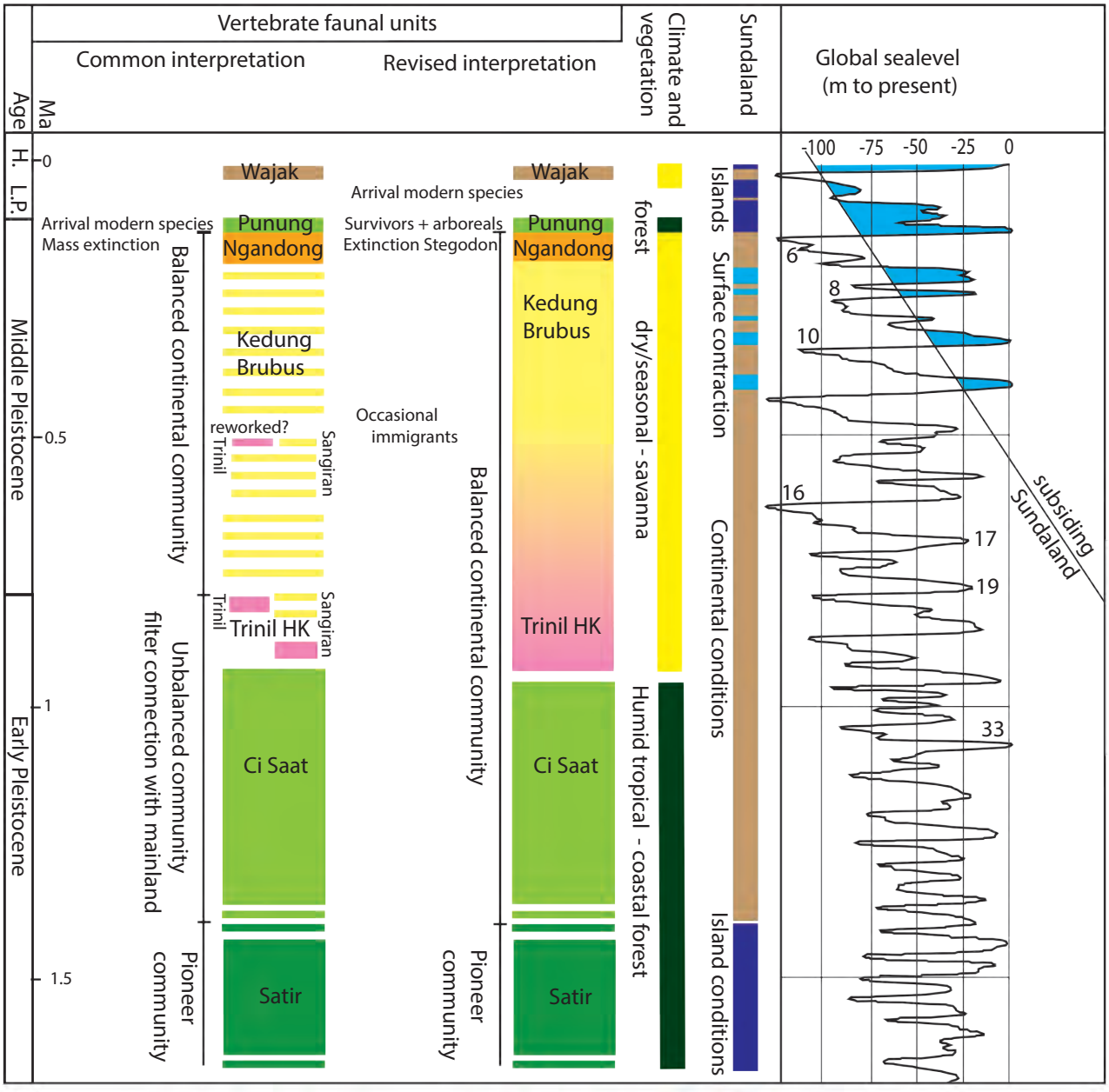


Fig. 6. The Pleistocene vertebrate biozonation of eastern Java: chronology, landscape and climate. Left column: common interpretation, with updated chronology. Right column: revised interpretation. Faunal units based on De Vos et al. (1982) and Sondaar (1984). Sea-level curve: Bintanja and Van der Wal (2008). Subsiding Sundaland: Sarr et al. (2019).

5. The hominin chronology of Java

5.1 The model of the long-standing lineage

From multiple species to a single taxon

The first Pleistocene hominin remains from Java were unearthed in the Wajak cave, in 1888 and 1890. The material, amongst which two partial skulls, was recognized as *Homo sapiens*, though remarkably robust (Storm, 1995; Dubois, 1920). Later in 1890, Dubois found a hominin mandible in Kedung Brubus. In 1891 and 1892, he made his great discoveries in Trinil: two hominin molars, a skullcap and a femur, which he assigned to a new species, *Pithecanthropus erectus* (Dubois, 1895). It took three decades before substantial new hominin fossils were found on the island. Between 1931 and 1933 thousands of vertebrate fossils were excavated from the Solo terrace of Ngandong, including 12 partial hominin crania, with a larger cranial capacity than the *Pithecanthropus* skullcap from Trinil. Oppenoorth (1932) assigned these fossils to a new, younger species, called *Homo soloensis*, which he regarded as a proto-Australian population. In 1936 a skull was found in Perning near Mojokerto. Von Koenigswald recognized it as a *Pithecanthropus* child, but after a dispute with Dubois, he changed this to *Homo mojokertensis* (Von Koenigswald, 1936a; 1936b). In 1937 and 1938, hominin fossils were discovered in the area around Sangiran, including a skullcap with a great morphological and metric similarity to the skullcap from Trinil. Von Koenigswald (1940) assigned all fossils to *Pithecanthropus erectus* and referred to the skullcap as *Pithecanthropus* II (today Sangiran 2). In the same period, Von Koenigswald also excavated fossil remains from the nearby Punung caves, amongst which he recognized a hominin tooth (Von Koenigswald, 1939). He regarded the fossils as contemporary with those from Trinil and assigned the hominin tooth to *Pithecanthropus erectus*.

In 1939, Von Koenigswald discovered a robust partial calvaria in Sangiran (Skull IV), and in 1941, a highly robust mandible fragment (Sangiran 6). Weidenreich (1945) assigned these new specimens to two new species*: Pithecanthropus gigantus* and *Meganthropus palaeojavanicus*, and regarded the hominin species from Sangiran as an evolutionary line, from *Meganthropus palaeojavanicus,* to *Pithecanthropus gigantus,* to *Pithecanthropus erectus*. However, the author acknowledged that the hominin species may also have existed side by side.

Meanwhile, hominin fossils had also been excavated in China, which had been described as *Sinanthropus pekinensis* (Weidenreich, 1943; Black, 1930) and a robust form, described as *Gigantopithecus* (Weidenreich, 1945). Weidenreich (1940) suggested that *Sinanthropus pekinensis* and *Pithecanthropus erectus* may be combined into one new species, *Homo erectus*. This became an accepted taxonomical became practice after the publications of Mayr (1950), who also proposed to sink all other Javanese forms, including *Meganthropus, Pithecanthropus gigantus* and *Homo soloensis* into this new taxon. Le Gros Clark (1964) expanded the definition of *Homo erectus*, by assigning similar hominin remains from Africa to the species, such as Olduvai 9, previously referred to as *Homo leakeyi*.

Chronological groups

All Early to Middle Pleistocene hominin fossils from Java are nowadays referred to as *Homo erectus*, but the fossil material is subdivided in chronological groups, which echo the former subdivision in species **(Table 3)**. Note, however, that the definition of these chronological groups does not align completely parallel among different authors. The most recent subdivision by Kaifu and Athreya (in press) distinguishes between an early and late *Homo erectus* of Java, and subdivide the early *Homo erectus* in two groups: the Sangiran Lower and Upper Group. The Lower Group covers the fossil material from the black clays and the Grenzbank, whereas the Upper Group covers the fossils from the sandstones overlying the Grenzbank, which they refer to as Bapang AG (above Grenzbank). The Sangiran Lower Group has a 'primitive' craniodental morphology, with relatively large molars, hyper-robust cranial bones, and a small cranial capacity. This group includes the specimens formerly regarded as *Meganthropus.* The Sangiran Upper Group includes Sangiran 2 and several well-preserved skulls discovered in Sangiran over the past decades, such as the Sangiran 17 and Skull IX.

The Late *Homo erectus* includes the material from Ngandong, formerly referred to as *Homo soloensis*, as well as four skulls discovered over the past decades: Sambungmacan 1, 3 and 4 and Ngawi 1. These crania are characterized by a widened frontal squama, a lengthened cranial base and a heightened cranial vault, resulting in an increased cranial capacity.

Phylogenetic discontinuity?

The morphological and metric diversity of the hominin fossils from Java has been the subject of a long discussion about their phylogenetic relation.

The oldest chronological group, the Sangiran Lower Group, contains robust mandibles and isolated dental remains that exceed the size range of the known *Homo erectus* sample world-wide, notably mandibles Sangiran 5 and 6, which were formerly regarded as *Pithecanthropus dubius* and *Meganthropus.* The same accounts for the extreme

thickness of cranium Sangiran 31. Robinson (1955, 1953) argued that the specimens are highly similar to *Paranthropus*, whereas Tobias and Von Koenigswald (1965) and Tyler (1995) noted an affinity with *Australopithecus* or *Homo habilis,* suggesting that the fossils represent an older, pre-*erectus* population.

A similar discussion was held over the phylogenetic position of the late *Homo erectus* of Java. Delson et al. (2001), Schwarz (2004), Schwartz and Tattersall (2003), Widianto and Zeitoun (2003), Baab (2011) and Baab and Zaim (2017) argued that the voluminous, vaulted brain case of this group points to the arrival of a new, more modern population, unrelated to the older *Homo erectus* of Java.

The single lineage model

Antón (2003, 2002), Baba et al. (2003), and Kaifu et al. (2017; 2008) regard all Pleistocene hominins from Java as a continuous evolutionary lineage, pointing to consistent cranial traits. According to these authors the Javanese *Homo erectus* is single population that lived isolated from other (mainland) populations, such as the Chinese *Homo erectus*. The chronological groups are regarded as time bands of this lineage (Kaifu and Athreya, in press). The robustness of some of the older specimens possibly reflects extreme sexual dimorphism (Kaifu et al., 2011), which may have been a primitive feature of the genus, also recognized in the Dmanisi population (Lordkipanidze et al., 2013).

The single-lineage model has today become commonly accepted. Remarkable is that in Africa and Eurasia, *Homo erectus* was replaced in the course of the Middle Pleistocene, by non-*erectus* hominins with a more voluminous, vaulted braincase, which may collectively be referred to as *Homo heidelbergensis* (Schwartz and Tattersall, 2003; Stringer, 2002). In eastern Asia, this morphologically diverse new population is referred to as archaic *Homo sapiens* (Antón, 2003), late Middle Pleistocene *Homo* (Rightmire et al., 2015), or late archaic *Homo* (Kaifu, 2017). The assumed continuation of the old *Homo erectus* lineage on Java implicates its survival on this remote part of the Sunda Shelf, as a relict population.

Extinction of the lineage and arrival of Homo sapiens

It is generally assumed that the Javanese *Homo erectus* lineage went extinct in the beginning of the Late Pleistocene, together with most other members of the Middle Pleistocene vertebrate community. This 'faunal turnover' is commonly linked to climate change, toward more humid conditions and a forested landscape (Rizal et al., 2020; Van den Bergh et al., 2001; Sondaar, 1984). Within this model, the Late Pleistocene Punung Fauna consists of modern species. This brings us back to the hominin tooth from the Punung cave, described by Von Koenigswald (1939) as *Pithecanthropus erectus*. Interestingly, Badoux (1959) recognized five other hominin teeth in the Punung collection, among material that had formerly been labeled as *Pongo.* The author assigned the specimens to *Homo* cf. *Pithecanthropus*. However, in line with the later interpretation of the Punung Fauna as a modern fauna, the hominin teeth were renamed *Homo sapiens* by Sondaar (1984), albeit without further anatomical justification. Storm et al. (2005) tried to trace back the hominin teeth in the Punung Collection of Von Koenigswald in the Senckenberg Museum of Frankfurt, but the specimens appeared to be lost. They did find a single hominin tooth in the collection, from which they assumed that it belongs to the Punung assemblage. The authors assigned this specimen to *H. sapiens* rather than *H. erectus*, referring to its relatively small size.

More reliable records of the arrival of anatomically modern *Homo sapiens* in the Sundaland region date from later in the Late Pleistocene and include the material from Niah Cave, Borneo, dated to ~37 ka (Curnoe et al., 2019) and from Java, such as the Wajak skulls, with a minimum age of 37.4 to 28.5 ka (Storm, 2013), and two femora from the youngest Solo terrace of Trinil, dated to 37-32 ka (Ruff et al., 2022).

The continental perspective

The new insights into the Quaternary paleogeography of Java and the Sunda Shelf urge us to reconsider the model of an isolated hominin lineage. Instead of an island with intermittent land bridges, eastern Java has been an integral part of emerged Sundaland, at least since 1.3 Ma, when a balanced, continental vertebrate community developed. It seems likely that the former island perspective of Java has also coloured our interpretation of the Javanese hominins. Most likely, the geographic range of the Pleistocene hominins was not restricted to present-day Java. The fossil assemblages of Java record the occasional arrival of new species, including herbivore taxa such as *Elephas* and *Rusa.* Apparently, these herbivore taxa could migrate over Sundaland. So, why would the *Homo erectus* population of Sundaland have remained isolated from mainland populations, for a period of time that exceeds one million years?

5.2 New insights

The early Homo erectus *and the complex stratigraphy of Trinil and Sangiran*

The early *Homo erectus* is mainly represented by fossil remains from Trinil and Sangiran. To understand their chronological relationships and the subdivision of this material into a Lower and Upper Group, it is relevant to dive into the

complex stratigraphy of both sites.

Fig. 7 shows a cross-section over the Solo valley near Trinil, with the Dubois excavation site on the left bank and the museum on the right bank. The right bank features a gravelly strath terrace that truncates a thick unit of parallel-bedded fluvial tuffs. The left river bank presents a lower, younger terrace, with its erosive base reaching almost down to low water level of the Solo. This terrace has a composite build-up. Its basal part reflects downcutting conditions, with gravelly channels and sandy point bars; its top part is a tuffaceous fill, reflecting a change to aggradation, which makes the terrace a fill terrace. The strath terrace of the right bank (T5) is an abrasion level of the oldest Solo, dating to around 375 ka and relates to MIS10. The terrace of the left bank (T2) reflects MIS6 downcutting, followed by aggradation which may relate to the MIS5 base-level rise and/or to increased volcanic supply **(Chapter 2 of this thesis)**.

At the Dubois excavation site, older strata are preserved below the erosive base of terrace T2. Among these are fossil-bearing lag deposits of incisive streams that pre-date the Solo drainage system. This level was formerly referred to as Haupt Knochenschicht. It consists of two superimposed channels, which we refer to as BBC-1 and BBC-2, dating to 830 – 773 ka and ~450 ka respectively (Hilgen et al., 2023). During the historic excavations, fossils from both channels have become mixed. Dubois' hominin fossils, the upper third molar (Trinil 1), the skullcap (Trinil 2) and two other teeth (Trinil 4 and 5) derive from either BBC-1 or BBC-2. However, this probably does not account for Trinil 3, also known as Femur I. A reconstruction of its find location indicates that it derives from a T2 channel that cuts through the older fossil-bearing channels (Pop et al., 2023a), which explains its modern, post-*erectus* morphology (Ruff et al., 2015). A prominent T2 channel is also visible east of the Dubois excavation site, at the site of Selenka Grube III. A fill of laminated clay shows that this must have been an abandoned channel. Unknowingly, the excavators missed the bone-bearing lag deposits and worked through the fill of this MIS6 Solo channel.

The Dubois collection also yielded hominin fossils that were only later recognized as such. Femora II-V (Dubois, 1932) have an erectus-type morphology and are in a fragmented state of preservation (Ruff et al., 2015), which is quite different from femur I, pointing to a provenance from BBC-1 or BBC-2. Joordens et al. (2015) described fresh water mollusks with opening traces, shell tools and an engraved shell, all deriving from the Dubois collection. The sandy fill of the shells was dated to ~ 450 ka, which ties the specimens to BBC-2.

Along the right river bank, the BBCs are mostly absent. The facies of the thick unit of bedded fluvial tuff resembles the fill of the T2 terrace of the left bank, however, the unit is tectonically tilted and reaches a much greater height than terrace T2. It is abraded by one of the oldest Solo terraces, indicating that it predates the origin of this river. We referred to this unit as the Trinil Formation. With an age of ~450 ka for BBC2 and a T5 terrace age of ~375 ka, there is only a relatively short time window for this prominent unit. Compared to the incised bone-bearing channels (the BBCs), the stacking of fluvially deposited tuff beds reflects a remarkable base-level rise. We postulated the formation of a volcanic barrier between the Lawu and the Kendeng, forming a lake basin that was quickly filled, by fluvial supply of volcanic ash **(Chapter 3 of this thesis)**.

Previously, the fluvial deposits of both river banks had been referred to as the Kabuh Formation. **Fig. 7** shows that it is a composite of deposits of varying ages and different landscape stages: the BBCs are rare traces of an old incisive landscape, the Trinil Formation is the thick tuffaceous fill of a subsequent lake basin, and the Solo terraces are a complex of progressive incision and fill structures.

In 1978, Jacob excavated two hominin femora (Trinil 9 and 10) from the right bank. Recently, the specimens were identified as *Homo sapiens* (Ruff et al., 2022). We were able to relocate their finding spot in a small erosion remnant of terrace T1. This is a poorly preserved fill terrace that correlates with the 31 ka Kendeng terrace (Rizal et al., 2020). Around Trinil, remnants of this terrace are 'glued' to the valley walls, marked by subtle irregularities or small preserved terrace surfaces at ca. 8 m above low water level.

The Sangiran stratigraphy is generally represented as a standard profile **(Fig. 8A)**. As explained in **Section 3.3**, the vertebrate-bearing stratigraphic range consists of black organic clays (Sangiran Formation) overlain by fluvial conglomerates and tuffaceous sandstones (Bapang Formation) forming stacked fluvial sequences. **Fig. 8B** shows the standard profile as a chronostratigraphic representation, based on the most recent chronology of Matsu'ura et al. (2020) and with references to other studies. The black clays offer a good age control, established through radiometrically dated tuff laminae, and by a normal polarity zone regarded as the Jaramillo subchron, in the top-range of the clay series. The overlying fluvial sequences also contain ash-dominated laminae that have been dated through multiple single-grain radiometric datings.

In the stratigraphy of (Itihara et al., 1985), the boundary between the black clays and the first conglomerate bed, known as the Grenzbank, is regarded as conformable, an interpretation that still holds strong in recent hominin literature. However, the Grenzbank is a basal lag deposit of an incisive, fluvial (and locally tidal) channel system and the contact with the underlying clays is obviously unconformable. This is confirmed by the available numerical ages: the top of the black clays contains the upper boundary of the Jaramillo subchron of 990 ka (Hyodo et al., 1993),

whereas a few meters higher, the base of the Grenzbank was dated to ~900 ka (Matsu'ura et al., 2020). A clay layer with a thickness of ~10 m is missing, likely due to erosion, resulting in a chronological hiatus of ~ 80 ka (Hilgen et al., 2022). Also the Bapang Formation is commonly regarded as a record of continuous deposition. In practice, there are probably short hiatuses between the individual fluvial sequences, each consecutive gravel bed being slightly incised into the previous sequence. The basal conglomerate bed, the Grenzbank, probably relates to the lowstand of MIS22. The second fluvial sequence was dated to ~780 ka. Possibly, the basal conglomerate of this sequence correlates with MIS20. The third sequence postdates the Brunhes – Matuyama polarity change and may be tied to MIS18 or MIS16.

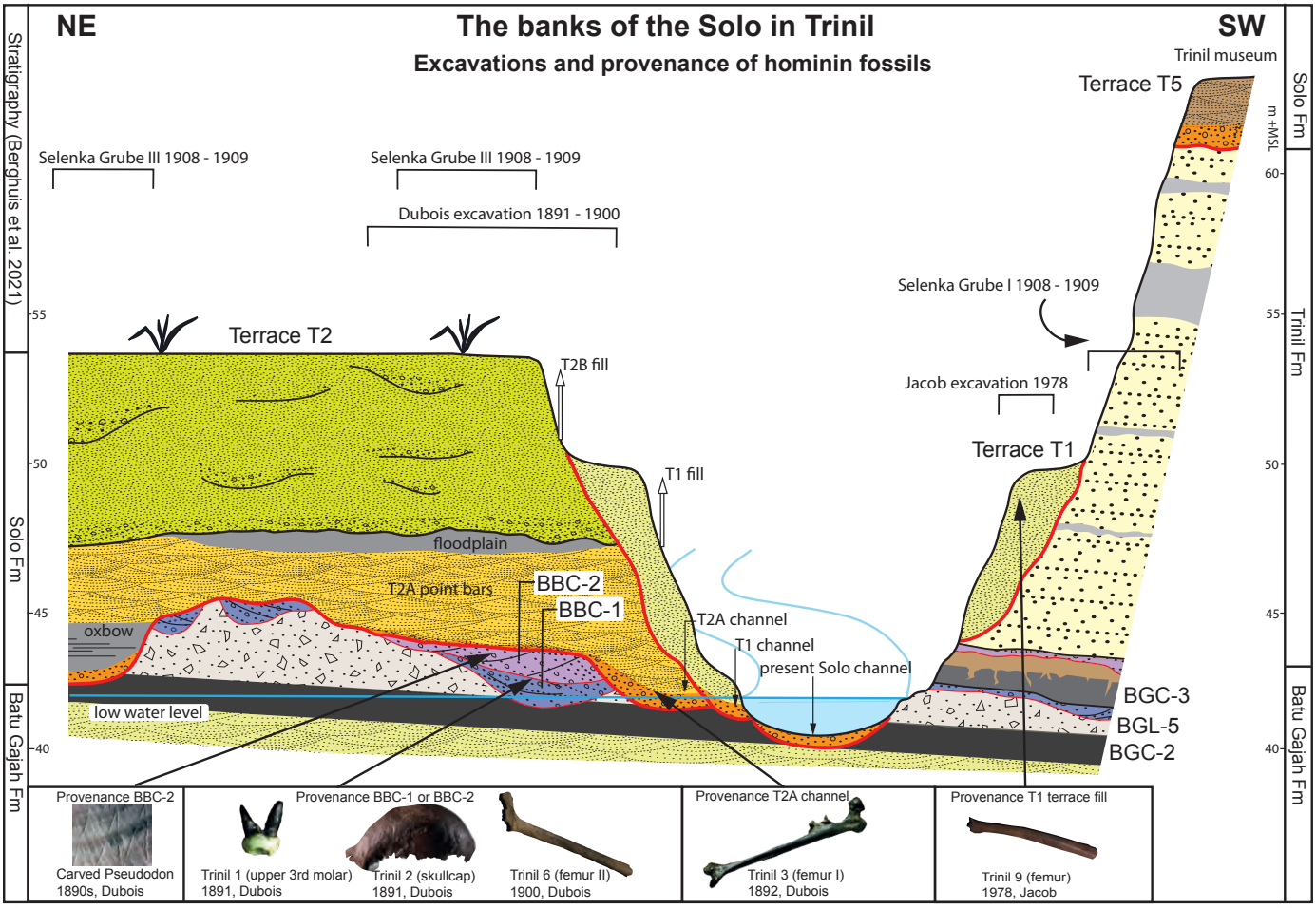
Most of the hominin fossils from Sangiran are surface finds, or in-situ finds with a poorly documented provenance. For some of these specimens, the stratigraphic provenance has been reconstructed. Hominin fossils derive from the top of the clays, with a proven first occurrence at ~ 1.1 Ma (Matsu'ura et al., 2020). This is the oldest reliable record of hominin presence in eastern Java. Likely, the stratigraphic range of hominin remains continues downwards to Tuff 8 (T8 in **Fig. 8**), dated to ~1.3 Ma (Matsu'ura et al., 2020). Hominin fossils are also reported from the basal two fluvial sequences of the Bapang Formation. However, hominin fossils are unknown from the third sequence, which post-dates the Brunhes – Matuyama polarity reversal.

The subdivision of the hominin material in a Sangiran Lower and Upper Group is stratigraphy-based. The Lower Group derives from the black clays and the Grenzbank. It is dominated by dental or gnathic remains, including the robust specimens formerly regarded as *Meganthropus*. Skull elements from this range are rare, but probably include Sangiran 4 and 31, as well as Bjg 1602, recently discovered in the Grenzbank (Widianto et al., 2023). These skulls are marked by an extremely-thickened cranial bone, as well as an extremely-pronounced nuchal torus, both of which are unknown from any other hominin species. The Upper Group derives from the fluvial sequences overlying the Grenzbank and consists of dentognathic remains as well as skulls, amongst which are the well-preserved crania Sangiran 10, 12, 17, Skull IX and Bukuran.

The question is, how do the hominin fossils from Trinil correlate chronologically to the fossils from Sangiran? **Fig. 8A** shows the standard stratigraphy of both sites, ordered by their correlation between the Grenzbank of Sangiran and the 'Haupt Knochenschicht' of Trinil. This correlation was proposed by Von Koenigswald (1939) and has survived the later stratigraphic and biostratigraphic revisions. Projected side-by-side, the correlation is certainly not unreasonable. At both sites, this conglomerate bed marks the transition from marshy coastal clays to channelled fluvial deposits. **Fig. 8B** shows the same profiles, but now with a chronological ordering. This shows that in Sangiran, the black clays offer a more or less continuous record, covering most of the Early Pleistocene. In Trinil, we only have a fragmented record of this period, which consists of volcanic breccias with ferralitic weathering profiles, levels of slight incision, and inter-bedded beds of organic clays. This marks a slightly higher position of Trinil in the paleo-landscape, closer to the foot of the Old Lawu, and suggests some subsidence of the Sangiran area during this same period. Moving to the overlying fluvial strata, we see again that the Sangiran stratigraphy offers a rather complete record, with a basal conglomerate dating to ~900 ka overlain by several fluvial sequences that appear to correlate with the sea-level curve from MIS22 onward. In Trinil we see this same transition, but the preservation is much less detailed. We only have two incisive conglomerates, BBC-1 and BBC-2, which together make up the former 'Haupt Knochenschicht'. BBC-1, with an age range between 830 and 773 ka, correlates chronologically with the second fluvial sequence of Sangiran. BBC-2 is much younger. If we move further upward in the stratigraphic record, we see that Trinil has a more complete record of the latest Middle Pleistocene than Sangiran, thanks to the occurrence of the lake-basin fill (the Trinil Formation) and the subsequent Solo terraces.

As a result of the former correlation between the Grenzbank of Sangiran and the 'Haupt Knochenschicht' of Trinil, and the practice of adding the Grenzbank specimens to the Lower Group, the 'Haupt Knochenschicht' hominin fossils from Trinil have commonly been regarded as part of the Lower Sangiran Group. This makes Trinil 2 a 'gracile member' of the archaic population. This is incorrect. If we assume that Trinil 2 derives from BBC-1, then it is age-equivalent to the hominin fossils from the second fluvial sequence of Sangiran, which are part of the Upper Sangiran Group. Yet, this correlation of Trinil 2 with the Lower Sangiran Group has confounded evolutionary interpretations. According to the prevalent model, the Lower and Upper Sangiran Groups represent an evolving lineage of *Homo erectus*, an interpretation that is based on the recognition of a shared cranial form. The problem is that reasonably intact crania from the black clays or the Grenzbank are not available, which makes Trinil 2 the best-preserved cranium of the Lower Group. Schwarz and Tattersal (2003) even refer to the Lower Group as the Trinil/Sangiran 2 morph. Nevertheless, Trinil 2 is certainly part of the younger group. Sangiran 2 is a skull of unknown stratigraphic provenance, but with a metric and morphological match with Trinil 2, indicating that it is most likely also a member of the younger group.

From a geological point of view, it is strange that the hominin fossils from the Grenzbank are added to the Lower Group. It is more realistic to regard this stratigraphic level as the base of the overlying fluvial series. However, from a taxonomic point of view, it is understandable. The Grenzbank yielded robust dentognathic remains, which are similar to the fossils from the underlying clays. The level also yielded Sangiran 4, the partial skull previously regarded as *Pithecanthropus robustus,* and the recently discovered robust skull Bjg 1602.



Left bank	Right bank	Sub-unit	Description	Interpretation	Polarity	Ar/Ar	OSL	Age-range
		Terrace 1 T-1	Cross-bedded tuffaceous sand.	Stacked channels and bars. Fluvial aggradation, high volcanic supply.				MIS2 or 4. T1 correlates the lowermost terrace of the Kendeng, OSL-dated 31 +/- 6 ka**
		Terrace 2 T-2B	Tuffaceous sand and fine pumice gravel; stacked channels and bars.	Stacked channels and bars. Fluvial aggradation, high volcanic supply.			95^{+36}_{-56} ka*	
		Terrace 2 T-2A	Crumbly, dark brown, rooted clay.	Floodplain deposit.				
		Terrace 2 T-2A	Bedded sand and fine gravel.	Point bars, incision and acretion, meandering river.	N.		129^{+64}_{-64} ka 188^{+32}_{-32} ka	MIS6. Correlates with Ngandong terrace and Madura Strait submerged valley
		Terrace 2 T-2A	Finely laminted grey clay.	Oxbox-lake fill.				
		Terrace 5 T-5	Bedded sand and fine gravel; point bar deposits.	Point bars, incision and acretion, meandering river.				
T-2A		T5	Conglomerate of rounded andesite gravel. Forms the basis of all terrace sequences.	Channel lag, incisive conditions. Partly confined or meandering conditions.				MIS10 ~375 ka Correlates with high terrace of Kendeng **
			Parallel bedded tuffaceous sand, shallow channel stuctures. Beds separated by clay drapes or clay layers. Rooted intervals and vertisols.	Lake basin, fluvial braidplains. High supply of ash, dry, seasonal conditions.				Window ~ 450 -375 ka
		Bone-bearing channel 2 BBC-2	Cross-bedded conglomerate. Poorly rounded clasts of weathered and fresh volcanite. Rich in reworked soil nodules, vertebrate bones and fresh-water molluscs.	Incision, local reworking and winnowing. Soil erosion. Dry, seasonal conditions. Contempory supply of ash.	N.	450+/-110 ka	430 +/- 50 ka#	480 - 380 ka or: ~ 450 ka
		Batu Gajah Clay 3 BGC-3	Massive grey clay, covered with vertisol rich in calcareous concretions.	Local pond in incision. Soil: dry, seasonal conditions.				
		Bone-bearing channel 1 BBC-1	Cross-bedded conglomerate with ash lenses. Poorly rounded clasts of weathered and fresh volcanite. Contains vertebrate bones and fresh-water molluscs.	Incision, local reworking and winnowing. Contemporary ash-supply.	R.	770 +/- 120 ka		830 - 773 ka
		Batu Gajah Lahar 5 BGL-5	Volcanic breccia: clayey matrix, clasts of weathered and unweathered volcanite.	Volcanic mass flow (lahar). Slope collapse of weathered dome.		710 +/- 120 ka		~ 830 ka
		Batu Gajah Clay 2 BGC-2	Massive black organic clay with dispersed fine pyrite and occasional gastropods.	Coastal marsh.				
			Cross-bedded tuffacceous sand.	Fluvially reworked volcanic ash.				

Fig. 7. The banks of the Solo in Trinil: stratigraphy, chronology, and provencane of hominin fossils. All numerical ages and magnetic polarities from Hilgen et al. (2023), except *: Berghuis et al. (2021), **: Rizal et al. (2020). #: Joordens et al. (2015).

In contrast, the hominin remains from the overlying part of the Bapang Formation are more gracile and conform better to the average metrics of *Homo erectus*. In theory, this may imply that the Grenzbank represents a stage of strong evolutionary change. However, the stratigraphy tells a different story. The robust specimens are only found in the basal conglomerate and not in the similarly aged top part of this lowest fluvial sequence. This indicates that the robust fossils may have been reworked from the underlying clays. Also, the incised top of the black clays and the chronological hiatus of ~ 80 ka points to this direction. This suggests that the Sangiran hominins may be subdivided in two chronological populations, with a clear morphological distinction: an archaic robust population and a subsequent more gracile population. Furthermore, the stratigraphic ranges of the fossils, prior to reworking, suggest that the robust population lived in the humid coastal forest, between ~1.3 Ma (or 1.1 Ma) and ~ 900 ka. The gracile population lived in the subsequent landscape stage, characterized by dry, grassy plains with local, partly incisive streams, from ~900 ka onward, and possibly disappeared from the area after 773 ka.

This provides a more logical subdivision of the two populations, with respect to morphology, chronology and landscape, but it does not yet answer the question of their phylogenetic relationship. Instead of looking at crania, it is better to compare dentognathic elements, which are available in larger numbers. Compared to the later, more gracile population, the archaic population is characterized by larger post-canine dentition, a thickened mandibular corpus and a relatively narrow dental arcade (Noerwidi et al., 2020; Zanolli et al., 2019; Kaifu et al., 2005). However, authors disagree about the evolutionary implications. Von Koenigswald and Tobias (1965) noted a similarity with the dentition of *Homo habilis*, and postulated an earlier migration wave from Africa. Zanolli et al. (2019) regarded some of the robust dental material as non-hominin and proposed to hold on to the taxon *Meganthropus palaeojavanicus*, as an ape species. Kramer (1994) regarded the dental elements as derived in comparison to *Homo habilis* or australopithine taxa and proposed a phylogenetic relation with the earliest *Homo erectus* of eastern Africa. Kaifu et al. (2005) came to a similar conclusion, but regarded the robust dentition from the Lower Sangiran Group as 'equally primitive to or more primitive than' the earliest *Homo erectus* from eastern Africa.

These interpretations point to an early out-of-Africa dispersal wave, of a population that may perhaps be regarded as 'earliest *Homo erectus*'. If we regard this early-migration wave of *Homo erectus* as the ancestral lineage of all Javanese *Homo erectus*, then the observed dentognathic reduction and arcade widening must have been a local evolutionary process, which in that case would have been a parallel evolutionary trend, taking place independently on Java and in Africa. The other option is that the earliest population of Java was replaced by a new, more derived *Homo erectus* population, representing a new migration wave.

The late Homo erectus *and the time gap*

The next question is, how does the typical *Homo erectus* from Sangiran and Trinil relate to the late *Homo erectus* from Ngandong, Sambungmacan, Ngawi and the Madura Strait? Today, the long discussion on phylogenetic continuity or discontinuity between these populations appears to have been settled in favour of the single-lineage model, referring to a common cranial form (Kaifu and Athreya, in press; Kaifu, 2017; Kaifu et al., 2008; Antón, 2002).

There are, however, two problems involved in this model. The first problem is that the single-lineage model is firmly based on the idea of Java as an island, with intermittent land connections during lowstands. However, as explained in **Section 2.1**, Java has probably been part of an exposed Sundaland throughout the Middle Pleistocene. Indeed, the remote setting along the far southeastern margin of Sundaland may have resulted in biogeographic isolation, for example through the occurrence of forest barriers. However, this is not what we see in the vertebrate fossil record, which reflects a stable continental community, lacks evidence of endemism, and records the occasional arrival of new herbivore species such as *Elephas hysudrindicus, Rusa* sp., and *Axis javanicus.* The second problem is that there is a huge gap in the fossil record. The *Homo erectus* remains from Sangiran date from the latest Early Pleistocene, between 900 and 773 ka. This also accounts for the material from Trinil, assuming that this derives from BBC-1 or may

have become reworked in BBC-2. With an age range of 140 – 130 ka for the late *Homo erectus* of Ngandong, we have a gap in the fossil record of >600 ka.

The time gap in the fossil record, however, is probably not as large as it seems **(Fig. 9)**. We know that hominins were present in Trinil around 450 ka, based on the dated shells with traces of consumption, shell tools and the carved shell (Joordens et al., 2015). Another chronologically intermediate and previously unknown group is known from its core stones and retouched flake tools, which Sander Hilgen found in Sogen, a few km downstream of Trinil, within the newly defined Trinil Formation, with an age range between 450 and 375 ka (Pop et al., 2023b). These are the oldest, unequivocal stone tools, found in an in-situ context on eastern Java. An intermediate-aged cranium may be Mojokerto 1, the child skull from Perning. Published radiometric ages for this bone bed gave very old ages, of 1.5 Ma (Morwood et al., 2003) or even 1.8 Ma (Swisher et al., 1994), which would make the skull the earliest record of *Homo erectus* on Java (Huffman, 2001; Morley et al., 2020). However, all signs point to a much younger age, which we estimated to ~450 ka **(Chapter 4 and 5 of the thesis)**.

Although these specimens point to hominin presence on eastern Java around 450 or 400 ka, the tools and the child skull do not give much clarity on evolutionary aspects. Interestingly, we may have adult crania from this period: Sambungmacan 1, 3 and 4 and Ngawi 1 were all found in the Solo Valley not far from Trinil. The field reports mention a provenance from 'fine-grained volcaniclastic sediment'. Within the revised Trinil stratigraphy, this may either be the bedded tuff of the Trinil Formation or one of the fill terraces of the Solo, likely T4 or T2. Therefore, reconstructing their exact find spots and stratigraphic provenance is essential **(see recommendations)**.

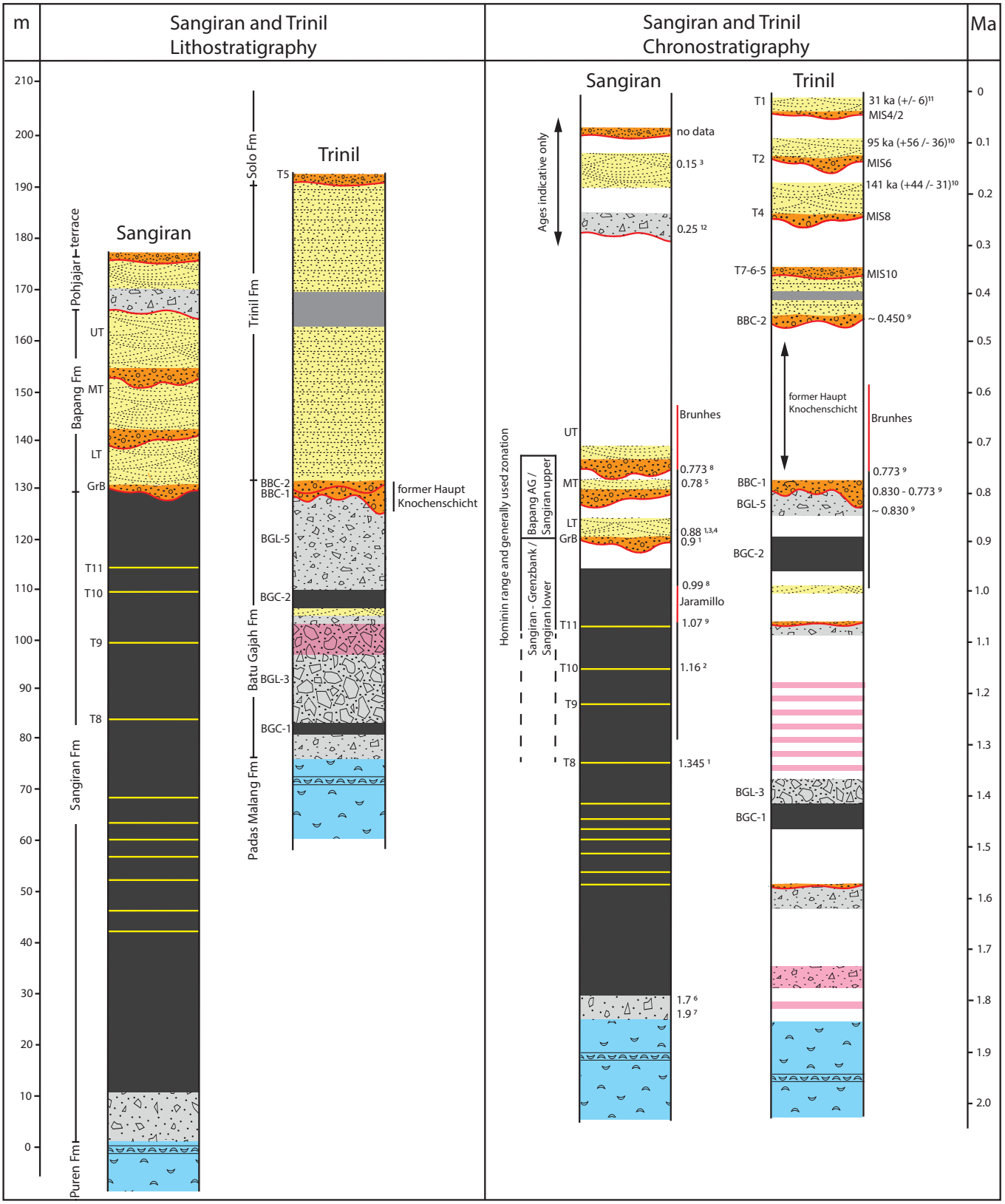


Fig. 8. The stratigraphy of Sangiran and Trinil. **A:** Lithostratigraphy based on Itihara et al. (1985) and Berghuis et al. (2021), with correlation between the Grenzbank and the 'Haupt Knochenschicht' as proposed by Von Koenigswald (1939). **B:** Chronostratigraphy based on 1: Matsu'ura et al. (2020). 2: Suzuki (1983). 3: Saleki et al. (1998). 4: Falguères et al. (2015). 5: Shimizu (1985). 6: Sémah et al. (2000). 7: Bettis et al. (2004). 8: Hyodo et al. (2011). 9: Hilgen et al. (2023). 10: Berghuis et al. (2021). 11: Rizal et al. (2020). 12: Suzuki and Wikarno (1982).

Most remarkable is the earliest gap in the hominin record. Why are hominin fossils absent in the third fluvial sequence of the Bapang Formation in Sangiran, post-dating the 773 ka Brunhes-Matuyama polarity change? Is this by chance or due to preservation issues, or does this signal the disappearance or even local extinction of the population?

The Punung hominins as the survivors of the older lineage

According to the prevailing models, the ancient Javanese *Homo erectus* lineage became extinct in MIS5e, together with most other members of the long-standing grass-land vertebrate community, due to the shift toward humid and forested conditions. As explained in **Section 4.3**, this must have been a combination of an island stage, causing strong reduction of the exposed land surface and an eastward shift of the forested zone. However, I also showed that the model of an MIS5e faunal turnover is largely incorrect. Except for *Stegodon,* most of the Middle Pleistocene taxa probably survived this island stage. Most of all, it must have been impossible for savanna-related vertebrate taxa to reach Java during peak MIS5e island conditions. The assignment of the Punung herbivore teeth to modern taxa, as has been common practice for the past 40 years, is a subjective taxonomical decision, apparently made to fit with the model of mass extinction and replacement, which makes this a form of circular reasoning. The same accounts for the hominin teeth from Punung. Their re-interpretation from *Pithecanthropus* to *Homo sapiens*, by Sondaar (1984) and later authors, has not been based on morphological evidence, but rather on an interpretation of the changed conditions.

As explained in **Section 4.3**, the only new arrivals of the MIS5e vertebrate community are arboreal species, which came along with the eastward-shifting forest zone. In theory, these may have included a population of forest-adapted archaic *Homo sapiens*, but this is highly hypothetical and requires strong fossil evidence. An alternative, much more likely explanation, is that the Punung hominins are the survivors of the preceding MIS6 population.

5.3 A new hominin framework for eastern Java

Referring to the morphological variety of the hominin fossil record and their chronostratigraphic ranges, and taking into account the major Pleistocene landscape stages of eastern Java and the larger Sundaland region, I tentatively propose a taxonomical re-interpretation of the Pleistocene populations of eastern Java **(Fig. 9)**.

Homo erectus palaeosondaicus*, the archaic Sundaland population*

Dental comparisons link the archaic hominins of eastern Java to the earliest *Homo erectus* of eastern Africa, which points to an early dispersal wave. They may have left their African territories ~2 Ma, with an oldest record outside Africa in Dmanisi ~1.8 Ma. Recent studies suggest multiple, even older hominin dispersal waves out of Africa to Eurasia, with earliest ages around 2.4 Ma (Curran et al., 2025; Scardia et al., 2021).

Homo erectus' arrival on eastern Java, as indicated by its earliest fossils in Sangiran at 1.1 Ma and likely ~ 1.3 Ma, has commonly been linked to lowstands and temporary land bridges. However, the under the revised regional landscape model, Sundaland was continuously exposed in this period. The first hominin record on eastern Java rather reflects the emergence of this marginal zone of Sundaland, a zone of complex tectonism and volcanism. It coincides with the establishment of a balanced, continental vertebrate community in this area, which shows that emerging eastern Java became a fixed part of the continental ecosystem. The fact that this archaic hominin population was part of this earliest continental vertebrate community of eastern Java suggests that the population was already present on Sundaland prior to 1.3 Ma, suggesting out-of-Africa dispersal along the Indian Ocean rim.

There are two aspects that set this archaic Sundaland population apart from all other known early *Homo* populations. First, its extremely thickened braincase. And second, its remarkable habitat in a humid, coastal forest. Although the first aspect has been drawn to attention by researchers as Tyler (1995) and Westaway et al. (2015), the second aspect has remained largely unnoticed. It completely changes our perception of the geographic ranges and migration routes of this population. These archaic hominins, with robust jaws, large post-canine dentition, and thickened cranial bones, may very well have populated the extensive coastlines of Early Pleistocene Sundaland.

Although its dentognathic characteristics can be linked to an ancestral population of eastern Africa, the thickened cranial vault and the coastal forest habitat are unique features. Possibly, these anatomic features developed in the Sunda region. Alternatively, this ancient Sundaland population may have been related to an ancestral, yet undiscovered, hominin population living in the eastern African coastal forest (see Joordens et al., 2019). In any case, the cranial and dental robustness of this population warrants a taxonomic subdivision. Weidenreich's *Meganthropus palaeojavanicus* is unsuitable, as this classification places the population outside the genus *Homo*. Tyler (2001) therefore proposed *Homo palaeojavanicus*. However, if we agree on a relation with the earliest *Homo* aff. *erectus* of eastern Africa, it is better to distinguish this robust archaic population at subspecies level. Moreover, I think it is relevant to highlight its background as an archaic species of Sundaland. Therefore, I propose to refer to this archaic hominin population as *Homo erectus palaeosondaicus*. A formal description and publication of this new subspecies name is yet to be made.

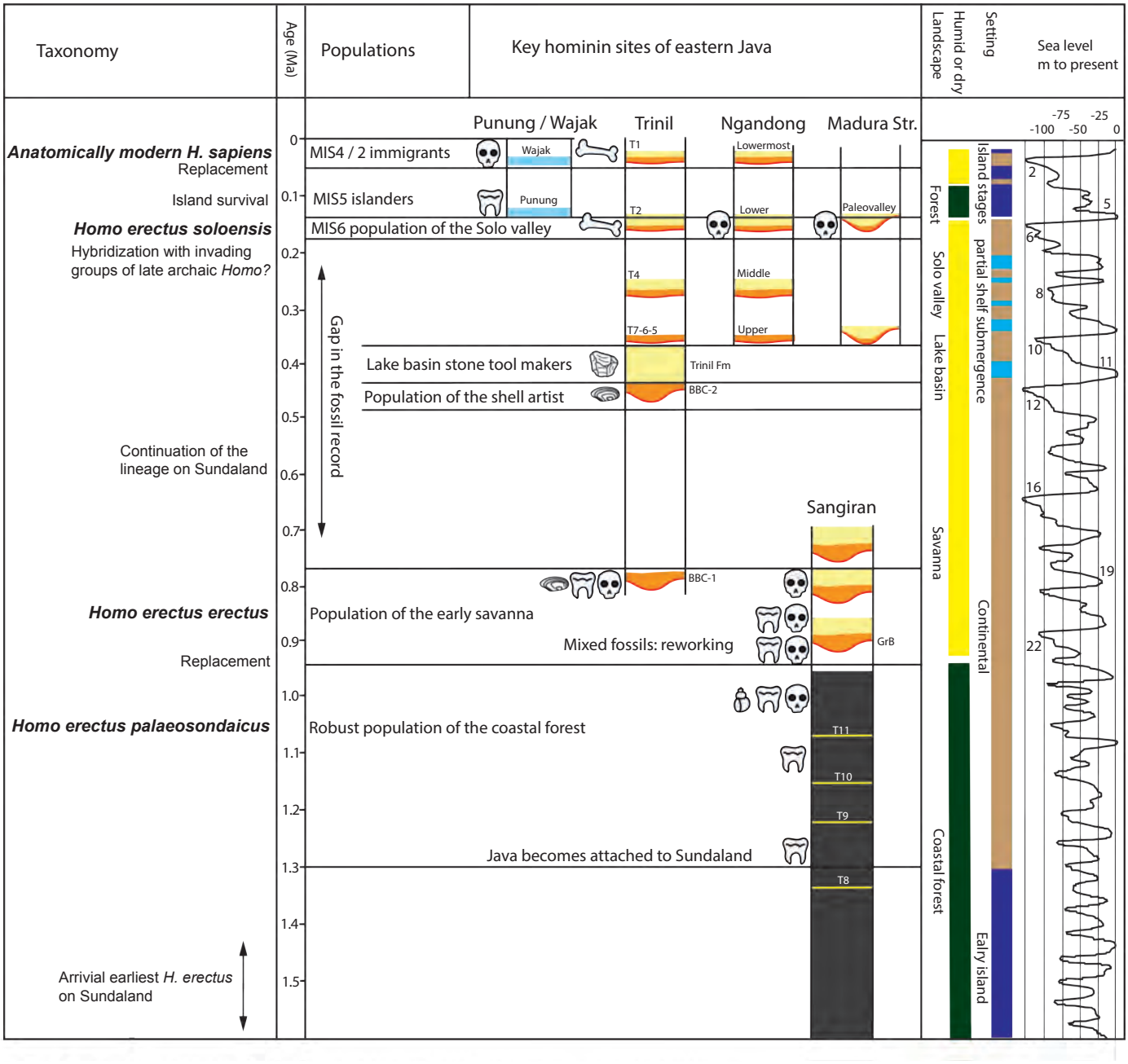


Fig. 9. The Pleistocene hominins of eastern Java: stratigraphy, chronology, populations, and revised taxonomy.

Little is known of the subsistence strategies of this earliest hominin population of Sundaland. Choi and Driwantoro (2007) described bones from the Sangiran black clays bearing cutmarks made by shell tools. Besides such butchering of land animals, I think it is likely that the population exploited aquatic resources, available on tidal flats, in tidal creeks and mangrove swamps, such as mollusks, crustaceans and fish. The coastal forest may also have offered fruit and other plant resources. Aquatic and plant resources are typically eaten by Burmese long-tailed macaques living in a coastal forest, which shows that such exploitation is within the primate repertoire (Haslam et al., 2022; Falótico et al., 2017).

Recently it was demonstrated that Mediterranean Neanderthals exploited aquatic resources and were engaged in diving for molluscan shells (Villa et al., 2020; Zilhão et al., 2020). This raises the question of whether the robust bone anatomy of this archaic Sundaland population relates to their coastal habitat. Verhaegen and Munro (2011), and Amson et al. (2018) suggested that the robust bone anatomy of *Homo erectus* may have been an adaptation for shallow-water breath-hold diving, with the increased bone mass (and thus body density) facilitating a neutral buoyancy with filled lungs at foraging depth (Houssaye and Botton-Divet, 2018). Indeed, *Homo erectus* had heavy cranial and postcranial bones, but evidence of a coastal habitat is scarce. With *Homo erectus palaeosondaicus* we have a population with an extremely robust anatomy, and a coastal habitat. This indeed opens the possibility that its hyper-robustness was a heritable adaptation to a partly aquatic lifestyle and littoral foraging.

Homo erectus erectus*, a new dispersal wave over Sundaland*

The Mid Pleistocene transition brought a drastic climate and landscape change to the Sundaland region. Forests largely disappeared and wide savannas became dominant. In the stratigraphy of Trinil and Sangiran, we see that the humid coastal forest disappeared around 900 ka. Irregular incisions, eroding soils and occasional events of volcanic ash fall give an impression of a relatively harsh environment. Nevertheless, a rich vertebrate fossil record shows that the local plains must have offered suitable living conditions for a vertebrate community dominated by herbivores such as bovids, cervids and *Stegodon*. Along with this drastic landscape change, there is a marked change in the hominin fossil record, toward a reduced cranial thickness, reduced tooth sizes, a more rounded dental arcade and a reduced thickness of the jaws. As this more gracile population includes cranium Trinil 2, the type specimen of *Homo erectus*, it may rightly be referred to as *Homo erectus erectus* (see Antón, 2003). Whether this is a local evolutionary process, possibly as an adaptation to the changed environmental conditions, or the arrival of a new population is hard to say based on the available fossil record.

Local evolution of a single, isolated Javanese lineage appears to be the convention nowadays. Again, I think this model is largely based on the previous 'island view' of Early Pleistocene Java. However, the new landscape model of a continuous Early Pleistocene mainland connection questions such prolonged isolation of a local hominin lineage. Comparative dental studies show that the post-900 ka hominins of Java have a closer affinity with the contemporary *Homo erectus* from China and eastern Africa than with the pre-900 ka robust population of Java (Zanolli et al., 2019; Kaifu et al., 2005). This may be a result of parallel evolution. However, it is more realistic to assume a second Asian-ward dispersal wave of *Homo erectus*, with a norther route into China as well as a southern route into Sundaland. Recently, Muttoni and Kent (2024) described rapid, climate-driven dispersal of *Homo erectus* into Eurasia during MIS22, around 900 ka, exactly the age of the great change in the hominin record of Java. I therefore postulate a new dispersal wave over Sundaland, of a population that was better adapted to dry, savanna-like conditions than the existing robust population of Sundaland. There may have been a tempory overlap or gene flow between the two populations. But we do see that, after the arrival of *Homo erectus erectus*, the archaic *Homo erectus palaeosondaicus* quickly disappears from the fossil record.

Systematic taphononic studies to the subsistence strategies of the late Early Pleistocene *Homo erectus erectus* have never been carried out. It would, for example, be interesting to look for indications of hunting or scavenging by this grass-land population. However, during our 2018 and 2019 studies in Trinil, José Joordens noted shells with opening-traces in BBC-1, similar to the shells described from BBC-2 (Joordens et al., 2015). Therefore, we can infer that this population exploited freshwater mollusks from local streams. at least from ~800 ka onwards.

Again, it is relevant to consider *Homo erectus erectus* as a Sundaland species rather than a Javanese species. This also provides a potential answer to the incomplete fossil record of eastern Java. Chronological gaps in the fossil record may represent temporary shifts of the geographic range of the population. The species, or individual communities of the species, may have temporarily left the volcanic foothills of present-day eastern Java, but may very well have persisted on the surrounding Sundaland plains. Such shifting territories may have been related to the availability of food resources, for example by shifts of vegetation zones or migration patterns of herbivores. Later in the Middle Pleistocene, highstands resulted in temporary contraction of the exposed land surface, with a concomitant eastward shift of forested zones, which may also have driven populations to present-day Java. This may explain the presence of the stone tool makers on Java, which coincides with the MIS11 highstand. Whether this Sundaland population of *Homo erectus erectus* indeed remained isolated from the mainland *Homo erectus* is unknown, in the absence of fossil remains from the early Middle Pleistocene.

The MIS6 population of the Solo valley, Homo erectus soloensis*, a hybrid hominin?*

The MIS6 Solo valley population is regarded as the last recorded *Homo erectus* of Java and the last worldwide representative of this successful hominin species. Looking at the abundance of fossil material, the population appears to have been flourishing. With the discovery of the Madura Strait specimens, we now know that the population lived along the banks of the Solo, not only on the present-day island of Java, but also along its lower reach on the Sunda Shelf, in the area of the present-day Madura Strait. This makes their attribution to *Homo erectus soloensis* (see Antón, 2003) indeed highly appropriate. Most likely, however, similar populations lived along the courses of other Sundaland rivers.

The consensus is that this MIS6 population is the direct descendant of the Early Pleistocene *Homo erectus erectus* of Sangiran and Trinil. However, is it reasonable to assume that this Sundaland population remained isolated for more than 600 ka, despite the continuous land connection? The MIS6 population of the Solo Valley dates from a period in which, on the Asian mainland, the older *Homo erectus* population had been replaced by a morphologically diverse population of larger-brained hominins that may be referred to as archaic *Homo sapiens* (Antón, 2003) or late archaic *Homo* (Kaifu, 2017). Most likely, this was a replacement by invading groups, which included Neanderthals and Deniso-

vans. Others argue for hybridization or even in-situ evolution of the Chinese *Homo erectus* (Wu et al., 2019; Li et al., 2017). With the open land connection, it would be remarkable if these mobile post-*erectus* mainland populations, did *not* disperse over Sundaland. The recent confirmation of the Penghu mandible, dredged up from the sea shelf just off Taiwan, as Denisovan (Tsutaya et al., 2025) shows just how close this coastal Asian mainland population was to Sundaland.

As a population of the submerged lowland plains of Sundaland, the MIS6 hominins from the Madura Strait form an interesting group to search for indications of invading mainland populations. In **Chapter 8** of this thesis we carried out an extensive morphological and metric comparison of Madura Strait 1 (MS1), a frontal fragment with a dextral supraorbital torus, with Pleistocene crania from the Java, Flores and the Asian mainland. The torus of MS1 is relatively gracile, but basically has a good metric and morphological match with the late *Homo erectus* crania from Java and differs from the late Middle Pleistocene mainland crania in several aspects. The Madura Strait hominins therefore appear to have been part of the larger Javanese or Sundaland population and the cranial fragments do not provide new indications for contact or hybridization with mainland populations.

Interestingly, a taphonomic analysis of the Madura Strait assemblage indicated that the hominin population may have been engaged in selective hunting. This is a modern hunting strategy, commonly associated with Neanderthals (Langdon, 2022; Speth, 2013, 2010b; Stiner, 2009; Domínguez-Rodrigo et al., 2007; Speth and Clark, 2006) or in China with other late Middle Pleistocene hominins, possibly Denisovans (Wang et al., 2022; Trinkaus and Wu, 2017; Li et al., 2017). The use of such hunting methods by the Madura Strait hominins may therefore, carefully, be regarded as indication of contact with post-*erectus* mainland populations.

Suppose that there has indeed been contact between the Sundaland *Homo erectus* and invading late Middle Pleistocene, post-*erectus* mainland hominins, then gene flow into the older, Sundaland *Homo erectus* population may provide an explanation for the increased cranial capacity of the late *H. erectus* (*H. erectus soloensis*) of Java, along with the persistence (and dominance) of an ancient *erectus*-type cranial morphology. There is a fossil that may shed a better light on this matter. For Dubois (1894), Femur I from Trinil was one of his key *Pithecanthropus erectus* finds, and his most convincing argument for an upright posture. As explained in **Section 5.2**, this specimen falls outside the morphological range of *Homo erectus,* and has more affinity with modern humans (Ruff et al., 2015). It derives from terrace T2, which is age-equivalent to the Ngandong terrace and the Madura Strait paleovalley. The modern, non-*erectus* anatomy of Femur I is therefore a strong indication that the MIS6 population was not a full, unmixed descendent of the older Javanese lineage. And, even if there were two separate populations living along the MIS6 Solo valley, then this still implies that there has been contact and possibly gene flow between the Javanese *Homo erectus* and an invading population.

Based on Denisovan introgression into the genome of present-day populations from island Southeast Asia and Oceania, we know that Denisovans must have been present in Southeast Asia before the Late Pleistocene arrival of anatomically modern *Homo sapiens* (Teixeira et al., 2021; Jacobs et al., 2019; Reich et al., 2011). It is interesting to think that Denisovans may have been among invading groups of late archaic *Homo* from the Asian mainland into Sundaland during MIS6, running into the existing population of Sundaland *Homo erectus.* This opens the possibility that *Homo erectus soloensis*, the MIS6 population of the Solo, was a hybrid or introgressed hominin, possibly carrying Denisovan genes.

The MIS5 island population

As explained in **Section 5.2**, I regard the Punung hominins of MIS5e as the survivors of the previous population of *Homo erectus soloensis.* Moreover, they may very well have been the first population that actually became isolated on island-stage Java.

Previously, it was assumed that *Homo erectus* would not have been able to forage under the forested conditions of MIS5e (Storm et al., 2005). It is, however, unsure whether eastern Java was indeed fully forested during MIS5e. More importantly, we have seen that during the preceding MIS6, the Solo population had probably been engaged in deliberate hunting of bovids. Bovids are common in the Punung island fauna, so this food resource remained available. Fruit and other plant-based food resources may even have been available in larger quantities than during the preceding grass-dominated stage. Moreover, the MIS6 population had partly relied on aquatic food resources, such as freshwater turtles, which must also have been available during the subsequent interglacial island-stage.

It is also relevant to note that the Sundaland *Homo erectus* appears to have persisted in this region for more than a million years, which points to a good capability to adapt to ecological changes. I noted that the earliest population of the coastal forest may have relied on littoral foraging. From the later populations, either *H. erectus erectus* from Sangiran and Trinil or *H. erectus soloensis* from Ngandong, Sambungmacan, and the Madura Strait, we only have fossils from fluvial contexts, suggesting that river valleys formed a preferential habitat. However, the Sundaland *H. erectus* may very well also have taken in other ecological niches, which did not yield fossil evidence. A diverse ecological

background would have made the population, as a whole, particularly resistant against climate or landscape changes and may explain its long persistence. It is interesting to think of *H. erectus* groups that continued to live along the Sundaland coast, practicing littoral foraging. Such groups may very well have had the abilities to survive the MIS5e island conditions of Java.

Anatomically modern Homo sapiens

The dispersal of anatomically modern *Homo sapiens* over Sundaland from MIS4 onward is undisputed. They may very well have run into an older population of *Homo erectus soloensis* that had survived MIS5e on island-stage Java, a population that may have carried genes from late archaic *Homo* populations that had arrived in this area during MIS6.

Remarkable is that the Late Pleistocene anatomically modern *Homo sapiens* of Java is represented by the finely-built femora 9 and 10 from Trinil, as well as the robust remains from Wajak, pointing to two contemporary but morphologically different populations (Ruff et al., 2022).

6. Recommendations further studies

The Pleistocene hominins of Java were Sundaland populations. Therefore, it is interesting to search for fossil evidence of these populations on the other Sundaland islands or the Malay peninsula.

The Kedung Brubus site forms a major blank spot in our understanding of the regional chronostratigraphy. Detailed dating studies and controlled fossil excavation from individual stratigraphic levels are urgently required and may provide valuable new insights into Middle Pleistocene vertebrate communities and hominin populations.

The hominin-bearing fluvial series from Mojokerto has a cyclic build-up, which I linked to the Middle Pleistocene Brantas. However, the debate is ongoing. Only a detailed dating study may provide final answers. Instead of looking at the series as a record of continuous deposition, it is better to date individual aggradational sequences. Multiple single-grain radiometric measurements, following the procedures of Hilgen et al. (2023), may be done on samples from the fine-grained tuffacous beds that make up the top of these sequences. The youngest sequences probably lie within the range of OSL-datings. Again, the series is promising from a palaeontological point of view, as it probably includes parts of the Middle Pleistocene that are not sufficiently covered by available studies of other sites.

The stratigraphic provenance of the Sambungmacan 1, 3 and 4 and Ngawi 1 skulls is to date unknown. Their allocation to the 'Kabuh Formation' is meaningless, as this unit name has been used in this area for a suite of fluvial deposits of various ages. In **Chapter 3** of this thesis, we subdivided these fluvial strata into three units, and provided field criteria to distinguish between these units. If it is possible to relocate the exact find sites of the skulls, it must also be possible to determine their stratigraphic provenance and age.

The hominin assemblage from Ngandong contains two tibiae. Moreover, Sambungmacan 2 is a tibia, possibly of similar age. A comparative morphometric study of these specimens is of great interest. It is possible that they have a post-*erectus* morphology, similar to the contemporary Femur I from Trinil. This would provide strong evidence for introgression by an invading non-erectus population.

Finally, it would be very interesting to devote more attention to the relatively understudied *Homo erectus palaeosondaicus*, and, as also suggested by Widianto and Noerwidi (2023), to explore for more and possibly even older fossils of this intriguing group.



The Madura Strait, view to the south from the coast of Madura, with the city of Surabaya in the distance and the Suramadu Bridge to the right. The sand extraction area lies at the other side of the bridge. At low water, an abrasion platform comes up, consisting of cemented coastal sandstones, which form interbeds in the Pleistocene clays, marking the margin of the basin. The strata have been slightly uplifted and tilted southwards.



Samenvatting
Summary

Dankwoord
Ucapan terima kasih
Acknowledgements

Curriculum vitae

References

SAMENVATTING

De fossiele beenderen van Java houden de wetenschappelijke wereld al meer dan een eeuw bezig. Met name het oostelijk deel van het eiland kent rijke vindplaatsen, waarvan sommige ook menselijke fossielen hebben opgeleverd, fossielen die vroeger zijn beschreven als *Pithecanthropus*, maar die we vandaag de dag beschouwen als *Homo erectus.* Wat maakt dit gebied zo rijk aan fossielen? Dit is een vraag die ik vaak krijg. Oostelijk Java kende vroeger duidelijk een rijke en diverse vertebratenfauna. Maar de kans dat botten van deze dieren uiteindelijk bewaard blijven is erg klein. Wat hielp is dat het gebied een relatief droog klimaat heeft gekend, met een lage verweringssnelheid van botten. Het kende ook een uitgesproken regenseizoen, waarin botten die tijdens de droge tijd verspreid over het land waren komen te liggen, werden samengespoeld in rivierbeddingen. Er was een hoge aanvoer van vulkanisch zand, wat leidde tot snelle sedimentatie en begraving van aanwezige botten in een rivierbedding. Oostelijk Java is ook een tektonisch actief gebied, met lokale bodemdaling, waardoor afzettingen bewaard bleven. Door diezelfde tectonische activiteit werden deze lagen later geplooid, zodat ze weer aan het oppervlak terecht kwamen. En ten slotte helpt het dat het gebied tot op de dag van vandaag een relatief droog klimaat kent, hetgeen tot een min of meer open landschap leidt, waarin tropische bodemverwering geen grote rol speelt.

De fossielen uit oostelijk Java geven een interessant inzicht in de evolutie en verspreiding van soorten over zuidoost-Azië gedurende het Pleistoceen. De westelijke eilanden van Indonesië, waaronder Java, maken deel uit van het Sunda Plat. In het verleden heeft dit gebied boven zeeniveau gelegen, waardoor een brede continentale zone ontstond die het westelijk deel van Indonesië verbond met het Aziatische vasteland. Dit verloren continent noemen we Sundaland. Zulke fasen waarin Sundaland boven water lag, zouden zijn gekoppeld aan ijstijden, oftewel glacialen. Omdat tijdens ijstijden veel water wordt vastgehouden in ijskappen, is dan wereldwijd het zeeniveau lager. *Homo erectus* zou Java onder dergelijke glaciale omstandigheden bereikt kunnen hebben. Dit maakte de ontdekking van een vindplaats op de zeebodem, in de Straat van Madura, heel bijzonder. Het is de eerste vindplaats van fossiele beenderen in dit overstroomde gebied, en biedt daarmee een uniek venster op de fauna van het Pleistocene Sundaland.

De fossielen werden bij toeval ontdekt tijdens een zandwinnings project. Zand werd gewonnen op de bodem van de Straat van Madura en vervolgens naar een kustlocatie vervoerd nabij Gresik, waar het werd gebruikt voor de aanleg van een nieuw haventerrein. In 2015, net na de voltooiing, was het terrein een zandvlakte, met een oppervlakte van meer dan 100 ha, helemaal verlaten en zuchtend in de zon. Het bleek bezaaid te zijn met fossiele beenderen. Het kostte me een paar maanden om alle fossielen van het oppervlak te verzamelen. Tegen het einde van het jaar had ik in totaal 6372 exemplaren verzameld.

Het verzamelen van de fossielen was nog maar het begin. De interpretatie van de vindplaats en haar fossielen bleek lastig binnen de geaccepteerde geologische en paleontologische beschrijvingen van Java. De stratigrafie, die de afzettingen op het eiland beschrijft en onderverdeelt in grotere eenheden, was tamelijk eenvoudig opgezet en hield geen rekening met de complexe landschapsontwikkeling van het eiland, onder invloed van vulkanisme, tektoniek, zeespiegelschommelingen en steeds veranderende drainagepatronen. Bovendien bleek er geen logisch verband te zijn tussen de stratigrafie van Java en de offshore stratigrafie van het omringende continentaal plat. Het eiland was altijd het domein geweest van paleontologen en archeologen, terwijl de ondiepe zee al decennia het domein was van oliemaatschappijen die het gebied afzoeken naar winbare olie- en gasvoorraden. Seismische studies in dit zeegebied laten zien dat de zeebodem bestaat uit een opstapeling van dikke mariene lagen, wat wijst op een opeenvolging van mariene fasen, met daartussen periodes waarin het gebied droog lag. Maar een dergelijke cycliciteit was nooit herkend in de geologie van Java. Dit is vreemd, temeer omdat paleontologen juist deze afwisseling van mariene en droge fasen van het Sunda Plat gebruiken om veranderingen in de fossiele fauna van Java te verklaren.

Om deze zaken op te lossen, besloot ik, samen met collega's uit Nederland en Indonesië, om de wijde omgeving van de beroemde vindplaatsen op oostelijk Java opnieuw te onderzoeken. Het bleek al gauw dat de geologische situatie inderdaad veel complexer is dan eerder werd aangenomen. Het lagenpakket bevat grote hiaten en er is een enorme laterale variatie, waardoor correlaties tussen vindplaatsen lastig zijn. In zo'n situatie is het weinig zinvol om met regionale stratigrafische eenheden te werken, zeker als die 'units' dan ook nog eens worden beschouwd als chronologische eenheden. Toch is dat hoe het nu al bijna een eeuw gaat, met als gevolg dat heel wat correlaties en interpretaties die tot op de dag van vandaag algemeen geaccepteerd zijn, flink herzien moesten worden.

Ter vervanging van het oude stratigrafische systeem definieerden wij nieuwe, lokale eenheden met een beperkte geografische geldigheid. Deze 'units' zijn telkens gebaseerd op goed herkenbare lithologische overgangen en vertegenwoordigen belangrijke fasen in de lokale landschapsontwikkeling. De units zijn uitdrukkelijk niet gedefinieerd als

chronologische eenheden. Maar, uiteraard is het wel relevant om inzicht te hebben in de ouderdommen van de stratigrafische eenheden en in de processen waaronder ze gevormd zijn. Daarom hebben we zoveel mogelijk geprobeerd

de nieuwe units in een chronologische context te plaatsen. Dat leidde hier en daar tot wel heel verrassende inzichten, die sterk afwijken van de tot dusver geldende interpretaties. Dat niet iedereen het daar zomaar mee eens was, is begrijpelijk.

Waarop zijn deze ouderdomsindicaties gebaseerd? Er zijn verschillende manieren om gesteentes te dateren, maar die hebben vaak wel hun beperkingen. Voor mariene afzettingen kunnen we terugvallen op gedateerde ranges van microfossielen. Voor terrestrische afzettingen in een vulkanisch gebied kunnen we radiometrische dateringsmethoden gebruiken, maar deze bepalen kristallisatie-ouderdommen, en die zijn niet noodzakelijkerwijs hetzelfde als afzettings-ouderdommen, zeker niet voor de rivierafzettingen waar we op Java veelal naar kijken. Een andere methode is OSL-datering. Deze bepaalt de tijd die is verstreken sinds een mineraal voor het laatst aan licht is blootgesteld, en geeft daarmee een maat voor de daadwerkelijke ouderdom van de afzetting. Maar de techniek werkt alleen voor specifieke sedimenttypen en voor ouderdommen jonger dan ca. 450 duizend jaar. Er zijn nog meer technieken, zoals het meten van de magnetische polariteit van het sediment. Deze kan je vervolgens koppelen aan gedateerde omkeringen van het aardmagnetisch veld. Al met al vormen de uitkomsten van deze bepalingen steeds slechts een stukje van de puzzel. Het is belangrijk om altijd het grotere geheel ogenschouw te nemen. Er zitten heel wat signalen in de stratigrafie waar je ook leeftijdscorrelaties mee kan doen, signalen die bijvoorbeeld wijzen op een grote vulkanische uitbarsting of een verandering van type vulkanisme. Ditzelfde geldt voor grote tektonische gebeurtenissen, klimaatverandering, of een verandering van riviergedrag. Dit soort processen hebben allemaal hun sporen nagelaten in het ‘geologisch archief’ en soms zelfs in het huidige landschap. Als je eenmaal grip krijgt op het verloop van deze landschapsvormende processen, hun representatie in de geologie, en de ouderdommen die erbij horen, dan kan je ook een ruwe chronologie koppelen aan de gesteentepakketten.

Een belangrijk patroon dat je kan herkennen in het de stratigrafie van Java is de cycliciteit die verband houdt met zeespiegelfluctuaties. Ook hiermee kan je goed correleren, zeker als je ergens een paar betrouwbare dateringen hebt. Maar boven alles biedt deze cycliciteit de lang gezochte verbinding tussen de geologie van het eiland en de geologie van de zeebodem van het continentaal plat. De situatie blijkt echter iets anders te zijn dan voorheen werd aangenomen. Recente studies hebben aangetoond dat het Sunda Plat geen tektonisch stabiel oppervlak vormt, maar onderhevig is aan bodemdaling. Het gebied lag waarschijnlijk helemaal boven de zee tijdens het Vroeg-Pleistoceen en kwam pas in de loop van het Midden-Pleistoceen binnen het bereik van zeespiegelfluctuaties. Dit was ook de periode waarin op oostelijk Java een ouder systeem van lokale kleine rivieren langzaam maar zeker opging in twee grote drainagesystemen die nu nog altijd bestaan: de Brantas en de Solo. Destijds waren die rivieren veel langer dan nu. Ze strekten zich oostwaarts uit tot aan de rand van het continentaal plat, over wat nu de zeebodem is van de Straat van Madura. Door de regionale bodemdaling kwam dit laagland langzaam maar zeker binnen het bereik van zeespiegelfluctuaties kwam te liggen, waardoor de benedenloop van deze rivieren soms verdronk, tijdens periodes met een hoge zeespiegel, dus tijdens interglacialen. Als de benedenloop van een rivier verdrinkt dan heeft dat gevolgen voor haar lengteprofiel. Een rivier reageert dan doorgaans door sediment af te zetten in haar bovenloop. Trekt de zee zich weer terug, dan begint de rivier zich weer in te snijden. Afhankelijk van de tektonische situatie kan dit proces, van afwisselende sedimentatie en insnijding, leiden tot de vorming van rivierterrassen (onder omstandigheden van opheffing) of tot begraven sets van dal-opvullingen (onder omstandigheden van bodemdaling). Beide kunnen in oostelijk Java worden waargenomen. In de aan bodemdaling onderhevige kustvlakte rond Jombang en Mojokerto vind je oude dalopvullingen van de Brantas, begraven onder het oppervlak. Erg interessant is dat deze dalopvullingen lokaal omhoog zijn geduwd, in jonge plooiruggen. Zandgroeves in dit gebied geven een prachtige zicht op dit cyclische gedrag van de Brantas, dat vrij goed gerelateerd kan worden aan de Midden-Pleistocene zeespiegelcurve. Hier liggen ook de vindplaatsen van Perning en Jetis, die onder andere de beroemde schedel van Mojokerto hebben opgeleverd. In de opgeheven vlakte rond Trinil en Ngawi heeft de Solo een mooie reeks fluviatiele terrassen gevormd, met fossielhoudende rivierafzettingen van verschillende ouderdommen. De terrassen zijn te volgen tot in de dwarsvallei door de Kendeng, waar zich het befaamde terras van Ngandong bevindt, waarschijnlijk de rijkste vindplaats van *Homo erectus*-schedels ter wereld. Ten noorden van de Kendeng bevindt zich de dalende Randublatung Vallei, die doorloopt tot aan de kustvlakte langs de Straat van Madura. De terrassen verdwijnen hier abrupt en gaan over in begraven dal-opvullingen.

De fluviatiele afzettingen van de Brantas en de Solo vormen een schitterende en goed aan de zeespiegelcurve te koppelen reeks, waarbij met name voor de Brantas nog aanvullende dateringen noodzakelijk zijn, ter verificatie van het voorgestelde raamwerk. Misschien nog wel belangrijker is dat hiermee ook een verbinding is gemaakt tussen de stratigrafie van Java en die van de zeebodem op het continentaal plat, volgens het principe dat de fluviatiele pakketten op het eiland en mariene pakketten op de zeebodem beide gerelateerd zijn aan periodes met een hoge zeespiegel en dus ruwweg met elkaar gecorreleerd kunnen worden.

De vallei-opvullingen van de Solo zijn oostwaarts te volgen tot in het kustgebied van de Straat van Madura. De nieuwe fossielenvindplaats in de Straat van Madura is zo’n oude vallei van de Solo. Op basis van reconstructies van insnijdings- en sedimentatiecycli konden we deze oude vallei koppelen aan het voorlaatste glaciaal. Dit werd bevestigd

door OSL-dateringen van het fluviatiele sediment. Deze wezen op een ouderdom van ca. 140 duizend jaar, iets jonger dan het glaciaal-maximum van deze ijstijd. Hiermee is de dalopvulling te relateren aan de fase waarin de zeespiegel weer steeg en de rivier zijn oude vallei begon op te vullen met sediment.

De fossielen in dit rivierzand zijn de overblijfselen van fluviatiele dieren, zoals rivierhaaien, krokodillen, schildpadden en nijlpaarden, gemengd met de overblijfselen van terrestrische dieren zoals runderen, herten, olifanten, neushoorns en zwijnen. In totaal konden 36 verschillende diersoorten worden geïdentificeerd, wat de collectie buitengewoon soortenrijk maakt. Alles bij elkaar vertegenwoordigt de collectie een laaglandfauna, die hoorde bij een savanne-achtige vlakte langs een grote, langzaam stromende rivier. Verschillende soorten pijlstaartroggen, haaien en schildpadden waren niet eerder beschreven van vindplaatsen op Java. Andere soorten waren wel eerder beschreven op Java, maar zijn uiterst zeldzaam, zoals makaken en Komodovaranen. Deze laatste soort was één van de belangrijkste roofdieren binnen het ecosysteem. Het laat zien dat zijn huidige territorium, op Komodo, Rinca en Flores, een overblijfsel is van een veel groter verspreidingsgebied. Van soorten als *Duboisia santeng* en *Epileptobos groeneveldtii* werd voorheen verondersteld dat ze al eerder waren uitgestorven, maar ze bleken tot ten minste 140 duizend jaar geleden te hebben overleefd op de laaglandvlakte van Sundaland. Een waardevol facet van ons onderzoek is dat alle geïdentificeerde skeletresten zijn opgemeten en beschreven, hetgeen een interessant inzicht geeft in lichaamsgrootte en evolutionaire trends per soort, en bovendien een goede referentie biedt voor toekomstige identificaties.

Onder de geïdentificeerde fossielen bevinden zich twee menselijke schedelfragmenten. Het materiaal dateert uit een periode van grote veranderingen in de menselijke populatie in Azië. Op het vasteland werd *Homo erectus* geleidelijk vervangen door binnenvallende groepen van meer moderne menssoorten, onder wie Denisoviërs en Neanderthalers. Op Java lijkt *Homo erectus* al deze tijd te hebben overleefd, als een relictpopulatie. Maar geldt dit ook voor de laaglandvlaktes van Sundaland? Sundaland was immers het grootste deel van deze tijd gewoon verbonden met het vasteland van Azië. We hebben een gedetailleerde metrische en morfologische vergelijking uitgevoerd tussen de nieuwe schedelfragmenten van de Straat van Madura en alle relevante schedels uit het Pleistoceen van China, India, Java en Flores. Hieruit blijkt dat de schedelfragmenten uit de Straat van Madura een grote verwantschap vertonen met de late *Homo erectus* van Java en niet zozeer met de even oude, maar morfologisch meer moderne populaties van het Aziatische vasteland. Dit toont aan dat de Javaanse *Homo erectus* een groter territorium had, dat zich uitstrekte over de laaglandvlaktes van Sundaland. In plaats van te spreken van de Java-mens, kunnen we misschien beter spreken van de Sunda-mens. Het roept echter wel de vraag op: waarom drongen de populaties van het vasteland niet door tot in Sundaland? Deze vraag is niet zo eenvoudig te beantwoorden. Een mogelijkheid is dat de savanne zich alleen over het zuidoostelijke deel van Sundaland uitstrekte, en dat dit gebied in het noorden werd afgeschermd door een dicht equatoriaal woud, dat een barrière vormde voor de verspreiding van soorten die zich het liefst ophouden in meer open terrein.

Snijsporen op fossiele botten tonen aan dat de *Homo erectus* van de Straat van Madura zich voedde met rivierschildpadden en runderen. De ledemaatbotten van de runderen werden gebroken om toegang te kijgen tot het beenmerg. Interessant is dat de meeste runderen in de collectie zijn gestorven als jongvolwassene. Dit is niet wat je onder natuurlijke omstandigheden zou verwachten en wijst op selectieve jacht door mensen, gericht op het doden van de meest vetrijke exemplaren binnen een kudde. In Europa en op het Aziatische vasteland wordt dit gedrag over het algemeen in verband gebracht met relatief moderne populaties zoals de Neanderthalers. Mogelijk ontwikkelde de Sunda Mens dit gedrag onafhankelijk. Maar het is ook mogelijk dat de Sunda Mens dit gedrag heeft overgenomen van binnenvallende modernere groepen. Hiermee is het ook nog steeds mogelijk dat de late *Homo erectus,* van Java en van de Straat van Madura, wel degelijk al genen droeg van deze meer moderne mensachtigen van het vasteland.

SUMMARY

The vertebrate fossils of eastern Java have fascinated the world for more than a century. The area holds some of the richest hominin sites of the world and yielded the type specimens of *Homo erectus*. What makes this area so rich in Pleistocene fossils? This is a question I often get from an interested audience. For sure, Java must have had a rich and diverse vertebrate community throughout the Pleistocene. But the chance that bones of terrestrial species end up as fossils is very small. What helped, is that most of the time eastern Java had a relatively dry climate, with low bone weathering rates. There was a pronounced rainy season, washing scattered bones into river channels. A high supply of volcanic sand caused efficient burial in fluvial sediment. Eastern Java is also a tectonically active zone, with local subsidence, which makes that such fluvial deposits were preserved. In later time, this same tectonism resulted in local folding and uplift, exposing the ancient deposits and their fossil content. And finally, it is helpful that eastern Java is, also today, relatively dry, which provides more or less open exposures, and it makes that there is no tropical weathering, which would quickly reduce embedded bones to clay.

The fossils from eastern Java give an interesting insight into the evolution and dispersal of species over Southeast Asia. The islands of western Indonesia, which include Java, are part of the Sunda Shelf. In the past, the shelf has been subaerially exposed, forming a wide continental zone that connected western Indonesia to the Asian mainland. We call this lost continent Sundaland. Stages of Sundaland exposure have been linked to ice ages, also known as glacials, by the mechanism that large volumes of water get stored in ice caps, resulting in a lower global sea-level. *Homo erectus* may have reached Java under such glacial conditions.

Against this background, the discovery of the Madura Strait vertebrate site was very exciting news. It is the first subsea fossil site of the Sunda Shelf, offering a unique window to the vertebrate community of the lowland plains of Sundaland. The fossils were excavated from the seabed during a sand extraction work. The extracted sand was transported to a coastal site in Gresik, where it was used to develop a new harbour terrain. In 2015, just after its completion, this site was a 100 ha-wide sandy plain, completely desolated and baking in the sun. Upon inspection, its surface appeared to be strewn with vertebrate fossils. It took me several months to pick them all up, collecting a total of 6372 specimens.

Collecting the fossils was only the beginning. The subsequent analysis and interpretation of the geology and the fossils proved to be difficult within the accepted geological and palaeontological models for Java. The stratigraphy of Java, which subdivides the depositional record of the island in larger units, was rather simple and seemed to ignore the complex landscape setting of the island, subject to volcanism, tectonism, sea-level fluctuations and changing drainage systems. Moreover, there appeared to be no connection between the island stratigraphy of Java and the offshore stratigraphy of the shelf. The island has been the domain of palaeontologists and archaeologists, whereas the shelf sea has been the domain of oil companies searching the area for hydrocarbon reserves. Their seismic surveys revealed a sub-seabed geology with cyclic build-up, of stacked sea-level related marine sequences, pointing to repeated stages of submergence and intermittent stages of shelf exposure. But a similar cyclicity was unknown from the depositional record of Java. This is strange, even more so because palaeontologists refer to such alternating stages of shelf submergence and shelf emergence to explain changes in the fossil record of Java.

To solve these matters, I started, together with colleagues from the Netherlands and Indonesia, a re-investigation of the geology of eastern Java and its vertebrate sites. Indeed, the depositional record of the island appeared to be much more complex than previously understood. It contains significant hiatuses and has considerable lateral variation. The previous use of regional chronostratigraphic units is largely incorrect. Instead, we defined local units. Units that follow major lithological changes and reflect important changes in the local depositional landscape. The units do not infer unproven regional age relations. Nevertheless, we did our best to place them in a chronological context, referring to available numerical ages. How do you know these ages? This is another frequently asked question. There are several ways to date deposits, but they usually come with uncertainties. For marine deposits we may refer to dated ranges of specific microfossils. For terrestrial deposits in a volcanic terrain, we may use radiometric dating techniques, but these determine crystallization ages, which are not necessarily the same as depositional ages, certainly not for fluvially re-deposited material, which is generally what we work with on Java. Another option is OSL-dating. This method determines the time that has passed since a mineral grain was last exposed to light. This gives an age of actual deposition, but the technique only works for specific sediment types, and for ages below around 450 thousand years. There are more techniques, such as measuring the magnetic polarity of sediment and linking this to dated reversals of the earth's magnetic field. Altogether, such ages only form pieces of the puzzle. It is important to also take into account other chronological information, such as major eruptions or a change of volcanic style, tectonic events, a changing climate, or a change of river behaviour. All these things left their traces in the depositional record and sometimes even in the present-day landscape, and can be used for correlations and age estimates.

One of the most important patterns in the geological record is a cyclicity related to sea-level fluctuations. It allows for correlations, and in combination with a few reliable numerical ages, forms a good framework. Most of all, it provides the long-sought connection with the off-shore geology. However, the situation proved to be a bit different than previously assumed. Recent studies have shown that the Sunda Shelf is not a tectonically stable surface, but instead has been subject to subsidence. The shelf was widely exposed during the Early Pleistocene, and only came within the reach of sea-level fluctuations in the course of the Middle Pleistocene. On eastern Java, this was the period in which the two large drainage systems developed, the Brantas and the Solo. These days, the rivers were much longer than they are today and extended eastwards all the way to the shelf edge, over what now is the seabed of the Madura Strait. Each time their lower reaches became flooded, the rivers responded by sedimentation in their higher reaches. And as the sea retreated again, the rivers incised new valleys. Depending on the tectonic situation, this process of alternating sedimentation and incision may have formed river terraces (under uplift conditions) or stacked and buried valley-fills (under conditions of subsidence). Both can be observed on eastern Java. In the subsiding plains area around Jombang and Mojokerto, the Brantas formed stacked fluvial sequences, buried below the surface of the plains. Interestingly, these have locally been pushed up in a series of young folds, providing beautiful exposures of these fluvial deposits, which contain the hominin-bearing bone beds of Perning and Jetis. In the uplifted plains around Trinil and Ngawi, the Solo formed a unique series of fluvial terraces, with fossil-bearing fluvial deposits of various ages. The terraces can be traced to the Kendeng traverse valley, where we find the famous hominin-bearing terrace of Ngandong. North of the Kendeng ridge, these terraces continue as stacked valley fills, buried in the coastal clays of the subsiding plains of the Randublatung Valley. For both rivers, the incision and aggradation cycles could be linked with the sea-level curve, forming a reliable age framework. The fluvial sequences of the Brantas and the Solo finally made it possible to establish a link between the stratigraphy of Java and the stacking of marine sequences of the central part of the shelf, by the principle that both are linked to sea-level highstands.

The buried Pleistocene valleys of the Solo can be traced eastwards to the Madura Strait seabed. The Madura Strait vertebrate site is one of the ancient valleys. Based on our reconstructions of incision-aggradation cycles and shelf subsidence, the valley might have been cut during the second last glacial. This was confirmed by OSL-datings of the sandstone fill, which gave an age of around 140 thousand years. This age slightly postdates the glacial maximum, and links the valley fill to the subsequent stage of rising sea level.

The skeletal elements in this fluvial sediment are the remains of fluvial vertebrates, such as river sharks, crocodilians, turtles and hippopotamids, mixed with the remains of terrestrial vertebrates, such as bovids, cervids, elephantoids, rhinos, and suids. A total of 36 different species could be identified, which makes the assemblage extremely rich in species. Altogether, the assemblage represents a lowland community, populating the grass-dominated terrain along a large, slow-moving river. Several species of stingrays, sharks and turtles were previously undescribed from Java. Other species are extremely rare within the Javanese fossil assemblages, such as macaques and Komodo dragons. The latter species was an important predator of the lowland plains of Pleistocene Sundaland, indicating that its current territories on Komomo, Rinca and Flores are a relict of a much larger geographic range. Species such as *Duboisia santang* and *Epileptobos groeneveldtii* were previously assumed to have gone extinct earlier in time, but were shown to have survived on the Sundaland plains up to at least 140 thousand years ago. A valuable feature of our faunal studies is that all identified remains have been measured in detail, which gives an interesting insight into size ranges and evolutionary trends per species and provides a reference for future identifications.

Among the identified fossils are two hominin skull fragments. The material dates from a period of great changes of the hominin population in Asia. On the mainland, the older *Homo erectus* population was replaced by invading more modern hominins, amongst which were Denisovans and Neanderthals. On Java, *Homo erectus* appeared to have survived as a relict population. But does this also account for the lowland plains of Sundaland? After all, Sundaland was openly connected to mainland Asia most of this time. To get a better grip on this interesting question, we carried out a detailed metric and morphological comparison of the new skull fragments with all relevant Pleistocene skulls from China, India, Java and Flores. This showed that the Madura Strait skull fragments have a great affinity with the late *Homo erectus* from Java and not so much with the contemporary, more modern populations from the Asian mainland. It shows that the Javanese *Homo erectus* had a larger territory, which extended over the lowland plains of Sundaland. Instead of Java Man, we may better speak of Sunda Man. This, however, brings up the question: why didn't the late Middle Pleistocene mainland hominins penetrate into Sundaland? This question is not so easy to answer. A possibility is that the Sundaland savanna only covered the southeastern part of Sundaland, and that it was shielded from the plains further to the north by a dense equatorial forest, which formed a barrier for species more adapted to an open terrain.

Cutmarks on fossil bones show that the Madura Strait hominins foraged on river turtles and bovids. Bovid limb bones were broken for collecting bone-marrow. Interestingly, the death assemblage of bovids is dominated by young adults. This is not what you would expect under natural conditions and points to selective hunting by hominins, aiming for the most fat-rich prey. In Europe and mainland Asia, this behaviour is generally linked to relatively modern popula-

tions such as Neanderthals. Possibly, Sunda man developed this behaviour independently. But it may also be possible that Sunda man copied this behaviour from invading more modern groups. This makes that we still cannot rule out that the late *Homo erectus* from Java, and from the Madura Strait, did already carry some genes of these mainland populations.

DANKWOORD

Dit onderzoek was een schitterende reis door het ongerepte Sundaland en het getoeter van het hedendaagse Java. Onderweg ben ik vele vertebraten tegengekomen en enkelen hebben me enorm geholpen. Zoals mijn drie begeleiders, Thijs van Kolfschoten, José Joordens en Tom Veldkamp.

Thijs, zonder jou was dit proefschrift er nooit gekomen. Jij durfde het aan om deze zwerver een promotieplekje aan te bieden. We maakten snoepreisjes naar Java en Japan. Overdag botjes ordenen in het museum, 's avonds een biertje op de veranda. Veel dank voor je anatomische lessen, je vertrouwen en positieve houding. Ons voortgangsoverleg hielden we doorgaans in een Utrechtse cappuccinobar met diverse taartjes. Ik hoop dat we die traditie voortzetten!

José, het was een geniaal idee om mijn studie in jouw project te integreren. Het voorzag mijn gepruts met fossieltjes van een brede context. Als ik weer 's verstrikt zat in een veel te vage hypothese en het allemaal nauwelijks onder woorden kon brengen, snapte jij meteen wat ik bedoelde. Zonder jouw coaching en slimme ingevingen had ik dit onderzoek nooit tot een goed einde kunnen brengen. Ik hoop dat we de komende jaren nog meer Javaanse ontdekkingen doen.

Tom, je hebt een bijzonder oog voor geologie en veranderende landschappen. In Trinil liet je dit zien in het veld. Maar je kon het ook voor sites waar je nooit bent geweest. Bij mij thuis, met een soepje en een broodje, en met mijn kaarten, profielen en foto's over de tafel uitgespreid, legde je met gemak de ontbrekende puzzelstukjes.

Dan zijn er nog heel wat anderen die een grote rol hebben gespeeld. Zoals Simon Troelstra; jouw biostratigrafie heeft de basis gelegd voor alle daaropvolgende papers. André Ramcharan, veel dank voor je lessen bot-identificatie en voor de gastvrijheid in jouw schitterende archeozoölogisch laboratorium. Tony Reimann en Alice Versendaal, zonder jullie dateringen had niemand het geloofd! Sander Hilgen en Eduard Pop, wij waren de drie kindjes van José. Onze Trinil-papers hebben de archeologische wereld op haar grondvesten doen schudden!

Botjes identificeren is leuk, maar er bleven altijd stukken liggen waar ik niet uitkwam. Gelukkig waren er dan echte experts aan wie ik een fotootje kon sturen. Thijs en André, maar ook Gert van den Bergh en Ivo Verheijen. 'Oh, dat is gewoon een …'.

Veel dank ben ik verschuldigd aan Peter van der Hulst en zijn collega's van Van Oord. Jullie hebben de botjes opgezogen, al was dat voor jullie bijvangst. Maar vervolgens mocht ik ook vrijelijk al jullie onderzoeksgegevens en baggerrapporten gebruiken.

Dan zijn er nog mijn wetenschappelijke helden: Dubois, Von Koenigswald, Duyfjes en Hooijer. In dit proefschrift wijs ik een heel enkele keer op kleine onjuistheden in jullie geschriften, maar dat doet niets af aan mijn grote ontzag.

Verder heb ik heel wat persoonlijke steun gehad. Lieve Odile, de meeste van mijn plannen hoon jij terecht weg. Maar, toen ik verkondigde dat ik wel een proefschrift wilde schrijven reageerde je gelijk enthousiast. Paar weken in het veld? Geen probleem, we pakken de agenda erbij! Inzinking? We maken een stappenplannetje! Mijn artikelen waren 'onleesbaar en te lang', maar gelukkig waren er ook nog door AI geconstrueerde samenvattingen en podcasts. Ada, Willemijn en Zwaantje, jullie weten niet beter dan dat je vader iets met fossielen doet en dat hij werkt aan iets wat nooit afkomt. Een paar jaar terug was het lockdown en zaten we met zijn allen gezellig aan de keukentafel te werken. Maar het is inderdaad vreemd dat iedereen in de jaren daarna weer lekker naar buiten ging, terwijl ik aan die keukentafel bleef zitten typen. Maar ik hield het vol, omdat we elke avond weer gezellig zaten te lachen aan diezelfde tafel.

UCAPAN TERIMA KASIH

Saya mengucapkan terima kasih kepada direksi Berlian Manyar Sejahtera: bapak Harry Purwanto, Hendiek Eko Setiantoro dan ibu Dewi Djunaidi, atas izin untuk mengumpulkan fosil di tempat reklamasi. Terima kasih juga kepada direksi dan pemimpin Pelindo 3, atas bantuan dan menyediakan data geoteknis: bapak Djarwo Surjanto, Didid Handoko, dan Heskiel Sasiang.

Terima khusus kepada direksi dan ilmuwan Museum Geologi dan Museum Trinil, atas pekerjaan sama dan persahabatan: bapak Isnu Hajar Sulistyawan, Iwan Kurniawan, Unggul Wibowo, Indra Sutisna, Halmi Insani dan Catur Hari Gumono. Dan saya mengucapkan terima kasih kepada Pusat Penelitian Arkeologi Nasional dan Badan Riset dan Inovasi Nasional, atas perizinan, pekerjaan sama dan persahabatan: bapak I Made Geria, Sofwan Noerwidi dan Shinatria Adhityatama.

Akhirnya, saya mengucapkan terima kasih kepada warga desa, atas keramahan, atas tempat istirahat, atas puluhan cangkir kopi tubruk, dan atas kekuatiran jika saya belum kembali dari hutan saat senja. Terima kasih khusus kepada Agus Hadi Widianto (Trinil) dan Sumani Parmin (Marmoyo), yang menemani saya di lapangan, selama berjalan jauh. Syukurlah kita tidak takut kaki basah!

ACKNOWLEDGEMENTS

It was a pleasure and great honour to work with Yousuke Kaifu. One day I would like to have a lab like yours, with cabinets full of comparative skulls... And I am grateful to the editors of Quaternary Environments and Humans, Andrea Zerboni and Silvia Bello, for their willingness to publish all Madura Strait-articles in one beautiful edition. For me a dream came true.

TENSLOTTE

De Maori’s weten dat rivieren een ziel hebben. In sommige landen is het gebruik in opkomst om rivieren als rechtspersonen te beschouwen. Dan vind ik het niet gek om een rivier te bedanken. De Solo leidt tegenwoordig een armzalig bestaan, als afvoerputje van allerhande troep. Maar nog altijd is zij schitterend, in al haar kronkels. Je voelt gewoon dat ze een sterke ziel heeft. Haar oevers vormen misschien wel de langst-bevolkte streek ter wereld. Dank je wel, lieve Solo, voor alles wat je mij en de mensheid hebt gegeven.

CURRICULUM VITAE

Harold Berghuis (Amstelveen, 1969) studied Geology at the Vrije Universiteit Amsterdam (1988-1993). After his graduation and military service, he started working at MH-Nederland, a Dutch geotechnical engineering company nowadays known as MH-Poly. In 2005 he set up his own company Sealand Coastal Consultancy, focussing on seabed dredging and port design. Indonesia became his main working area, with projects such as the relocation and deepening of the Barito approach channel (South-Kalimantan) and the deepening and extension of the ports of Surabaya (East-Java) and Belawan (North-Sumatra).

In 2015, Harold collected more than 6,000 fossils during a dredging and reclamation work in Surabaya. This sparked his interest for the palaeontology of Java. In 2018, he started his PhD trajectory at the Faculty of Archaeology of Leiden University, supervised by professor Thijs Van Kolfschoten, to study the geology and vertebrate palaeontology of eastern Java.

Harold is married and has three daughters. He is interested in history, languages, landscapes, sports and music.

REFERENCES

Adhityatama, S., Yarista, A.S., 2019. Potensi arkeologi lanskap bawah air Indonesia. Kalpataru 28, 55–71.

Aimi, Aziz, 1985. Vertebrate fossils from the Sangiran dome, Mojokerto, Trinil and Sambungmacan areas. Quaternary geology of the hominid fossil bearing formations in Java.

Albab, A., Aryanto, N.C.D., 2017. Seismic Facies of Pleistocene–Holocene Channel-fill Deposits in Bawean Island and Adjacent Waters, Southeast Java Sea. Bulletin Of the marine Geology 32, 230193.

Ali, Abdullah, Nor, Pau, Kulaimi, Naim, 2021. A review of the genus Rusa in the indo-malayan archipelago and conservation efforts. Saudi Journal of Biological Sciences.

Alqahtani, F.A., Johnson, H.D., Jackson, C.A.-L., Som, M.R.B., 2015. Nature, origin and evolution of a Late Pleistocene incised valley-fill, Sunda Shelf, Southeast Asia. sedimentology 62, 1198–1232.

Amson, E., Billet, G., De Muizon, C., 2018. Evolutionary adaptation to aquatic lifestyle in extinct sloths can lead to systemic alteration of bone structure. Proc. R. Soc. B. 285, 20180270. https://doi.org/10.1098/rspb.2018.0270

Andrews, P., Jalvo, Y.F., 1997. Surface modifications of the Sima de los Huesos fossil humans. Journal of Human Evolution 33, 191–217.

Antoine, P.-O., 2012. Pleistocene and Holocene rhinocerotids (Mammalia, Perissodactyla) from the Indochinese Peninsula. Comptes Rendus Palevol 11, 159–168.

Antoine, P.-O., Reyes, M.C., Amano, N., Bautista, A.P., Chang, C.-H., Claude, J., De Vos, J., Ingicco, T., 2022. A new rhinoceros clade from the Pleistocene of Asia sheds light on mammal dispersals to the Philippines. Zoological Journal of the Linnean Society 194, 416–430.

Antón, S.C., 2003. Natural history of Homo erectus. Am. J. Phys. Anthropol. 122, 126–170. https://doi.org/10.1002/ajpa.10399

Antón, S.C., 2002. Evolutionary significance of cranial variation in Asian *Homo erectus*. American J Phys Anthropol 118, 301–323. https://doi.org/10.1002/ajpa.10091

Ashworth, P.J., Best, J.L., Leddy, J.O., 1994. The physical modelling of braided rivers and deposition of fine-grained sediment, in: Process Models and Theoretical Geomorphology§. Wiley and sons, Chichester, pp. 115–139.

Athreya, S., Hopkins, A., 2021. Conceptual issues in hominin taxonomy: *Homo heidelbergensis* and an ethnobiological reframing of species. American J Phys Anthropol 175, 4–26. https://doi.org/10.1002/ajpa.24330

Athreya, S., Wu, X., 2017. A multivariate assessment of the Dali hominin cranium from China: Morphological affinities and implications for Pleistocene evolution in East Asia. American J Phys Anthropol 164, 679–701. https://doi.org/10.1002/ajpa.23305

Auclair, M., Lamothe, M., Huot, S., 2003. Measurement of anomalous fading for feldspar IRSL using SAR. Radiation measurements 37, 487–492.

Aziz, F., de Vos, J., 1999. The fossil faunas from the Citarum area, West Java, Indonesia. Deinsea 7, 21–32.

Baab, K.L., 2011. Cranial Shape in Asian Homo erectus: Geographic, Anagenetic, and Size-Related Variation, in: Norton, C.J., Braun, D.R. (Eds.), Asian Paleoanthropology, Vertebrate Paleobiology and Paleoanthropology. Springer Netherlands, Dordrecht, pp. 57–79. https://doi.org/10.1007/978-90-481-9094-2_6

Baab, K.L., Zaim, Y., 2017. Global and local perspectives on cranial shape variation in Indonesian Homo erectus. Anthropological Science 125, 67–83.

Baba, H., Aziz, F., Kaifu, Y., Suwa, G., Kono, R.T., Jacob, T., 2003. *Homo erectus* Calvarium from the Pleistocene of Java. Science 299, 1384–1388. https://doi.org/10.1126/science.1081676

Badgley, C., 1986. Taphonomy of mammalian fossil remains from Siwalik rocks of Pakistan. Paleobiology 12, 119–142.

Badoux, D.M., 1959. Fossil mammals from two deposits at Punung (Java). Ph. D. thesis.

Bae, C.J., Wu, X., 2024. Making sense of eastern Asian Late Quaternary hominin variability. Nature communications 15, 9479.

Bailey, G., Cawthra, H.C., 2023. The significance of sea-level change and ancient submerged landscapes in human dispersal and development: A geoarchaeological perspective. Oceanologia 65, 50–70.

Balzeau, A., 2006. Are thickened cranial bones and equal participation of the three structural bone layers autapomorphic traits of Homo erectus? Bulletins et mémoires de la Société d'Anthropologie de Paris. BMSAP 18, 145–163.

Balzeau, A., Albessard-Ball, L., Kubicka, A.M., Filippo, A., Beaudet, A., Santos, E., Bienvenu, T., Arsuaga, J.-L., Bartsiokas, A., Berger, L., Bermúdez De Castro, J.M., Brunet, M., Carlson, K.J., Daura, J., Gorgoulis, V.G., Grine, F.E., Harvati, K., Hawks, J., Herries, A., Hublin, J.-J., Hui, J., Ives, R., Joordens, J.A., Kaifu, Y., Kouloukoussa, M., Léger, B., Lordkipanidze, D., Margvelashvili, A., Martin, J., Martinón-Torres, M., May, H., Mounier, A., Du Plessis, A., Rae, T., Röding, C., Sanz, M., Semal, P., Stratford, D., Stringer, C., Tawane, M., Temming, H., Tsoukala, E., Zilhão, J., Zipfel, B., Buck, L.T., 2022. Frontal sinuses and human evolution. Sci. Adv. 8, eabp9767. https://doi.org/10.1126/sciadv.abp9767

Bandy, O.L., 1972. Neogene planktonic foraminiferal zones, California, and some geologic implications. Palaeogeography, Palaeoclimatology, Palaeoecology 12, 131–150. https://doi.org/10.1016/0031-0182(72)90010-7

Bartstra, G., 1982. Tbe river-laid strata near Trinil, site of Homo erectus, Java, Indonesia. Modern Quaternary Research in Southeast Asia Vol 7, 97–130.

Bartstra, G.-J., 1988. The age of Solo Man and Java Man, in: Early Man in the Southern Hemisphere. pp. 12–22.

Bartstra, G.J., 1983. The vertebrate-bearing deposits of Kedungbrubus and Trinil, Java, Indonesia. Geologie en Mijnbouw 62, 329–336.

Bartstra, G.-J., 1978. The age of the Djetis beds in East and Central Java. Antiquity 52, 56.

Behrensmeyer, A.K., 1988. Vertebrate preservation in fluvial channels. Palaeogeography, Palaeoclimatology, Palaeoecology 63, 183–199.

Behrensmeyer, A.K., 1984. Taphonomy and the fossil record: the complex processes that preserve organic remains in rocks also leave their own traces, adding another dimension of information to fossil samples. American Scientist 72, 558–566.

Behrensmeyer, A.K., 1978. Taphonomic and ecologic information from bone weathering. Paleobiology 4, 150–162.

Behrensmeyer, A.K., Gordon, K.D., Yanagi, G.T., 1986. Trampling as a cause of bone surface damage and pseudo-cutmarks. Nature 319, 768–771.

Behrensmeyer, A.K., Western, D., Boaz, D.E.D., 1979. New perspectives in vertebrate paleoecology from a recent bone assemblage. Paleobiology 5, 12–21.

Ben-Dor, Gopher, Hershkovitz, Barkai, 2011. Man the Fat Hunter: The Demise of Homo erectus and the Emergence of a New Hominin Lineage in the Middle Pleistocene (ca. 400 kyr) Levant. Plos One.

Berggren, W.A., Hilgen, F.J., Langereis, C.G., Kent, D.V., Obradovich, J.D., Raffi, I., Raymo, M.E., Shackleton, N.J., 1995. Late Neogene chronology: New perspectives in high-resolution stratigraphy. GSA Bulletin 107, 1272–1287. https://doi.org/10.1130/0016-7606(1995)107<1272:LNCNPI>2.3.CO;2

Berggren, W.A., Kent, D.V., Flynn, J.J., Couvering, J. a. V., 1985. Cenozoic geochronology. GSA Bulletin 96, 1407–1418. https://doi.org/10.1130/0016-7606(1985)96<1407:CG>2.0.CO;2

Berghuis, H.W.K., Veldkamp, A., Shinatria Adhityatama, Reimann, T., Versendaal, A., Kurniawan, I., Pop, E., Van Kolfschoten, T., Joordens, J.C.A., 2025a. A late Middle Pleistocene lowstand valley of the Solo River on the Madura Strait seabed, geology and age of the first hominin locality of submerged Sundaland. Quaternary Environments and Humans.

Berghuis, H.W.K., Adhityatama, S., Troelstra, S.R., Noerwidi, S., adi Suriyanto, R., prasetyo Wibowo, U., Pop, E., Kurniawan, I., Veldkamp, A., Joordens, J.C., 2023. Response to the comment by Huffman and Zaim. Quaternary science reviews 307, 108059.

Berghuis, H.W.K., Kaifu, Y., Prasetyo Wibowo, U., Van Kolfschoten, T., Sutisna, I., Noerwidi, S., Shinatria Adhityatama, Van den Bergh, G., Pop, E., Suriyanto, R.A., Veldkamp, A., Joordens, J.C.A., Kurniuawan, I., 2025d. The late Middle Pleistocene Homo erectus of the Madura Strait, first hominin fossils from submerged Sundaland. Quaternary Environments and Humans.

Berghuis, H.W.K., Troelstra, S.R., Zaim, Y., 2019. Plio-Pleistocene foraminiferal biostratigraphy of the eastern Kendeng Zone (Java, Indonesia): The Marmoyo and Sumberingin Sections. Palaeogeography, Palaeoclimatology, Palaeoecology 528, 218–231. https://doi.org/10.1016/j.palaeo.2019.05.008

Berghuis, H.W.K., Van den Bergh, G., Van Kolfschoten, T., Prasetyo Wibowo, U., Kurniawan, I., Shinatria Adhityatama, Sutisna, I., Verheijen, I., Pop, E., Veldkamp, A., Joordens, J.C.A., 2025b. First vertebrate faunal record from submerged Sundaland: the late Middle Pleistocene, hominin-bearing fauna of the Madura Strait. Quaternary Environments and Humans.

Berghuis, H.W.K., Van Kolfschoten, T., Adhityatama, S., Troelstra, S.R., Noerwidi, S., Suriyanto, R.A., Wibowo, U.P., Pop, E., Kurniawan, I., Hilgen, S.L., 2022. The eastern Kendeng Hills (Java, Indonesia) and the hominin-bearing beds of Mojokerto, a re-interpretation. Quaternary science reviews 295, 107692.

Berghuis, H.W.K., Van Kolfschoten, T., Prasetyo Wibowo, U., Kurniawan, I., Shinatria Adhityatama, Sutisna, I., Pop, E., Joordens, J.C.A., 2025c. The taphonomy of the Madura Strait fossil assemblage, a record of selective hunting and marrow processing by late Middle Pleistocene Sundaland hominins. Quaternary Environments and Humans.

Berghuis, H.W.K., Veldkamp, A., Adhityatama, S., Hilgen, S.L., Sutisna, I., Barianto, D.H., Pop, E.A., Reimann, T., Yurnaldi, D., Ekowati, D.R., 2021. Hominin homelands of East Java: Revised stratigraphy and landscape reconstructions for Plio-Pleistocene Trinil. Quaternary Science Reviews 260, 106912.

Bhattacharya, J.P., 2006. Deltas.

Binford, L.R., 1981. Bones: ancient men and modern myths. Academic press.

Bintanja, R., van de Wal, R.S.W., 2008. North American ice-sheet dynamics and the onset of 100,000-year glacial cycles. Nature 454, 869–872. https://doi.org/10.1038/nature07158

Bird, M.I., Taylor, D., Hunt, C., 2005. Palaeoenvironments of insular Southeast Asia during the Last Glacial Period: a savanna corridor in Sundaland? Quaternary Science Reviews 24, 2228–2242.

Black, D., 1930. Discovery of Skull of Adult Sinanthropus at Chou Kou Tien. Anthropologischer Anzeiger 358–359.

Blasco, R., Rosell, J., Peris, J.F., Cáceres, I., Vergès, J.M., 2008. A new element of trampling: an experimental application on the Level XII faunal record of Bolomor Cave (Valencia, Spain). Journal of Archaeological Science 35, 1605–1618.

Blasco, Rosell, Smith, Maul, Sañudo, Barkai, Gopher, 2016. Tortoises as a dietary supplement: A view from the Middle Pleistocene site of Qesem Cave, Israel. Quaternary Science Reviews 133, 165–182.

Blow, W.H., 1969. Late Middle Eocene to Recent planktonic foraminiferal biostratigraphy, in: Proceedings of the First International Conference on Planktonic Microfossils. EJ Brill Leiden, pp. 199–422.

Blumenschine, Cavallo, 1992. Scavenging and Human Evolution. Scientific American 267, 90–97.

Blumenschine, R.J., 1995. Percussion marks, tooth marks, and experimental determinations of the timing of hominid and carnivore access to long bones at FLK Zinjanthropus, Olduvai Gorge, Tanzania. Journal of human Evolution 29, 21–51.

Blumenschine, R.J., 1988. An experimental model of the timing of hominid and carnivore influence on archaeological bone assemblages. Journal of archaeological science 15, 483–502.

Blumenschine, R.J., 1986. Carcass consumption sequences and the archaeological distinction of scavenging and hunting. journal of Human Evolution 15, 639–659.

Blumenschine, R.J., Selvaggio, M.M., 1988. Percussion marks on bone surfaces as a new diagnostic of hominid behaviour. Nature 333, 763–765.

Boaz, N.T., Ciochon, R.L., Xu, Q., Liu, J., 2004. Mapping and taphonomic analysis of the Homo erectus loci at Locality 1 Zhoukoudian, China. Journal of Human Evolution 46, 519–549.

Bolli, H.M., 1966. The planktonic foraminifera in well Bodjonegoro-1 of Java. Geologisches Institut der Eidg. Technischen Hochschule und der Universität ….

Bolli, H.M., Saunders, J.B., Perch-Nielsen, K., 1989. Plankton Stratigraphy: Volume 1, Planktic Foraminifera, Calcareous Nannofossils and Calpionellids. CUP Archive.

Boomgaart, L., 1949. Smaller foraminifera from Bodjonegoro, Java.

Bourdon, J., Wright, K., Lucas, S.G., Spielmann, J.A., Pence, R., 2011. Selachians from the Upper Cretaceous (Santonian) Hosta Tongue of the Point Lookout Sandstone, central New Mexico: Bulletin 52. New Mexico Museum of Natural History and Science.

Bourgeon, Burke, Higham, 2017. Earliest human presence in North America dated to the last glacial maximum: new radiocarbon dates from Bluefish Caves, Canada. Plos One.

Bowen, D.W., Weimer, P., 2003. Regional sequence stratigraphic setting and reservoir geology of Morrow incised-valley sandstones (lower Pennsylvanian), eastern Colorado and western Kansas. AAPG bulletin 87, 781–815.

Brasseur, B., Sémah, F., Sémah, A.-M., Djubiantono, T., 2011. Approche paléopédologique de l'environnement des hominidés fossiles du dôme de Sangiran (Java central, Indonésie). Quaternaire 22, 13–34.

Braun, D.R., Harris, J.W.K., Levin, N.E., McCoy, J.T., Herries, A.I.R., Bamford, M.K., Bishop, L.C., Richmond, B.G., Kibunjia, M., 2010. Early hominin diet included diverse terrestrial and aquatic animals 1.95 Ma in East Turkana, Kenya. Proc. Natl. Acad. Sci. U.S.A. 107, 10002–10007. https://doi.org/10.1073/pnas.1002181107

Brongersma, Leo Daniel, 1937. Some Comments Upon HC Raven's Paper:" Wallace's Line and the Distribution of Indo-Australian Mammals". Archives néerlandaises de zoologie 2, 240–256.

Brongersma, Léo Daniël, 1937. On fossil remains of a hyaenid from Java. Zoologische Mededelingen 20, 186–202.

Brongersma, L.D., 1935. Notes on some recent and fossil cats, chiefly from the Malay Archipelago. Zoologische Mededelingen 18, 1–89.

Brongersma-Sanders, M., 1957. Mass mortality in the sea. Geological Society of America Memoirs 67, 941–1010.

Brouwer, J., 1966. Stratigraphy of the younger Tertiary in North-East Java and Madura. Bataafse Internationale Petroleum Maatschappij.

Brown, P., Sutikna, T., Morwood, M.J., Soejono, R.P., Jatmiko, Wayhu Saptomo, E., Awe Due, R., 2004. A new small-bodied hominin from the Late Pleistocene of Flores, Indonesia. Nature 431, 1055–1061.

Bull, W.B., 1990. Stream-terrace genesis: implications for soil development. Geomorphology 3, 351–367.

Bunn, H.T., 2019. Large ungulate mortality profiles and ambush hunting by Acheulean-age hominins at Elandsfontein, Western Cape Province, South Africa. Journal of archaeological science 107, 40–49.

Bunn, H.T., Gurtov, A.N., 2014. Prey mortality profiles indicate that Early Pleistocene Homo at Olduvai was an ambush predator. Quaternary International 322, 44–53.

Bunn, H.T., Kroll, E.M., Ambrose, S.H., Behrensmeyer, A.K., Binford, L.R., Blumenschine, R.J., Klein, R.G., McHenry, H.M., O'Brien, C.J., Wymer, J.J., 1986. Systematic Butchery by Plio/Pleistocene Hominids at Olduvai Gorge, Tanzania [and Comments and Reply]. Current Anthropology 27, 431–452. https://doi.org/10.1086/203467

Bunn, H.T., Pickering, T.R., 2010. Methodological recommendations for ungulate mortality analyses in paleoanthropology. Quaternary Research 74, 388–394.

Burckle, L.H., 1982. Diatom biostratigraphy of Late Miocene and Pliocene sediments of eastern Java (Indonesia). Marine Micropaleontology 7, 363–368. https://doi.org/10.1016/0377-8398(82)90012-3

Buylaert, J.-P., Jain, M., Murray, A.S., Thomsen, K.J., Thiel, C., Sohbati, R., 2012. A robust feldspar luminescence dating method for Middle and Late P leistocene sediments. Boreas 41, 435–451.

Cameron, D., Patnaik, R., Sahni, A., 2004. The phylogenetic significance of the Middle Pleistocene Narmada hominin cranium from central India. Intl J of Osteoarchaeology 14, 419–447. https://doi.org/10.1002/oa.725

Capaldo, Blumenschine, 1994. A Quantitative Diagnosis of Notches Made by Hammerstone Percussion and Carnivore Gnawing on Bovid Long Bones. America Antiquity 59, 724–748.

Cappetta, H., 1987. Chondrichthyer II, mesozoic and cenozoic elasmobranchii. Handbook of paleoichthyology, 3B 19.

Carthaus, E., 1911. Zur Geologie von Java, insbesondere des Ausgrabungsgebietes, in: Selenka and Blanckenhorn Die Pithecanthropusschichten Auf Java Geologische Und Palaontologische Ergebnisse De Trinil-Expedition (1907 Und 1908) Verlag Von Wilhelm Engelmann, Leipzig. pp. 1–33.

Cas, R.A.F., Wright, J.V., 1987. Volcanic successions: Ancient and modern. Allen and Unin, London.

Cattaneo, A., Steel, R.J., 2003. Transgressive deposits: a review of their variability. Earth-Science Reviews 62, 187–228.

Chaiyarat, R., Sriphonkrang, N., Khamsirinan, P., Nakbun, S., Youngpoy, N., 2023. Age structure, development and population Viability of Banteng (Bos javanicus) in captive breeding for ex-situ conservation and reintroduction. Animals 13, 198.

Chamero, B., Buscalioni, Á.D., Marugán-Lobón, J., Sarris, I., 2014. 3D Geometry and Quantitative Variation of the Cervico-Thoracic Region in Crocodylia. The Anatomical Record 297, 1278–1291. https://doi.org/10.1002/ar.22926

Choi, K., Driwantoro, D., 2007. Shell tool use by early members of Homo erectus in Sangiran, central Java, Indonesia: cut mark evidence. Journal of Archaeological Science 34, 48–58.

Claeson, K.M., O'Leary, M.A., Roberts, E.M., Sissoko, F., Bouaré, M., Tapanila, L., Goodwin, D., Gottfried, M.D., 2010. First Mesozoic record of the stingray Myliobatis wurnoensis from Mali and a phylogenetic analysis of Myliobatidae incorporating dental characters. Acta Palaeontologica Polonica 55, 655–674.

Claude, J., Tong, H., van der Geer, A., Antoine, P.-O., Reyes, M., de Vos, J., Ingicco, T., 2024. The origin of the Malesian fossil turtle diversity: Fossil versus molecular data, in: Annales de Paléontologie. Elsevier, p. 102665.

Cleghorn, Marean, 2007. The destruction of skeletal elements by carnivores: the growth of a general model for skeletal element destruction and survival in zooarchaeological assemblages. Sociology and Anthropology Faculty Publications.

Clements, B., Hall, R., Smyth, H.R., Cottam, M.A., 2009. Thrusting of a volcanic arc: a new structural model for Java. Petroleum Geoscience 15, 159–174.

Coil, R., Yezzi-Woodley, K., Tappen, M., 2020. Comparisons of impact flakes derived from hyena and hammerstone long bone breakage. Journal of Archaeological Science 120, 105167.

Colbert, E.H., Hooijer, D.A., 1953. Pleistocene mammals from the limestone fissures of Szechwan, China.

Compagno, L.J., 2001. Sharks of the world: an annotated and illustrated catalogue of shark species known to date. Food & Agriculture Org.

Cooper, A., Stringer, C.B., 2013. Did the Denisovans Cross Wallace's Line? Science 342, 321–323. https://doi.org/10.1126/science.1244869

Cordain, Watkins, Mann, 2001. Fatty acid composition and energy density of foods available to African hominids'.

Cosijn, J., 1932. Tweede mededeeling over het voorkomen van fossiele beenderen in het heuvelland ten Noorden van Djetis en Perning (Java). Geol. Mijnbouwk. Gen. en Kol., Geol. 135–148.

Cosijn, J., 1931. Voorlopige mededeeling omtrent het voorkomen van fossiele beenderen in het heuvelterrein ten Noorden van Djetis en Perning. Verh. Geol. Mijnbouwk. Gen. en Kol., Geol. 113–119.

Costamagno, S., Soulier, M.-C., Val, A., Chong, S., 2019. The reference collection of cutmarks. Palethnologie. Archéologie et sciences humaines.

Cui, Y., Wu, X., 2015. A geometric morphometric study of a Middle Pleistocene cranium from Hexian, China. Journal of Human Evolution 88, 54–69.

Cuny, G., Piyapong, C., 2007. Tail spine characteristics of stingrays (order myliobatiformes): a comment to Schwartz (2005). Electronic Journal of Ichthyology 3, 15–17.

Curnoe, D., Datan, I., Goh, H.M., Sauffi, M.S., 2019. Femur associated with the Deep Skull from the west mouth of the Niah Caves (Sarawak, Malaysia). Journal of Human Evolution 127, 133–148.

Curran, S.C., Drăguşin, V., Pobiner, B., Pante, M., Hellstrom, J., Woodhead, J., Croitor, R., Doboş, A., Gogol, S.E., Ersek, V., 2025. Hominin presence in Eurasia by at least 1.95 million years ago. Nature Communications 16, 836.

Dalrymple, R.W., 1992. Tidal depositional systems. Facies models response to sea-level change. 195–218.

Dam, M.A., 1994. The late Quaternary evolution of the Bandung basin, west Java, Indonesia. Thesis VU Amsterdam.

D'Amore, D.C., Blumenschine, R.J., 2009. Komodo monitor (Varanus komodoensis) feeding behavior and dental function reflected through tooth marks on bone surfaces, and the application to ziphodont paleobiology. Paleobiology 35, 525–552.

Damuth, J.E., 1980. Use of high-frequency (3.5–12 kHz) echograms in the study of near-bottom sedimentation processes in the deep-sea: a review. Marine Geology 38, 51–75.

Darmadi, Y., Willis, B.J., Dorobek, S.L., 2007. Three-dimensional seismic architecture of fluvial sequences on the low-gradient Sunda Shelf, offshore Indonesia. Journal of Sedimentary Research 77, 225–238.

de Visser, J.A., 2008. The extinct genus Hexaprotodon Falconer & Cautley, 1836 (Mammalia, Artiodactyla, Hippopotamidae) in Asia: paleoecology and taxonomy (PhD Thesis).

De Vos, D.E., 1983. The Pongo faunas from Java and Sumatra and their significance for biostratigraphical and paleoecological interpretations. Proceedings B 86, 417–425.

De Vos, J., Sartono, Hardja-Sasmita, 1982. The fauna from Trinil, type locality of Homo erectus: a reinterpretation. Geol. Mijnb. 61, 207–211.

De Vos, J., Sondaar, P., 1994. Dating hominid sites in Indonesia. Science 266, 1726–1727.

Dean et al., 2015. Abrupt termination of Marine Isotope Stage 16 (Termination VII) at 631.5 ka in Santa Barbara Basin, California - Dean - 2015 - Paleoceanography - Wiley Online Library. Paleoceanography and paleoclimatology.

Defen, H., Chunhua, X., 2016. Pleistocene mammalian faunas of China, in: Paleoanthropology and Paleolithic Archaeology in the People's Republic of China. Routledge, pp. 267–289.

Delfino, M., De Vos, J., 2010. A revision of the Dubois crocodylians, *Gavialis bengawanicus* and *Crocodylus ossifragus* , from the Pleistocene *Homo erectus* beds of Java. Journal of Vertebrate Paleontology 30, 427–441. https://doi.org/10.1080/02724631003617910

Delson, E., Harvati, K., Reddy, D., Marcus, L.F., Mowbray, K., Sawyer, G.J., Jacob, T., Márquez, S., 2001. The Sambungmacan 3 *Homo erectus* calvaria: A comparative morphometric and morphological analysis. Anat. Rec. 262, 380–397. https://doi.org/10.1002/ar.1048

Dennell, R., 2009. The Palaeolithic Settlement of Asia. Cambridge University Press.

Dennell, R., 2008. The palaeolithic settlement of Asia. Cambridge University Press.

D'Errico, F., 2003. The invisible frontier. A multiple species model for the origin of behavioral modernity. Evolutionary Anthropology 12, 188–202. https://doi.org/10.1002/evan.10113

Détroit, F., Mijares, A.S., Corny, J., Daver, G., Zanolli, C., Dizon, E., Robles, E., Grün, R., Piper, P.J., 2019. A new species of Homo from the Late Pleistocene of the Philippines. Nature 568, 181–186.

Dhani Irwanto, 2016. Atlantis in the Java Sea, last galcial vegetation of Sundaland.

Diedrich, C.G., 2012. An Ice Age spotted hyena *Crocuta crocuta spelaea* (Goldfuss 1823) population, their excrements and prey from the Late Pleistocene hyena den of the Sloup Cave in the Moravian Karst, Czech Republic. Historical Biology 24, 161–185. https://doi.org/10.1080/08912963.2011.591491

Discamps, E., Costamagno, S., 2015. Improving mortality profile analysis in zooarchaeology: a revised zoning for ternary diagrams. Journal of Archaeological Science 58, 62–76.

Domínguez-Rodrigo, Barba, Egeland, 2007. Deconstructing Olduvai: a taphonomic study of the Bed I sites. Springer, the Netherlands.

Domínguez-Rodrigo, M., 2002. Hunting and Scavenging by Early Humans: The State of the Debate. Journal of World Prehistory 16, 1–54. https://doi.org/10.1023/A:1014507129795

Domínguez-Rodrigo, M., Baquedano, E., Organista, E., Cobo-Sánchez, L., Mabulla, A., Maskara, V., Gidna, A., Pizarro-Monzo, M., Aramendi, J., Galán, A.B., 2021. Early Pleistocene faunivorous hominins were not kleptoparasitic, and this impacted the evolution of human anatomy and socio-ecology. Scientific Reports 11, 16135.

Domínguez-Rodrigo, M., Courtenay, L.A., Cobo-Sánchez, L., Baquedano, E., Mabulla, A., 2022. A case of hominin scavenging 1.84 million years ago from Olduvai Gorge (Tanzania). Annals of the New York Academy of Sciences 1510, 121–131. https://doi.org/10.1111/nyas.14727

Domínguez-Rodrigo, M., Pickering, T.R., 2003. Early hominid hunting and scavenging: A zooarcheological review. Evolutionary Anthropology 12, 275–282. https://doi.org/10.1002/evan.10119

Dozy, C.M., 1911. Bemerkungen zur Stratigraphie der Sedimente in der Triniler Gegend, in: Selenka and Blanckenhorn: Die Pithecanthropus-Schichten Auf Java. Geologische Und Paläontologische Ergebnisse Der Trinil-Expedition (1907 Und 1908). Verlag Von Wilhelm Engelmann, Leipzig.

Driver, J.C., Maxwell, D., 2013. Bison death assemblages and the interpretation of human hunting behaviour. Quaternary International 297, 100–109.

Dubois, 1908. Das geologische Alter der Kendeng-oder Trinil-fauna. Tijdschrift van het Koninklijk Nederlandsch Aardrijkskundig Genootschap 1235–1270.

Dubois, 1907. Eenige van Nederlandschen kant verkregen uitkomsten met betrekking tot de kennis der Kendeng-fauna (fauna van Trinil). Tijdschrift van het Koninklijk Nederlandsch Aardrijkskundig Genootschap 449–458.

Dubois, 1896. On Pithecanthropus erectus: A Transitional form Between Man and the Apes. The scientific transactions of the Royal Dublin Society 1–18.

Dubois, 1895. Pithecanthropus erectus, betrachtet als eine wirkliche Uebergangsform und als Stammform des Menschen. Zeitschrift für Ethnologie 723–738.

Dubois, 1894a. Pithecanthropus erectus: eine menschenaehnliche Uebergangsform aus Java. Landesdruckerei.

Dubois, 1894b. Palaeontologische onderzoekingen op Java. Verslag van het Mijnwezen.

Dubois, 1893. Palaeontologische onderzoekingen op Java. Verslag van het Mijnwezen.

Dubois, 1891. Paleontologische onderzoekingen op java. verslag van het mijnwezen 14–18.

Dubois, E., 1932. The distinct organization of Pithecanthropus of which the femur bears evidence, now confirmed from other individuals of the described species. (No Title).

Dubois, E., 1920. De proto-Australische fossiele mensch van Wadjak (Java). Koninklijke Akademie van Wetenschappen, Amsterdam 19, 88–105.

Dunham, R.J., 1962. Classification of Carbonate Rocks According to Depositional Textures 38, 108–121.

Durcan, J.A., King, G.E., Duller, G.A., 2015. DRAC: Dose Rate and Age Calculator for trapped charge dating. Quaternary Geochronology 28, 54–61.

Duyfjes, J., 1936. Zur Geologie und Stratigraphie des Kendenggebietes zwischen Trinil und Soerabaja (Java). De Ingenieur ned.-Indie 4, 136–149.

Duyfjes, J., 1938a. Toelichting bij Blad 110 (Modjokerto), Geologische Kaart van Java Schaal 1: 100.000. Bandung. Dienst van den Mijnbouw in Nederlandsch-Indie.

Duyfjes, J., 1938b. Toelichting bij blad 115 (Surabaya) van de Geologische Kaart van Java.

Egeland, C.P., Domínguez-Rodrigo, M., Barba, R., 2007. The Hunting-versus-scavenging debate, in: Deconstructing Olduvai: A Taphonomic Study of the Bed I Sites, Vertebrate Paleobiology and Paleoanthropology. Springer Netherlands, Dordrecht, pp. 11–22. https://doi.org/10.1007/978-1-4020-6152-3_2

Egi, N., Nakatsukasa, M., Kalmykov, N.P., MASCHENKO, E.N., Takai, M., 2007. Distal humerus and ulna of Parapresbytis (Colobinae) from the Pliocene of Russia and Mongolia: phylogenetic and ecological implications based on elbow morphology. Anthropological Science 115, 107–117.

Elbert, 1908. Ueber das Alter der Kendeng-Schichten mit Pihecanhropus erecus Dubois. Neues Jahrbuch fur Mineralogie, Geologie und Paleontlogie 648–662.

Elliott, T., 1986. Siliciclastic shorelines. Sedimentary environments and facies 615–155.

Ericson, D.B., Wollin, G., Wollin, J., 1955. Coiling direction of Globorotalia truncatulinoides in deep-sea cores. Deep Sea Research (1953) 2, 152–158. https://doi.org/10.1016/0146-6313(55)90018-6

Espigares, Palmqvist, Guerra-Merchán, Ros-Montoya, García-Aguilar, Rodríguez-Gómez, Serrano, Martínez-Navarro, 2019. The earliest cut marks of Europe: a discussion on hominin subsistence patterns in the Orce sites (Baza basin, SE Spain). Nature Scientific Reports.

Espinoza, E.O., Mann, M.-J., 1993. The History and Significance of the Schreger Pattern in Proboscidean Ivory Characterization. Journal of the American Institute for Conservation 32, 241–248. https://doi.org/10.1179/019713693806124866

Evans, D.L., Quinton, J.N., Tye, A.M., Rodés, Á., Davies, J.A.C., Mudd, S.M., Quine, T.A., 2019. Arable soil formation and erosion: a hillslope-based cosmogenic nuclide study in the United Kingdom. SOIL 5, 253–263.

Falconer, Cautley, 1836. On the fossil hippopotamus of the Siwalik Hills. Asiatic Researches Vol. XIX, 39–53.

Falconer, H., Cautley, P.T., 1846. Fauna antiqua Sivalensis, being the fossil zoology of the Sewalik hills in the north of India, by H. Falconer and PT Cautley. Smith, Elder and Company.

Falótico, T., Spagnoletti, N., Haslam, M., Luncz, L.V., Malaivijitnond, S., Gumert, M., 2017. Analysis of sea almond (*Terminalia catappa*) cracking sites used by wild Burmese long-tailed macaques (*Macaca fascicularis aurea*). American J Primatol 79, e22629. https://doi.org/10.1002/ajp.22629

FAO, 2015. World reference base for soil resources 2014, International soil classification system for naming soils and creating legends for soil maps Update 2015, world soil resources reports. Food and Agriculture Organization of the United Nations.

Farani, G.L., Nogueira, M.M., Johnsson, R., Neves, E., 2015. The salt tolerance of the freshwater snail Melanoides tuberculata (Mollusca, Gastropoda), a bioinvader gastropod. Pan-American Journal of Aquatic Sciences 10, 212–221.

Fauzi, M.R., Ansyori, M.M., Prastiningtyas, D., Intan, M.F.S., Wibowo, U.P., Wulandari, Rahmanendra, H., Widianto, H., Simanjuntak, T., 2016. Matar: A forgotten but promising Pleistocene locality in East Java. Quaternary International, Southeast Asia: human evolution, dispersals and adaptation 416, 183–192. https://doi.org/10.1016/j.quaint.2015.12.091

Ferreira, T.O., Nóbrega, G.N., Albuquerque, A.G., Sartor, L.R., Gomes, I.S., Artur, A.G., Otero, X.L., 2015. Pyrite as a proxy for the identification of former coastal lagoons in semiarid NE Brazil. Geo-Marine Letters 35, 355–366.

Fisher, J.W., 1995. Bone surface modifications in zooarchaeology. J Archaeol Method Theory 2, 7–68. https://doi.org/10.1007/BF02228434

Fisher, R.V., Schmincke, H.-U., 1984. Pyroclastic rocks. Springer Science & Business Media.

Flemming, N.C., 2021. Global experience in locating submerged prehistoric sites and their relevance to research on the American continental shelves. The Journal of Island and Coastal Archaeology 16, 170–193. https://doi.org/10.1080/15564894.2020.1781712

Fourvel, J.-B., Thackeray, J.F., Brink, J.S., O'regan, H., Braga, J., 2018. Taphonomic interpretations of a new Plio-Pleistocene hominin-bearing assemblage at Kromdraai (Gauteng, South Africa). Quaternary Science Reviews 190, 81–97.

Gaudzinski, Roebroeks, 2000. Adults only. Reindeer hunting at the middle palaeolithic site salzgitter lebenstedt, northern Germany. Journal of human evolution.

Gemel, R., Haring, E., 2011. On two shells of trionychid turtles in the collection of the" Zoologische Staatssammlung Munchen" with remarks about morphological differences between Chitra GRAY, 1844 and Pelochelys GRAY, 1864 (Testudines: Trionychidae). HERPETOZOA 23, 67–77.

Genevraye, P.D., Samuel, L., 1972. Geology of the Kendeng Zone (Central & East Java). Indonesian Petroleum Association, Annual Convention Proceedings 1, 17–30.

Geraads, D., 1979. Nouvelles données sur Hyaena brevirostris bathygnatha Dubois (Carnivora, Mammalia) du pléistocène de Java. Compte rendu sommaire des séances de la Société géologique de France 2, 80.

Gibbard, P.L., Lewin, J., 2002. Climate and related controls on interglacial fluvial sedimentation in lowland Britain. Sedimentary Geology 151, 187–210.

Gilson, S.-P., St-Pierre, C.G., Lominy, M., Lessa, A., 2021. Shark teeth used as tools: An experimental archaeology study. Journal of Archaeological Science: Reports 35, 102733.

Grubb, P., 2005. Order artiodactyla. Mammal Species of the World. A Taxonomic and Geographic Reference 3rd edition 1, 637–722.

Gruwier, B., de Vos, J., Kovarovic, K., 2015. Exploration of the taxonomy of some Pleistocene Cervini (Mammalia, Artiodactyla, Cervidae) from Java and Sumatra (Indonesia): a geometric-and linear morphometric approach. Quaternary Science Reviews 119, 35–53.

Guérin, C., 1980. Les rhinocéros (Mammalia, Perissodactyla) du Miocène terminal au Pléistocène supérieur en Europe occidentale. Comparaison avec les espèces actuelles (fascicule 1). Travaux et Documents des Laboratoires de Géologie de Lyon 79, 3–421.

Hall, R., 2013. The palaeogeography of Sundaland and Wallacea since the Late Jurassic. 1 e1–e1. https://doi.org/10.4081/jlimnol.2013.s2.e1

Hall, R., Smyth, H.R., 2008. Cenozoic arc processes in Indonesia: identification of the key influences on the stratigraphic record in active volcanic arcs.

Hall, R., Spakman, W., 2015. Mantle structure and tectonic history of SE Asia. Tectonophysics 658, 14–45.

Hamilton, W.B., Pertambangan, I.D., Development, U.S.A. for I., 1979. Tectonics of the Indonesian region. U.S. Govt. Print. Off.

Hampton, B.A., Horton, B.K., 2007. Sheetflow fluvial processes in a rapidly subsiding basin, Altiplano plateau, Bolivia. Sedimentology 54, 1121–1148. https://doi.org/10.1111/j.1365-3091.2007.00875.x

Hardjasasmita, H.S., 1987. Taxonomy and phylogeny of the Suidae (Mammalia) in Indonesia. Scripta geologica 85, 1–68.

Harrison, T., 1989. New postcranial remains of Victoriapithecus from the middle Miocene of Kenya. Journal of Human Evolution 18, 3–54.

Harrison, T., 1982. Small-bodied apes from the Miocene of East Africa (PhD Thesis). University of London Ph. D. thesis.

Hartono, U., 1994. The petrology and geochemistry of the Wilis and Lawu volcanoes, East Java, Indonesia (phd). University of Tasmania.

Haslam, M., Malaivijitnond, S., Gumert, M.D., 2022. Stone-tool-assisted hunting by a wild monkey (Macaca fascicularis aurea). Behaviour 159, 1365–1373.

Heaney, L.R., 1991. A synopsis of climatic and vegetational change in Southeast Asia, in: Tropical Forests and Climate. Springer, pp. 53–61.

Heintz, E., 1970. Les Cervides Villafrachiens de France et s' Espagne. Memoires du Museun National D'Histoire Naturelle Serie, Nouvelle Serie C, Sciences de la Terre.

Heinzelin, J.D., Clark, J.D., White, T., Hart, W., Renne, P., WoldeGabriel, G., Beyene, Y., Vrba, E., 1999. Environment and Behavior of 2.5-Million-Year-Old Bouri Hominids. Science 284, 625–629. https://doi.org/10.1126/science.284.5414.625.

Hennig, 1911. Die Fischreste, in: E . Selenka & M . Blanckenhorn, Die Pithecanthropus Schichten Auf Java. Pp. 54-60, Pi. X L. W. Engelmann, Leipzig.

Herman, J., Hovestadt-Euler, M., Hovestadt, D.C., Stehmann, M., 1994. Contributions to the study of the comparative morphology of teeth and other relevant ichthyodorulites in living supra-specific taxa of Chondrichthyan fishes. Part B: Batomorphi 165–207.

Hertler, C., Volmer, R., 2008. Assessing prey competition in fossil carnivore communities—a scenario for prey competition and its evolutionary consequences for tigers in Pleistocene Java. Palaeogeography, Palaeoclimatology, Palaeoecology 257, 67–80.

Hijma, M.P., Cohen, K.M., Roebroeks, W., Westerhoff, W.E., Busschers, F.S., 2012. Pleistocene Rhine–Thames landscapes: geological background for hominin occupation of the southern North Sea region. J Quaternary Science 27, 17–39. https://doi.org/10.1002/jqs.1549

Hilgen et al., under review. The stratigraphy and age of the classic Homo erectus-bearing succession at Trinil (Java, Indonesia). Journal of Human Evolution.

Hilgen, S.L., Hilgen, F.J., Adhityatama, S., Kuiper, K.F., Joordens, J.C., 2022. Towards an astronomical age model for the Lower to Middle Pleistocene hominin-bearing succession of the Sangiran Dome area on Java, Indonesia. Quaternary Science Reviews 297, 107788.

Hilgen, S.L., Pop, E., Adhityatama, S., Veldkamp, T.A., Berghuis, H.W., Sutisna, I., Yurnaldi, D., Dupont-Nivet, G., Reimann, T., Nowaczyk, N., 2023. Revised age and stratigraphy of the classic Homo erectus-bearing succession at Trinil (Java, Indonesia). Quaternary Science Reviews 301, 107908.

Hillson, S., 2005. Teeth. Cambridge university press.

Hocknull, S.A., Piper, P.J., van den Bergh, G.D., Due, R.A., Morwood, M.J., Kurniawan, I., 2009. Dragon's paradise lost: palaeobiogeography, evolution and extinction of the largest-ever terrestrial lizards (Varanidae). PLoS One 4, e7241.

Hoffman, J.S., Clark, P.U., Parnell, A.C., He, F., 2017. Regional and global sea-surface temperatures during the last interglaciation. Science 355, 276–279. https://doi.org/10.1126/science.aai8464

Holman, J.A., 2000. Fossil snakes of North America: origin, evolution, distribution, paleoecology. Indiana University Press.

Hooijer, 1962b. Report upon a collection of Pleistocene mammals from tin-bearing deposits in a limestone cave near Ipoh, Kinta Valley, Perak. Federation of Malaya.

Hooijer, D.A., 1983. Remarks upon the Dubois collection of fossil mammals from Trinil and Kedungbrubus in Java. Geologie en Mijnbouw 62, 337–338.

Hooijer, D.A., 1972. Varanus (Reptilia, Sauria) from the Pleistocene of Timor. Zoologische Mededelingen 47, 445–448.

Hooijer, D.A., 1964. New records of mammals from the Middle Pleistocene of Sangiran, Central Java. Zoologische Mededelingen 40, 73–88.

Hooijer, D.A., 1958a. Fossil Bovidae from the Malay archipelago and the Punjab. Brill.

Hooijer, D.A., 1958b. A. The Pleistocene Vertebrate Fauna of Celebes. Asian Perspectives 2, 71–76.

Hooijer, D.A., 1955. Fossil Proboscidea from the Malay archipelago and the Punjab. EJ Brill.

Hooijer, D.A., 1954. Pleistocene vertebrates from celebes. IX, elasmobranchii.

Hooijer, D.A., 1950. The fossil Hippopotamidae of Asia, with notes on the recent species. Zoologische Verhandelingen 8, 1–124.

Hooijer, D.A., 1946. Prehistoric and fossil rhinoceroses from the Malay Archipelago and India. Brill Archive.

Hooijer, D.A., 1962a. Quaternary langurs and macaques from the Malay Archipelago. Zoologische verhandelingen 55, 1–64.

Hooijer, D.A., Kurtén, B., 1984. Trinil and Kedungbrubus: the Pithecanthropus-bearing fossil faunas of Java and their relative age. Annales Zoologici Fennici 21, 135–141.

Houssaye, A., Botton-Divet, L., 2018. From land to water: evolutionary changes in long bone microanatomy of otters (Mammalia: Mustelidae). Biological Journal of the Linnean Society 125, 240–249.

Howell, F.C., 1999. Paleo-Demes, Species Clades, and Extinctions in the Pleistocene Hominin Record. Journal of Anthropological Research 55, 191–243. https://doi.org/10.1086/jar.55.2.3631209

Hublin, J.-J., Weston, D., Gunz, P., Richards, M., Roebroeks, W., Glimmerveen, J., Anthonis, L., 2009. Out of the North Sea: the Zeeland Ridges Neandertal. Journal of human evolution 57, 777–785.

Huffman, F., Buffler, R., Kappelman, J., Ruez, D., 2007. Sedimentological and paleogeographical context of the Mojokerto hominin site, East Java.

Huffman, O.F., 2001a. Geologic context and age of the Perning/Mojokerto Homo erectus, East Java. Journal of Human Evolution 40, 353–362. https://doi.org/10.1006/jhev.2001.0464

Huffman, O.F., 2001b. Plio-Pleistocene environmental variety in eastern Java and early Homo erectus paleoecology–a geological perspective. Sangiran: Man, Culture, and Environment in Pleistocene Times 231–256.

Huffman, O.F., De Vos, J., Berkhout, A.W., Aziz, F., 2010. Provenience reassessment of the 1931–1933 Ngandong Homo erectus (Java), confirmation of the bone-bed origin reported by the discoverers. PaleoAnthropology 2010, 1–60.

Huffman, O.F., Shipman, P., Hertler, C., de Vos, J., Aziz, F., 2005. Historical Evidence of the 1936 Mojokerto Skull Discovery, East Java. Journal of Human Evolution 48, 321–363. https://doi.org/10.1016/j.jhevol.2004.09.001

Huffman, O.F., Zaim, J., 2023. Geological age estimate for the Mojokerto child's skull Homo erectus. Comment on Berghuis et al."The eastern Kendeng Hills (Java, Indonesia) and the hominin-bearing beds of Mojokerto, a re-interpretation"[Quat. Sci. Rev. 295 (2022) 107692]. Quaternary Science Reviews 108058.

Huffman, O.F., Zaim, Y., 2003. Mojokerto Delta, East Jawa; paleoenvironment of Homo modjokertensis–first results. Journal of Mineral Technology 10, 53–82.

Huffman, O.F., Zaim, Y., Kappelman, J., Ruez Jr, D.R., De Vos, J., Rizal, Y., Aziz, F., Hertler, C, 2006. Relocation of the 1936 Mojokerto skull discovery site near Perning, East Java. Journal of Human Evolution 50, 431–451.

Hüneke, H., Henrich, R., 2011. Chapter 4 - Pelagic Sedimentation in Modern and Ancient Oceans, in: HüNeke, H., Mulder, T. (Eds.), Developments in Sedimentology, Deep-Sea Sediments. Elsevier, pp. 215–351. https://doi.org/10.1016/B978-0-444-53000-4.00004-4

Huntley, D.J., Baril, M.R., 1997. The K content of the K-feldspars being measured in optical dating or in thermoluminescence dating. Ancient Tl 15, 11–13.

Husein, S., Kakda, K., Aditya, H.F.N., 2015. Mekanisme Perlipatan En-Echelon di Antiklinorium Rembang Utara, in: Prosiding Seminar Nasional Kebumian Ke-8 Jurusan Teknik Geologi Fakultas Teknik Universitas Gadjah Mada, Yogyakarta, GEO41. pp. 224–234.

Husson, L., Boucher, F.C., Sarr, A.-C., Sepulchre, P., Cahyarini, S.Y., 2020. Evidence of Sundaland's subsidence requires revisiting its biogeography. Journal of Biogeography 47, 843–853.

Husson, L., Salles, T., Lebatard, A.-E., Zerathe, S., Braucher, R., Noerwidi, S., Aribowo, S., Mallard, C., Carcaillet, J., Natawidjaja, D.H., 2022. Javanese Homo erectus on the move in SE Asia ca. 1.8 Ma. Nature scientific reports.

Hyodo, M., Watanabe, N., Sunata, W., Susanto, E.E., Wahyono, H., 1993. Magnetostratigraphy of hominid fossil bearing formations in Sangiran and Mojokerto, Java. Anthropological Science 101, 157–186.

Ikeda, T., 2007. A comparative morphological study of the vertebrae of snakes occurring in Japan and adjacent regions. Current Herpetology 26, 13–34.

Indriati et al., 2011. The Age of the 20 Meter Solo River Terrace, Java, Indonesia and the Survival of Homo erectus in Asia. PlosOne.

Ingicco, T., de Vos, J., Huffman, O.F., 2014. The oldest gibbon fossil (hylobatidae) from insular Southeast Asia: evidence from Trinil,(East Java, Indonesia), lower/middle Pleistocene. PloS one 9, e99531.

Iqbal, M., Setiawan, A., Windusari, Y., Yustian, I., Zulkifli, H., 2020. Updating status of the distributional records of giant freshwater stingray Urogymnus polylepis (Bleeker, 1852) in Indonesia, in: AIP Conference Proceedings. AIP Publishing.

Itihara, M., HASIBUAN, F., KAGEMORI, Y., KADAR, D., SHIBASAKI, T., 1985. Geology and stratigraphy of the Sangiran area.

Jacob, T., Curtis, G.H., 1971. Preliminary potassium-argon dating of early man in Java. Contributions of the University of California Archaeological research facility 12, 50.

Jacobs, G.S., Hudjashov, G., Saag, L., Kusuma, P., Darusallam, C.C., Lawson, D.J., Mondal, M., Pagani, L., Ricaut, F.-X., Stoneking, M., 2019. Multiple deeply divergent Denisovan ancestries in Papuans. Cell 177, 1010–1021.

Jaeckel, 1911. Die fossilen Schildkrötenreste von Trinil, in: Die Pitheoanthropusschichten Auf Java,. Herg. Selenka, M. S. u. Blanckenhorn, M., Verlag von W. Engelmann, Leipzig.

Jalvo, Y., Andrews, P., 2016. Atlas of taphonomic identifications: 1001+ images of fossil and recent mammal bone modification. Springer.

Janensch, 1911a. Die Reptilienreste (exkl. Schildkrõten), in: Selenka and Blanckenhorn Die Pithecanthropusschichten Auf Java Geologische Und Palaontologische Ergebnisse De Trinil-Expedition (1907 Und 1908) Verlag Von Wilhelm Engelmann, Leipzig.

Janensch, W., 1911b. Die Proboscidier-Schadel der Trinil-Expeditions-Sammlung; ML Selenka & M, in: Selenka and Blanckenhorn Die Pithecanthropusschichten Auf Java Geologische Und Palaontologische Ergebnisse De Trinil-Expedition (1907 Und 1908) Verlag Von Wilhelm Engelmann, Leipzig.

Janssen, R., Joordens, J.C., Koutamanis, D.S., Puspaningrum, M.R., de Vos, J., Van Der Lubbe, J.H., Reijmer, J.J., Hampe, O., Vonhof, H.B., 2016. Tooth enamel stable isotopes of Holocene and Pleistocene fossil fauna reveal glacial and interglacial paleoenvironments of hominins in Indonesia. Quaternary Science Reviews 144, 145–154.

Jenkins, D.G., 1967. Recent distribution, origin, and coiling ratio changes in Globorotalia pachyderma (Ehrenberg). Micropaleontology 195–203.

Johnson, E., 1985. Current developments in bone technology, in: Advances in Archaeological Method and Theory. Elsevier, pp. 157–235.

Joordens, J.C., d'Errico, F., Wesselingh, F.P., Munro, S., de Vos, J., Wallinga, J., Ankjærgaard, C., Reimann, T., Wijbrans, J.R., Kuiper, K.F., 2015. Homo erectus at Trinil on Java used shells for tool production and engraving. Nature 518, 228–231.

Joordens, J.C., Feibel, C.S., Vonhof, H.B., Schulp, A.S., Kroon, D., 2019. Relevance of the eastern African coastal forest for early hominin biogeography. Journal of Human Evolution 131, 176–202.

Joordens, J.C., Wesselingh, F.P., de Vos, J., Vonhof, H.B., Kroon, D., 2009. Relevance of aquatic environments for hominins: a case study from Trinil (Java, Indonesia). Journal of Human Evolution 57, 656–671.

Junghuhn, F., 1857. Over fossiele zoogdierbeenderen te Patihajam, in de residentie Djapara, eiland Java. Natuurkundig Tijdschrift voor Nederlansch-Indië 14, 215–219.

Kaifu, Y., 2017. Archaic Hominin Populations in Asia before the Arrival of Modern Humans: Their Phylogeny and Implications for the "Southern Denisovans." Current Anthropology 58, S418–S433. https://doi.org/10.1086/694318

Kaifu, Y., Athreya, S., in press. What's in a Name? Late Middle and Early Late Pleistocene Hominin Systematics Diversity and Evolution of Archaic Eastern Asian Hominins: A Synthetic Model of the Fossil and Genetic Records. PaleoAnthropology.

Kaifu, Y., Aziz, F., Indriati, E., Jacob, T., Kurniawan, I., Baba, H., 2008. Cranial morphology of Javanese Homo erectus: new evidence for continuous evolution, specialization, and terminal extinction. Journal of Human Evolution 55, 551–580.

Kaifu, Y., Baba, H., Aziz, F., Indriati, E., Schrenk, F., Jacob, T., 2005. Taxonomic affinities and evolutionary history of the early Pleistocene hominids of Java: Dentognathic evidence. American J Phys Anthropol 128, 709–726. https://doi.org/10.1002/ajpa.10425

Kaifu, Y., Baba, H., Sutikna, T., Morwood, M.J., Kubo, D., Saptomo, E.W., Awe, R.D., Djubiantono, T., 2011b. Craniofacial morphology of Homo floresiensis: description, taxonomic affinities, and evolutionary implication. Journal of Human Evolution 61, 644–682.

Kaifu, Y., Indriati, E., Aziz, F., Kurniawan, I., Baba, H., 2011. Cranial Morphology and Variation of the Earliest Indonesian Hominids, in: Norton, C.J., Braun, D.R. (Eds.), Asian Paleoanthropology, Vertebrate Paleobiology and Paleoanthropology. Springer Netherlands, Dordrecht, pp. 143–157. https://doi.org/10.1007/978-90-481-9094-2_11

Kaifu, Y., Kurniawan, I., Kubo, D., Sudiyabudi, E., Putro, G.P., Prasanti, E., Aziz, F., Baba, H., 2015. Homo erectus calvaria from Ngawi (Java) and its evolutionary implications. Anthropological Science 123, 161–176.

Kaifu, Y., Kurniawan, I., Mizushima, S., Sawada, J., Lague, M., Setiawan, R., Sutisna, I., Wibowo, U.P., Suwa, G., Kono, R.T., 2024. Early evolution of small body size in Homo floresiensis. Nature Communications 15, 6381.

Kaifu, Y., Kurniawan, I., Yurnaldi, D., Setiawan, R., Setiyabudi, E., Insani, H., Takai, M., Nishioka, Y., Takahashi, A., Aziz, F., 2022. Modern human teeth unearthed from below the 128,000-year-old level at Punung, Java: A case highlighting the problem of recent intrusion in cave sediments. Journal of Human Evolution 163, 103122.

Karl, H.V., 1987. Revision der fossilen schildkröten (Reptilia, Testudines) von Jawa. Gothaer Museumsheft 14, 37–44.

Kars, R.H., Reimann, T., Ankjærgaard, C., Wallinga, J., 2014. Bleaching of the post-IR IRSL signal: new insights for feldspar luminescence dating. Boreas 43, 780–791. https://doi.org/10.1111/bor.12082

Keenan, S.W., 2016. From bone to fossil: A review of the diagenesis of bioapatite. American Mineralogist 101, 1943–1951. https://doi.org/10.2138/am-2016-5737

Kelsey, H.M., Nelson, A.R., Hemphill-Haley, E., Witter, R.C., 2005. Tsunami history of an Oregon coastal lake reveals a 4600 yr record of great earthquakes on the Cascadia subduction zone. Geological Society of America Bulletin 117, 1009–1032.

Kent, B.W., 2018. The cartilaginous fishes (chimaeras, sharks, and rays) of Calvert Cliffs, Maryland, USA. The Geology and Vertebrate Paleontology of Calvert Cliffs, Maryland, USA. Smithsonian Contributions to Paleobiology 100, 45–157.

Khurniawan, S., 2019. Discriminating the molariform characteristics of fossil Bovidae from Java, Indonesia: A contribution to increase the resolution of faunal identification at hominin environment. Thesis, Faculty of Archaeology, Leiden University.

Kidder, J.H., Durband, A.C., 2004. A re-evaluation of the metric diversity within Homo erectus. Journal of Human Evolution 46, 297–313.

Kidwell, S.M., 1986. Models for fossil concentrations: paleobiologic implications. Paleobiology 12, 6–24.

Kleemann, K.H., 1980. Boring bivalves and their host corals from the Great Barrier Reef. Journal of molluscan Studies 46, 13–54.

Klein, R.G., Cruz-Uribe, K., 1983. The computation of ungulate age (mortality) profiles from dental crown heights. Paleobiology 9, 70–78.

Kocsis, L., 2024. The Elasmobranch fossil record of the Indo-Australian archipelago since the Miocene. Diversity.

Kocsis, L., Razak, H., Briguglio, A., Szabó, M., 2019. First report on a diverse Neogene cartilaginous fish fauna from Borneo (Ambug Hill, Brunei Darussalam). Journal of Systematic Palaeontology 17, 791–819. https://doi.org/10.1080/14772019.2018.1468830

Kolfschoten, T. van, Essen, H. van, 2004. Palaeozoological heritage from the bottom of the North Sea (Chapter 9).

Kolfschoten, T. van, Laban, C., 1995. Pleistocene terrestrial mammal faunas from the North Sea. Mededelingen/Rijks Geologische Dienst 52, 135.

Kottelat, M., 2013. The fishes of the inland waters of Southeast Asia: a catalogue and core bibliography of the fishes known to occur in freshwaters, mangroves and estuaries. Raffles Bulletin of Zoology.

Koumans, F.P., 1949. On some fossil fish remains from Java. Zoologische Mededelingen 30, 77–82.

Kozuch, L., Fitzgerald, C., 1989. A guide to identifying shark centra from southeastern archaeological sites. Southeastern Archaeology 146–157.

Kramer, A., 1994. A critical analysis of claims for the existence of Southeast Asian australopithecines. Journal of human evolution 26, 3–21.

Kreutzer, L.A., 1988. Megafaunal butchering at Lubbock Lake, Texas: a taphonomic reanalysis. Quaternary Research 30, 221–231.

Krumbein, W.C., 1942. Criteria for subsurface recognition of unconformities. AAPG Bulletin 26, 36–62.

Kucera, M., 2007. Planktonic Foraminifera as Tracers of Past Oceanic Environments, in: Hillaire–Marcel, C., De Vernal, A. (Eds.), Developments in Marine Geology, Proxies in Late Cenozoic Paleoceanography. Elsevier, pp. 213–262. https://doi.org/10.1016/S1572-5480(07)01011-1

Kumai, H., 1985. Geology and stratigraphy of the Mojokerto area. Quaternary geology of the hominid fossil bearing formations in Java 55–61.

Kurtén, B., 1962. The sabre-toothed cat Megantereon from the Pleistocene of Java. Zoologische Mededelingen 38, 101–104.

Kurtén, B., 1956. The status and affinities of Hyaena sinensis Owen and Hyaena ultima Matsumoto. American Museum novitates; no. 1764.

Kurtén, B., 1953. On the variation and population dynamics of fossil and recent mammal populations (PhD Thesis). Societas pro fauna et flora Fennica.

Kusumastuti, A., Van Rensbergen, P., Warren, J.K., 2002. Seismic sequence analysis and reservoir potential of drowned Miocene carbonate platforms in the Madura Strait, East Java, Indonesia. AAPG bulletin 86, 213–232.

Laj, C., Channell, J.E., 2007. Geomagnetic excursions. Geomagnetism 5, 373–416.

Lamb, J.L., Beard, J.H., 1972. Late Neogene planktonic foraminifers in the Caribbean, Gulf of Mexico, and Italian stratotypes.

Langbroek, M., Roebroeks, W., 2000. Extraterrestrial evidence on the age of the hominids from Java. J. Hum. Evol. 38, 595–600. https://doi.org/10.1006/jhev.1999.0394

Langdon, J.H., 2022. Behavior in the Middle Pleistocene, in: Human Evolution, Springer Texts in Social Sciences. Springer International Publishing, Cham, pp. 461–494. https://doi.org/10.1007/978-3-031-14157-7_16

Lavigne, F., Thouret, J.-C., Hadmoko, D.S., Sukatja, C.B., 2007. Lahars in Java: Initiations, dynamics, hazard assessment and deposition processes. Forum Geografi Vol 21, 17–32.

Lazar, O.R., Bohacs, K.M., Macquaker, J.H.S., Schieber, J., Demko, T.M., 2015. Capturing Key Attributes of Fine-Grained Sedimentary Rocks In Outcrops, Cores, and Thin Sections: Nomenclature and Description Guidelines. Journal of Sedimentary Research 85, 230–246. https://doi.org/10.2110/jsr.2015.11

LeGros Clark, W.E., 1964. The fossil evidence for human evolution. Chicago, Illinois University of Chicago.

Lehmann, H., 1936. Morphologische studien auf Java. Engelhorn.

Leinders, J.J.M., 1985. The age of the hominid-bearing deposits of Java: state of the art. Geologie en Mijnbouw 64, 167–173.

Li, Z.-Y., Wu, X.-J., Zhou, L.-P., Liu, W., Gao, X., Nian, X.-M., Trinkaus, E., 2017. Late Pleistocene archaic human crania from Xuchang, China. Science 355, 969–972. https://doi.org/10.1126/science.aal2482

Lin, C.-Y., Lin, C.-H., Shimada, K., 2022. A previously overlooked, highly diverse early Pleistocene elasmobranch assemblage from southern Taiwan. PeerJ 10, e14190.

Liu, W., Athreya, S., Xing, S., Wu, X., 2022. Hominin evolution and diversity: a comparison of earlier-Middle and later-Middle Pleistocene hominin fossil variation in China. Phil. Trans. R. Soc. B 377, 20210040. https://doi.org/10.1098/rstb.2021.0040

Liu, W., Martinón-Torres, M., Kaifu, Y., Wu, X., Kono, R.T., Chang, C., Wei, P., Xing, S., Huang, W., Bermúdez De Castro, J.M., 2017. A mandible from the Middle Pleistocene Hexian site and its significance in relation to the variability of Asian *Homo erectus*. American J Phys Anthropol 162, 715–731. https://doi.org/10.1002/ajpa.23162

Liu, W., Wu, X., 2022. Morphological diversities and evolutionary implications of the Late Middle Pleistocene hominins in China. Acta Anthropologica Sinica 41, 563.

Liu, W., Zhang, Y., Wu, X., 2005. Middle Pleistocene human cranium from Tangshan (Nanjing), Southeast China: A new reconstruction and comparisons withHomo erectus from Eurasia and Africa. Am. J. Phys. Anthropol. 127, 253–262. https://doi.org/10.1002/ajpa.20066

Liu, Wu, Xing, Zhang, 2014. Human Fossils in China. Science Press, Beijing.

Lopes, M.S., Bertucci, T.C.P., Rapagnã, L., Tubino, R. de A., Monteiro-Neto, C., Tomas, A.R.G., Tenório, M.C., Lima, T., Souza, R., Carrillo-Briceño, J.D., 2016. The path towards endangered species: prehistoric fisheries in southeastern Brazil. PloS one 11, e0154476.

Lopes, R.P., 2012. Bioerosion and bioincrustation in body fossils from the Coastal Plain of Rio Grande do Sul State, Southern Brazil. Ichnology of Latin America–Selected Papers. Sociedade Brasileira de Paleontologia, Série Monografias 2, 179–194.

Lordkipanidze, D., Ponce De León, M.S., Margvelashvili, A., Rak, Y., Rightmire, G.P., Vekua, A., Zollikofer, C.P.E., 2013. A Complete Skull from Dmanisi, Georgia, and the Evolutionary Biology of Early *Homo*. Science 342, 326–331. https://doi.org/10.1126/science.1238484.

Lourens, L., 2004. 21 The Neogene Period. A Geologic Time Scale 2004 409–440.

Louys, J., 2018. Practice and prospects in underwater palaeontology.

Louys, J., 2014. The large terrestrial carnivore guild in Quaternary Southeast Asia. Quaternary Science Reviews 96, 86–97.

Louys, J., Duval, M., Price, G.J., Westaway, K., Zaim, Y., Rizal, Y., Aswan, Puspaningrum, M., Trihascaryo, A., Breitenbach, S.F.M., Kwiecien, O., Cai, Y., Higgins, P., Albers, P.C.H., De Vos, J., Roberts, P., 2022. Speleological and environmental history of Lida Ajer cave, western Sumatra. Phil. Trans. R. Soc. B 377, 20200494. https://doi.org/10.1098/rstb.2020.0494

Louys, J., Kealy, S., 2024. How did Homo erectus reach Java? Least-cost pathway models and a consideration of possible Sumatran routes. Quaternary Palaeontology and Archaeology of Sumatra 199.

Louys, J., Meijaard, E., 2010. Palaeoecology of Southeast Asian megafauna-bearing sites from the Pleistocene and a review of environmental changes in the region. Journal of Biogeography 37, 1432–1449. https://doi.org/10.1111/j.1365-2699.2010.02297.x

Louys, J., Roberts, P., 2020. Environmental drivers of megafauna and hominin extinction in Southeast Asia. Nature 1–5.

Louys, J., Turner, A., 2012. Environment, preferred habitats and potential refugia for Pleistocene Homo in Southeast Asia. Comptes Rendus Palevol 11, 203–211.

Lunt, P., 2013. The sedimentary geology of Java. Indonesian Petroleum Association.

Lyman, R.L., 1994. Vertebrate taphonomy. Cambridge University Press.

Maddy, D., Veldkamp, A., Jongmans, A.G., Candy, I., Demir, T., Schoorl, J.M., van der Schriek, T., Stemerdink, C., Scaife, R.G., van Gorp, W., 2012. Volcanic disruption and drainage diversion of the palaeo-Hudut River, a tributary of the Early Pleistocene Gediz River, Western Turkey. Geomorphology 165–166, 62–77. https://doi.org/10.1016/j.geomorph.2011.12.032

Maglio, V.J., 1973. Origin and evolution of the Elephantidae. Transactions of the American Philosophical Society 63, 1–149.

Makaske, B., 2001. Anastomosing rivers: a review of their classification, origin and sedimentary products. Earth-Science Reviews 53, 149–196.

Mallon, J.C., Henderson, D.M., McDonough, C.M., Loughry, W.J., 2018. A “bloat-and-float” taphonomic model best explains the upside-down preservation of ankylosaurs. Palaeogeography, palaeoclimatology, palaeoecology 497, 117–127.

Marean, Spencer, 1991. Impact of Carnivore Ravaging on Zooarchaeological Measures of Element Abundance. America Antiquity.

Marin, J., Saladié, P., Rodríguez-Hidalgo, A., Carbonell, E., 2017. Neanderthal hunting strategies inferred from mortality profiles within the Abric Romaní sequence. PloS one 12, e0186970.

Martin, J.E., Buffetaut, E., Naksri, W., Lauprasert, K., Claude, J., 2012. Gavialis from the Pleistocene of Thailand and its relevance for drainage connections from India to Java.

Martin, K., 1886. Fossile Säugethierreste von Java und Japan. Sammlungen des Geologischen Reichs-Museums in Leiden. Serie 1, Beiträge zur Geologie Ost-Asiens und Australiens 4, 25–69.

Matsu’ura, S., Kondo, M., Danhara, T., Sakata, S., Iwano, H., Hirata, T., Kurniawan, I., Setiyabudi, E., Takeshita, Y., Hyodo, M., 2020. Age control of the first appearance datum for Javanese Homo erectus in the Sangiran area. Science 367, 210–214.

Mayr, E., 1950. Taxonomic categories in fossil hominids, in: Cold Spring Harbor Symposia on Quantitative Biology. Cold Spring Harbor Laboratory Press, pp. 109–118.

Mazzini, A., Svensen, H., Akhmanov, G.G., Aloisi, G., Planke, S., Malthe-Sørenssen, A., Istadi, B., 2007. Triggering and dynamic evolution of the LUSI mud volcano, Indonesia. Earth and Planetary Science Letters 261, 375–388.

McCord, W.P., Pritchard, P.C., 2002. A review of the softshell turtles of the genus Chitra, with the description of new taxa from Myanmar and Indonesia (Java). HAMADRYAD-MADRAS- 27, 11–56.

McGrath, S.M., Clemens, S.C., Huang, Y., 2023. Pleistocene Sunda Shelf submersion-exposure cycles initiate vegetation Walker Circulation feedback. Geology 51, 1053–1056.

Meijaard, E., 2003. Mammals of south-east Asian islands and their Late Pleistocene environments. Journal of Biogeography 30, 1245–1257. https://doi.org/10.1046/j.1365-2699.2003.00890.x

Meijaard, E., Groves, C.P., 2004. Morphometrical relationships between South-east Asian deer (Cervidae, tribe Cervini): evolutionary and biogeographic implications. Journal of Zoology 263, 179–196.

Meikle, W.E., Parker, S.T., 1994. Naming Our Ancestors: An Anthology of Hominid Taxonomy. Waveland PressInc.

Miall, A.D., 2014. Fluvial depositional systems. Springer, Berlin.

Miall, A.D., 1996. The geology of fluvial sediments. Springer, Berlin.

Miall, A.D., 1977. Fluvial Sedimentology: An Historical Review 1–47.

Milan, J., Lindow, B.E., Lauridsen, B.W., 2011. Bite traces in a turtle carapace fragment from the middle Danian (Lower Paleocene) bryozoan limestone, Faxe, Denmark. Bulletin of the Geological Society of Denmark 59, 61–67.

Milne, N., Granatosky, M.C., 2021. Ulna Curvature in Arboreal and Terrestrial Primates. J Mammal Evol 28, 897–909. https://doi.org/10.1007/s10914-021-09566-5

Moigne, A.-M., Awe, R.D., Sémah, F., Sémah, A.-M., 2004. The cervids from the Ngebung site ('Kabuh'series, Sangiran Dome, Central Java) and their biostratigraphical significance, in: Modern Quaternary Research in Southeast Asia, Volume 18. CRC Press, pp. 31–44.

Moigne, A.-M., Malassé, A.D., Singh, M., Kaur, A., Gaillard, C., Karir, B., Pal, S., Bhardwaj, V., Abdessadok, S., Sao, C.C., 2016. The faunal assemblage of the paleonto-archeological localities of the late Pliocene Quranwala Zone, Masol formation, Siwalik range, NW India. Comptes Rendus Palevol 15, 359–378.

Mol, D., Bakker, R., 2022. Quaternary terrestrial megafaunal remains and their localities in the southern bight of the North Sea between the British Isles and The Netherlands: an overview. Staringia 17, 88–127.

Molengraaff, G.A.F., Weber, M., 1921. On the relation between the pleistocene glacial period and the origin of the Sunda sea (Java and South China-sea), and its influence on the distribution of coralreefs and on the land-and freshwater fauna. Koninklijke Nederlandse Akademie van Wetenschappen Proceedings Series B Physical Sciences 23, 395–439.

Moll, E.O., Platt, S.G., Chan, E.H., Horne, B.D., Platt, K., Praschag, P., Chen, P.N., Van Dijk, P.P., 2021. Batagur affinis (Cantor 1847)–Southern River Terrapin, Tuntong.

Montgelard, C., Catzeflis, F.M., Douzery, E., 1997. Phylogenetic relationships of artiodactyls and cetaceans as deduced from the comparison of cytochrome b and 12S rRNA mitochondrial sequences. Molecular Biology and Evolution 14, 550–559.

Moormann and van Bremen, 1978. Rice: soil, water, land. International rice research institute.

Morlan, R.E., 1980. Taphonomy and archaeology in the Upper Pleistocene of the Northern Yukon Territory: A glimpse of the peopling of the New World. University of Ottawa Press.

Morley, R.J., Morley, H.P., Swiecicki, T., 2017. Constructing Neogene Palaeogeographical Maps for the Sunda Region 7.

Morley, R.J., Morley, H.P., Swiecicki, T., 2016. Mio-Pliocene Palaeogeography, Uplands And River Systems of the Sunda Region Based on Mapping Within a Framework of Vim Depositional Cycles.

Morley, R.J., Morley, H.P., Zaim, Y., Huffman, O.F., 2020. Palaeoenvironmental setting of Mojokerto Homo erectus, the palynological expressions of Pleistocene marine deltas, open grasslands and volcanic mountains in East Java. Journal of Biogeography 47, 566–583.

Morwood, M.J., O'Sullivan, P., Susanto, E.E., Aziz, F., 2003. Revised age for Mojokerto 1, an early *Homo* erectus cranium from East Java, Indonesia. Australian Archaeology 57, 1–4. https://doi.org/10.1080/03122417.2003.11681757

Mulder, T., Syvitski, J.P., 1995. Turbidity currents generated at river mouths during exceptional discharges to the world oceans. The Journal of Geology 103, 285–299.

Müller, L., 1923. Crocodilus siamensis Schneid. und Crocodilus ossifragus Dubois. [sn]@.

Munson, P.J., Garniewicz, R.C., 2003. Age-mediated survivorship of ungulate mandibles and teeth in canid-ravaged faunal assemblages. Journal of Archaeological Science 30, 405–416.

Musliki and Saratman, 1996. A Late Pliocene Shallowing Upward Carbonate Sequence and Its Reservoir Potential, Northeast Java Basin.

Muttoni, G., Kent, D.V., 2024. Hominin population bottleneck coincided with migration from Africa during the Early Pleistocene ice age transition. Proc. Natl. Acad. Sci. U.S.A. 121, e2318903121. https://doi.org/10.1073/pnas.2318903121

Nelson, J.S., Grande, T.C., Wilson, M.V., 2016. Fishes of the World. John Wiley & Sons.

Nemec, W., 1990. Aspects of sediment movement on steep delta slopes. Coarse-grained deltas 10, 29–73.

Ng, H.H., Kottelat, M., 2013. Revision of the Asian catfish genus Hemibagrus Bleeker, 1862 (Teleostei: Siluriformes: Bagridae). Raffles Bulletin of Zoology 61.

Ni, X., Ji, Q., Wu, W., Shao, Q., Ji, Y., Zhang, C., Liang, L., Ge, J., Guo, Z., Li, J., 2021. Massive cranium from Harbin in northeastern China establishes a new Middle Pleistocene human lineage. The Innovation 2.

Niekus, M.J.L.Th., Kozowyk, P.R.B., Langejans, G.H.J., Ngan-Tillard, D., Van Keulen, H., Van Der Plicht, J., Cohen, K.M., Van Wingerden, W., Van Os, B., Smit, B.I., Amkreutz, L.W.S.W., Johansen, L., Verbaas, A., Dusseldorp, G.L., 2019. Middle Paleolithic complex technology and a Neandertal tar-backed tool from the Dutch North Sea. Proc. Natl. Acad. Sci. U.S.A. 116, 22081–22087. https://doi.org/10.1073/pnas.1907828116

Nishimura, A.C., Russo, G.A., Nengo, I.O., Miller, E.R., 2022. Morphological affinities of a fossil ulna (KNM-WS 65401) from Buluk, Kenya. Journal of Human Evolution 166, 103177.

Nishioka, Y., Vidthayanon, C., 2018. First occurrence of Duboisia (Bovidae, Artiodactyla, Mammalia) from Thailand. Fossil Record 21, 291–299.

Njau, J., Gilbert, H., 2016. Standardizing terms for crocodile-induced bite marks on bone surfaces in light of the frequent bone modification equifinality found to result from crocodile feeding behavior, stone tool modification, and trampling. FOROST (Forensic Osteology) Occasional Publications 3, 1–13.

Noerwidi, S., Suriyanto, R.A., Prayudi, A., Widianto, H., 2021. Hominin Femur finding from Banjarejo: Its morphological character and taxonomical position. Berita Sedimentologi 47, 8–16.

Noerwidi, S., Vialet, A., Widianto, H., Kurniawan, I., Zaim, J., Suriyanto, R.A., Joordens, J., Lorenzo, C., Simanjuntak, T., Sémah, F., 2020. Exploring the diversity of fossil hominin dental patterns in the western Indonesian archipelago during the Quaternary by Geometric Morphometric Analysis. Application on second upper and lower molars. L'anthropologie 124, 102791.

Noya e.a., 1992. Geological map of The Mojokerto quadrangle, Jawa - Google Scholar [WWW Document]. URL https://scholar.google.com/scholar_lookup?title=Geological%20map%20of%20the%20Mojokerto%20quadrangle%2C%20Jawa&author=Y.%20Noya&author=T.%20Suwarti&author=Sarmili%20L.%20Suharsono&publication_year=1992 (accessed 3.28.19).

Ocal, M.K., Sevil, F., Parin, U., 2004. A quantitative study on the digital bones of cattle. Annals of Anatomy-Anatomischer Anzeiger 186, 165–168.

O'Connell, J.F., Hawkes, K., Jones, N.B., 1988. Hadza Hunting, Butchering, and Bone Transport and Their Archaeological Implications. Journal of Anthropological Research 44, 113–161. https://doi.org/10.1086/jar.44.2.3630053

Oliver, 1994. Estimates of hominid and carnivore involvement in the FLK Zinjanthropus fossil assemblage: some socioecological implications. Journal of Human Evolutiom 27, 267–294.

Oppenoorth, 1932. Een nieuwe fossiele mensch van Java. Tijdschrift van het Koninklijk Nederlandsch Aardrijkskundig Genootschap. 704–708.

Pales, L., Garcia, M.A., Lambert, C., 1971. Atlas ostéologique pour servir à l'identification des mammifères du Quaternaire. (No Title).

Palmqvist, P., Martínez-Navarro, B., Pérez-Claros, J.A., Torregrosa, V., Figueirido, B., Jiménez-Arenas, J.M., Espigares, M.P., Ros-Montoya, S., De Renzi, M., 2011. The giant hyena Pachycrocuta brevirostris: modelling the bone-cracking behavior of an extinct carnivore. Quaternary International 243, 61–79.

Pannekoek, A.J., 1949. Outline of the geomorphology of Java.

Pante, M.C., Blumenschine, R.J., 2010. Fluvial transport of bovid long bones fragmented by the feeding activities of hominins and carnivores. Journal of Archaeological Science 37, 846–854.

Pardo, A., Keller, G., 2008. Biotic effects of environmental catastrophes at the end of the Cretaceous and early Tertiary: Guembelitria and Heterohelix blooms. Cretaceous Research, Life and the environment during the Cretaceous 29, 1058–1073. https://doi.org/10.1016/j.cretres.2008.05.031

Paredes, J.M., Foix, N., Piñol, F.C., Nillni, A., Allard, J.O., Marquillas, R.A., 2007. Volcanic and climatic controls on fluvial style in a high-energy system: the Lower Cretaceous Matasiete Formation, Golfo San Jorge basin, Argentina. Sedimentary Geology 202, 96–123.

Pfretzschner, H.-U., 2004. Fossilization of Haversian bone in aquatic environments. Comptes Rendus Palevol 3, 605–616.

Pickering, Egeland, 2006. Experimental patterns of hammerstone percussion damage on bones: implications for inferences of carcass processing by humans. Journal of Archaeological Science 459e469.

Pincheira-Donoso, D., Bauer, A.M., Meiri, S., Uetz, P., 2013. Global taxonomic diversity of living reptiles. PloS one 8, e59741.

Plummer, Bishop, 2016. Oldowan Hominin Behavior and Ecology at Kanjera South, Kenya. Journal of Anthropological Sciences 2–12.

Pobiner, 2007. Hominin-carnivore interactions: evidence from modern carnivore bone modification and Early Pleistocene archaeofaunas (Koobi Fora, Kenya; Olduvai …. Rutgers University, New Jersey.

Pobiner, B.L., 2020. The zooarchaeology and paleoecology of early hominin scavenging. Evolutionary Anthropology 29, 68–82. https://doi.org/10.1002/evan.21824

Pobiner, Rogers, Monahan, Harris, 2008. New evidence for hominin carcass processing strategies at 1.5 Ma, Koobi Fora, Kenya. Journal of Human Evolution 55, 103–130.

Podhade, Vaish, Yogita Panday, 2019. GROSS ANATOMICAL AND MORPHOMETRICAL STUDY ON SCAPULA OF THE LEOPARD (Panthera pardus). The bioscan.

Polhaupessy, A.A., 1990. Late Cenozoic palynological studies on Java (PhD Thesis). University of Hull.

Pons, L.J., Van Breemen, N., Driessen, P.M., 1982. Physiography of coastal sediments and development of potential soil acidity. Acid Sulfate Weathering 10, 1–18.

Pop, E., Hilgen, S., Adhityatama, S., Berghuis, H., Veldkamp, T., Vonhof, H., Sutisna, I., Alink, G., Noerwidi, S., Roebroeks, W., 2023a. Reconstructing the provenance of the hominin fossils from Trinil (Java, Indonesia) through an integrated analysis of the historical and recent excavations. Journal of Human Evolution 176, 103312.

Pop, E., Noerwidi, S., Spoor, F., 2024. Naming Homo erectus: A review. Journal of Human Evolution 190, 103516.

Pop et al., under review. Reconstructing the provenance of the hominin fossils from Trinil (Java, Indonesia) through an integrated analysis of the historical and recent excavations. Journal of Human Evolution.

Pop, Noerwidi, S., Hafsari, M., dhityatama, S., Veldkamp, A., Schoorl, J.M., Khurniawan, S., Berghuis, H., Hilgen, S., Drespriputra, O., Yuwono, P., Sutisna, I., Perwira Shidqi, Joordens, J.C.A., 2023b. Digging Trinil's hominin backyard: Sogen, a promising Middle Pleistocene archaeological site along the Solo River [abstract). PaleoAnthropology 2, 374.

Postma, G., Colella, A., Prior, D.B., 1990. Coarse-grained deltas. Int. Assoc. Sedimentol. Spec. Publ 10, 13–27.

Potts, Shipman, Ingall, 1988. Taphonomy, paleoecology, and hominids of Lainyamok, Kenya. Journal of Human Evolution.

Pradeep, H.D., Swapnil, S.S., Nashad, M., Venu, S., Ranjan, K.R., Sumitha, G., Devi, S.M., Farejiya, M.K., 2018. First record and DNA barcoding of Oman cownose ray, Rhinoptera jayakari Boulenger, 1895 from Andaman Sea, India. Zoosystema 40, 67–74.

Pringgoprawiro and Baharuddin, 1979. Biostratigrafi Foraminifera Planktonic dan Bidang-Bidang Pengenal Kaenozoikum-Akhirdari Sumur-Sumur Tobo, Cepu, Jawa Timur. Proceedings PIT VIII Ikatan Ahli Geologi Indonesia, Jakarta 21–31.

Pringgoprawiro, H., 1983. Biostratigrafi dan Paleogeografi Cekungan Jawa Timur Utara Suatu Pendekatan Baru. Disertasi ITB. Bandung.

Pritchard, P.C.H., Rabett, R.J., Piper, P.J., 2009. Distinguishing species of geoemydid and trionychid turtles from shell fragments: evidence from the Pleistocene at Niah Caves, Sarawak. Intl J of Osteoarchaeology 19, 531–550. https://doi.org/10.1002/oa.1038

Prothero, D.R., Domning, D., Fordyce, R.E., Foss, S., Janis, C., Lucas, S., Marriott, K.L., Metais, G., Naish, D., Padian, K., Rössner, G., Solounias, N., Spaulding, M., Stucky, R.M., Theodor, J., Uhen, M., 2022. On the Unnecessary and Misleading Taxon "Cetartiodactyla." J Mammal Evol 29, 93–97. https://doi.org/10.1007/s10914-021-09572-7

Puspaningrum, M.R., van den Bergh, G.D., Chivas, A.R., Setiabudi, E., Kurniawan, I., 2020. Isotopic reconstruction of Proboscidean habitats and diets on Java since the Early Pleistocene: Implications for adaptation and extinction. Quaternary Science Reviews 228, 106007. https://doi.org/10.1016/j.quascirev.2019.106007

Railsback, L.B., Gibbard, P.L., Head, M.J., Voarintsoa, N.R.G., Toucanne, S., 2015. An optimized scheme of lettered marine isotope substages for the last 1.0 million years, and the climatostratigraphic nature of isotope stages and substages. Quaternary Science Reviews 111, 94–106. https://doi.org/10.1016/j.quascirev.2015.01.012

Reich, D., Green, R.E., Kircher, M., Krause, J., Patterson, N., Durand, E.Y., Viola, B., Briggs, A.W., Stenzel, U., Johnson, P.L., 2010. Genetic history of an archaic hominin group from Denisova Cave in Siberia. Nature 468, 1053–1060.

Reich, D., Patterson, N., Kircher, M., Delfin, F., Nandineni, M.R., Pugach, I., Ko, A.M.-S., Ko, Y.-C., Jinam, T.A., Phipps, M.E., 2011. Denisova admixture and the first modern human dispersals into Southeast Asia and Oceania. The American Journal of Human Genetics 89, 516–528.

Reinhold, T., 1937. Fossil duiatoms of the Neogene of Java and their zonal distribution. Verhandel. Geol. -Mijinbow. Geol. Ser. 12, 43–133.

Rhodin, A.G., Thomson, S., Georgalis, G.L., Karl, H.V., Danilov, I.G., Takahashi, A., de la Fuente, M.S., Bourque, J., Delfino, M., Bour, R., 2015. Turtles and tortoises of the world during the rise and global spread of humanity: first checklist and review of extinct Pleistocene and Holocene chelonians.

Rightmire, G.P., 1990. The evolution of Homo erectus: comparative anatomical studies of an extinct human species. Cambridge University Press.

Rightmire, G.P., Henke, W., Tattersall, I., 2015. Handbook of Paleoanthropology.

Rizal, Y., Westaway, K.E., Zaim, Y., van den Bergh, G.D., Bettis, E.A., Morwood, M.J., Huffman, O.F., Grün, R., Joannes-Boyau, R., Bailey, R.M., Sidarto, Westaway, M.C., Kurniawan, I., Moore, M.W., Storey, M., Aziz, F., Suminto, Zhao, J., Aswan, Sipola, M.E., Larick, R., Zonneveld, J.-P., Scott, R., Putt, S., Ciochon, R.L., 2020. Last appearance of Homo erectus at Ngandong, Java, 117,000–108,000 years ago. Nature 577, 381–385. https://doi.org/10.1038/s41586-019-1863-2

Robinson, J.T., 1955. Further remarks on the relationship between "Meganthropus" and australopithecines. American J Phys Anthropol 13, 429–445. https://doi.org/10.1002/ajpa.1330130304

Robinson, J.T., 1953. Meganthropus, australopithecines and hominids. American J Phys Anthropol 11, 1–38. https://doi.org/10.1002/ajpa.1330110112

Rogers, Kidwell, 2007. A conceptual framework for the genesis and analysis of vertebrate skeletal concentrations. Bonebeds: Genesis, Analysis, and Paleobiological Significance: University of Chicago Press, Chicago 1–63.

Rogers, R.R., Eberth, D.A., Fiorillo, A.R., 2010. Bonebeds: genesis, analysis, and paleobiological significance. University of Chicago Press.

Rogers, R.R., Kidwell, S.M., 2000. Associations of Vertebrate Skeletal Concentrations and Discontinuity Surfaces in Terrestrial and Shallow Marine Records: A Test in the Cretaceous of Montana. The Journal of Geology 108, 131–154. https://doi.org/10.1086/314399

Roth, V.L., Shoshani, J., 1988. Dental identification and age determination in *Elephas maximus*. Journal of Zoology 214, 567–588. https://doi.org/10.1111/j.1469-7998.1988.tb03760.x

Roychoudhury, A.N., Kostka, J.E., Van Cappellen, P., 2003. Pyritization: a palaeoenvironmental and redox proxy reevaluated. Estuarine, Coastal and Shelf Science 57, 1183–1193.

Rozzi, R., Winkler, D.E., De Vos, J., Schulz, E., Palombo, M.R., 2013. The enigmatic bovid Duboisia santeng (Dubois, 1891) from the Early–Middle Pleistocene of Java: A multiproxy approach to its paleoecology. Palaeogeography, Palaeoclimatology, Palaeoecology 377, 73–85.

Ruff, C.B., Puymerail, L., Macchiarelli, R., Sipla, J., Ciochon, R.L., 2015. Structure and composition of the Trinil femora: Functional and taxonomic implications. Journal of Human Evolution 80, 147–158. https://doi.org/10.1016/j.jhevol.2014.12.004

Ruff, C.B., Sylvester, A.D., Rahmawati, N.T., Suriyanto, R.A., Storm, P., Aubert, M., Joannes-Boyau, R., Berghuis, H., Pop, E., Batenburg, K.J., 2022. Two Late Pleistocene human femora from Trinil, Indonesia: Implications for body size and behavior in Southeast Asia. Journal of Human Evolution 172, 103252.

Sáez, A., Valero-Garcés, B.L., Moreno, A., Bao, R., Pueyo, J.J., González-Sampériz, P., Giralt, S., Taberner, C., Herrera, C., Gibert, R.O., 2007. Lacustrine sedimentation in active volcanic settings: the Late Quaternary depositional evolution of Lake Chungará (northern Chile). Sedimentology 54, 1191–1222. https://doi.org/10.1111/j.1365-3091.2007.00878.x

Saint-Marc, P., Suminta, 1979. Biostratigraphy of late Miocene and Pliocene deep water sediments of eastern Java (Indonesia). The Journal of Foraminiferal Research 9, 106–117. https://doi.org/10.2113/gsjfr.9.2.106

Sala, N., Martínez, I., Lorenzo, C., García, R., Carretero, J.M., Rodríguez, L., Gómez-Olivencia, A., Aranburu, A., García, N., Quam, R., Gracia, A., Ortega, M.C., Arsuaga, J.L., 2024. Taphonomic skeletal disturbances in the Sima de los Huesos postcranial remains. The Anatomical Record 307, 2437–2450. https://doi.org/10.1002/ar.25197

Saléh, R., 1867. Over fossiele beenderen van den Pandan. Natuurkundig Tijdschrift voor Nederlansch Indië 29, 422–423.

Salles, T., Mallard, C., Husson, L., Zahirovic, S., Sarr, A.-C., Sepulchre, P., 2021. Quaternary landscape dynamics boosted species dispersal across Southeast Asia. Communications Earth & Environment 2, 240.

Santa Luca, A.P., 1980. The Ngandong fossil hominids: a comparative study of a far eastern Homo erectus group. Yale Peabody Museum.

Sanyoto, S., 2009. Biostratigrafi dan biodatum foraminifera planktonik sumur-95 di daerah Cepu Kabupaten Blora, Jawa Tengah.

Sarr, A.-C., Husson, L., Sepulchre, P., Pastier, A.-M., Pedoja, K., Elliot, M., Arias-Ruiz, C., Solihuddin, T., Aribowo, S., Susilohadi, 2019. Subsiding Sundaland. Geology 47, 119–122. https://doi.org/10.1130/G45629.1

Sartono, S., 1981. The age of Homo modjokertensis. Mod. Quaternary Res. SE Asia 6, 91–102.

Satrya, T.R., 2014. Engineering Geological Mapping at Center of Surabaya Region by Developing Geo-Tomography Image Analysis, in: Celeb. Int. Conf. Earth Sci., No.

Satyana, A.H., 2007. Central Java, Indonesia–A "Terra Incognita" in petroleum exploration: New considerations on the tectonic evolution and petroleum implications.

Satyana, A.H., Armandita, C., 2004. Deepwater Plays of Java, Indonesia: Regional Evaluation on Opportunities and Risks.

Satyana, A.H., Erwanto, E., Prasetyadi, C., 2004. Rembang-Madura-Kangean-Sakala (RMKS) Fault Zone, East Java Basin: The Origin and Nature of A Geologic Border. Proc. IAGI, 33rd., Ann. Conv. And Exh., Bandung.

Scardia, G., Neves, W.A., Tattersall, I., Blumrich, L., 2021. What kind of hominin first left Africa? Evolutionary Anthropology 30, 122–127. https://doi.org/10.1002/evan.21863

Schiebel, R., Hemleben, C., 2005. Modern planktic foraminifera. Paläontol Z 79, 135–148. https://doi.org/10.1007/BF03021758

Schmid, E., Garraux, O., 1972. Atlas of animal bones: for prehistorians, archaeologists and quaternary geologists= Knochenatlas: für Prähistoriker, Archäologen und Quartärgeologen. (No Title).

Schwartz, F.J., 2007. Tail spine characteristics of stingrays (Order Myliobatiformes) frequenting the FAO Fishing Area 61 (20°N 120 E-50°N 150 E) of the Northwest Pacific Ocean. The Raffles Bulletin of Zoology 121–130.

Schwartz, J.H., 2004. Getting to Know *Homo erectus*. Science 305, 53–54. https://doi.org/10.1126/science.1099989

Schwartz, J.H., Tattersall, I., 2003. Craniodental morphology of genus Homo (Africa and Asia). New York Wiley.

Scott, K.M., 1988. Origins, behavior, and sedimentology of lahars and lahar-runout flows in the Toutle-Cowlitz River System.

Scott, K.M., Macías, J.L., Naranjo, J.A., Rodríguez, S., McGeehin, J.P., 2001. Catastrophic Debris Flows Transformed from Landslides in Volcanic Terrains: Mobility, Hazard Assessment, and Mitigation Strategies. U.S. Department of the Interior, U.S. Geological Survey.

Selenka, L., Blanckenhorn, M.L.P., 1911a. Die Pithecanthropus-Schichten auf Java: Geologische und paläontologische Ergebnisse der Trinil-Expedition (1907 und 1908), ausgeführt mit Unterstützung der Akademischen Jubiläumsstiftung der Stadt Berlin und der Königlich bayerischen Akademi der Wissenschaften. W. Engelmann.

Selenka, L., Blanckenhorn, M.L.P., 1911b. Die Pithecanthropus-Schichten auf Java: Geologische und paläontologische Ergebnisse der Trinil-Expedition (1907 und 1908), ausgeführt mit Unterstützung der Akademischen Jubiläumsstiftung der Stadt Berlin und der Königlich bayerischen Akademi der Wissenschaften. W. Engelmann.

Sellés-Martínez, J., 1996. Concretion morphology, classification and genesis. Earth-Science Reviews 41, 177–210.

Selvaggio, M.M., 1998. Evidence for a three-stage sequence of hominid and carnivore involvement with long bones at FLKZinjanthropus, Olduvai Gorge, Tanzania. Journal of Archaeological Science 25, 191–202.

Sémah, A.-M., Sémah, F., 2012. The rain forest in Java through the Quaternary and its relationships with humans (adaptation, exploitation and impact on the forest). Quaternary International 249, 120–128. https://doi.org/10.1016/j.quaint.2011.06.013

Sémah, A.-M., Sémah, F., Djubiantono, T., Brasseur, B., 2010. Landscapes and Hominids' environments: changes between the Lower and the Early Middle Pleistocene in Java (Indonesia). Quaternary International 223, 451.

Setiyabudi, E., Kurniawan, I., Insani, H., Takahashi, A., 2021. Late Pleistocene fossil record of Cuora amboinensis (Testudines: Geoemydidae) from the Wajak site, East Java, Indonesia, and its paleozoogeographic and archeozoological implications. Paleontological Research 25, 25–31.

Setiyabudi, E., Takahashi, A., Kaifu, Y., 2016. First certain fossil record of Orlitia borneensis (Testudines: Geoemydidae) from the Pleistocene of central Java, Indonesia. Current herpetology 35, 75–82.

Shipman, P., Rose, J.J., 1988. Bone tools: an experimental approach, in: Scanning Electron Microscopy in Archaeology. pp. 303–335.

Silver, 1963. The ageing of domestic animals. Agricultural and Food Sciences, Environmental Science.

Sipola, M.E., 2018. Formation of the Ngandong paleoanthropological site and Solo River terrace sequence, Central Java, Indonesia.

Smart, C.W., Thomas, E., 2006. The enigma of early Miocene biserial planktic foraminifera. Geology 34, 1041–1044. https://doi.org/10.1130/G23038A.1

Smith, H.E., Price, G.J., Duval, M., Westaway, K., Zaim, J., Rizal, Y., Puspaningrum, M.R., Trihascaryo, A., Stewart, M., Louys, J., 2021. Taxonomy, taphonomy and chronology of the Pleistocene faunal assemblage at Ngalau Gupin cave, Sumatra. Quaternary International 603, 40–63.

Smith, R., Kitching, J., 1997. Sedimentology and vertebrate taphonomy of the Tritylodon acme zone: a reworked palaeosol in the Lower Jurassic Elliot Formation, Karoo Supergroup, South Africa. Palaeogeography, Palaeoclimatology, Palaeoecology 131, 29–50.

Smith, T., Smith, R., 2003. Terrestrial mammals as biostratigraphic indicators in upper Paleocene-lower Eocene marine deposits of the southern North Sea Basin. SPECIAL PAPERS-GEOLOGICAL SOCIETY OF AMERICA 513–520.

Smyth, H., Hall, R., Hamilton, J., Kinny, P., 2005. East Java: Cenozoic basins, volcanoes and ancient basement, in: Proceedings of the Indonesian Petroleum Association, 30th Annual Convention. Indonesian Petroleum Association, pp. 251–266.

Smyth, H.R., Hall, R., Nichols, G.J., 2008. Cenozoic volcanic arc history of East Java, Indonesia: the stratigraphic record of eruptions on an active continental margin. Special-Papers-Geological society of America 436, 199.

Soeradi et al., 1985. Geology and stratigraphy of the Trinil area, in: Quaternary Geology of the Hominid Fossil Bearing Formations in Java,. Geological Research and Development Centre Special Publication, Bandung, pp. 49–53.

Soeria-Atmadja, R., Maury, R.C., Bellon, H., Pringgoprawiro, H., Polve, M., Priadi, B., 1994. Tertiary magmatic belts in Java. Journal of southeast asian earth sciences 9, 13–27.

Sonakia, A., 1984. The skull cap of early man and associated mammalian fauna from Narmada Valley alluvium, Hoshangabad area, Madhya Pradesh, India. Records of the Geological survey of India 113, 159–172.

Sondaar, P.Y., 1984. Faunal evolution and the mammalian bio stratigraphy of Java. The Early Evolution of Man with Special Emphasis on Southeast Asia and Africa. Cour. Forsch. Inst. Senckenberg, Frankfurt am Main 69, 219–235.

Spehar, S.N., Sheil, D., Harrison, T., Louys, J., Ancrenaz, M., Marshall, A.J., Wich, S.A., Bruford, M.W., Meijaard, E., 2018. Orangutans venture out of the rainforest and into the Anthropocene. Sci. Adv. 4, e1701422. https://doi.org/10.1126/sciadv.1701422

Speth, J., Clark, J., 2006. Hunting and overhunting in the Levantine Late Middle Palaeolithic. Before Farming 2006, 1–42. https://doi.org/10.3828/bfarm.2006.3.1

Speth, J.D., 2013. Middle Paleolithic Large-Mammal Hunting in the Southern Levant, in: Clark, J.L., Speth, J.D. (Eds.), Zooarchaeology and Modern Human Origins, Vertebrate Paleobiology and Paleoanthropology. Springer Netherlands, Dordrecht, pp. 19–43. https://doi.org/10.1007/978-94-007-6766-9_3

Speth, J.D., 2010a. Big-Game Hunting: Protein, Fat, or Politics?, in: The Paleoanthropology and Archaeology of Big-Game Hunting, Interdisciplinary Contributions to Archaeology. Springer New York, New York, NY, pp. 149–161. https://doi.org/10.1007/978-1-4419-6733-6_12

Speth, J.D., 2010b. The Paleoanthropology and Archaeology of Big-Game Hunting, Interdisciplinary Contributions to Archaeology. Springer New York, New York, NY. https://doi.org/10.1007/978-1-4419-6733-6

Spinage, C.A., 1973. A review of the age determination of mammals by means of teeth, with especial reference to Africa. African Journal of Ecology 11, 165–187. https://doi.org/10.1111/j.1365-2028.1973.tb00081.x

Sprintall, J., Chong, J., Syamsudin, F., Morawitz, W., Hautala, S., Bray, N., Wijffels, S., 1999. Dynamics of the South Java Current in the Indo-Australian Basin. Geophysical Research Letters 26, 2493–2496. https://doi.org/10.1029/1999GL002320

Steele, 2003. Using mortality profiles to infer behavior in the fossil record. Journal of Mammalogy.

Stewart, M., Louys, J., Breeze, P.S., Clark-Wilson, R., Drake, N.A., Scerri, E.M., Zalmout, I.S., Al-Mufarreh, Y.S., Soubhi, S.A., Haptari, M.A., 2020. A taxonomic and taphonomic study of Pleistocene fossil deposits from the western Nefud Desert, Saudi Arabia. Quaternary Research 95, 1–22.

Stiner, 2009. The antiquity of large game hunting in the Mediterranean Paleolithic. Evidence from mortality patterns. Transitions in prehistory: Papers in honor of Ofer Bar-Yosef.

Stiner, M.C., 2013. An Unshakable Middle Paleolithic?: Trends versus Conservatism in the Predatory Niche and Their Social Ramifications. Current Anthropology 54, S288–S304. https://doi.org/10.1086/673285

Stiner, M.C., 1990. The use of mortality patterns in archaeological studies of hominid predatory adaptations. Journal of anthropological archaeology 9, 305–351.

Stiner, M.C., Barkai, R., Gopher, A., 2009. Cooperative hunting and meat sharing 400–200 kya at Qesem Cave, Israel. Proc. Natl. Acad. Sci. U.S.A. 106, 13207–13212. https://doi.org/10.1073/pnas.0900564106

Storm, P., 2001. The evolution of humans in Australasia from an environmental perspective. Palaeogeography, Palaeoclimatology, Palaeoecology 171, 363–383.

Storm, P., 1995. The evolutionary significance of the Wajak skulls. Scripta Geologica 110, 1–248.

Storm, P., 1994. De morfologie van Homo modjokertensis. Cranium 11, 97–102.

Storm, P., Aziz, F., de Vos, J., Kosasih, D., Baskoro, S., van den Hoek Ostende, L.W., 2005. Late Pleistocene Homo sapiens in a tropical rainforest fauna in East Java. Journal of Human Evolution 49, 536–545.

Storm, P., Wood, R., Stringer, C., Bartsiokas, A., De Vos, J., Aubert, M., Kinsley, L., Grün, R., 2013. U-series and radiocarbon analyses of human and faunal remains from Wajak, Indonesia. Journal of human evolution 64, 356–365.

Stremme, H., 1911. 191 I. Die Säugetiere mit Ausnahme der Proboscidier, in: Selenka and Blanckenhorn Die Pithecanthropusschichten Auf Java Geologische Und Palaontologische Ergebnisse De Trinil-Expedition (1907 Und 1908) Verlag Von Wilhelm Engelmann, Leipzig. pp. 82–150.

Stringer, C., 2002. Modern human origins: progress and prospects. Phil. Trans. R. Soc. Lond. B 357, 563–579. https://doi.org/10.1098/rstb.2001.1057

Sukardi, 1992. Peta Geologi Lembar Surabaya dan Sapulu, Jawa. Pusat Penelitian dan Pengembangan Geologi.

Suraprasit, K., Jaeger, J.-J., Chaimanee, Y., Chavasseau, O., Yamee, C., Tian, P., Panha, S., 2016. The middle Pleistocene vertebrate fauna from Khok Sung (Nakhon Ratchasima, Thailand): biochronological and paleobiogeographical implications. ZooKeys 1.

Susilohadi, 1995. Late Tertiary and Quaternary Geology of the East Java Basin, Indonesia (PhD Thesis). University of Wollongong.

Swisher, C.C., Curtis, G.H., Jacob, T., Getty, A.G., Suprijo, A., Widiasmoro, 1994. Age of the earliest known hominids in Java, Indonesia. Science 263, 1118–1121. https://doi.org/10.1126/science.8108729

Taylor, P.D., Wilson, M.A., 2003. Palaeoecology and evolution of marine hard substrate communities. Earth-Science Reviews 62, 1–103.

Tebbens, L.A., Veldkamp, A., Westerhoff, W., Kroonenberg, S.B., 1999. Fluvial incision and channel downcutting as a response to Late-glacial and Early Holocene climate change: the lower reach of the River Meuse (Maas), The Netherlands. Journal of Quaternary Science: Published for the Quaternary Research Association 14, 59–75.

Teixeira, J.C., Jacobs, G.S., Stringer, C., Tuke, J., Hudjashov, G., Purnomo, G.A., Sudoyo, H., Cox, M.P., Tobler, R., Turney, C.S., 2021. Widespread Denisovan ancestry in Island Southeast Asia but no evidence of substantial super-archaic hominin admixture. Nature Ecology & Evolution 5, 616–624.

Ter Haar, C., 1934. Het Ngandong Terras, Rapport over Ontdekking, Uitgraving en Geologische Ligging er van uitgebracht [The Ngandong Terrace, Report on the Discovery, Excavation and Geological relationships]. Geological Library (prepared for signature on 27 July.

Thiede, J., 1975. Distribution of foraminifera in surface waters of a coastal upwelling area. Nature 253, 712. https://doi.org/10.1038/253712a0

Tobias, P.V., Von Koenigswald, G.H.R., 1965. A Comparison Between the Olduvai Hominines and Those of Java and Some Implications for Hominid Phylogeny. Current Anthropology 6, 427–431. https://doi.org/10.1086/200630.

Trinkaus, Wu, 2017. External auditory exostoses in the Xuchang and Xujiayao human remains: Patterns and implications among eastern Eurasian Middle and Late Pleistocene …. Plos One.

Trooster, 1937. Nota betreffende Ir. J. Duyfjes “Zur Geologie und Statigraphie ders Kendenggebietes zwischen Trinil und Soerabaia. Bataafse Internationale Petroleum Maatschappij.

Tseng, Z.J., Chang, C.-H., 2007. A study of new material of Crocuta crocuta ultima (Carnivora: Hyaenidae) from the Quaternary of Taiwan. Collection and Research 20, 9–19.

Tsutaya, T., Sawafuji, R., Taurozzi, A.J., Fagernäs, Z., Patramanis, I., Troché, G., Mackie, M., Gakuhari, T., Oota, H., Tsai, C.-H., Olsen, J.V., Kaifu, Y., Chang, C.-H., Cappellini, E., Welker, F., 2025. A male Denisovan mandible from Pleistocene Taiwan. Science 388, 176–180. https://doi.org/10.1126/science.ads3888.

Tucker, M.E., 1985. Shallow-marine carbonate facies and facies models. Geological Society, London, Special Publications 18, 147–169.

Turner, A., Antón, M., 1996. The giant hyaena, Pachycrocuta brevirostris (Mammalia, Carnivora, Hyaenidae). Geobios 29, 455–468.

Tyler, D.E., 2001. "Meganthropus" cranial fossils from Java. Human evolution 16, 81–101.

Tyler, D.E., 1995. The current picture of hominid evolution in Java. Acta Anthropologica Sinica 14, 313.

Vallance, J.W., 2005. Volcanic debris flows, in: Debris-Flow Hazards and Related Phenomena. Springer, pp. 247–274.

van Bemmelen, R.W., 1949. The geology of Indonesia. 1, A. General geology of Indonesia and adjacent archipelagoes. US Government Printing Office.

Van Benthem Jutting, 1937. Non marine Mollusca from fossil horizons in Java with special reference to the Trinil fauna. Zoologische Mededelingen, Vol 20, 83–180.

Van den Bergh, 1988. Duboisia Santeng, the endemic Pleistocene Bovid from Java.

Van den Bergh, G.D., 1999. The Late Neogene elephantoid-bearing faunas of Indonesia and their palaeozoogeographic implications. Scripta Geologica 117, 1–419.

Van Den Bergh, G.D., 1999. The Late Neogene elephantoid-bearing faunas of Indonesia and their palaeozoogeographic implications. Scripta Geologica 117, 1–419.

Van den Bergh, G.D., de Vos, J., Sondaar, P.Y., 2001. The Late Quaternary palaeogeography of mammal evolution in the Indonesian Archipelago. Palaeogeography, Palaeoclimatology, Palaeoecology 171, 385–408.

Van den Bergh, G.D., de Vos, J., Sondaar, P.Y., Aziz, F., 1996. Pleistocene zoogeographic evolution of Java (Indonesia) and glacio-eustatic sea level fluctuations: a background for the presence of Homo. Bulletin of the Indo-Pacific Prehistory Association 14, 7–21.

Van den Bergh, G.D., Kaifu, Y., Kurniawan, I., Kono, R.T., Brumm, A., Setiyabudi, E., Aziz, F., Morwood, M.J., 2016. Homo floresiensis-like fossils from the early Middle Pleistocene of Flores. Nature 534, 245–248.

Van den Brink, L.M., 1982. On the mammal fauna of the Wajak Cave, Java (Indonesia). Mod. Quat. Res. SE Asia 7, 177–193.

Van der Geer, A., Lyras, G., De Vos, J., Dermitzakis, M., 2011. Evolution of island mammals: adaptation and extinction of placental mammals on islands. John Wiley & Sons.

Van der Geer, A.A., 2019. Selenka and Blanckenhorn Die Pithecanthropusschichten Auf Java Geologische Und Palaontologische Ergebnisse De Trinil-Expedition (1907 Und 1908) Verlag Von Wilhelm Engelmann, Leipzig. PeerJ 7, e6894.

Van der Geer, A.A., Lyras, G.A., Volmer, R., 2018. Insular dwarfism in canids on Java (Indonesia) and its implication for the environment of Homo erectus during the Early and earliest Middle Pleistocene. Palaeogeography, Palaeoclimatology, Palaeoecology 507, 168–179.

Van der Kaars, S., Wang, X., Kershaw, P., Guichard, F., Setiabudi, D.A., 2000. A Late Quaternary palaeoecological record from the Banda Sea, Indonesia: patterns of vegetation, climate and biomass burning in Indonesia and northern Australia. Palaeogeography, Palaeoclimatology, Palaeoecology 155, 135–153.

Van der Kaars, W.A., Dam, M.A.C., 1995. A 135,000-year record of vegetational and climatic change from the Bandung area, West-Java, Indonesia. Palaeogeography, Palaeoclimatology, Palaeoecology 117, 55–72.

Van der Maarel, F.H., 1932. Contributions to the knowledge of the fossil mammalian fauna of Java. Wet. Med. Dienst. Mijnb. Ned. Indie 15, 1–208.

Van Es, L.J.C., 1931. The age of Pithecanthropus. Springer.

Van Gorsel, J.T., Troelstra, S.R., 1981. Late Neogene planktonic foraminiferal biostratigraphy and climatostratigraphy of the Solo River section (Java, Indonesia). Marine Micropaleontology 6, 183–209. https://doi.org/10.1016/0377-8398(81)90005-0

Veldkamp, A., Schoorl, J.M., Wijbrans, J.R., Claessens, L., 2012. Mount Kenya volcanic activity and the Late Cenozoic landscape reorganisation in the upper Tana fluvial system. Geomorphology 145, 19–31.

Veldkamp, A., Tebbens, L.A., 2001. Registration of abrupt climate changes within fluvial systems: insights from numerical modelling experiments. Global and Planetary Change 28, 129–144.

Veldkamp, A., van Dijke, J.J., 2000. Simulating internal and external controls on fluvial terrace stratigraphy: a qualitative comparison with the Maas record. Geomorphology 33, 225–236. https://doi.org/10.1016/S0169-555X(99)00125-7

Verhaegen, M., Munro, S., 2011. Pachyosteosclerosis suggests archaic Homo frequently collected sessile littoral foods. Homo 62, 237–247.

Vialet, A., Guipert, G., Jianing, H., Xiaobo, F., Zune, L., Youping, W., Tianyuan, L., de Lumley, M.-A., de Lumley, H., 2010. Homo erectus from the Yunxian and Nankin Chinese sites: Anthropological insights using 3D virtual imaging techniques. Comptes Rendus Palevol 9, 331–339.

Villa, P., Mahieu, E., 1991. Breakage patterns of human long bones. Journal of human evolution 21, 27–48.

Villa, P., Soriano, S., Pollarolo, L., Smriglio, C., Gaeta, M., D'orazio, M., Conforti, J., Tozzi, C., 2020. Neandertals on the beach: Use of marine resources at Grotta dei Moscerini (Latium, Italy). PloS one 15, e0226690.

Volmer, R., Hertler, C., van der Geer, A., 2016. Niche overlap and competition potential among tigers (Panthera tigris), sabertoothed cats (Homotherium ultimum, Hemimachairodus zwierzyckii) and Merriam's Dog (Megacyon merriami) in the Pleistocene of Java. Palaeogeography, Palaeoclimatology, Palaeoecology 441, 901–911.

Volz, W., 1907. Das geologische Alter der Pithecanthropus-Schichten bei Trinil, Ost-Java. Schweizerbart.

Von den Driesch, A., 1976. A guide to the measurement of animal bones from archaeological sites. Peabody Museum Press.

Von Koenigswald, 1939. Dan Pleistozän Javas, Quartär.

von Koenigswald, G.H.R., 1940. Neue Pithecanthropus Funde 1936-1938; Ein Beitrag zur Kenntnis der Prae-Hominiden. Wet. Meded. Dienst Mijnb. Ned. Indie 28, 1–232.

Von Koenigswald, G.H.R., 1935. Die Saugetierfaunen Javas. Proc. Kon. Akad.v. Wetensch, Amsterdam 38, 188–198.

Von Koenigswald, G.H.R., 1934. Zur Stratigraphie des Javanischen Pleistocan. De Ingenieur in Nederlands-Indie 1, 185–201.

Von Koenigswald, G.H.R., 1933. Beitrag zur Kenntnis der fossilen Wirbeltiere Javas I. Teil. Wet. Med. Dienst. Mijnb. Ned. Indie 23, 1–127.

Von Koenigswald, G.H.R., 1936a. Ein fossiler hominide aus dem Altpleistocan Ostjavas. De Ingenieur ned.-Indie 4, 149–157.

von Koenigswald, G.H.R., 1936b. Erste Mitteilung über einen fossilen Hominiden aus dem Altpleistocän Ostjavas. Verh. K. Akad. Van Wet. 39, 1000.

Voorhies, M.R., 1969. Taphonomy and population dynamics of an early Pliocene vertebrate fauna, Knox County, Nebraska.

Voris, H.K., 2000. Maps of Pleistocene sea levels in Southeast Asia: shorelines, river systems and time durations. Journal of Biogeography 27, 1153–1167. https://doi.org/10.1046/j.1365-2699.2000.00489.x

Vos, J. de, Sondaar, P., C. C. Swisher, I.I.I., 1994. Dating hominid sites in Indonesia [WWW Document]. Science. URL http://link.galegroup.com/apps/doc/A15948857/AONE?sid=googlescholar (accessed 3.28.19).

Wade, B.S., Pearson, P.N., Berggren, W.A., Pälike, H., 2011. Review and revision of Cenozoic tropical planktonic foraminiferal biostratigraphy and calibration to the geomagnetic polarity and astronomical time scale. Earth-Science Reviews 104, 111–142.

Wang, M., Zong, Y., 2020. Significant SST differences between peak MIS5 and MIS1 along the low-latitude western North Pacific margin. Quaternary Science Reviews 227, 106060.

Wang, Z. Li, T. Tong, T. van Kolfschoten, 2022. Hominin paleoenvironment in East Asia: The Middle Paleolithic Xuchang-Lingjing (China) mammalian evidence. Quaternary International.

Weaver, C.E., 1989. Clays, muds, and shales. Elsevier.

Weidenreich, F., 1951. Morphology of Solo man. Anthropological Paper of the American Museum of Natural History 43, 205–290.

Weidenreich, F., 1945. Giant early man from Java and South China. Anthrop. Pap. Am. Mus. Nat. Hist. 40, 1–134.

Weidenreich, F., 1943. The skull of Sinanthropus pekinensis; a comparative study on a primitive hominid skull. Palaeontologica. Sinica 10, 1–298.

Weidenreich, F., 1940. Some problems dealing with ancient man. American Anthropologist 42, 375–383.

Weinand, D.C., 2005. A reevaluation of the paleoenvironmental reconstructions associated with Homo erectus from Java, Indonesia, based on the functional morphology of fossil bovid astragali (PhD Thesis). The University of Tennessee.

Wells, J.W., 1944. Middle Devonian bone beds of Ohio. Bulletin of the Geological Society of America 55, 273–302.

Wentworth, C.K., 1922. A scale of grade and class terms for clastic sediments. The journal of geology 30, 377–392.

Westaway, K.E., Morwood, M.J., Roberts, R.G., Rokus, A.D., Zhao, J.-X., Storm, P., Aziz, F., Van den Bergh, G., Hadi, P., De Vos, J., 2007. Age and biostratigraphic significance of the Punung Rainforest Fauna, East Java, Indonesia, and implications for Pongo and Homo. Journal of Human Evolution 53, 709–717.

Westaway, M.C., Durband, A., Lambert, D., 2015. Human evolution in Sunda and Sahul and the continuing contributions of Professor Colin Groves.

Widianto, H., Noerwidi, S., 2023. Long journey of Indonesian Homo erectus: Arrival and dispersal in Java Island. L'Anthropologie 127, 103167.

Widianto, H., Noerwidi, S., Hascaryo, A.T., 2023. New Hominin calvaria discovery from Grenzbank Layer of Sangiran Dome (Java, Indonesia): The last archaic Homo erectus lived in Java. L'Anthropologie 127, 103165.

Widianto, H., Zeitoun, V., 2003. Morphological description, biometry and phylogenetic position of the skull of Ngawi 1 (east Java, Indonesia). Intl J of Osteoarchaeology 13, 339–351. https://doi.org/10.1002/oa.694

Williston, S.W., 1925. The osteology of the reptiles. Harvard University Press.

Wilson, D.E., Reeder, D.M., 2005. Mammal species of the world: a taxonomic and geographic reference. JHU press.

Wintle, A.G., Murray, A.S., 2006. A review of quartz optically stimulated luminescence characteristics and their relevance in single-aliquot regeneration dating protocols. Radiation measurements 41, 369–391.

Wright, V.P., 1984. Peritidal carbonate facies models: a review. Geological Journal 19, 309–325.

Wu, X., Athreya, S., 2013. A description of the geological context, discrete traits, and linear morphometrics of the Middle Pleistocene hominin from Dali, Shaanxi Province, China. American J Phys Anthropol 150, 141–157. https://doi.org/10.1002/ajpa.22188

Wu, X., Bräuer, G., 1993. Morphological comparison of archaic Homo sapiens crania from China and Africa. Zeitschrift für Morphologie und Anthropologie 241–259.

Wu, X., Pei, S., Cai, Y., Tong, H., Xing, S., Jashashvili, T., Carlson, K.J., Liu, W., 2021. Morphological description and evolutionary significance of 300 ka hominin facial bones from Hualongdong, China. Journal of Human Evolution 161, 103052.

Wu, X.-J., Pei, S.-W., Cai, Y.-J., Tong, H.-W., Li, Q., Dong, Z., Sheng, J.-C., Jin, Z.-T., Ma, D.-D., Xing, S., Li, X.-L., Cheng, X., Cheng, H., De La Torre, I., Edwards, R.L., Gong, X.-C., An, Z.-S., Trinkaus, E., Liu, W., 2019. Archaic human remains from Hualongdong, China, and Middle Pleistocene human continuity and variation. Proc. Natl. Acad. Sci. U.S.A. 116, 9820–9824. https://doi.org/10.1073/pnas.1902396116

Wu, X.-J., Schepartz, L.A., Liu, W., Trinkaus, E., 2011. Antemortem trauma and survival in the late Middle Pleistocene human cranium from Maba, South China. Proc. Natl. Acad. Sci. U.S.A. 108, 19558–19562. https://doi.org/10.1073/pnas.1117113108

Wyrtki, K., 1961. Physical Oceanography of the Southeast Asian waters.

Xing, S., Martinón-Torres, M., Bermúdez de Castro, J.M., 2018. The fossil teeth of the Peking Man. Scientific Reports 8, 2066.

Yudha, D.S., Aritona, F.T.S., Eprilurahman, R., 2020a. Characteristics of Shell Bone as an Identification Tool for Turtle Species (Reptiles: Testudines) in Java, Borneo, and Sumatra. Journal of Tropical Biodiversity and Biotechnology 5, 35–43.

Yudha, D.S., Prabowo, M.A., Suriyanto, R.A., Barianto, D.H., 2020b. The diversity of ray-finned fishes (Actinopterygii) in Plio-Pleistocene Java. Journal of Tropical Biodiversity and Biotechnology 5, 149–156.

Yudha, D.S., Ramadhani, R., Suriyanto, R.A., Novian, M.I., 2018. The diversity of sharks fossils in Plio-Pleistocene of Java, Indonesia, in: AIP Conference Proceedings. AIP Publishing.

Zagwijn, W.H., 1989. The Netherlands during the Tertiary and the Quaternary: A case history of Coastal Lowland evolution, in: Van Der Linden, W.J.M., Cloetingh, S.A.P.L., Kaasschieter, J.P.K., Van De Graaff, W.J.E., Vandenberghe, J., Van Der Gun, J.A.M. (Eds.), Coastal Lowlands. Springer Netherlands, Dordrecht, pp. 107–120. https://doi.org/10.1007/978-94-017-1064-0_6

Zahirovic, S., Flament, N., Dietmar Müller, R., Seton, M., Gurnis, M., 2016a. Large fluctuations of shallow seas in low-lying S outheast A sia driven by mantle flow. Geochemistry, Geophysics, Geosystems 17, 3589–3607.

Zahirovic, S., Matthews, K.J., Flament, N., Müller, R.D., Hill, K.C., Seton, M., Gurnis, M., 2016b. Tectonic evolution and deep mantle structure of the eastern Tethys since the latest Jurassic. Earth-Science Reviews 162, 293–337.

Zaim, Y., 2010. Geological evidence for the earliest appearance of hominins in Indonesia, in: Out of Africa I. Springer, pp. 97–110.

Zaim, Y., Ciochon, R.L., Polanski, J.M., Grine, F.E., Bettis III, E.A., Rizal, Y., Franciscus, R.G., Larick, R.R., Heizler, M., Eaves, K.L., 2011. New 1.5 million-year-old Homo erectus maxilla from Sangiran (Central Java, Indonesia). Journal of human evolution 61, 363–376.

Zanolli, C., Kaifu, Y., Pan, L., Xing, S., Mijares, A.S., Kullmer, O., Schrenk, F., Corny, J., Dizon, E., Robles, E., 2022. Further analyses of the structural organization of Homo luzonensis teeth: Evolutionary implications. Journal of Human Evolution 163, 103124.

Zanolli, C., Kullmer, O., Kelley, J., Bacon, A.-M., Demeter, F., Dumoncel, J., Fiorenza, L., Grine, F.E., Hublin, J.-J., Nguyen, A.T., 2019. Evidence for increased hominid diversity in the Early to Middle Pleistocene of Indonesia. Nature ecology & evolution 3, 755–764.

Zavala, C., 2020. Hyperpycnal (over density) flows and deposits. Journal of Palaeogeography 9, 1–21.

Zhang, S., Li, Z., Zhang, Y., Gao, X., 2009. Mortality profiles of the large herbivores from the Lingjing Xuchang Man Site, Henan Province and the early emergence of the modern human behaviors in East Asia. Chin. Sci. Bull. 54, 3857–3863. https://doi.org/10.1007/s11434-009-0648-7

Zilhão, J., Angelucci, D.E., Igreja, M.A., Arnold, L.J., Badal, E., Callapez, P., Cardoso, J.L., d'Errico, F., Daura, J., Demuro, M., Deschamps, M., Dupont, C., Gabriel, S., Hoffmann, D.L., Legoinha, P., Matias, H., Monge Soares, A.M., Nabais, M., Portela, P., Queffelec, A., Rodrigues, F., Souto, P., 2020. Last Interglacial Iberian Neandertals as fisher-hunter-gatherers. Science 367, eaaz7943. https://doi.org/10.1126/science.aaz7943

Zolitschka, B., Francus, P., Ojala, A.E., Schimmelmann, A., 2015. Varves in lake sediments–a review. Quaternary Science Reviews 117, 1–41.

